LIFE AND DEATH: NEW PERSPECTIVES AND APPLICATIONS IN FORENSIC SCIENCE

EDITED BY: Gulnaz T. Javan, M. Eric Benbow and
T. Komang Ralebitso-Senior

PUBLISHED IN: Frontiers in Ecology and Evolution and Frontiers in Microbiology

frontiers Research Topics

frontiers

ISSN 1664-8714
ISBN 978-2-88971-489-6
DOI 10.3389/978-2-88971-489-6

About Frontiers

Frontiers is more than just an open-access publisher of scholarly articles: it is a pioneering approach to the world of academia, radically improving the way scholarly research is managed. The grand vision of Frontiers is a world where all people have an equal opportunity to seek, share and generate knowledge. Frontiers provides immediate and permanent online open access to all its publications, but this alone is not enough to realize our grand goals.

Frontiers Journal Series

The Frontiers Journal Series is a multi-tier and interdisciplinary set of open-access, online journals, promising a paradigm shift from the current review, selection and dissemination processes in academic publishing. All Frontiers journals are driven by researchers for researchers; therefore, they constitute a service to the scholarly community. At the same time, the Frontiers Journal Series operates on a revolutionary invention, the tiered publishing system, initially addressing specific communities of scholars, and gradually climbing up to broader public understanding, thus serving the interests of the lay society, too.

Dedication to Quality

Each Frontiers article is a landmark of the highest quality, thanks to genuinely collaborative interactions between authors and review editors, who include some of the world's best academicians. Research must be certified by peers before entering a stream of knowledge that may eventually reach the public - and shape society; therefore, Frontiers only applies the most rigorous and unbiased reviews.
Frontiers revolutionizes research publishing by freely delivering the most outstanding research, evaluated with no bias from both the academic and social point of view. By applying the most advanced information technologies, Frontiers is catapulting scholarly publishing into a new generation.

What are Frontiers Research Topics?

Frontiers Research Topics are very popular trademarks of the Frontiers Journals Series: they are collections of at least ten articles, all centered on a particular subject. With their unique mix of varied contributions from Original Research to Review Articles, Frontiers Research Topics unify the most influential researchers, the latest key findings and historical advances in a hot research area! Find out more on how to host your own Frontiers Research Topic or contribute to one as an author by contacting the Frontiers Editorial Office: frontiersin.org/about/contact

LIFE AND DEATH: NEW PERSPECTIVES AND APPLICATIONS IN FORENSIC SCIENCE

Topic Editors:
Gulnaz T. Javan, Alabama State University, United States
M. Eric Benbow, Michigan State University, United States
T. Komang Ralebitso-Senior, Liverpool John Moores University, United Kingdom

Citation: Javan, G. T., Benbow, M. E., Ralebitso-Senior, T. K., eds. (2021). Life and Death: New Perspectives and Applications in Forensic Science. Lausanne: Frontiers Media SA. doi: 10.3389/978-2-88971-489-6

Table of Contents

frontiers in Ecology and Evolution

EDITORIAL
published: 25 August 2021
doi: 10.3389/fevo.2021.725046

Editorial: Life and Death: New Perspectives and Applications in Forensic Science

Gulnaz T. Javan[1]*, *M. Eric Benbow*[2,3,4,5] and *T. Komang Ralebitso-Senior*[6]

[1] Department of Physical Sciences and Forensic Science Programs, Alabama State University, Montgomery, AL, United States, [2] Department of Entomology, Michigan State University, East Lansing, MI, United States, [3] Department of Osteopathic Medical Specialties, Michigan State University, East Lansing, MI, United States, [4] AgBioResearch, Michigan State University, East Lansing, MI, United States, [5] Ecology, Evolution and Behavior Program, Michigan State University, East Lansing, MI, United States, [6] School of Pharmacy and Biomolecular Sciences, Liverpool John Moores University, Liverpool, United Kingdom

Keywords: microbial ecology, next-generation sequencing, vertebrate decomposition, necrobiome, thanatomicrobiome, forensic science

Editorial on the Research Topic

Life and Death: New Perspectives and Applications in Forensic Science

INTRODUCTION

Death is a universal phenomenon and what happens after life has led to extensive forensic ecology research. Consequently, we now know that the shell of the once living provides fertile ground for other life forms, spanning prokaryotic microbes to large, vertebrate scavengers. This ephemeral patch of newly available resources also provides rich sources of evidence that can be used in death investigation. In recent years there have been substantial advances in technology that have facilitated the research and application of human remains decomposition in ways that harness theory and basic understanding of the ecological and evolutionary sciences (Tomberlin et al., 2011). To that end, this special issue covers the most recent perspectives and research that explores the complex ways that the once living can provide important information to the forensic sciences, in ways that can ultimately be applied to the judicial system and its processes. It is within this context of linking basic research in death and decomposition to applications of forensics that the special topic was born.

THE RESEARCH TOPIC

This Research Topic evaluates our understanding of the structure and function of necrobiome communities associated with the postmortem decomposition of vertebrate carrion. Mammalian hosts and their microbiomes undergo a process of ecological reciprocal adaptation. Changes in decomposition and postmortem perturbations may influence differentially dispersed populations of bacteria, fungi, and other microbes, resulting in dynamic changes or succession of postmortem microbial communities that also mediate how other scavengers (e.g., insects) detect and use the resource. Although there are several factors that affect this process, there is abundant evidence that understanding these communities can provide data of forensic importance. Some of that evidence lies within the papers that represent this special topic where the focus is both the basic understanding, and value, of using postmortem necrobiome and thanatomicrobiome communities in forensics.

OPEN ACCESS

Edited and reviewed by:
Mark A. Elgar,
The University of Melbourne, Australia

***Correspondence:**
Gulnaz T. Javan
gjavan@alasu.edu

Specialty section:
This article was submitted to Evolutionary and Population Genetics, a section of the journal Frontiers in Ecology and Evolution

Received: *14 June 2021*
Accepted: *09 August 2021*
Published: *25 August 2021*

Citation:
Javan GT, Benbow ME and Ralebitso-Senior TK (2021) Editorial: Life and Death: New Perspectives and Applications in Forensic Science. Front. Ecol. Evol. 9:725046. doi: 10.3389/fevo.2021.725046

Forensic investigators are in need of modern tools to assist in constructing postmortem timelines, trace evidence relationships among subjects, and the circumstances of death or body relocation. The molecular tools used to evaluate the postmortem microbiome have potential to provide data for answering such questions of forensic importance including postmortem interval (PMI), i.e., the time elapsed since death or the postmortem submergence interval (PMSI). Current studies demonstrate the feasibility of using postmortem metrics of invertebrates, vertebrates, microbes, and their molecules as forensic tools, ranging from PMI estimates to trace evidence biomarkers. This Research Topic has brought fresh and innovative science for solving death investigations, using cutting-edge technologies concerning the community of organisms that detect and use carcasses in ways that can be studied to inform forensic investigations. We use the collection to highlight how the microbial, soil, scavengers, and mRNA transcript census in and/or around the vertebrate body changes postmortem as a function of time and temperature.

PERSPECTIVES OF STATE OF THE ART AND ITS FUTURE

It is important to reflect on the scientific journey of using micro- and macroorganisms in forensic science, the technology and methods that are driving this discipline, and the future potential while fully cognizant of the limitations. Such perspectives are provided by Jordan and Mills on the history of different DNA typing methods as applied to human and non-human DNA, and Roy et al. with a comprehensive review on thanatogenomics as a tool of enormous potential in forensic medicine.

POSTMORTEM HUMAN MICROBIOME

Saliva is an essential body fluid and trace evidence, while the human buccal cavity is an established go-to area of sampling for human DNA in crime scenes as a means of identifying the victim of crime (e.g., bites, sexual assault, missing persons) or the suspected offender. It is sensible, therefore, to profile the microbiome of the oral cavity to determine time since deposition (López et al. *re* saliva and multiplex qPCR assay) and postmortem interval relative to the decomposition timeline (Ashe et al. who used a suite of culture-based, metagenomics and metatranscriptomic methods). Similarly, Ahannach et al. provided a comprehensive review highlighting the value, and hurdles that must be addressed, of microbial forensic analyses of skin, mouth and vaginal samples to complement and strengthen forensic investigations, particularly for sexual assault and femicide cases.

The manner and cause of death is central to autopsy within human pathology. Forensic pathology is an established science for the resolution of crimes, particularly in instances of unexplained deaths. Kaszubinski et al. studied postmortem microbiomes following deaths from a range of causes and identified the potential role of microbial community dynamics to help determine manner and cause of death (M/COD), including relative to antemortem health status.

Applying cutting-edge technologies for knowledge development in new contexts typically leads to further seminal research questions. For example: Are there organs that are better or more accurate sources of the thanatomicrobiome for enhanced PMI calculations?; Is there a point or interval since death at which organ-based microbiome can no longer be used reliably for accurate PMI determination? Thus Lutz et al. studied the thanatomicrobiome of six human reproductive and non-reproductive organs during extended postmortem interval, and identified several significant relationships between PMI, organ group type and relative abundances of the four most abundant bacterial orders (Burkholderiales, Clostridiales, MLE1-12, Saprospirales).

THE ROLE OF ANIMAL MODELS

Although certain questions cannot be answered fully with using mammalian surrogates, many global regions and countries do not yet have the ethical framework required to conduct forensic decomposition, postmortem research and field experiments using human remains. As a result, requisite and essential research is being implemented with the use of different animals, mostly pigs (*Sus scrofa*), laboratory mice (*Mus musculus* Linnaeus), and rats (*Rattus norvegicus* Berkenhout), as surrogates for the human cadaver. While the benefits of mammalian proxies are well-recognized, the transferability of animal-derived data to human postmortem ecology e.g., postmortem interval, postburial interval (PBI), and PMSI determinations is justifiably under the microscope (Matuszewski et al., 2019). This, therefore, necessitates special scrutiny as shown by DeBruyn et al. who compared the decomposition of human cadavers and pigs as mammalian surrogates.

Research and knowledge development cannot stop until the required ethical approvals and guidelines are in place. As a result, Gates et al. presented their work within a medicolegal context using pigs to understand the role and/or occurrence of postmortem bacterial translocation in sudden unexplained death in infants (SUDI).

Carter et al. (2007) defined the concept of a cadaver decomposition island (CDI) and highlighted the need to understand this unique ecosystem as part of extending the forensic toolkit. To this end, Bisker et al., in the first of such studies, applied a combination of Hill ecological indices (Chao et al., 2010, 2014), metagenomics, physicochemical and edaphic factor analyses to determine PMI during a 24-month subsurface decomposition of *Sus scrofa domesticus*. In a similar context, Procopio et al. evidenced the importance of fungal metabarcoding and showed that mycoforensics needs to be given similar attention and utility as bacteria-based microbial ecology forensics.

METHOD DEVELOPMENT AND CROSS-DISCIPLINARY WORK

Successful resolution of unexplained death, or that resulting from criminal activity, is a process that inherently crosses (forensic) disciplines and scientific practices. This Research Topic has

highlighted how contemporary techniques have substantially advanced the forensic field. For example, forensic entomology is one of the earliest and most established disciplines where minimum time since death ($_{min}$PMI) has been used globally for the resolution of crimes (Tomberlin and Benbow, 2015; Byrd and Tomberlin, 2019), where early approaches typically measured the developmental rates and successional patterns of insects (e.g., Archer and Elgar, 2003). Presently, Pimsler et al. applied qPCR-based transcriptomics to understand the decompositional role of *Chrysomya rufifacies* at a molecular level, thus demonstrating the core theme in our Research Topic; that of the role of adopting cutting-edge techniques to advance translational forensic science.

AUTHOR CONTRIBUTIONS

GJ, ME, and TR-S contributed to the writing and editing of this manuscript.

FUNDING

While this Editorial was written, GJ was funded by the National Science Foundation (NSF) grant HRD 2011764 and the National Institute of Justice (NIJ) 2017-MU-MU-4042. MB was supported by a grant from the National Institute of Justice, Office of Justice Programs, U.S. Department of Justice awarded (2020-75-CX-0012). TR-S was supported by the QR-Global Challenges Research Fund (2019/2020) of Liverpool John Moores University.

ACKNOWLEDGMENTS

We are grateful to the 25 authors from around the world who contributed to this Research Topic and provided expert coverage of new perspectives and applications in forensic science through 12 original research and review articles. Also, we warmly thank all the dedicated reviewers for their contributions to this eBook and the editorial support of the Journal.

REFERENCES

Archer, M. S., and Elgar, M. A. (2003). Yearly activity patterns in southern Victoria (Australia) of seasonally active carrion insects. *Forensic Sci. Int.* 132, 173–176. doi: 10.1016/S0379-0738(03)00034-3

Byrd, J. H., and Tomberlin, J. K. (2019). *Forensic Entomology: The Utility of Arthropods in Legal Investigations*. Boca Raton, FL: CRC Press.

Carter, D. O., Yellowlees, D., and Tibbett, M. (2007). Cadaver decomposition in terrestrial ecosystems. *Naturwissenschaften* 94, 12–24. doi: 10.1007/s00114-006-0159-1

Chao, A., Chiu, C. -H., and Jost, L. (2010). Phylogenetic diversity measures based on Hill numbers. *Philos. Trans. R. Soc. B Biol. Sci.* 365, 3599–3609. doi: 10.1098/rstb.2010.0272

Chao, A., Chiu, C. -H., and Jost, L. (2014). Unifying species diversity, phylogenetic diversity, functional diversity, and related similarity and differentiation measures through Hill numbers. *Annu. Rev.* 45, 297–324. doi: 10.1146/annurev-ecolsys-120213-091540

Matuszewski, S., Hall, M. J. R., Moreau, G., Schoenly, K. G., Tarone, A. M., and Villet, M. H. (2019). Pigs vs people: the use of pigs as analogues for humans in forensic entomology and taphonomy research. *Int. J. Legal Med.* 134, 798–810. doi: 10.1007/s00414-019-02074-5

Tomberlin, J. K., and Benbow, M. E. (2015). *Forensic Entomology: International Dimensions and Frontiers*. Boca Raton, FL: CRC Press.

Tomberlin, J. K., Benbow, M. E., Tarone, A. M., and Mohr, R. M. (2011). Basic research in evolution and ecology enhances forensics. *Trends Ecol. Evol.* 26, 53–55. doi: 10.1016/j.tree.2010.12.001

Author Disclaimer: Points of view in this document are those of the authors and do not necessarily represent the official position or policies of the U.S. Department of Justice.

Conflict of Interest: The authors declare that the research was conducted in the absence of any commercial or financial relationships that could be construed as a potential conflict of interest.

Publisher's Note: All claims expressed in this article are solely those of the authors and do not necessarily represent those of their affiliated organizations, or those of the publisher, the editors and the reviewers. Any product that may be evaluated in this article, or claim that may be made by its manufacturer, is not guaranteed or endorsed by the publisher.

frontiers in Microbiology

ORIGINAL RESEARCH
published: 24 July 2020
doi: 10.3389/fmicb.2020.01686

Soil Fungal Communities Investigated by Metabarcoding Within Simulated Forensic Burial Contexts

Noemi Procopio[1†], Stefano Ghignone[2], Samuele Voyron[2,3], Marco Chiapello[2], Anna Williams[4], Andrew Chamberlain[5], Antonietta Mello[2*] and Michael Buckley[1,5]*

[1] Manchester Institute of Biotechnology, The University of Manchester, Manchester, United Kingdom, [2] Istituto per la Protezione Sostenibile delle Piante, CNR, Turin, Italy, [3] Dipartimento di Scienze della Vita e Biologia dei Sistemi, Università degli Studi di Torino, Turin, Italy, [4] School of Applied Sciences, University of Huddersfield, Huddersfield, United Kingdom, [5] School of Natural Sciences, The University of Manchester, Manchester, United Kingdom

Decomposition of animal bodies in the burial environment plays a key role in the biochemistry of the soil, altering the balance of the local microbial populations present before the introduction of the carcass. Despite the growing number of studies on decomposition and soil bacterial populations, less is known on its effects on fungal communities. Shifts in the fungal populations at different post-mortem intervals (PMIs) could provide insights for PMI estimation and clarify the role that specific fungal taxa have at specific decomposition stages. In this study, we buried pig carcasses over a period of 1- to 6-months, and we sampled the soil in contact with each carcass at different PMIs. We performed metabarcoding analysis of the mycobiome targeting both the internal transcribed spacer (ITS) 1 and 2, to elucidate which one was more suitable for this purpose. Our results showed a decrease in the fungal taxonomic richness associated with increasing PMIs, and the alteration of the soil fungal signature even after 6 months post-burial, showing the inability of soil communities to restore their original composition within this timeframe. The results highlighted taxonomic trends associated with specific PMIs, such as the increase of the Mortierellomycota after 4- and 6-months and of Ascomycota particularly after 2 months, and the decrease of Basidiomycota from the first to the last time point. We have found a limited number of taxa specifically associated with the carrion and not present in the control soil, showing that the major contributors to the recorded changes are originated from the soil and were not introduced by the carrion. As this is the first study conducted on burial graves, it sets the baseline for additional studies to investigate the role of fungal communities on prolonged decomposition periods and to identify fungal biomarkers to improve the accuracy of PMI prediction for forensic applications.

Keywords: microbial ecology, next-generation sequencing, fungal communities, necrobiome, post-mortem interval, vertebrate decomposition, forensic science

OPEN ACCESS

Edited by:
Gulnaz T. Javan, Alabama State University, United States

Reviewed by:
DeEtta Kay Mills, Florida International University, United States
Sheree J. Finley, Alabama State University, United States

****Correspondence:***
Noemi Procopio
noemi.procopio@northumbria.ac.uk; noemi.procopio@gmail.com
Antonietta Mello
antonietta.mello@ipsp.cnr.it

†Present address:
Noemi Procopio, The Forensic Science Unit, Faculty of Health and Life Sciences, School of Applied Sciences, Northumbria University, Newcastle Upon Tyne, United Kingdom

Specialty section:
This article was submitted to Systems Microbiology, a section of the journal Frontiers in Microbiology

Received: *06 May 2020*
Accepted: *29 June 2020*
Published: *24 July 2020*

Citation:
Procopio N, Ghignone S, Voyron S, Chiapello M, Williams A, Chamberlain A, Mello A and Buckley M (2020) Soil Fungal Communities Investigated by Metabarcoding Within Simulated Forensic Burial Contexts. Front. Microbiol. 11:1686. doi: 10.3389/fmicb.2020.01686

INTRODUCTION

The introduction of a cadaver in a terrestrial environment has a strong effect on the ecosystem, providing a nutrient-rich source of food that is consumed by plants and scavengers, and generating an impact on the overall soil microbial dynamics (Barton et al., 2013). Changes in the microbial community can be used as an indicator of the time elapsed since death (also known as post-mortem interval, PMI) of the carrion, particularly in case of cadavers exposed on the soil surface (Hawksworth and Wiltshire, 2015; Bellini et al., 2016; Javan et al., 2016; Javan and Finley, 2018; Metcalf, 2019). Evaluating the PMI is a key factor in forensic investigations as it can provide important information on the timing and hence circumstances of death. However, numerous taphonomic factors (Christensen et al., 2014) play a significant role in the decomposition of organic remains, making the correct estimation of the PMI more challenging and limited in its accuracy, particularly in the case of heavily decomposed remains (Swift, 2006). For this reason, there is a requirement for the development of additional tools to improve the estimation of the PMI, which could complement existing ones (for an overview of the methods available for PMI estimation using microbiota see Metcalf, 2019). Recently, several independent studies have demonstrated the applicability of this type of study to the estimation of PMI by investigating the effects of different hosts (e.g., decomposing human, Parkinson et al., 2009; Cobaugh et al., 2015; Finley et al., 2016; Metcalf et al., 2016b; Szelecz et al., 2018; swine, Pechal et al., 2013; Guo et al., 2016; Procopio et al., 2018a; or rodents, Metcalf et al., 2013, 2016b; Guo et al., 2016), different burial conditions (e.g., exposed on the surface, Parkinson et al., 2009; Metcalf et al., 2013, 2016b; Pechal et al., 2013; Cobaugh et al., 2015; Finley et al., 2016; Guo et al., 2016; Szelecz et al., 2018 or shallow burials, Finley et al., 2016; Procopio et al., 2018a), different environments (e.g., indoor laboratory environments, Metcalf et al., 2013, 2016b or outdoor environments in different geographical locations, Parkinson et al., 2009; Pechal et al., 2013; Cobaugh et al., 2015; Finley et al., 2016; Guo et al., 2016; Metcalf et al., 2016b; Procopio et al., 2018a; Szelecz et al., 2018), and different substrates (e.g., in/on the carcass, Metcalf et al., 2013, 2016b; Pechal et al., 2013; Guo et al., 2016; Szelecz et al., 2018 or in the cadaver-associated soil, Parkinson et al., 2009; Metcalf et al., 2013, 2016b; Cobaugh et al., 2015; Finley et al., 2016; Procopio et al., 2018a; Szelecz et al., 2018). In general, it has been shown that, despite the obvious differences between different experimental designs, some microbial taxa are regularly associated with specific decomposition stages, and that specific taxa appear or increase in abundance at selected time points post-mortem in a similar manner across several independent studies (Procopio et al., 2018a; Metcalf, 2019). These results motivate additional research to improve the methods and to explore the possibility of applying this methodology in medico-legal investigations (Metcalf, 2019).

Metabarcoding analysis of soil microbial communities has been the subject of numerous studies not only in soil ecology and biochemistry, but also in forensic science, particularly due to the advent of next-generation sequencing (NGS) technologies that allow the characterization of the soil microbiome for numerous applications (Zhou and Bian, 2018). Metabarcoding refers to the characterization of operational taxonomic units (OTUs) by targeting specific "barcodes" in the microbial genome (Orgiazzi et al., 2013, 2015), either the bacterial one (selectively amplifying the hypervariable regions of the16S rRNA gene, e.g., V4) (Klindworth et al., 2013) or the fungal one [targeting the internal transcribed spacer (ITS) genomic regions] (Schoch et al., 2012). These approaches usually involve DNA extraction from soil, amplification via polymerase chain reaction (PCR) of a genomic region of interest (e.g., the "barcode" region), sequencing of the resulting amplicons, bioinformatic processing of the information and taxonomic evaluation of the analyzed samples (Taberlet et al., 2012).

Using microbes to estimate PMI is particularly promising (Metcalf, 2019) and may have particular utility when the body is heavily decomposed (e.g., dry or skeletonised remains) due to the current difficulty in the estimation of a precise PMI for skeletonised remains. In fact, in those cases PMI estimation often relies on the morphological examination of the remains, thus lacking objectivity and quantifiability, and numerous variables (e.g., temperature, humidity, exposure to sun, presence/absence, and type of soil) can strongly affect and ultimately impair the correctness of the estimations (Buekenhout et al., 2018). However, only in a few cases were long time frames investigated via microbial metabarcoding (Cobaugh et al., 2015; Finley et al., 2016; Metcalf et al., 2016b; Procopio et al., 2018a), leaving gaps in current knowledge. In particular, most previous studies have focused principally on the bacterial communities, despite some of them showing the potential of investigating both the bacterial and the fungal communities (Parkinson et al., 2009; Metcalf et al., 2016b) to maximize the success of addressing PMI from a microbial perspective. Parkinson et al. (2009) performed a combined analysis of both bacterial and fungal communities in cadaver-associated soil beneath two human cadavers using terminal restriction fragment length polymorphism (T-RFLP) on the ITS region. They noted the presence of specific succession patterns during several decomposition stages, although the intrinsic limits of the analysis performed did not allow them to identify specific fungal taxa associated with the observed temporal trend. Chimutsa et al. (2015) specifically investigated the fungal community changes in tanks filled with garden soil and a decomposing domestic pig (*Sus scrofa*) leg positioned at three different depths and at three time points after burial (3, 28, and 77 days). The fungal communities were characterized using PCR and denaturing gradient gel electrophoresis (PCR-DGGE) of the 18S rRNA gene. They did not find any statistically significant shift in fungal community diversity or numerical dominance in either the presence or the absence of the carcass, leading the authors to recommend different approaches such as the use of NGS to overcome the limitations of their study. Metcalf et al. (2016b) carried out a wider study including both mice (in laboratory settings) and decomposing human bodies exposed in outdoor settings at the Sam Houston State University (Southeast Texas Applied Forensic Science Facility). They evaluated at different PMIs the succession of bacteria, archaea, and fungi both on skin and within the cadaver-associated soil, highlighting the presence of several patterns characteristic for specific bacterial and fungal

succession in the grave soil analyzed at increasing PMIs. Fu et al. (2015) performed metabarcoding analyses of the fungal communities associated with the decomposition of rat carcasses at three selected time points, and found significant correlations between the time elapsed since death and the fungal succession on the carcasses. More recently, Fu et al. (2019) also performed a similar experiment on juvenile pigs both exposed in outdoor conditions (in China, during the summer period, sampled from day 0 to day 14 post-mortem) and left to decompose indoors as a proxy to estimate PMI from the fungal shift. Also in this case, they found trends between specific decomposition stages and specific fungal taxa, suggesting potential for this type of analysis to estimate PMI.

Due to the important effect that environmental variables can have on the decomposition rate (Metcalf, 2019), it is crucial to perform additional outdoor studies in different geographical locations in order to test the possibility of building a regression model for PMI estimation from metabarcoding analyses that may be suitable for a wide range of environmental conditions, and to include temperature records in the model to take into account also the seasonality within the same environment (Metcalf, 2019). It is unclear whether forensic metabarcoding studies that were done in other, warmer and drier environments will provide models that are accurate in Britain with its cooler and less seasonal climate, and this phenomenon limits the applicability of the results found by other groups in this country. Britain has a markedly colder climate than the sites where similar studies have been conducted so far (e.g., Texas or China) and therefore it is crucial to investigate the microbial changes associated with decomposition in this specific environment to potentially obtain new insights on the estimation of PMI. Furthermore, this type of study has never been conducted on burial scenarios before, but only on exposed cadavers on soil; this weakness strongly affects the potential application of results obtained by other groups when working on buried remains. For this reason, we performed an experimental shallow outdoor burial of four pig carcasses at a rural site within Britain and investigated PMIs ranging from 1 to 6 months. In particular, we collected soil samples from the graves after 1, 2, 4, and 6 months post-mortem and conducted metabarcoding analyses on the samples. Our primary aim was to obtain a complete profile of the fungal populations associated with specific PMIs, to understand the impact that a buried carcass has on the soil biodiversity in a climate such as the British one and to evaluate if similar fungal successions were observed in different climates and for exposed cadavers. Secondary aims were to evaluate if there were differences in terms of the performance of the ITS1 and ITS2 regions of the fungal genome in this study, and ultimately to make recommendations for the design of similar experiments in other environmental conditions in the future.

MATERIALS AND METHODS

Experimental Design

The experimental design of the study has been already described in detail in Procopio et al. (2018a), and is summarized here. Four juvenile pigs (*Sus scrofa*) (named P1, P2, P3, and P4) were buried under approximately 40 cm soil at the HuddersFIELD outdoor taphonomy facility (University of Huddersfield, United Kingdom) between May and November 2016. The experiment was conducted in accordance with the guidelines of the United Kingdom Department for Environment, Food and Rural Affairs (DEFRA). Animals used for this study died from natural causes prior to the experiment and were not euthanized for the purpose of the research. Soil physicochemical and biological characteristics on a control sample taken at approximately 40 cm in depth prior to the burials were undertaken by the C.N.R. – Institute for the Study of the Ecosystems, Pisa, Italy. Sample characteristics were electrical conductivity (0.53 dS m^{-1}), total N (0.448%), total organic C (6.29%), total P (1.95 g/kg), available P (62.93 mg/kg), NO^{3-} (69.84 mgNO^{3-}/kg), NH_3 (1.93 mgNH3/kg), dehydrogenase activity (0.96 μgINTF/gss*h), β-glucosidase activity (34 μmolMUB/g*h), phosphatase activity (31 μmolMUB/g*h), arylsulfatase activity (314 μmolMUB/g*h), protease activity (15 μmolAMC/g*h). Pigs of similar age (3–5 weeks old) and weight (4.5–11 kg), which had died from natural causes were kept frozen after death until their burial. Despite the freeze-thawing process having been shown to have an effect on the anaerobic bacterial communities of frozen/thawed mice allowed to decompose on the surface (Hyde et al., 2017), difference in body size between mice and pigs and in the depositional environment chosen (surface *versus* burial) make these findings potentially not applicable to our study. Furthermore, the effects of changes in the bacterial biota on the fungal community are not known, so despite there may be a change in the fungal community (due to the competition of bacteria and fungi for the same carcass), no one has demonstrated whether this actually occurs. The experiment time was set to zero when the cadavers were allowed to de-frost and were placed within soil graves, and subsequently each pig was left in the grave for a specific amount of time post-mortem (P1 = 1 month, P2 = 2 months, P3 = 4 months, and P4 = 6 months). The decomposition stages and the morphological aspects of the carcasses were evaluated and described in Procopio et al. (2018a). Briefly, after 1 month, P1 was in putrefaction, but overall the carcass shape was still recognizable; after 2 months, P2 was in the putrefaction/liquefaction stage of decomposition with bones still attached to ligaments; after 4 months, P3 was partially skeletonised with still some soft tissues present; after 6 months, P4 was fully skeletonised and disarticulated.

At each selected PMI, the graves were excavated and the carcasses sampled to collect soil samples for the metabarcoding. Soil samples in contact with the superior surface of the carcass (taken from the fore-limb area, the abdominal area and the hind-limb area of the body to maximize the microbial varieties sampled, e.g., taking into account potential microbial differences associated with different anatomical areas) were pooled in one bag per individual/burial at the selected PMI, and frozen at −20°C after their collection until further analysis. Three technical replicates per bag (i.e., one bag per grave) were subsampled from each bag and used for metabarcoding analyses. Additionally, control soil samples (taken at similar soil depths but without a carcass being present) were collected at locations

2 and 6 m away from the graves in order to exclude microbial contaminations from the graves. The control samples were obtained concurrently with the last sampling performed in November 2016 (6 months PMI), to provide a representative record of the background microbial activity within the field used for the experiment without direct microbial contamination from the graves. According to Metcalf et al. (2016b), the observable differences within the microbial community associated with the close proximity of a decomposing body are larger and more significant than those caused by variations in local environmental conditions (linked with seasonality, temperature, and rainfall). For this reason, our control samples were collected at different distances from the graves but at a single time point. Control soil samples were frozen at −20°C until further analysis. Metabarcoding samples totaled 18 (three samples per grave plus six controls). Soil pHs were recorded and reported in Procopio et al. (2018a), as well as soil temperatures and local temperatures and rainfalls (Procopio et al., 2018b).

DNA Extraction, Amplification, and Sequencing

In order to characterize the fungal communities in the most efficient and reliable way, we targeted both ITS1 and ITS2 according to Mello et al. (2011). In fact, previous works showed contrasting results when dealing with ITS1 or ITS2. While Blaalid et al. (2013) obtained similar results when using either ITS1 or ITS2 to perform fungal metabarcoding with environmental data, Banchi et al. (2018b) showed discrepancies and biases in the detection of Basidiomycota when ITS1 or ITS2 were used as metabarcode for lichen mycobiomes, and suggested the complementary analysis of both ITS1 and ITS2 to reliably estimate the taxonomic diversity of the samples. In similar studies, Wang et al. (2015) concluded conversely that ITS1 provides a better DNA barcode than ITS2 allowing a better species discrimination efficiency, whereas the ITS2 has been specifically selected and preferred to ITS1 in another study to catch fungal diversity in airborne samples (Banchi et al., 2018a). It is clear that an *a priori* choice of the region/s to target was not ideal, and for this reason, our analysis of the fungal communities targeted specifically both the ITS1 and the ITS2 regions.

Genomic DNA was extracted from 500 mg of soil sample using the FastDNA SPIN Kit for Soil (MP Biomedicals, Europe), following the guidelines provided by the manufacturer, and fungal communities were specifically targeted amplifying the ITS regions in the nuclear ribosomal repeat unit ITS1 and ITS2. Forward ITS1-F (CTTGGTCATTTAGAGGAAGTAA) and reverse ITS2 (GCTGCGTTCTTCATCGATGC) primers for ITS1 (Gardes and Bruns, 1993) and forward fITS9 (GAACGCAGCRAAIIGYGA) and reverse ITS4 (TCCTCCGCTTATTGATATGC) primers (Sigma-Aldrich, United Kingdom) for ITS2 (Ihrmark et al., 2012 and White et al., 1990, respectively) were used in combination with 8 bp unique tags (**Supplementary Table S1**). The expected amplicon size was ∼250–600 bp for ITS1 (Bokulich and Mills, 2013; Hoggard et al., 2018) and ∼240–460 for ITS2. Primers and tags used for the subsequent analyses both for ITS1 and for ITS2 amplifications have been listed in **Supplementary Table S2**. Degeneracies were allowed in the primers to decrease eventual biases and to increase the ability to detect organisms characterized by slight modifications in their binding site's sequences. PCR negative controls were run in each analysis to perform a quality check of the amplifications and in all cases these controls gave negative results. PCR reaction mixtures were set up as follows: 12.5 μL master mix (Platinum Hot Start PCR Master Mix 2×, Thermo Fisher, United Kingdom), 0.5 μL forward primer (10 μM), 0.5 μL reverse primer (10 μM), and 0.5–1.5 μL (2.0–5.0 ng/μL) template DNA in a final reaction volume of 25 μL. The thermal cycler (T3000, Biometra GmbH, Göttingen, Germany) conditions were set up as follows: denaturation at 94°C for 2 min; 35 cycles of denaturation at 94°C for 30 s, annealing at 52°C for 40 s, and extension at 68°C for 30 s; final extension at 68°C for 10 min and maintenance of the samples at 4°C. The PCR products obtained were checked on 1.5% (w/v) agarose gels (Sigma-Aldrich, United Kingdom), purified (Wizard SV Gel and PCR Clean-UpSystem, Promega, United Kingdom), quantified with Qubit (Qubit Fluorometric Quantitation, Thermo Fisher Scientific, United Kingdom) and sent to IGA Technology Services (Udine, Italy) for paired-end sequencing using the Illumina MiSeq technology (2 × 300 bp). The company ligated our tagged PCR products with a couple of Illumina adapters, and generated two libraries named "Library A" and "Library B" for ITS1 and ITS2, respectively, due to the different length of the amplicons expected for ITS1 and ITS2 as previously mentioned.

DNA Data Analysis

Paired−end reads from each library were merged using Pear v.0.9.2 (Zhang et al., 2013), with the quality score threshold for trimming the low−quality part of a read set at 28, the minimum length of reads after the trimming process set at 200 bp and the minimum possible length of the assembled sequences set at 200 bp. Unix bash commands were used to select assembled sequences beginning with recognizable forward primer (no mismatch allowed), to trim initial and terminal 19 and 20 bases (corresponding to forward and reverse primers, respectively) and to assign a sample specific progressive count to each fragment. Assembled sequences from each library were clustered into OTUs using a *de novo* clustering strategy with QIIME v1.91 (Caporaso et al., 2010) and VSEARCH[1] v2.3.4 (Rognes et al., 2016) at 97% similarity. Taxonomic assignment to OTUs was performed using the full "UNITE + INSD" dataset v.8.2 (released 2019-02-02; Nilsson et al., 2019) as a reference, and using BLAST and UCLUST, implemented in QIIME, as assignment methods. A consensus of the two assignment methods has been manually inspected and edited by mycologists and used for subsequent statistical analyses.

Statistical Analyses

Numerical ecology statistical analyses were performed within the computing environment R[2] (R Core Team, 2013). As previously described in Procopio et al. (2018a),

[1]https://github.com/torognes/vsearch

[2]https://www.R-project.org/

control samples collected from two different locations were extracted in triplicate (replicate #1, #2, and #3) from each location (overall six DNA samples extracted), and during the data analysis they have been unified arbitrarily into a single control sample, summing up the reads of each of the three replicates to obtain our three replicates for control samples.

A number of filtering steps were applied to gather the final OTU dataset: OTUs with fewer than 50 reads were filtered out as well as samples with fewer than 20 reads and OTUs showing a coefficient of variation greater than 3.0 were also removed.

In order to standardize sampling efforts and to allow for comparisons of samples with non-uniform coverage, the OTU table has been normalized by subsampling at even sequencing depth from each sample using the minimal number of sequences obtained between the two libraries as value for the rarefaction (59,413 sequences) by means of the *rarefy_even_depth* function in the R package phyloseq v.1.22.3 (McMurdie and Holmes, 2013). The rarefaction effects on an OTU table are commonly rendered by means of the rarefaction curves, in order to graphically estimate species richness. Raw species richness counts can only be compared when the species richness has reached a clear asymptote; all the species present in a sample are well described when the curve ascribed to each sample reaches its plateau. Rarefaction curves were rendered by means of the function *ggrare*, provided by the richness. R script from the phyloseq extension package by Mahendra Mariadassou[3]. All taxon abundances were calculated and graphically plotted using the R package phyloseq v.1.28.0 (McMurdie and Holmes, 2013).

Biodiversity analyses were carried out by comparing the richness (number of species) and evenness (richness taking into account relative abundances) of microbial communities of the PMIs. Within-sample (alpha) diversity was assessed by six estimators: "observed number of species," "Chao1," "abundance-based coverage estimators (ACE)," "Shannon," "Simpson," "Fisher." The alpha diversity indices were calculated and plotted by means of the functions *estimate_richness* and *plot_richness* implemented in the R package phyloseq (McMurdie and Holmes, 2013).

In order to test whether communities were statistically different from each other, a multivariate homogeneity of group dispersions among the different Control and PMI groups was first assessed by means of the *betadisper* and *permutest* (with 9,999 permutations) functions in the R package vegan v.2.5.2 (Oksanen et al., 2018). The differences in the composition of fungal communities in PMIs for both libraries were rendered by means of a nonmetric multidimensional scaling ordination (NMDS), to visualize Bray–Curtis distances, using the functions *vegdist* and *metaMDS* in the R package vegan (Oksanen et al., 2018).

The permutational multivariate analysis of variance (PERMANOVA, 9,999 permutations), as implemented in the *adonis* function of the vegan package of R (Oksanen et al., 2018), were applied to assess whether communities were statistically different from each other. Indicator species analysis [a classification-based method to measure associations between species and groups of sites (Dufrêne and Legendre, 1997)] was carried out using the *multipatt* function in the indicspecies v.1.7.6 R package, with 9,999 permutations (Cáceres and De Legendre, 2009) in order to assess whether OTUs (and if so, which ones) were significantly associated with a particular PMI.

To explore the shifts in the fungal basal communities at different decomposition stages, we evaluated which families showed statistically significant differences in the alpha diversity using the Kruskal–Wallis test and the Dunn's pairwise tests, and in beta diversity and in the abundances at different PMIs applying the Student's *t*-test with Benjamini and Hochberg False Discovery Rate (FDR) correction (Benjamini and Hochberg, 1995) with the T.TEST and P.ADJUST functions in R. This correction generated both *p* values and adjusted *p* values (*q* values), that were used to evaluate the statistical significance of the results reported in the work.

RESULTS

Metabarcoding Analysis of Soil Fungi

Within the 18 samples analyzed, we respectively obtained 1,529,090 sequences after Library A pre-processing and 1,827,776 sequences after Library B pre-processing. Soil controls yielded overall 1,144,877 sequences (from 71,600 to 102,938 for Library A and from 46,536 to 141,094 for Library B), while grave soil samples yielded overall 2,211,989 sequences (from 60,085 to 113,214 for Library A and from 67,102 to 140,992 sequences for Library B). After the *de novo* clustering, sequences with 97% identity were clustered providing 1,640 initial OTUs for Library A and 2,569 initial OTUs for Library B. We identified overall two kingdoms within Library A and 12 within Library B (**Supplementary Table S2**), showing that the ITS2 pair of primers allowed wider amplification spectrum than the ITS1 pair. OTUs belonging to "Fungi" kingdom were respectively 99.7% in Library A (1,264 out of 1,268) and 81.8% in Library B (1,543 out of 1,885); all the OTUs belonging to different kingdoms were not considered for further analyses. Also, in terms of the number of reads, Library A showed slightly fewer reads for Fungi (∼1,500,000) than Library B (∼1,700,000), as well as fewer OTUs than Library B (**Supplementary Figure S1**). After the filtration step that removed OTUs whose cluster size was smaller than 50 reads (overall 601 OTUs for Library A and 857 OTUs for Library B were withheld after the filtration) and OTUs whose Coefficient of Variation was greater than 3.0, we obtained a final number of 571 OTUs for Library A and 749 OTUs for Library B (**Supplementary Data S1**). The sequence coverage obtained for both libraries showed adequacy for the proposed study (**Supplementary Figure S2**) and that, for both libraries, the control samples were the highest in terms of species

[3]https://github.com/mahendra-mariadassou/phyloseq-extended

richness, followed by P1, and then by P2–P4 that showed similarities to each other.

Fungal Community Changes During Progressive Stages of Decomposition

To account for richness and evenness of the microbial taxa associated with different PMIs, we calculated the Shannon–Wiener index and used boxplots to represent the species distribution among samples, with replicates grouped together in terms of raw species number (**Figure 1**). Other indices for alpha diversity such as Chao1, ACE, Simpson's and Fisher's index have been also applied, as recommended by Bandeira et al. (2013), in order to better define the communities (**Supplementary Figure S3**).

The Shannon–Wiener diversity indices (**Figure 1A**) showed statistical differences between the mean ranks of the groups for Library A and B (Kruskal–Wallis test, p = 0.027 and 0.012, respectively). However, after *post hoc* Wilcoxon test with Bonferroni correction the only statistical difference found was between controls and P2 for Library B (q = 0.014). We also calculated the linear regression models for both libraries (**Supplementary Figure S4**). The regression lines calculated for each library did not meet at any point in the graph, meaning that the Shannon–Wiener diversity indices for Library A and B were not statistically different from each other.

Taxonomic richness data were normally distributed (Shapiro–Wilk test, p = 0.13), and have been consequently evaluated using an analysis of variance (ANOVA) test (which showed a significant change for both libraries, $p < 0.0001$) followed by *post hoc* Tukey tests (**Table 1**).

Library B samples showed smaller standard deviations in the fungal richness (**Figure 1B**) and allowed for a better discrimination between the various time points than Library A. To test whether fungal communities were statistically different from each other, we evaluated the homogeneity of dispersion among groups (**Figure 2A**) and then ran a PERMANOVA test. The test provided significant results (p = 1e-04 for Library A and p = 1e-04 for Library B), thus indicating that the dissimilarity was influenced by difference in composition between groups. Consequently, we analyzed the differences in the taxonomic abundances from different samples to evaluate the beta diversity between different samples and we used a NMDS plot to visualize Bray-Curtis dissimilarities (**Figure 2B**). Samples collected from the same location clustered better in Library B, with the only exceptions being for P1 and P4, where the clusters were less scattered in Library A (**Figure 2B**). Overall, P1 was closer to the control, as previously reported also for bacterial data (Procopio et al., 2018a), whereas samples collected with increasing PMIs showed an ordered distribution from the control from the left to the right on the plot, with P2 being more distant, P3 being the most distant one and P4 being closer again to the control (**Figure 2B**).

To give a comparison of the NMDS ordinations of Bray–Curtis distances for Library A and B, we performed the Procrustes

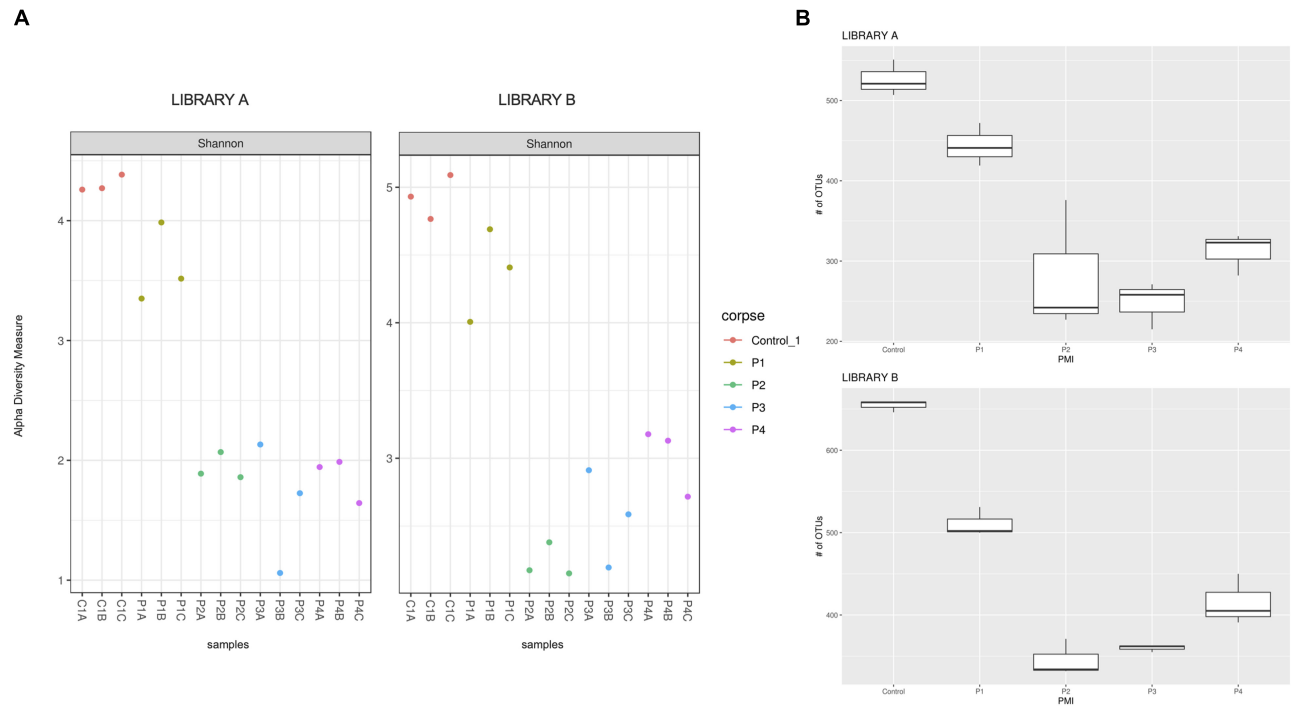

FIGURE 1 | (A) Shannon alpha diversity measure of the samples collected after 1 (P1), 2 (P2), 4 (P3), and 6 (P4) months post-mortem for Library A (left) and Library B (right) and **(B)** box plot of the fungal richness of soil samples showing the raw number of OTUs per sample for Library A (top) and Library B (bottom), with standard deviations represented with vertical error bars and medians represented with a bold line in each box.

TABLE 1 | *Post hoc* Tukey test results for taxonomic richness calculated for Library A and B.

Library A	Control	P1	P2	P3	P4	Library B	Control	P1	P2	P3	P4
Control	–	$p > 0.05$	$p = 0.001$	$p = 0.001$	$p = 0.001$	Control	–	$p = 0.001$	$p = 0.001$	$p = 0.001$	$p = 0.001$
P1	$p > 0.05$	–	$p = 0.004$	$p = 0.001$	$p = 0.017$	P1	$p = 0.001$	–	$p = 0.001$	$p = 0.001$	$p = 0.001$
P2	$p = 0.001$	$p = 0.004$	–	$p > 0.05$	$p > 0.05$	P2	$p = 0.001$	$p = 0.001$	–	$p > 0.05$	$p = 0.001$
P3	$p = 0.001$	$p = 0.001$	$p > 0.05$	–	$p > 0.05$	P3	$p = 0.001$	$p = 0.001$	$p > 0.05$	–	$p = 0.003$
P4	$p = 0.001$	$p = 0.017$	$p > 0.05$	$p > 0.05$	–	P4	$p = 0.001$	$p = 0.001$	$p = 0.001$	$p = 0.003$	–

Non-significant values have been reported in red. Significant values are reported in green.

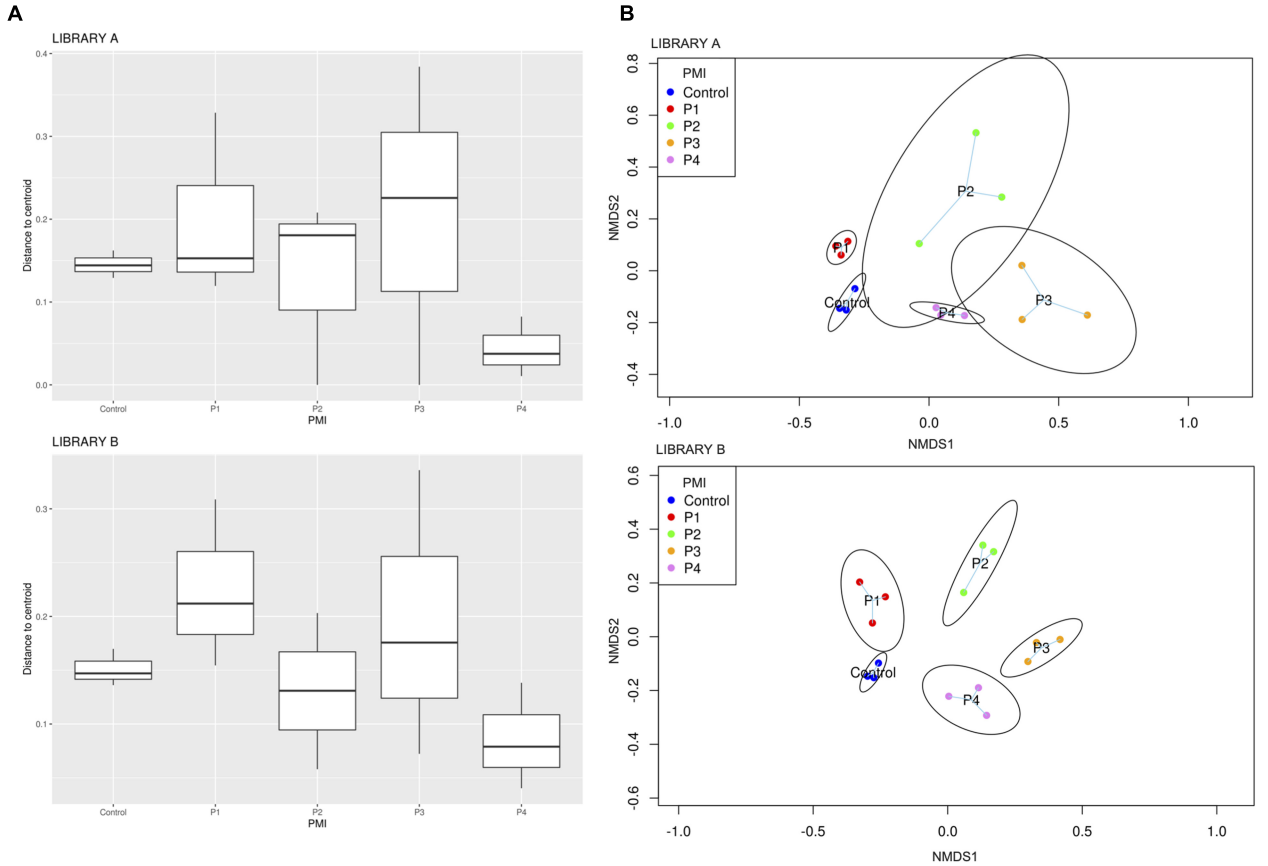

FIGURE 2 | (A) Boxplot showing Bray-Curtis dissimilarity of the replicates from the centroid for specific PMIs for Library A (top) and Library B (bottom) and **(B)** NMDS plot showing an increase in beta diversity between the control soil and the grave soil, represented by expanded ellipses for P1, P2, P3, and P4 (P1 = 1 month, P2 = 2 months, P3 = 4 months, and P4 = 6 months). Standard deviation is represented by the dimension of the ellipses. Library A is at the top of the figure, and Library B at the bottom. The homogeneity of dispersion among groups was supported by a non-significant result in permutest (*p*-value = 0.48 for Library A and 0.31 for Library B).

analysis that provides a plot where the same samples are connected by vector arrows. Results showed that the degree of concordance between Library A and B is statistically significant (p = 1e-04), meaning that the ordination of the data is similar between the two libraries (**Supplementary Figure S5**).

To characterize the differences found between the samples, we looked at the relative abundance of phyla (**Supplementary Figure S6**). Due to the incompleteness of the database for fungal species, we were not able to identify all of the species sequenced, and so we had to accept some unidentified phyla in the data.

When looking at specific PMIs, there were some noticeable trends with increasing time elapsed since death at phyla (**Figure 3**) and family level (**Table 2**, **Figure 4**, **Supplementary Figure S7**, and **Supplementary Data S2**). Ascomycota showed a notable increase in abundance after 2-months and a decrease after 4- and 6-months post-mortem compared with the controls for both libraries, despite their abundance decreasing after 2-months and slowly starting to increase again from 4-months onward. In particular, abundance of Pyronemataceae increased significantly in P2 in comparison with the control, and decreased after 4 months post-mortem. Abundance of Melanommataceae,

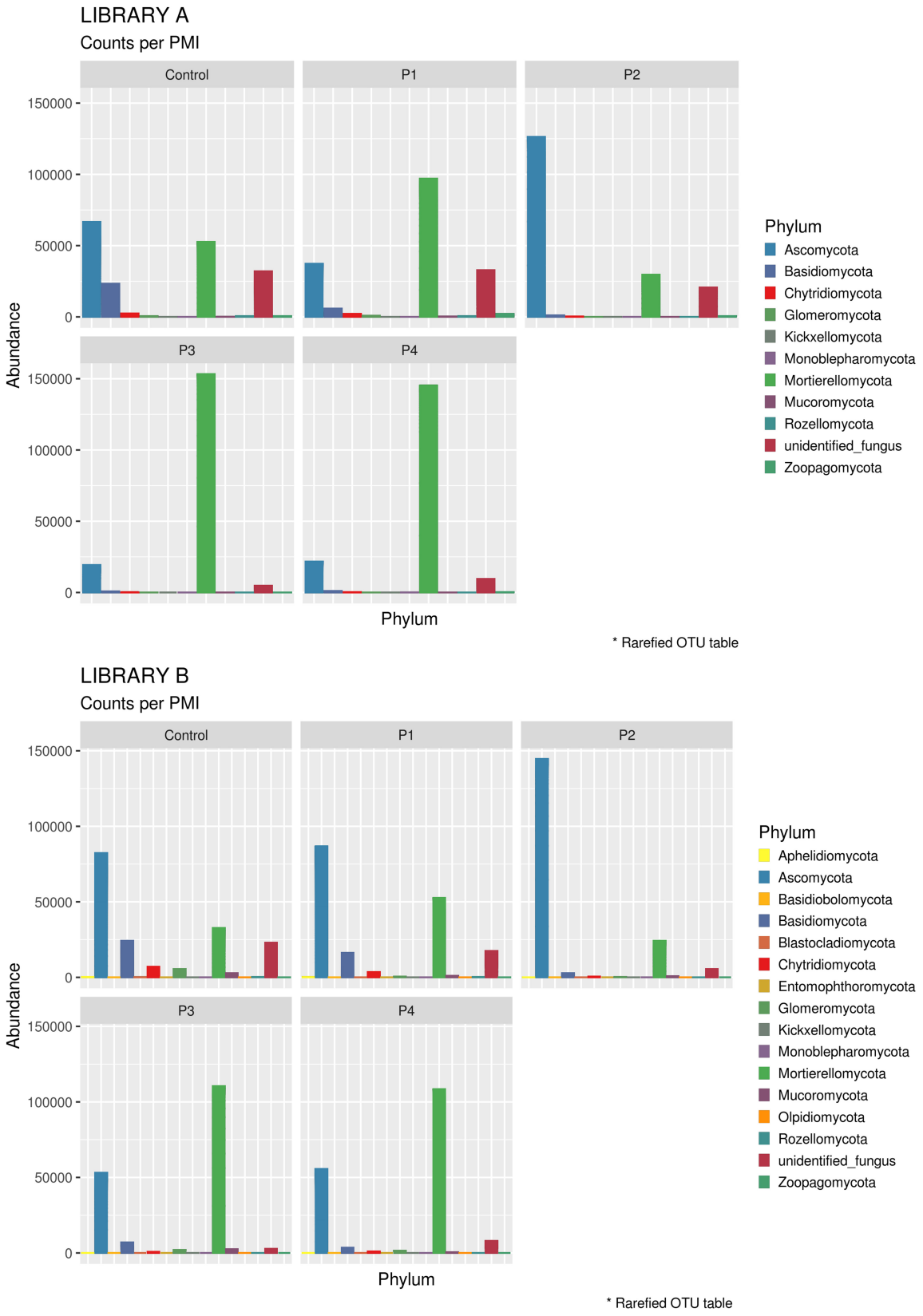

FIGURE 3 | Bar chart with abundances of taxa at a phylum level associated with control soil and with the experimental samples in Library A **(top)** and Library B **(bottom)**. The order of the phyla represented in the legend is the same of the bars in the plot.

TABLE 2 | Families grouped according to their phylum showing statistical differences between the control and the various time points (P1 to P4).

	Library A				Library B			
	P1	**P2**	**P3**	**P4**	**P1**	**P2**	**P3**	**P4**
Ascomycota								
Massarinaceae	↓ $p = 0.004$	↓ $p = 0.0006$	↓ $p = 0.0007$	↓ $p = 0.001$	↓ $p = 0.002$	↓ $p = 0.0009$	↓ $p = 0.0008$	↓ $p = 0.005$
Pyronemataceae	–	↑ $p = 0.002$	–	–	–	↑ $p = 0.003$	–	–
Melanommataceae	–	↓ $p = 0.004$	↓ $p = 0.004$	↓ $p = 0.004$	–	–	–	–
Bionectriaceae	–	↓ $p = 0.002$	↓ $p = 0.003$	↓ $p = 0.002$	–	–	–	–
Onygenaceae	–	↓ $p = 0.002$	–	–	–	–	–	–
Pseudeurotiaceae	–	–	–	–	–	↓ $p = 0.004$	↓ $p = 0.005$	–
Coniochaetaceae	–	–	–	–	–	↓ $p = 0.003$	↓ $p = 0.003$	↓ $p = 0.005$
Gymnoascaceae	–	–	–	–	–	↓ $p = 0.004$	–	–
Chaetomiaceae	–	–	–	–	–	↓ $p = 0.003$	–	↓ $p = 0.004$
Zoopagomycota								
Piptocephalidaceae	↑ $p = 0.004$	–	–	–	–	–	–	–
Zygomycota								
Mortierellaceae	–	–	–	↑ $p = 0.003$	–	–	–	–
Basidiomycota								
Entolomataceae	–	–	–	–	–	↓ $p = 0.005$	–	–
Psathyrellaceae	–	–	–	–	–	↓ $p = 0.0009$	↓ $p = 0.0008$	↓ $p = 0.004$
Glomeromycota								
Diversisporaceae	–	–	–	–	–	↓ $p = 0.005$	↓ $p = 0.005$	↓ $p = 0.005$

Statistical significance was calculated via Student's t-test with False Discovery Rate (FDR) correction. Results reported here were selected for p value ≤ 0.005. The symbol "↑" indicates an increase in comparison to the control, and the symbol "↓" a decrease. Non-significant values have been reported with the symbol "–."

Bionectriaceae, Massarinaceae, Onygenaceae, Pseudeurotiaceae, Coniochaetaceae, Gymnoascaceae, Chaetomiaceae, and Nectriaceae on the other hand showed a decline in P2, P3, and P4 compared with the control. Basidiomycota, with in particular Entolomataceae and Psathyrellaceae, constantly decreased with increasing PMIs. Mortierellomycota increased in abundance in P1 (in particular the Mortierellaceae family), then decreased in P2 and were the most abundant phylum at P3 and P4.

Identification of Endogenous Mammalian Fungal Communities and Basal Communities

In order to identify specifically basal fungal communities that vary depending on the PMI of the bodies, excluding the taxa introduced in the cadaveric soil by the carcass (e.g., skin fungi present in and on the bodies), we evaluated which taxa were uniquely present in the cadaveric soil and not in the control samples, and then excluded these unique OTUs from the analysis of the "basal community." In summary, for Library A we found 569 different OTUs present within the basal microbiome (**Supplementary Data S3**) and only two taxa specifically associated with the bodies (not identified in the control; **Supplementary Data S4**), and for Library B we found 735 different OTUs present within the basal microbiome (**Supplementary Data S3**) and 14 taxa specifically associated with the bodies (not identified in the control; **Supplementary Data S4**). It can be noted here that primers used for Library B allowed the identification of a higher number of fungi OTUs associated with the decomposing carcass than primers for Library A. For this reason, we will discuss results regarding the mycobiome introduced by the carcass only with reference to Library B (**Figure 5**). The results showed that the carcass' fungal community that was abundant in soil at the first time point, almost disappeared with advanced decomposition stages, apart from some outliers such as the Onygenales order

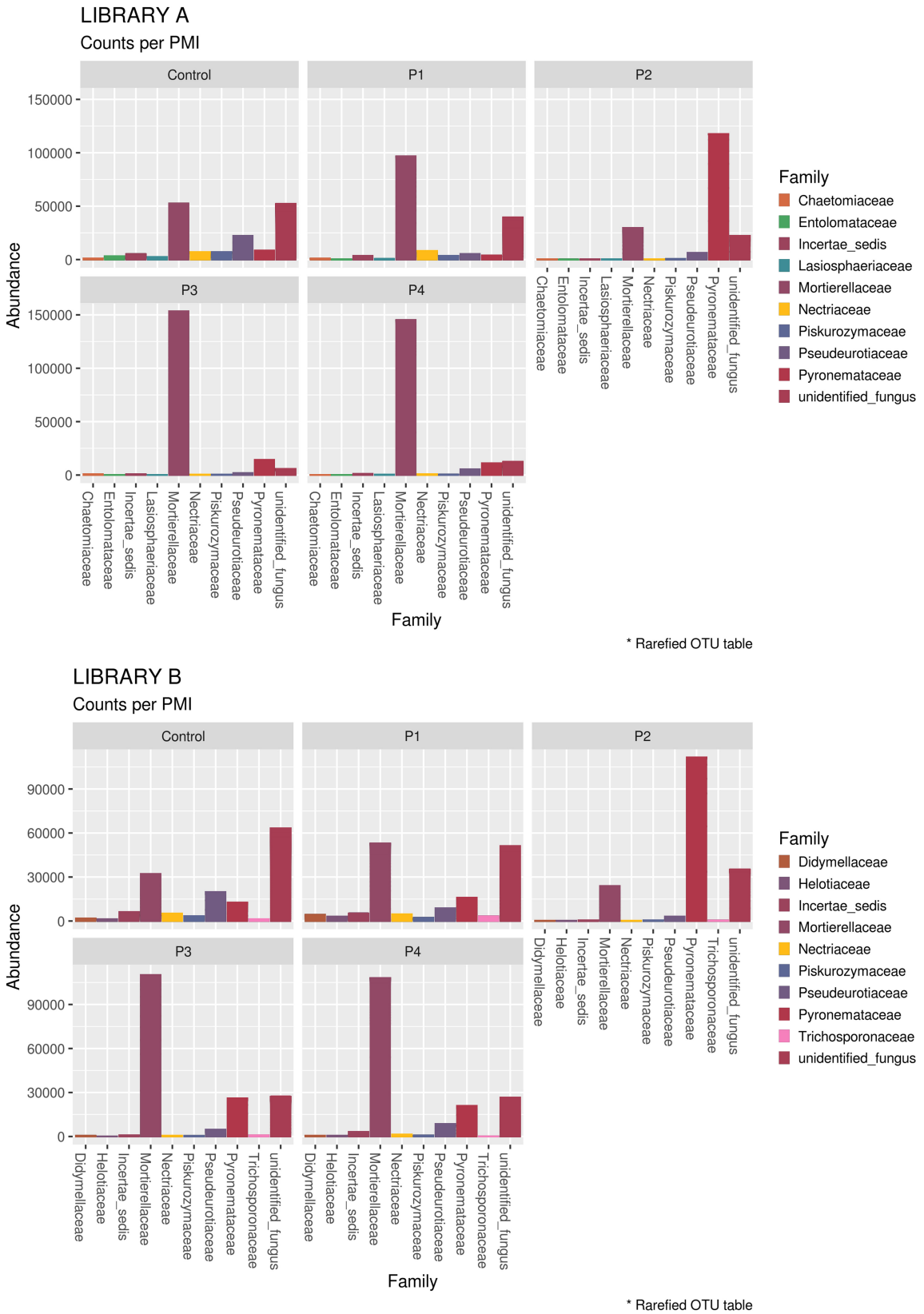

FIGURE 4 | Bar chart with abundances of the top 10 taxa at a family level associated with control soil and with the experimental samples in Library A **(top)** and Library B **(bottom)**. The order of the families represented in the legend is the same of the bars in the plot.

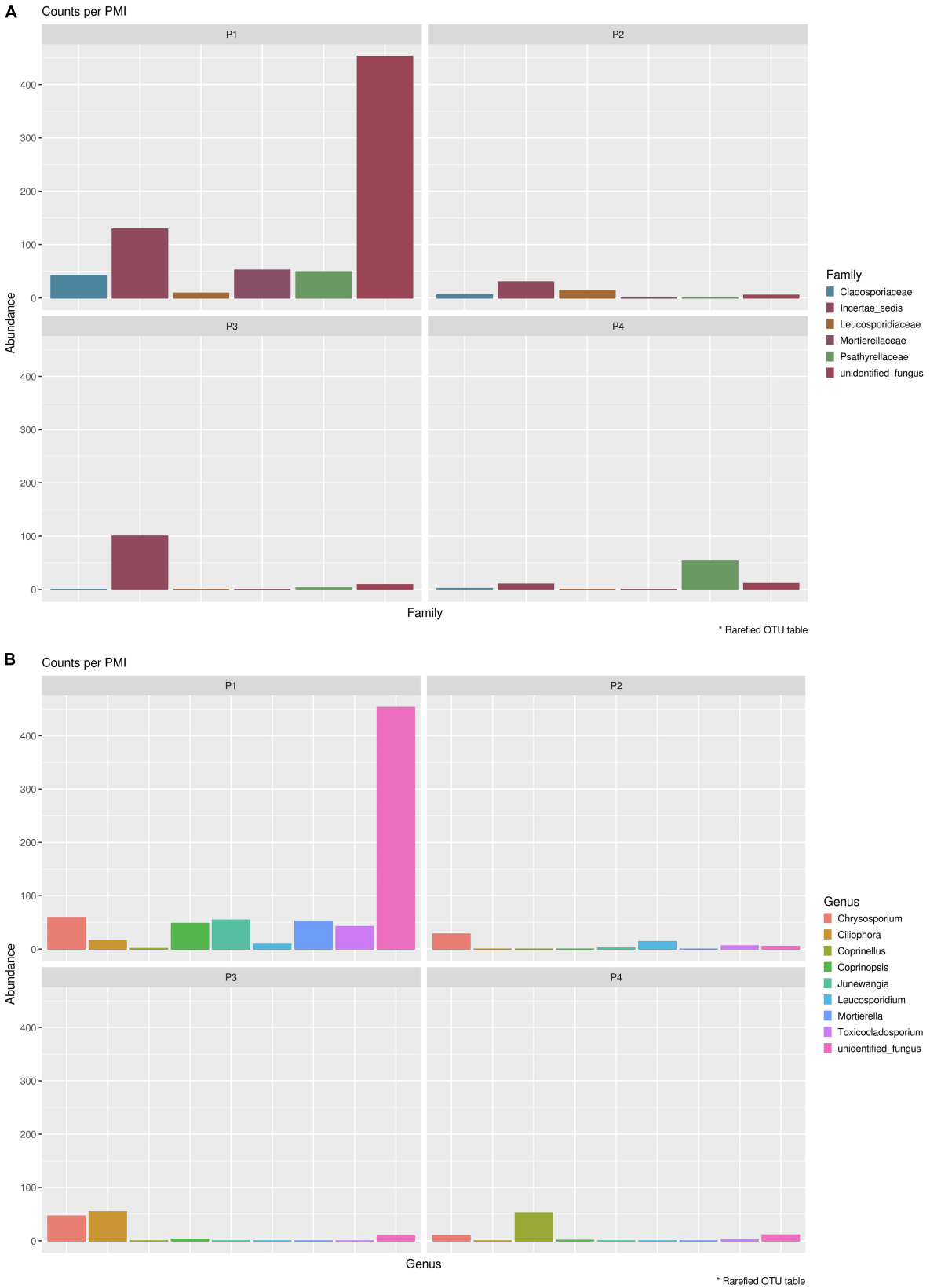

FIGURE 5 | Mycobiome associated uniquely with the mammalian carcasses and not identified within the control sample at **(A)** family level and **(B)** genus level. Abundances per each family or genus were reported in different colors (see legend). The order of the families and genus represented in the legend is the same of the bars in the plot.

(family "Incertae sedis," genus *Chrysosporium*) which were more abundant in P1 and P3, and the Psathyrellaceae (genus *Coprinellus*) which started to increase only after 6 months. The term "Incertae sedis" found in **Figure 5** is a mycological term used to combine together different taxa which have not been classified yet into a specific family, and that for this reason can only be grouped in this way.

Indicator species analysis was also undertaken to evaluate which species were significantly associated specifically with the basal microbiome or with the carcasses (significance level = 5%) (**Supplementary Data S5**). Overall, the analysis showed that 253 OTUs for Library A and 295 species for Library B contributed to explain the differences observed between the control and the grave soil (p value $\leq$ 0.05), and that two OTUs contributed significantly to discriminate carrion-associated fungi from the basal fungal communities for Library B, but none for Library A. To report only taxa associated with significant increases or decreases at selected PMIs, we performed a Student's t-test with FDR correction. Results obtained were almost identical to the ones showed in **Table 2**, with the same families having significant differences between the control and the various PMIs (**Supplementary Figures S8–S11** and **Supplementary Data S6**).

DISCUSSION

The introduction of a decomposing carcass in the burial environment significantly alters the structure of the soil fungal communities, causing measurable changes such as an overall decrease in the richness of the fungal community with increasing PMIs. These findings are similar to what has been already found for bacteria in the burial environment (Procopio et al., 2018a), for fungal communities in soil underneath decomposing exposed pigs (Fu et al., 2019) and for bacterial communities present in different anatomical locations of human cadavers (Pechal et al., 2018). This result suggests that the presence of a decomposing carcass has a negative impact on the diversity of the fungal communities present in the soil, and the effect is particularly exacerbated when the body reaches the putrefaction/liquefaction stage of decomposition, where the least richness has been recorded. The biotic and abiotic factors in the soil environment are altered due to the release of organic compounds in the soil at different decomposition stages (Vass et al., 2004), and fungal species present in the environment as well as fungi originating from the microflora of the body are subjected to a growth inhibition and potentially to inter-specific competition that can result in sequential changes to the composition of the fungal community (Parkinson et al., 2009; Pechal et al., 2018). Fungal communities seem to be more sensitive than bacteria to alterations of soil environment, with significant reductions in species richness being already observed between the controls and the soil collected at the first time point, in contrast to what was observed for bacteria (Procopio et al., 2018a). Fungi also appear to start returning toward the original community structure (i.e., the one existing previously to the introduction of the carcass) faster than do the bacteria (Procopio et al., 2018a), as shown by the significant increase in the taxonomic richness of the samples collected after 6 months PMI. This finding could be due to their reduced sensitivity to strict pH parameters in comparison with bacteria (Finley et al., 2015) and to their potential better adaptation to new environments (Selbmann et al., 2013). Despite the quicker return to the original conditions for fungi compared to bacteria, more than 6 months appeared to be necessary for both fungi and bacteria to return to their original "basal" state; an observation that may be particularly useful in the investigation of clandestine movements of buried bodies from their original grave to a secondary grave.

We were able to identify specific trends for different phyla that might be good indicators for specific PMIs of buried cadavers. In particular, we found a significant increase in the abundance of Pyronemataceae (Ascomycota) after 2-months PMI that may be specific to buried cadavers. In fact, the increase of the abundance of Ascomycota during the first stages of decomposition was not reported by Fu et al. (2019) within soil collected underneath exposed pig cadavers. Ascomycota are decomposers able to break down the animal tissues into major organic compounds, and they have already been identified as fungal decomposers particularly active during the active decay of the carcass (Metcalf et al., 2016a). Recently, Bruns et al. (2020) have postulated that the post-fire microbial habitat is structured by a thermo-chemical gradient, which cause two main effects: a temperature gradient that causes differential mortality with soil depth, and a chemical gradient that structures resources available to recolonizing microbes. On this basis, we can postulate that the rise of temperature originated by the decomposition process in the burial environment that, even if lower than that caused by a fire, is extended in time (e.g., at least 2 months in our study), could cause the same effects, thus leading to the strong presence of fungi belonging to the family Pyronemataceae recorded here.

Basidiomycota on the other hand showed a constant decrease in their abundance starting from a greater amount and variety of families in control samples and ending in a significantly lower amount with prolonged PMIs. This result is in contrast with that of Metcalf et al. (2016a), who suggested that Basidiomycota are particularly abundant during the active decay stage, but is in agreement with Fu et al. (2015), who noticed a decrease in the abundance of this phylum in the rectum of decomposing rats with increasing time after death. In our case, the carcasses reached the active stage of decomposition between 1 and 2 months, but Basidiomycota decreased rapidly with the introduction of the carcass into the soil (from control to P1), with the Piskurozymaceae family being the most abundant one after 1 month, and with all the families, including Entolomataceae and Psathyrellaceae disappearing completely after 2, 4-, and 6-months post-mortem, suggesting their limited role during the active decomposition of the carcasses in this study. The same happened for the Glomeromycota phylum, where Diversisporaceae constantly decreased from P2 onward.

Mortierellomycota, and in particular the Mortierellaceae family, were previously found to be particularly active in between the active decay and the dry remains stages (Metcalf et al., 2016a). Our results are partially in agreement with this finding, with an increase of Mortierellaceae in P3 and P4, however, we also found an increase from the control to P1, suggesting that they also may

have a role during the early decomposition stages of the carcasses, particularly when in the presence of buried carcasses.

We did not find an increase in Zygomycota and in Chytridiomycota with time, as found in contrast by Fu et al. (2015) in the rectum of decomposing rats, indicating that the soil fungal communities may act in a different way from the internal communities.

Unfortunately, the very limited amount of metabarcoding data available on fungal communities associated with cadaveric decomposition does not allow us to perform a comprehensive comparison between different studies. However, we found some similarities with the results of the study conducted by Metcalf et al. (2016a) on human cadavers in Texas, also with the one conducted by Fu et al. (2015) on rat carcasses in China and with the subsequent study conducted by the same group on exposed pigs (Fu et al., 2019), despite the fact that in all cases these studies were conducted with exposed remains instead of with buried ones as was the case in our study. So, it could be argued that the fungal succession during the various decomposition stages appears reproducible and reliable despite different geographical areas, different carrion species and different post-mortem conditions (e.g., buried vs non-buried). This highlights the potential for this type of analysis to provide a complementary fungal "clock of death" similar to the one already proposed for bacteria (Metcalf et al., 2013), provided that further studies are conducted in different geographical areas, with a higher number of timepoints and in different depositional environments in order to build a regression model that could assist in the prediction of the PMI.

Considering the fungal taxa introduced into the burial environment by the carcass, we noticed that the cadaveric soil is not a favorable environment for the survival and for the growth of these introduced species, and that overall fungi introduced by the body are replaced by soil fungi in less than 2 months. Similar findings were presented also by Fu et al. (2019), who showed that the variety of soil fungi present after 1-day post-mortem was higher than the one found during the decomposition of the carcasses. An example of this is represented by the Cladosporiaceae family. This family has been found to be a physiologic inhabitant of the intestine of the pig (Hurst, 2016), and our results showed that Cladosporiaceae species are not able to survive with advancing decomposition stages. Surprisingly, we did not find evidence in living pigs for the other families found to be abundant in P1, raising a question around the decrease, and then the eventual increase after several months, of some of these fungal families in the cadaveric soils. Interestingly, specific members of the Mortierellaceae family were found to be more abundant in P1 and then disappeared at prolonged PMIs. Although this may seem to contradict the previous findings, it should be noted that the specific taxa mentioned in this section of the work are the ones not found in the control soil and exclusively brought in by the carcass itself. So, despite some taxa of this family not being able to survive after prolonged PMIs, other members of the Mortierellaceae family already present in the soil showed the ability to take advantage of the organic nutrients released with the decomposition of the carcasses to become the most abundant species in the cadaveric soil after 4- and 6-months post mortem.

When looking for species significantly associated specifically with the basal microbiome or with the carcasses, only two OTUs were found to have contributed to discriminate carrion-associated fungi from the basal fungal communities, proving how limited the contribution to the soil fungal communities introduced by the carrion is, and supporting the potential to extend these findings to future applications involving the presence of other carrions (including humans).

In order to achieve fungal taxonomic identification, ITS1 and ITS2 loci are normally the standard sequences of choice, despite different authors having contrasting opinions regarding their efficiency and, in particular, about which one is the best performing one. When comparing the performance of ITS1 and ITS2 loci, we found sometimes specific results for the specific library investigated (e.g., some families were found to be statistically significant only for one of the two libraries), but the trends found were always in agreement between the two (e.g., Massarinaceae decreased constantly and significantly both for Library A and B). Overall results showed that ITS1 and ITS2 performed similarly in the characterization of the various samples, despite the lower variation between the replicates found for ITS2 in comparison with ITS1.

CONCLUSION

This study has shown that shifts in the fungal communities present in the grave soil of pig carcasses, like the results for bacterial communities, have the potential to reveal information about the PMI of buried carcasses from 1- to 6-months post mortem. Here we were able to demonstrate that specific fungal families, such as the Mortierellaceae or the Massarinaceae, may be ideal for the estimation of the PMI, providing that additional research with additional bodies and time points is done to confirm the findings presented here. According to our results, the decrease of the abundance of Masssarinaceae families in cadaveric soil compared to a control soil may indicate the presence of a decomposing body, and the reduction in abundance of specific Ascomycota families such as Melanommataceae, Bionectriaceae, Pseudeurotiaceae, Coniochaetaceae, and Chaetomiaceae, Basidiomycota families such as Psathyrellaceae and Glomeromycota families such as Diversisporaceae may indicate the presence of a body in active or advanced decomposition stages. On the contrary, the presence of an increased abundance of Pyronemataceae in the soil, in comparison with a control, may indicate the presence of a body in the active decomposition stage, whereas an increase of Piptocephalidaceae might indicate the presence of a body at the beginning of its decomposition, and the increase of Mortierellaceae might indicate the presence of a body in an advanced decomposition stage. We have also shown here that the specific analysis of the ITS1 or the ITS2 sites provide similar results, but that the range of data obtained with ITS2 is generally wider when compared to ITS1, allowing for a better characterization of the distinct PMIs. For this reason,

we recommend here that in future work either the combination of the two ITS sites, or exclusively the ITS2 region should be targeted instead of using the ITS1 only. Despite the constraints found, including the limited availability of metabarcoding fungal data in forensic casework and the lack of curated databases, we were able in this study to provide interesting insights on the fungal shifts in the burial environment in temperate climates, finding some good correlations also with the results of other experiments conducted on different carrion species and in different environments. Overall, this pilot study showed the great potential that fungal metabarcoding has for forensic investigations, and should be the starting point for additional research to improve the estimation of PMI through the analysis of changes in soil fungal communities.

AUTHOR'S NOTE

This manuscript has been released as a pre-print at ResearchSquare (Procopio et al., 2020).

DATA AVAILABILITY STATEMENT

The datasets generated for this study can be found in the NCBI Sequence Read Archive (SRA-NCBI; https://www.ncbi.nlm.nih.gov/sra) under project accession number PRJNA594906 and BioSample accession numbers SAMN13816975–SAMN13816980.

ETHICS STATEMENT

The animal study was reviewed and approved by the School of Applied Sciences, University of Huddersfield. The tissues (carcasses) used in the experiment were fallen stock (animals that had died of natural causes). National regulations (DEFRA) were adhered to in all aspects of the experiments. Pig burials took place on a facility with a DEFRA license for such activity. The work adhered to any other regulations that may apply to experimental work undertaken at the various universities where analyses were undertaken.

AUTHOR CONTRIBUTIONS

NP, AM, and MB designed the study. NP, AC, AW, and MB performed the experimental burial and the soil samplings. NP and AM performed the extraction and amplification of DNA. SG, SV, and MC performed the bioinformatic analysis of the results. NP, SG, and SV performed the data interpretation. NP was the major contributor in writing the manuscript. AC, MB, and AW performed the proofreading of the manuscript. All authors read and approved the final manuscript.

FUNDING

We are grateful to the Royal Society for funding both a doctoral studentship (NP) and University Research Fellowship (MB) under grants RG130453 and UF120473, respectively. We would also like to acknowledge the UKRI for funding a Future Leaders Fellowship (NP) under grant MR/S032878/1. The funding body did not have any role in the design of the study, in the collection, analysis and interpretation of data, or in writing the manuscript.

ACKNOWLEDGMENTS

We would like to thank the HuddersFIELD taphonomic facility for giving us the possibility to conduct this study.

SUPPLEMENTARY MATERIAL

The Supplementary Material for this article can be found online at: https://www.frontiersin.org/articles/10.3389/fmicb.2020.01686/full#supplementary-material

REFERENCES

Banchi, E., Ametrano, C. G., Stanković, D., Verardo, P., Moretti, O., Gabrielli, F., et al. (2018a). DNA metabarcoding uncovers fungal diversity of mixed airborne samples in Italy. *PLoS One* 13:e0194489. doi: 10.1371/journal.pone.0194489

Banchi, E., Stankovic, D., Fernández-Mendoza, F., Gionechetti, F., Pallavicini, A., and Muggia, L. (2018b). ITS2 metabarcoding analysis complements lichen mycobiome diversity data. *Mycol. Prog.* 17, 1049–1066. doi: 10.1007/s11557-018-1415-4

Bandeira, B., Jamet, J.-L., Jamet, D., and Ginoux, J.-M. (2013). Mathematical convergences of biodiversity indices. *Ecol. Indic.* 29, 522–528. doi: 10.1016/j.ecolind.2013.01.028

Barton, P. S., Cunningham, S. A., Lindenmayer, D. B., and Manning, A. D. (2013). The role of carrion in maintaining biodiversity and ecological processes in terrestrial ecosystems. *Oecologia* 171, 761–772. doi: 10.1007/s00442-012-2460-3

Bellini, E., Ambrosio, E., Zotti, M., Nucci, G., Gabbrielli, M., and Vanezis, P. (2016). The usefulness of cadaveric fungi as an investigation tool. *Am. J. Forensic Med. Pathol.* 37:23. doi: 10.1097/PAF.0000000000000210

Benjamini, Y., and Hochberg, Y. (1995). Controlling the false discovery rate: a practical and powerful approach to multiple testing. *J. R. Stat. Soc. Ser. B* 51, 289–300. doi: 10.1111/j.2517-6161.1995.tb02031.x

Blaalid, R., Kumar, S., Nilsson, R. H., Abarenkov, K., Kirk, P. M., and Kauserud, H. (2013). ITS1 *versus* ITS2 as DNA metabarcodes for fungi. *Mol. Ecol. Resour.* 13, 218–224. doi: 10.1111/1755-0998.12065

Bokulich, N. A., and Mills, D. A. (2013). Improved selection of internal transcribed spacer-specific primers enables quantitative, ultra-high-throughput profiling of fungal communities. *Appl. Environ. Microbiol.* 79, 2519–2526. doi: 10.1128/AEM.03870-12

Bruns, T. D., Chung, J. A., Carver, A. A., and Glassman, S. I. (2020). A simple pyrocosm for studying soil microbial response to fire reveals a rapid, massive response by *Pyronema* species. *PLoS One* 15:e0222691. doi: 10.1371/journal.pone.0222691

Buekenhout, I., Cravo, L., Vieira, D. N., Cunha, E., and Ferreira, M. T. (2018). Applying standardized decomposition stages when estimating the PMI of buried remains: reality or fiction? *Aust. J. Forensic Sci.* 50, 68–81. doi: 10.1080/00450618.2016.1212268

Cáceres, M., and De Legendre, P. (2009). Associations between species and groups of sites: indices and statistical inference. *Ecology* 90, 3566–3574. doi: 10.1890/08-1823.1

Caporaso, J. G., Kuczynski, J., Stombaugh, J., Bittinger, K., Bushman, F. D., Costello, E. K., et al. (2010). QIIME allows analysis of high-throughput community sequencing data. *Nat. Methods* 7, 335–336. doi: 10.1038/nmeth.f.303

Chimutsa, M., Olakanye, A. O., Thompson, T. J. U., and Ralebitso-Senior, T. K. (2015). Soil fungal community shift evaluation as a potential cadaver decomposition indicator. *Forensic Sci. Int.* 257, 155–159. doi: 10.1016/j.forsciint.2015.08.005

Christensen, M. A., Passalacqua, N., and Bartelink, E. (2014). "Forensic taphonomy," in *Forensic Anthropology Current Methods and Practice*, ed. A. E. Rattenbury (Cambridge, MA: Academic Press), 119–147.

Cobaugh, K. L., Schaeffer, S. M., and DeBruyn, J. M. (2015). Functional and structural succession of soil microbial communities below decomposing human cadavers. *PLoS One* 10:e0130201. doi: 10.1371/journal.pone.0130201

Dufrêne, M., and Legendre, P. (1997). Species assemblages and indicator species: the need for a flexible asymmetrical approach. *Ecol. Monogr.* 67, 345–366. doi: 10.1890/0012-9615(1997)067[0345:saaist]2.0.co;2

Finley, S. J., Benbow, M. E., and Javan, G. T. (2015). Potential applications of soil microbial ecology and next-generation sequencing in criminal investigations. *Appl. Soil Ecol.* 88, 69–78. doi: 10.1016/j.apsoil.2015.01.001

Finley, S. J., Pechal, J. L., Benbow, M. E., Robertson, B. K., and Javan, G. T. (2016). Microbial signatures of cadaver gravesoil during decomposition. *Microb. Ecol.* 71, 524–529. doi: 10.1007/s00248-015-0725-1

Fu, X., Guo, J., Finkelbergs, D., He, J., Zha, L., Guo, Y., et al. (2019). Fungal succession during mammalian cadaver decomposition and potential forensic implications. *Sci. Rep.* 9:12907. doi: 10.1038/s41598-019-49361-0

Fu, X. L., Guo, J. J., Zhu, Z. Y., Ding, Z. Y., Zha, L., and Cai, J. F. (2015). The potential use of fungi community in postmortem interval estimation in China. *Forensic Sci. Int. Genet. Suppl. Ser.* 5, e476–e478. doi: 10.1016/J.FSIGSS.2015.09.189

Gardes, M., and Bruns, T. D. (1993). ITS primers with enhanced specificity for basidiomycetes - application to the identification of mycorrhizae and rusts. *Mol. Ecol.* 2, 113–118. doi: 10.1111/j.1365-294X.1993.tb00005.x

Guo, J., Fu, X., Liao, H., Hu, Z., Long, L., Yan, W., et al. (2016). Potential use of bacterial community succession for estimating post-mortem interval as revealed by high-throughput sequencing. *Sci. Rep.* 6:24197. doi: 10.1038/srep24197

Hawksworth, D. L., and Wiltshire, P. (2015). Forensic mycology: current perspectives. *Res. Rep. Forensic Med. Sci.* 5, 75–83. doi: 10.2147/RRFMS.S83169

Hoggard, M., Vesty, A., Wong, G., Montgomery, J. M., Fourie, C., Douglas, R. G., et al. (2018). Characterizing the human mycobiota: a comparison of small subunit rRNA. ITS1, ITS2, and large subunit rRNA genomic targets. *Front. Microbiol.* 9:2208. doi: 10.3389/fmicb.2018.02208

Hurst, C. J. (ed.) (2016). *Advances in Environmental Microbiology*. Berlin: Springer.

Hyde, E. R., Metcalf, J. L., Bucheli, S. R., Lynne, A. M., and Knight, R. (2017). "Microbial communities associated with decomposing corpses," in *Forensic Microbiol*, ed. D. O. Carter John (Hoboken, NJ: Wiley Sons Ltd), 245–273. doi: 10.1002/9781119062585.ch10

Ihrmark, K., Bödeker, I. T. M., Cruz-Martinez, K., Friberg, H., Kubartova, A., Schenck, J., et al. (2012). New primers to amplify the fungal ITS2 region - evaluation by 454-sequencing of artificial and natural communities. *FEMS Microbiol. Ecol.* 82, 666–677. doi: 10.1111/j.1574-6941.2012.01437.x

Javan, G. T., and Finley, S. J. (2018). "What is the 'ŸThanatomicrobiome' and what is its relevance to forensic investigations?," in *Forensic Ecogenomics*, ed. T. K. Ralebitso-Senior (Elsevier), 13–143.

Javan, G. T., Finley, S. J., Can, I., Wilkinson, J. E., Hanson, J. D., and Tarone, A. M. (2016). Human thanatomicrobiome succession and time since death. *Sci. Rep.* 6:29598.

Klindworth, A., Pruesse, E., Schweer, T., Peplies, J., Quast, C., Horn, M., et al. (2013). Evaluation of general 16S ribosomal RNA gene PCR primers for classical and next-generation sequencing-based diversity studies. *Nucleic Acids Res.* 41:e1. doi: 10.1093/nar/gks808

McMurdie, P. J., and Holmes, S. (2013). phyloseq: an R package for reproducible interactive analysis and graphics of microbiome census data. *PLoS One* 8:e61217. doi: 10.1371/journal.pone.0061217

Mello, A., Napoli, C., Murat, C., Morin, E., Marceddu, G., and Bonfante, P. (2011). ITS-1 *versus* ITS-2 pyrosequencing: a comparison of fungal populations in truffle grounds. *Mycologia* 103, 1184–1193. doi: 10.3852/11-027

Metcalf, J. L. (2019). Estimating the postmortem interval using microbes: knowledge gaps and a path to technology adoption. *Forensic Sci. Int. Genet.* 38, 211–218. doi: 10.1016/J.FSIGEN.2018.11.004

Metcalf, J. L., Carter, D. O., and Knight, R. (2016a). Microbiology of death. *Curr. Biol. Mag.* 26, R543–R576. doi: 10.1016/j.cub.2016.03.042

Metcalf, J. L., Xu, Z. Z., Weiss, S., Lax, S., Van Treuren, W., Hyde, E. R., et al. (2016b). Microbial community assembly and metabolic function during mammalian corpse decomposition. *Science* 351, 158–162. doi: 10.1126/science.aad2646

Metcalf, J. L., Parfrey, L. W., Gonzalez, A., Lauber, C. L., Knights, D., Ackermann, G., et al. (2013). A microbial clock provides an accurate estimate of the postmortem interval in a mouse model system. *eLife* 2:e01104.

Nilsson, R. H., Larsson, K.-H., Taylor, A. F. S., Bengtsson-Palme, J., Jeppesen, T. S., Schigel, D., et al. (2019). The UNITE database for molecular identification of fungi: handling dark taxa and parallel taxonomic classifications. *Nucleic Acids Res.* 47, D259–D264. doi: 10.1093/nar/gky1022

Oksanen, J., Blanchet, F. G., Friendly, M., Kindt, R., Legendre, P., McGlinn, D., et al. (2018). *Vegan: Community Ecology Package. R package version 2.4–6*.

Orgiazzi, A., Bianciotto, V., Bonfante, P., Daghino, S., Ghignone, S., Lazzari, A., et al. (2013). 454 pyrosequencing analysis of fungal assemblages from geographically distant, disparate soils reveals spatial patterning and a core mycobiome. *Diversity* 5, 73–98. doi: 10.3390/d5010073

Orgiazzi, A., Dunbar, M. B., Panagos, P., de Groot, G. A., and Lemanceau, P. (2015). Soil biodiversity and DNA barcodes: opportunities and challenges. *Soil Biol. Biochem.* 80, 244–250. doi: 10.1016/J.SOILBIO.2014.10.014

Parkinson, R. A., Dias, K.-R., Horswell, J., Greenwood, P., Banning, N., Tibbett, M., et al. (2009). "Microbial community analysis of human decomposition on soil," in *Criminal and Environmental Soil Forensics*, eds K. Ritz, L. Dawson, and D. Miller (Berlin: Springer), 379–394. doi: 10.1007/978-1-4020-9204-6_24

Pechal, J. L., Crippen, T. L., Tarone, A. M., Lewis, A. J., Tomberlin, J. K., and Benbow, M. E. (2013). Microbial community functional change during vertebrate carrion decomposition. *PLoS One* 8:e79035. doi: 10.1371/journal.pone.0079035

Pechal, J. L., Schmidt, C. J., Jordan, H. R., and Benbow, M. E. (2018). A large-scale survey of the postmortem human microbiome, and its potential to provide insight into the living health condition. *Sci. Rep.* 8, 1–15.

Procopio, N., Ghignone, S., Voyron, S., Chiapello, M., Williams, A., Chamberlain, A., et al. (2020). *Soil Fungal Communities Investigated by Metabarcoding within Simulated Forensic Burial Contexts*. Preprint. Available online at: https://www.researchsquare.com/article/rs-13445/v1

Procopio, N., Ghignone, S., Williams, A., Chamberlain, A., Mello, A., and Buckley, M. (2018a). Metabarcoding to investigate changes in soil microbial communities within forensic burial contexts. *Forensic Sci. Int. Genet.* 39, 73–85. doi: 10.1016/j.fsigen.2018.12.002

Procopio, N., Williams, A., Chamberlain, A. T., and Buckley, M. (2018b). Forensic proteomics for the evaluation of the post-mortem decay in bones. *J. Proteomics* 177, 21–30. doi: 10.1016/j.jprot.2018.01.016

R Core Team (2013). *R: A Language and Environment for Statistical Computing*. Vienna: R Core Team.

Rognes, T., Flouri, T., Nichols, B., Quince, C., and Mahé, F. (2016). VSEARCH: a versatile open source tool for metagenomics. *PeerJ* 4:e2584. doi: 10.7717/peerj.2584

Schoch, C. L., Seifert, K. A., Huhndorf, S., Robert, V., Spouge, J. L., Levesque, C. A., et al. (2012). Nuclear ribosomal internal transcribed spacer (ITS) region as a universal DNA barcode marker for Fungi. *Proc. Natl. Acad. Sci. U.S.A.* 109, 6241–6246. doi: 10.1073/pnas.1117018109

Selbmann, L., Egidi, E., Isola, D., Onofri, S., Zucconi, L., de Hoog, G. S., et al. (2013). Biodiversity, evolution and adaptation of fungi in extreme environments. *Plant Biol.* 147, 237–246. doi: 10.1080/11263504.2012.753134

Swift, B. (2006). "The timing of death," in *Essentials of Autopsy Practice*, ed. G. N. Rutty (London: Springer), 189–214. doi: 10.1007/b136465

Szelecz, I., Lösch, S., Seppey, C. V. W., Lara, E., Singer, D., Sorge, F., et al. (2018). Comparative analysis of bones, mites, soil chemistry, nematodes and soil micro-eukaryotes from a suspected homicide to estimate the post-mortem interval. *Sci. Rep.* 8:25. doi: 10.1038/s41598-017-18179-z

Taberlet, P., Prud'Homme, S., Campione, E., Roy, J., Miquel, C., Shehzad, W., et al. (2012). Soil sampling and isolation of extracellular DNA from large amount of starting material suitable for metabarcoding studies. *Mol. Ecol.* 21, 1816–1820. doi: 10.1111/j.1365-294X.2011.05317.x

Vass, A. A., Smith, R. R., Thompson, C. V., Burnett, M. N., Wolf, D. A., Synstelien, J. A., et al. (2004). Decompositional odor analysis database. *J. Forensic Sci.* 49, 760–769.

Wang, X.-C., Liu, C., Huang, L., Bengtsson-Palme, J., Chen, H., Zhang, J.-H., et al. (2015). ITS1: a DNA barcode better than ITS2 in eukaryotes? *Mol. Ecol. Resour.* 15, 573–586. doi: 10.1111/1755-0998.12325

White, T. J., Bruns, T., Lee, S., and Taylor, J. (1990). "Amplification and direct sequencing of fungal ribosomal RNA genes for phylogenetics,"in *PCR Protocols: A Guide to Methods and Applications*, eds M. A. Innis, D. H. Gelfand, J. J. Sninsky, and T. J. White (Academic Press), 315–322. doi: 10.1016/B978-0-12-372180-8.50042-1

Zhang, J., Kobert, K., Flouri, T., and Stamatakis, A. (2013). PEAR: a fast and accurate illumina paired-end reAd mergeR. *Bioinformatics* 30, 614–620. doi: 10.1093/bioinformatics/btt593

Zhou, W., and Bian, Y. (2018). Thanatomicrobiome composition profiling as a tool for forensic investigation. *Forensic Sci. Res.* 3, 105–110. doi: 10.1080/20961790.2018.1466430

Conflict of Interest: The authors declare that the research was conducted in the absence of any commercial or financial relationships that could be construed as a potential conflict of interest.

frontiers in Microbiology

ORIGINAL RESEARCH
published: 04 September 2020
doi: 10.3389/fmicb.2020.555347

Dysbiosis in the Dead: Human Postmortem Microbiome Beta-Dispersion as an Indicator of Manner and Cause of Death

*Sierra F. Kaszubinski[1], Jennifer L. Pechal[2], Katelyn Smiles[2], Carl J. Schmidt[3,4], Heather R. Jordan[5], Mariah H. Meek[1,6,7] and M. Eric Benbow[2,7,8]**

[1] Department of Integrative Biology, Michigan State University, East Lansing, MI, United States, [2] Department of Entomology, Michigan State University, East Lansing, MI, United States, [3] Wayne County Medical Examiner's Office, Detroit, MI, United States, [4] Department of Pathology, University of Michigan, Ann Arbor, MI, United States, [5] Department of Biological Sciences, Mississippi State University, Starkville, MS, United States, [6] AgBio Research, Michigan State University, East Lansing, MI, United States, [7] Ecology, Evolutionary Biology and Behavior Program, Michigan State University, East Lansing, MI, United States, [8] Department of Osteopathic Medical Specialties, Michigan State University, East Lansing, MI, United States

OPEN ACCESS

Edited by:
Spyridon Ntougias, Democritus University of Thrace, Greece

Reviewed by:
Michael S. Allen, University of North Texas Health Science Center, United States
Konstantinos Papadimitriou, University of Peloponnese, Greece

***Correspondence:**
M. Eric Benbow
benbow@msu.edu

Specialty section:
This article was submitted to Systems Microbiology, a section of the journal Frontiers in Microbiology

Received: *24 April 2020*
Accepted: *19 August 2020*
Published: *04 September 2020*

Citation:
Kaszubinski SF, Pechal JL, Smiles K, Schmidt CJ, Jordan HR, Meek MH and Benbow ME (2020) Dysbiosis in the Dead: Human Postmortem Microbiome Beta-Dispersion as an Indicator of Manner and Cause of Death. Front. Microbiol. 11:555347. doi: 10.3389/fmicb.2020.555347

The postmortem microbiome plays an important functional role in host decomposition after death. Postmortem microbiome community successional patterns are specific to body site, with a significant shift in composition 48 h after death. While the postmortem microbiome has important forensic applications for postmortem interval estimation, it also has the potential to aid in manner of death (MOD) and cause of death (COD) determination as a reflection of antemortem health status. To further explore this association, we tested beta-dispersion, or the variability of microbiomes within the context of the "Anna Karenina Principle" (AKP). The foundational principle of AKP is that stressors affect microbiomes in unpredictable ways, which increases community beta-dispersion. We hypothesized that cases with identified M/CODs would have differential community beta-dispersion that reflected antemortem conditions, specifically that cardiovascular disease and/or natural deaths would have higher beta-dispersion compared to other deaths (e.g., accidents, drug-related deaths). Using a published microbiome data set of 188 postmortem cases (five body sites per case) collected during routine autopsy in Wayne County (Detroit), MI, we modeled beta-dispersion to test for M/COD associations *a priori*. Logistic regression models of beta-dispersion and case demographic data were used to classify M/COD. We demonstrated that beta-dispersion, along with case demographic data, could distinguish among M/COD – especially cardiovascular disease and drug related deaths, which were correctly classified in 79% of cases. Binary logistic regression models had higher correct classifications than multinomial logistic regression models, but changing the defined microbial community (e.g., full vs. non-core communities) used to calculate beta-dispersion overall did not improve model classification or M/COD. Furthermore, we tested our analytic approach on a case study that predicted suicides from other deaths, as well as distinguishing MOD (e.g., homicides vs. suicides) within COD (e.g., gunshot

wound). We propose an analytical workflow that combines postmortem microbiome indicator taxa, beta-dispersion, and case demographic data for predicting MOD and COD classifications. Overall, we provide further evidence the postmortem microbiome is linked to the host's antemortem health condition(s), while also demonstrating the potential utility of including beta-dispersion (a non-taxon dependent approach) coupled with case demographic data for death determination.

Keywords: postmortem microbiome, forensic microbiology, manner of death, cause of death, microbial communities, beta-dispersion, Anna Karenina Principle, necrobiome

INTRODUCTION

The organisms represented in microbiomes have important functional roles for host life – influencing health status, development, and disease susceptibility, among many others (Turnbaugh et al., 2007; Zaneveld et al., 2017). Microbes also play an important functional role in the decomposition process (Pechal et al., 2014), as the communities change with dispersal, competition, and other interactions after host death (Pechal et al., 2014, 2018; Metcalf et al., 2016). These dynamic, yet predictable (Belk et al., 2018; Pechal et al., 2018), microbial community profile changes after death make the postmortem microbiome a potential forensic resource for postmortem interval (PMI) estimation. PMI estimation is indeed the most studied forensic application of the postmortem microbiome (Metcalf et al., 2013; Pechal et al., 2014); but, this community has additional potential for other forensic applications as well, like indicating antemortem health conditions (e.g., cardiovascular disease or violent death) (Pechal et al., 2018) and the living environment (e.g., neighborhood blight) (Pearson et al., 2019).

The postmortem microbiome is structured in part by a decedents' antemortem health condition and the suite of stressors that impact the human host. These stressors include drug/alcohol abuse or high stress lifestyle conditions like neighborhood blight (e.g., abandoned building, inactivity, and dumping), that are associated with certain manners of death (e.g., homicide) (Pechal et al., 2018; Pearson et al., 2019; Zhang et al., 2019). Importantly, the adult human postmortem microbiome does not significantly change from the antemortem microbiome for approximately 48 h after death when tested in a single geographic region (Pechal et al., 2018). Due to the stability of the postmortem microbiome within 48 h of death, and the potential connection to lifestyle condition, microbial community metrics (e.g., diversity) were associated with certain manners of deaths (MOD) or causes of deaths (COD) (Pechal et al., 2018; Zhang et al., 2019). However, fewer studies have tested associations of postmortem microbial community variability with MOD or COD (Pechal et al., 2018; Pearson et al., 2019; Zhang et al., 2019).

In past work, microbial diversity and indicator taxa were shown to reflect antemortem health conditions and MOD (Pechal et al., 2018; Pearson et al., 2019; Zhang et al., 2019). In some cases, lower microbial alpha-diversity was associated with cardiovascular disease, non-violent deaths, and neighborhood blight (Pechal et al., 2018; Pearson et al., 2019); however, it is difficult to capture the variability in a large sample set using alpha-diversity metrics alone (e.g., richness), as they do not account for taxon relative composition. Zhang et al. (2019) combined microbial indicator taxa and case demographic data found in autopsy reports (e.g., decedents age, sex, race, etc.) to test machine learning models for classifying M/COD (Zhang et al., 2019). While indicator taxa are a useful reflection of antemortem conditions, microbial indicator taxa may not be present in all cases (e.g., *Haemophilus influenzae*), or they may be ubiquitous (e.g., *Staphylococcus*), and so less useful for a generalizable tool for M/COD determination (Pechal et al., 2018). For this study, we tested a metric that captures microbial variability while not specifically relying on indicator taxa: beta-dispersion. Our goal was to determine how postmortem microbiome beta-dispersion could be an additional tool for predicting M/CODs during death investigation.

Following the conceptual context of the "Anna Karenina Principle" (AKP), after prolonged exposure to any array of stressors, the microbiomes of unhealthy individuals becomes more variable compared to the microbial communities of healthy individuals (Zaneveld et al., 2017). For example, beta-dispersion increased among living individuals with a history of obesity, infection, and smoking (Barbian et al., 2015; Zaneveld et al., 2017). In other words, increased variation in the microbial communities reflects dysbiosis, and this community variability can be quantified through calculations of beta-dispersion (Barbian et al., 2015; Zaneveld et al., 2017). Beta-dispersion is calculated, within the context of a dataset, using a multivariate distance from the centroid for each case sample, as defined by a grouping factor (e.g., body site, PMI, weight status) (Oksanen et al., 2019). Based on the link between increased beta-dispersion and health status in living populations, we considered M/COD as grouping factors to quantify microbial signatures and develop metrics associated with M/COD determinations. Such association of beta-dispersion with M/COD could conceivably be additional evidence in future death investigation.

Microbial community metrics could potentially aid medical examiners and other certifiers of death (referred to as "medical examiners"), as determining M/COD can be error prone. While COD spans a variety of causes relating to the injury/disease a person died from, MOD encompasses only five major categories: natural, accident, suicide, homicide, and indeterminate (Randy et al., 2002). Medical examiners qualify their MOD determination with incremental degrees of certainty considering the available evidence (Randy et al., 2002). Given the possibility for mismatch between the MOD determination and the actual MOD, the postmortem microbiome could provide another potential piece of evidence to document M/COD determination.

To evaluate how postmortem microbiome variability is associated with M/CODs, we modeled postmortem microbiome beta-dispersion from five body sites of 188 routine autopsy with known M/COD (as determined by a board-certified forensic pathologist). We predicted that certain M/CODs, such as natural deaths and cardiovascular disease, would have higher beta-dispersion than other M/CODs due to the previous antemortem health condition links found in previous studies (Pechal et al., 2018). However, the effect of life environment was predicted to increase beta-dispersion as well, in a way that could potentially factor into deaths classified as homicide, for example, those due to blunt force trauma or gunshot wounds (Pearson et al., 2019). Quantifying beta-dispersion, using M/COD as a grouping factor, could provide reliable and usable tool in death investigation for M/COD determination.

MATERIALS AND METHODS

Sample Collection, DNA Extraction, and Sequencing

The postmortem microbiome data used in this study were acquired from Pechal et al. (2018) but re-analyzed to test M/COD determination from beta-dispersion. This dataset contains postmortem microbiome samples obtained from 188 Wayne County Medical Examiner's Office autopsy cases (Detroit, MI, 2014–2016), representing multiple MODs (accident, homicide, suicide, natural) and CODs (asphyxiation, blunt force trauma, cardiovascular disease, drug-related deaths, gunshot wounds, etc.) (**Supplementary Table S1**) (Pechal et al., 2018). The cases also represent a cross-section of the greater Detroit metropolitan area population and were nearly evenly divided among females and males (83:105) and black and white (90:98) (**Supplementary Table S1**). Cases comprised of adults (18–88 years) with a body mass index (BMI) ranging from 8.5–67.5 kg/m^2 (**Supplementary Table S1**). The dataset is the largest postmortem microbiome available to test beta-dispersions potential to aid in M/COD determination.

Detailed methods for sample collection, DNA extraction, and sequencing can be found in Pechal et al. (2018). To summarize, trained personnel at Wayne County Medical Examiner's Office collected microbial community swab samples from five body sites (nose, mouth, rectum, ears, and eyes) during routine autopsy. Microbial DNA was extracted and sequenced to characterize the microbial communities. The Michigan State University (MSU) Genomics Core Facility (East Lansing, MI, United States) sequenced the 16S rRNA V4 region using an Illumina MiSeq standard flow cell (v2) using a 500-cycle reagent cartridge.

Data Analysis and Bioinformatics

Sequence reads from postmortem microbiome samples were analyzed with QIIME2 (v2018.11) (Bolyen et al., 2019), following the methodology outlined in Kaszubinski et al. (2019). DADA2 v1.8.0 (Callahan et al., 2016) was used for denoising. Sequences were aligned using MAFFT v7.397 (Katoh and Standley, 2013), and FastTree v2.1 (Price et al., 2010). Taxonomy and amplicon sequencing variant (ASV) tables were exported as comma separated values (csv) files to be used as input data for all downstream analysis. ASV and taxonomy files were combined with demographic data obtained from autopsy reports (age, sex, race, BMI, etc.) as *phyloseq* (v1.28.0) objects in R (v3.6.1) (McMurdie and Holmes, 2013; R Core Team, 2018). ASVs less than 0.01% of the mean library size were trimmed, removing 22,214 ASVs for a total of 8,692 ASVs. *Phyloseq* objects were split among the body sites (nose, mouth, rectum, ears, and eyes) and analyzed separately.

Method Selection

To determine the optimal methodology for calculating beta-dispersion before moving forward with classifying M/COD, we compared standardization approaches of the microbial communities, distance matrices, and alpha-diversity to select the optimal method for beta-dispersion calculation. For standardization, rarefying (randomly subsampling ASVs to a specified minimum library size) and normalizing (non-rarefaction based method; removing ASVs not present in a specified percentage of samples) were compared for each body site using three minimum library sizes (3,000, 5,000, and 7,000 sequences) and sample percentage cut off (1%, 3%, 10%), respectively. We wanted to determine not only which standardization strategy was optimal, but also how sensitive the standardizations were (minimum library size and sample percentage cut off). While rarefaction has been debated (McMurdie and Holmes, 2014; Weiss et al., 2017), we sought to eliminate bias associated with different library sizes that could inflate differences in beta-dispersion among M/CODs (Kaszubinski et al., 2019). Specifically, library size differences can mask biologically meaningful results especially for unweighted distance matrices (Weiss et al., 2017). Normalization (as referenced in this manuscript), is a common non-rarefaction technique used in ecology studies (Poos and Jackson, 2012). However, this leads to different library sizes among samples, which may be an artifact in some analyses.

We also compared unweighted and weighted UniFrac distances matrices for calculating beta-dispersion to determine whether considering abundances (weighted UniFrac) would affect the beta-dispersion calculation and should be considered for downstream modeling; UniFrac (weighted and unweighted) is commonly used in forensic studies (Javan et al., 2017; Pechal et al., 2018). Beta-dispersion was calculated among MODs and CODs using the *vegan* package (v2.5-5) in R at each minimum library size and sample percentage cutoff (Oksanen et al., 2019). The *betadisper* function from vegan reports the distance from the centroid for each sample, as defined by a grouping factor (in this dataset M/COD). Each postmortem microbiome sample had two corresponding beta-dispersion values, with either MOD or COD as a grouping factor. Kruskal–Wallis, Fligner-Killeen, and *post hoc* Nemenyi tests among beta-dispersion values tested differences among M/CODs and were reported with a Bonferroni correction (Pohlert, 2018). Additionally, alpha-diversity metrics (Chao1 and Shannon diversity) were calculated using *phyloseq* for each minimum library size and sample percentage cutoff level.

We then selected a methodology [standardization of input data analysis (rarefaction or normalization) and distance matrix] for calculating beta-dispersion based on the number of significant differences in beta-dispersion (among M/CODs) identified by Kruskal–Wallis and *post hoc* Nemenyi tests as well as the highest alpha-diversity (see the section "Method Selection" in "Results"). This standardization approach was identified for its potential to distinguish M/COD, while maintaining microbial diversity. For subsequent analyses, microbial communities were rarefied to 5,000 sequences and beta-dispersion was calculated using unweighted UniFrac distance.

Model Selection

We built multinomial logistic regression models to classify M/COD from beta-dispersion values and case demographic data (Böhning, 1992) using the *lme4* (v1.1-21) and *mlogit* package (v1.0-1) (Bates et al., 2019; Croissant, 2019). Logistic regression is an analysis commonly used in clinical settings because it has distinct advantages (de Jong et al., 2019). Logistic regression does not assume normality, linearity, or homoscedasticity (even variance) (Harrell et al., 1996; Steyerberg et al., 2001). Logistic regression is prone to overfitting, especially in cases with small datasets (de Jong et al., 2019). However, goodness-of-fit metrics, such as R^2 and model comparison can be used to evaluate the validity of models (Pohlert, 2018; de Jong et al., 2019).

Full multinomial logistic regression models included all categories of interest for classifying M/COD (e.g., homicide, suicide, natural, and accidental death for MOD; cardiovascular disease, drug related deaths, blunt force trauma, asphyxiation, gunshot wounds, and "other deaths" for COD). Demographic data of interest [age, BMI, sex, race, PMI (<48 h; >49 h), season, and event location (outdoors, indoors, hospital, vehicular)] were summarized (**Table 1**) and demographic means were tested among M/CODs (Kruskal–Wallis with a Bonferroni correction) to identify potential significant ($p < 0.05$) covariates for inclusion in model building (Pohlert, 2018). Multicollinearity was evaluated among the covariates using a correlation test, which found the covariates to be independent, meeting model assumptions (**Supplementary Figure S1**) (Steyerberg et al., 2001).

Multiple logistic regression models classifying M/COD were built and tested for each body site. We used a stepwise selection with backward elimination of predictors to determine significant covariates (Steyerberg et al., 2001). Only those models with significant ($p < 0.1$) beta-dispersion contribution as a covariate were selected for further modeling with case demographic data. We chose a more conservative p-value for the beta-dispersion covariate cut off to avoid excluding potentially relevant models for further evaluation, as recommended in other studies (Steyerberg et al., 2001). However, overall model significance was considered at $p < 0.05$. The best performing models were identified based on goodness-of-fit metric McFadden R^2 (excellent fit ranges from 0.2-0.4) (McFadden, 1979), model comparison using Akaike information criterion (AIC) (lower AIC = better model) (Bozdogan, 1987), and classification success (correct classifications/total number of samples). Based on these initial model building results,

TABLE 1 | Case demographic data stratified by M/COD.

	Age (y)		BMI		Sex		Race		PMI		Event location			Season			
	Mean	SD	Mean	SD	Female	Male	Black	White	<48 h	>49 h	Hospital	Indoors	Outdoors	Vehicular	Autumn	Spring	Summer	Winter
Manner of death																		
Accident (n = 71)	39.9	13.8	30	8.48	35	36	26	45	62	9	10	51	7	3	4	41	17	9
Homicide (n = 39)	36.2	12.3	26.9	6.42	9	30	34	5	37	2	9	14	12	4	2	20	6	11
Natural (n = 57)	53.7	10.7	29.8	10.1	25	32	29	28	45	12	6	49	1	1	2	33	14	8
Suicide (n = 22)	44.9	15.6	27.2	6.57	11	12	3	20	21	2	1	18	3	1	2	10	6	5
Cause of death																		
Asphyxiation (n = 11)	46.5	20.1	25.4	4.35	4	7	2	9	10	1	1	7	2	1	1	3	3	4
Blunt force trauma (n = 21)	42.6	14.7	28.9	10.3	12	9	14	7	21	0	4	7	8	2	4	9	3	5
Cardiovascular disease (n = 42)	54.5	11.6	29.9	9.56	20	22	23	19	34	8	6	35	1	0	2	26	7	7
Drug-related deaths (n = 70)	41	12.7	29.7	7.51	34	36	22	48	58	12	5	60	3	2	2	43	17	8
Gunshot wounds (n = 30)	33.8	11.8	27.5	6.34	5	25	24	6	28	2	7	10	9	4	1	16	6	7
Other (n = 16)	47.3	12	28.8	12.1	5	11	7	9	14	2	3	13	0	0	0	7	7	2

Mean (±SD) age (years) and body mass index (BMI; kg/m^2) for 188 cases included in this study. Sex, race, postmortem interval (PMI) estimate, death event location, and time of year (season) for death discovery were reported as count data.

models could be improved (see the section "Model Selection" in "Results").

To improve logistic regression models, we considered three microbial community types for beta-dispersion calculation: full communities, random forest indicator communities, and "non-core" communities. While the grouping factor (M/COD) remained the same, the microbial communities used to calculate beta-dispersion differed. "Full community" beta-dispersion was calculated from the standardized community input data within each body site. "Random forest indicators," as determined by *Boruta* (v6.0.0) in R, used confirmed and tentative taxa of importance ($p < 0.05$) (Kursa and Rudnicki, 2018), and beta-dispersion was calculated from this set of significant indicator taxa. Random forest classification error was determined using the *randomForest* package (v4.6-14) in R (Breiman et al., 2018). While the definition of a "core microbiome" is widely debated (Shade and Handelsman, 2012), we defined "non-core" taxa in this study as taxa present in only one M/COD. The taxa had to be present in at least one case, for example the genus *Turicella* was present in only one homicide case, while the family Streptococcaceae was represented in several homicide cases. "Core" taxa were removed, and beta-dispersion was calculated from the remaining 'non-core' taxa.

Lastly, we tested binary logistic regression (classifying between two categories) compared to multinomial logistic regression (multiple categories). Binary logistic regression models were also built using the *lme4* (v1.1-21) and *mlogit package* (v1.0-1) in R (Bates et al., 2019; Croissant, 2019), and the best performing models were considered based on AIC (Bozdogan, 1987), McFadden R^2, and classification success (correct classifications/total number of samples). Beta-dispersion differences were visualized using principal coordinate analysis (PCoA) plots created in *phyloseq*, and potential beta-dispersion differences were assessed using permutational multivariate analysis of variance (PERMANOVA) (Anderson, 2017).

Case Studies

Using the methodology outlined above, we tested data from two case studies for classifying MOD from nose communities to showcase the forensic potential beta-dispersion has as a tool for medical examiners. For the first case study (Case Study #1), a matched design with paired cases of similar age, race, and sex, to limit the effect of demographic data (**Supplementary Table S2**), were examined to compare suicides ($n = 22$) against other manners of death ($n = 21$ accident, homicide, or natural). For the second case study (Case Study #2), we examined MOD within COD, specifically examining homicides ($n = 25$) vs. suicides ($n = 4$) resulting from gunshot wounds (**Supplementary Table S1**). Potential indicator taxa for each grouping (MOD) were identified using *Boruta* in R. We also evaluated the potential beta-dispersion differences between MODs using PERMANOVA (Anderson, 2017), and classified MOD using binary logistic regression. We calculated achieved power using *G*Power 3* v3.0.5 (Faul et al., 2007). Case study beta-dispersion was compared using the mean and standard deviation using an independent mean two−tailed *t*-test ($\alpha = 0.05$).

RESULTS

Method Selection

Unweighted UniFrac distances, compared to weighted UniFrac distances, were the optimum distance matrix for these data. In summary, unweighted UniFrac had three-times as many significant comparisons (identified mean differences of beta-dispersion among M/CODs by Kruskal–Wallis and *post hoc* Nemenyi $p < 0.05$) across rarefied and normalized communities, four-times as fewer deviations of variance (identified variance differences of beta-dispersion among M/CODs by Fligner-Killeen $p < 0.05$), and lack of library size bias (**Supplementary Figures S2, S3** and **Supplementary Tables S3, S4**). Unifrac distances were more robust against rarefying and normalizing, as significant comparisons occurred with both standardization methods (Kruskal–Wallis and *post hoc* Nemenyi $p < 0.05$; **Supplementary Figure S3** and **Supplementary Table S3**). Rarefaction was the more appropriate standardization strategy than normalization for this dataset as well. While normalizing the data had more than double the significant comparisons than rarefying, normalizing microbial communities led to a significant decrease in alpha-diversity compared to rarefying (Kruskal–Wallis and *post hoc* Nemenyi $p < 0.05$; **Supplementary Figures S2, S4** and **Supplementary Tables S3, S5**). For normalizing combined with Weighted Unifrac, we found a bias of library size among the significant comparisons (**Supplementary Table S4**). Most of the significant comparisons (7 out of 10) had differential library sizes, reflecting that M/COD differences in beta-dispersion may have been related to library size using our normalization approach (Kruskal–Wallis and *post hoc* Nemenyi $p < 0.05$; **Supplementary Table S4**). A minimum library size of 5,000 sequences was selected for model comparisons, as more body sites yielded significant comparisons (Kruskal–Wallis $p < 0.05$) than other library sizes (7,000: 3 body sites, 5,000: 5 body sites; 3,000: 1 body site; **Supplementary Figure S2**) and was the appropriate minimum library size based on alpha-rarefaction curves of sequencing depth (**Supplementary Tables S3, S5** and **Supplementary Figures S5, S6**).

Model Comparison

Beta-dispersion significantly differed among body sites and M/CODs (Kruskal–Wallis $p < 0.05$, **Figure 1** and **Supplementary Table S6**). Every postmortem microbiome sample had two corresponding beta-dispersion values (distances from centroid), with either MOD or COD as the grouping factor. On average, eye microbiomes had the highest beta-dispersion [MOD: 0.646 (SD = 0.0346); COD: 0.642 (SD = 0.0346); **Supplementary Table S6**], while mouth communities had the lowest beta-dispersion [MOD: 0.567 (SD = 0.0779); COD: 0.563 (SD = 0.0800); **Supplementary Table S6**]. Beta-dispersion was significantly different among all body site communities, except the ears and eyes, but we considered all body sites for downstream modeling with logistic regression to not prematurely remove body sites from consideration (Kruskal–Wallis $p < 0.05$; **Supplementary Table S6**). Natural

death postmortem microbiomes had the highest average beta-dispersion [0.628 (SD = 0.0560); **Supplementary Table S6**] compared to homicides [0.606 (SD = 0.0694)] and accidents [0.608 (SD = 0.0683); Kruskal–Wallis $p < 0.05$; **Supplementary Table S6**]. Microbiomes of cases with cardiovascular disease had significantly higher beta-dispersion among all body sites [0.625 (SD = 0.0565); **Supplementary Table S6**] compared to gunshot wounds [0.605 (SD = 0.0708)], blunt force trauma [0.601 (SD = 0.0624)] and drug-related deaths [0.611 (SD = 0.0684); Kruskal–Wallis $p < 0.1$; **Supplementary Table S6**]. While beta-dispersion means differed significantly among MODs and CODs, there was overlap among beta-dispersion values, indicating that other variables contribute to microbiome beta-dispersion (**Figure 1**). Therefore, we considered additional case demographic data for downstream modeling. Age, sex, race, and event location were significantly different among MODs/CODs (Kruskal–Wallis $p < 0.05$; **Table 1**; **Supplementary Table S7**); however, so as to not prematurely remove potentially important demographic data we included all demographic data of interest in downstream modeling [age, BMI, sex, race, PMI (<48 h; >49 h), season, and event location (outdoors, indoors, hospital, vehicular)].

Multinomial logistic regression models were useful for initially determining which body site beta-dispersion had the best classification potential for M/COD. Classifying among all MODs, nose and mouth beta-dispersion were significant covariates, while nose, mouth, and ear beta-dispersion were a significant covariate for classifying all COD categories ($p < 0.1$; **Supplementary Table S8**). Nose community beta-dispersion, on average, successfully classified MODs at 61.1% (SD = 0.872), while ears and nose beta-dispersion successfully classified CODs on average 62.3% (SD = 0.599) and 62.5% (SD = 0.291), respectively (**Supplementary Table S8**). Based on these results, we only used those body sites with statistically significant

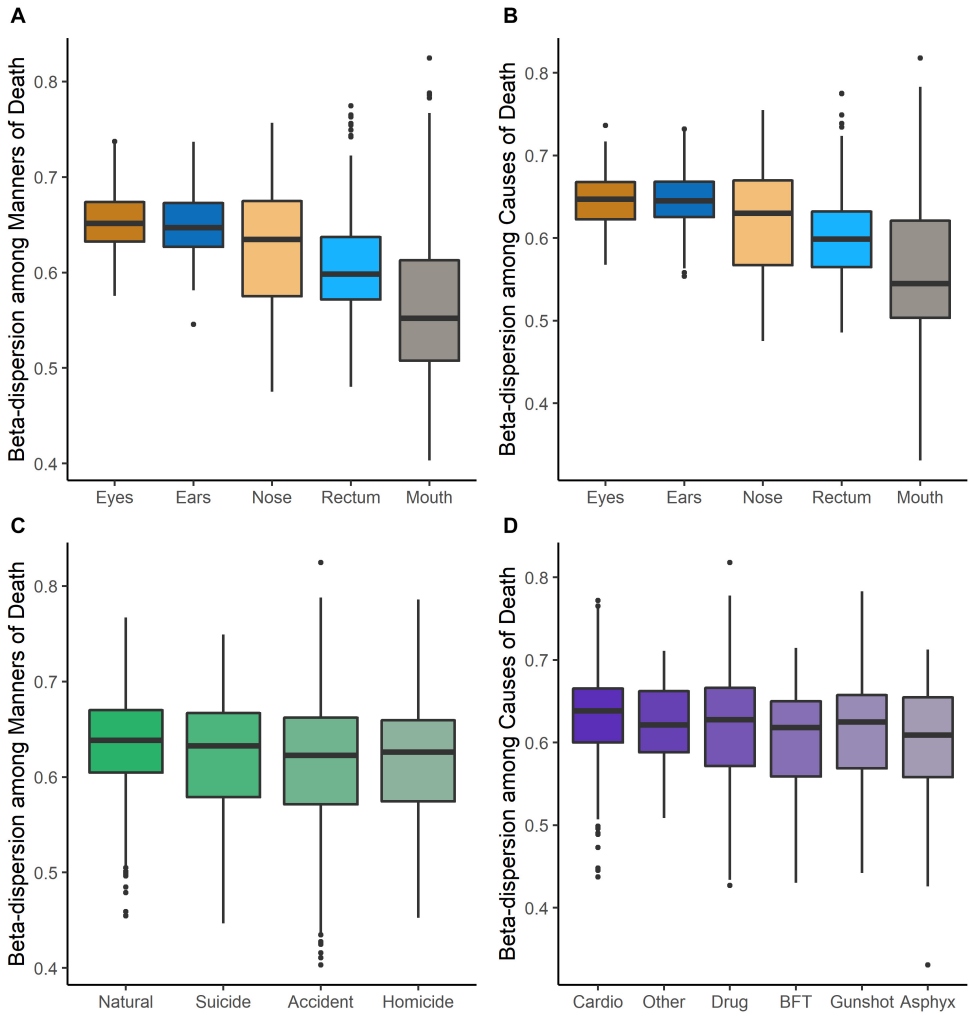

FIGURE 1 | Beta-dispersion values (distances from the centroid) for each postmortem sample, stratified among body sites and MODs/CODs. **(A)** Beta-dispersion values with MOD as the grouping factor and stratified among body sites. **(B)** COD as the grouping factor and stratified among body sites. **(C)** Beta-dispersion values for all postmortem samples with MOD as the grouping factor, **(D)** with COD as the grouping factor (cardio, cardiovascular disease; drug, drug-related deaths; BFT, blunt force trauma; asphyx, asphyxiation).

($p < 0.05$) models among M/CODs for further model building: nose, mouth, and ears.

While initial multinomial logistic regression models were able to classify among all M/CODs at higher success rate than random (overall average 50.2%; random chance: MOD: 25.0%; COD: 16.7%), models could be improved (**Supplementary Table S8**). Models classifying M/COD with only beta-dispersion (no case demographic data) were significant ($p < 0.05$) but had low classification success and model fit (∼40% average classification success; McFadden R^2 of ∼ 0.0244; **Supplementary Table S8**). Adding case demographic data to the models led to better classification success and model fit (∼60% average classification success; McFadden R^2: ∼0.298; **Supplementary Table S8**). However, we attempted to improve our models by testing different microbial communities to calculate beta-dispersion (full communities, random forest indicator communities, and "non-core" communities) and binary logistic regression rather than multinomial logistic regression.

Overall, microbial community type (full communities, random forest indicator communities, and "non-core" communities) did not improve logistic regression models (**Figure 2** and **Supplementary Tables S9, S10**). Models using "non-core" community beta-dispersion were not significant ($p > 0.05$) and so thus removed from further consideration and downstream modeling (**Supplementary Table S9**). Even though random forest indicator communities were specific to M/COD, multinomial logistic regression models were not more successful than full communities at classifying M/COD, and were less successful in some cases [percent correct classifications for full: 59.1% (SD = 2.64); RF: 57.8% (SD = 3.06); **Figure 2**; **Supplementary Table S10**]. For the random forest indicator communities and full communities, all models were within 7% of each other for McFadden R^2, a metric of model fit [full: 0.298 (SD = 0.0367); RF: 0.318 (SD = 0.0445); **Figure 2**; **Supplementary Table S10**].

For some M/COD comparisons (natural vs. accidental death; cardiovascular disease vs. drug-related death; disease vs. non-diseased state), binary logistic regression models performed best with an average classification success of 83.2% (SD = 5.50) (**Supplementary Table S11**) for full community and random forest indicator communities ("non-core" communities were not modeled for binary logistic regression due to poor results in the multinomial logistic regression models). For nose communities, beta-dispersion was a significant covariate ($p < 0.1$) between natural vs. accidental death, cardiovascular disease vs. drug-use, and diseased (natural deaths) vs. non-diseased (accidental, homicide, suicide) deaths (**Table 2** and **Supplementary Table S11**). While random forest indicator communities had marginally higher successful classification compared to full communities (full: 78.9%; RF: 83.6%) and higher McFadden R^2 (full: 0.347; RF: 0.369), the sample size of cases included in the random forest models was smaller (**Table 2** and **Supplementary Table S11**), as some samples were discarded if they did not have the RF indicator taxa. Therefore, we considered full community beta-dispersion as the most appropriate metric (**Figure 3**). There was no distinct visual clustering of samples suggesting that misclassification was randomly distributed among samples (PERMANOVA $p > 0.05$; **Figure 3**). In summary, we have compiled the best performing multinomial and binary logistic regression models for this dataset, based on the percent correct classifications, McFadden R^2, and AIC (**Supplementary Table S12**).

Case Studies

Case Study #1

Of the 188 cases, we matched nose communities of 22 cases by age [43 years (SD = 14)], sex (21 females; 22 males), and race (6 blacks; 37 whites) with other deaths (natural, homicide, and accidental) for a total of 43 cases (**Supplementary Table S2**). We identified three significant indicator taxa of suicide (*Boruta* $p < 0.05$; **Supplementary Table S13**). Suicide communities had higher beta-dispersion [0.659 (SD = 0.0433)] than non-suicides [0.654 (SD = 0.0427); **Supplementary Table S13**] but there were no significant differences in beta-dispersion among suicides (PERMANOVA permuted $p = 0.144$; **Supplementary Table S13**). Logistic regression of beta-dispersion without demographic data classified suicide cases with a 58.1% success rate (**Supplementary Table S13**), likely associated with low power (1–β: 0.0660). For future studies, we proposed a potential workflow using this matched-design case study for other researchers to use as a reference (**Figure 4** and **Supplementary Table S13**).

Case Study #2

Despite the low sample sizes, we identified ten potential indicator taxa for homicide vs. suicide resulting from gunshot wounds (*Boruta* $p < 0.05$; **Supplementary Table S14**). Beta-dispersion among gunshot wound homicides was significantly higher [0.626 (SD = 0.0491)] than gunshot wound suicides [0.543 (SD = 0.0959); PERMANOVA permuted $p < 0.05$; **Supplementary Table S14**]. Furthermore, we found significant logistic regression models of homicides vs. suicides with gunshot wounds accurately classified 93.1% of the time (**Supplementary Table S14**), despite uneven and low sample sizes ($n = 25$ homicides; $n = 4$ suicides; **Supplementary Table S14**), we achieved moderate power (1–β: 0.469).

DISCUSSION

In previous research, the AKP concept was tested with distinct treatment vs. control groups based on living health conditions and in living hosts (Zaneveld et al., 2017). However, we postulated the postmortem microbiome of various M/CODs would correspond with differential beta-dispersion, which could potentially be used as additional evidence in future forensic investigations. We hypothesized that cardiovascular disease and/or natural deaths would have the highest beta-dispersion, as AKP correlates with disease state in the antemortem life condition (Barbian et al., 2015; Zaneveld et al., 2017). Higher microbiome beta-dispersion was also predicted to be related to a stressful life environment, which is often associated with homicides, gunshot wounds, and blunt force trauma deaths (Pearson et al., 2019). Our best performing models were binary logistic regression models that confirmed the medical

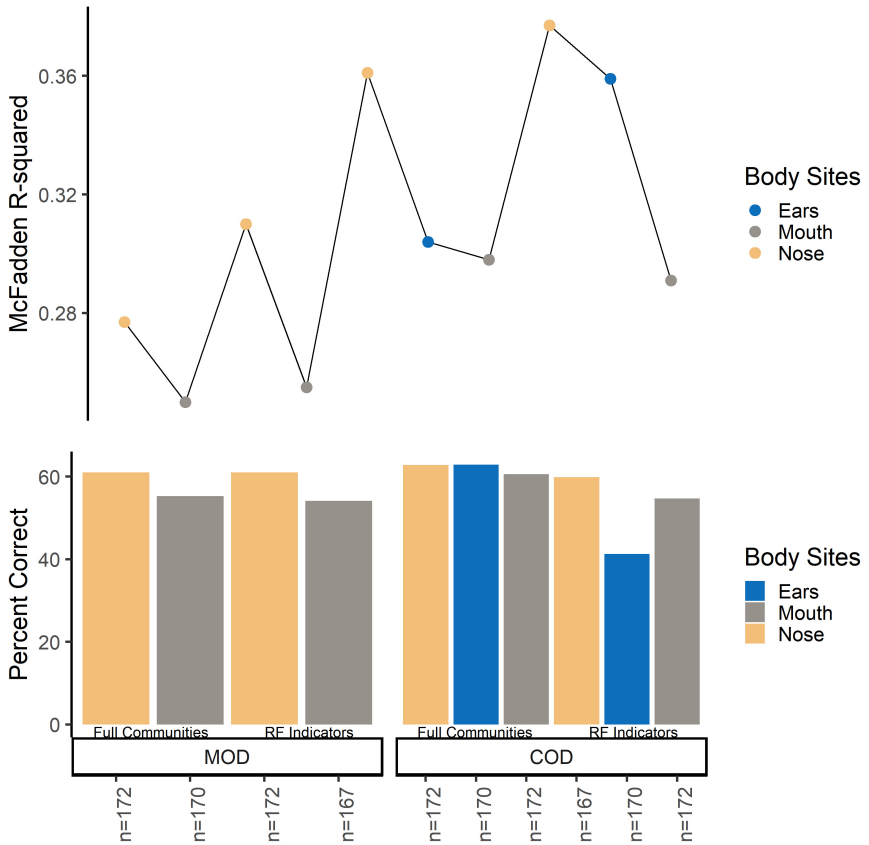

FIGURE 2 | Multinomial logistic regression model comparison among full communities and random forest indicator communities beta-dispersion for MODs/CODs. For the bottom panel, the y-axis indicates percent correct, or the number of correct classifications/total number of samples. Each bar represents a multinomial logistic model. For the top panel, the y axis indicates McFadden R^2 for the corresponding multinomial logistic regression model.

examiner's M/COD assessment ∼79% of the time, specifically for cardiovascular disease vs. drug-related deaths. Multinomial logistic regression models confirmed the medical examiner's M/COD assessment nearly 62% of the time. While better than random chance, including all M/CODs during classification (with uneven sample sizes) likely resulted in reduced classification accuracy for the multinomial logistic regression models.

Our dataset represents a cross-section of deaths from a large metropolitan area, with multiple body sites, using targeted sequencing of the 16S rRNA gene. The cases included were predominately natural cardiovascular disease deaths and accidental drug-related deaths. Therefore, direct comparison of the results of this study would be most applicable for cities with similar demographics (U.S. Census Bureau, 2020a), such as Chicago, IL (U.S. Census Bureau, 2020b) or Cincinnati, OH (U.S. Census Bureau, 2020c). While the demographic data lends classification ability in multinomial logistic regression, areas with differing demographics will require the creation of independent baseline models. It is also important to note that beta-dispersion is calculated in reference to the samples included in the dataset (Anderson et al., 2006). Therefore, future work should include data and cases from multiple geographic areas that include a range of socio-economic diversity and overall living conditions.

While we included five body site (ears, nose, mouth, eyes, and rectum) communities that showed differential success in classifying M/COD with beta-dispersion, there are more body sites of interest for the forensic community. As body site drives the microbial community composition more than any other factor (Pechal et al., 2018), comparisons to other body sites may be limited. For example, body sites sampled for the internal organs and blood (Javan et al., 2016) or skin microbiome (Kodama et al., 2019) could harbor different microbial communities than the ones included in this study, and provide different predictive power using this modeling approach. Beta-dispersion among all body sites was significantly different, but mouth, nose, and ears from this data set showed the most potential for downstream forensic applications. This is due to beta-dispersion from these body sites being significant covariates in logistic regression models, but also because these body sites are exposed to the environment and can potentially be affected by ambient conditions (Dewhirst et al., 2010). Dysbiosis of the oral cavity (nose, mouth, ears) has also been linked to systemic diseases such as cardiovascular disease (Seymour et al., 2007), and could link to the results we report here with higher beta-dispersion in cardiovascular disease and natural deaths.

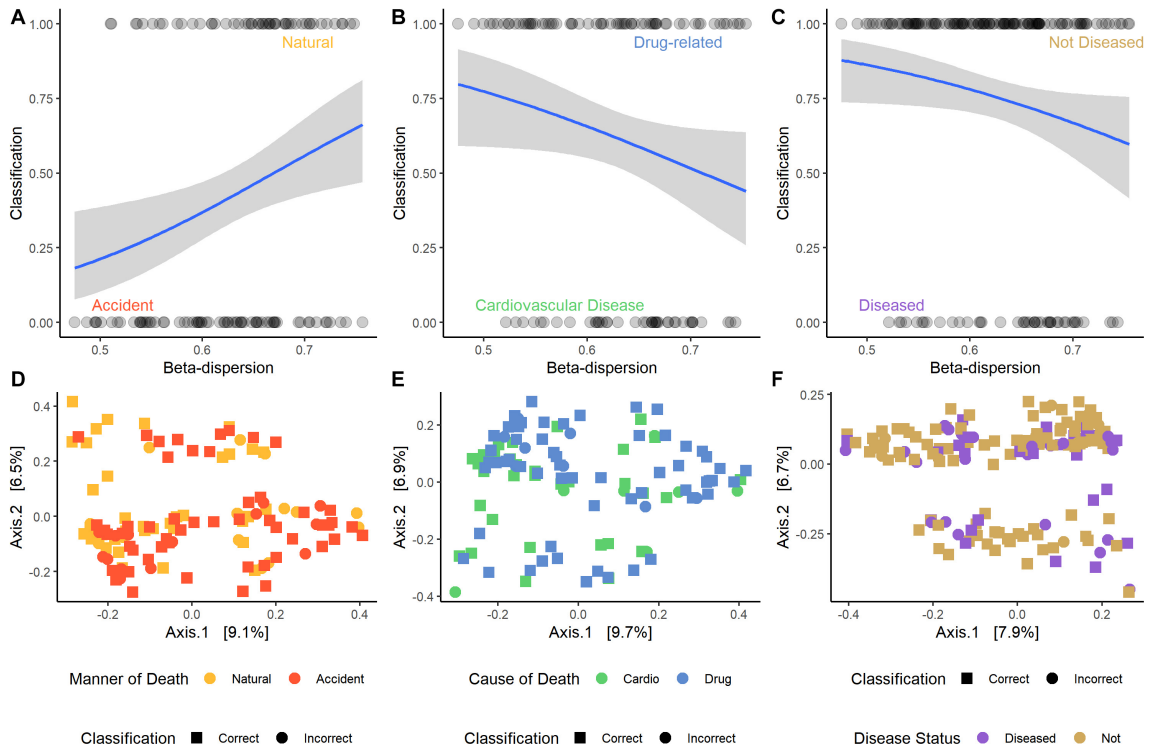

FIGURE 3 | Logistic regression models of the best performing pair-wise comparisons. Nose samples were selected, as well as beta-dispersion from full communities. **(A–C)** Logistic regression models with a 95% confidence interval of beta-dispersion on the *x*-axis and the binary classification on the *y*-axis. **(A)** Accident: 0, natural: 1. **(B)** Cardiovascular disease: 0, drug-related: 1. **(C)** Disease: 0, non-diseased: 1. **(D–F)** Principal coordinate analysis (PCoA) plots of microbial samples included in the logistic regression model. Colors correspond with the M/COD, while shape indicates if the sample was correctly classified by the model. **(D)** Natural vs. accidental deaths. **(E)** Drug-related vs. cardiovascular disease deaths. **(F)** Diseased vs. non-diseased deaths.

TABLE 2 | Summary of binary logistic regression models classifying natural vs. accident, cardiovascular vs. drug-use, and disease vs. non-diseased state.

Comparison	Beta-dispersion community profile	Significant demographic data	McFadden R^2	Degrees of freedom	χ^2	*P*	Accuracy
Natural – Accident	Full community (*n* = 120)	Race + event location + age	0.314	6	51.9	<< 0.05	0.783
	Random forest indicators (*n* = 117)	Event location + age	0.388	5	62.5	<< 0.05	0.829
Cardio – Drug	Full community (*n* = 107)	BMI + event location + PMI + age	0.399	5	56.9	<< 0.05	0.804
	Random forest indicators (*n* = 100)	BMI + age	0.356	3	47.6	<< 0.05	0.820
Disease – Non	Full community (*n* = 172)	BMI + race + event location + age	0.328	5	70.3	<< 0.05	0.779
	Random forest indicators (*n* = 163)	BMI + race + event location + age	0.364	7	73.1	<< 0.05	0.859

Significance of the model was determined by the p. For model comparisons, the McFadden R^2 and model accuracy (correct classifications/total number of samples) were considered within each body site.

This work revealed that beta-dispersion has potential to inform the M/COD decision making process during death determination. Accidental deaths, which were predominately drug related deaths in this dataset, had overall lower beta-dispersion than natural deaths, mirroring the dysbiosis found in non-forensic studies (Meckel and Kiraly, 2019). Accidental deaths and homicides were not distinguishable by beta-dispersion. While we hypothesized that high-stress lifestyle associated with homicidal deaths would increase beta-dispersion (Pearson et al., 2019), homicides had the lowest beta-dispersion among MODs. The antemortem link of high-stress lifestyle was not as strong as antemortem disease status in this study, compared to previous results that indicated higher microbial diversity associated with neighborhood blight and vacancy (Pearson et al., 2019). This may be because those decedents who were victims of homicide lived relatively healthy lifestyles and were, overall, younger when compared to decedents with a disease status. However, we do not have access to that specific information, as we were constrained to the contents of the autopsy reports.

In suicides, postmortem microbiomes of the nose, while representing the lowest sample size, had similar beta-dispersion to natural deaths, which was similar to other antemortem studies (Naseribafrouei et al., 2014; Liang et al., 2018). Microbiomes of suicidal people in living populations have higher diversity than healthy controls, specifically increased taxa associated with

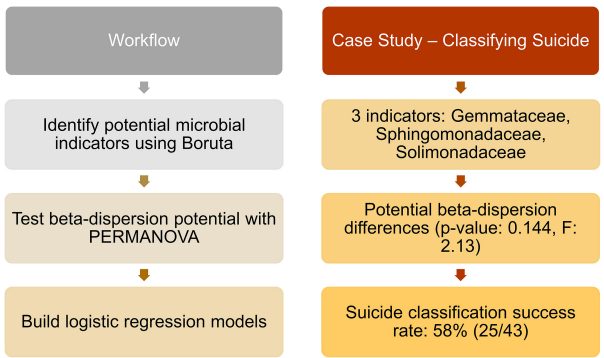

FIGURE 4 | Proposed workflow with suicide matched-design case study. **Left** column indicates potential steps researchers and practitioners can follow for future studies. **Right** column provides results from the matched-design case study, following the workflow. Twenty-three suicide cases were matched by age, sex, and race with other deaths (natural, homicide, and accidental), and nose samples were included in the analyses. Indicator taxa were identified by *Boruta*, while beta-dispersion was calculated using UniFrac distances and tested with PERMANOVA. A logistic regression model of beta-dispersion was constructed to classify suicide vs. non-suicide deaths.

inflammation (Naseribafrouei et al., 2014). Therefore, there is a potential link between high microbial beta-dispersion and mental health that would be a promising area of future research. Previous work documented the association of postmortem microbiome diversity and other metrics to heart disease (Pechal et al., 2018). In the current research, cardiovascular disease had significantly higher beta-dispersion than any other type of death. Dysbiosis in the microbiomes of people with cardiovascular disease has been documented, as there may be a microbiome link to disease pathogenesis (Wilson Tang and Hazen, 2017). Based on our results, some deaths may benefit from microbial evidence more than others. Specifically, drug-related deaths, cardiovascular disease, and suicides prompt further investigation with the postmortem microbiome. It is important to note that other MOD/CODs may not preclude the decedent from having cardiovascular disease antemortem (i.e., a homicide victim could have cardiovascular disease), which could in turn affect the microbiome. In future studies, it would be pertinent to explore the interaction between cardiovascular disease and other MODs/CODs.

We chose multinomial logistic regression as a simple model that is often used in clinical settings (de Jong et al., 2019). However, multinomial logistic regression has limitations, and biases toward classifying categories with larger sample sizes (de Jong et al., 2019); thus, future modeling approaches may provide improved predictive ability for forensic use. We achieved marginal improvement of classification in these models with random forest indicator taxa compared to models using the full microbial community data set. This result was not entirely unexpected, as random forest model error rates ranged from: 53.1–64.4% (**Supplementary Table S15**). Random forest indicators derived from random forest models with high error (>50% error rate) did not improve multinomial regression models classifying M/COD. This illustrates that beta-dispersion can be calculated in a variety of ways, which has downstream effects on distinguishing categories of interest. Therefore, an objective approach to selecting beta-dispersion calculation should be used, as outlined in this study.

Instead, binary logistic regression models were most effective at improving model success. The categories with the highest classification success also had the largest sample size (natural deaths/accidents; cardiovascular disease/drug-related deaths), and were highly correlated, as most natural deaths were cardiovascular disease (42/57) and most accidents were drug-related deaths (59/71). There was some overlap in pathology among cardiovascular disease deaths and drug-related deaths (Molina et al., 2020), showcasing how our best performing logistic regression models have potential applications in forensic death determination. While our case studies would benefit from further exploration with larger datasets, we provided strong evidence that other comparisons differentiating MOD, such as suicide vs. non-suicides, could also prove useful for forensic death determination. Additionally, future research efforts may involve novel approaches to model parameterization better informed by the specific M/COD and underlying case context and characteristics.

While not the first study to classify M/COD from microbial communities (Pechal et al., 2018; Kaszubinski et al., 2019; Zhang et al., 2019), this is the first study to compare random forest classification and logistic regression performance using beta-dispersion. MOD classification success with microbial community random forest indicators alone (Kaszubinski et al., 2019) were comparable to multinomial logistic regression models built with only beta-dispersion (∼40%). Inclusion of case demographic data improved multinomial logistic regression model, which was consistent with previous random forest regression model accuracy of ears and nose body site communities (>60%) (Zhang et al., 2019). A strength of the MLR approach, is that it does not depend on specific indicator postmortem microbial taxa, which can vary across studies (Pechal et al., 2018; Kaszubinski et al., 2019). Furthermore, we suggest that microbial community information, either taxon dependent (e.g., indicator taxa) or not (e.g., beta-dispersion), could be an additional piece of evidence in M/COD determination. We wanted to identify if demographic data were indicative of certain M/CODs (e.g., age significantly higher in natural deaths or for cardiovascular disease) and were useful to supplement beta-dispersion in downstream modeling. We chose a slightly less conservative p-value so that potentially important demographic data were not prematurely removed. By including demographic data into our models, successful classification was improved rather than using microbial data alone, which is something to consider in future death investigation.

CONCLUSION

Microbial community metrics, such as beta-dispersion, have potential forensic use in contributing to classification of M/COD during death investigation. This reflection is due to the

antemortem link to the postmortem microbiome. We showed beta-dispersion increased based on disease status (cardiovascular disease) according to AKP, and beta-dispersion reflected M/COD, especially for cardiovascular disease and drug related deaths. While random forest is a useful tool for these types of datasets, MLR with beta-dispersion produced comparable results without reliance on specific microbial indicator taxa. Furthermore, we demonstrated circumstances where beta-dispersion could be used to distinguish MOD using two case studies; however, low and uneven sample size was an issue for all case studies. Despite the reduced power of these case studies, this workflow may be useful for other forensic practitioners to test within their own sample set, that encompass new locations and demographic data, to strengthen the antemortem link to the postmortem microbiome. As sample sizes increase for postmortem microbial studies, it may be necessary for large databases, or geographically and demographically specific data to train models with high success rates for practical use in forensic contexts. The methods outlined in this study serve as a guide to developing non-taxonomic indicator microbiome tools for other researchers and medical examiners in different geographic locations and investigation contexts. Ultimately, modeling beta-dispersion with case demographic data is a potential tool that could be useful for medical examiners during death investigation to combine with other methods of M/COD determination. The future of using postmortem microbiomes in forensic sciences continues to show promise.

DATA AVAILABILITY STATEMENT

Sequence data were archived through the European Bioinformatics Institute European Nucleotide Archive (www.ebi.ac.uk/ena) under accession number: PRJEB22642. The microbial community analyses are available as R code on GitHub (https://github.com/sierrakasz/AKP-betadisp-paper).

AUTHOR CONTRIBUTIONS

SK performed the data analysis and wrote the manuscript. JP, CS, HJ, and MB acquired the data. JP and KS helped design the case studies. JP, MM, and MB critically revised intellectual content. SK, JP, KS, CS, HJ, MM, and MB edited the manuscript and approved the final version. All authors contributed to the article and approved the submitted version.

FUNDING

This research was funded by a grant from the National Institute of Justice, Office of Justice Programs, U.S. Department of Justice awarded (2014-DN-BX-K008) to JP, CS, HJ, and MB. SK was funded by the Department of Defense SMART Scholarship program. Points of view in this document are those of the authors and do not necessarily represent the official position or policies of the U.S. Department of Justice or Department of Defense.

ACKNOWLEDGMENTS

The authors thank M. M. Brewer and C. R. Weatherbee for help with sample processing and S. E. Evans for comments on the final manuscript.

SUPPLEMENTARY MATERIAL

The Supplementary Material for this article can be found online at: https://www.frontiersin.org/articles/10.3389/fmicb.2020.555347/full#supplementary-material

REFERENCES

Anderson, M. J. (2017). *Permutational Multivariate Analysis of Variance (PERMANOVA)*. Chichester: John Wiley & Sons, Ltd, 1–15. doi: 10.1002/9781118445112.stat07841

Anderson, M. J., Ellingsen, K. E., and McArdle, B. H. (2006). Multivariate dispersion as a measure of beta diversity. *Ecol. Lett.* 9, 683–693. doi: 10.1111/j.1461-0248.2006.00926.x

Barbian, H. J., Li, Y., Ramirez, M., Klase, Z., Lipende, I., Mjungu, D., et al. (2015). Destabilization of the gut microbiome marks the end-stage of simian immunodeficiency virus infection in wild chimpanzees. *Am. J. Primatol.* 80, 1–29. doi: 10.1002/ajp.22515

Bates, D., Maechler, M., Bolker, B., Walker, S., Christensen, R. H. B., Singmann, H., et al. (2019). Fitting linear mixed-effects models using lme4. *J. Stat. Softw.* 67, 1–48. doi: 10.18637/jss.v067.i01 (accessed December 17, 2019).

Belk, A., Xu, Z. Z., Carter, D. O., Lynne, A., Bucheli, S., Knight, R., et al. (2018). Microbiome data accurately predicts the postmortem interval using random forest regression models. *Genes* 9:104. doi: 10.3390/genes9020104.

Böhning, D. (1992). Multinomial logistic regression algorithm. *Ann. Inst. Stat. Math.* 44, 197–200. doi: 10.1007/BF00048682

Bolyen, E., Rideout, J. R., Dillon, M. R., Bokulich, N. A., Abnet, C. C., Al-Ghalith, G. A., et al. (2019). Reproducible, interactive, scalable and extensible microbiome data science using QIIME 2. *Nat. Biotechnol.* 37, 852–857. doi: 10.1038/s41587-019-0209-9

Bozdogan, H. (1987). Model selection and Akaike's Information Criterion (AIC): The general theory and its analytical extensions. *Psychometrika* 52, 345–370. doi: 10.1007/BF02294361

Breiman, L., Cutler, A., Liaw, A., and Wiener, M. (2018). *Package "randomForest."*. Available online at: https://www.stat.berkeley.edu/$\sim$breiman/RandomForests/

Callahan, B. J., McMurdie, P. J., Rosen, M. J., Han, A. W., Johnson, A. J. A., and Holmes, S. P. (2016). DADA2: High-resolution sample inference from Illumina amplicon data. *Nat. Methods* 13, 581–583. doi: 10.1038/nmeth.3869

Croissant, Y. (2019). *Package "mlogit."*. Available from: https://r-forge.r-project.org/projects/mlogit/

de Jong, V. M. T., Eijkemans, M. J. C., van Calster, B., Timmerman, D., Moons, K. G. M., Steyerberg, E. W., et al. (2019). Sample size considerations and predictive performance of multinomial logistic prediction models. *Stat. Med.* 38, 1601–1619. doi: 10.1002/sim.8063

Dewhirst, F. E., Chen, T., Izard, J., Paster, B. J., Tanner, A. C. R., Yu, W. H., et al. (2010). The human oral microbiome. *J. Bacteriol.* 192, 5002–5017. doi: 10.1128/JB.00542-10

Faul, F., Erdfelder, E., Lang, A. G., and Buchner, A. (2007). "G*Power 3: A flexible statistical power analysis program for the social, behavioral, and

biomedical sciences," in *Behavior Research Methods*, Ed. M. Brysbaert (Madison: Psychonomic Society Inc), 175–191. doi: 10.3758/BF03193146

Harrell, F., Lee, K., and Mark, D. (1996). Multivariable prognostic models: issues in developing models, evaluating assumptions and adequacy, and measuring and reducing errors. *Stat. Med.* 15, 361–387. doi: 10.1002/(SICI)1097-0258(19960229)15:4<361::AID-SIM168>3.0.CO;2-4

Javan, G. T., Finley, S. J., Can, I., Wilkinson, J. E., Hanson, J. D., and Tarone, A. M. (2016). Human thanatomicrobiome succession and time since death. *Sci. Rep.* 6:29598. doi: 10.1038/srep29598

Javan, G. T., Finley, S. J., Smith, T., Miller, J., and Wilkinson, J. E. (2017). Cadaver thanatomicrobiome signatures: the ubiquitous nature of Clostridium species in human decomposition. *Front. Microbiol.* 8:2096. doi: 10.3389/fmicb.2017.02096

Kaszubinski, S. F., Pechal, J. L., Schmidt, C. J., Heather, J. R., Benbow, M. E., and Meek, M. H. (2019). Evaluating bioinformatic pipeline performance for forensic microbiome analysis. *J. Forensic Sci.* 65, 513–525. doi: 10.1111/1556-4029.14213

Katoh, K., and Standley, D. M. (2013). MAFFT multiple sequence alignment software version 7: Improvements in performance and usability. *Mol. Biol. Evol.* 30, 772–780. doi: 10.1093/molbev/mst010

Kodama, W. A., Xu, Z., Metcalf, J. L., Song, S. J., Harrison, N., Knight, R., et al. (2019). Trace Evidence Potential in Postmortem Skin Microbiomes: From Death Scene to Morgue. *J. Forensic Sci.* 64, 791–798. doi: 10.1111/1556-4029.13949

Kursa, M. B., and Rudnicki, W. R. (2018). *Package "Boruta"*. Available from: https://notabug.org/mbq/Boruta/

Liang, S., Wu, X., Hu, X., Wang, T., and Jin, F. (2018). Recognizing depression from the microbiota–gut–brain axis. *Int. J. Mol. Sci.* 19:1592. doi: 10.3390/ijms19061592

McFadden, D. (1979). "Chapter 15: quantitative methods for analyzing travel behaviour on individuals: some recent developments," in *Behavioural Travel Modelling*, eds D. Hensher, P. Stopher, and C. Helm (London: Croom Helm).

McMurdie, P. J., and Holmes, S. (2013). Phyloseq: an R package for reproducible interactive analysis and graphics of microbiome census data. *PLoS One* 8:e61217. doi: 10.1371/journal.pone.0061217

McMurdie, P. J., and Holmes, S. (2014). Waste not, want not: why rarefying microbiome data is inadmissible. *PLoS Comput. Biol.* 10:e3531. doi: 10.1371/journal.pcbi.1003531

Meckel, K. R., and Kiraly, D. D. (2019). A potential role for the gut microbiome in substance use disorders. *Psychopharmacology* 236, 1513–1530. doi: 10.1007/s00213-019-05232-0

Metcalf, J. L., Parfrey, L. W., Gonzalez, A., Lauber, C. L., Knights, D., Ackermann, G., et al. (2013). A microbial clock provides an accurate estimate of the postmortem interval in a mouse model system. *eLife* 2013, 1–19. doi: 10.7554/eLife.01104

Metcalf, J. L., Xu, Z. Z., Weiss, S., Lax, S., Treuren, W., Van Hyde, E. R., et al. (2016). Microbial community assembly and metabolic function during mammalian corpse decomposition. *Science* 351, 158–162. doi: 10.1126/science.aad2646

Molina, D. K., Vance, K., Coleman, M. L., and Hargrove, V. M. (2020). Testing an age-old adage: can autopsy findings be of assistance in differentiating opioid versus cardiac deaths? *J. Forensic Sci.* 65, 112–116. doi: 10.1111/1556-4029.14174

Naseribafrouei, A., Hestad, K., Avershina, E., Sekelja, M., Linløkken, A., Wilson, R., et al. (2014). Correlation between the human fecal microbiota and depression. *Neurogastroenterol. Motil.* 26, 1155–1162. doi: 10.1111/nmo.12378

Oksanen, J., Blanchet, F. G., Friendly, M., Kindt, R., Legendre, P., Mcglinn, D., et al. (2019). *vegan: Community Ecology Package. R Package Version 2.5-5*. Available online at: https://CRAN.R-project.org/package=vegan (accessed October 23, 2019).

Pearson, A. L., Rzotkiewicz, A., Pechal, J. L., Schmidt, C. J., Jordan, H. R., Zwickle, A., et al. (2019). Initial Evidence of the Relationships between the Human Postmortem Microbiome and Neighborhood Blight and Greening Efforts. *Ann. Am. Assoc. Geogr.* 109, 958–978. doi: 10.1080/24694452.2018.1519407

Pechal, J. L., Crippen, T. L., Benbow, M. E., Tarone, A. M., Dowd, S., and Tomberlin, J. K. (2014). The potential use of bacterial community succession in forensics as described by high throughput metagenomic sequencing. *Int. J. Legal. Med.* 128, 193–205. doi: 10.1007/s00414-013-0872-1

Pechal, J. L., Schmidt, C. J., Jordan, H. R., and Benbow, M. E. (2018). A large-scale survey of the postmortem human microbiome, and its potential to provide insight into the living health condition. *Sci. Rep.* 8, 1–15. doi: 10.1038/s41598-018-23989-w

Pohlert, T. (2018). *The Pairwise Multiple Comparison of Mean Ranks Package (PMCMR). R package* Available online at: https://CRAN.R-project.org/package=PMCMR (accessed October 23, 2019).

Poos, M. S., and Jackson, D. A. (2012). Addressing the removal of rare species in multivariate bioassessments: The impact of methodological choices. *Ecol. Indic.* 18, 82–90. doi: 10.1016/j.ecolind.2011.10.008

Price, M. N., Dehal, P. S., and Arkin, A. P. (2010). FastTree 2–approximately maximum-likelihood trees for large alignments. *PLoS One* 5:e9490. doi: 10.1371/journal.pone.0009490

R Core Team (2018). *R: A Language and Environment for Statistical Computing*. Vienna: R Core Team.

Randy, H., Hunsaker, I. I. I. J. C., and Davis, G. J. (2002). *A Guide For Manner Of Death Classification*. Alanta: National Association of Medical Examiners

Seymour, G., Ford, P., Cullinan, M., Leishman, S., and Yamazaki, K. (2007). Relationship between periodontal infections and systemic disease. *Clin. Microbiol. Infect.* 4, 3–10. doi: 10.1111/j.1469-0691.2007.01798.x

Shade, A., and Handelsman, J. (2012). Beyond the Venn diagram: the hunt for a core microbiome. *Environ. Microbiol.* 14, 4–12. doi: 10.1111/j.1462-2920.2011.02585.x

Steyerberg, E. W., Eijkermans, M. J. C., Harrell, F. E. Jr., and Habbema, J. D. F. (2001). Prognostic Modeling with Logistic Regression Analysis: In Search of a Sensible Strategy in Small Data Sets. *Med. Decis. Making* 21, 45–56. doi: 10.1177/0272989X0102100106

Turnbaugh, P. J., Ley, R. E., Hamady, M., Fraser-Liggett, C. M., Knight, R., and Gordon, J. I. (2007). The Human Microbiome Project. *Nature* 449, 804–810. doi: 10.1038/nature06244

U.S. Census Bureau (2020a). *QuickFacts: Detroit city, Michigan*. Suitland, MD: U.S. Census Bureau.

U.S. Census Bureau (2020b). *QuickFacts: Chicago city, Illinois*. Suitland, MD: U.S. Census Bureau.

U.S. Census Bureau (2020c). *QuickFacts: Cincinnati city, Ohio*. Suitland, MD: U.S. Census Bureau.

Weiss, S., Xu, Z. Z., Peddada, S., Amir, A., Bittinger, K., Gonzalez, A., et al. (2017). Normalization and microbial differential abundance strategies depend upon data characteristics. *Microbiome* 5, 1–18. doi: 10.1186/s40168-017-0237-y

Wilson Tang, W. H., and Hazen, S. L. (2017). The Gut Microbiome and Its Role in Cardiovascular Diseases. *Circulation* 135, 1008–1010. doi: 10.1161/CIRCULATIONAHA.116.024251

Zaneveld, J. R., McMinds, R., and Thurber, R. V. (2017). Stress and stability: applying the Anna Karenina principle to animal microbiomes. *Nat. Microbiol.* 2, 1–8. doi: 10.1038/nmicrobiol.2017.121

Zhang, Y., Pechal, J. L., Schmidt, C. J., Jordan, H. R., Wang, W. W., Eric Benbow, M., et al. (2019). Machine learning performance in a microbial molecular autopsy context: a cross-sectional postmortem human population study. *PLoS One* 14:e0213829. doi: 10.1371/journal.pone.0213829

Conflict of Interest: The authors declare that the research was conducted in the absence of any commercial or financial relationships that could be construed as a potential conflict of interest.

frontiers in Microbiology

ORIGINAL RESEARCH
published: 08 December 2020
doi: 10.3389/fmicb.2020.569630

Effects of Extended Postmortem Interval on Microbial Communities in Organs of the Human Cadaver

Holly Lutz[1,2], Alexandria Vangelatos[3], Neil Gottel[1,2], Antonio Osculati[4], Silvia Visona[4], Sheree J. Finley[5], Jack A. Gilbert[1,2] and Gulnaz T. Javan[5]**

[1] Department of Pediatrics, University of California, San Diego, La Jolla, CA, United States, [2] Scripps Institution of Oceanography, University of California, San Diego, La Jolla, CA, United States, [3] Biological Sciences Division, University of Chicago, Chicago, IL, United States, [4] Department of Public Health, Experimental and Forensic Medicine, University of Pavia, Pavia, Italy, [5] Physical Sciences Department, Forensic Science Programs, Alabama State University, Montgomery, AL, United States

Human thanatomicrobiota studies have shown that microorganisms inhabit and proliferate externally and internally throughout the body and are the primary mediators of putrefaction after death. Yet little is known about the source and diversity of the thanatomicrobiome or the underlying factors leading to delayed decomposition exhibited by reproductive organs. The use of the V4 hypervariable region of bacterial 16S rRNA gene sequences for taxonomic classification ("barcoding") and phylogenetic analyses of human postmortem microbiota has recently emerged as a possible tool in forensic microbiology. The goal of this study was to apply a 16S rRNA barcoding approach to investigate variation among different organs, as well as the extent to which microbial associations among different body organs in human cadavers can be used to predict forensically important determinations, such as cause and time of death. We assessed microbiota of organ tissues including brain, heart, liver, spleen, prostate, and uterus collected at autopsy from criminal casework of 40 Italian cadavers with times of death ranging from 24 to 432 h. Both the uterus and prostate had a significantly higher alpha diversity compared to other anatomical sites, and exhibited a significantly different microbial community composition from non-reproductive organs, which we found to be dominated by the bacterial orders MLE1-12, Saprospirales, and Burkholderiales. In contrast, reproductive organs were dominated by Clostridiales, Lactobacillales, and showed a marked decrease in relative abundance of MLE1-12. These results provide insight into the observation that the uterus and prostate are the last internal organs to decay during human decomposition. We conclude that distinct community profiles of reproductive versus non-reproductive organs may help guide the application of forensic microbiology tools to investigations of human cadavers.

Keywords: thanatomicrobiome, cadaver, 16S rRNA, internal organs, manner of death

OPEN ACCESS

Edited by:
George Tsiamis, University of Patras, Greece

Reviewed by:
Heather Rose Jordan, Mississippi State University, United States
Jonathan J. Parrott, Arizona State University West campus, United States

****Correspondence:***
Gulnaz T. Javan
gjavan@alasu.edu
Holly Lutz
hllutz@health.ucsd.edu;
hlutz@fieldmuseum.org

Specialty section:
This article was submitted to Systems Microbiology, a section of the journal Frontiers in Microbiology

Received: *04 June 2020*
Accepted: *16 November 2020*
Published: *08 December 2020*

Citation:
Lutz H, Vangelatos A, Gottel N, Osculati A, Visona S, Finley SJ, Gilbert JA and Javan GT (2020) Effects of Extended Postmortem Interval on Microbial Communities in Organs of the Human Cadaver. Front. Microbiol. 11:569630. doi: 10.3389/fmicb.2020.569630

INTRODUCTION

During life, the human microbiome serves important health-related functions including nutrient acquisition, pathogen defense, energy salvage, and immune defense training (Gilbert et al., 2016). The microbiome has also been linked to cardiovascular, metabolic, and immune diseases, as well as mental health disorders via the gut-brain-axis (GBA; Gilbert et al., 2018). The microbiota GBA is

a complex, bidirectional circuit that links the neural, endocrine, and immunological systems with the microbial communities in the gut (Grenham et al., 2011; Cryan and Dinan, 2012; Meckel and Kiraly, 2019). After death, microbial communities present within and on the body are exposed to radical environmental changes, and recent studies have shown that microbial succession among mammalian cadavers follows a metabolically predictable progression (Metcalf et al., 2016; Javan et al., 2019).

Forensic microbiology is an emerging field of study in which microorganisms serve as forensic tools to potentially address unanswered forensic questions such as cause and time of death. The detection of pathogenic microbes has evidential value in medicolegal evaluations pertaining to etiological determinations of pathological death. However, the connection between postmortem microbial communities and violent death (homicide, suicide, and overdoses) is still in its infancy. Postmortem microbial communities' succession related to human remains has been proven to be predictable and applicable for forensic science and criminal investigations (Damann et al., 2015; DeBruyn and Hauther, 2017; Pechal et al., 2018). By determining the intricate relationships between microbial abundances in specific organs, thanatomicrobiome (microbiome of death) studies have the potential to resolve knowledge gaps in a death investigation that could match specific taxa to a point on a "microbial clock" in a regression model (Metcalf, 2019). Advances in DNA sequencing technologies paired with increased understanding of the human postmortem microbiome have hinted at the possibility that the cadre of microbes could be used as a predominant drivers of decay (Metcalf et al., 2016; Buresova et al., 2019) and as trace evidence to link distinct people to objects with which they have previously interacted (Fierer et al., 2010; Lax et al., 2015; Park et al., 2017; Schmedes et al., 2017; Kodama et al., 2019). Recent studies have also shown that the microbiome may be used to estimate the amount of time that has elapsed since death, referred to as the postmortem interval (PMI), allowing investigators to establish a potential timeline of death (Maujean et al., 2013; Pechal et al., 2014; Cobaugh et al., 2015; Hauther et al., 2015; Burcham et al., 2016; Javan et al., 2016; Metcalf et al., 2016; Javan et al., 2017).

The microbial composition and abundance associated with internal organ tissues are dependent on temperature, and PMI, since bacteria have different growth optima based on the physicochemical constraints of their environment (Deutscher, 2008; Ercolini et al., 2009; Rakoff-Nahoum et al., 2016). Also, microbial abundances associated with the body antemortem may play a role in decay, as a cadaver of an aged adult human, with approximately 40 trillion microbial cells, decays more rapidly than a deceased fetus or newborn (Campobasso et al., 2001), which usually has reduced microbial colonization density (Dunn et al., 2017). Of course, as suggested by Campobasso et al. (2001), these trends are contingent upon the medications and disease state of the individual prior to death. In Italy, as with other localities in the world, the determination of the cause of death is essential for legal documentation and public health in regard to epidemiological surveillance. For example, in the United States, the causes of death are classified as accident, homicide, natural, suicide, and undetermined. In contrast to United States death certificates, Italian death certificates do not offer an undetermined cause of death. Death investigation systems serve as conduits for epidemiological data collection and as an important sentinel system in the event of mass pandemics of fatal diseases as in the recent cases of novel coronavirus (severe acute respiratory syndrome coronavirus-2, SARS-CoV-2, or COVID-19).

The cause of death is used to clarify the circumstances surrounding how a person died or how an injury was sustained. Here we focus on Italian cadavers due to their extended PMIs (up to 24–432 h) compared to those of other geographic locations (e.g., the United States). There was an even spread of PMIs: 22 cases with PMIs less than 72 h and 18 with PMIs 72–432 h. The Italian Regolamento di Polizia Mortuaria, Law number 285, Article 8 of 1990 prohibits an autopsy prior to 24 h of discovering a dead body (Frati et al., 2006). In the current study, we hypothesized that microbial taxa composition in postmortem internal organ tissues are dependent on temporal (PMI) and forensic (cause of death) influences. To test this hypothesis, the V4 hypervariable region of the 16S rRNA gene was probed to investigate the extent to which microbial associations among different body organs in human cadavers can be used to predict the cause of death and/or PMI. By sampling different anatomical body sites of human cadavers with various causes of death (accident, natural, suicide, and homicide), we were able to ascertain that cause of death has a significant influence on microbial community composition of postmortem tissues, and that despite these differences, commonalities may still be identified among tissues.

MATERIALS AND METHODS

Collection of Autopsy Specimens

Sequencing of amplicons of the 16S rRNA V4 hypervariable region was performed using microbial DNA from postmortem organ tissue from 40 Italian cadavers including brain, heart, liver, spleen, prostate, and uterus collected at autopsy from criminal casework cadavers. All cadaver samples were collected before the COVID-19 outbreak in Wuhan, China; therefore, COVID-19 specimens were not a part of this study. Careful precautions were taken to reduce contamination and maintain hygienic laboratory conditions. Bodies were kept in the morgue at 1°C at the Department of Public Health, Experimental and Forensic Medicine at the University of Pavia in Pavia, Italy (**Supplementary Table 1**). The study included 14 females and 26 male cadavers, and the youngest case was in the range 15–20 and the oldest 85–90. All PMIs were confirmed by official Daily Crime Logs with the shortest PMI was 24 h and the longest was 18 days. Cadavers were categorized into four groups according to cause of death: accidental, homicide, natural, and suicide. Autopsies were performed in the morgue with ambient temperatures between 8 and 10°C. Postmortem samples were uniformly excised from an identical section of each tissue of the brain, heart, liver, spleen, prostate, and uterus of each cadaver. For example, cardiac tissue was homogeneously removed from the left ventricle area of the

hearts. During autopsies, tissues that were extracted from internal organs were placed into labeled sterile polyethylene bags. After collection, samples were transported on dry ice to the Thanatos Laboratory, a core facility on the campus of Alabama State University in Montgomery, AL, United States, and stored at −80°C until further analysis. Using sterile, disposable surgical scalpels, a representative sample of 40–50 mg of tissue was aliquoted from each organ for microbial analyses. Tissues were collected using protocols approved by Alabama State University's Institutional Review Board (2018400) in accordance with Italian laws regarding personal data treatment. The reference Italian law is the authorization n9/2016 of the guarantor of privacy. This authorization was then replaced by Regulation (EU) 2016/679 of the European Parliament and of the Council. The specimens were anonymized before transferring to the Thanatos Lab at Alabama State University. In cases of deceased subjects, consent is not required, as the samples were taken for clinical/forensic purposes and because it is not possible to contact the next of kin in anonymized circumstances.

DNA Extraction and Sequencing

DNA was extracted from internal organs using conventional chemical and physical disruption protocols (Urakawa et al., 2010) using the phenol chloroform method, which is specifically optimized for recovery of microbial DNA from low-yield, highly decayed postmortem samples (Can et al., 2014). We used the standard 515F and 806R primers (Caporaso et al., 2011, 2012; Kozich et al., 2013) to amplify the V4 region of the 16S rRNA gene, using mitochondrial blockers to reduce amplification of host mitochondrial DNA (*sensu* Lutz et al., 2019). Sequencing was performed using paired-end 150 base reads on an Illumina HiSeq sequencing platform. Following standard demultiplexing and quality filtering using the Quantitative Insights Into Microbial Ecology pipeline (QIIME2; Caporaso et al., 2010) and vsearch8.1 (Rognes et al., 2016). Chimeric sequences were removed and absolute sequence variants (ASVs) were identified using Deblur (Amir et al., 2017), and taxonomy was assigned using the Greengenes Database (May 2013 release).[1]

Analysis of 16S rRNA Sequencing Data

Following quality filtering and taxonomy assignment, libraries were rarefied to an even read depth of 1000 reads per library; these libraries were used for all subsequent analyses. Alpha diversity was calculated using the Shannon index and measured species richness based on actual observed ASV diversity. Significance of differing mean values for each diversity calculation was determined using the Kruskal–Wallis rank sum test, followed by a *post hoc* Dunn test with Benjamini–Hochberg corrected *p*-values. Two measures of beta diversity (unweighted UniFrac and weighted UniFrac) were calculated using relative abundances of each ASV (calculated as ASV read depth divided by total library read depth). The adonis2 function was used in the R package Vegan v2.4.2 (Oksanen et al., 2018) for PERMAONVA analysis of marginal effects for organ type, sex, age, cause of death, PMI, BMI, with Bonferroni correction for multiple comparisons. In the case of marginal effects of organ type, non-independence of samples was accounted for from the same cadavers by using the strata function available in ADONIS, whereby strata = "case number" was set. Analysis of composition of microbiome (ANCOM) was performed to assess significance of differential abundance based on log2fold change measures between organs and between different causes of death (Mandal et al., 2015). To examine relationships between PMI and the four most abundant bacterial orders, one-way analysis of variance (ANOVA) was performed on independent linear regression models for each bacterial order and human organ. While alpha diversity of each bacterial order (as with alpha diversity of all bacterial taxa) examined exhibited a normal distribution across PMI values [ANOVA, $Pr(>F) > 0.05$], we did identify a significant interaction between organs and PMI [two-way ANOVA, $Pr(>F) = 0.05$]. Additional R packages used for analyses and figure generation included vegan (Oksanen et al., 2018), ggplot2 (Wickham, 2009), and dplyr (Wickham et al., 2018). For a complete list of packages and codes for microbiome analyses.[2] All 16S rRNA sequence and sample metadata are publicly available via the QIITA platform[3] under study identifier (ID) 13450 and the European Bioinformatics Institute (EBI) under accession number ERP125301.

RESULTS

Sampling and Library Quality

Sampling spanned PMIs of 24–432 h [avg (SD) = 111 (± 93) h] and included tissues from cadavers corresponding to different causes of death grouped into four categories according to each internal organ: accidental (n = 51), natural (n = 63), homicide (n = 13), and suicide (n = 31) (**Table 1**). Following sequence deblurring, quality filtering, and rarefaction a total of 853,850 16S

[1]http://greengenes.lbl.gov

[2]http://github.com/hollylutz/CadaverMP

[3]http://qiita.ucsd.edu

TABLE 1 | Samples of human cadavers by organ, and cause of death.

	Cause of Death (*n*)				
Organ	**Natural**	**Accident**	**Homicide**	**Suicide**	**Total (*n*)**
Female brain	7	7	2	6	22
Male brain	8	3	1	1	13
Female heart	4	6	2	6	18
Male heart	5	4	1	1	11
Female liver	7	8	2	6	23
Male liver	7	4	1	1	13
Female spleen	6	3	1	4	14
Male spleen	6	3	1	0	10
Prostate	5	10	1	5	21
Uterus	8	3	1	1	13
Total	63	51	13	31	158

n, number of libraries post-filtering.

rRNA V4 amplicon sequences comprising 771 ASV reads were generated from 158 sample libraries.

Alpha and Beta Diversity

Alpha diversity varied significantly ($p < 0.05$; Kruskal–Wallis rank sum test with Bonferroni correction) between reproductive organs (prostate and uterus) and non-reproductive organs (brain, heart, and liver, with the exception of spleen) (**Figure 1**). The two reproductive organs exhibited both higher observed ASV richness values by organ (**Figure 1A**) and Shannon index of microbial richness and evenness values by organ than non-reproductive organs (**Figure 1B**).

PERMANOVA analysis of factors contributing to variation among weighted UniFrac beta diversity metrics included organ, sex, PMI, and body mass index (BMI), while factors contributing to variation among unweighted UniFrac beta diversity metrics included organ, age, and cause of death (**Table 2**). Organ type was the strongest factor contributing to both weighted and unweighted UniFrac beta diversity

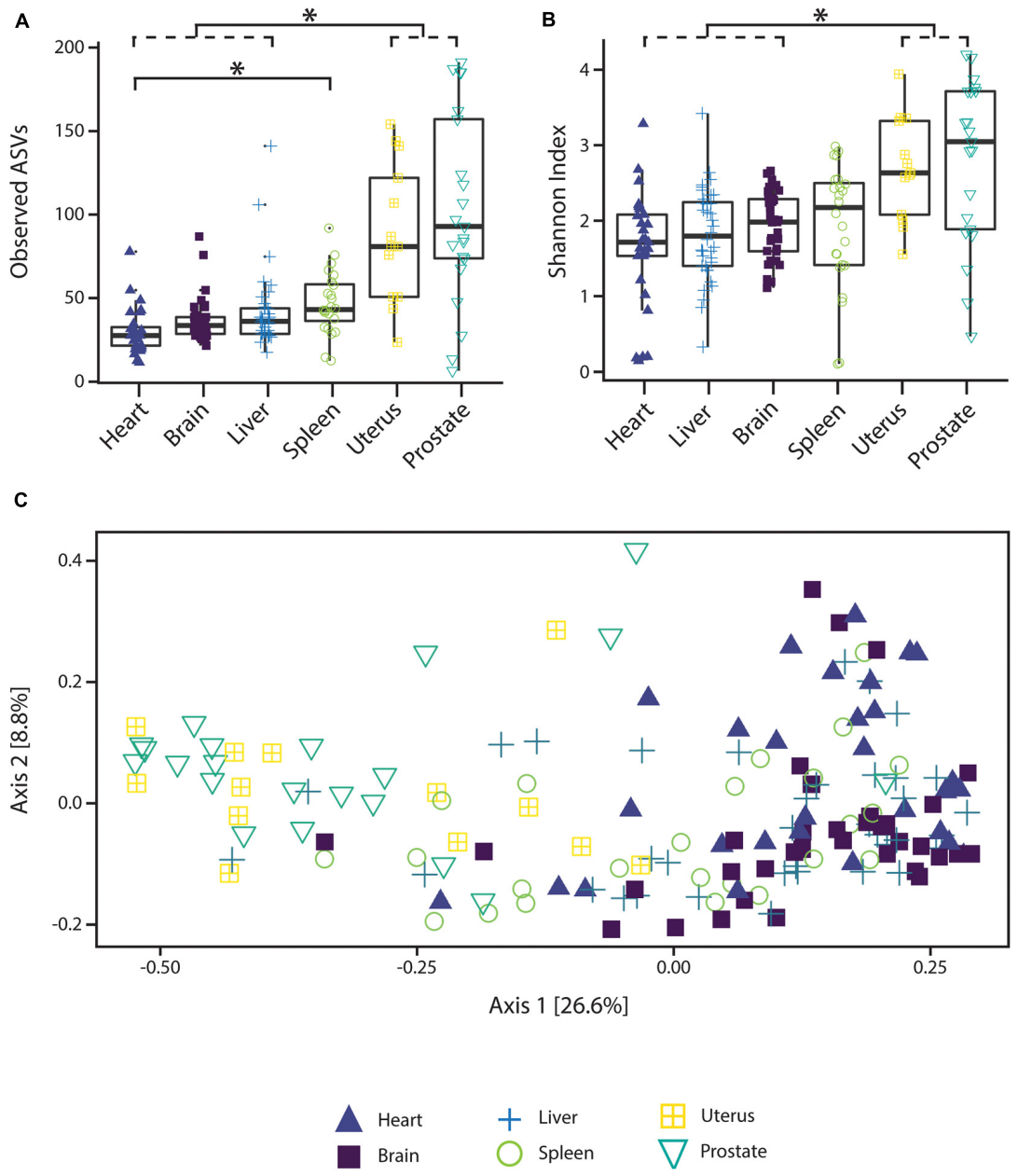

FIGURE 1 | Alpha and beta diversity measures of microbial communities by organ. **(A)** Observed ASV richness by organ, **(B)** Shannon index of microbial richness and evenness by organ. Asterisk indicates $p < 0.05$ Kruskal–Wallis rank sum test with Bonferroni correction. **(C)** PCoA based on unweighted UniFrac measures of microbial dissimilarity by organ.

TABLE 2 | PERMANOVA analysis assessing marginal effects of variables on weighted and unweighted UniFrac beta diversity.

	Df	SumOfSqs	R^2	F	p-value
Weighted UniFrac					
Organ	5	1.03	0.12	4.50	0.001*
Sex	1	0.44	0.05	10.05	0.006*
Age	–	0.09	0.01	2.16	0.270
Cause of death	3	0.24	0.03	1.81	0.186
PMI	–	0.29	0.03	6.61	0.006*
BMI	–	0.19	0.02	4.39	0.018*
Unweighted UniFrac					
Organ	5	5.03	0.16	6.00	0.001*
Sex	1	0.31	0.01	2.21	0.102
Age	–	0.39	0.01	2.81	0.042*
Cause of death	3	0.85	0.03	2.02	0.018*
PMI	–	0.41	0.01	2.92	0.048
BMI	–	0.30	0.01	2.17	0.180

*Indicate Bonferroni adjusted p-value < 0.05.

(R^2 = 0.12 and R^2 = 0.16, respectively) was identified by multidimensional scaling, specifically, principle coordinate analysis (PCoA) analysis (**Figure 1C**). Although significant, other factors including age, sex, PMI, BMI, and cause of death each explained 1–5% of beta diversity. Differing PERMANOVA results between weighted and unweighted UniFrac for cause of death suggest that specific bacteria may be associated with the cause of death, but that these differences are negligible when taking into account the relative abundance of bacterial taxa; weighted UniFrac measures suggest that although taxonomic composition may not vary significantly between different causes of death the relative abundance of specific taxa vary significantly.

Bacterial Community Composition and Differential Abundance Between Organs and Cause of Death

In general, non-reproductive organs were dominated by the bacterial orders MLE1-12 (*Candidatus* Melainabacteria), Saprospirales, and Burkholderiales, while reproductive organs were dominated by Clostridiales, Lactobacillalaes, and showed a marked decrease in relative abundance of MLE1-12 (**Figure 2**). Analysis of composition of microbiomes between organs confirmed significant differences in relative abundance (measured as the log2fold change in 16S rRNA ASV relative abundance) of multiple bacterial taxa (**Figure 3**). Specifically, reproductive organs showed significant reduction in a single ASV belonging to the family MLE1-12 and ASVs belonging to the family Chitinophagaceae, including one ASV belonging to the genus *Sediminibacterium*. The prostate also showed a significant reduction in a single ASV in the family Moraxellaceae, belonging to species *Acinetobacter rhizosphaerae*. Both prostate and uterus showed an increased relative abundance of ASVs in the family Bacteroidaceae, identified to species as *Bacteroides fragilis* in the prostate and only as *Bacteroides* sp. in the uterus. A single ASV in the family Streptococcaceae, genus *Streptococcus*, was also found to be increased in both organs. Lastly, both prostate and uterus showed increased relative abundance of ASVs in the family Lachnospiraceae, with one ASV showing an increase in both organs and two other ASVs belonging to the genus *Blautia* showing an increase in the uterus only. Among non-reproductive organs there were no marked patterns. Only three ASVs were identified as being slightly reduced in the brain. Two of these ASVs belonging to the families Chitinophagaceae and MLE1-12 were also reduced in both reproductive organs, and the third ASV belonging to the family Sphingomonadaceae, species *Sphingomonas yabuuchiae*, was also reduced in the uterus. The heart showed a decrease in one ASV belonging to the family Veillonellaceae, species *Veillonella dispar*, and increases in two ASVs belonging to the families Pseudomonadaceae and Enterobacteriaceae. Only one ASV belonging to the family Clostridiaceae, species *Clostridium perfringens*, was found to be significantly reduced in the liver, with no ASVs identified as significantly increased. Lastly, only two ASVs were found to be increased in the spleen, belonging to the families Peptostreptococcaceae and Chitinophagaceae, genus *Sediminibacterium*.

Analysis of composition of microbiomes analyses identified very few meaningful differences in bacterial relative abundance between causes of death, but several differences are worthy of remark. We observed an increased relative abundance (>20 log2 fold change relative to other causes of death) of ASVs belonging to the families MLE1-12, Enterobacteriaceae, and Chitinophagaceae among individuals who died of natural causes. Accidental deaths showed no meaningful differences from other manners of death, while death by homicide appeared to be slightly negatively associated (∼5 log2 fold change) with ten unique ASVs belonging to the class Bacilli, primarily in the families Streptococcaceae and Lactobacillaceae. Lastly, death by suicide showed a strong negative association with an ASV in the family Peptostreptococcaceae (>20 log2 fold change relative to other manners of death).

Association Between PMI and Bacterial Relative Abundances

Regression analyses of PMI and relative abundances of the four most abundant bacterial orders across all six human organs identified several significant relationships (**Figure 4**). Within the heart, ASVs belonging to the order Burkholderiales showed a significant increase in relative abundance with increasing PMI (R^2 = 0.11; p = 0.04). Among all organs except the uterus, ASVs belonging to the order Clostridiales showed increased relative abundance with increasing PMI, but these trends were significant only for the brain (R^2 = 0.38; p = 5.2e-5), liver (R^2 = 0.09; p = 0.04), and spleen (R^2 = 0.28; p = 0.01). Among the brain, heart, liver, and spleen, ASVs in the order MLE1-12 showed a slight decrease in relative abundance with increasing PMI, but these results were not significant. Lastly, ASVs belonging to the order Saprospirales showed no discernable trends in relation to PMI.

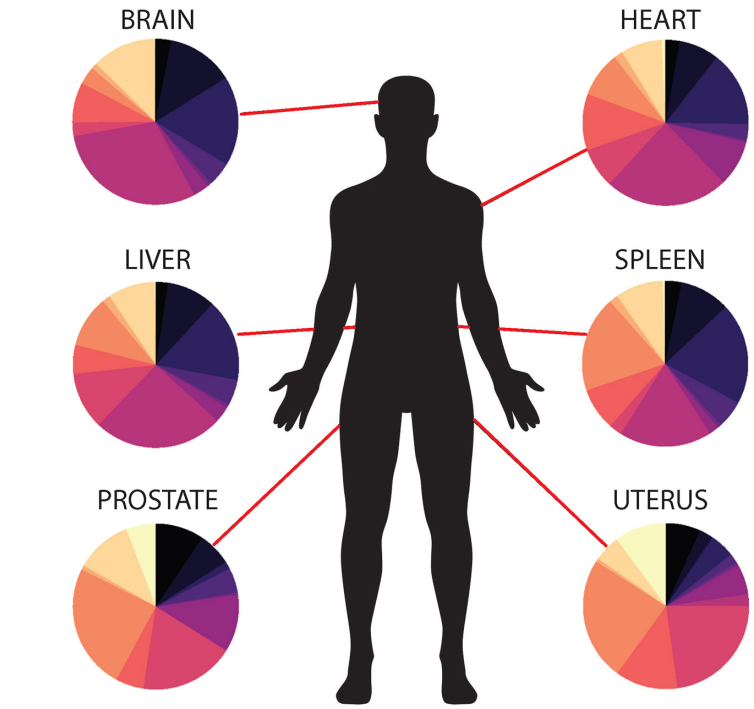

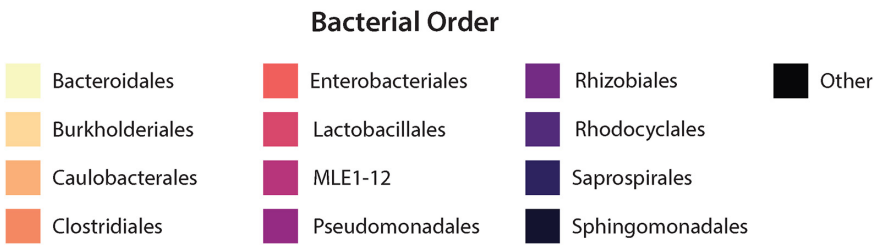

FIGURE 2 | Mean relative abundance of top 10 bacterial orders identified within each organ.

DISCUSSION

The utilization of genetic (Javan et al., 2020) and microbial data in the context of forensic investigations holds great promise for the field of forensic science (Bell et al., 2018; Oliveira and Amorim, 2018). Identification of taxa that are associated with PMI, specific causes of death, or other traits such as age, sex, and BMI may allow investigators to refine the circumstantial details surrounding the death of an individual. In this study, we found the order Clostridiales and the family Saprospiraceae to be among the most dominant putrefactive taxa in the cadre of bacteria that comprise the cadaver internal organ microbiome. Specifically, brain and spleen samples demonstrated significant increases in relative abundances of Clostridiales, as well as increases observed in heart, liver, and prostate tissues. These results, with the exception of uterus, at various times of death confirmed the Postmortem *Clostridium* Effect (PCE) which points to the observation of Clostridia in internal organ tissues (Javan et al., 2017; Pechal et al., 2018; Burcham et al., 2019; Junkins et al., 2019). Further, we also identify a number of cadaver-specific traits (sex, PMI, BMI, and cause of death) to be associated with microbial alpha and beta diversity, as well as bacterial taxa that are differentially associated with these traits.

Postmortem observations of human reproductive organs have demonstrated that the nulligravid uterus and prostate are the last organs to putrefy during decomposition (Casper, 1861; Scott et al., 2020). The prostate's anatomy is juxtaposed to the urethra, and it is exposed to microorganisms residing in the urinary tract (Shrestha et al., 2018). Also, the uterus's anatomy has the greatest content of muscle fibers found in the corpus uteri (Schwalm and Dubrauszky, 1966). There is a limited number of microorganisms (e.g., *Clostridium* spp.) that have collagenolytic proteases essential for the degradation of the collagen coating surrounding the prostate and uterus thereby lending to the resistance to their decay (Suzuki et al., 2006). In the natural order of decomposition, human decay is first visible on the abdominal wall, where gut bacteria, such as coliforms and *Clostridium*, proliferate and decompose hemoglobin into greenish compounds that stain the skin. Decomposition typically begins at the gut area unless the cause of death involves asphyxiation by hanging, inflammation of the protective membranes covering the brain and spinal cord (meningitis), drowning, and sun poisoning due to an increase of

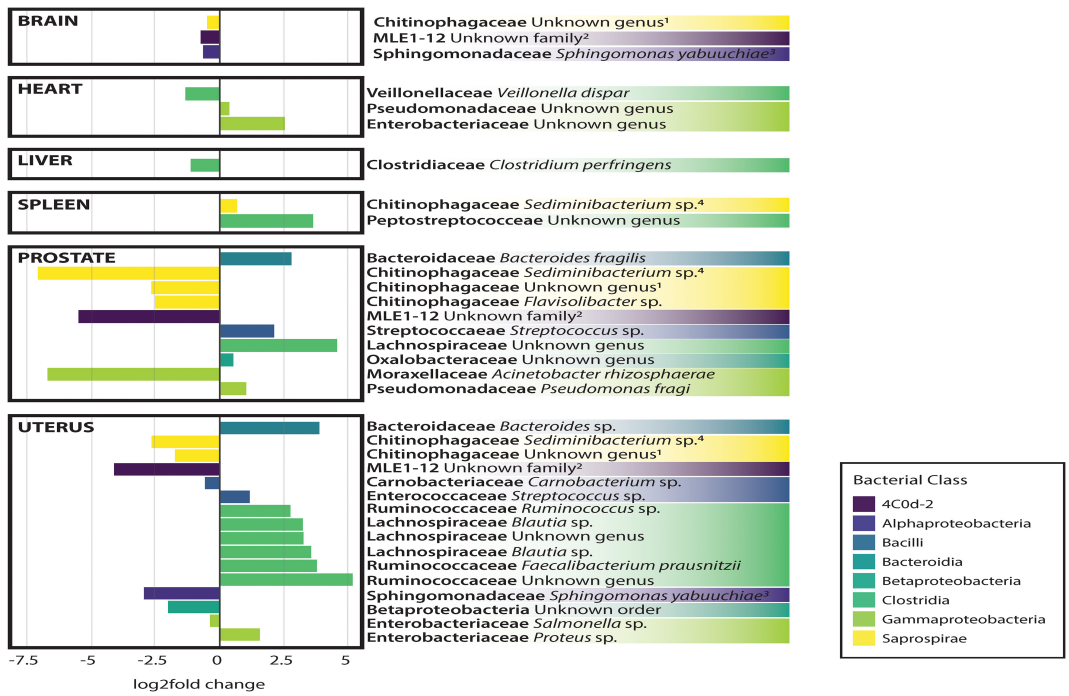

FIGURE 3 | Log2Fold change in differential abundance of individual bacterial OTUs between each organ compared to all other organs. Negative and positive values correspond to under- and over-representation of ASVs in each organ, respectively.

blood to the skull. Internal organs (liver, pancreas, spleen), that are in close proximity to the gut will immediately begin to putrefy in a particular natural order of decomposition.

Also of interest in this thanatomicrobiome study is the Saprospirales order. These bacteria did not conform to the stereotypical examples of decomposers. Saprospirae are large, filamentous microorganisms that are isolated from aquatic environments, predominantly marine-associated, but also freshwater and activated sludge. Members in this family breakdown polysaccharides and use the products of hydrolysis for the conversion of nutrients into bacterial biomass (Xia et al., 2008) which are important processes in human putrefaction. The helical gliding strains of this family are also associated with predation of other bacteria producing selective forces that increase their abundance. These bacteria are isolated most frequently from environmental sources; however, the study of the thanatomicrobiome of internal organs is not directly influenced by the same environmental abiotic factors (i.e., pH and temperature) and biotic factors (i.e., insects and scavenger activities) that are encountered by the other environmental samples (Javan et al., 2016). Some studies have shown that internal body sites with restricted access to environmental taxa decay in a relatively normal fashion; however, they decompose more slowly than body sites invaded by taxa from gravesoil and aquatic ecosystems (Preiswerk et al., 2018).

The significant patterns observed in the current study that are associated with cause of death warrant reinforcement from additional investigations to elucidate the origin of these associations. A retrospective study of Italian criminal cases demonstrated that 34% of decedents had no documented or an inaccurate cause of death (Di Vella and Campobasso, 2015). The majority of inaccuracies are results of over-diagnoses of natural deaths, specifically ischemic heart disease, hypertensive cardiovascular disease, and cancer. The risk of misdiagnoses is particularly high in traumatic deaths that do not include blood samples for toxicological testing and/or radiological imaging.

Microbes colonizing organs would decompose them differently depending in the manner of death classification (natural, suicide, homicide, or accident). Host bodies that died as result of natural death (e.g., cancer, cardiovascular disease, diabetes) will generally putrefy more slowly than death due to breaches in the skin (e.g., gunshot wounds, blunt force trauma) that permit entry of environmental bacteria and abiotic and biotic factors (Javan et al., 2019). In a recent study to determine how postmortem microbiome beta dispersion could be an additional forensic tool for predicting cause and manner of death in medicolegal investigations, a surprising finding demonstrated that the beta diversity significantly differed among body sites and causes and manners of death. For example, microorganisms detected in cardiovascular disease cases had significantly increased beta dispersion among all body locations (eyes, ears, nose, rectum, and mouth) (Kaszubinski et al., 2020). Therefore, the increase in microorganisms in cardiovascular disease cases demonstrates dysbiosis in the dead, and that microbial signature variability may be measured through beta-dispersion calculations (e.g., Kruskal–Wallis).

To date, a universal approach to determine the cause of death remains an enigma. There are only a few methods

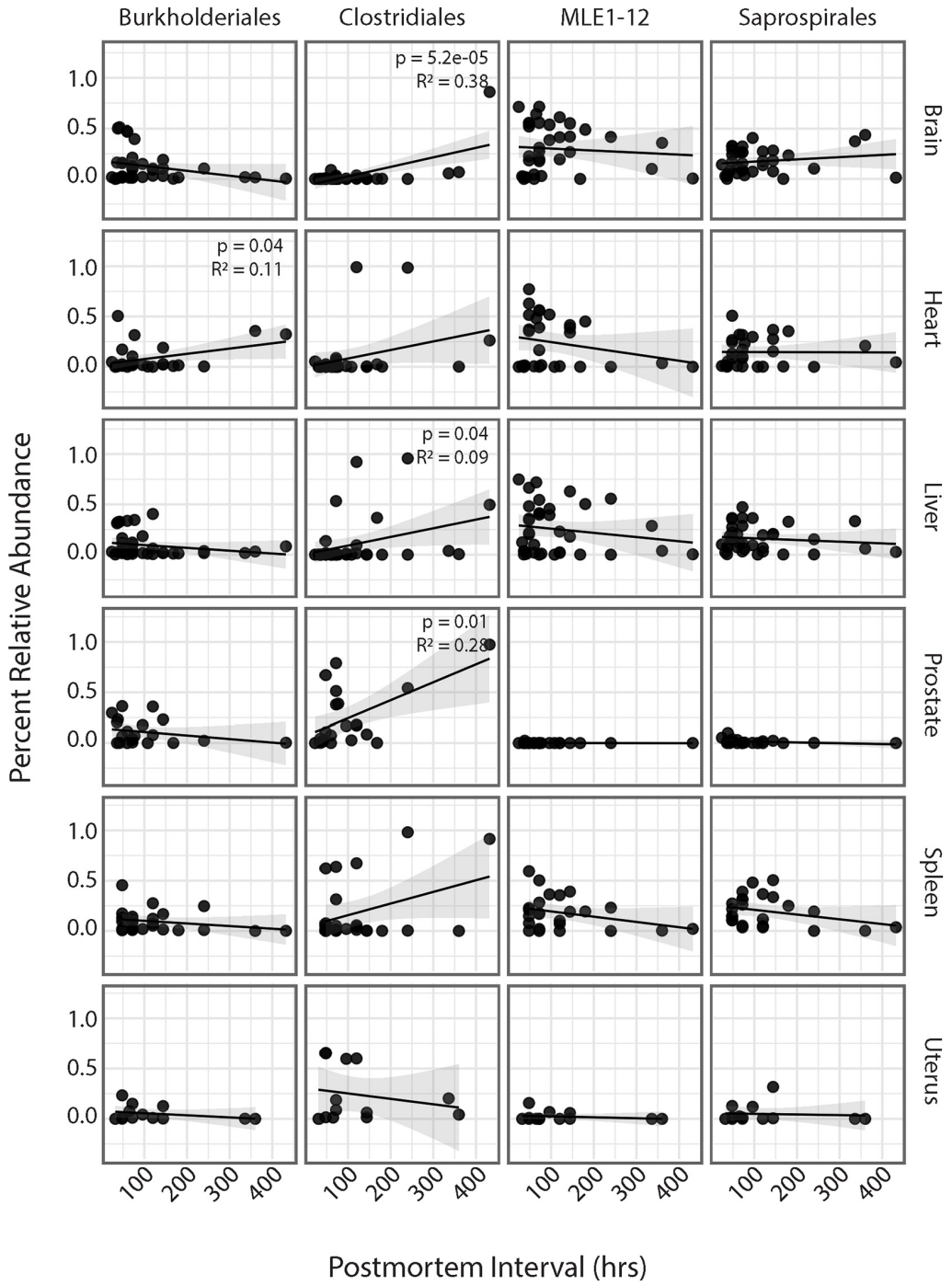

FIGURE 4 | Linear regression of relative abundance of four most abundant bacterial orders by PMI across each organ. Significance values are annotated in top right corner for each regression. Non-significant values not labeled.

presently used that employ molecular biology to diagnose the cause of death. Ackerman et al. (2001) coined the term "molecular autopsy" to describe the studies of DNA extracted from cadaveric blood and tissue samples to establish the cause of death in autopsy-negative cases. During molecular autopsies, specimens are taken from the cadaver and DNA is extracted using commercially available DNA extraction kits. Sequencing of the extracted DNA is analyzed via traditional Sanger sequencing and

high-throughput next-generation platforms to detect disease-causing mutations (Boczek et al., 2012). The sequencing and bioinformatics techniques described in the current study suggest that an increased subject size and varying times of death will provide insights for the utility of this methodology to determine the cause of death.

There are limitations of this methodology which include the paucity of known reference genomes for sequence comparisons (Pechal et al., 2014). Furthermore, despite the efficacy of this novel approach to molecular autopsy, a larger sample size of deceased cases is needed to further account for variation in postmortem microbial communities associated with human decomposition in different habitats.

CONCLUSION

The advancement of the thanatomicrobiome as a forensic indicator of the cause of death requires investigation of unknown relationships between human remains, fundamental decomposition processes, and internal microorganisms. There are a variety of abiotic and biotic factors obtained from cadavers that have been investigated as biomarkers to assist forensic pathologists in the determination of the cause of death. Current medicolegal investigative techniques have their merits; but in reality, most of the molecular approaches are limited to the approximation of PMI and the cause of death. Furthermore, the approaches do not provide definitive determinations of the cause of death, which remain an enigma. Future experiments using our thanatos model system that include a larger cohort of samples from both violent and pathological deaths and more internal organs will be necessary to determine the potential impact of the relationship between postmortem microbial succession and the cause of death. Finding a new method which takes the human error out of PMI calculations and determinations of the cause of death would be a milestone in solving questionable criminal cases. Robust statistical models have to be applied to account for the microbial variability demonstrated among different causes of death. Furthermore, in the era of COVID-19, accurate autopsies are crucial in order to determine the cause of death in decedents who test positive for SARS-CoV-2 and to discriminate between those who died *from* COVID-19 and who died *with* COVID-19.

DATA AVAILABILITY STATEMENT

The datasets presented in this study can be found in online repositories. The names of the repository/repositories and accession number(s) can be found in the article/ **Supplementary Material**. The EBI Accession Number is PRJEB41511.

ETHICS STATEMENT

The study was approved by the Committee for the Protection of Human Subjects, Alabama State University Institutional Review Board (IRB) number 2020100. Methods were in accordance with relevant guidelines and regulations regarding working with cadavers. Written informed consent was obtained from next-of-kin relatives of the cases.

AUTHOR CONTRIBUTIONS

GJ and JG designed the study. SV and AO collected the human corpses. GJ and SF extracted the genomic DNA, PCR, and gel electrophoresis the postmortem samples. NG performed the MiSeq sequencing. HL performed the bioinformatic data analysis. HL, GJ, and SF wrote and edited the amnuscript. All authors read and approved the final manuscript.

FUNDING

This work was supported by the National Science Foundation (NSF) grant HRD 2011764 and the National Institute of Justice (NIJ) 2017-MU-MU-4042.

SUPPLEMENTARY MATERIAL

The Supplementary Material for this article can be found online at: https://www.frontiersin.org/articles/10.3389/fmicb.2020.569630/full#supplementary-material

Supplementary Table 1 | Demographic data for each of the 40 cadavers. The cases were collected at the Department of Public Health, Experimental and Forensic Medicine at the University of Pavia in Pavia, Italy.

REFERENCES

Ackerman, M. J., Tester, D. J. and Driscoll, D. J. (2001). Molecular autopsy of sudden unexplained death in the young. *Am. J. Forensic Med.* 22, 105–111. doi: 10.1097/00000433-200106000-00001

Amir, A., McDonald, D., Navas-Molina, J. A., Kopylova, E., Morton, J. T., Xu, Z. Z., et al. (2017). Deblur rapidly resolves single-nucleotide community sequence patterns. *MSystems* 2:e00191-16. doi: 10.1128/mSystems.00191-16

Bell, C. R., Wilkinson, J. E., Robertson, B. K., and Javan, G. T. (2018). Sex-related differences in the thanatomicrobiome in postmortem heart samples using bacterial gene regions V1-2 and V4. *Lett. Appl. Microbiol.* 67, 144–153. doi: 10.1111/lam.13005

Boczek, N. J., Tester, D. J., and Ackerman, M. J. (2012). The molecular autopsy: an indispensable step following sudden cardiac death in the young? *Herzschrittmacherther Elektrophysiol.* 23, 167–173. doi: 10.1007/s00399-012-0222-x

Burcham, Z. M., Hood, J. A., Pechal, J. L., Krausz, K. L., Bose, J. L., Schmidt, C. J., et al. (2016). Fluorescently labeled bacteria provide insight on post-mortem microbial transmigration. *Forensic Sci. Int.* 264, 63–69. doi: 10.1016/j.forsciint.2016.03.019

Burcham, Z. M., Pechal, J. L., Schmidt, C. J., Bose, J. L., Rosch, J. W., Benbow, M. E., et al. (2019). Bacterial community succession, transmigration, and differential gene transcription in a controlled vertebrate decomposition model. *Front. Microbiol.* 10:745. doi: 10.3389/fmicb.2019.00745

Buresova, A., Kopecky, J., Hrdinkova, V., Kamenik, Z., Omelka, M., and Sagova-Mareckova, M. (2019). Succession of microbial decomposers is determined by litter type, but site conditions drive decomposition rates. *Appl. Environ. Microbiol.* 85, e001760-19.

Campobasso, C. P., Di Vella, G., and Introna, F. (2001). Factors affecting decomposition and Diptera colonization. *Forensic Sci. Int.* 120, 18–27. doi: 10.1016/s0379-0738(01)00411-x

Can, I., Javan, G. T., Pozhitkov, A. E., and Noble, P. A. (2014). Distinctive thanatomicrobiome signatures found in the blood and internal organs of humans. *J. Microbiol. Methods* 106, 1–7. doi: 10.1016/j.mimet.2014.07.026

Caporaso, J. G., Kuczynski, J., Stombaugh, J., Bittinger, K., Bushman, F. D., Costello, E. K., et al. (2010). QIIME allows analysis of high-throughput community sequencing data. *Nat. Methods* 7, 335–336.

Caporaso, J. G., Lauber, C. L., Walters, W. A., Berg-Lyons, D., Huntley, J., Fierer, N., et al. (2012). Ultra-high-throughput microbial community analysis on the Illumina HiSeq and MiSeq platforms. *ISME J.* 6, 1621–1624. doi: 10.1038/ismej.2012.8

Caporaso, J. G., Lauber, C. L., Walters, W. A., Berg-Lyons, D., Lozupone, C. A., Turnbaugh, P. J., et al. (2011). Global patterns of 16S rRNA diversity at a depth of millions of sequences per sample. *Proc. Natl. Acad. Sci. U.S.A.* 108, 4516–4522. doi: 10.1073/pnas.1000080107

Casper, J. L. (1861). *A Handbook Of The Practice Of Forensic Medicine: Based Upon Personal Experience*. Norderstedt: hansebooks.

Cobaugh, K. L., Schaeffer, S. M., and DeBruyn, J. M. (2015). Functional and structural succession of soil microbial communities below decomposing human cadavers. *PLoS One* 10:e0130201. doi: 10.1371/journal.pone.0130201

Cryan, J. F., and Dinan, T. G. (2012). Mind-altering microorganisms: the impact of the gut microbiota on brain and behaviour. *Nat. Rev. Neurosci.* 13, 701–712. doi: 10.1038/nrn3346

Damann, F. E., Williams, D. E., and Layton, A. C. (2015). Potential use of bacterial community succession in decaying human bone for estimating postmortem interval. *J. Forensic Sci.* 60, 844–850. doi: 10.1111/1556-4029.12744

DeBruyn, J. M., and Hauther, K. A. (2017). Postmortem succession of gut microbial communities in deceased human subjects. *PeerJ* 5:e3437. doi: 10.7717/peerj.3437

Deutscher, J. (2008). The mechanisms of carbon catabolite repression in bacteria. *Curr. Opin. Microbiol.* 11, 87–93. doi: 10.1016/j.mib.2008.02.007

Di Vella, G., and Campobasso, C. P. (2015). Death investigation and certification in Italy. *Acad. Forensic Pathol.* 5, 454–461. doi: 10.23907/2015.050

Dunn, A. B., Jordan, S., Baker, B. J., and Carlson, N. S. (2017). The maternal infant microbiome: considerations for labor and birth. *MCN Am. J. Matern. Child Nurs.* 42, 318–325.

Ercolini, D., Russo, F., Nasi, A., Ferranti, P., and Villani, F. (2009). Mesophilic and psychrotrophic bacteria from meat and their spoilage potential *in vitro* and in beef. *Appl. Environ. Microbiol.* 75, 1990–2001. doi: 10.1128/aem.02762-08

Fierer, N., Lauber, C. L., Zhou, N., McDonald, D., Costello, E. K., and Knight, R. (2010). Forensic identification using skin bacterial communities. *Proc. Natl. Acad. Sci. U.S.A.* 107, 6477–6481. doi: 10.1073/pnas.1000162107

Frati, P., Frati, A., Salvati, M., Marinozzi, S., Frati, R., Angeletti, L. R., et al. (2006). Neuroanatomy and cadaver dissection in Italy: history, medicolegal issues, and neurosurgical perspectives: historical vignette. *J. Neurosurg.* 105, 789–796. doi: 10.3171/jns.2006.105.5.789

Gilbert, J. A., Blaser, M. J., Caporaso, J. G., Jansson, J. K., Lynch, S. V., and Knight, R. (2018). Current understanding of the human microbiome. *Nat. Med.* 24, 392–400. doi: 10.1038/nm.4517

Gilbert, J. A., Quinn, R. A., Debelius, J., Xu, Z. Z., Morton, J., Garg, N., et al. (2016). Microbiome-wide association studies link dynamic microbial consortia to disease. *Nature* 535, 94–103. doi: 10.1038/nature18850

Grenham, S., Clarke, G., Cryan, J. F., and Dinan, T. G. (2011). Brain–gut–microbe communication in health and disease. *Front. Physiol.* 2:94. doi: 10.3389/fphys.2011.00094

Hauther, K. A., Cobaugh, K. L., Jantz, L. M., Sparer, T. E., and DeBruyn, J. M. (2015). Estimating time since death from postmortem human gut microbial communities. *J. Forensic Sci.* 60, 1234–1240. doi: 10.1111/1556-4029.12828

Javan, G. T., Finley, S. J., Can, I., Wilkinson, J. E., Hanson, J. D., and Tarone, A. M. (2016). Human thanatomicrobiome succession and time since death. *Sci. Rep.* 6:29598.

Javan, G. T., Finley, S. J., Smith, T., Miller, J., and Wilkinson, J. E. (2017). Cadaver thanatomicrobiome signatures: the ubiquitous nature of *Clostridium* species in human decomposition. *Front. Microbiol.* 8:2096. doi: 10.3389/fmicb.2017.02096

Javan, G. T., Finley, S. J., Tuomisto, S., Hall, A., Benbow, M. E., and Mills, D. (2019). An interdisciplinary review of the thanatomicrobiome in human decomposition. *Forensic Sci. Med. Pathol.* 15, 75–83. doi: 10.1007/s12024-018-0061-0

Javan, G. T., Hanson, E., Finley, S. J., Visonà, S. D., Osculati, A., and Ballantyne, J. (2020). Identification of cadaveric liver tissues using thanatotranscriptome biomarkers. *Sci. Rep.* 10, 1–8.

Junkins, E. N., Speck, M., and Carter, D. O. (2019). The microbiology, pH, and oxidation reduction potential of larval masses in decomposing carcasses on Oahu, Hawaii. *J. Forensic Leg. Med.* 67, 37–48. doi: 10.1016/j.jflm.2019.08.001

Kaszubinski, S. F., Pechal, J. L., Smiles, K., Schmidt, C. J., Jordan, H. R., Meek, M. H., et al. (2020). Dysbiosis in the dead: human postmortem microbiome beta-dispersion as an indicator of manner and cause of death. *Front. Microbiol.* 11:2212. doi: 10.3389/fmicb.2020.555347

Kodama, W. A., Xu, Z., Metcalf, J. L., Song, S. J., Harrison, N., Knight, R., et al. (2019). Trace evidence potential in postmortem skin microbiomes: from death scene to morgue. *J. Forensic Sci.* 64, 791–798. doi: 10.1111/1556-4029.13949

Kozich, J. J., Westcott, S. L., Baxter, N. T., Highlander, S. K., and Schloss, P. D. (2013). Development of a dual-index sequencing strategy and curation pipeline for analyzing amplicon sequence data on the MiSeq Illumina sequencing platform. *Appl. Environ. Microbiol.* 79, 5122–5130.

Lax, S., Hampton-Marcell, J. T., Gibbons, S. M., Colares, G. B., Smith, D., Eisen, J. A., et al. (2015). Forensic analysis of the microbiome of phones and shoes. *Microbiome* 3:21.

Lutz, H. L., Jackson, E. W., Webala, P. W., Babyesiza, W. S., Peterhans, J. C. K., Demos, T. C., et al. (2019). Ecology and host identity outweigh evolutionary history in shaping the bat microbiome. *mSystems* 4, e00511–e00519.

Mandal, S., Van Treuren, W., White, R. A., Eggesbø, M., Knight, R., and Peddada, S. D. (2015). Analysis of composition of microbiomes: a novel method for studying microbial composition. *Microb. Ecol. Health Dis.* 26:27663.

Maujean, G., Guinet, T., Fanton, L., and Malicier, D. (2013). The interest of postmortem bacteriology in putrefied bodies. *J. Forensic Sci.* 58, 1069–1070. doi: 10.1111/1556-4029.12155

Meckel, K. R., and Kiraly, D. D. (2019). A potential role for the gut microbiome in substance use disorders. *Psychopharmacology* 236, 1513–1530. doi: 10.1007/s00213-019-05232-0

Metcalf, C. J. E., Xu, Z. Z., Weiss, S., Lax, S., Van Treuren, W., Hyde, E. R., et al. (2016). Microbial community assembly and metabolic function during mammalian corpse decomposition. *Science* 351, 158–162. doi: 10.1126/science.aad2646

Metcalf, J. L. (2019). Estimating the postmortem interval using microbes: knowledge gaps and a path to technology adoption. *Forensic Sci. Int. Genet.* 38, 211–218. doi: 10.1016/j.fsigen.2018.11.004

Oksanen, J., Blanchet, F. G., Friendly, M., Kindt, R., Legendre, P., McGlinn, D., et al. (2018). *vegan: Community Ecology Package, vR package version 2.5-2*. https://CRAN.R-project.org/package=vegan (accessed February 18, 2017).

Oliveira, M., and Amorim, A. (2018). Microbial forensics: new breakthroughs and future prospects. *Appl. Microbiol. Biotechnol.* 102, 10377–10391. doi: 10.1007/s00253-018-9414-6

Park, J., Kim, S. J., Lee, J. A., Kim, J. W., and Kim, S. B. (2017). Microbial forensic analysis of human-associated bacteria inhabiting hand surface. *Forensic Sci. Int. Genet.* 6, e510–e512.

Pechal, J. L., Crippen, T. L., Benbow, M. E., Tarone, A. M., Dowd, S., and Tomberlin, J. K. (2014). The potential use of bacterial community succession in forensics as described by high throughput metagenomic sequencing. *Int. J. Legal Med.* 128, 193–205. doi: 10.1007/s00414-013-0872-1

Pechal, J. L., Schmidt, C. J., Jordan, H. R., and Benbow, M. E. (2018). A large-scale survey of the postmortem human microbiome, and its potential to provide insight into the living health condition. *Sci. Rep.* 8:5724.

Preiswerk, D., Walser, J. C., and Ebert, D. (2018). Temporal dynamics of microbiota before and after host death. *ISME* 12, 2076–2085. doi: 10.1038/s41396-018-0157-2

Rakoff-Nahoum, S., Foster, K. R., and Comstock, L. E. (2016). The evolution of cooperation within the gut microbiota. *Nature* 533, 255–259. doi: 10.1038/nature17626

Rognes, T., Flouri, T., Nichols, B., Quince, C., and Mahé, F. (2016). VSEARCH: a versatile open source tool for metagenomics. *PeerJ* 4:e2584. doi: 10.7717/peerj.2584

Schmedes, S. E., Woerner, A. E., and Budowle, B. (2017). Forensic human identification using skin microbiomes. *Appl. Environ. Microbiol.* 83, e001672-17.

Schwalm, H., and Dubrauszky, V. (1966). The structure of the musculature of the human uterus—muscles and connective tissue. *Am. J. Obstet. Gynecol.* 94, 391–404. doi: 10.1016/0002-9378(66)90661-2

Scott, L., Finley, S. J., Watson, C., and Javan, G. T. (2020). Life and death: a systematic comparison of antemortem and postmortem gene expression. *Gene* 731:44349.

Shrestha, E., White, J. R., Yu, S. H., Kulac, I., Ertunc, O., De Marzo, A. M., et al. (2018). Profiling the urinary microbiome in men with positive versus negative biopsies for prostate cancer. *J. Urol.* 199, 161–171. doi: 10.1016/j.juro.2017.08.001

Suzuki, Y., Tsujimoto, Y., Matsui, H., and Watanabe, K. (2006). Decomposition of extremely hard-to-degrade animal proteins by thermophilic bacteria. *J. Biosci. Bioeng.* 102, 73–81. doi: 10.1263/jbb.102.73

Urakawa, H., Martens-Habbena, W., and Stahl, D. A. (2010). High abundance of ammonia-oxidizing Archaea in coastal waters, determined using a modified DNA extraction method. *Appl. Environ. Microbiol.* 76, 2129–2135. doi: 10.1128/aem.02692-09

Wickham, H. (2009). *ggplot2: Elegant Graphics for Data Analysis*. New York, NY: Springer.

Wickham, H., Francois, R., Henry, L., and Müller, K. (2018). dplyr: a grammar of data manipulation. *R. Pack. Version* 0.7, 8.

Xia, Y., Kong, Y., Thomsen, T. R., and Nielsen, P. H. (2008). Identification and ecophysiological characterization of epiphytic protein-hydrolyzing Saprospiraceae ("*Candidatus Epiflobacter*" spp.) *in activated sludge. Appl. Environ. Microbiol.* 74, 2229–2238. doi: 10.1128/aem.02502-07

Conflict of Interest: The authors declare that the research was conducted in the absence of any commercial or financial relationships that could be construed as a potential conflict of interest.

frontiers in Microbiology

ORIGINAL RESEARCH
published: 13 January 2021
doi: 10.3389/fmicb.2020.608856

Comparative Decomposition of Humans and Pigs: Soil Biogeochemistry, Microbial Activity and Metabolomic Profiles

Jennifer M. DeBruyn[1], Katharina M. Hoeland[2], Lois S. Taylor[1], Jessica D. Stevens[1], Michelle A. Moats[1], Sreejata Bandopadhyay[1†], Stephen P. Dearth[2], Hector F. Castro[3], Kaitlin K. Hewitt[2†], Shawn R. Campagna[3], Angela M. Dautartas[4†], Giovanna M. Vidoli[4], Amy Z. Mundorff[4] and Dawnie W. Steadman[4]*

[1] Department of Biosystems Engineering and Soil Science, The University of Tennessee, Knoxville, Knoxville, TN, United States, [2] Department of Chemistry, The University of Tennessee, Knoxville, Knoxville, TN, United States, [3] Biological and Small Molecule Mass Spectrometry Core, Department of Chemistry, The University of Tennessee, Knoxville, Knoxville, TN, United States, [4] Department of Anthropology, The University of Tennessee, Knoxville, Knoxville, TN, United States

Vertebrate decomposition processes have important ecological implications and, in the case of human decomposition, forensic applications. Animals, especially domestic pigs (*Sus scrofa*), are frequently used as human analogs in forensic decomposition studies. However, recent research shows that humans and pigs do not necessarily decompose in the same manner, with differences in decomposition rates, patterns, and scavenging. The objective of our study was to extend these observations and determine if human and pig decomposition in terrestrial settings have different local impacts on soil biogeochemistry and microbial activity. In two seasonal trials (summer and winter), we simultaneously placed replicate human donors and pig carcasses on the soil surface and allowed them to decompose. In both human and pig decomposition-impacted soils, we observed elevated microbial respiration, protease activity, and ammonium, indicative of enhanced microbial ammonification and limited nitrification in soil during soft tissue decomposition. Soil respiration was comparable between summer and winter, indicating similar microbial activity; however, the magnitude of the pulse of decomposition products was greater in the summer. Using untargeted metabolomics and lipidomics approaches, we identified 38 metabolites and 54 lipids that were elevated in both human and pig decomposition-impacted soils. The most frequently detected metabolites were anthranilate, creatine, 5-hydroxyindoleacetic acid, taurine, xanthine, *N*-acetylglutamine, acetyllysine, and sedoheptulose 1/7-phosphate; the most frequently detected lipids were phosphatidylethanolamine and monogalactosyldiacylglycerol. Decomposition soils were also significantly enriched in metabolites belonging to amino acid metabolic pathways and the TCA cycle. Comparing humans and pigs, we noted several differences in soil biogeochemical responses. Soils under humans decreased in pH as decomposition progressed, while under pigs, soil pH increased. Additionally, under pigs we observed significantly higher ammonium and protease activities compared to

OPEN ACCESS

Edited by:
T. Komang Ralebitso-Senior, Liverpool John Moores University, United Kingdom

Reviewed by:
Sheree J. Finley, Alabama State University, United States
Qinru Sun, Xi'an Jiaotong University, China

***Correspondence:**
Jennifer M. DeBruyn
jdebruyn@utk.edu

†Present address:
Sreejata Bandopadhyay, Department of Microbiology and Molecular Genetics, Michigan State University, East Lansing, MI, United States
Kaitlin K. Hewitt, Department of Chemistry, Jackson State University, Jackson, MS, United States
Angela M. Dautartas, Department of Anthropology, Sociology, and Criminology, Troy University, Troy, AL, United States

Specialty section:
This article was submitted to Systems Microbiology, a section of the journal Frontiers in Microbiology

Received: *21 September 2020*
Accepted: *17 December 2020*
Published: *13 January 2021*

Citation:
DeBruyn JM, Hoeland KM, Taylor LS, Stevens JD, Moats MA, Bandopadhyay S, Dearth SP, Castro HF, Hewitt KK, Campagna SR, Dautartas AM, Vidoli GM, Mundorff AZ and Steadman DW (2021) Comparative Decomposition of Humans and Pigs: Soil Biogeochemistry, Microbial Activity and Metabolomic Profiles. Front. Microbiol. 11:608856. doi: 10.3389/fmicb.2020.608856

humans. We identified several metabolites that were elevated in human decomposition soil compared to pig decomposition soil, including 2-oxo-4-methylthiobutanoate, sn-glycerol 3-phosphate, and tryptophan, suggesting different decomposition chemistries and timing between the two species. Together, our work shows that human and pig decomposition differ in terms of their impacts on soil biogeochemistry and microbial decomposer activities, adding to our understanding of decomposition ecology and informing the use of non-human models in forensic research.

Keywords: soil microbiology, carcass, forensic taphonomy, soil biogeochemistry, metabolomics, lipidomics, human decomposition, forensic anthropology

INTRODUCTION

Carrion decomposition is a critical component in biogeochemical cycling in all ecosystems. In terrestrial ecosystems, animals left to decompose on the soil surface are a nutrient and moisture-rich resource, creating a "hot spot" of enhanced biological activity (Keenan et al., 2018b). This ultimately serves to increase biodiversity and heterogeneity across landscapes. These decomposition hot spots have profound effects on the local soils, microorganisms, and plants (Towne, 2000; Carter et al., 2007; Bump et al., 2009; Parmenter and MacMahon, 2009; Yang et al., 2010; Barton et al., 2012, 2013a,b; Cobaugh et al., 2015; van Klink et al., 2020). Increases in ammonium, dissolved organic carbon, dissolved organic nitrogen, and phosphate are routinely documented (Cobaugh et al., 2015; Barton et al., 2016; Fancher et al., 2017; Keenan et al., 2018a). Concomitant with this is temporal succession of local biological communities, including arthropods, plants, microbes and microfauna (Schoenly and Reid, 1987; Barton et al., 2013a; Macdonald et al., 2014; Cobaugh et al., 2015; Finley et al., 2016; Szelecz et al., 2016; Keenan et al., 2018a; Taylor et al., 2020).

While certain patterns have emerged from these studies of carcass decomposition, it is also generally noted that there can be wide variability in soil physicochemical responses. For example, soil pH in decomposition-impacted soils does not exhibit predictable patterns: Some studies reported decreased pH associated with surface decomposition (Towne, 2000; Aitkenhead-Peterson et al., 2012), others report an increase (Benninger et al., 2008; Meyer et al., 2013; Keenan et al., 2018b; Szelecz et al., 2018), and still others found no significant change (Cobaugh et al., 2015; Fancher et al., 2017). This variability in soil pH is important because soil pH controls not only the soil chemistry, it is also a key driver of bacterial community structure generally (Lauber et al., 2009), ultimately influencing the composition of the decomposer community.

Understanding patterns and processes of mammalian decomposition has important forensic applications. Forensic taphonomy research often focuses on using patterns of decomposition to improve estimates of postmortem interval (PMI) or time since death estimations (e.g., Carter and Tibbett, 2003; Tibbett and Carter, 2003; Metcalf et al., 2013; Pechal et al., 2013; Hauther et al., 2015; Johnson et al., 2016; von der Lühe et al., 2017). Because of challenges in obtaining, and/or restrictions on use of, human cadavers, many forensic taphonomy studies use animal carcasses as proxies. Therefore, much of our knowledge of decomposition timing and processes have relied on various animal carcasses, including pigs (Hopkins et al., 2000; Wilson et al., 2007; Howard et al., 2010; Meyer et al., 2013; Pechal et al., 2013; Forger et al., 2019; Matuszewski et al., 2020), mice (Metcalf et al., 2013; Lauber et al., 2014), rats (Carter et al., 2010), dogs (Reed, 1958), and other vertebrate wildlife (Towne, 2000; Parmenter and MacMahon, 2009; Macdonald et al., 2014; Risch et al., 2020). Domestic pigs (*Sus scrofa*) are often cited as the most useful analog for humans in decomposition studies, given their physiological and anatomical similarities, including mass, hairiness, and pigmentation (Schoenly et al., 2007; Matuszewski et al., 2020). Studies using pigs often have greater replication, and have been formative in establishing proof-of-concept for forensic methods (Matuszewski et al., 2020). In general, studies have revealed that pigs and humans host similar postmortem insect communities (Schoenly et al., 2007; Wang et al., 2017; Matuszewski et al., 2020). Species similarities in postmortem soil and decomposer dynamics are less well understood. Pigs and humans are both monogastric omnivores, having a relatively similar gut microbiome composition (Ley et al., 2008) in comparison to carnivores or herbivores. However, different species of mammalian carcasses each have their own unique composition: For example, pigs have a greater moisture content while humans have greater nitrogen content (Carter et al., 2007). Additionally, pigs have higher levels of total saturated fatty acids compared to humans, contributing to differences in adipocere formation between pigs and humans (Notter et al., 2009). There is also evidence that the suite of volatile organic compounds responsible for decomposition odors differs between species (Vass et al., 2008); a fact that is exploited by canines trained in human remains detection.

Despite the evidence that decomposition processes may differ between different species, most of the existing studies have confounding variables that hamper interpretation (Matuszewski et al., 2020). Only a few studies have made direct comparisons: one study compared 10 non-human vertebrates ranging in mass from 6 g (deer mouse) to 13 kg (mule deer), revealing that mass loss rates were variable between species and not correlated to initial body mass (Parmenter and MacMahon, 2009). Another study comparing buried skeletal muscle tissue from four mammals (including humans) showed that while soil nutrient enrichment patterns associated with decomposition followed the same overall temporal patterns, there were differences in nitrogen flux; namely soil ammonium concentrations associated with porcine and bovine tissues were twice as high as human tissue

(Stokes et al., 2013). To address the question of whether pigs can be used as proxies in forensic taphonomy research, a study was undertaken at the University of Tennessee Anthropology Research Facility (ARF). Over three seasonal trials which directly compared humans, pigs, and rabbits, the study quantified gross morphological changes via the Total Body Score method (Megyesi et al., 2005). This study revealed that pigs do not exhibit the same decomposition patterns as humans, and noted that humans had greater variability, scavenging, and mummification compared to animals (Dautartas et al., 2018; Steadman et al., 2018). This finding was corroborated by a similar study conducted in an arid environment, which also concluded that humans and pigs displayed differential decomposition (Connor et al., 2018).

Given that humans and pigs have differential morphological decomposition patterns, the objective of our study was to determine if human and pig decomposition have similar effects on soil. Our null hypothesis was that because of their similar mass, the decomposition of these two species under identical environmental conditions should have similar effects on soil physicochemistry, microbial activity, biogeochemistry and decomposition products. To address our hypothesis, we measured several soil physicochemical parameters and indicators of microbial activity, including respiration, protease activity and untargeted metabolomic profiles during two comparative human and pig decomposition trials conducted at the ARF (reported in Dautartas et al., 2018; Steadman et al., 2018). Untargeted metabolomics has emerged as a powerful tool in systems biology, focusing on the identification and quantitation of low molecular weight metabolites present in a system (<1,000 Da). More recently, it has been applied to characterize microbial communities from various environmental samples, including soil (e.g., Randewig et al., 2019; Withers et al., 2020). Here, we applied an untargeted metabolomics and lipidomics approach to soil collected in close proximity to decomposing carcasses to characterize decomposition products. Together, our work provides a direct comparison of human and pig decomposition in terms of their impacts on soil biogeochemistry and microbial decomposer communities, adding to our understanding of decomposition ecology and providing important information for evaluating the use of non-human analogs in forensic research.

MATERIALS AND METHODS

Study Design

Two comparative decomposition trials conducted at the University of Tennessee Anthropology Research Facility (ARF) were the focus of this study, conducted in the summer of 2014 and the winter of 2014–2015. The ARF, located in Knoxville, Tennessee (35° 56′ 28″ N, 83° 56′ 25″ W), is a nearly 3-acre outdoor laboratory dedicated to the study of human decomposition. The site is a temperate deciduous forest with well-drained fine textured soils (Damann et al., 2012). The textural class of the soils at this site based on particle size analysis was silt loam (>55% silt) (L. S. Taylor, *personal comm.*).

The human subjects were donations to the University of Tennessee Forensic Anthropology Center[1]. As no living human subjects were involved, this work was exempt from review by the University of Tennessee Institutional Review Board. No preference was employed for donor sex, age, or ancestry. The University of Tennessee protocol for accepting donations ensured the individuals did not have communicable diseases. The bodies were not autopsied or embalmed, nor had signs of external trauma. All subjects were placed in a 4°C morgue cooler for at least 24 h before placement to equalize body temperature. The human donors consisted of six adult females and four males, with weights ranging from 53 to 107 kg, and all died of natural causes. Ten pig (*S. scrofa*) carcasses were obtained from a local farm near Knoxville, Tennessee. The summer trial used three female and two male pigs, ranging from 40 to 59 kg in weight. The winter trial used two female and three male pigs, ranging from 47 to 57 kg. A veterinarian euthanized the animals via injection; all protocols for animal handling and euthanasia were approved by the University of Tennessee Institutional Animal Care and Use Committee (IACUC). Full details on the donors, carcasses, and euthanasia protocols are provided in Dautartas et al. (2018).

The experimental design has been described in detail previously (Dautartas et al., 2018; Steadman et al., 2018). In each trial, five human subjects and five pig (*S. scrofa*) carcasses were placed on virgin soils that had not previously been used for decomposition experiments at the ARF. They were placed in a randomized block design, along with domestic rabbit (*Oryctolagus cuniculus*) carcasses which were not included as part of our current study (**Supplementary Figure 1**). Carcasses were placed with a minimum of 3 m between each carcass. Internal temperatures for human donors were monitored using Tiny Tag data loggers (Gemini Data Loggers, United Kingdom) with probes inserted rectally. Soil temperatures for both pigs and humans were recorded with Tiny Tag data loggers inserted 5–10 cm into the soil immediately adjacent to the donors. Ambient temperature and humidity were recorded hourly using Tiny Tag loggers suspended from nearby trees, and used to calculate Accumulated Degree Days (ADD) as described in Dautartas et al. (2018). Morphological changes and tissue loss of the carcasses was scored using the Total Body Score (TBS) (Megyesi et al., 2005).

Soil Sampling

Soil samples were collected prior to carcass placement, and then from the area immediately adjacent to each carcass during decomposition. Due to physical site constraints that limited access to soils (terrain and thick vegetation), the summer trial included four human subjects and three pigs; the winter trial included five humans and five pigs. Soils were additionally collected from control sites that were at least 5 m from the carcasses and had not been previously exposed to decomposition. Five meters was reasonably assumed to be beyond the zone of influence of the carcasses: Past research at the ARF and nearby sites has revealed minimal (<1 m) lateral translocation of decomposition products or effects on soil biota beyond the

[1]https://fac.utk.edu/

area of visible decomposition fluid saturation (Keenan et al., 2018a, 2019); other researchers have also reported that soil communities were affected up to 1 m away from human cadavers, but unaffected at 5 m (Singh et al., 2018). For the summer trial, samples were collected weekly for 5 weeks, which corresponded to approximately 400 ADD and TBS of approximately 28 for pigs and 24 for humans (Dautartas et al., 2018). For the winter trial, weekly samples were collected for the first 2 months, when decomposition was most variable. Following that, soils were collected monthly for a total of 21 weeks, which corresponded to approximately 600 ADD and TBS of 15 for pigs and 25 for humans (Dautartas et al., 2018). Soils were collected from the top 0–5 cm using sterile 15 mm plastic corers, following the method of Cobaugh et al. (2015). At each sampling time point, approximately 20 core samples were taken from the area around each donor which was visibly discolored by decomposition fluids, up to 30 cm away from each donor. Core sample locations were selected throughout the visible decomposition zone to ensure uniform coverage of the area (i.e., equal number of cores were taken from the head, torso, and limb areas). The core samples were composited in a sterile Whirl-pak® bag, and transported back to the lab for immediate processing. Soils were thoroughly homogenized prior to laboratory analyses, and subsamples stored at −20°C for enzyme assays and −80°C for metabolomics analyses.

Soil Physicochemical Analyses

Gravimetric soil moisture was determined by oven-drying soils at 105°C for at least 48 h. Soil pH was measured at 20°C using a 1:2 soil to deionized water (dH_2O) slurry and an Orion multiparameter meter (Orion Star A329, Thermo Scientific). Water soluble nutrients were extracted from soils by mixing soils 1:5 in dH_2O and shaking for 4 h at 170 rpm. Samples were centrifuged at 188 rcf at 20°C for 25 min to settle soils, and supernatants were filtered through grade GF/F glass microfiber filters (Whatman™) to remove suspended particulates. Extracts were stored at −20°C until analysis. Ammonium concentrations in soil extracts were quantified following a microplate protocol after a 2 h incubation, with minor modifications (Rhine et al., 1998). The ammonium standard [$(NH_4)_2SO_4$] was dissolved in dH_2O to account for potential matrix effects. In addition, 70 μl (instead of the 50 μl specified in original protocol) of each soil extract or standard were pipetted into the microplate, and 50 μl of deionized water was used (instead of 100 μl). Nitrate concentrations were determined (in triplicate) using a colorimetric method (Doane and Horwáth, 2003) using 50 μl of the NO_3^- color reagent and 70 μl of the soil extracts in a 96-well plate. Absorbance values were measured using a plate reader at 543 nm after incubating for at least 10 min at room temperature (Doane and Horwáth, 2003). Data analysis of physicochemical parameters was done in R v3.2.0 using R Studio v0.99.491. An initial screen with a mixed model showed that time was a significant factor, so subsequent analyses focused on comparing the treatments for each date separately. ANOVAs followed by a *post hoc* TukeyHSD comparison test were used to identify significant differences between treatments for each date.

Soil Biological Activity

Soil respiration rates over 24 h were determined by incubating 10 g (wet weight) soils in sealed 70 ml vials fitted with septa. At the beginning and end of incubation, 0.25 ml headspace samples were taken in duplicate and manually injected and read on a LiCor LI-820 CO_2 Analyzer (LiCor Inc., Lincoln, NE, United States). As a proxy for protein degradation activity, leucine amino peptidase activity was measured, according to Bell et al. (2013). Briefly, 2.75 g of soil was slurried with 91 ml Tris buffer (pH 6.7) in a blender. L-leucine-7-amido-4-methylcoumarin hydrochloride (200 μl) was added to the slurries in a 96-deep-well plate. Plates were incubated for 3 h at 20°C, then centrifuged to settle soil particles. 250 μl of the supernatant was transferred to a new 96-well plate and read on a Synergy H1 plate reader (BioTek, Winooski, VT, United States). Data analysis of microbial activity rates was performed as described for soil physicochemical parameters.

Metabolomics and Lipidomics

Extraction Method

Metabolomics and lipidomics were only performed on soil samples from the winter trial, as these soils had been appropriately flash-frozen and preserved at −80°C. Unfortunately, soil samples from the summer trial had been stored at −20°C, which is not recommended for long term storage of samples for metabolomics (Pinto et al., 2014; Hernandes et al., 2017), and therefore we were not able to perform metabolomic and lipidomic analysis for the summer trial. For the winter trial samples, the entirety of the extraction process was performed at 4°C unless otherwise stated. Soil samples were crushed with mortar and pestle under liquid nitrogen and weighed (approximately 100 mg) into individual 2 ml microcentrifuge tubes. To each tube, 1.3 ml of extraction solvent consisting of 40:40:20 HPLC grade methanol, acetonitrile, and water with 0.1 M formic acid (Thermo Fisher Scientific, Waltham, MA, United States) was added (Rabinowitz and Kimball, 2007). Soil particles were suspended by vortexing before extraction was carried out for 20 min while being shaken in an orbital platform shaker (Bellco, Vineland, NJ, United States). Following extraction, samples were centrifuged for 5 min at 16,100 rcf and the supernatant was removed and combined with the supernatant from the first extraction in new microcentrifuge tubes. The remaining soil was resuspended in 200 μl of extraction solvent and incubated for another 20 min while being shaken. Following extraction, samples were centrifuged for 5 min at 16,100 rcf before the supernatant was again transferred to the same microcentrifuge tubes. The samples were evaporated to dryness under a stream of nitrogen gas. The resulting dried residue was resuspended in 300 μl of sterile Milli-Q® grade water and transferred to autosampler vials for subsequent mass spectrometric analysis. Lipidomics extractions followed a modified version of the procedure described by Bligh and Dyer (1959). The method used two extraction solvents, 1:1 (v/v) 0.1 N hydrochloric acid: methanol (solvent 1), and 100% chloroform (solvent 2), which were added to approximately 50–100 mg of crushed soil samples. 800 μl of solvent 1 and 400 μl of solvent

2 were mixed and added to the soil samples. Samples were vortexed for 10 s and centrifuged at 16,100 rcf for 5 min. The chloroform layer was isolated and dried under nitrogen and resuspended in 9:1 (v/v) methanol: chloroform in autosampler vials prior to analysis.

Mass Spectrometry Methods

Mass spectrometry methods were adapted from Lu et al. (2010) for soil samples as we have described previously (Mueller et al., 2020). Autosampler vials were placed in autosampler trays (Ultimate 3000 RS Autosampler, Dionex, Sunnyvale, CA, United States) maintained at 4°C. A 10 μl aliquot from each vial was injected through a Synergi 2.5 μ reverse-phase Hydro-RP 100, 100 mm × 2.00 mm liquid chromatography column (Phenomenex, Torrance, CA, United States) maintained at 25°C. Chromatographic elution was ionized via electrospray ionization (Spray voltage: 2 kV, nitrogen sheath gas: 10, capillary temperature: 320°C) and introduced to an Exactive Plus Orbitrap mass spectrometer (Thermo Fisher Scientific, Waltham, MA, United States). LC-MS analysis was performed in negative ionization mode with a full-scan covering a window of 85 to 800 *m/z* from 0 to 9 min and 110 to 1,000 from 9 to 25 min. The resolution was set to 140,000 and the acquisition gain control target to 3e6. Solvent A was composed of 97:3 water: methanol with 10 mM tributylamine and 15 mM acetic acid. Solvent B consisted of methanol. The gradient was as follows: 0 to 5 min: 0% B, 5 to 13 min: 20% B, 13 to 15.5 min: 55% B, 15.5 to 19 min: 95% B, 19 to 25 min: 0% B using a constant flow rate of 200 μl min^{-1}.

Metabolomics Data Processing and Analysis

Mass spectrometry data files generated by Xcalibur were converted to mzML format (Martens et al., 2011) using the Proteowizard package (Chambers et al., 2012). Sample non-linear retention time correction, metabolite identification, and chromatogram integration were performed using MAVEN (Melamud et al., 2010; Clasquin et al., 2012). Metabolites were manually selected based on known standards (±5 ppm mass tolerance and ≤1.5 retention time tolerance). Unidentified spectral features were annotated using MAVEN's automatic peak detection algorithms with the settings as follows: Mass domain resolution was 10 ppm, time domain resolution was 10 scans, and EIC smoothing was 5 scans with 0.5 min peak grouping. Baseline smoothing was 5 scans and the top 80% of intensities were dropped from chromatogram for baseline calculation. Peak scoring was performed based on a trained classifier model looking for 4 minimum peaks per group, 5 minimum signal-to-noise, 5 minimum signal-to-blank, 10,000 minimum signal intensity, and 5 scan minimum peak width. Spectral features were normalized by soil dry weight. For each metabolite identified, relative intensity was calculated as the intensity in a given sample normalized to intensities in all samples. Relative intensities were uploaded to MetaboAnalyst online statistical analyzer for further analyses. Partial least squares-discriminant analysis (PLS-DA) and variable importance in projection (VIP) scores were calculated using MetaboAnalyst (Chong et al., 2019). MetaboAnalyst was also used to determine metabolic pathways using a human metabolic reference map that is available through KEGG (Kyoto Encyclopedia of Genes and Genomes). Heatmaps were generated in R v1.1.423 using ggplot2 (Wickham, 2009). The metabolomics profiling data is available in the MetaboLights database[2] under study MTBLS2254.

RESULTS

Ambient, Soil, and Internal Donor Temperatures

For the summer trial (June 2014), the mean ambient air temperature was 24.4°C. The ambient mean maximum was 38.5°C (day 4) and mean minimum was 15.0°C (day 34). Soil temperatures were recorded hourly from sensors placed in soil adjacent to human donors; the soil sensor associated with donor number 7 failed during the experiment, so these data were not used for analyses. The mean soil temperature for the study was 25.3°C (**Supplementary Figure 2A**). Soil temperatures in decomposition soils were slightly elevated in comparison with ambient temperatures during days 4 through 17. Soil temperatures reached a mean maximum of 33.9°C on study day 8, and a mean minimum of 19.1°C on study day 1. Temperature probes were placed inside human donors to measure internal temperature fluctuations during decomposition progression. Internal donor temperatures mirrored those of soil temperatures, diverging from ambient air temperatures. The internal temperature mean for the duration of the study was 26.1°C, and reached a mean maximum temperature of 39.8°C on study day 7 (1 day prior to mean maximum soil temperatures) (**Supplementary Figure 2A**). The internal mean minimum was 7.1°C at the beginning of the study (day 1).

For the winter trial (starting in December 2014), the mean ambient temperature was 4.7°C, with a mean maximum of 33.4°C, and mean minimum of −16.5°C. Soil temperatures closely followed ambient temperatures, although with less daily variation; the mean soil temperature over the course of the study was 6.2°C (**Supplementary Figure 2B**). Soil temperatures reached a mean maximum of 15.9°C on study day 123 (week 17) and minimum of −0.13°C on day 81 (week 12). Internal donor temperatures did not vary appreciably from either soil or ambient air temperatures; the overall study mean was 6.3°C. Internal donor temperatures reached a mean maximum of 27.7°C on study day 114 (week 16) and mean minimum of −2.8°C on day 82 (week 12) (**Supplementary Figure 2B**).

Soil Physicochemistry

For the winter trial, all ten study plots were intended to be replicates and were in the same local area and on the same soil type. However, we retrospectively noted some variability in the response of several measured parameters, and that this variability was dependent on the location of the plot. Namely, six of the plots (three human and three pig) were on undisturbed forest soils with a visible O horizon and neutral pH (pH 6 to 7) (hereafter referred

[2]https://www.ebi.ac.uk/metabolights

to as "lower site"). The other four plots (two human and two pig) were placed closer to a fence line (hereafter, "upper site") where soils had been previously disturbed from construction activities nearby. These upper site soils were visibly lighter in color: They did not have an O horizon, were lower in organic matter, and had a higher pH at the start of the study (pH 7 to 8). In order to account for the confounding factor of location, we first tested all variables for a plot location effect. Where a significant effect was observed (for pH, LAP activity, and metabolite profiles), we split the dataset by location and analyzed the two sites separately. Where no location effect was observed (nitrate, ammonium, and respiration), the data were analyzed together.

During the summer trial, soils became more alkaline under pigs, and more acidic under humans starting at week 3 (approximately 438 ADD; **Supplementary Table 1**). At this time, pigs were slightly more decomposed, with a TBS of 29 compared to human TBS of 25 (**Supplementary Table 1**). pH differences continued for the duration of sampling (**Figure 1A** and **Supplementary Table 2**). pH was significantly different between humans, pigs, and controls (ANOVA $p < 0.05$). During the winter, the pH was not as strongly affected: there were no significant changes over the first 5 weeks of the winter trial. After this time, at both the lower and upper sites, the decomposition soils had slightly reduced pH compared to controls; though this was only significant at weeks 5 (229 ADD) and 21 for the lower sites and week 17 (738 ADD) for the upper site (**Figures 1B,C** and **Supplementary Table 3**).

Ammonium concentrations were significantly elevated in decomposition soils in both the summer and winter trials (**Figures 2A,B**). The magnitude of this pulse was much higher in summer, with maximum concentrations reaching >1,000 μgN gdw^{-1} at week 2 (297 ADD); in the winter, peak concentrations were 60 to 125 μgN gdw^{-1} at week 9 (315 ADD). During the summer trial, pigs resulted in a significantly greater pulse of ammonium to the soil compared to controls starting in week 2 and through the remainder of the trial. Human treatments had elevated soil ammonium concentrations, but because of high variability between individuals (**Supplementary Table 2**), were not significantly different from the control soils in the summer (**Figure 2A**). In the winter trial, elevated ammonium was observed under decomposing pigs, with maximum concentrations reached at weeks 9 and 17 (315 and 738 ADD) (**Figure 2B** and **Supplementary Table 3**). Nitrate concentrations did not significantly change in any of the treatments for either trial (**Figures 2C,D** and **Supplementary Tables 2**, **3**). Control sites (i.e., background soils) were not significantly different between summer and winter trials for pH, ammonium, or nitrate.

Soil Microbial Activity

Decomposition resulted in elevated soil respiration rates starting in the first week of the summer trial and continuing throughout the experiment. Both human and pig treatments had significantly higher soil respiration rates compared to control soils, and pig-decomposition soils were significantly higher than human-decomposition soils in the summer (**Figure 3A** and **Supplementary Table 2**). In the winter trial, elevated respiration rates started during the fifth week (230 ADD), and peaked at weeks 17 through 21 following a period of spring warming (**Figure 3B** and **Supplementary Table 3**). Despite differences in ambient temperatures, the magnitude of the increases in soil respiration rates were comparable between summer and winter trials. We also noted that respiration rates were strongly correlated to TBS scores reported by Dautartas et al. (2018): In the summer trial, Pearson's $r = 0.54$, 0.85 for humans and pigs, respectively; in the winter, $r = 0.85$, 0.84 for humans and pigs, respectively.

We additionally measured leucine aminopeptidase (LAP) activity as a proxy for potential protease (i.e., protein degradation) capacity of the soil communities. During the summer trial, we observed elevated LAP potential activity in soils below pigs, but not below humans (**Figure 4A** and **Supplementary Table 2**). LAP activity was significantly correlated to pH (Spearman rank correlation coefficient $R_s = 0.739$, $p < 0.001$, **Supplementary Figure 3**). During the winter trial, enzyme rates were highly variable. Interestingly, during the first half of the experiment, LAP rates were elevated as a result of decomposition on the organic matter-rich soil of the lower site, but decreased as a result of decomposition in the disturbed soil at the upper site (**Figures 4B,C** and **Supplementary Table 3**). Control sites (i.e., background soils) were not significantly different between summer and winter trials for respiration or LAP.

Metabolomics and Lipidomics (Winter Trial)

To explore the impact of decomposition on microbial community function and decomposition products, metabolite and lipid profiles were generated for the winter trial soil samples (summer trial samples were not stored at −80°C and therefore could not be used for metabolomics). As with pH and LAP, PLS-DA analysis for metabolomics and lipidomics showed significantly different metabolic profiles in decomposition soil from the upper and lower sites (**Supplementary Figure 4**), thus we analyzed the two locations separately. Metabolomics analysis revealed a total of 84 metabolites identified from human and pig decomposition soils (**Figure 5**). PLS-DA of metabolite profiles at each sample timepoint showed significant changes in decomposition soils compared to control soils (**Figures 6A–C** and **Supplementary Figures 5**, **6**). Individual metabolites responsible for driving the differences in the PLS-DA were identified by variable importance in projection (VIP) scores: Metabolites with VIP scores greater than 1 were identified for each timepoint and used for further analyses. Based on VIP scores, each metabolite was categorized as being high or low in abundance in the three treatments (human, pig, and control) (**Figures 6D–F**). At the lower site (undisturbed soil), 66 metabolites with VIP > 1 increased in the decomposition treatments compared to control soils, with anthranilate, creatine, 5-hydroxyindoleacetic acid 5 (HIAA), taurine, and xanthine being the most frequently detected (detected in at least 5 out of 13 weeks). In the upper disturbed sites, 48 metabolites with VIP > 1 were identified. Here, *N*-acetylglutamine, acetyllysine, creatine, HIAA, and sedoheptulose 1/7-phosphate were the most

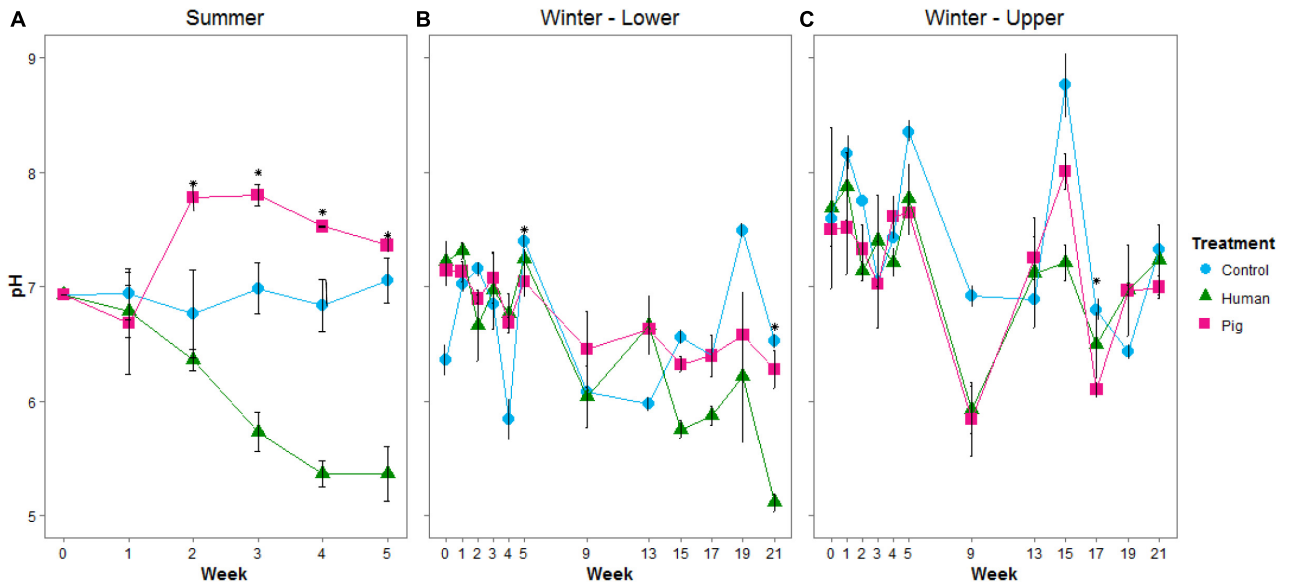

FIGURE 1 | Mean pH of soils below decomposing humans and pigs during the summer **(A)** and winter **(B,C)** trials. The lower site **(B)** refers to undisturbed forest soil, while the upper site **(C)** had disturbed soil. Error bars show standard deviations. Asterisks indicate sample times with significant differences between the three treatments ($p < 0.05$).

frequently detected (detected in at least 4 out of 13 weeks) (**Supplementary Figure 7**). Combining the two sites, we found a total of 38 metabolites elevated in decomposition soil (**Supplementary Table 4**). We further assessed those metabolites by matching them to KEGG pathways using the pathway enrichment tool in MetaboAnalyst. Decomposition soils were significantly enriched in metabolites belonging to metabolic pathways of amino acids (e.g., alanine, aspartate, and glutamate, as well as arginine and proline metabolism), and the citric acid (TCA) cycle (**Figure 7**). We detected multiple amino acids in decomposition soils, such as alanine, aspartate, gamma aminobutyric acid (GABA), glutamate, glutamine, isoleucine, leucine, methionine, phenylalanine, proline, serine, threonine, tyrosine, and valine (**Figure 5**).

A similar approach was taken for analyzing the lipidomics data via multivariate analysis. The focus was directed to six lipid classes, namely phosphatidylglycerol (PG), phosphatidylethanolamine (PE), phosphatidylinositol (PI), phosphatidic acid (PA), and phosphatidylserine (PS), all known to be major components of bacterial membranes, as well as monogalactosyldiacylglycerol (MGDG), a lipid class present in plants with roles in photosynthesis. Soil from the lower site revealed a total of 84 lipids, whereas the upper location had 57. In detail, we were able to identify 16 PS lipids, 9 PI, 5 PG, 16 PE, 12 PA, and 26 MGDG for the lower site. A similar trend was noticed for the upper sampling location with 11 PS, 7 PI, 3 PG, 14 PE, 5 PA, and 17 MGDG. Combining both results, 54 lipids were elevated in decomposition soils compared to the control soils (**Supplementary Table 5**).

Comparing the human and pig treatments, we saw that by the second week of decomposition, the metabolite profiles in the soils below human and pigs significantly diverged, and these differences continued through the end of the 22-week experiment (**Supplementary Figures 5**, **6**). To determine if there was a difference between human and pig decomposition products, we identified features that were differentially abundant between human and pig plots. Metabolites that were frequently elevated in human decomposition soils compared to pig soils included 2-oxo-4-methylthiobutanoate, sn-glycerol 3-phosphate and tryptophan; these metabolites were elevated at four or more of our sampling time points (**Figure 8**).

DISCUSSION

Signatures of Decomposition-Impacted Soils

Soils beneath decomposing pigs and humans were impacted in terms of the chemical parameters measured in our study. In contrast to controls, which were not exposed to decomposition, we observed significant changes in pH, nutrients, microbial activity and metabolites. The pH change was variable in response and differed between seasons, with pH being affected more drastically in the summer. It was also notable that the pH change was opposite for pigs and humans; pH increased under pigs, but decreased under humans. This variability in soil pH is important to note because soil pH has been determined to be a predictor of bacterial community structure (Lauber et al., 2009), and thus would ultimately influence the composition of the bacterial decomposer communities. Other studies examining the impact of animal or human decomposition on soils have also reported mixed results with respect to pH. For example, depending on the study, decomposing humans on soil surfaces resulted in decreased pH (Aitkenhead-Peterson et al., 2012) or

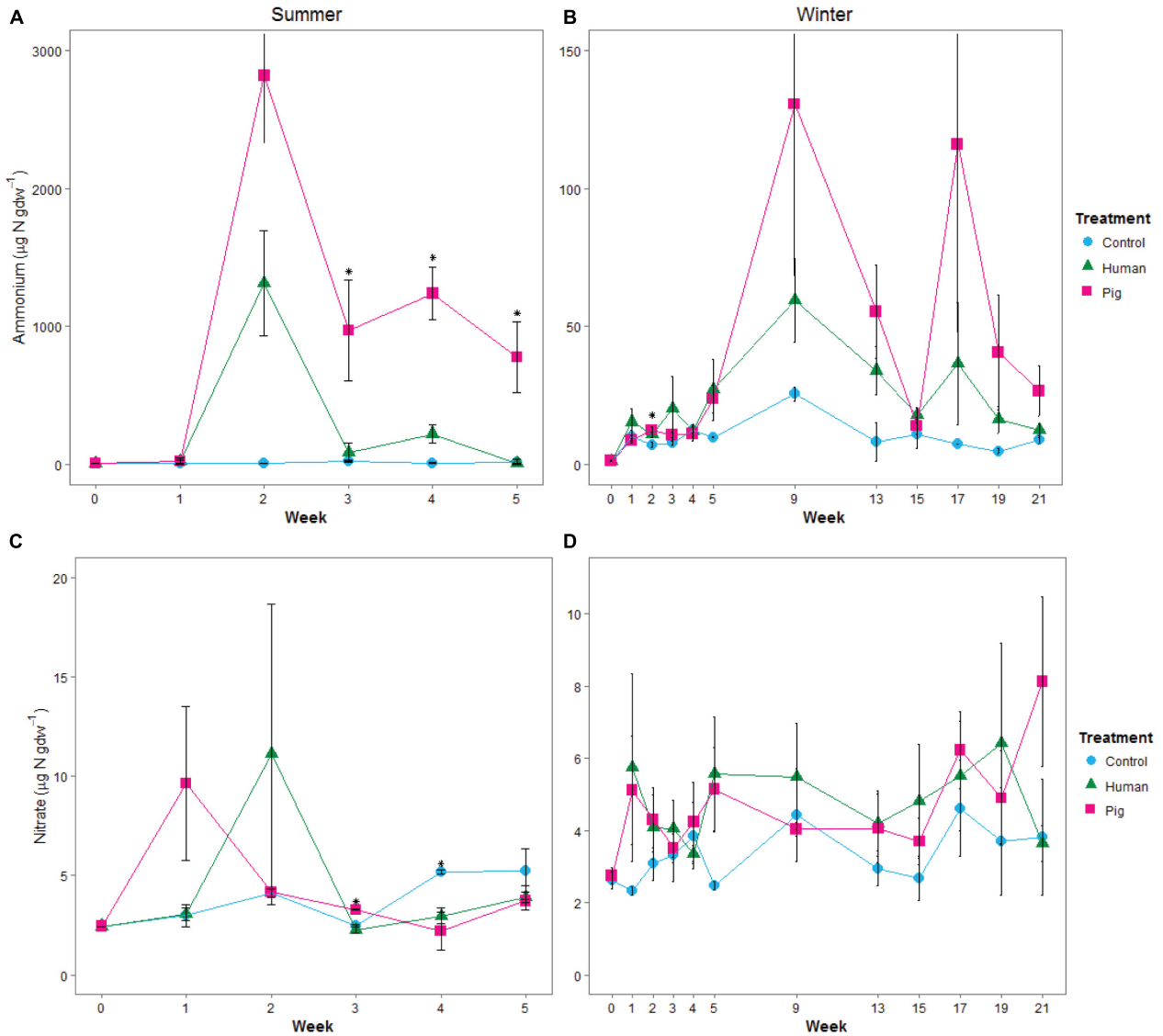

FIGURE 2 | Mean concentrations of ammonium **(A,B)** and nitrate **(C,D)** in soils below decomposing humans and pigs during the summer **(A,C)** and winter **(B,D)** trials. Error bars show standard deviations. Asterisks indicate sample times with significant differences between the three treatments ($p < 0.05$).

no significant change in pH (Cobaugh et al., 2015; Fancher et al., 2017). Decomposing pigs have been reported to increase soil pH (Benninger et al., 2008; Meyer et al., 2013; Szelecz et al., 2018). Decomposing rabbits also resulted in an increase in pH (Quaggiotto et al., 2019). It has also been noted that buried carcasses (both animal and human) generally cause an increase in pH (Hopkins et al., 2000; Wilson et al., 2007; Stokes et al., 2013; Keenan et al., 2018a). Our study has added to the growing body of observations that the response of soil pH to mammalian decomposition is not predictable and seems to depend on species and local environmental and edaphic conditions.

In the decomposition-impacted soils, we observed an expected increase in soil respiration as an indicator of increased microbial metabolism, which correlated with previously published Total Body Score data, a scale used to score extent of visible morphological decomposition (Dautartas et al., 2018). Many of the metabolites enriched in decomposition soils were intermediates of the TCA cycle, the central energy-generating cycle of aerobic organisms, indicating increased aerobic metabolism. We also observed multiple lines of evidence of protein decomposition and ammonification, including increased protease activity and products of proteolysis, including amino acids and ammonium. We were able to detect several amino acids in the decomposition soils, and pathway analysis showed that many of the enriched metabolites in decomposition soils belonged to amino acid pathways. Our observation is consistent with other studies that have detected amino acids in porcine decomposition fluids (Swann et al., 2012), and soils impacted by human and other mammalian decomposition (Vass et al., 2002; Macdonald et al., 2014). In our study, the

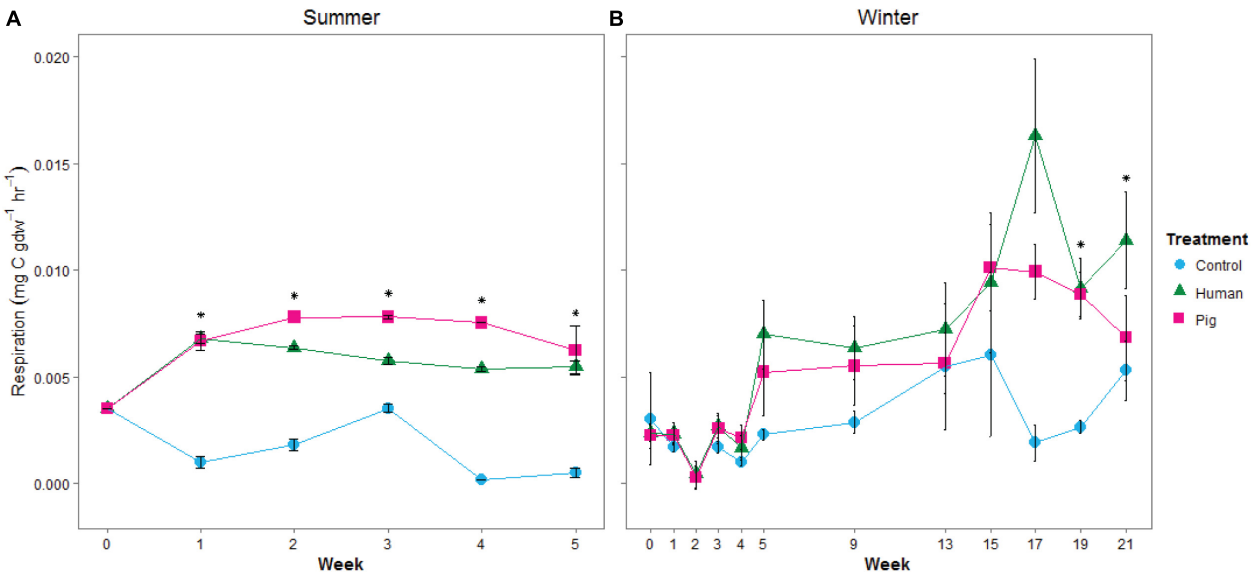

FIGURE 3 | Mean soil respiration rates, estimated from 24-h incubations at 20°C, from soils under decomposing humans and pigs during **(A)** summer and **(B)** winter trials. Error bars show standard deviations. Asterisks indicate significant differences between the three treatments ($p < 0.05$).

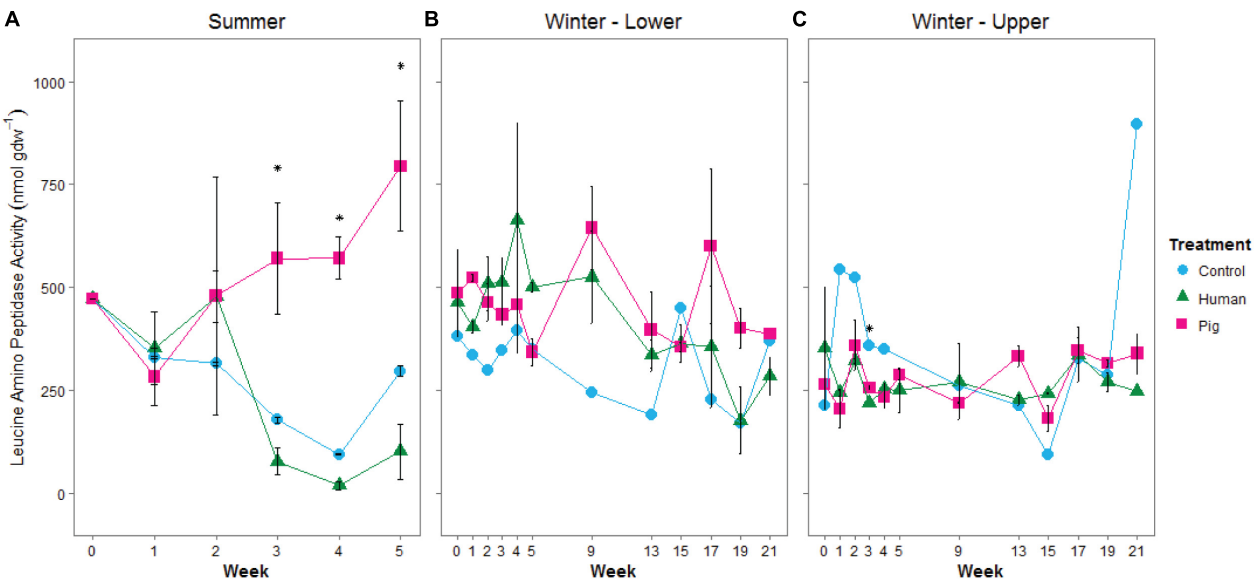

FIGURE 4 | Mean leucine aminopeptidase potential activity in soils below decomposing humans and pigs during summer **(A)** and winter **(B,C)** trials. The lower site **(B)** refers to undisturbed forest soil, while the upper site **(C)** had disturbed soil. Error bars show standard deviations. Asterisks indicated significant differences between the three treatments ($p < 0.05$).

most consistently detected amino acids in decomposition soils (both human and pig) were creatine, alanine, proline, taurine and GABA. Creatine is a non-protein amino acid involved in ATP generation in muscle tissue. Studies with rats and mice have shown marked increases in creatine in blood and tissues over the early (24–72 h) postmortem interval (Dai et al., 2019; Mora-Ortiz et al., 2019). Taurine is particularly abundant in bile and the large intestines of mammals. Alanine and proline are two of the more common amino acids that make up proteins in vertebrates and have been detected in the serum, blood and tissues of mice and rats in the first 72 h postmortem (Sato et al., 2015; Kaszynski et al., 2016; Dai et al., 2019; Mora-Ortiz et al., 2019). While human cell autolytic processes would be responsible for the production of amino acids and ammonium early in decomposition, the elevated microbial respiration and protease activities measured in our soils indicated microbially-mediated decomposition was occurring as well.

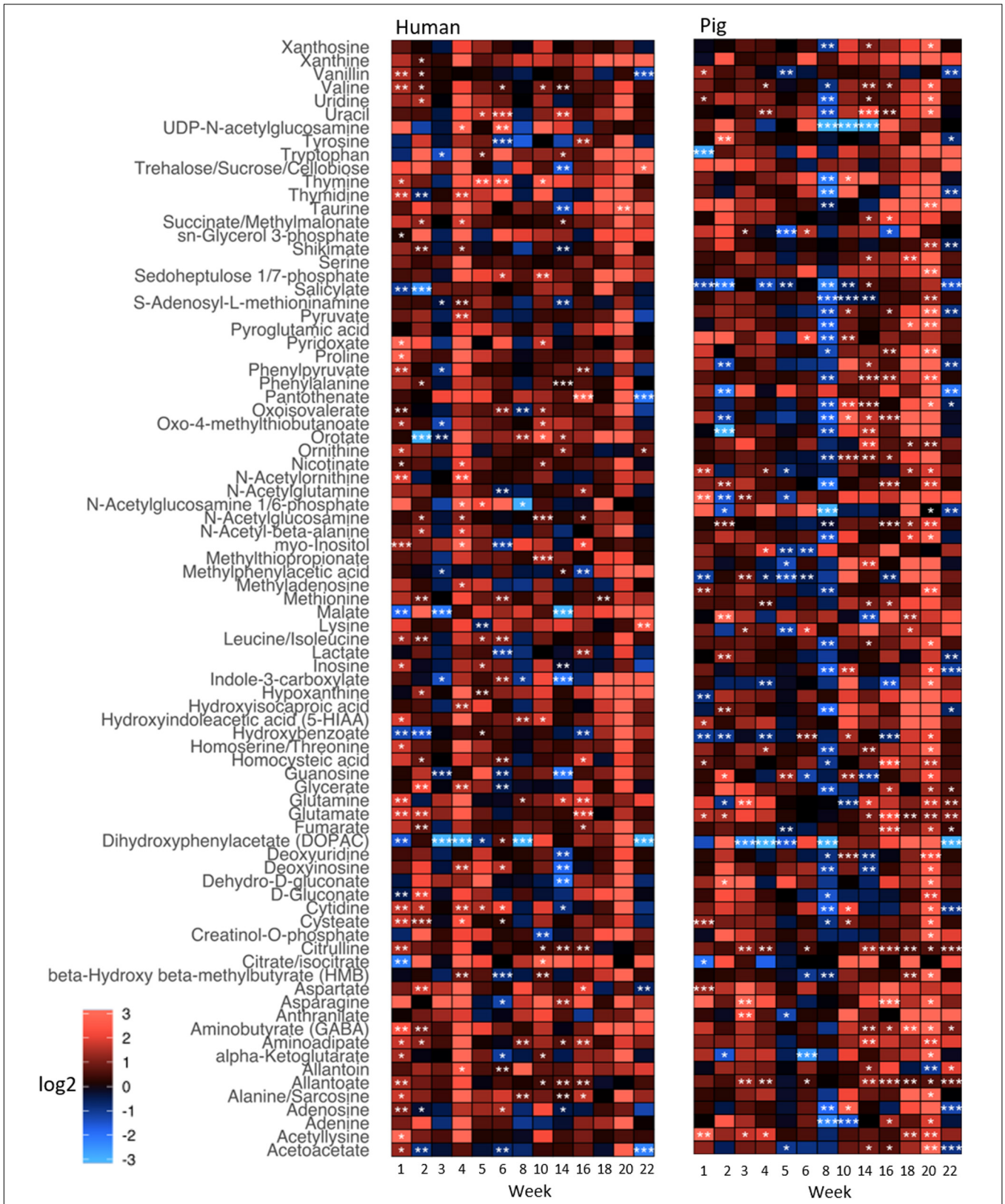

FIGURE 5 | Heatmap depicting relative intensities of metabolites detected in soils below decomposing humans and pigs relative to control soils for the winter trial. Shades of red and blue show an increase and decrease of metabolite intensities, respectively, relative to the control (i.e., fold change). The color scale represents the magnitude of a log2-fold change. Different significance levels (Student's *t*-test) are indicated with asterisks: $*p \leq 0.1$, $**p \leq 0.05$, $***p \leq 0.01$.

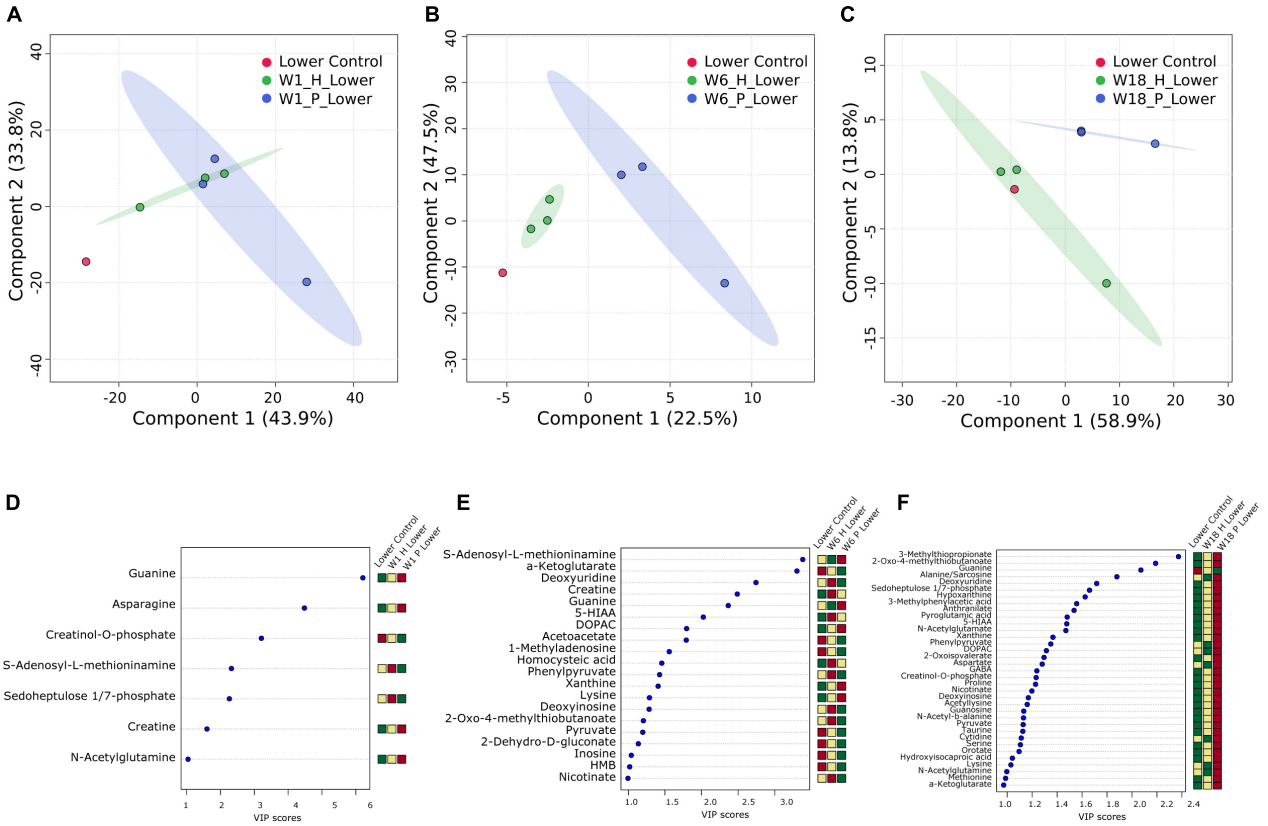

FIGURE 6 | Multivariate analysis of decomposition and control soil from the lower site for week 1 **(A,D)**, week 6 **(B,E)**, and week 18 **(C,F)** for the winter trial. PLS-DA plots **(A–C)** and VIP score plots **(D–F)** for metabolites with VIP > 1 are shown. Heatmaps indicate high (red) and low (green) relative intensity of particular metabolites in human (H) and pig (P) decomposition soil in comparison to control soil.

The proteolytic conversion of proteins into amino acids and ammonium (via both autolytic and microbial-mediated processes) is what ultimately contributes to the pulse of nitrogen introduced to the environment and available to microbes and plants (Macdonald et al., 2014). Ammonium can then be converted to nitrate by nitrification (mediated by nitrifying bacteria and/or archaea); however, only minimal changes in nitrate concentrations were observed here. Elevated ammonium concentrations without a concurrent increase in nitrate concentrations has been consistently observed during the mass loss period of both human and animal carcass decomposition (Macdonald et al., 2014; Cobaugh et al., 2015; Keenan et al., 2018a,b). Longer term studies have noted increases in soil nitrate during skeletonization, once soil oxygen levels have returned and ammonia concentrations have declined (Metcalf et al., 2016; Keenan et al., 2018b; Szelecz et al., 2018), however, our study was not long enough in duration to observe this. Nitrification is an oxygen-dependent process, and elevated respiration in decomposition soils during soft tissue decomposition draws down soil oxygen, limiting nitrification (Geets et al., 2006; Keenan et al., 2018b). In addition, high concentrations of ammonium can be toxic to nitrifying microbes (Vadivelu et al., 2007). Together, our results confirm that mammalian decomposition initially results in enhanced microbial ammonification and limited nitrification in soil during soft tissue decomposition.

Seasonal Differences in Decomposition Soils

We observed different responses in soil physicochemistry between the summer and winter trials. Notably, pH and nutrient concentrations were more affected in summer: Ammonium concentrations were an order of magnitude higher and nitrate concentrations were twice as high in the summer compared to winter. Soil and internal temperatures during the summer study were elevated during the early stages of decomposition, as has been documented in other studies (Keenan et al., 2018b; Quaggiotto et al., 2019), concurrent with the period of peak fly larvae activity. Larval masses have been shown to generate heat in excess of 10°C above ambient temperatures (Weatherbee et al., 2017). Because of warmer temperatures, increased insect activity, and reduced scavenging, decomposition progressed more rapidly in the summer (Dautartas et al., 2018; Steadman et al., 2018). In the winter, lower ambient temperatures and little to no insect activity (Dautartas et al., 2018) resulted in a slower release of decomposition products over time. This would have given the soil microbial populations more time to assimilate and oxidize

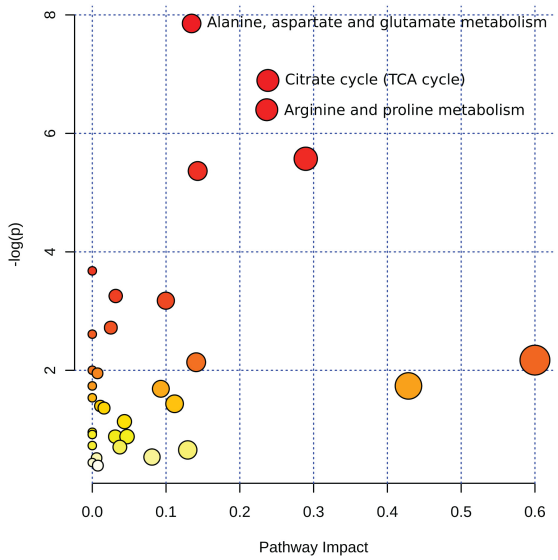

FIGURE 7 | Summary of pathway analysis from 38 metabolites detected in decomposition soil for the winter trial. Circles represent matched pathways according to *p*-values from the pathway enrichment analysis and pathway impact values from the pathway topology analysis. The *x*-axis shows the pathway impact value computed from the pathway topological analysis, also represented by the size of the circle, with larger circles indicating greater pathway impact value. The *y*-axis shows the log of the *p*-values obtained from pathway enrichment analysis, also represented in color, with darker colors indicating lower *p*-values. Alanine, aspartate, and glutamate metabolism: $p < 0.001$, impact value = 0.13462; TCA cycle $p < 0.001$, impact value = 0.23804; arginine and proline metabolism: $p < 0.001$, impact value = 0.23652.

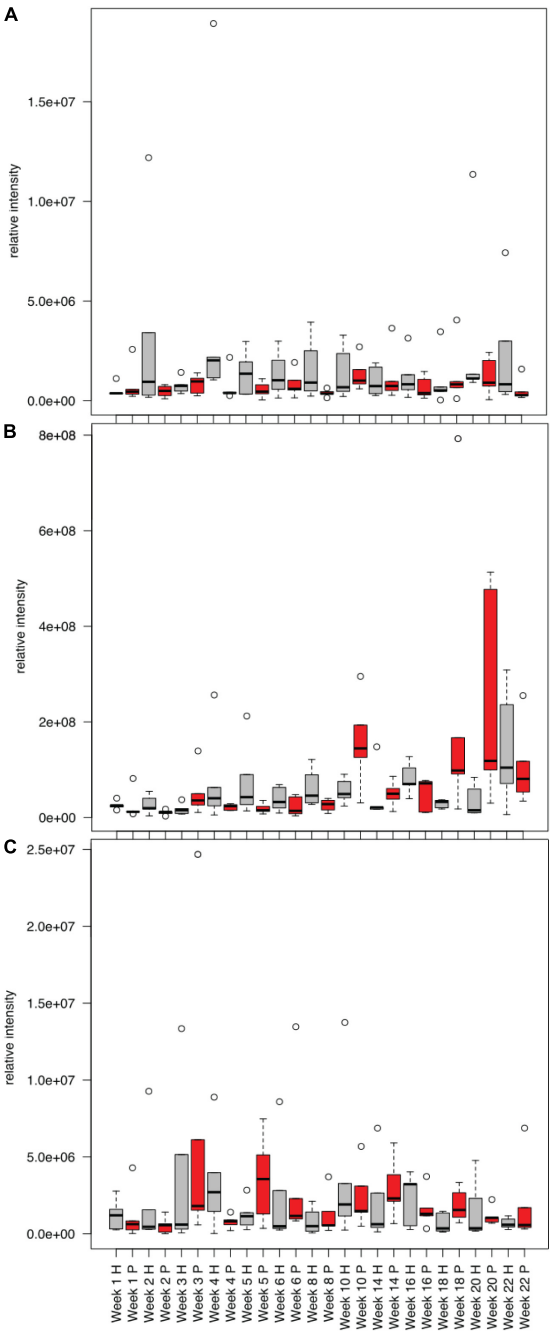

FIGURE 8 | Mean relative intensities of metabolites detected in decomposition soil that were elevated in humans (H, gray) compared to pigs (P, red) for the winter trials: **(A)** sn-glycerol 3-phosphate, **(B)** 2-Oxo-4-methyladenosine, **(C)** tryptophan.

the available ammonium. Interestingly, despite differences in ambient temperatures and decomposition rates between summer and winter, levels of microbial activity (i.e., respiration) were comparable between the two seasons.

The elevated microbial activities corresponded to increased soil temperatures in both trials. It was also notable that despite relatively similar microbial respiration rates, we had higher protease activity in the summer compared to winter. This higher degree of specific protease activity in summer is likely due to the more concentrated pulse of decomposition products in soil over a shorter period of time (i.e., higher substrate concentrations). The large larval masses feeding on the donors in the summer may also have contributed to elevated protease activities, as these larvae are known to secrete proteases (Pinilla et al., 2013). Other decomposition studies have reported seasonal differences in decomposition processes, for example, different microbial community compositions (Breton et al., 2016), number and abundance of volatile organic compounds produced (Forbes et al., 2014) and differential transformation of fatty acids in decomposition fluid (Ueland et al., 2018).

Comparison of Human and Pig Decomposition Soils

The soil biogeochemical responses measured in our study were not the same between pigs and human. Pig decomposition sites had higher ammonium, pH, and LAP activity compared to humans. In addition, the suite of metabolites measured were significantly different between the two species. Metabolites that were frequently elevated in human decomposition soils compared to pig decomposition soils included: 2-Oxo-4-methyladenosine (a modified tRNA), sn-glycerol 3-phosphate

(a component of glycerophospholipids that make up biological membranes) and the amino acid tryptophan. Humans and pigs generally attract similar postmortem insect communities (Matuszewski et al., 2020), so the difference we observed between the two species may be because of more extensive scavenging of humans compared to pigs, which would have diverted more of the resource away from decomposers toward scavengers (Steadman et al., 2018). The differences may also have been due to differences in body composition and/or microbiome between the two species. Pigs tend to have higher moisture content (Carter et al., 2007), which might explain increased microbial activity and mobilization of decomposition products into the soil. Pigs also have higher levels of total saturated fatty acids (Notter et al., 2009) and produce different volatile organic compounds during decomposition (Vass et al., 2008) indicating that different body compositions may influence decomposers and their processes. Both humans and pigs are monogastric omnivores and have similar gut microflora compared to other species (Ley et al., 2008). However, the microbiomes of humans and pigs are not identical, and therefore it could be hypothesized that different microflora, which are active participants in postmortem decomposition, could result in different decomposition rates and pathways/metabolites between the two species.

Importance of Edaphic Properties in Decomposition Response

An unintentional confounding factor in this experiment was discovered once the winter trial was already underway: Some of the subjects had been placed on undisturbed, O/A-horizon soil forest soil, while others were placed on a section where the soil had been disturbed and B horizon subsoil was present. While soil type and parent material were the same, the two sites had different pH and organic matter content. Thus, this allowed us to determine if the starting soil chemistry had an effect on the decomposition response. During decomposition, pH and protease responses were significantly different between the two sites: Decomposition in the soil organic matter (SOM)-rich acidic topsoil resulted in a slight increase in pH and LAP activity, while decomposition in the SOM-poor disturbed subsoil resulted in a slight decrease in pH and LAP activity. This suggests that some of the effects of decomposition on soils may be dependent on soil chemistry or organic matter, and may be an explanation for the inconsistent effects on soil pH that have been previously reported in the literature (Vass et al., 1992; Towne, 2000; Benninger et al., 2008; Aitkenhead-Peterson et al., 2012; Cobaugh et al., 2015; Fancher et al., 2017). SOM can buffer added acids, preventing pH decreases (Jiang et al., 2018), which may explain why we saw an increase in pH in the SOM-rich site and decrease at the SOM-poor site. We additionally show here that protease activity and metabolite profiles were different at the two sites, indicating that the biological communities were also differentially affected.

Study Limitations

As with many field taphonomy studies conducted at anthropology research facilities, we were limited in terms of donor numbers (n = 5 in each treatment group) and spatial constraints (vegetation and terrain) rendered it difficult to sample some soils. Despite best attempts to standardize the placement locations of the donors and carcasses, it was discovered after the winter trial was underway that because of background environmental heterogeneity, there was a significant block (plot) effect that had to be taken into account in the statistical analyses. Finally, storage of the summer trial samples at a higher temperature (−20°C instead of −80°C) left them unsuitable for metabolomics analyses, so unfortunately, we were not able to make a seasonal comparison of metabolomic and lipidomic profiles.

CONCLUSION

A direct comparison of humans and pigs has shown that their decomposition dynamics (Dautartas et al., 2018) and impacts on soils (this study) are not identical. Given the accepted use of animal analogs in forensic taphonomy research, this study further contributes to the growing understanding of limitations with this practice. This work also has implications in ecosystems ecology. Decaying carcasses are an important part of nutrient cycling in ecosystems; differences between species in terms of nutrient redistribution may be important to consider as animal populations change in space and time. Finally, an unintended finding of our study was the differential decomposition response between organic matter rich topsoil and organic matter poor subsoil, demonstrating that microbial and biogeochemical responses may be dependent on local edaphic properties; an aspect which should be investigated in future studies.

DATA AVAILABILITY STATEMENT

The datasets generated for this study can be found in the **Supplementary Material** and in online repositories. The names of the repository/repositories and accession number(s) can be found below: MetaboLights Database, (https://www.ebi.ac.uk/metabolights) under ID MTBLS2254.

ETHICS STATEMENT

The studies involving human participants were reviewed and approved by University of Tennessee Institutional Review Board. Written informed consent for participation was not required for this study in accordance with the national legislation and the institutional requirements. The animal study was reviewed and approved by University of Tennessee Institutional Animal Care and Use Committee. Written informed consent was obtained from the owners for the participation of their animals in this study.

AUTHOR CONTRIBUTIONS

The study was conceived by JD, DS, AM, and GV. Resources were provided by JD, DS, AM, and SC. Field experiments, sampling, and laboratory analyses were conducted by JD, AD, JS, MM, and SB. Metabolomics and lipidomics laboratory and data analyses were conducted by KH, MM, SD, HC, and KH. Data analysis was conducted by JD, KH, LT, JS, and AD. Manuscript writing was led by JD, KH, and LT with input from all authors.

FUNDING

This work was funded by NSF Award 1549726 to JD, NIJ Grant #2013-DN-BX-K037 to DS, AM, and JD, and NIJ Grant # 2018-DU-BX-0180 to DS, JD, and SC. NSF REU Site Awards 1156644 supported MM (2015), and CHE-1262767 supported both MM (2014) and KH (2015). Publication fees were granted by the University of Tennessee Libraries Open Publishing Support Fund.

ACKNOWLEDGMENTS

We thank the donors and their families, and the support of the University of Tennessee Forensic Anthropology Center personnel. We also thank S. Schaeffer, R. York, and D. Williams for their assistance in laboratory analyses and soil sampling.

SUPPLEMENTARY MATERIAL

The Supplementary Material for this article can be found online at: https://www.frontiersin.org/articles/10.3389/fmicb.2020.608856/full#supplementary-material

REFERENCES

Aitkenhead-Peterson, J. A., Owings, C. G., Alexander, M. B., Larison, N., and Bytheway, J. A. (2012). Mapping the lateral extent of human cadaver decomposition with soil chemistry. *Forensic Sci. Int.* 216, 127–134. doi: 10.1016/j.forsciint.2011.09.007

Barton, P., Cunningham, S., Lindenmayer, D., and Manning, A. (2012). The role of carrion in maintaining biodiversity and ecological processes in terrestrial ecosystems. *Oecologia* 171, 761–772. doi: 10.1007/s00442-012-2460-3

Barton, P. S., Cunningham, S., Macdonald, B., McIntyre, S., Lindenmayer, D., and Manning, A. (2013a). Species traits predict assemblage dynamics at ephemeral resource patches created by carrion. *PLoS One* 8:e53961. doi: 10.1371/journal.pone.0053961

Barton, P. S., Cunningham, S. A., Lindenmayer, D. B., and Manning, A. D. (2013b). The role of carrion in maintaining biodiversity and ecological processes in terrestrial ecosystems. *Oecologia* 171, 761–772. doi: 10.1007/s00442-012-2460-3

Barton, P. S., McIntyre, S., Evans, M. J., Bump, J. K., Cunningham, S. A., and Manning, A. D. (2016). Substantial long-term effects of carcass addition on soil and plants in a grassy eucalypt woodland. *Ecosphere* 7:11. doi: 10.1002/ecs2.1537

Bell, C. W., Fricks, B. E., Rocca, J. D., Steinweg, J. M., McMahon, S. K., and Wallenstein, M. D. (2013). High-throughput fluorometric measurement of potential soil extracellular enzyme activities. *J. Vis. Exp.* 81:e50961. doi: 10.3791/50961

Benninger, L. A., Carter, D. O., and Forbes, S. L. (2008). The biochemical alteration of soil beneath a decomposing carcass. *Forensic Sci. Int.* 180, 70–75. doi: 10.1016/j.forsciint.2008.07.001

Bligh, E. G., and Dyer, W. J. (1959). A rapid method of total lipid extraction and purification. *Can. J. Biochem. Physiol.* 37, 911–917. doi: 10.1139/o59-099

Breton, H., Kirkwood, A. E., Carter, D. O., and Forbes, S. L. (2016). The impact of carrion decomposition on the fatty acid methyl ester (FAME) profiles of soil microbial communities in southern Canada. *Can. Soc. Forensic Sci. J.* 49, 1–18. doi: 10.1080/00085030.2015.1108036

Bump, J., Webster, C., Vucetich, J., Peterson, R., Shields, J., and Powers, M. (2009). Ungulate carcasses perforate ecological filters and create biogeochemical hotspots in forest herbaceous layers allowing trees a competitive advantage. *Ecosystems* 12, 996–1007. doi: 10.1007/s10021-009-9274-0

Carter, D., and Tibbett, M. (2003). Taphonomic mycota: fungi with forensic potential. *J. Forensic Sci.* 48, 1–4. doi: 10.1520/JFS2002169

Carter, D., Yellowlees, D., and Tibbett, M. (2007). Cadaver decomposition in terrestrial ecosystems. *Naturwissenschaften* 94, 12–24. doi: 10.1007/s00114-006-0159-1

Carter, D., Yellowlees, D., and Tibbett, M. (2010). Moisture can be the dominant environmental parameter governing cadaver decomposition in soil. *Forensic Sci. Int.* 200, 60–66. doi: 10.1016/j.forsciint.2010.03.031

Chambers, M. C., Maclean, B., Burke, R., Amodei, D., Ruderman, D. L., Neumann, S., et al. (2012). A cross-platform toolkit for mass spectrometry and proteomics. *Nat. Biotech.* 30, 918–920. doi: 10.1038/nbt.2377

Chong, J., Yamamoto, M., and Xia, J. G. (2019). Metaboanalystr 2.0: from raw spectra to biological insights. *Metabolites* 9:10. doi: 10.3390/metabo9030057

Clasquin, M. F., Melamud, E., and Rabinowitz, J. D. (2012). LC-MS data processing with MAVEN: a metabolomic analysis and visualization engine. *Curr. Protoc. Bioinformatics* 37, 14.11.1–14.11.23. doi: 10.1002/0471250953.bi1411s37

Cobaugh, K. L., Schaeffer, S. M., and DeBruyn, J. M. (2015). Functional and structural succession of soil microbial communities below decomposing human cadavers. *PLoS One* 10:e0130201. doi: 10.1371/journal.pone.0130201

Connor, M., Baigent, C., and Hansen, E. S. (2018). Testing the use of pigs as human proxies in decomposition studies. *J. Forensic Sci.* 63, 1350–1355. doi: 10.1111/1556-4029.13727

Dai, X. H., Fan, F., Ye, Y., Lu, X., Chen, F., Wu, Z. G., et al. (2019). An experimental study on investigating the postmortem interval in dichlorvos poisoned rats by GC/MS-based metabolomics. *Legal Med.* 36, 28–36. doi: 10.1016/j.legalmed.2018.10.002

Damann, F. E., Tanittaisong, A., and Carter, D. O. (2012). Potential carcass enrichment of the University of Tennessee Anthropology Research Facility: a baseline survey of edaphic features. *Forensic Sci. Int.* 222, 4–10. doi: 10.1016/j.forsciint.2012.04.028

Dautartas, A., Kenyhercz, M. W., Vidoli, G. M., Meadows Jantz, L., Mundorff, A., and Steadman, D. W. (2018). Differential decomposition among pig, rabbit, and human remains. *J. Forensic Sci.* 63, 1673–1683. doi: 10.1111/1556-4029.13784

Doane, T. A., and Horwáth, W. R. (2003). Spectrophotometric determination of nitrate with a single reagent. *Anal. Lett.* 36, 2713–2722. doi: 10.1081/AL-120024647

Fancher, J. P., Aitkenhead-Peterson, J. A., Farris, T., Mix, K., Schwab, A. P., Wescott, D. J., et al. (2017). An evaluation of soil chemistry in human cadaver decomposition islands: potential for estimating postmortem interval (PMI). *Forensic Sci. Int.* 279, 130–139. doi: 10.1016/j.forsciint.2017.08.002

Finley, S. J., Pechal, J. L., Benbow, M. E., Robertson, B. K., and Javan, G. T. (2016). Microbial signatures of cadaver gravesoil during decomposition. *Microb. Ecol.* 71, 524–529. doi: 10.1007/s00248-015-0725-1

Forbes, S. L., Perrault, K. A., Stefanuto, P. H., Nizio, K. D., and Focant, J. F. (2014). Comparison of the decomposition VOC profile during winter and summer in a moist, mid-latitude (cfb) climate. *PLoS One* 9:11. doi: 10.1371/journal.pone.0113681

Forger, L. V., Woolf, M. S., Simmons, T. L., Swall, J. L., and Singh, B. (2019). A eukaryotic community succession based method for postmortem

interval (PMI) estimation of decomposing porcine remains. *Forensic Sci. Int.* 302:109838. doi: 10.1016/j.forsciint.2019.05.054

Geets, J., Boon, N., and Verstraete, W. (2006). Strategies of aerobic ammonia-oxidizing bacteria for coping with nutrient and oxygen fluctuations. *FEMS Microbiol. Ecol.* 58, 1–13. doi: 10.1111/j.1574-6941.2006.00170.x

Hauther, K., Cobaugh, K., Jantz, L., Sparer, T., and Debruyn, J. (2015). Estimating time since death from postmortem human gut microbial communities. *J. Forensic Sci.* 60, 1234–1240. doi: 10.1111/1556-4029.12828

Hernandes, V. V., Barbas, C., and Dudzik, D. (2017). A review of blood sample handling and pre-processing for metabolomics studies. *Electrophoresis* 38, 2232–2241. doi: 10.1002/elps.201700086

Hopkins, D., Wiltshire, P., and Turner, B. (2000). Microbial characteristics of soils from graves: an investigation at the interface of soil microbiology and forensic science. *Appl. Soil Ecol.* 14, 283–288. doi: 10.1016/S0929-1393(00)00063-9

Howard, G., Duos, B., and Watson-Horzelski, E. (2010). Characterization of the soil microbial community associated with the decomposition of a swine carcass. *Int. Biodeterior. Biodegradation* 64, 300–304. doi: 10.1016/j.ibiod.2010.02.006

Jiang, J., Wang, Y. P., Yu, M. X., Cao, N. N., and Yan, J. H. (2018). Soil organic matter is important for acid buffering and reducing aluminum leaching from acidic forest soils. *Chem. Geol.* 501, 86–94. doi: 10.1016/j.chemgeo.2018.10.009

Johnson, H. R., Trinidad, D. D., Guzman, S., Khan, Z., Parziale, J. V., DeBruyn, J. M., et al. (2016). A machine learning approach for using the postmortem skin microbiome to estimate the postmortem interval. *PLoS One* 11:e0167370. doi: 10.1371/journal.pone.0167370

Kaszynski, R. H., Nishiumi, S., Azuma, T., Yoshida, M., Kondo, T., Takahashi, M., et al. (2016). Postmortem interval estimation: a novel approach utilizing gas chromatography/mass spectrometry-based biochemical profiling. *Anal. Bioanal. Chem.* 408, 3103–3112. doi: 10.1007/s00216-016-9355-9

Keenan, S. W., Emmons, A. L., Taylor, L. S., Phillips, G., Mason, A. R., Mundorff, A. Z., et al. (2018a). Spatial impacts of a multi-individual grave on microbial and microfaunal communities and soil biogeochemistry. *PLoS One* 13:e0208845. doi: 10.1371/journal.pone.0208845

Keenan, S. W., Schaeffer, S. M., and DeBruyn, J. M. (2019). Spatial changes in soil stable isotopic composition in response to carrion decomposition. *Biogeosciences* 16, 3929–3939. doi: 10.5194/bg-16-3929-2019

Keenan, S. W., Schaeffer, S. M., Jin, V. L., and DeBruyn, J. M. (2018b). Mortality hotspots: nitrogen cycling in forest soils during vertebrate decomposition. *Soil Biol. Biochem.* 121, 165–176. doi: 10.1016/j.soilbio.2018.03.005

Lauber, C., Metcalf, J., Keepers, K., Ackermann, G., Carter, D., and Knight, R. (2014). Vertebrate decomposition is accelerated by soil microbes. *Appl. Environ. Microbiol.* 80, 4920–4929. doi: 10.1128/AEM.00957-14

Lauber, C. L., Hamady, M., Knight, R., and Fierer, N. (2009). Pyrosequencing-based assessment of soil ph as a predictor of soil bacterial community structure at the continental scale. *Appl. Environ. Microbiol.* 75:5111. doi: 10.1128/AEM.00335-09

Ley, R. E., Hamady, M., Lozupone, C., Turnbaugh, P. J., Ramey, R. R., Bircher, J. S., et al. (2008). Evolution of mammals and their gut microbes. *Science* 320, 1647–1651. doi: 10.1126/science.1155725

Lu, W., Clasquin, M. F., Melamud, E., Amador-Noguez, D., Caudy, A. A., and Rabinowitz, J. D. (2010). Metabolomic analysis via reversed-phase ion-pairing liquid chromatography coupled to a stand alone orbitrap mass spectrometer. *Anal. Chem.* 82, 3212–3221. doi: 10.1021/ac902837x

Macdonald, B. C. T., Farrell, M., Tuomi, S., Barton, P. S., Cunningham, S. A., and Manning, A. D. (2014). Carrion decomposition causes large and lasting effects on soil amino acid and peptide flux. *Soil Biol. Biochem.* 69, 132–140. doi: 10.1016/j.soilbio.2013.10.042

Martens, L., Chambers, M., Sturm, M., Kessner, D., Levander, F., Shofstahl, J., et al. (2011). Mzml—a community standard for mass spectrometry data. *Mol. Cell. Proteomics* 10:R110.000133. doi: 10.1074/mcp.R110.000133

Matuszewski, S., Hall, M. J. R., Moreau, G., Schoenly, K. G., Tarone, A. M., and Villet, M. H. (2020). Pigs vs people: the use of pigs as analogues for humans in forensic entomology and taphonomy research. *Int. J. Legal Med.* 134, 793–810. doi: 10.1007/s00414-019-02074-5

Megyesi, M. S., Nawrocki, S. P., and Haskell, N. H. (2005). Using accumulated degree-days to estimate the postmortem interval from decomposed human remains. *J. Forensic Sci.* 50, 618–626. doi: 10.1520/JFS2004017

Melamud, E., Vastag, L., and Rabinowitz, J. D. (2010). Metabolomic analysis and visualization engine for LC-MS data. *Anal. Chem.* 82, 9818–9826. doi: 10.1021/ac1021166

Metcalf, J., Wegener Parfrey, L., Gonzalez, A., Lauber, C., Knights, D., Ackermann, G., et al. (2013). A microbial clock provides an accurate estimate of the postmortem interval in a mouse model system. *eLife* 2:e01104. doi: 10.7554/eLife.01104.016

Metcalf, J. L., Xu, Z. Z., Weiss, S., Lax, S., Van Treuren, W., Hyde, E. R., et al. (2016). Microbial community assembly and metabolic function during mammalian corpse decomposition. *Science* 351:158. doi: 10.1126/science.aad2646

Meyer, J., Anderson, B., and Carter, D. (2013). Seasonal variation of carcass decomposition and gravesoil chemistry in a cold (Dfa) climate. *J. Forensic Sci.* 58, 1175–1182. doi: 10.1111/1556-4029.12169

Mora-Ortiz, M., Trichard, M., Oregioni, A., and Claus, S. P. (2019). Thanatometabolomics: introducing nmr-based metabolomics to identify metabolic biomarkers of the time of death. *Metabolomics* 15:11. doi: 10.1007/s11306-019-1498-1

Mueller, L. O., Borstein, S. R., Tague, E. D., Dearth, S. P., Castro, H. F., Campagna, S. R., et al. (2020). Populations of populus angustifolia have evolved distinct metabolic profiles that influence their surrounding soil. *Plant Soil* 448, 399–411. doi: 10.1007/s11104-019-04405-2

Notter, S. J., Stuart, B. H., Rowe, R., and Langlois, N. (2009). The initial changes of fat deposits during the decomposition of human and pig remains. *J. Forensic Sci.* 54, 195–201. doi: 10.1111/j.1556-4029.2008.00911.x

Parmenter, R. R., and MacMahon, J. A. (2009). Carrion decomposition and nutrient cycling in a semiarid shrub–steppe ecosystem. *Ecol. Monogr.* 79, 637–661. doi: 10.1890/08-0972.1

Pechal, J., Crippen, T., Tarone, A., Lewis, A., Tomberlin, J., and Benbow, M. (2013). Microbial community functional change during vertebrate carrion decomposition. *PLoS One* 8:e79035. doi: 10.1371/journal.pone.0079035

Pinilla, Y. T., Moreno-Perez, D. A., Patarroyo, M. A., and Bello, F. J. (2013). Proteolytic activity regarding *S. magellanica* (diptera: Calliphoridae) larval excretions and secretions. *Acta Trop.* 128, 686–691. doi: 10.1016/j.actatropica.2013.09.020

Pinto, J., Domingues, M. R. M., Galhano, E., Pita, C., Almeida, M. D., Carreira, I. M., et al. (2014). Human plasma stability during handling and storage: impact on nmr metabolomics. *Analyst* 139, 1168–1177. doi: 10.1039/C3AN02188B

Quaggiotto, M. M., Evans, M. J., Higgins, A., Strong, C., and Barton, P. S. (2019). Dynamic soil nutrient and moisture changes under decomposing vertebrate carcasses. *Biogeochemistry* 146, 71–82. doi: 10.1007/s10533-019-00611-3

Rabinowitz, J. D., and Kimball, E. (2007). Acidic acetonitrile for cellular metabolome extraction from *Escherichia coli*. *Anal. Chem.* 79, 6167–6173. doi: 10.1021/ac070470c

Randewig, D., Marshall, J. D., Nasholm, T., and Jamtgard, S. (2019). Combining microdialysis with metabolomics to characterize the in situ composition of dissolved organic compounds in boreal forest soil. *Soil Biol. Biochem.* 136:9. doi: 10.1016/j.soilbio.2019.107530

Reed, H. (1958). A study of dog carcass communities in Tennessee, with special reference to the insects. *Am. Midl. Nat.* 59, 213–245. doi: 10.2307/2422385

Rhine, E. D., Sims, G. K., Mulvaney, R. L., and Pratt, E. J. (1998). Improving the berthelot reaction for determining ammonium in soil extracts and water. *Soil Sci. Soc. Am. J.* 62, 473–480. doi: 10.2136/sssaj1998.03615995006200020026x

Risch, A. C., Frossard, A., Schutz, M., Frey, B., Morris, A. W., and Bump, J. K. (2020). Effects of elk and bison carcasses on soil microbial communities and ecosystem functions in Yellowstone. *USA. Funct. Ecol.* 34, 1933–1944. doi: 10.1111/1365-2435.13611

Sato, T., Zaitsu, K., Tsuboi, K., Nomura, M., Kusano, M., Shima, N., et al. (2015). A preliminary study on postmortem interval estimation of suffocated rats by gc-ms/ms-based plasma metabolic profiling. *Anal. Bioanal. Chem.* 407, 3659–3665. doi: 10.1007/s00216-015-8584-7

Schoenly, K., and Reid, W. (1987). Dynamics of heterotrophic succession in carrion arthropod assemblages: discrete seres or a continuum of change? *Oecologia* 73, 192–202. doi: 10.1007/BF00377507

Schoenly, K. G., Haskell, N. H., Hall, R. D., and Gbur, J. R. (2007). Comparative performance and complementarity of four sampling methods and arthropod preference tests from human and porcine remains at the Forensic Anthropology Center in Knoxville, Tennessee. *J. Med. Entomol.* 44, 881–894. doi: 10.1093/jmedent/44.5.881

Singh, B., Minick, K. J., Strickland, M. S., Wickings, K. G., Crippen, T. L., Tarone, A. M., et al. (2018). Temporal and spatial impact of human cadaver decomposition on soil bacterial and arthropod community structure and function. *Front. Microbiol.* 8:02616. doi: 10.3389/fmicb.2017.02616

Steadman, D. W., Dautartas, A., Kenyhercz, M. W., Jantz, L. M., Mundorff, A., and Vidoli, G. M. (2018). Differential scavenging among pig, rabbit, and human subjects. *J. Forensic Sci.* 63, 1684–1691. doi: 10.1111/1556-4029.13786

Stokes, K. L., Forbes, S. L., and Tibbett, M. (2013). Human versus animal: contrasting decomposition dynamics of mammalian analogues in experimental taphonomy. *J. Forensic Sci.* 58, 583–591. doi: 10.1111/1556-4029.12115

Swann, L. M., Busetti, F., and Lewis, S. W. (2012). Determination of amino acids and amines in mammalian decomposition fluid by direct injection liquid chromatography-electrospray ionisation-tandem mass spectrometry. *Anal. Methods* 4, 363–370. doi: 10.1039/C1AY05447C

Szelecz, I., Koenig, I., Seppey, C. V. W., Le Bayon, R. C., and Mitchell, E. A. D. (2018). Soil chemistry changes beneath decomposing cadavers over a one-year period. *Forensic Sci. Int.* 286, 155–165. doi: 10.1016/j.forsciint.2018.02.031

Szelecz, I., Sorge, F., Seppey, C. V. W., Mulot, M., Steel, H., Neilson, R., et al. (2016). Effects of decomposing cadavers on soil nematode communities over a one-year period. *Soil Biol. Biochem.* 103, 405–416. doi: 10.1016/j.soilbio.2016.09.011

Taylor, L. S., Phillips, G., Bernard, E. C., and DeBruyn, J. M. (2020). Soil nematode functional diversity, successional patterns, and indicator taxa associated with vertebrate decomposition hotspots. *PLoS One* 15:e0241777. doi: 10.1371/journal.pone.0241777

Tibbett, M., and Carter, D. O. (2003). Mushrooms and taphonomy: the fungi that mark woodland graves. *Mycologist* 17, 20–24. doi: 10.1017/S0269915X03001150

Towne, E. G. (2000). Prairie vegetation and soil nutrient responses to ungulate carcasses. *Oecologia* 122, 232–239. doi: 10.1007/PL00008851

Ueland, M., Forbes, S. L., and Stuart, B. H. (2018). Seasonal variation of fatty acid profiles from textiles associated with decomposing pig remains in a temperate Australian environment. *Forensic Chem.* 11, 120–127. doi: 10.1016/j.forc.2018.10.008

Vadivelu, V. M., Keller, J., and Yuan, Z. (2007). Free ammonia and free nitrous acid inhibition on the anabolic and catabolic processes of nitrosomonas and nitrobacter. *Water Sci. Technol.* 56, 89–97. doi: 10.2166/wst.2007.612

van Klink, R., Van Laar-Wiersma, J., Vorst, O., and Smit, C. (2020). Rewilding with large herbivores: positive direct and delayed effects of carrion on plant and arthropod communities. *PLoS One* 15:17. doi: 10.1371/journal.pone.0226946

Vass, A. A., Barshick, S. A., Sega, G., Caton, J., Skeen, J. T., Love, J. C., et al. (2002). Decomposition chemistry of human remains: a new methodology for determining the postmortem interval. *J. Forensic Sci.* 47, 542–553.

Vass, A. A., Bass, W. M., Wolt, J. D., Foss, J. E., and Ammons, J. T. (1992). Time since death determinations of human cadavers using soil solution. *J. Forensic Sci.* 37, 1236–1253. doi: 10.1520/JFS13311J

Vass, A. A., Smith, R. R., Thompson, C. V., Burnett, M. N., Dulgerian, N., and Eckenrode, B. A. (2008). Odor analysis of decomposing buried human remains. *J. Forensic Sci.* 53, 384–391. doi: 10.1111/j.1556-4029.2008.00680.x

von der Lühe, B., Fiedler, S., Mayes, R. W., and Dawson, L. (2017). Temporal fatty acid profiles of human decomposition fluid in soil. *Org. Geochem.* 111, 26–33. doi: 10.1016/j.orggeochem.2017.06.004

Wang, Y., Ma, M. Y., Jiang, X. Y., Wang, J. F., Li, L. L., Yina, X. J., et al. (2017). Insect succession on remains of human and animals in Shenzhen, China. *Forensic Sci. Int.* 271, 75–86. doi: 10.1016/j.forsciint.2016.12.032

Weatherbee, C. R., Pechal, J. L., and Benbow, M. E. (2017). The dynamic maggot mass microbiome. *Ann. Entomol. Soc. Am.* 110, 45–53. doi: 10.1093/aesa/saw088

Wickham, H. (2009). *ggplot2: Elegant Graphics for Data Analysis*. New York: Springer, 182. doi: 10.1007/978-0-387-98141-3

Wilson, A., Janaway, R., Holland, A., Dodson, H., Baran, E., Pollard, A. M., et al. (2007). Modelling the buried human body environment in upland climes using three contrasting field sites. *Forensic Sci. Int.* 169, 6–18. doi: 10.1016/j.forsciint.2006.07.023

Withers, E., Hill, P. W., Chadwick, D. R., and Jones, D. L. (2020). Use of untargeted metabolomics for assessing soil quality and microbial function. *Soil Biol. Biochem.* 143:9. doi: 10.1016/j.soilbio.2020.107758

Yang, L., Edwards, K., Byrnes, J., Bastow, J., Wright, A., and Spence, K. (2010). A meta-analysis of resource pulse– consumer interactions. *Ecol. Monogr.* 80, 125–151. doi: 10.1890/08-1996.1

Conflict of Interest: The authors declare that the research was conducted in the absence of any commercial or financial relationships that could be construed as a potential conflict of interest.

frontiers in Ecology and Evolution

REVIEW
published: 04 March 2021
doi: 10.3389/fevo.2021.630397

Microbiome in Death and Beyond: Current Vistas and Future Trends

Dipayan Roy[1], Sojit Tomo[1], Purvi Purohit[1] and Puneet Setia[2]**

[1] Department of Biochemistry, All India Institute of Medical Sciences, Jodhpur, Jodhpur, India, [2] Department of Forensic Medicine and Toxicology, All India Institute of Medical Sciences, Jodhpur, Jodhpur, India

Forensic medicine has, for a long time, been relying on biochemical, anthropologic, and histopathologic evidences in solving various investigations. However, depending on the method used, lengthy sample processing time, scanty sample, and less sensitivity and accuracy pervade these procedures. Accordingly, newer arenas such as the thanatomicrobiome have come forward to aid in its quandaries; furthermore, the parallel advances in genomic and proteomic techniques have complemented and are still emerging to be used in forensic experiments and investigations. Postmortem interval (PMI) is one of the most important aspects of medico-legal investigations. The current trend in PMI estimation is toward genomic analyses of autopsy samples. Similarly, determination of cause of death, although a domain of medical sciences, is being targeted as the next level of forensic casework. With the current trend in laboratory sciences moving to the discovery of newer disease-specific markers for diagnostic and prognostic purposes, the same is being explored for the determination of the cause of death by using techniques such as Real-Time PCR, DNA micro-array, to Next-Gen Sequencing. Establishing an individual's biological profile has been done using medicolegal methods and anthropology as well as bar-bodies/Davidson bodies (gender determination); and in cases where the determination of age/gender is a challenge using morphological characteristics; the recent advances in the field of genomics and proteomics have played a significant role, e.g., use of mitochondrial DNA in age estimation and in maternity disputes. The major hurdle forensic medical research faces is the fact that most of the studies are conducted in animal models, which are often difficult to mimic in human and real-time scenarios. Additionally, the high accuracy required in criminal investigations to be used in a court of law as evidence has prevented these results to come out of the labs and be used to the optimum. The current review aims at giving a comprehensive and critical account of the various molecular biology techniques including "thanatogenomics," currently being utilized in the veritable fields of forensic medicine.

Keywords: postmortem interval (PMI), next-generation sequencing, thanatomicrobiome, thanatogenomics, thanatoproteomics, postmortem submersion interval, microbial clock, gut microbiome

OPEN ACCESS

Edited by:
Gulnaz T. Javan, Alabama State University, United States

Reviewed by:
Matteo Moretti, University of Pavia, Italy
Eric Crubezy, Université Toulouse III - Paul Sabatier, France

****Correspondence:***
Purvi Purohit
dr.purvipurohit@gmail.com
Puneet Setia
puneetsetia@gmail.com

Specialty section:
This article was submitted to Evolutionary and Population Genetics, a section of the journal Frontiers in Ecology and Evolution

Received: *17 November 2020*
Accepted: *29 January 2021*
Published: *04 March 2021*

Citation:
Roy D, Tomo S, Purohit P and Setia P (2021) Microbiome in Death and Beyond: Current Vistas and Future Trends. Front. Ecol. Evol. 9:630397. doi: 10.3389/fevo.2021.630397

INTRODUCTION

Death eventuates the emergence of a vast, complex ecosystem. The natural process of decomposition after death comprises of physical and biochemical changes that provide critical information about time since death, location, and manner of death. Understanding this process entails an understanding of the human genetic, physiologic, metabolic, and, most importantly, environmental diversity imparted and shared by our microbial cohabitants. The term microbiome was suggested by Lederberg "to signify the ecological community of commensal, symbiotic, and pathogenic microorganisms that share our body space" (Lederberg and McCray, 2001; NIH HMP Working Group et al., 2009). The substantially sizeable spatiotemporal diversity of the human microbiome is not only dynamic but also often predictable, which makes them potential candidates to serve as markers for various intrinsic and extrinsic factors (Grice and Segre, 2011; Human Microbiome Project Consortium, 2012a; David et al., 2014; Chevalier et al., 2015; Zhou and Bian, 2018). On the one hand, they influence our health and disease predispositions and, on the other hand, play an essential role in the decay process (Hyde et al., 2013). It has revolutionized our perception of the complex dynamics that unfold after death.

Earlier, much of our knowledge used to come from culture-based approaches which, although species-specific, cannot account for the majority of the uncultivable microbes and their diversity (Zhou et al., 2004; Bik et al., 2006). The advent of high-throughput or next-generation sequencing (NGS) has brought about the necessary alternative to study the human microbiome as well as expand its practice in forensic genetic investigations. Metagenomic sequencing studies carried out as part of the Human Microbiome Project have helped us identify several body sites harboring complex and significantly different microbial communities within and among individuals (Human Microbiome Project Consortium, 2012a).

Thanatomicrobiome is the microbial community associated with the host after its death and is named after the Greek god of death, Thanatos (Javan et al., 2016a). It characterizes the microbial succession in and around dead biomass and contributes significantly to modulating decomposition (Javan et al., 2017). In parallel, the potential of using genomic data in forensic medicine has increased manifold, giving rise to thanatogenomics. Even though the human microbiome essentially includes bacteria, fungi, viruses, and other unicellular organisms, it is the bacteria which are of utmost importance in the forensic context because of their diversity and their primary role in the decay process (American Society for Microbiology, 2013). Moreover, they are not only spread throughout the different parts of the body but are also consolidated in certain areas such as the oral cavity and intestine, creating particular niches. The internal organs such as the heart, liver, and spleen are sterile in healthy humans, but within 24 h of the postmortem period, there is a proliferation of the microbiome in the internal organs (Gevers, 1975). The overall progression of the decay process is dependent upon several external and internal factors and plays an important role in determining the accuracy of the predictive methods in forensic sciences. The thanatomicrobial community has two distinctive components: the microbiome of the internal organs of cadavers and the microbiome associated with external body surfaces, the latter also termed epinecrotic microbiome (Javan et al., 2016a). With the aid of genomic and molecular advances in the past decade, the thanatomicrobiome has emerged as a tool of enormous potential in the arsenal of forensic medicine (Alan and Sarah, 2012).

In this review, we have attempted a comprehensive account of the potential applications of the thanatomicrobiome in forensic medicine, primarily on the postmortem interval (PMI), and cause of death, focusing on the possible microbial marker profiles and their robustness as well as limitations. The estimation of time since death is fundamental in establishing useful information regarding the time of death, necessary information that needs to be presented in the court of law. It is also one of the *ad rem* challenges for forensic specialists all over the world as far too many variables affect the postmortem changes, making it difficult to rely on one specific method. In the early postmortem period, temperature nomogram, rigor mortis, and hypostasis are considered as the standard tools in day-to-day practice (Madea, 2016). The temperature nomograms use algor mortis as the basis for calculating time since death, the Henssge's nomogram being one of the most popular methods (Henssge, 1988). The other methods in early postmortem period include histopathological and biochemical methods. Degenerative changes in the skin, which initiates as vacuolation of the corpus basale and spinosum, start appearing 6 h after death. The disintegration of the dermis is complete by 18 h (Bardale et al., 2012). The biochemical methods include postmortem biochemical markers in tissue and body fluids (Donaldson and Lamont, 2014). The body fluids include vitreous humor, synovial fluid, pericardial fluid, and cerebrospinal fluid. Some of these markers which are well investigated in the literature are potassium, sodium, urea, chloride, hypoxanthine, and cardiac troponin T (Meurs et al., 2019). In the late postmortem period, the body starts disintegrating, and this is known as decomposition. This period is divided into fresh, bloat, early decay, advanced decay, and skeletal remains (Metcalf, 2019). During this period, when ample time has passed after death, PMI estimates with the available methods of algor, rigor, or livor mortis may no longer be applicable, and various other methods, such as forensic entomology and molecular assessment, have to be relied upon, which all have their own limitations and weaknesses (Pittner et al., 2020). The determination of the cause of death is, again, vital in narrowing down the circumstances in which a person died or suffered an injury. In autopsy-negative cases, the DNA can be extracted from the blood and tissue samples of the cadaver to possibly analyze the cause of death, a method termed as "molecular autopsy" (Ackerman et al., 2001). Similarly, the thanatomicrobial samples can be collected and analyzed through the available high-throughput platforms to aid in forensic investigations. These methods, too, come with their own pitfalls and limitations.

Our literature search included the keywords "thanatomicrobiome," "microbiome," "forensic medicine," "postmortem interval," "postmortem submersion interval," "cause of death," and "gut microbiome" on the PubMed, Embase,

and Scopus databases between October 2019 and December 2020. The search results were sorted for the articles which focused on the application of thanatomicrobiome in forensic medicine. Most of the articles dealt with PMI as it is the most extensively studied area for the thanatomicrobiome (**Figure 1**). Additionally, we have briefed upon the various technologies and methods that have been in use for microbial profiling and the newer approaches and practices that are coming up in thanatomicrobiome studies.

THE INTERTWINED ODYSSEY OF FORENSICS, GENOMICS, AND THE HUMAN THANATOMICROBIOME

Forensic medicine and genomics go a long way back. Minisatellites and microsatellites were proposed for human identification by Sir Alec Jeffreys. Restriction fragment length polymorphism (RFLP), which required intact DNA in micrograms, was primarily used for human identification (Børsting and Morling, 2016). Next came the highly sensitive polymerase chain reaction (PCR)-based mitochondrial DNA (mtDNA) sequencing which could be used to type even degraded samples in trace amounts, e.g., hair shafts (Sullivan et al., 1992). This technique has been extensively in use and gave rise to the creation of the European DNA Profiling Group's mtDNA population database project (EMPOP) (Parson and Bandelt, 2007). With further advances in sequencing methods such as Sanger's chain termination method and capillary electrophoresis, eventually, short tandem repeat (STR) assays took over, followed by single-nucleotide polymorphism base extension (Mitchelson, 2003; Børsting and Morling, 2016). These methods have been used extensively in forensic casework (Phillips et al., 2007; Børsting et al., 2009; Walsh et al., 2014). Because of their polymorphic nature, STRs are given high weight in human identification. Overall, the current applications for DNA profiling include identification of crime suspects, identification of dead bodies or human remains, matching with profiles of criminals, e.g., the Combined DNA Indexing System (CODIS) of the Federal Bureau of Investigation (FBI), and genealogical DNA testing with microsatellites on the Y-chromosome, respectively. CODIS is a database of more than 12 million human DNA profiles and has aided in countless criminal investigations. This only emphasizes the importance of genomic technologies in forensic medicine. However, the applications of genomic technologies in forensics are not limited to human samples alone and involve the amalgamation of multiple disciplines (Arenas et al., 2017; Javan et al., 2019).

Micro-organisms show intra- and inter-individual variation in terms of number and distribution in different body sites (Human Microbiome Project Consortium, 2012a). Hence, comprehensive microbial profiling, which is an essential step in identifying relevant markers in forensic medicine, includes both characterizing the species that are present and the extent of their abundance (Human Microbiome Project Consortium, 2012b; Zhou and Bian, 2018).

In the pre-NGS era, accurate microbial profiling involved simple culturing and finding out interactions between co-cultured taxa; these methods were constrained by their limited number of taxa and interactions as well as failed to provide the dynamics of the entire community (Malla et al., 2019). Culture-independent methods have several advantages in this regard: direct extraction of the genetic material from the sample of interest, discovery and characterization of a vast number of microbial species which were otherwise unidentifiable or undefined with previous techniques, and obtaining a high-throughput profile of the microbial community by genome sequencing (Gill et al., 2006; Schloissnig et al., 2013; Adserias-Garriga et al., 2017a; Almeida et al., 2019). Massively parallel sequencing, aided further by robust bioinformatics pipelines, has evolved as a boon by allowing microbial analysis and overcoming the challenges of identifying unknown and low-abundance microorganisms (Schmedes et al., 2016). Due to its high throughput, low cost, and reduced turnaround time, it is a powerful technique to gain insight into the human thanatomicrobiome, possibly to infer into existing disease states as well as past medical conditions, human identification, PMI estimation, and decomposition analysis (Cho and Blaser, 2012; Schmedes et al., 2016).

Currently Available Techniques: An Overview

Overall, the currently available tools for the genetic profiling of the thanatomicrobiome have shown a distinct shift toward the newer and advanced molecular biology techniques. These include DNA extraction kits as well as group-specific PCR primers and metagenomics and whole-genome sequencing (**Figure 2**). Some commercially available DNA isolation techniques are the QIAamp DNA stool minikit (Qiagen), Inhibitor Removal Technology column (Carlsbad), and PowerSoil® DNA isolation kit (MoBio Laboratories, Inc.) (Finley et al., 2015; Hauther et al., 2015; Lawrence et al., 2019). To identify the relative quantities of key microbial groups for the suitability of PMI estimation, group-specific primers have been developed and used successfully (Matsuki et al., 2002; Liszt et al., 2009).

There are two primary metagenomic (direct genetic analysis of entire communities of organisms) approaches (**Figure 3**) that have been in use: marker gene- or amplicon-based sequencing and shotgun whole genome sequencing (WGS). In the former, a genomic region is amplified, which is conserved within a taxon but variable among taxa. Common marker genes include 16S rRNA gene for prokaryotes, 18S rRNA gene for eukaryotes, and internal transcribed spacer for fungi (Zhou and Bian, 2018). The most commonly used bacterial genetic marker to identify microbial taxa present in a community is the 16S rRNA gene. It is a single phylogenetic marker which can provide a more in-depth coverage but cannot differentiate at the species level. The reasons for which it is widely used for molecular identification are as follows: (a) the relatively short 16S rRNA gene has hypervariable regions appropriately sized for the metagenomic platforms and (b) the conserved regions of this gene allow for designing universal primers to target the hypervariable regions

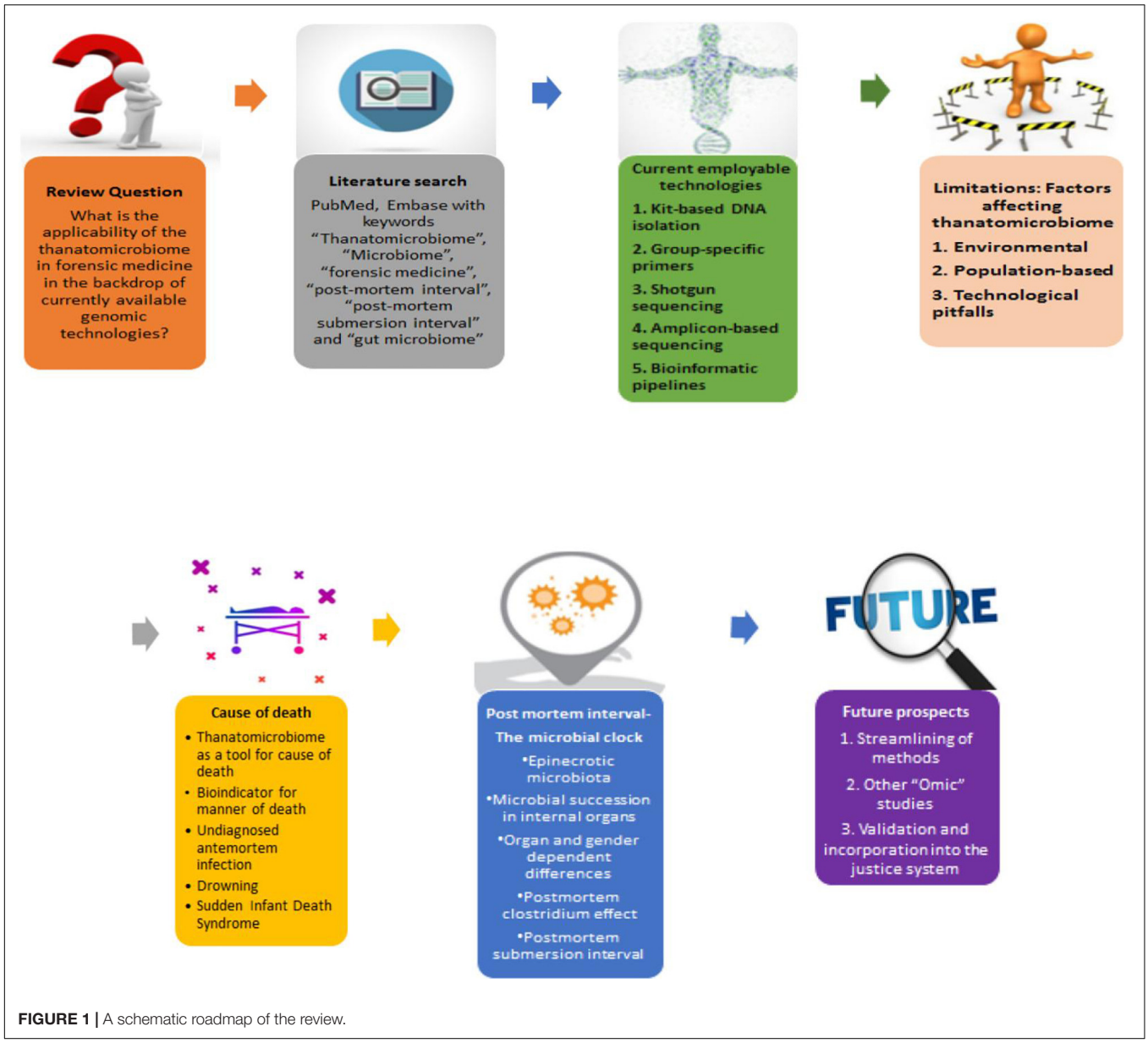

FIGURE 1 | A schematic roadmap of the review.

describing the microbial diversity (Bell et al., 2018). It has been observed that the V4 hypervariable region is the most sensitive for microbial signatures. The segments juxtaposed to V2 and V4 hypervariable regions have, again, the highest accuracy for taxonomic determination (Chakravorty et al., 2007; Bell et al., 2018). However, this approach has certain limitations. 16S rRNA data profiling has low discriminatory power for some taxa, and it cannot provide higher than genus-level resolution (Mignard and Flandrois, 2006). It is also limited to the marker gene regions; hence, the functional traits of the community are left out of the investigation. Finally, there are technical issues like the purity of the isolates and primer selection bias (Janda and Abbott, 2007).

Shotgun sequencing of the metagenome, on the other hand, accounts for higher taxonomic resolution and less bias and provides a greater level of diversity (Jovel et al., 2016; Malla et al., 2019). WGS also gives a functional inference about the microbial community as it engages in a genome-wide approach using strings of genomic DNA sequences and matching them to an annotated database of known DNA sequences. It can provide strain-level characterization by producing sequence reads of strain-specific markers (Schmedes et al., 2016). For strain-specific microbial identification alongside functional profiling, the GSMer approach and the HuMiChip2 microarray platform have been developed (Tu et al., 2014, 2017). Multi locus sequence typing (MLST)-based identification methods such as MetaMLST can characterize single strains of known species (Zolfo et al., 2018) and can be applied to profile the human thanatomicrobiome communities. However, analysis of this massive scale of data usually requires the development of efficient and accurate computational pipelines

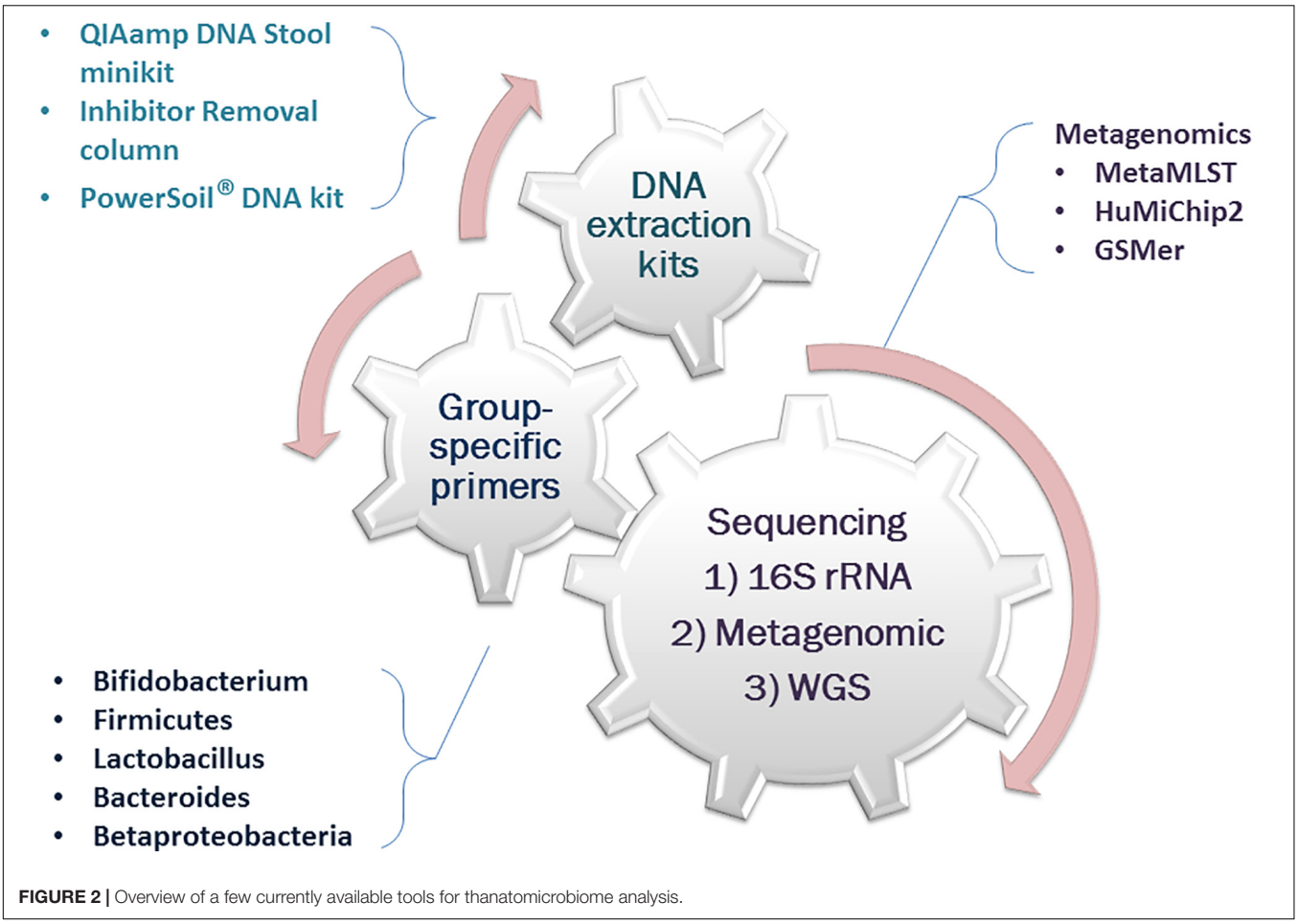

FIGURE 2 | Overview of a few currently available tools for thanatomicrobiome analysis.

and comprehensive annotation of reference databases, which pose a challenge in itself (Quince et al., 2017). The processing decisions required for the data analyses involve a series of transformations using executable standard line software. These decisions ultimately have downstream effects on the results and interpretation of the data; hence, any application of the thanatomicrobiome in the criminal justice system would require streamlined standard operating procedures (Leipzig, 2016; Kaszubinski et al., 2020a).

For the 16S amplicon sequencing analysis, taxonomy, and community characterization, the standard process uses operational taxonomic unit-based or amplicon sequence variant (ASV)-based clustering tools, such as Quantitative Insights Into Microbial Ecology 2 (QIIME2), Mothur, and Divisive Amplicon Denoising Algorithm (DADA2) (Nguyen et al., 2016; Bharti and Grimm, 2019). Current studies mainly employ 16S rRNA sequencing considering that it can provide consistent estimates, is economical and time-saving, and is suitable for a large number of samples to screen microbial markers for estimating time and location of death. Other approaches involving transcriptome and proteome analysis are also gaining popularity.

Finally, while metagenomic analyses give insights about community structure, meta-transcriptomic investigation sheds light upon the functional profiles of the community. Both of these analytic methods together, at varying stages of decomposition, have shown potential in PMI estimations (Burcham et al., 2019a,b). Moreover, total RNA sequencing can prove to be a cost-effective method compared to WGS, as it is equally reliable and has fewer chances of overestimating microbial diversity from sequencing errors (Kunin et al., 2010; Burcham et al., 2019a).

CONSTRAINTS AND KNOWLEDGE GAPS: WHAT LIES AHEAD AND HOW TO OVERCOME THEM

Being ubiquitous and having erectable ecologies, there is no denying the potential of microbes as physical evidence for forensic science. However, several hurdles in forensic sciences still need to be overcome. Metcalf has outlined some lacunae that need to be filled before utilizing the thanatomicrobiome in the estimation of PMI (Metcalf, 2019). The same can be extended to other potential medicolegal applications. These include the time frames in which microbes can be most informative, the external variables that need to be incorporated in the microbial models, the sample types and sample location ideal for addressing a particular problem, the stage of investigation in which the microbial sample should be collected, and the most robust

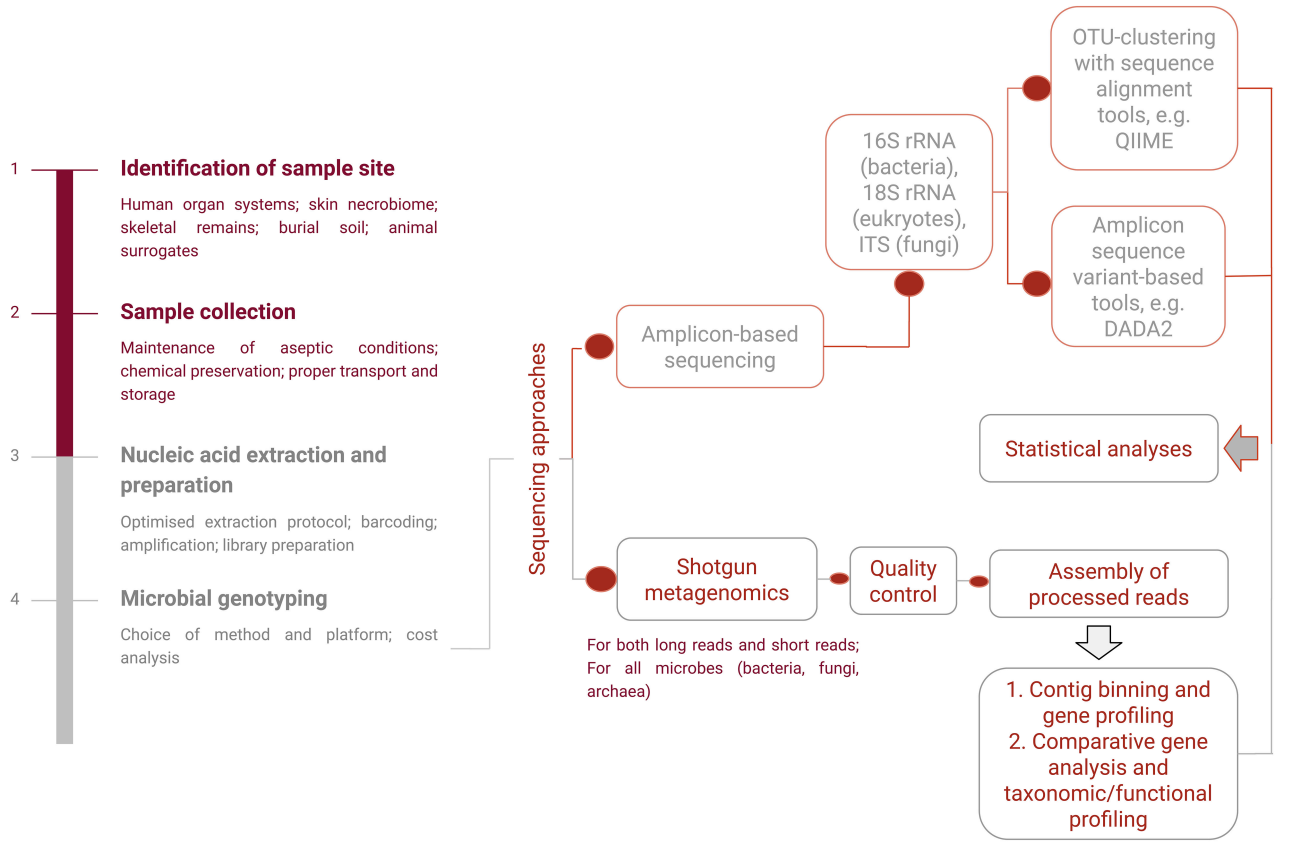

FIGURE 3 | A schematic representation of amplicon-based and shotgun metagenomic sequencing procedures.

modeling methods. These issues, along with particular other challenges, are discussed below.

Environmental and Population-Based Diversity

The highly diverse human microbial community shows high inter-individual variability depending upon food habits, age and sex, ethnicity, geographical provenance, and presence of pathological conditions, among other factors, and this potentially affects the thanatomicrobiome composition and, consequently, the microbial succession (Arumugam et al., 2011; Wu et al., 2011; David et al., 2014; Dehingia et al., 2015; Rehman et al., 2016; Gupta et al., 2017; Angelakis et al., 2018; Gaulke and Sharpton, 2018; Senghor et al., 2018; de la Cuesta-Zuluaga et al., 2019). These can grossly be divided into abiotic and biotic factors. A clear understanding of these factors and their interactions will help in devising generalized models for use in forensics.

The abiotic factors include time, temperature, humidity, pH, and antemortem living habits, e.g., diet and drugs. The biotic factors, on the other hand, include insects, scavenger population, commensals, and antemortem infections (Dash and Das, 2020).

An increase in temperature considerably changes the decomposition process in dead bodies (Benbow et al., 2018). It also significantly alters the bacterial colonization of tissues (Iancu et al., 2018). Furthermore, the rate and degree of decomposition are greatly increased if the cadaver is exposed to water (Abad Santos, 2019). Generally, the decomposition process happens faster in humid climates. Hence, a colder environment and lesser relative humidity will thwart microbial proliferation to a degree (Jordan and Tomberlin, 2017).

The gut microbiota, in its composition and diversity, is closely related to dietary habits and food products. Bacteroidetes and Actinobacteria populations are positively associated with a fat-rich diet but negatively with fibers, whereas Firmicutes and Proteobacteria have a reverse association (Wu et al., 2011; Senghor et al., 2018). A comparative study of animal- and plant-based diets showed that the former led to a decrease in Firmicutes (*Roseburia* spp., *E. rectale*, and *R. bromii*), while the latter increased the abundance of *Bacteroides* spp. and *Bilophila* spp. (David et al., 2014). Accordingly, there is country-based diversity; the gut microbiome in western populations with a more prevalent protein- and fat-rich diet is rich in Firmicutes (*Blautia*, *Roseburia*, *Ruminococcus*, and *Clostridium difficile*), Actinobacteria (*B. adolescentis* and *B. catenulatum*), and Bacteroidetes (*Bacteroides*), while Asian people have an intermediate gut microbial diversity with dominant species being *Prevotella*, *Butyrivibrio*, and *Staphylococcus aureus* (Arumugam et al., 2011; Senghor et al., 2018). This variability extends within the different regions of the same country as well, as shown in

an NGS-based study on Indian populations of distinct cultures, traditions, and diet (Dehingia et al., 2015). However, the sizeable microbial diversity among populations of different countries cannot be explained by diet alone (Nishijima et al., 2016). Other factors such as lifestyle and subsistence strategies, host genetics, and altitude of living are also involved (Nam et al., 2011; Schnorr et al., 2014; Das et al., 2018; Jha et al., 2018).

The use of antibiotics is of considerable significance in thanatomicrobiome analysis. The alteration of the gut microbiota in prolonged antibiotic use is well established. The effects are twofold: (1) it makes the host susceptible to other infections, e.g., *C. difficile* colitis (Norén, 2010) and (2) it causes colonization of the gut by antibiotic-resistant organisms (Keeney et al., 2014; Nogueira et al., 2019). In a recent study, *Clostridium* was found to be the most abundant genus in the liver and spleen of drug overdose victims (Brackett, 2018). Additionally, *Bacteroides* and *Alistipes* were found abundantly in the gut of individuals on laxatives (Vila et al., 2020). Thus, antibiotic use during the lifetime has to be taken into account while looking for thanatomicrobiome signatures.

Other environmental variables like soil type and insect activity may also affect the predictable microbial succession during decomposition. However, even though the decomposer community is derived from soil, soil type itself is not an independent factor for community development, and thus decomposition is a sufficiently reproducible process (Metcalf et al., 2016). In the presence and absence of insect populations, the microbial succession process during decomposition can be identified by specific taxa for each group (Guo et al., 2016). Finally, body mass can be a pivotal factor, as it has been seen that larger carcasses decompose slower and release higher levels of nitrogen required for the growth of microbial communities after the death of the host (Spicka et al., 2011; Deel et al., 2020). On the contrary, the characterization of soil microbial communities of four different *Sus scrofa* carcasses revealed no significant differences through decomposition (Weiss et al., 2016). These instances show that, even though environmental variables can influence microbial communities, they may not necessarily affect the succession all the time. However, these studies had only a handful of samples and were carried out with animal models, and further human studies are necessary to understand how these and other factors impact the succession of microbial communities and the accuracy of the microbial clock.

Technological Limitations

High-throughput sequencing technologies have opened new frontiers in a cost-effective analysis of the microbial communities. However, it is not without its share of shortcomings. Firstly, the characterization of the microbiome in most studies has been achieved at the upper taxonomic ranks. This alone cannot serve the purpose of individualistic human identification we are ultimately aiming for. Secondly, sample preparation methods involving nucleic acid extraction remain a notable area of creating a bias toward various microbial taxa (Yuan et al., 2012). Most studies cited in the latter sections of this review have used the 16S rRNA gene amplicon sequencing. The conserved regions of the gene, the available databases, and a large number of studies on this marker in the existing literature make it an attractive target (Schmedes et al., 2016). Nevertheless, it suffers from insufficient species resolution, sequence and copy number variation in a single bacterium, PCR bias, inaccurate relationships based on variability outside of the marker region, and horizontal transfer of the gene region (Fox et al., 1992; Suzuki and Giovannoni, 1996; Wang et al., 1997; Klappenbach et al., 2000; Schouls et al., 2003; Janda and Abbott, 2007; Soergel et al., 2012). These may lead to misclassified reads, inaccurate quantification, and confounded analyses. Bioinformatic tools like Phylogenetic Investigation of Communities by Reconstruction of Unobserved States (PICRUSt), which can predict functional gene profiles from the relative abundance of all known taxa, can be handy but only for known species (Langille et al., 2013). Shotgun metagenomics, on the other hand, can differentiate at the species level, but it has less depth of coverage for particular sites of the genome. Complex samples, containing thousands of species, will suffer from limited coverage of particular genomes, especially those communities with low abundance and coming from a trace amount of samples.

Additionally, the sequencing platform used can itself be a source of technical bias and hinder the accurate determination of microbial composition and functional profile (Rutty et al., 2015; Hao et al., 2017). For instance, 454 technology has a low yield, a variable length of sequence reads, and a high rate of insertion/deletion errors, whereas the ion torrent platform has a higher rate of sequencing errors (Salipante et al., 2014; Hao et al., 2017). Earlier, Illumina sequencers, although with high throughput, could produce reads only 100 bases in length and hence could not provide enough taxonomic information for reliable species-level resolution. In comparison, the 454 pyrosequencing system has a longer read length (Liu et al., 2012). Computational limitations also include high cost and sufficiently large computing power. Moreover, algorithms that are capable of analyzing the data in a biologically relevant manner are on demand (Rothberg and Leamon, 2008; Petrosino et al., 2009). Identifying the microbe of interest within a highly complex metagenomic sample also requires its resolution from its near neighbors as well as from a vast community creating background noise. A highly sensitive and accurate detection technique is imperative in this scenario. Such targeted markers or marker panels should not only provide species-level resolution but must also be developed in a cost-effective method, balancing the sequence coverage and throughput. Newly developed technologies in implementation should be validated, and sample analysis has to focus more on a molecular level to identify specific and individualized microbial signatures. Last but not least, the variability in the working knowledge of the technicians and engineers and, subsequently, the inter-laboratory variation that exists, but difficult to evaluate, have to be taken into account. The development of novel quality control metrics, especially for cases where a high-quality reference is not available, could be useful in reducing the sequencing errors (Trivedi et al., 2014).

To apply the thanatomicrobial profiles in the veritable field of forensic sciences, universally applicable models should be in place with validated protocols, which incorporate temporal and seasonal microbial changes while taking care of other

sources of variation (**Figure 4**), such as host characteristics and environments. These models are challenging to establish due to the limited amount of available data as well as a lack in the generalization of existing model systems. A great barrier for the applicability of the thanatomicrobiome in creating such models for PMI estimation is the lack of human cadaver-associated data sets from different environments encompassing diverse populations. Many experiments are carried out using pigs as animal surrogate models as they are similar to humans in diet, body fat, and body hair coverage (Schoenly et al., 2006). However, pig and human bacterial communities are non-comparable (Furet et al., 2009). Comparative fecal metagenomics revealed that the pig fecal phyla are closer to that of cow rumen and chicken cecum (Lamendella et al., 2011). A comparison of the skeletal muscle tissue decomposition between human, pork, beef, and lamb showed that no single analog could precisely predict human decomposition in the soil, although they are all close approximations of the human decomposition dynamics (Stokes et al., 2013). Moreover, most studies on human thanatomicrobiome so far have been limited to the North American population. In the context of this enormous diversity and associated shortcomings, efforts should be focused on (a) studies including populations from diverse geographical and ethnic backgrounds, (b) individualizing the microbiome profiles while trying to incorporate the existing variables and chalking out the microbes common to humans, (c) determining the portions of these microbes which vary due to the environmental and living conditions mentioned above, and (d) selecting those bacteria which are relatively abundant to reduce stochastic sampling effects. Moreover, while building multivariate models with the thanatomicrobiome data, care should be taken not to overfit. Adding a new covariate is desirable only when it improves the model significantly over the expected natural increase in precision associated with it, or we risk losing the generalizability of the model. Overall, these advances will result in the development of a defined set of markers for the human microbiome and target genes or sequences containing sufficient variation to generate a profile that can provide a sufficient degree of individualization of the donor(s) of biological evidence for aiding in human identity testing, PMI estimation, and determination of the cause of death.

To summarize, the limitations pertaining to these upcoming methods are twofold: on the one hand, they deal with extreme population variation as well as ecological diversities and, on the other, the technological aspects still have a lot of area for improvement in creating more human cadaver-associated databases and streamlining the bioinformatic pipelines. By extension, the current knowledge gaps in the applicability of the thanatomicrobiome in forensic medicine are (a) the sample types and locations most fitting to provide the best possible evidence in

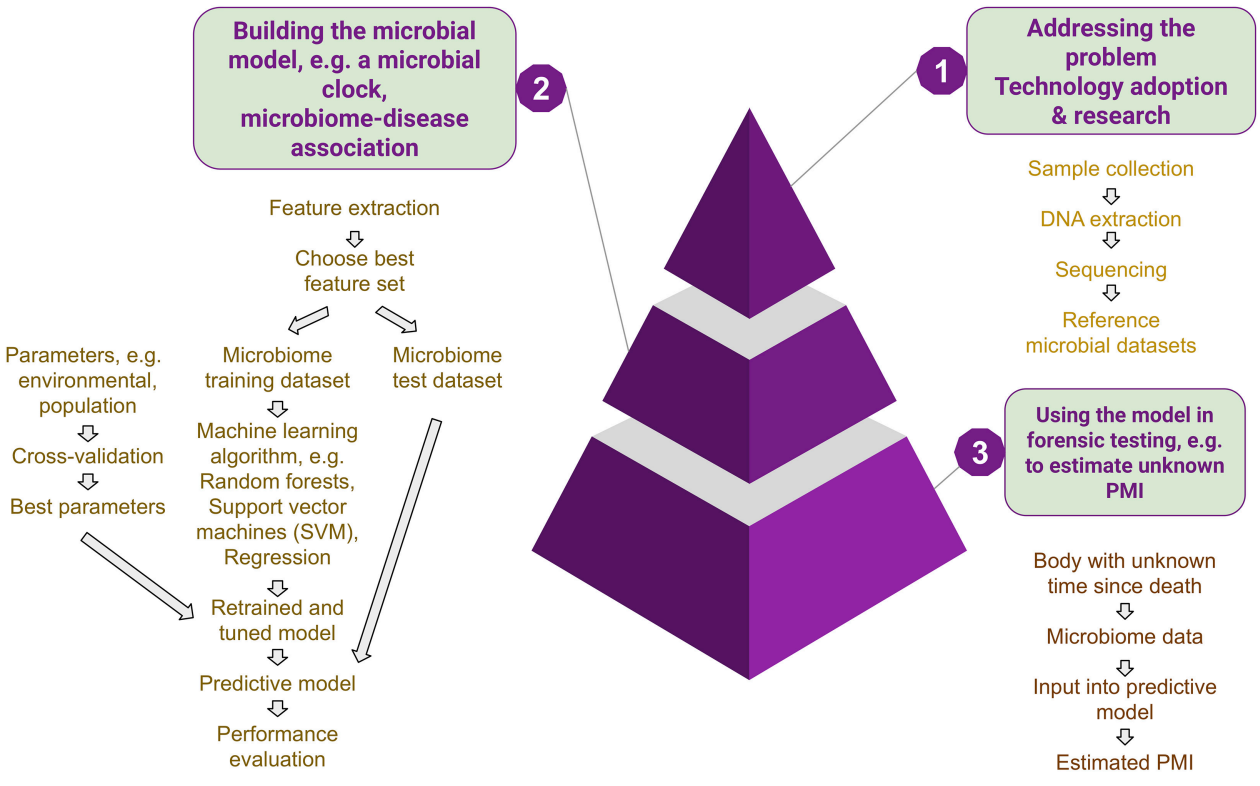

FIGURE 4 | Development of microbial models. To address the gaps in knowledge, new technology is adopted, and research is carried out on microbial community succession and functionality. Data obtained from these experiments are used to build machine learning models (with training and validation sets), which are then fine-tuned with available best parameters to eventually be used for unknown microbial samples.

criminal cases, (b) the time frames in which microbial evidence is most informative, (c) the most robust predictive models, and (d) standard bioinformatic pipelines. In the following sections, these issues have been addressed in order to differentiate (1) anecdotal cases or cases based on certain environments and (2) identify those having a more general scope in forensic and medicolegal investigations.

THANATOMICROBIOME AS A TOOL FOR PREDICTING CAUSE OF DEATH

The presence of specific microbes can act as hidden evidence or bioindicator for the cause of death. In general, if we recover a single microbial species from body fluids at autopsy, it is suggestive of an infection incurred during life, while a mixed profile points toward a postmortem invasion (Alan and Sarah, 2012). This can prove to be useful in confirming the diagnosis of an antemortem infection, identifying the etiological agent of a previously undiagnosed infectious disease, or identifying microbial markers for particular types of death (Ventura Spagnolo et al., 2019) (**Table 1**).

Dysbiosis in Cause of Death

A recent multinational study focused on different anatomical sites in human cadavers with various causes of death such as accident, suicide, and homicide found that the manner of death has a significant influence on the microbial community in various postmortem organs, e.g., brain, liver, uterus, and prostate (Lutz et al., 2020). The PMI and cause of death were associated with the alpha and beta diversity of the tissue microbial profiles (Lutz et al., 2020). Similar associations were observed previously where the beta dispersion differed significantly between anatomical body sites and causes and manners of death (Kaszubinski et al., 2020b). A different microbial signature was also observed in cardiovascular disease cases. For the associations between relative bacterial abundance and manners of death, ASVs from the families MLE1-12, Enterobacteriaceae, and Chitinophagaceae were positively associated in natural deaths, whereas 10 unique ASVs from the Bacilli class were negatively associated with homicide (Lutz et al., 2020). These findings imply that microbial signature variability could be measured through beta diversity in predicting the cause or manner of death.

An extensive study on 336 body fluid samples from 129 autopsies, involving bacterial culture, 16S rRNA identification, and matrix-assisted laser desorption/ionization-time of flight (MALDI-TOF), to establish a correlation between microbial isolates and cause of death found correlations in six out of eight seawater drowning cases. Enterococcus and Enterobacter were isolated in the cardiac blood and peritoneal fluid of a patient who died of colon perforation and cardiopulmonary arrest, showing the migration of the colon communities of Enterobacteriaceae to peritoneal fluid and cardiac blood (Na et al., 2017). A kinetic postmortem survey of the microbiota in culture-positive extra-intestinal tissue found bacterial translocation to extra-intestinal compartments such as mesenteric lymph nodes (MLNs), spleen, liver, kidney, and cardiac blood 5 min after death, the highest rates being in MLNs (Heimesaat et al., 2012). The highest detection rate was observed in organs for *Lactobacillus* at 3 and 12 h postmortem. Such rapid translocation of intestinal bacteria could be useful in distinguishing between primary pathogenic bacteria and secondary putrefactive contaminants not only while investigating causes of unknown deaths but also for screening tissue donors before allogeneic transplantation. Investigating the dynamics of bacterial translocation and intestinal dysbiosis in contributing to the early stages of liver disease, Fouts et al. (2012) found that there is an increase in intestinal permeability independent of microbiome changes or endotoxin and translocation of families Enterobacteriaceae, Enterococcaceae, and Bacillaceae, primarily to the MLNs, in cholestatic liver injury. The postmortem transmigration of *Staphylococcus aureus* and *Clostridium perfringens* during murine decomposition can help in determining the cause of death and track down the origins associated with the geographic location of the human remains during postmortem investigations (Burcham et al., 2016). In 10 heart samples from individuals who died of cardiac arrest, Bell et al. (2018) studied the heart thanatomicrobiome and found sex-related differences in male and female corpses at the bacterial phylum (Firmicutes in males and Proteobacteria in females), class (Bacilli in males and γ-Proteobacteria in females), order (Lactobacillales and Rhizobiales only detected in males and Pseudomonadales in females), family (Streptococcaceae only detected in males), and genus (*Streptococcus* and *Lactobacillus* in males) levels, which demonstrated that microbial populations form ecological niches differently in the hearts of males and females after death (Bell et al., 2018). They also found Proteobacteria to have the highest abundance, which indicates a relationship between heart thanatomicrobiome and cardiac diseases; as Proteobacteria, usually found in the gut, can act as precursors to inflammation; it can also cause dysbiosis and an increased risk of heart disease, as it has been shown as an independent marker of risk of cardiovascular disease in previous antemortem studies (Amar et al., 2013; Metcalf et al., 2013; Shin et al., 2015). From a cross-sectional study of an urban–industrial population, decreased phylogenetic diversity was a significant predictor of heart disease in a <24-h time window, where the dominant taxa were Streptococcus, Prevotella, Fusobacterium, and Rothia (Pechal et al., 2018). Furthermore, Rothia, along with other additional community metrics, can be used as a biomarker for hosts with chronic dysbiosis (Pechal et al., 2018). Such qualitative and quantitative changes in the microbiome can pave new ways of identifying existing disease conditions of the deceased.

In Drowning

The presence of diatoms in blood or organs (e.g., lungs) has long since been the gold-standard indicator to diagnose drowning and whether it is antemortem or postmortem. However, in rare cases, when identification through diatoms is impractical, other microbes can aid in providing informative results. In the past, methods employed to identify these organisms have included light and electron microscopy, bacterial culture, and PCR (Lunetta et al., 1998; He et al., 2008; Lucci et al., 2008; Tie et al., 2010; Huys et al., 2012; Sitthiwong et al., 2014;

TABLE 1 | Potential applications of thanatomicrobiome in diagnosing cause of death.

Specimen type	Sample size (*n*)	Method	Characteristic finding(s)	Application(s)	References
SKH-1 Elite female mice; liver, spleen, heart, stomach, kidney, intestine	90	Whole body fluorescent imaging	*Staphylococcus aureus*—highest concentration at 5–7 days pm and undetectable by culture on day 30	(1) Cause of death (2) Geolocation	Burcham et al., 2016
Mice (hfa); ileum and colon	–	RT-qPCR	Enterococci, enterobacteria	(1) Presence of ante-mortem acute and chronic intestinal inflammation (2) Screening donor tissues before allogenic transplant	Heimesaat et al., 2012
Male BALB/c mice; gastro-intestinal tract, liver	12	16S rRNA sequencing	Enterobacteriaceae, Enterococcaceae, Bacillaceae, Lactobacillaceae	(1) Bacterial translocation in cholestatic liver injury (2) Toxic liver injury	Fouts et al., 2012
Human heart	10	16S rRNA amplicon sequencing	Distinct cardiac bacterial phyla in male (*Streptococcus*) and female corpses (*Clostridium*, *Pseudomonas*)	(1) Relation between cardiac thanatomicrobiome and cardiac diseases (2) Postmortem clostridium effect	Bell et al., 2018
Human • Ears, eyes, mouth, nose, rectum	188	(1) 16S rRNA amplicon (2) MiSeq PICRUSt (for predictive function) (3) QIIME2, DADA2	*Streptococcus*, *Haemophilus*, *Veillonella*, *Rothia*, *Fusobacterium*, *Prevotella*	(1) Microbial diversity is an indicator of antemortem host health (2) Beta-dispersion is an indicator of manner of death	Pechal et al., 2018; Kaszubinski et al., 2020b
Human • Liver, mesenteric lymph node, portal vein blood, pericardial fluid	33	Bacterial culture; RT-qPCR	*Staphylococcus*, *Streptococcus*, *Clostridium*, *Enterococcus*, *Escherichia* (most common among 21 different genera)	(1) Liver and pericardial fluid are ideal internal sampling sites for antecedent bacterial infection (2) Sampling time < 5 days	Tuomisto et al., 2013
Human • Blood • Lung, kidney, liver • Water	2	(1) Culture 16S rRNA gene analysis (2) 454 pyrosequencing	*Cyanobacteria*, *Bacillariophyceae*, *Dictyochophyceae*, *Chrysophyceae*, *Trebouxiophyceae*	Cause of death: drowning	Kakizaki et al., 2012
Human • Blood • Bone marrow • Lung	93 (three drowned cases, 90 non-drowned controls)	(1) Bacterial culture (2) PCR	(1) *Aeromonas* as non-commensal indicator of drowning (negative for all control samples) (2) Bone marrow as sampling matrix (3) Aseptic sternal puncture as alternative sampling technique	Cause of death: drowning	Huys et al., 2012
Male Sprague Dawley rats • Lungs • Liver, kidney • Cardiac blood	10 (four drowned, four postmortem immersions, two controls)	(1) IHC (2) 16S rRNA amplicon; MiSeq (3) MALDI-TOF	Predominance of: • *Brucella*, *Pseudomonas*, *Rhodococcus*, *etc*. (seawater group) • *Clostridium* (freshwater group)	Cause of death: drowning	Lee et al., 2017

(Continued)

TABLE 1 | Continued

Specimen type	Sample size (*n*)	Method	Characteristic finding(s)	Application(s)	References
Human • Blood • Water	(1) Ten antemortem drowning cases (five seawater, five saltwater) (2) Three postmortem drowning	Microbial culture	Fecal coliforms and fecal streptococci as diagnostic markers for antemortem drowning	Cause of death: drowning	Lucci et al., 2008
Human • Blood • Lung, kidney, liver	43 (41 drowned and two not drowned)	Multiplex qPCR with Taqman probes	• Aeromonas (freshwater drowning) • *Vibrio* and *Photobacteria* (seawater drowning)	(1) Differentiation of immersed and non-immersed victims (2) Molecular diagnostic test for drowning as the cause of death	Uchiyama et al., 2012
Human • Brain, lungs, spleen, kidney, liver	20 drowned	Multiplex qPCR with Taqman probes	12 out of 16 drowning cases correctly showed the respective bacterioplankton in their habitat	Molecular diagnostics for drowning as the cause of death	Rutty et al., 2015
Human • Liver, lung, kidney, spleen, heart, brain, trachea • CSF • Body fluids	64	Serology, nested PCR, electron microscopy, viral culture	Virological infection in two cases	Ruling out infectious cause of SIDS	Fernández-Rodríguez et al., 2006
Human • FFPE of lung, brain, kidney, spleen, thymus, thyroid, lymphoid tissue, and heart	20 (11 SIDS and nine controls)	RT-qPCR	Epstein–Barr virus and HHV-6 are significantly more frequent in SIDS compared to controls	Ruling out infectious cause of SIDS	Alvarez-Lafuente et al., 2008
Human • Bone fragment	1	(1) Laser microdissection (2) PCR (3) 16S rRNA deep sequencing	*Pseudomonas*, most abundant genus from Pseudomonadaceae family	Possible cause of death: *Pseudomonas* osteomyelitis	D'Argenio et al., 2017

Rácz et al., 2016). A culture study with 10 drowning victims and three postmortem submersions revealed fecal coliform (*E. coli*) and fecal streptococci (*E. faecalis*) to be useful markers for drowning (Lucci et al., 2008). Aeromonads in the blood can also be considered as a potential marker for freshwater drowning, as it has been shown by another culture study (Huys et al., 2012). Uchiyama et al. (2012) developed a multiplex real-time PCR protocol for assaying bacterioplankton in drowning cases. In 43 victims, they found related microbes, e.g., Aeromonas for freshwater drowning and Vibrio and Photobacterium for seawater drowning in all lung samples compared to non-drowning victims. This method was further applied to 20 cadavers, where it was found that this method can potentially be used as a high-throughput supportive diagnostic test for antemortem drowning (Rutty et al., 2015). Kakizaki et al. (2012) used the 454 pyrosequencing approach to ascertain the cause of death of two drowning cases and found that it is possible to determine diverse aquatic microbes in drowning victims that can point toward the aquatic environment in which the drowning occurred. An animal study sampled for lungs, kidney, liver, and blood, and found significant aquatic microbial presence in the drowned group compared to closed organs of postmortem immersion group (Lee et al., 2017). Aquatic bacterial communities were further dominated by Proteobacteria (seawater), Bacteroidetes (freshwater), Actinobacteria, and Bacillariophyta (Lee et al., 2017).

In Sudden Infant Death Syndrome

The risk factors for sudden infant death syndrome (SIDS), defined by the unexpected death of an otherwise healthy infant aged less than 1 year, include genetic predisposition, immunological disorder, exogenous stressors, and undiagnosed infections/sepsis. The common microbial agents associated with SIDS are human herpes virus, enterovirus, respiratory syncytial virus, adenovirus, cytomegalovirus, Epstein–Barr virus, *Streptococcus pneumoniae*, *Bordetella pertussis*, *Haemophilus influenzae*, and *Neisseria meningitidis* (Fernández-Rodríguez et al., 2006; Alvarez-Lafuente et al., 2008; Oliveira and Amorim, 2018; Ventura Spagnolo et al., 2019). SIDS has been part of many a legal investigation because of the possibility of crime in infants of this age group. Routine postmortem protocols exist in the form of serology testing and PCR assays for many bacteria and

viruses in specimens from autopsies. However, comprehensive microbial profiling has not yet been developed in this arena, and it can potentially provide us with etiology-specific disease diagnoses. Such a panel, accompanying autopsy findings and antemortem clinical information, can be a handy tool to ascertain causes of death due to infection and rule out other causes in criminal investigations.

However, it is worth noting that microorganisms can be influenced by environmental conditions, and variation in microbial population will exist at different PMI; hence, considering these, utmost care must be practiced while relying on a microbial signature solely for the cause of death. Furthermore, using a combination of laser microdissection and microbial typing, the cause of death of a child from the 18th century was resolved to be osteomyelitis caused by *Pseudomonas aeruginosa* (D'Argenio et al., 2017). Such findings should prompt us to preserve samples of unknown clinical cases for future innovative technologies.

THANATOMICROBIOME IN POSTMORTEM INTERVAL—"THE MICROBIAL CLOCK"

Reliable methods of PMI estimation is of utmost importance, as it has invaluable relevance to the inceptive phase of criminal investigations. Inferring the PMI has long been based on observatory data from direct body inspection, *viz*., body cooling, postmortem lividity, and rigor mortis, to name a few (Salam et al., 2012). However, beyond the compound method, many other methods have come up in the aid of PMI (Sharma et al., 2015; Madea et al., 2019). Accumulated degree days (ADD), a unit representing the amount of time an organism spends at a temperature within its development threshold, can be a useful tool in that it can be practiced for decomposition data across various environments and regions (Megyesi et al., 2005). Biochemical assessment can be advantageous after cellular death and when redistribution of electrolytes has set in. A commonly used biochemical test is the vitreous humor potassium concentration (Adjutantis and Goutselinis, 1972). A combination of multiple methods can be useful, e.g., vitreous humor potassium, combined with vitreous humor hypoxanthine and ambient temperature, has shown encouraging results (Rognum et al., 2016). However, biochemical markers come with their own limitations due to the variability in age, sex, cause of death, and other factors. Furthermore, time dependency plays a pivotal role in the usability of these markers in PMI estimation (Woydt et al., 2018). Most biochemical markers have predictive ability if the cadaver is still in the early phases of its postmortem period. As time progresses and the body enters the advanced phases of decomposition, the PMI estimation becomes more difficult.

Methods and technology that can objectively measure with high accuracy and precision are being considered (Donaldson and Lamont, 2014). Moreover, the potential of ecological succession patterns of small organisms or insect species as an indicator of PMI has been long established (Tomberlin et al., 2011). Forensic entomology is an integral part of forensic investigations when the time since death is beyond 3 days (Kashyap and Pillai, 1989). However, due to their seasonal and developmental variation, it is difficult to practically impose them in all circumstances. Information on the geographical variation of many of these forensically important insects is also unknown (Klong-Klaew et al., 2018). Henceforth, the postmortem microbiome has shown much promise as a novel, alternative, and precise method to aid in the estimation of PMI, as they are ubiquitous and have predictable ecologies, on the premise that bacterial succession changes in a predictable and clock-like manner across mammalian species within the same environment in response to the changes in a decomposing resource (Deel et al., 2020).

Thanatomicrobiome in Human Remains

Research revolving around the applicability of the human microbial community in PMI includes sampling from different organs (**Figure 5** and **Table 2**), as the pattern of community succession differs at various time points of decomposition according to the location (Deel et al., 2020).

The Epinecrotic Community

External locations facilitate an easily accessible, non-invasive manner of sampling for the epinecrotic microbial community. In this regard, the skin is the most important site in forensic applications. It also provides specific locations on the human body with their own niche of microorganisms. This is important because the microbial population in a particular site, e.g., oral cavity is, at the same time, different from that of the other body locations and similar across individuals. In a study carried out at the Southeast Texas Applied Forensic Science laboratory, two human corpses each were allowed to decompose in spring and winter seasons, which revealed that a suite of bacterial and fungal groups form a reproducible network that emerges on a predictable time scale and, hence, can serve as estimators of PMI (Metcalf et al., 2016). Two other human subjects were sampled from the internal left buccal region, external left/right cheeks, external left/right biceps, torso, and rectum (Hyde et al., 2015). With the progress of decomposition, the microbial diversity and richness for both bodies were similar for the skin, mouth, and rectal samples. Besides that, Acinetobacter of γ-Proteobacteria class was abundant in both bodies in the late decomposition stages. Another study by the same group found that communities from the mouth and oral cavity differ in pre-bloat and end-bloat stages of decomposition (Hyde et al., 2013). Oral microbial community sampling from three donated individuals showed different dynamics in bacterial composition as the decomposition process progresses through fresh, bloat, active and advanced decay, and dry remains stages and had similar overall successional changes. Firmicutes and Actinobacteria were predominant in the fresh stage, while Clostridiales and Bacillaceae were the principal representatives of Firmicutes from bloat to advanced decay (Adserias-Garriga et al., 2017b). Although the sample sizes for the aforementioned studies are less and variable, the similarity in the microbial succession across the different stages of decomposition is a pivotal finding, as it reflects the possibility

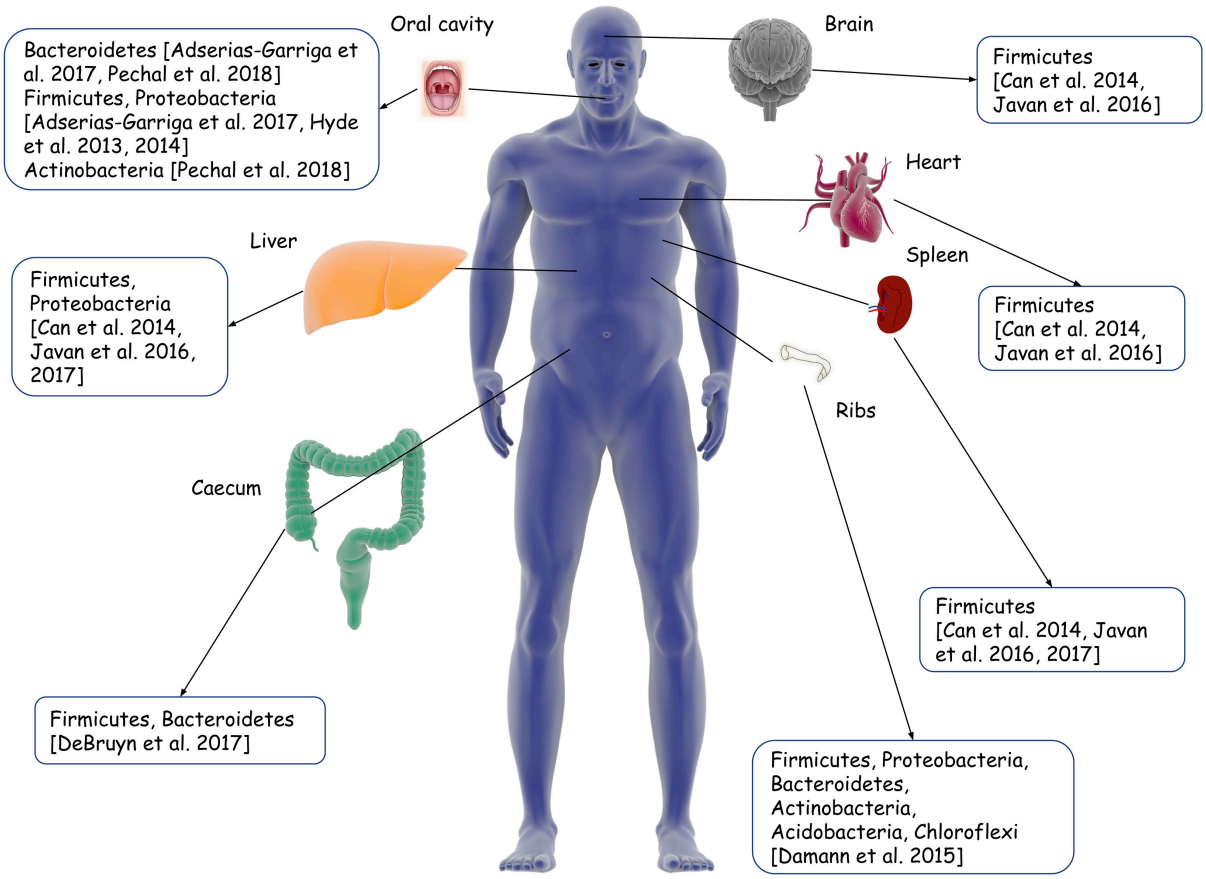

FIGURE 5 | Illustration of different body sites for thanatomicrobiome sampling from existing studies. Boxes indicate the dominant phyla in the microbial communities in that respective organ/body part.

of using the oral microbiome in PMI estimation. An analysis of the surface communities residing in the ear and nasal canals of 17 cadavers led to the successful development of a *k*-nearest neighbor regression model, which could accurately predict the true PMI to within 55 ADD (Johnson et al., 2016). In a larger study involving 188 subjects, samples were collected from various sites such as the eyes, ear, nose, mouth, and rectum and analyzed to show that predictive models from composition and functional profiles, in the context of each sample location, could be used to estimate PMI within the time frame of less than as well as greater than 2 days (Pechal et al., 2018). Zhang et al. (2019) utilized the datasets from the study mentioned above and employed machine learning algorithms in an attempt to predict PMI and found that *xgboost method* resulted in highest accuracy compared to random forest and neural network while incorporating all anatomical areas. The *xgboost method* is a tree-based machine learning method which grows sequentially into a single tree by fitting on residuals. The accuracy of this method was 0.745 for PMI and 0.876 for the location of death. It is worth noting that cases do not always allow for a sample collection from all anatomical sites. Therefore, the aforementioned studies simultaneously serve the purpose of highlighting the anatomical areas which are most important in postmortem casework and the types of sample that must be collected to provide the best possible information. A meta-analysis using the QIITA open-source platform and subsequent model testing using data from the first 25 sample days of each included study indicated that skin data using the 16S rRNA genetic marker performs reasonably in accurately predicting PMI at the phylum level (Belk et al., 2018). Another recent study demonstrated that, upon repeated sampling, the postmortem skin microbiome is stable for up to 60 h (Kodama et al., 2019). They studied 16 scenes of death to see whether objects present at the scene can be linked to the decedents and found that, overall, it could be traced three-fourth of the time with single-user based items, such as smoking pipes and medical devices being the most accurate. The findings are similar to those of previous studies which identified mobile phones as having personal microbial signatures of the user (Meadow et al., 2014; Lax et al., 2015). Overall, these findings point toward the skin and the oral cavity being potentially promising sites to build an accurate microbial clock upon. Furthermore, the skin microbiome can also be extended to act as complementary evidence to establish associations and identifications, e.g., for the analysis of partial or smudged fingerprints for better comparison. Notably, skin commensals are highly resistant to humidity; hence, the epinecrotic thanatomicrobiome signatures can be utilized

TABLE 2 | Assessment of human thanatomicrobiome in estimation of time since death.

Sampling site	Sample size (*n*)	Sample characteristics	Methodology	Time of decomposition/PMI	References
Ears, eyes, mouth, nose, rectum	188	• Median age 43 (18–88) years • M:F = 1.3 • 90 black, 98 white	(1) 16S rRNA amplicon; MiSeq (2) PICRUSt (for predictive function)	24 h to >73 h	Pechal et al., 2018
Ears, eyes, mouth, nose, rectum	188	Two datasets • Metadata of the collected samples • Microbial taxonomic information through Illumina MiSeq	Three machine learning algorithms: xgboost, random forest, and neural network	24 h to > 73 h	Zhang et al., 2019
Nostril and ear canal	21	–	(1) 16S rRNA amplicon; Illumina (2) Statistical regression models to predict PMI	800 ADD	Johnson et al., 2016
Skin and gravesoil	4	–	16S rRNA amplicon, 18S rRNA amplicon, internal transcribed spacer, HiSeq, MiSeq	82 days during spring; 143 days during winter	Metcalf et al., 2016
Mouth, rectum (pre-bloat) Mouth, rectum, gastro-intestinal tract (post-bloat)	2	• 68 and 52 years • M:F = 2.0	16S rRNA amplicon and 454 pyrosequencing	30 days	Hyde et al., 2013
Mouth, cheeks, biceps, torso, rectum	2	• 55 and 85 years • M:F = 1.0	16S rRNA amplicon and 454 pyrosequencing	979 CDH	Hyde et al., 2015
Lower rib	12	• Median age 57 (26–88) years • M:F = 11.0	16S rRNA amplicon and 454 pyrosequencing	571–18,918 ADD	Damann et al., 2015
(1) Brain, heart, liver, spleen (2) Blood	11	• Median age 47 (20–67) years • M:F = 2.7	16S rRNA amplicon and 454 pyrosequencing	20–240 h	Can et al., 2014
(1) Brain, heart, liver, spleen (2) Blood (3) Buccal cavity	27	• Median age 48 (17–82) years • M:F = 1.2	16S rRNA amplicon; MiSeq	3.5–240 h	Javan et al., 2016b
Liver, spleen	45	• Median age 41 (16–82) years • M:F = 1.6	16S rRNA amplicon; MiSeq	4–78 h	Javan et al., 2017
Brain, heart, liver, spleen, prostate, uterus	40	• Age range 15–20 years for youngest and 85–90 for oldest • M:F = 1.86	16S rRNA sequencing	1–18 days	Lutz et al., 2020
Proximal large intestine	12	• Median age 65 (51–88) years • M:F = 0.5 • 12 white	qPCR	9–20 days	Hauther et al., 2015
Proximal large intestine/cecum	4	Age range 62–67 years 4 white	16S rRNA amplicon; MiSeq	0–800 CDH	DeBruyn and Hauther, 2017
Oral cavity	3	• Median age 80 (20–81) years • M:F = 0.5 • 4 white	16S rRNA amplicon; MiSeq	0–12 days	Adserias-Garriga et al., 2017b
Burial soil	3	• Median age 80 (20–81) years • M:F = 0.5 • 4 white	16S rRNA amplicon; MiSeq	0–12 days	Adserias-Garriga et al., 2017a
Burial soil	18	–	16S rRNA amplicon; MiSeq	3–303 days	Finley et al., 2016

for deducing models of PMI estimation (Javan et al., 2016b). However, the small number of cadavers available for some of these studies, as well as the inability to account for the PMI in donated cadavers, requires further evaluation of the skin microbiome (Javan et al., 2016a). The skin microbiome is also in a state of dynamic flux due to its constant exposure to the environment. Therefore, the microbial community may not always be exclusive to the individual, and the skin bacterial population truly representative of a particular environment, e.g., coryneforms in moist environments, should also be taken into consideration.

Internal Organs

Contrary to external body surfaces, internal organs are not directly under the influence of external environmental factors in the initial stages of decomposition. The decomposition of the various human organs also happen in a different order of progression, where organs such as the stomach, intestine, liver, and pancreas undergo decomposition first and that of tendons, bones, and nulligravid uterus happen last (Javan et al., 2016b). Characteristic microbial succession in the internal sites and organs can thus be utilized to predict PMI. In 11 cases in which the PMI ranged from 20 to 240 h, organ thanatomicrobiome analyses suggested that facultative anaerobes, such as *Lactobacillus*, predominate in cadavers with short PMI (29.5 h), while cadavers with long PMI (240 h) have a predominance of obligate anaerobes like *Clostridium* (Can et al., 2014). In a cross-sectional study involving 27 human cadavers from criminal cases with known PMI, statistically significant organ-, sex-, and time-dependent differences were found in the thanatomicribome communities of the brain, heart, liver, spleen, buccal cavity, and blood (Javan et al., 2016b). With the increase in the depth of taxonomic levels, the prediction models could better explain (65% at the species level compared to 21% at the family and genus level) the variance in PMI due to different variables. Notably, Firmicutes (e.g., *Clostridium*, *Peptoniphilus*, and *Bacillus*) was a stable biomarker across microbial communities derived from different body locations. Thus, organ-specific microbial signatures can possibly be useful in PMI estimation. Species-specific identification of microbes must also be emphasized upon when going for thanatomicrobiome signatures. However, ambient-temperature exposure, which imparts significant influence on the microbial community, was not accounted for in this study (Javan et al., 2016b).

A postmortem microbiome of liver and spleen revealed *Clostridium* sp. in 95% of the samples. In the 16S rRNA gene, the V4 hypervariable region could sufficiently discriminate *Clostridium* sp. in postmortem tissue, where it predominates in both short (4 h) and long (10 days) PMIs (Javan et al., 2016b, 2017). This ubiquity of *Clostridium* sp. is explained by its rapid generation times, the proteolytic activity resulting in transmigration to other tissues, and hypoxic environment, together known as the postmortem clostridium effect. In line with this finding, *Clostridium* spp. was the most abundant organism isolated from the postmortem liver and spleen tissues of drug overdose subjects (Brackett, 2018). Moreover, the preponderance of *Pseudomonas* sp. was detected exclusively in internal organs such as the brain, heart, liver, spleen as well as the blood of female cadavers, while males contained the facultative anaerobe Rothia (Javan et al., 2016b). This organ- as well as sex-specific difference is also important for pathologists working on decomposing human bodies for location, identity, and possible cause of death.

A targeted qPCR study from human large intestinal microflora showed that *Bacteroides* and *Lactobacillus* declined exponentially with increasing PMI (Hauther et al., 2015). In contrast, *Bifidobacterium* did not show any significant trends, pointing out the potential of the former two microbes as quantitative indicators of PMI. This was further validated by an amplicon sequencing experiment, which revealed a microbial succession over time toward a common decay community in four bodies, wherein *Bacteroides* and *Parabacteroides* decreased, while *Clostridium* and *Anaerosphaera*, as well as *Ignatzschineria* and *Wohlfahrtiimonas*, increased significantly (DeBruyn and Hauther, 2017). Notably, the latter two are fly associated γ-Proteobacteria, and therefore they could provide a better understanding of PMI estimation by augmenting the existing options. Overall, these findings may help build predictive models of different thanatomicrobiome communities according to the internal organ microbial signatures.

Skeletal Remains and Burial Soil

As a potential extension of the microbial clock from internal organs to skeletal remains, Damann et al. (2015) collected the lower rib from 12 decomposing bodies. An interstage taxonomic succession of Firmicutes, Bacteroidetes, Actinobacteria, and Acidobacteria from partially skeletonized remains to dry remains was observed. For each successive decay stage, α-Proteobacteria increased, while γ-Proteobacteria decreased. The communities associated with the partially skeletonized remains (PMI of 27–284 days) were closer to those of the human gut (Firmicutes and Bacteroidetes), while those of the dry remains (PMI of 554–1,692 days) mimicked that of the soil (Actinobacteria and Acidobacteria). Similar findings were obtained from the soil samples of three cadavers: Proteobacteria and Bacteroidetes dominated the first 6 days of decomposition, after which there was a sudden shift to an increase in Firmicutes, with a concomitant decrease in Proteobacteria (Adserias-Garriga et al., 2017a).

The decomposition soil of 18 human subjects showed increased taxon richness and decreased evenness and a consistent diversity with buried remains, whereas surface cadavers showed a decrease in all parameters, alluding to the importance of the depth of burial as it can affect the microbial community composition and, subsequently, PMI estimations (Finley et al., 2016). Moreover, the microbial succession of the soil communities is complete by at least 420 days after burial (Thomas et al., 2017). Hence, in longer PMI or dry remains stage, the soil communities are analogous with varying depths. It is still well to remember that the decomposition process varies widely depending on hot or cold environmental conditions, as a colder climate can preserve intact cadavers

for longer periods of time. Hence, the anatomical location of sampling is crucial as is the surrounding environment, as external body sites which allow for non-invasive sample collections, despite providing an accurate microbial clock, are more prone to environmental changes, especially in hotter climates, whereas internal body sites, although less impacted by the environment, require invasive sampling. A 2013 study demarcated liver and pericardial fluid as best sampling sites and concluded that postmortem sampling is to be done within 5 days (Tuomisto et al., 2013). This is because pericardial fluid aspiration needs no handling of organs in the abdominal cavity and can be easily carried out with a sterile needle. For estimating longer PMI, the microbial successions of bones or burial soil are, again, better choices. A combination of all these parameters can be taken into account after careful consideration of the location of death, time frame, and convenience of sampling.

Supportive Evidence in Animal Surrogates

Many research groups have employed animal models such as swine (Dickson et al., 2011) and mice models (Dong et al., 2019) (**Table 3**), as these are similar to human bodies to the extent that they can provide a better understanding of the decomposition process in humans whereas being more readily available at the same time compared to human bodies (Javan et al., 2016a; Zhou and Bian, 2018). They are also low in cost compared to carrying out experiments on human cadavers.

Metcalf et al. (2013) in five dead and decomposing mice over 48 days at eight time-points each, used high-throughput sequencing to study samples taken from the abdominal cavity, skin of head and torso, and associated grave soil to infer that the succession of prokaryotic and eukaryotic microbial communities may be useful in the estimation of PMI in early stages of decomposition, especially within 3 days (Metcalf et al., 2013). They suggested a microbial clock to provide an accurate PMI estimate as shifts in the presence and abundance of specific bacterial and eukaryotic taxa in skin and soil sites were consistent during the decomposition stages. Epinecrotic community composition and succession analyses showed that relatively abundant phyla like Proteobacteria, Firmicutes, Bacteroidetes, and Actinobacteria, under their notable variation during the decomposition process, can aid in PMI estimation (Guo et al., 2016). Indeed, metagenomic sequencing of epinecrotic bacterial communities showed that phylum- and family-level taxonomic resolution could explain 62.1 and 78.5% variation in physiological time, respectively, throughout decomposition (Pechal et al., 2014). A phylum-level taxonomic resolution in a random forest model with Campylobacteraceae, Moraxellaceae, Aerococcaceae, Micrococcaceae, Clostridiales Incertae Sedis XI, Comamonadaceae, and Fusobacteriaceae was the better choice to distinguish between days of decomposition (Pechal et al., 2014). The oral bacterial community, in a study on adult mice, showed distinct characteristic features at different taxonomic levels. Within 10 days after death, Proteobacteria and Firmicutes dominate, with γ-Proteobacteria showing a strong positive linear correlation with PMI. At the family and genus levels, the relative abundance of Enterobacteriaceae and Proteus increased with an increase in PMI (Dong et al., 2019). Furthermore, the postmortem microbiome in 20 Dutch rabbits showed organ- and temperature-specific changes in the community, which is in line with the findings in human cadavers. The intestinal thanatomicrobiome was also different in composition compared to those of the kidneys and lungs (Lawrence et al., 2019). Another study on the postmortem structure and function dynamics of *Staphylococcus aureus* by whole-body fluorescent imaging and culture-based methods showed that it reaches its highest concentration on 5–7 days postmortem and, thus, can potentially be tracked to determine PMI ranges (Burcham et al., 2016).

In gnotobiotic mice associated with human microbiota (hfa), enterococci and enterobacteria thrived in ileal lumen 3 and 24 h postmortem, respectively, pointing toward the fact that these microbes can possibly be used to precisely define PMI under specific ambient conditions (Heimesaat et al., 2012). The intestinal flora diversity in SD rats reduced again up to the 30th day postmortem, whereas the intragroup similarity showed a downward trend, indicating that the succession of intestinal flora is related to PMI (Li et al., 2018). With a T-RFLP approach, decomposing pork loin showed a stable abundance of Enterobacteriaceae 24 h onward (Handke et al., 2017). β-Proteobacteria was present within the first few days, while α-Proteobacteria became abundant 15 days onward. Firmicutes were present in the beginning as well as on 40-, 50-, and 60-day samples, thus making them significant in the estimation of prolonged PMI. However, Comamonadaceae and Clostridiaceae were only present up to 24 h, which was contradictory to previous findings from other groups. This difference can either be attributed to environmental variation or the different techniques used by other groups, primarily 454 pyrosequencing or Illumina sequencing technologies. The proteomic analysis of the same sample could identify several bacterial subspecies and strains, namely *Rhodopseudomonas palustris* strain BisB18 and *Baizongia pistaciae* strain Bp (Handke et al., 2017). However, high signals from muscle peptides prevent the possibility of appropriately identifying bacteria-specific peaks. Overall, these studies indicate that Proteobacteria and Firmicutes show significant variability in abundance with time after death, and may be considered as potentially useful in the estimation of PMI. Finally, an RNA-based denaturing gradient gel electrophoresis analysis of an isolated pig leg bacterial community in the context of soil bacterial profile revealed that soil communities were significantly different compared to control soil (fresh sandy loam garden soil without any carcass), especially in the advanced phase of decay, implying the importance of soil bacterial community profiling to identify secret burials (Bergmann et al., 2014). The terrestrial communities' analysis in the form of transcriptome or proteome of the microbes can also prove to be a useful tool in PMI estimation. However, accuracy can be badly affected by the mode of sample collection and environmental temperature.

TABLE 3 | Mammalian model systems for estimation of time since death using microbiome data.

Specimen type	Sample size (*n*)	Technique(s) used	Characteristic finding(s)	References
B6C3F1 mice; abdominal cavity, skin, and burial soil	Five replicates over eight time-points	NGS	• Burkholderia, Proteobacteria, Sphingobacteria (soil and skin), *Clostridium*, *Lactobacillus* (abdomen)—increase in abundance with time • Bacilli, Bacteroidia (abdomen), Pseudomonadales, Epsilonproteobacteria (skin)—decrease in abundance with time	Metcalf et al., 2013
C57BL/6 mice and hfa mice	–	RT-qPCR of 16S rRNA variable region	Enterococci—significantly higher in 3, 6, 48, and 72 h pm Enterobacteria—significantly higher between 12 and 24 h pm	Heimesaat et al., 2012
Swine; buccal cavity, skin, interior anal cavity	3	454 FLX Titanium pyrosequencing	• Bacteroidetes, Proteobacteria, Actinobacteria, Firmicutes—significant indicator phyla • Bacteroidaceae, Moraxellaceae, Bacillaceae, and Clostridiales Incertae Sedis XI—significant indicator families for decomposition	Pechal et al., 2014
SKH-1 Elite female mice; Liver, spleen, heart, stomach, kidney, intestine	90	Whole-body fluorescent imaging	*Staphylococcus aureus*—highest concentration at 5–7 days pm, and undetectable by culture on day 30	Burcham et al., 2016
Mice; bone marrow, stomach, heart, intestine	45	High-throughput RNA sequencing	• In stomach and intestines, Lactobacillaceae increased after 26 h, whereas Clostridiaceae increased after 170 h • Clostridiaceae dominated after 26 h in bone marrow and 9 h in the heart	Burcham et al., 2019
Mice; heart, intestine, lungs, bone marrow	63	Whole metagenome and metatranscriptome sequencing	Clostridium—in lungs, heart, and bone marrow at 7 days	Burcham et al., 2019
Dutch rabbits; ileum, cecum, kidney, lung	20	RT-qPCR and Illumina sequencing	• Firmicutes and Bacteroidetes dominated intestinal microbiome • Proteobacteria were highly abundant in lung and kidney at specific times and temperatures	Lawrence et al., 2019
Swine; cheek skin, snout, neck	3	ABI capillary electrophoresis sequencing	• γ- Proteobacteria- predominant on wound sites • Bacteroidetes—abundant on cheek and snouts	Dickson et al., 2011
Piglet; skin over abdomen and rib cage	3	454 FLX Titanium pyrosequencing	Variation of Proteobacteria (increasing) and Firmicutes (decreasing) over decomposition process during both summer and winter	Benbow et al., 2015
Piglet; skin and carcass	4	ARISA	Epinecrotic biofilm communities have distinctive shifts in the first and second weeks pm	Lang et al., 2016
SD Rats	–	PCR, DGGE, and sequencing	• *Enterococcus* sp. abundant on 1st and 5th day • *Bacillus thuringiensis* abundant on 10th, 15th, and 20th day • *Enterococcus faecalis* on 25th and 30th day after death	Li et al., 2018
Adult female Sprague–Dawley rats; buccal cavity, rectum	18	NGS	With the progress of decomposition, γ-Proteobacteria became predominant in the buccal cavity and the rectum, while Firmicutes and Bacteroidetes gradually decreased	Guo et al., 2016

(Continued)

TABLE 3 | Continued

Specimen type	Sample size (*n*)	Technique(s) used	Characteristic finding(s)	References
Sprague–Dawley rats; epinecrotic, epilithic and environmental water specimens	9	Illumina MiSeq sequencing	• In epinecrotic samples, Proteobacteria and Firmicutes were dominant phylum; Clostridiaceae was the most abundant taxon • In epilithic samples, Proteobacteria was the dominant phylum, while Comamonadaceae was the dominant taxon	He et al., 2019
Pig leg (*Sus scrofa domesticus*)	1	RT-PCR and DGGE	Species variation compared to soil bacterial community during active (day 28) and advanced decay (day 77)	Bergmann et al., 2014
Adult mice (strain ICR); oral cavity	24	NGS	Proteobacteria and Firmicutes dominate at phylum level, Enterobacteriaceae (family level) and Proteus (genus level) dominate as PMI increases	Dong et al., 2019
Pork loin	3	T-RFLP, capillary electrophoresis and LC-Orbitrap MS	Proteobacteria, Firmicutes	Handke et al., 2017

In the Estimation of Postmortem Submersion Interval

Postmortem submersion interval (PMSI), which is the amount of time human remains have been partially or fully submerged in an aquatic environment, demands a different approach as the decomposition process in water bodies is slower with adipocere formation due to anaerobic environment when compared with that of a terrestrial environment due to the effect of water temperature, salinity, tides, depth, mobility of the carcass, and scavengers (Caruso, 2016; He et al., 2019). Epinecrotic community from *S. scrofa* carcasses revealed not only significant temporal shifts in the bacterial communities at the phyletic and generic levels with the progression of the decomposition process but also significant seasonal variation between summer and winter (Benbow et al., 2015). Furthermore, using automated ribosomal intergenic spacer analysis method on *S. scrofa* carcasses, epinecrotic biofilms were shown to exhibit significant succession during the first 2 weeks, implying its possible use to estimate PMSI (Lang et al., 2016). An experiment on three swine heads for the bacterial succession data across two seasons, five stages of decomposition, and bacterial communities showed site- and season-specific preponderance and colonization (Dickson et al., 2011). Proteobacteria, Firmicutes, Bacteroidetes, and Actinobacteria were found to be the predominant phyla in epinecrotic rat samples, which showed dynamic variation, with Proteobacteria decreasing while Firmicutes increasing during decomposition, the latter becoming the dominant phylum on days 5 and 6 (He et al., 2019).

Furthermore, Clostridiaceae and Comamonadaceae were the most abundant families which displayed different succession patterns, as the former was abundant on days 1, 4, 5, and 6, while the latter decreased from day 4 onward. Thus, the detection of a combination of Clostridiaceae with Comamonadaceae could help narrow down the PMSI estimation (He et al., 2019). Currently, PMSI estimation is mainly derived from the inspection of the gross morphological findings of the recovered remains, like ADDs and total aquatic decomposition score (De Donno et al., 2014). Nevertheless, the abovementioned studies point toward the possibilities of novel methods which can bring about PMSI estimation not only for whole bodies but also for separated body parts as a result of pre- or post-submersion dismemberment.

Although mammalian models provide an idea of the applicability of the microbiome in PMI estimation, these experiments are carried out in tightly controlled, predictable environments, which means that the data have to be validated on human cadavers before making its way into the forensic toolbox. It is, therefore, well to remember that studies on animal models can only be able to support certain proposals made on humans and must not be treated as equivalent to human studies.

TOWARD LEGAL MEDICINE: THE NEXT STEP

We have to pay attention to adopting the new methods into the medicolegal system, the path to which will not be a smooth one. Currently, no laws exist as such regarding the use of thanatomicrobiome evidence in criminal investigations. The collection of microbial evidence from the crime scene or the individual for comparison is sure to bring newer legal and ethical concerns. The first steps in incorporating the thanatomicrobiome into the courtroom are the admissibility of microbial evidence and collection of samples. This depends largely upon the existing laws and regulations holding up the standards of the criminal justice system in a country, but as long as the method (a) has been widely tested, (b) has widely accepted operation standards, (c) is generally accepted in the scientific community, and (d) has known potential quantifiable error rates, the thanatomicrobiome could be made admissible as expert testimony. One other issue likely to present itself as a hurdle, as microbial evidence starts being introduced into the courtroom, is the complexity of the statistical analysis, as it

can potentially confuse and distract the jury. The standards for statistical analyses, therefore, need to be stricter, accompanied by sound theory, but long before these issues can be delved into in depth, solid groundwork needs to be carried out to regularize the entire process.

Metcalf has suggested a step-by-step approach on how this can be achieved—by identifying the needs, primary research, prototype development, and validation and acceptance, leading to adoption (Metcalf, 2019). This requires communication between the researcher and the medicolegal community to identify the main factors that need to be addressed by microbial technologies. The stakeholders, in this case, are the forensic community including law enforcers and medical examiners, the research community, the technology manufacturers, and the decision-makers. Basic research in collaboration with the forensic community and connecting to the legal system by the proper use of technology will help overcome many limitations. First, practical needs such as the sample collection stage or collection site need to be identified to be incorporated into the forensic workflow. Then, the research community can connect to the end-users in the justice and legal system by communicating their findings and help develop newer, robust, and cost-effective technologies. Currently, coordinated efforts, such as the American Gut Project, Earth Microbiome Project, QIIME2 platform with options for machine learning analysis, rapid drop in sequencing costs, and more and more standardized datasets coming up, can help the transition of a prototype from an academic lab to a practitioner a lot easier, taking into consideration that sampling and data generation methods undergo rigorous quality control, which is still challenging. Validation is essential in the development of any new technology, more so in forensic medicine since these methods affect the conviction or acquittal of individuals, policy decisions, and government actions on a larger scale (Schmedes et al., 2016). Every method, therefore, must be validated, including but not limited to its sensitivity, specificity, accuracy, the limit of detection, and error rate, before implementation. Moreover, this must happen on a local level, in connection with the end-users and legal community, since thanatomicrobial tools are always likely to be developed based on data from a particular population and specific geolocation. Hence, the need of the hour is the validation of large, population-, ethnicity-, and location-based datasets.

Future Perspectives—"The Road Less Traveled"

To realize the potential of human thanatomicrobiome characterization in forensic sciences, we should incorporate additional methods already available to or recently coming up to expand the horizons. More advanced sequencing methods can be developed and streamlined for data elucidation from complex metagenomic samples. Genomic data alone is not sufficient to get the picture beyond the species richness of the microbial communities. The level of gene transcription and the functional protein profiles are unknown even when we identify the genomic DNA of a species. Other "omic" studies, such as transcriptomics, proteomics, and metabolomics, have become far more accessible than before, and these areas should be further ventured into thanatomicrobiome research. Whole transcriptome analysis of the microbes is an exciting prospect, as it provides insights into gene expression and function in an organ-, tissue-, or condition-specific manner (D'Argenio, 2018; Heintz-Buschart and Wilmes, 2018). In fact, mRNA transcripts degrade differently for different tissues depending upon postmortem gene regulation and expression signatures (Scott et al., 2020). Publicly available bioinformatic pipelines like SAMSA have been developed for meta-transcriptomic data analysis (Westreich et al., 2016). The high sensitivity, rapidity, and its broad spectrum in characterizing microorganisms make mass spectrometry an intriguing option to be utilized in thanatomicrobiome work. Bottom-up proteomics approaches like MALDI-TOF and LC-MS/MS have already been used successfully in identifying bacteria (Fenselau, 2013; Handke et al., 2017). Proteomics can also rule out causes of infection by investigating the presence of bacterial protein components. Finally, it can help in elucidating the functionality, understanding, and succession of the gut microbiome in disease states and postmortem (Toscano et al., 2018). These prospects make metaproteomics and thanatoproteomics potential and forthcoming major areas in forensic microbiology research.

Microbial succession after death is a complex process, and different independent estimates could throw light on the same forensic variable. These estimates, then, can be combined within a Bayesian framework to improve the accuracy of the said variable. Such statistical frameworks can draw from several observations and need not necessarily be confined to the thanatomicrobiome alone to resolve the problem at hand, such as time since death. Furthermore, machine learning methods are being widely employed, keeping in pace with the massive amount of data that is being generated and will only grow with time. These methods can help in the prediction of pre-existing pathological conditions; as we know, many diseases affect human colonies. They can also link microbial communities' host phenotypes and other environmental parameters (Qu et al., 2019). As we incorporate multiple "omic" data types and diverse human thanatomicrobiome datasets and continue to grow upon our computational arsenal, we will improve our understanding of the succession of the thanatomicrobial communities.

CONCLUSION

Determining the time of death within a narrow window has always been of utmost importance and equally challenging. We have often pondered as death investigators, as we are always coerced to do a retrospective search from tremendously variable and often incomplete medical reliquiae, whether it is even possible to develop foolproof technologies. Nevertheless, the promise of applicability is there, in PMI estimation through different phases of decomposition, in studying aquatic microbial succession as a tool for PMSI, as well as to differentiate between antemortem and postmortem and between freshwater and saltwater drowning, in quantifying the human epinecrotic

communities, and in diagnosing or ruling out infectious causes of death. Newly developing technologies and the parallel development of computational pipelines are promising and have made it possible for the facilitation of generalizable microbial models, specific for each environment, into the medicolegal system and aid in forensic investigations, to exist in our foreseeable future.

AUTHOR CONTRIBUTIONS

PS and PP conceived the manuscript. DR and ST conducted the literature and designed the tables and figures. PP, DR, and ST drafted the manuscript. PS and PP edited the manuscript. All the authors contributed to the article and approved the submitted version.

REFERENCES

Abad Santos, J. (2019). Decomposition of pig carcasses at varying room temperature. *Themis* 7:3.

Ackerman, M. J., Tester, D. J., and Driscoll, D. J. (2001). Molecular autopsy of sudden unexplained death in the young. *Am. J. Forensic Med. Pathol.* 22, 105–111. doi: 10.1097/00000433-200106000-00001

Adjutantis, G., and Goutselinis, A. (1972). Estimation of the time of death by potassium levels in the vitreous humour. *Forensic Sci.* 1, 55–60. doi: 10.1016/0300-9432(72)90147-1

Adserias-Garriga, J., Hernández, M., Quijada, N. M., Rodríguez Lázaro, D., Steadman, D., and Garcia-Gil, J. (2017a). Daily thanatomicrobiome changes in soil as an approach of postmortem interval estimation: an ecological perspective. *Forensic Sci. Int.* 278, 388–395. doi: 10.1016/j.forsciint.2017.07.017

Adserias-Garriga, J., Quijada, N. M., Hernandez, M., Rodríguez Lázaro, D., Steadman, D., and Garcia-Gil, L. J. (2017b). Dynamics of the oral microbiota as a tool to estimate time since death. *Mol. Oral Microbiol.* 32, 511–516. doi: 10.1111/omi.12191

Alan, G., and Sarah, J. P. (2012). Microbes as forensic indicators. *Trop Biomed.* 29, 311–330.

Almeida, A., Mitchell, A. L., Boland, M., Forster, S. C., Gloor, G. B., Tarkowska, A., et al. (2019). A new genomic blueprint of the human gut microbiota. *Nature* 568, 499–504. doi: 10.1038/s41586-019-0965-1

Alvarez-Lafuente, R., Aguilera, B., Suárez-Mier, M. A., Morentin, B., Vallejo, G., Gómez, J., et al. (2008). Detection of human herpesvirus-6, Epstein-Barr virus and cytomegalovirus in formalin-fixed tissues from sudden infant death: a study with quantitative real-time PCR. *Forensic Sci. Int.* 178, 106–111. doi: 10.1016/j.forsciint.2008.02.007

Amar, J., Lange, C., Payros, G., Garret, C., Chabo, C., Lantieri, O., et al. (2013). Blood microbiota dysbiosis is associated with the onset of cardiovascular events in a large general population: the D.E.S.I.R. study. *PloS One* 8:e54461. doi: 10.1371/journal.pone.0054461

American Society for Microbiology (2013). *FAQ: Human Microbiome.* Washington, DC. Available online at: https://www.ncbi.nlm.nih.gov/books/NBK562894/ (accessed January 7, 2021).

Angelakis, E., Bachar, D., Yasir, M., Musso, D., Djossou, F., Melenotte, C., et al. (2018). Comparison of the gut microbiota of obese individuals from different geographic origins. *New Microbes New Infect.* 27, 40–47. doi: 10.1016/j.nmni.2018.11.005

Arenas, M., Pereira, F., Oliveira, M., Pinto, N., Lopes, A. M., Gomes, V., et al. (2017). Forensic genetics and genomics: much more than just a human affair. *PLoS Genet.* 13:e1006960. doi: 10.1371/journal.pgen.1006960

Arumugam, M., Raes, J., Pelletier, E., Le Paslier, D., Yamada, T., Mende, D. R., et al. (2011). Enterotypes of the human gut microbiome. *Nature* 473, 174–180. doi: 10.1038/nature09944

Bardale, R. V., Tumram, N. K., Dixit, P. G., and Deshmukh, A. Y. (2012). Evaluation of histologic changes of the skin in postmortem period. *Am. J. Forensic. Med. Pathol.* 33, 357–361. doi: 10.1097/PAF.0b013e31822c8f21

Belk, A., Xu, Z. Z., Carter, D. O., Lynne, A., Bucheli, S., Knight, R., et al. (2018). Microbiome data accurately predicts the postmortem interval using random forest regression models. *Genes* 9:104. doi: 10.3390/genes9020104

Bell, C. R., Wilkinson, J. E., Robertson, B. K., and Javan, G. T. (2018). Sex-related differences in the thanatomicrobiome in postmortem heart samples using bacterial gene regions V1-2 and V4. *Lett. Appl. Microbiol.* 67, 144–153. doi: 10.1111/lam.13005

Benbow, M. E., Barton, P. S., Ulyshen, M. D., Beasley, J. C., DeVault, T. L., Strickland, M. S., et al. (2018). Necrobiome framework for bridging decomposition ecology of autotrophically and heterotrophically derived organic matter. *Ecol. Monogr.* 89:e01331. doi: 10.1002/ecm.1331

Benbow, M. E., Pechal, J. L., Lang, J. M., Erb, R., and Wallace, J. R. (2015). The potential of high-throughput metagenomic sequencing of aquatic bacterial communities to estimate the postmortem submersion interval. *J. Forensic Sci.* 60, 1500–1510. doi: 10.1111/1556-4029.12859

Bergmann, R. C., Ralebitso-Senior, T. K., and Thompson, T. J. (2014). An RNA-based analysis of changes in biodiversity indices in response to Sus scrofa domesticus decomposition. *Forensic Sci. Int.* 241, 190–194. doi: 10.1016/j.forsciint.2014.06.001

Bharti, R., and Grimm, D. G. (2019). Current challenges and best-practice protocols for microbiome analysis. *Brief Bioinform.* 22, 178–193. doi: 10.1093/bib/bbz155

Bik, E. M., Eckburg, P. B., Gill, S. R., Nelson, K. E., Purdom, E. A., Francois, F., et al. (2006). Molecular analysis of the bacterial microbiota in the human stomach. *Proc. Natl. Acad. Sci. U.S.A.* 103, 732–737. doi: 10.1073/pnas.0506655103

Børsting, C., and Morling, N. (2016). "Genomic applications in forensic medicine," in *Medical and Health Genomics, 1st edn* (Elsevier), 295–309. doi: 10.1016/b978-0-12-420196-5.00022-8

Børsting, C., Rockenbauer, E., and Morling, N. (2009). Validation of a single nucleotide polymorphism (SNP) typing assay with 49 SNPs for forensic genetic testing in a laboratory accredited according to the ISO 17025 standard. *Forensic Sci. Int. Genet.* 4, 34–42. doi: 10.1016/j.fsigen.2009.04.004

Brackett, E. (2018). *Thanatomicrobiome Signatures in Drug Overdose Cases*. Thesis, Honors College of Middle Tennessee State University, Murfreesboro, TN.

Burcham, Z. M., Cowick, C. A., Baugher, C. N., Pechal, J. L., Schmidt, C. J., Rosch, J. W., et al. (2019a). Total RNA analysis of bacterial community structural and functional shifts throughout vertebrate decomposition. *J. Forensic Sci.* 64, 1707–1719. doi: 10.1111/1556-4029.14083

Burcham, Z. M., Pechal, J. L., Schmidt, C. J., Bose, J. L., Rosch, J. W., Benbow, M. E., et al. (2019b). Bacterial community succession, transmigration, and differential gene transcription in a controlled vertebrate decomposition model. *Front. Microbiol.* 10:745. doi: 10.3389/fmicb.2019.00745

Burcham, Z. M., Hood, J. A., Pechal, J. L., Krausz, K. L., Bose, J. L., Schmidt, C. J., et al. (2016). Fluorescently labeled bacteria provide insight on post-mortem microbial transmigration. *Forensic Sci. Int.* 264, 63–69. doi: 10.1016/j.forsciint.2016.03.019

Can, I., Javan, G. T., Pozhitkov, A. E., and Noble, P. A. (2014). Distinctive thanatomicrobiome signatures found in the blood and internal organs of humans. *J. Microbiol. Methods* 106, 1–7. doi: 10.1016/j.mimet.2014.07.026

Caruso, J. L. (2016). Decomposition changes in bodies recovered from water. *Acad. Forensic Pathol.* 6, 19–27. doi: 10.23907/2016.003

Chakravorty, S., Helb, D., Burday, M., Connell, N., and Alland, D. (2007). A detailed analysis of 16S ribosomal RNA gene segments for the diagnosis of pathogenic bacteria. *J. Microbiol. Methods* 69, 330–339. doi: 10.1016/j.mimet.2007.02.005

Chevalier, C., Stojanović, O., Colin, D. J., Suarez-Zamorano, N., Tarallo, V., Veyrat-Durebex, C., et al. (2015). Gut microbiota orchestrates energy homeostasis during cold. *Cell* 163, 1360–1374. doi: 10.1016/j.cell.2015.11.004

Cho, I., and Blaser, M. J. (2012). The human microbiome: at the interface of health and disease. *Nat. Rev. Genet.* 13, 260–270. doi: 10.1038/nrg3182

Damann, F. E., Williams, D. E., and Layton, A. C. (2015). Potential use of bacterial community succession in decaying human bone for estimating postmortem interval. *J. Forensic Sci.* 60, 844–850. doi: 10.1111/1556-4029.12744

D'Argenio, V. (2018). Human microbiome acquisition and bioinformatic challenges in metagenomic studies. *Int. J. Mol. Sci.* 19:383. doi: 10.3390/ijms19020383

D'Argenio, V., Torino, M., Precone, V., Casaburi, G., Esposito, M. V., Iaffaldano, L., et al. (2017). The cause of death of a child in the 18th century solved by bone microbiome typing using laser microdissection and next generation sequencing. *Int. J. Mol. Sci.* 18:109. doi: 10.3390/ijms18010109

Das, B., Ghosh, T. S., Kedia, S., Rampal, R., Saxena, S., Bag, S., et al. (2018). Analysis of the Gut microbiome of rural and urban healthy indians living in sea level and high altitude areas. *Sci. Rep.* 8:10104. doi: 10.1038/s41598-018-28550-3

Dash, H. R., and Das, S. (2020). Thanatomicrobiome and epinecrotic community signatures for estimation of post-mortem time interval in human cadaver. *Appl. Microbiol. Biotechnol.* 104, 9497–9512. doi: 10.1007/s00253-020-10922-3

David, L. A., Maurice, C. F., Carmody, R. N., Gootenberg, D. B., Button, J. E., Wolfe, B. E., et al. (2014). Diet rapidly and reproducibly alters the human gut microbiome. *Nature* 505, 559–563. doi: 10.1038/nature12820

De Donno, A., Campobasso, C. P., Santoro, V., Leonardi, S., Tafuri, S., and Introna, F. (2014). Bodies in sequestered and non-sequestered aquatic environments: a comparative taphonomic study using decompositional scoring system. *Sci. Justice* 54, 439–446. doi: 10.1016/j.scijus.2014.10.003

de la Cuesta-Zuluaga, J., Kelley, S. T., Chen, Y., Escobar, J. S., Mueller, N. T., Ley, R. E., et al. (2019). Age- and sex-dependent patterns of gut microbial diversity in human adults. *mSystems* 4:e261-19. doi: 10.1128/mSystems.00261-19

DeBruyn, J. M., and Hauther, K. A. (2017). Postmortem succession of gut microbial communities in deceased human subjects. *PeerJ* 5:e3437. doi: 10.7717/peerj.3437

Deel, H., Bucheli, S., Belk, A., Ogden, S., Lynne, A., Carter, D. O., et al. (2020). "Using microbiome tools for estimating the postmortem interval," in *Microbial Forensics, 3rd edn.* (Elsevier), 171–191. doi: 10.1016/B978-0-12-815379-6.00012-X

Dehingia, M., Devi, K. T., Talukdar, N. C., Talukdar, R., Reddy, N., Mande, S. S., et al. (2015). Gut bacterial diversity of the tribes of India and comparison with the worldwide data. *Sci. Rep.* 5:18563. doi: 10.1038/srep18563

Dickson, G. C., Poulter, R. T., Maas, E. W., Probert, P. K., and Kieser, J. A. (2011). Marine bacterial succession as a potential indicator of postmortem submersion interval. *Forensic Sci. Int.* 209, 1–10. doi: 10.1016/j.forsciint.2010.10.016

Donaldson, A. E., and Lamont, I. L. (2014). Estimation of post-mortem interval using biochemical markers. *Aust. J. Forensic Sci.* 46, 8–26. doi: 10.1080/00450618.2013.784356

Dong, K., Xin, Y., Cao, F., Huang, Z., Sun, J., Peng, M., et al. (2019). Succession of oral microbiota community as a tool to estimate postmortem interval. *Sci. Rep.* 9:13063. doi: 10.1038/s41598-019-49338-z

Fenselau, C. C. (2013). Rapid characterization of microorganisms by mass spectrometry—what can be learned and how? *J. Am. Soc. Mass Spectrom.* 24, 1161–1166. doi: 10.1007/s13361-013-0660-7

Fernández-Rodríguez, A., Ballesteros, S., de Ory, F., Echevarría, J. E., Alvarez-Lafuente, R., Vallejo, G., et al. (2006). Virological analysis in the diagnosis of sudden children death: a medico-legal approach. *Forensic Sci. Int.* 161, 8–14. doi: 10.1016/j.forsciint.2005.10.012

Finley, S. J., Lorenco, N., Mulle, J., Robertson, B. K., and Javan, G. T. (2015). Assessment of microbial DNA extraction methods of cadaver soil samples for criminal investigations. *Aust. J. Forensic Sci.* 48, 265–272. doi: 10.1080/00450618.2015.1063690

Finley, S. J., Pechal, J. L., Benbow, M. E., Robertson, B. K., and Javan, G. T. (2016). Microbial signatures of cadaver gravesoil during decomposition. *Microb. Ecol.* 71, 524–529. doi: 10.1007/s00248-015-0725-1

Fouts, D. E., Torralba, M., Nelson, K. E., Brenner, D. A., and Schnabl, B. (2012). Bacterial translocation and changes in the intestinal microbiome in mouse models of liver disease. *J. Hepatol.* 56, 1283–1292. doi: 10.1016/j.jhep.2012.01.019

Fox, G. E., Wisotzkey, J. D., and Jurtshuk, P. Jr. (1992). How close is close: 16S rRNA sequence identity may not be sufficient to guarantee species identity. *Int. J. Syst. Bacteriol.* 42, 166–170. doi: 10.1099/00207713-42-1-166

Furet, J. P., Firmesse, O., Gourmelon, M., Bridonneau, C., Tap, J., Mondot, S., et al. (2009). Comparative assessment of human and farm animal faecal microbiota using real-time quantitative PCR. *FEMS Microb. Ecol.* 68, 351–362. doi: 10.1111/j.1574-6941.2009.00671.x

Gaulke, C. A., and Sharpton, T. J. (2018). The Influence of ethnicity and geography on human gut microbiome composition. *Nat. Med.* 24, 1495–1496. doi: 10.1038/s41591-018-0210-8

Gevers, W. (1975). Biochemical aspects of cell death. *Forensic Sci.* 6, 25–29. doi: 10.1016/0300-9432(75)90220-4

Gill, S. R., Pop, M., Deboy, R. T., Eckburg, P. B., Turnbaugh, P. J., Samuel, B. S., et al. (2006). Metagenomic analysis of the human distal gut microbiome. *Science* 312, 1355–1359. doi: 10.1126/science.1124234

Grice, E. A., and Segre, J. A. (2011). The skin microbiome. *Nat. Rev. Microbiol.* 9, 244–253. doi: 10.1038/nrmicro2537

Guo, J., Fu, X., Liao, H., Hu, Z., Long, L., Yan, W., et al. (2016). Potential use of bacterial community succession for estimating post-mortem interval as revealed by high-throughput sequencing. *Sci. Rep.* 7:24197. doi: 10.1038/srep24197

Gupta, V. K., Paul, S., and Dutta, C. (2017). Geography, ethnicity or subsistence-specific variations in human microbiome composition and diversity. *Front. Microbiol.* 8:1162. doi: 10.3389/fmicb.2017.01162

Handke, J., Procopio, N., Buckley, M., van der Meer, D., Williams, G., Carr, M., et al. (2017). Successive bacterial colonisation of pork and its implications for forensic investigations. *Forensic Sci. Int.* 281, 1–8. doi: 10.1016/j.forsciint.2017.10.025

Hao, Y., Pei, Z., and Brown, S. M. (2017). Bioinformatics in microbiome analysis. *Methods Microbiol.* 44, 1–18. doi: 10.1016/bs.mim.2017.08.002

Hauther, K. A., Cobaugh, K. L., Jantz, L. M., Sparer, T. E., and DeBruyn, J. M. (2015). Estimating time since death from postmortem human gut microbial communities. *J. Forensic Sci.* 60, 1234–1240. doi: 10.1111/1556-4029.12828

He, F., Huang, D., Liu, L., Shu, X., Yin, H., and Li, X. (2008). A novel PCR-DGGE-based method for identifying plankton 16S rDNA for the diagnosis of drowning. *Forensic Sci. Int.* 176, 152–156. doi: 10.1016/j.forsciint.2007.08.005

He, J., Guo, J., Fu, X., and Cai, J. (2019). Potential use of high-throughput sequencing of bacterial communities for postmortem submersion interval estimation. *Braz. J. Microbiol.* 50, 999–1010. doi: 10.1007/s42770-019-00119-w

Heimesaat, M. M., Boelke, S., Fischer, A., Haag, L. M., Loddenkemper, C., Kühl, A. A., et al. (2012). Comprehensive postmortem analyses of intestinal microbiota changes and bacterial translocation in human flora associated mice. *PLoS One* 7:e40758. doi: 10.1371/journal.pone.0040758

Heintz-Buschart, A., and Wilmes, P. (2018). Human gut microbiome: function matters. *Trends Microbiol.* 26, 563–574. doi: 10.1016/j.tim.2017.11.002

Henssge, C. (1988). Death time estimation in case work. I. The rectal temperature time of death nomogram. *Forensic Sci. Int.* 38, 209–236. doi: 10.1016/0379-0738(88)90168-5

Human Microbiome Project Consortium (2012a). A framework for human microbiome research. *Nature* 486, 215–221. doi: 10.1038/nature11209

Human Microbiome Project Consortium (2012b). Structure, function and diversity of the healthy human microbiome. *Nature* 486, 207–214. doi: 10.1038/nature11234

Huys, G., Coopman, V., Van Varenbergh, D., and Cordonnier, J. (2012). Selective culturing and genus-specific PCR detection for identification of *Aeromonas* in tissue samples to assist the medico-legal diagnosis of death by drowning. *Forensic Sci. Int.* 221, 11–15. doi: 10.1016/j.forsciint.2012.03.017

Hyde, E. R., Haarmann, D. P., Lynne, A. M., Bucheli, S. R., and Petrosino, J. F. (2013). The living dead: bacterial community structure of a cadaver at the onset and end of the bloat stage of decomposition. *PLoS One* 8:e77733. doi: 10.1371/journal.pone.0077733

Hyde, E. R., Haarmann, D. P., Petrosino, J. F., Lynne, A. M., and Bucheli, S. R. (2015). Initial insights into bacterial succession during human decomposition. *Int. J. Legal Med.* 129, 661–671. doi: 10.1007/s00414-014-1128-4

Iancu, L., Dean, D. E., and Purcarea, C. (2018). Temperature influence on prevailing Necrophagous diptera and bacterial taxa with forensic implications for postmortem interval estimation: a review. *J. Med. Entomol.* 55, 1369–1379. doi: 10.1093/jme/tjy136

Janda, J. M., and Abbott, S. L. (2007). 16S rRNA gene sequencing for bacterial identification in the diagnostic laboratory: pluses, perils, and pitfalls. *J Clin. Microbiol.* 45, 2761–2764. doi: 10.1128/JCM.01228-07

Javan, G. T., Finley, S. J., Abidin, Z., and Mulle, J. G. (2016a). The thanatomicrobiome: a missing piece of the microbial puzzle of death. *Front. Microbiol.* 7:225. doi: 10.3389/fmicb.2016.00225

Javan, G. T., Finley, S. J., Can, I., Wilkinson, J. E., Hanson, J. D., and Tarone, A. M. (2016b). Human thanatomicrobiome succession and time since death. *Sci. Rep.* 6:29598. doi: 10.1038/srep29598

Javan, G. T., Finley, S. J., Smith, T., Miller, J., and Wilkinson, J. E. (2017). Cadaver thanatomicrobiome signatures: the ubiquitous nature of clostridium species in human decomposition. *Front. Microbiol.* 8:2096. doi: 10.3389/fmicb.2017.02096

Javan, G. T., Finley, S. J., Tuomisto, S., Hall, A., Benbow, M. E., and Mills, D. (2019). An interdisciplinary review of the thanatomicrobiome in human decomposition. *Forensic Sci. Med. Pathol.* 15, 75–83. doi: 10.1007/s12024-018-0061-0

Jha, A. R., Davenport, E. R., Gautam, Y., Bhandari, D., Tandukar, S., Ng, K. M., et al. (2018). Gut microbiome transition across a lifestyle gradient in Himalaya. *PLoS Biol.* 16:e2005396. doi: 10.1371/journal.pbio.2005396

Johnson, H. R., Trinidad, D. D., Guzman, S., Khan, Z., Parziale, J. V., DeBruyn, J. M., et al. (2016). A machine learning approach for using the postmortem skin microbiome to estimate the postmortem interval. *PLoS One* 11:e0167370. doi: 10.1371/journal.pone.0167370

Jordan, H. R., and Tomberlin, J. K. (2017). Abiotic and biotic factors regulating inter-kingdom engagement between insects and microbe activity on vertebrate remains. *Insects* 8:54.

Jovel, J., Patterson, J., Wang, W., Hotte, N., O'Keefe, S., Mitchel, T., et al. (2016). Characterization of the Gut microbiome using 16S or shotgun metagenomics. *Front. Microbiol.* 7:459. doi: 10.3389/fmicb.2016.00459

Kakizaki, E., Ogura, Y., Kozawa, S., Nishida, S., Uchiyama, T., Hayashi, T., et al. (2012). Detection of diverse aquatic microbes in blood and organs of drowning victims: first metagenomic approach using high-throughput 454-pyrosequencing. *Forensic Sci. Int.* 220, 135–146. doi: 10.1016/j.forsciint.2012.02.010

Kashyap, V. K., and Pillai, V. V. (1989). Efficacy of entomological method in estimation of post mortem interval: a comparative analysis. *Forensic Sci. Int.* 40, 245–250. doi: 10.1016/0379-0738(89)90182-5

Kaszubinski, S. F., Pechal, J. L., Schmidt, C. J., Jordan, H. R., Benbow, M. E., and Meek, M. H. (2020a). Evaluating bioinformatic pipeline performance for forensic microbiome analysis. *J. Forensic Sci.* 65, 513–525. doi: 10.1111/1556-4029.14213

Kaszubinski, S. F., Pechal, J. L., Smiles, K., Schmidt, C. J., Jordan, H. R., Meek, M. H., et al. (2020b). Dysbiosis in the dead: human postmortem microbiome beta-dispersion as an indicator of manner and cause of death. *Front. Microbiol.* 11:555347. doi: 10.3389/fmicb.2020.555347

Keeney, K. M., Yurist-Doutsch, S., Arrieta, M. C., and Finlay, B. B. (2014). Effects of antibiotics on human microbiota and subsequent disease. *Annu. Rev. Microbiol.* 68, 217–235. doi: 10.1146/annurev-micro091313-103456

Klappenbach, J. A., Dunbar, J. M., and Schmidt, T. M. (2000). rRNA operon copy number reflects ecological strategies of bacteria. *Appl. Environ. Microbiol.* 66, 1328–1333. doi: 10.1128/aem.66.4.1328-1333.2000

Klong-Klaew, T., Ngoen-Klan, R., Moophayak, K., Sukontason, K., Irvine, K. N., Tomberlin, J. K., et al. (2018). Predicting geographic distribution of forensically significant blow flies of subfamily chrysomyinae (*Diptera*: *Calliphoridae*) in Northern Thailand. *Insects* 9:106. doi: 10.3390/insects9030106

Kodama, W. A., Xu, Z., Metcalf, J. L., Song, S. J., Harrison, N., Knight, R., et al. (2019). Trace evidence potential in postmortem skin microbiomes: from death scene to morgue. *J. Forensic Sci.* 64, 791–798. doi: 10.1111/1556-4029.13949

Kunin, V., Engelbrektson, A., Ochman, H., and Hugenholtz, P. (2010). Wrinkles in the rare biosphere: pyrosequencing errors can lead to artificial inflation of diversity estimates. *Environ. Microbiol.* 12, 118–123. doi: 10.1111/j.1462-2920.2009.02051.x

Lamendella, R., Domingo, J. W., Ghosh, S., Martinson, J., and Oerther, D. B. (2011). Comparative fecal metagenomics unveils unique functional capacity of the swine gut. *BMC Microbiol.* 11:103. doi: 10.1186/1471-2180-11-103

Lang, J. M., Erb, R., Pechal, J. L., Wallace, J. R., McEwan, R. W., and Benbow, M. E. (2016). Microbial biofilm community variation in flowing habitats: potential utility as bioindicators of postmortem submersion intervals. *Microorganisms* 4:1. doi: 10.3390/microorganisms4010001

Langille, M. G., Zaneveld, J., Caporaso, J. G., McDonald, D., Knights, D., Reyes, J. A., et al. (2013). Predictive functional profiling of microbial communities using 16S rRNA marker gene sequences. *Nat. Biotechnol.* 31, 814–821. doi: 10.1038/nbt.2676

Lawrence, K. E., Lam, K. C., Morgun, A., Shulzhenko, N., and Löhr, C. V. (2019). Effect of temperature and time on the thanatomicrobiome of the cecum, ileum, kidney, and lung of domestic rabbits. *J. Vet. Diagn. Invest.* 31, 155–163. doi: 10.1177/1040638719828412

Lax, S., Hampton-Marcell, J. T., Gibbons, S. M., Colares, G. B., Smith, D., Eisen, J. A., et al. (2015). Forensic analysis of the microbiome of phones and shoes. *Microbiome* 3:21. doi: 10.1186/s40168-015-0082-9

Lederberg, J., and McCray, A. T. (2001). Ome sweet 'omics– a genealogical treasury of words. *Scientist* 15:8.

Lee, S. Y., Woo, S. K., Lee, S. M., Ha, E. J., Lim, K. H., Choi, K. H., et al. (2017). Microbiota composition and pulmonary surfactant protein expression as markers of death by drowning. *J. Forensic Sci.* 62, 1080–1088. doi: 10.1111/1556-4029.13347

Leipzig, J. (2016). A review of bioinformatic pipeline frameworks. *Brief. Bioinform.* 18, 530–536. doi: 10.1093/bib/bbw020

Li, H., Liu, R. N., Zhang, S. R., Yuan, L., and Xu, J. R. (2018). Succession law of intestinal flora after death in SD rats. *Fa Yi Xue Za Zhi* 34, 482–486. doi: 10.12116/j.issn.1004-5619.2018.05.005

Liszt, K., Zwielehner, J., Handschur, M., Hippe, B., Thaler, R., and Haslberger, A. G. (2009). Characterization of bacteria, clostridia and *Bacteroides* in faeces of vegetarians using qPCR and PCR-DGGE fingerprinting. *Ann. Nutr. Metab.* 54, 253–257. doi: 10.1159/000229505

Liu, L., Li, Y., Li, S., Hu, N., He, Y., Pong, R., et al. (2012). Comparison of next-generation sequencing systems. *J. Biomed. Biotechnol.* 2012:251364. doi: 10.1155/2012/251364

Lucci, A., Campobasso, C. P., Cirnelli, A., and Lorenzini, G. (2008). A promising microbiological test for the diagnosis of drowning. *Forensic Sci. Int.* 182, 20–26. doi: 10.1016/j.forsciint.2008.09.004

Lunetta, P., Penttilä, A., and Hällfors, G. (1998). Scanning and transmission electron microscopical evidence of the capacity of diatoms to penetrate the alveolo-capillary barrier in drowning. *Int. J. Legal Med.* 111, 229–237. doi: 10.1007/s004140050159

Lutz, H., Vangelatos, A., Gottel, N., Osculati, A., Visona, S., Finley, S. J., et al. (2020). Effects of extended postmortem interval on microbial communities in organs of the human cadaver. *Front. Microbiol.* 11:569630. doi: 10.3389/fmicb.2020.569630

Madea, B. (2016). Methods for determining time of death. *Forensic Sci. Med. Pathol.* 12, 451–485. doi: 10.1007/s12024-016-9776-y

Madea, B., Ortmann, J., and Doberentz, E. (2019). Estimation of the time since death-Even methods with a low precision may be helpful in forensic casework. *Forensic Sci. Int.* 302:109879. doi: 10.1016/j.forsciint.2019.109879

Malla, M. A., Dubey, A., Kumar, A., Yadav, S., Hashem, A., and Abd Allah, E. F. (2019). Exploring the human microbiome: the potential future role of next-generation sequencing in disease diagnosis and treatment. *Front. Immunol.* 9:2868. doi: 10.3389/fimmu.2018.02868

Matsuki, T., Watanabe, K., Fujimoto, J., Miyamoto, Y., Takada, T., Matsumoto, K., et al. (2002). Development of 16S rRNA-genetargeted group-specific primers for the detection and identification of predominant bacteria in human feces. *Appl. Environ. Microbiol.* 68, 5445–5451. doi: 10.1128/aem.68.11.5445-5451.2002

Meadow, J. F., Altrichter, A. E., and Green, J. L. (2014). Mobile phones carry the personal microbiome of their owners. *PeerJ.* 2:e447. doi: 10.7717/peerj.447

Megyesi, M. S., Nawrocki, S. P., and Haskell, N. H. (2005). Using accumulated degree-days to estimate the postmortem interval from decomposed human remains. *J. Forensic Sci.* 50, 618–626.

Metcalf, J. L. (2019). Estimating the postmortem interval using microbes: knowledge gaps and a path to technology adoption. *Forensic Sci. Int. Genet.* 38, 211–218. doi: 10.1016/j.fsigen.2018.11.004

Metcalf, J. L., Wegener Parfrey, L., Gonzalez, A., Lauber, C. L., Knights, D., Ackermann, G., et al. (2013). A microbial clock provides an accurate estimate of the postmortem interval in a mouse model system. *eLife* 2:e01104. doi: 10.7554/eLife.01104

Metcalf, J. L., Xu, Z. Z., Weiss, S., Lax, S., Van Treuren, W., Hyde, E. R., et al. (2016). Microbial community assembly and metabolic function during mammalian corpse decomposition. *Science* 351, 158–162. doi: 10.1126/science.aad2646

Meurs, J., Krap, T., and Duijst, W. (2019). Evaluation of postmortem biochemical markers: completeness of data and assessment of implication in the field. *Sci. Justice* 59, 177–180. doi: 10.1016/j.scijus.2018.09.002

Mignard, S., and Flandrois, J. P. (2006). 16S RRNA sequencing in routine bacterial identification: a 30-month experiment. *J. Microbiol. Methods* 67, 574–581. doi: 10.1016/j.mimet.2006.05.009

Mitchelson, K. R. (2003). The use of capillary electrophoresis for DNA polymorphism analysis. *Mol. Biotechnol.* 24, 41–68. doi: 10.1385/MB:24:1:41

Na, J. Y., Park, J. H., Kim, S. H., and Park, J. T. (2017). Bacteria as normal flora in postmortem body fluid samples. *Korean J. Leg. Med.* 41:87. doi: 10.7580/kjlm.2017.41.4.87

Nam, Y. D., Jung, M. J., Roh, S. W., Kim, M. S., and Bae, J. W. (2011). Comparative analysis of Korean human gut microbiota by barcoded pyrosequencing. *PLoS One* 6:e22109. doi: 10.1371/journal.pone.0022109

Nguyen, N. P., Warnow, T., Pop, M., and White, B. (2016). A perspective on 16S rRNA operational taxonomic unit clustering using sequence similarity. *NPJ Biofilms Microbiomes* 2:16004. doi: 10.1038/npjbiofilms.2016.4

NIH HMP Working Group, Peterson, J., Garges, S., Giovanni, M., McInnes, P., Wang, L., et al. (2009). The NIH human microbiome project. *Genome Res.* 19, 2317–2323. doi: 10.1101/gr.096651.109

Nishijima, S., Suda, W., Oshima, K., Kim, S. W., Hirose, Y., Morita, H., et al. (2016). The gut microbiome of healthy Japanese and its microbial and functional uniqueness. *DNA Res.* 23, 125–133. doi: 10.1093/dnares/dsw002

Nogueira, T., David, P. H. C., and Pothier, J. (2019). Antibiotics as both friends and foes of the human gut microbiome: the microbial community approach. *Drug Dev. Res.* 80, 86–97. doi: 10.1002/ddr.21466

Norén, T. (2010). Clostridium difficile and the disease it causes. *Methods Mol. Biol.* 646, 9–35. doi: 10.1007/978-1-60327-365-7_2

Oliveira, M., and Amorim, A. (2018). Microbial forensics: new breakthroughs and future prospects. *Appl. Microbiol. Biotechnol.* 102, 10377–10391. doi: 10.1007/s00253-018-9414-6

Parson, W., and Bandelt, H. J. (2007). Extended guidelines for mtDNA typing of population data in forensic science. *Forensic Sci. Int. Genet.* 1, 13–19. doi: 10.1016/j.fsigen.2006.11.003

Pechal, J. L., Crippen, T. L., Benbow, M. E., Tarone, A. M., Dowd, S., and Tomberlin, J. K. (2014). The potential use of bacterial community succession in forensics as described by high throughput metagenomic sequencing. *Int. J. Legal Med.* 128, 193–205. doi: 10.1007/s00414-013-0872-1

Pechal, J. L., Schmidt, C. J., Jordan, H. R., and Benbow, M. E. (2018). A large-scale survey of the postmortem human microbiome, and its potential to provide insight into the living health condition. *Sci. Rep.* 8:5724. doi: 10.1038/s41598-018-23989-w

Petrosino, J. F., Highlander, S., Luna, R. A., Gibbs, R. A., and Versalovic, J. (2009). Metagenomic pyrosequencing and microbial identification. *Clin. Chem.* 55, 856–866. doi: 10.1373/clinchem.2008.107565

Phillips, C., Salas, A., Sánchez, J. J., Fondevila, M., Gómez-Tato, A., Alvarez-Dios, J., et al. (2007). Inferring ancestral origin using a single multiplex assay of ancestry-informative marker SNPs. *Forensic Sci. Int. Genet.* 1, 273–280. doi: 10.1016/j.fsigen.2007.06.008

Pittner, S., Bugelli, V., Weitgasser, K., Zissler, A., Sanit, S., Lutz, L., et al. (2020). A field study to evaluate PMI estimation methods for advanced decomposition stages. *Int. J. Legal Med.* 134, 1361–1373. doi: 10.1007/s00414-020-02278-0

Qu, K., Guo, F., Liu, X., Lin, Y., and Zou, Q. (2019). Application of machine learning in microbiology. *Front. Microbiol.* 10:827. doi: 10.3389/fmicb.2019.00827

Quince, C., Walker, A. W., Simpson, J. T., Loman, N. J., and Segata, N. (2017). Shotgun metagenomics, from sampling to analysis. *Nat. Biotechnol.* 35, 833–844. doi: 10.1038/nbt.3935

Rácz, E., Könczöl, F., Tóth, D., Patonai, Z., Porpáczy, Z., Kozma, Z., et al. (2016). PCR-based identification of drowning: four case reports. *Int. J. Legal Med.* 130, 1303–1307. doi: 10.1007/s00414-016-1359-7

Rehman, A., Rausch, P., Wang, J., Skieceviciene, J., Kiudelis, G., Bhagalia, K., et al. (2016). Geographical patterns of the standing and active human gut microbiome in health and IBD. *Gut* 65, 238–248. doi: 10.1136/gutjnl-2014-308341

Rognum, T. O., Holmen, S., Musse, M. A., Dahlberg, P. S., Stray-Pedersen, A., Saugstad, O. D., et al. (2016). Estimation of time since death by vitreous humor hypoxanthine, potassium, and ambient temperature. *Forensic Sci. Int.* 262, 160–165. doi: 10.1016/j.forsciint.2016.03.001

Rothberg, J. M., and Leamon, J. H. (2008). The development and impact of 454 sequencing. *Nat. Biotechnol.* 26, 1117–1124. doi: 10.1038/nbt1485

Rutty, G. N., Bradley, C. J., Biggs, M. J., Hollingbury, F. E., Hamilton, S. J., Malcomson, R. D., et al. (2015). Detection of bacterioplankton using PCR probes as a diagnostic indicator for drowning; the Leicester experience. *Leg. Med.* 17, 401–408. doi: 10.1016/j.legalmed.2015.06.001

Salam, H. F. A., Shaat, E. A., Aziz, M. H. A., MoneimSheta, A. A., and Hussein, H. A. S. M. (2012). Estimation of postmortem interval using thanatochemistry and postmortem changes. *Alex. J. Med.* 48, 335–344. doi: 10.1016/j.ajme.2012.05.004

Salipante, S. J., Kawashima, T., Rosenthal, C., Hoogestraat, D. R., Cummings, L. A., Sengupta, D. J., et al. (2014). Performance comparison of Illumina and ion torrent next-generation sequencing platforms for 16S rRNA-based bacterial community profiling. *Appl. Environ. Microbiol.* 80, 7583–7591. doi: 10.1128/AEM.02206-14

Schloissnig, S., Arumugam, M., Sunagawa, S., Mitreva, M., Tap, J., Zhu, A., et al. (2013). Genomic variation landscape of the human gut microbiome. *Nature* 493, 45–50. doi: 10.1038/nature11711

Schmedes, S. E., Sajantila, A., and Budowle, B. (2016). Expansion of microbial forensics. *J. Clin. Microbiol.* 54, 1964–1974. doi: 10.1128/JCM.00046-16

Schnorr, S. L., Candela, M., Rampelli, S., Centanni, M., Consolandi, C., Basaglia, G., et al. (2014). Gut microbiome of the Hadza hunter-gatherers. *Nat Commun.* 5:3654. doi: 10.1038/ncomms4654

Schoenly, K. G., Haskell, N. H., Mills, D. K., Bieme-Ndi, C., Larsen, K., and Lee, Y. (2006). recreating death's acre in the school yard: using pig carcasses as model corpses, to teach concepts of forensic entomology & ecological succession. *Am. Biol. Teach.* 68, 402–410. doi: 10.2307/4452028

Schouls, L. M., Schot, C. S., and Jacobs, J. A. (2003). Horizontal transfer of segments of the 16S rRNA genes between species of the *Streptococcus anginosus* group. *J. Bacteriol.* 185, 7241–7246. doi: 10.1128/jb.185.24.7241-7246.2003

Scott, L., Finley, S. J., Watson, C., and Javan, G. T. (2020). Life and death: a systematic comparison of antemortem and postmortem gene expression. *Gene* 731:144349. doi: 10.1016/j.gene.2020.144349

Senghor, B., Sokhna, C., Ruimy, R., and Lagier, J. C. (2018). Gut microbiota diversity according to dietary habits and geographical provenance. *Hum. Microbiome J.* 7, 1–9. doi: 10.1016/j.humic.2018.01.001

Sharma, R., Garg, R. K., and Gaur, J. R. (2015). Various methods for the estimation of the post mortem interval for *Calliphoridae*: a review. *Egyp. J. Forensic Sci.* 5, 1–12. doi: 10.1016/j.ejfs.2013.04.002

Shin, N. R., Whon, T. W., and Bae, J. W. (2015). *Proteobacteria*: microbial signature of dysbiosis in gut microbiota. *Trends Biotechnol.* 33, 496–503. doi: 10.1016/j.tibtech.2015.06.011

Sitthiwong, N., Ruangyuttikarn, W., Vongvivach, S., and Peerapornpisal, Y. (2014). Detection and identification of diatoms in tissue samples of drowning victims. *Chiang Mai J. Sci.* 41, 1020–1031.

Soergel, D. A., Dey, N., Knight, R., and Brenner, S. E. (2012). Selection of primers for optimal taxonomic classification of environmental 16S rRNA gene sequences. *ISME J.* 6, 1440–1444. doi: 10.1038/ismej.2011.208

Spicka, A., Johnson, R., Bushing, J., Higley, L. G., and Carter, D. O. (2011). Carcass mass can influence rate of decomposition and release of ninhydrin-reactive nitrogen into gravesoil. *Forensic Sci. Int.* 209, 80–85. doi: 10.1016/j.forsciint.2011.01.002

Stokes, K. L., Forbes, S. L., and Tibbett, M. (2013). Human versus animal: contrasting decomposition dynamics of mammalian analogues in experimental taphonomy. *J. Forensic Sci.* 58, 583–591. doi: 10.1111/1556-4029.12115

Sullivan, K. M., Hopgood, R., and Gill, P. (1992). Identification of human remains by amplification and automated sequencing of mitochondrial DNA. *Int. J. Legal Med.* 105, 83–86. doi: 10.1007/BF02340829

Suzuki, M. T., and Giovannoni, S. J. (1996). Bias caused by template annealing in the amplification of mixtures of 16S RRNA genes by PCR. *Appl. Environ. Microbiol.* 62, 625–630. doi: 10.1128/AEM.62.2.625-630.1996

Thomas, T. B., Finley, S. J., Wilkinson, J. E., Wescott, D. J., Gorski, A., and Javan, G. T. (2017). Postmortem microbial communities in burial soil layers of skeletonized humans. *J. Forensic Leg. Med.* 49, 43–49. doi: 10.1016/j.jflm.2017.05.009

Tie, J., Uchigasaki, S., Haseba, T., Ohno, Y., Isahai, I., and Oshida, S. (2010). Direct and rapid PCR amplification using digested tissues for the diagnosis of drowning. *Electrophoresis* 31, 2411–2415. doi: 10.1002/elps.200900754

Tomberlin, J. K., Mohr, R., Benbow, M. E., Tarone, A. M., and VanLaerhoven, S. (2011). A roadmap for bridging basic and applied research in forensic entomology. *Annu. Rev. Entomol.* 56, 401–421. doi: 10.1146/annurev-ento-051710-103143

Toscano, M., de Grandi, R., and Drago, L. (2018). Proteomics: the new era of microbiology. *Microbiol. Med.* 32, 183–184. doi: 10.4081/mm.2017.7348

Trivedi, U. H., Cézard, T., Bridgett, S., Montazam, A., Nichols, J., Blaxter, M., et al. (2014). Quality control of next-generation sequencing data without a reference. *Front. Genet.* 5:111. doi: 10.3389/fgene.2014.00111

Tu, Q., He, Z., and Zhou, J. (2014). Strain/species identification in metagenomes using genome-specific markers. *Nucleic Acids Res.* 42:e67. doi: 10.1093/nar/gku138

Tu, Q., Li, J., Shi, Z., Chen, Y., Lin, L., Li, J., et al. (2017). HuMiChip2 for strain level identification and functional profiling of human microbiomes. *Appl. Microbiol. Biotechnol.* 101, 423–435. doi: 10.1007/s00253-016-7910-0

Tuomisto, S., Karhunen, P. J., Vuento, R., Aittoniemi, J., and Pessi, T. (2013). Evaluation of postmortem bacterial migration using culturing and real-time quantitative PCR. *J. Forensic Sci.* 58, 910–916. doi: 10.1111/1556-4029.12124

Uchiyama, T., Kakizaki, E., Kozawa, S., Nishida, S., Imamura, N., and Yukawa, N. (2012). A new molecular approach to help conclude drowning as a cause of death: simultaneous detection of eight bacterioplankton species using real-time PCR assays with TaqMan probes. *Forensic Sci. Int.* 222, 11–26. doi: 10.1016/j.forsciint.2012.04.029

Ventura Spagnolo, E., Stassi, C., Mondello, C., Zerbo, S., Milone, L., and Argo, A. (2019). Forensic microbiology applications: a systematic review. *Leg. Med.* 36, 73–80. doi: 10.1016/j.legalmed.2018.11.002

Vila, A. V., Collij, V., Sanna, S., Sinha, T., Imhann, F., Bourgonje, A. R., et al. (2020). Impact of commonly used drugs on the composition and metabolic function of the gut microbiota. *Nat. Commun.* 11:362. doi: 10.1038/s41467-019-14177-z

Walsh, S., Chaitanya, L., Clarisse, L., Wirken, L., Draus-Barini, J., Kovatsi, L., et al. (2014). Developmental validation of the HIrisPlex system: DNA-based eye and hair colour prediction for forensic and anthropological usage. *Forensic Sci. Int. Genet.* 9, 150–161. doi: 10.1016/j.fsigen.2013.12.006

Wang, Y., Zhang, Z., and Ramanan, N. (1997). The actinomycete Thermobispora bispora contains two distinct types of transcriptionally active 16S rRNA genes. *J. Bacteriol.* 179, 3270–3276. doi: 10.1128/jb.179.10.3270-3276.1997

Weiss, S., Carter, D. O., Metcalf, J. L., and Knight, R. (2016). Carcass mass has little influence on the structure of gravesoil microbial communities. *Int. J. Leg. Med.* 130, 253–263. doi: 10.1007/s00414-015-1206-2

Westreich, S. T., Korf, I., Mills, D. A., and Lemay, D. G. (2016). SAMSA: a comprehensive metatranscriptome analysis pipeline. *BMC Bioinformatics* 17:399. doi: 10.1186/s12859-016-1270-8

Woydt, L., Bernhard, M., Kirsten, H., Burkhardt, R., Hammer, N., Gries, A., et al. (2018). Intra-individual alterations of serum markers routinely used in forensic pathology depending on increasing post-mortem interval. *Sci. Rep.* 8:12811. doi: 10.1038/s41598-018-31252-5

Wu, G. D., Chen, J., Hoffmann, C., Bittinger, K., Chen, Y.-Y., Keilbaugh, S. A., et al. (2011). Linking long-term dietary patterns with gut microbial enterotypes. *Science* 334, 105–108. doi: 10.1126/science.1208344

Yuan, S., Cohen, D. B., Ravel, J., Abdo, Z., and Forney, L. J. (2012). Evaluation of methods for the extraction and purification of DNA from the human microbiome. *PLoS One* 7:e33865. doi: 10.1371/journal.pone.0033865

Zhang, Y., Pechal, J. L., Schmidt, C. J., Jordan, H. R., Wang, W. W., Benbow, M. E., et al. (2019). Machine learning performance in a microbial molecular autopsy context: a cross-sectional postmortem human population study. *PLoS One* 14:e0213829. doi: 10.1371/journal.pone.0213829

Zhou, W., and Bian, Y. (2018). Thanatomicrobiome composition profiling as a tool for forensic investigation. *Forensic Sci. Res.* 3, 105–110. doi: 10.1080/20961790.2018.1466430

Zhou, X., Bent, S. J., Schneider, M. G., Davis, C. C., Islam, M. R., and Forney, L. J. (2004). Characterization of vaginal microbial communities in adult healthy women using cultivation-independent methods. *Microbiology* 150, 2565–2573. doi: 10.1099/mic.0.26905-0

Zolfo, M., Asnicar, F., Manghi, P., Pasolli, E., Tett, A., and Segata, N. (2018). Profiling microbial strains in urban environments using metagenomic sequencing data. *Biol. Direct.* 13:9. doi: 10.1186/s13062-018-0211-z

Conflict of Interest: The authors declare that the research was conducted in the absence of any commercial or financial relationships that could be construed as a potential conflict of interest.

frontiers in Ecology and Evolution

MINI REVIEW
published: 22 March 2021
doi: 10.3389/fevo.2021.646130

Past, Present, and Future of DNA Typing for Analyzing Human and Non-Human Forensic Samples

Deidra Jordan[1,2] *and DeEtta Mills*[1,2]*

[1] Department of Biological Sciences, Florida International University, Miami, FL, United States, [2] International Forensic Research Institute, Florida International University, Miami, FL, United States

Forensic DNA analysis has vastly evolved since the first forensic samples were evaluated by restriction fragment length polymorphism (RFLP). Methodologies advanced from gel electrophoresis techniques to capillary electrophoresis and now to next generation sequencing (NGS). Capillary electrophoresis was and still is the standard method used in forensic analysis. However, dependent upon the information needed, there are several different techniques that can be used to type a DNA fragment. Short tandem repeat (STR) fragment analysis, Sanger sequencing, SNapShot, and capillary electrophoresis-single strand conformation polymorphism (CE-SSCP) are a few of the techniques that have been used for the genetic analysis of DNA samples. NGS is the newest and most revolutionary technology and has the potential to be the next standard for genetic analysis. This review briefly encompasses many of the techniques and applications that have been utilized for the analysis of human and nonhuman DNA samples.

Keywords: forensic genetics, DNA typing, metabarcoding, soil, microbes, minisatellites, next-generation sequencing

OPEN ACCESS

Edited by:
Gulnaz T. Javan, Alabama State University, United States

Reviewed by:
Carla Santos, University of Minho, Portugal
Antonio Amorim, University of Porto, Portugal

***Correspondence:**
DeEtta Mills
millsd@fiu.edu

Specialty section:
This article was submitted to Evolutionary and Population Genetics, a section of the journal Frontiers in Ecology and Evolution

Received: *25 December 2020*
Accepted: *02 March 2021*
Published: *22 March 2021*

Citation:
Jordan D and Mills D (2021) Past, Present, and Future of DNA Typing for Analyzing Human and Non-Human Forensic Samples. Front. Ecol. Evol. 9:646130. doi: 10.3389/fevo.2021.646130

INTRODUCTION

Forensic genetics applies genetic tools and scientific methodology to solve criminal and civil litigations (Editorial, 2007). Locard's Exchange Principle states that every contact leaves a trace, making any evidence a key component in forensic analysis. Biological evidence can comprise of cellular material or cell-free DNA from crime scenes, and as technologies improved, genetic methodologies were expanded to include human and non-human forensic analyses. Although these methodologies can be used for any genome, the prevalence of databases and standard guidelines has allowed human DNA typing to become the gold standard. This review will discuss the historical progression of DNA analysis techniques, strengths and limitations, and their possible forensic applications applied to human and non-human genetics.

METHODOLOGIES TO DETECT GENETIC DIFFERENCES IN HUMANS IS THE "GOLD STANDARD"

"DNA Fingerprinting": The Beginning of Human Forensic DNA Typing

"DNA fingerprinting" was serendipitously discovered in 1984 (Jeffreys, 2013). What they found propelled DNA "fingerprinting," or DNA typing, to the forefront in legal cases to become the "gold

standard" for forensic genetics in a court of law. Jeffreys first used restriction enzymes to fragment DNA, a method in which restriction endonucleases (RE) enzymes fragment the genomic DNA, producing restriction fragment length polymorphisms (RFLP) patterns. Since each RE recognizes specific DNA sequences to enzymatically cut the DNA, then inherent differences between gene sequences, due to evolutionary changes, will produce different fragment lengths. If the enzyme site is present in one individual but has changed in a different individual, the fragment lengths, once separated and visualized, will differ. While this technique was useful for some studies, Jeffreys did not find it useful for his particular genetic studies. Subsequently when working with the myoglobin gene in seals, he discovered that a short section of that gene – a minisatellite – was conserved and when isolated and cloned could be used to detect inherited genetic lineages as well as individualize a subject. Fragment length separation by electrophoresis, followed by transfer to Southern blot membranes, hybridized with a specific or non-specific complementary isotopic DNA probe, allowed for DNA fragments visualization (Jeffreys et al., 1985b). Upon careful analysis, Jeffreys determined that the fragments represented different combinations of DNA repetitive elements, unique to each individual, and could be used to better identify individuals or kinship lineages (Jeffreys et al., 1985b). Jeffreys' technology was used in several subsequent paternity, immigration, and forensic genetics cases (Gill et al., 1985; Jeffreys et al., 1985a; Evans, 2007). This was just the beginning of a whole new era in DNA typing.

Restriction Fragment Length Polymorphism (RFLP) Analysis: The Past

After Jeffreys' discoveries, many DNA analyses methods involving electrophoretic fragment separation were discovered. Many were based on RFLP principles (Botstein et al., 1980), e.g., amplified fragment length polymorphism (AFLP) (Vos et al., 1995), and terminal restriction fragment length polymorphism (TRFLP) (Liu et al., 1997). Others like length heterogeneity-polymerase chain reaction (LH-PCR) (Suzuki et al., 1998) were based on intrinsic insertions and deletions of bases within specific genetic markers. Sanger sequencing (Sanger and Coulson, 1975), and single-strand conformational polymorphism (SSCP) analysis (Orita et al., 1989), while separated by electrophoresis, are theoretically based on single base sequence changes rather than insertions, deletions or RE site differences. While Jeffrey's DNA fingerprinting method provided a very high power of discrimination, the main limitations were it was very time-consuming and required at least 10–25 ng of DNA to be successful (Wyman and White, 1980). With these limitations, RFLP was not always feasible for forensic cases.

Short Tandem Repeat (STR) Analysis: The Present

The polymerase chain reaction (PCR) was discovered by Kary Mullis in 1985 and helped transform all DNA analyses (Mullis et al., 1986). The current standard for human DNA typing is short tandem repeat (STR) analysis (McCord et al., 2019). This method amplifies highly polymorphic, repetitive DNA regions by PCR and separates them by amplicon length using capillary electrophoresis. These inheritable markers are a series of 2–7 bases tandemly repeated at a specific locus, often in non-coding genetic regions. Forensic STRs are commonly tetranucleotide repeats (Goodwin et al., 2011), chosen because of their technical robustness and high variation among individuals (Kim et al., 2015). The combined DNA index system (CODIS) uses 20 core STR loci, expanded in 2017, and several commercial kits are available that contain these STRs (Oostdik et al., 2014; Ludeman et al., 2018). After amplification, different fluorochromes on each primer set allow for visualization of STRs after deconvolution, creating a STR profile consisting of a combination of genotypes (Gill et al., 2015). This method has become the gold standard for human forensics. Its greatest strength is the standardization of loci used by all laboratories and an extremely large searchable database of genetic profiles. However, some limitations and challenges are faced when dealing with highly degraded or low template DNA samples. To overcome these technical challenges, standardized mini-STR kits have been developed which use shorter versions of the core STRs and can be used in the same manner for forensic cases (Butler et al., 2007; Constantinescu et al., 2012). Keep in mind, DNA typing of humans – a single species – is the gold standard because of (a) the concerted scientific effort to standardize loci to analyze, (b) the development of commercial kits that can produce the same results regardless of instrumentation or laboratory performing the work, (c) a compatible and very large database that provides allelic frequencies for all sub-populations of humans, (d) standardized statistical methods used to report the results and (e) many court cases that have accepted human DNA typing evidence in a court of law – setting the precedent for future cases to use DNA typing results.

METHODOLOGIES TO DETECT GENETIC DIFFERENCES IN NON-HUMANS: PAST AND PRESENT

Amplified Fragment Length Polymorphism (AFLP) Analysis

It was not long before scientists realized that non-human DNA could provide informative genetic evidence in forensic cases. Applications include bioterrorism, wildlife crimes, human identification through skin microorganisms, and so much more (Arenas et al., 2017). Since large quantities of biological materials are frequently not found at crime scenes, successful RFLP analyses were unlikely. Combining restriction enzymes and PCR technology, a process known as AFLP analysis (Vos et al., 1995), became a method for DNA fingerprinting using minute amounts of unknown sourced DNA. REs digest genomic DNA, then ligation of a constructed adapter sequence to the ends of all fragments allows the annealing of primers designed to recognize the adaptor sequences. Subsequent amplification generates many amplicons ranging in length when separated and visualized in an electropherogram or on a gel (Vos et al., 1995; Butler, 2012).

AFLP markers for plant forensic DNA typing have been used because it provides high discrimination, requires only small amounts of DNA and the method is reproducible, all forensically important characteristics (Datwyler and Weiblen, 2006). For example, since most cannabis is clonally propagated, subsequent generations will have identical genetic profiles as seen with AFLP (Miller Coyle et al., 2003), providing useful intelligence links back to the source population. But there are significant variation between cultivars and within populations, so not having a standard database representing the species' diversity for statistical comparisons greatly limits the method's applicability. Another forensic example of its use is differentiating between marijuana and hemp, two morphologically and genetically similar plants, one an illicit drug while the other is not. In this study, three populations of hemp and one population of marijuana were analyzed with AFLP producing 18 bands that were specific to hemp samples. Additionally, 51.9% of molecular variance occurred within populations indicating these polymorphisms were useful for forensic individualization (Datwyler and Weiblen, 2006).

Terminal Restriction Fragment Length Polymorphism (TRFLP) Analysis

As a result of the anthrax letter attacks of 2001, microbial forensics came to the forefront (Schmedes et al., 2016), a discipline that combines multiple scientific specialties – microbiology, genetics, forensic science, and analytical chemistry. One method used to compare microbial communities is TRFLP (Liu et al., 1997; Osborn et al., 2000; Butler, 2012). With this method, the DNA is amplified using "universal," highly conserved primer sequences shared across all organisms of interest, i.e., the 16S rRNA genes in bacteria and Archaea, and then uses REs to fragment the PCR products (**Table 1**). Separated by capillary electrophoresis, only the fluorescently tagged terminal restricted fragments are visualized (Mrkonjic Fuka et al., 2007), reducing the profile complexity and providing high discrimination. TRFLP has been used to characterize complex microbial communities for forensic applications by linking the similarity of the amplicon patterns generated from the intrinsic soil communities to the evidence from a crime scene (Meyers and Foran, 2008; Habtom et al., 2017). This method does provide a distinct pattern reflective of the microbial community, useful for forensic genetics but the method does not provide any sequence information. Another limitation is no standardization of which primer pairs or REs are used, making direct comparisons between studies difficult. This lack of standardization also hinders the development of a database for species identification. Additionally, the method is time-consuming due to the additional step of restriction digestion and the possibility of incomplete enzymatic digestion can complicate the interpretation of results (Osborn et al., 2000; Moreno et al., 2006).

Length Heterogeneity-Polymerase Chain Reaction (LH-PCR)

Another methodology has been used to characterize microbial communities is length heterogeneity- polymerase chain reaction (LH-PCR) (Suzuki et al., 1998). Universal primers complementary to highly conserved domains within genomes are used to amplify hypervariable sequences within specific sequence domains. The 16S/18S rRNA genes, the chloroplast genes or Internal Transcribed Spacer (ITS) regions are commonly used. This technique is based on the natural sequence length variation due to insertions and deletions of bases that occur within a domain (Moreno et al., 2006). It has been used to characterize microbial communities for forensic soil applications where a correlation between geographic location and microbial profiles has proven to be more discriminating than elemental soil analysis (Moreno et al., 2006, 2011; Damaso et al., 2018). With LH-PCR, metagenomic DNA extracted from the soil is amplified using fluorescently labeled universal primers with amplicon peaks within the electropherogram representing the minimum diversity within the community. However, specific sequence information is not known as many peaks of the same size could represent more than one species, thereby masking the community's actual taxonomic diversity. A recent study showed the intrinsic diversity of a microbial mat, masked by LH-PCR, could be further resolved by the inherent sequence differences using capillary electrophoresis-single strand conformational polymorphism (CE-SSCP) analysis (Damaso et al., 2014) and confirmed by sequencing. The advantage of LH-PCR is it is a fast and reproducible method that can correlate geographical areas to microbial patterns with bioinformatics (Damaso et al., 2018); but a soil database would need to be developed to be useful beyond specific geographical areas.

METHODOLOGIES TO DETECT INTERSEQUENCE VARIATION: THE PAST AND PRESENT

Sanger Sequencing and Single Nucleotide Polymorphism (SNP) Variation

The basis of genomic differentiation is the intrinsic order of base pairs within a region that can be evaluated by sequencing. Sanger sequencing has been the gold standard since the 1970s (Sanger and Coulson, 1975). Sanger sequencing was termed the gold standard because of the ability for single base pair resolution allowing for full sequence information to be determined. Robust and extensive databases are also readily available for comparison, i.e., GenBank, to identify an organism. However, it does have some limitations such as the short length (<500–700 bp) and it cannot sequence mixtures of organisms, for example, without cloning, so it would not be useful for sequencing complex microbial communities without intense time, effort and cost.

Other approaches use the ability to identify intrinsic single base sequence variation using single nucleotide polymorphisms (SNPs) within four forensically relevant SNP classes: identity-testing, ancestry informative, phenotype informative, and lineage informative. SNPs are particularly useful when typing degraded DNA or increasing the amount of genetic information retrieved from a sample (Budowle and van Daal, 2008;

TABLE 1 | The basis of differentiation, advantages, and disadvantages of past and current technologies.

Analysis technique	Basis of differentiation	Advantages	Disadvantages
Restriction Fragment Length Polymorphism (RFLP)	Restriction site sequence and fragment length	– High power of discrimination – Reproducible – No prior sequence information required – Can differentiate between homozygotes and heterozygotes	– Time-consuming – Partial digests – Need at least 10–25 ng of DNA – Genetic mutations only identified at restriction cut sites – Not ideal for whole genome variation identification – Requires radioisotopes
Amplified Restriction Fragment Length Polymorphism (AFLP)	Restriction fragment length	– Reproducible – Amplify small amounts of DNA – Species ID not known – Detects dominant bi-allelic markers – No prior sequence information required – Uses capillary electrophoresis techniques	– Time-consuming – Partial digests – Multiple steps can lead to unreproducible results – Genetic mutations only identified at restriction cut sites – Not ideal for whole genome variation identification – Unable to differentiate between heterozygous and homozygous alleles
Terminal-Restriction Fragment Length Polymorphism (TRFLP)	Restriction fragment length	– Less complex results – Amplicon based PCR – Uses capillary electrophoresis techniques	– Partial digests – Genetic mutations only identified at restriction cut sites – Peaks can be representative of more than one species – Not ideal for whole genome variation identification
Length Heterogeneity-PCR(LH-PCR)	Gene fragment length	– Easy, fast results – Reproducible – Uses universal primers – Uses capillary electrophoresis techniques – Provides a quick screening or monitoring tool for community changes	– May underestimate community/mixture complexity – Lack of database hinders species identification – PCR bias can reduce detection of lower DNA template concentrations
Short Tandem Repeat (STR)	STR fragment length	– Fast – Highly reproducible – High level of discrimination, codominant alleles – Standardized across forensic laboratories – Uses low DNA amounts for amplification – Database of genetic profiles and allelic frequencies for statistical comparisons	– Mixture deconvolution not easy – PCR artifacts can complicate results – Challenges with highly degraded or low template DNA
Sanger Sequencing	Sequences every base	– Gold standard for sequence analyses – Uses capillary electrophoresis techniques	– Low throughput – Only 500–700 bases sequenced at a time – Cannot sequence mixtures without cloning
SNaPshot™	Single base changes	– Detects bi-allelic and multi-allelic SNP markers – Able to distinguish between heterozygotes and homozygotes – Human SNP database for statistical comparisons	– Time-consuming – Need to know SNP sequence in advance to design primers – Multiple markers required for high level of discrimination
Single-strand Conformational Polymorphism (SSCP)	2° structure of single-stranded DNA caused by base changes alters strand migration on CE	– Simple – High specificity – Screen potential variations	– Short fragments – Temperature-and mutation sensitive – Nucleotide change not identifiable – DNA strands can reanneal after denaturation affecting mobility during electrophoresis
Next-Generation Sequencing (NGS)	Massive parallel sequencing using various technologies	– High throughput – Deconvolve mixtures – Sequence entire genomes/metagenomes – Simultaneous detection of STR amplicon lengths and SNPs within the amplicon – Used for any DNA (human, non-human, viral, microbes)	– Massive data output that may be challenging to analyze – Analysis algorithms not standardized – Difficult with some technologies to analyze metagenomes to species level

Goodwin et al., 2011). SNaPshot™ is a commercially available SNP kit that can identify known SNPs using single base extension (SBE) technology (Daniel et al., 2015; Fondevila et al., 2017). Wildlife forensics has used SNaPshot™ to identify endangered or trafficked species that are illegally poached to support criminal prosecutions. Elephant species identification from ivory and ivory products (Kitpipit et al., 2017) or differentiating wolf species from dog subspecies (Jiang et al., 2020) are both examples of SNaPshot™ assays developed for wildlife forensics. By using species-specific SNPs, the samples could be identified. But yet again, the limitation becomes the need for species-specific reference databases and the monumental task of developing a robust database for each species. Human SNPs databases with allele frequencies, as seen in dbSNP, however, are available making their forensic application more feasible in some cases.

Next-Generation Sequencing: The Present

Massively parallel sequencing (MPS) or next-generation sequencing (NGS) allows for mixtures of genomes of any species to be sequenced in one analysis (Ansorge, 2009). This technology can sequence thousands of genomic regions simultaneously, allowing for whole-genome, metagenomic sequencing or targeted amplicon sequencing (Gettings et al., 2016). Various NGS technologies are available each using slightly different technologies to sequence DNA (Heather and Chain, 2016). Verogen has developed kits explicitly for human forensic genomics using Illumina's MiSeq FGx system (Guo et al., 2017; Moreno et al., 2018). The FBI recently approved DNA profiles generated by Verogen forensic technology to be uploaded into the National DNA Index System (NDIS) (SWGDAM, 2019), making it the first NGS technology approved for NDIS.

Short tandem repeat mixture deconvolution, degraded, low template samples, and even microbial community samples are just a few of the potential NGS applications for forensic genomics and metagenomics (Borsting and Morling, 2015). In human STR analyses, the greatest challenge is mixture deconvolution. NGS technology presents an increased power of discrimination of STR alleles using the intrinsic SNPs genetic microhaplotypes – a combination of 2–4 closely linked SNPs within an allele (Kidd et al., 2014; Pang et al., 2020). However, the acceptance of analyses programs to deconvolve mixtures has not been standardized to the same level as it has for STRs.

Microbes are the first responders to changes in any environment because they are rapidly affected by the availability of nutrients and their intrinsic habitats. This makes them excellent indicators for studies investigating post-mortem interval (PMI) or as an indicator of soil geographical provenance (Giampaoli et al., 2014; Finley et al., 2015). In decaying organisms, shifts in epinecrotic communities or the thanatomicrobiome are becoming increasingly critical components in investigating PMI (Javan et al., 2016). Sequencing of the thanatomicrobiome revealed the *Clostridium* spp. varied during different stages human decomposition, the "Postmortem Clostridium Effect" (PCE), providing a time signature of the thanatomicrobiome, which could only have been uncovered through NGS (Javan et al., 2017). However, the lack of consensus in analyses techniques must be addressed before NGS methodologies can be introduced into the justice system (**Table 1**).

FUTURE DIRECTIONS AND CONCLUDING REMARKS

Forensic DNA typing has progressed quickly within a short timeframe (**Figure 1**), which can be attributed to the many advancements in molecular biology technologies. As these techniques advance, forensic scientists will analyze more atypical forms of evidence to answer questions deemed unresolvable with traditional DNA analyses. For example, epigenetics and DNA methylation markers have been proposed to estimate age, determine the tissue type, and even differentiate between monozygotic twins (Vidaki and Kayser, 2018). However, since epigenetic patterns are also influenced by environmental factors, they can be dynamic, and a number of confounding factors have the potential to affect predictions and must be taken into account when preparing prediction models (i.e., age estimation). Additionally, phenotype informative SNPs across the genome can infer physical characteristics like eye, hair, and skin color, even age, from an unknown source of DNA retrieved from a crime scene. But this technology could pose an "implicit bias" toward minorities, especially in "societies where racism and xenophobia are now on the rise" (Schneider et al., 2019) if not ethically and judicially implemented. With the increased sensitivity of NGS, low biomass samples from environmental DNA (eDNA) – DNA from soil, water, air – can complement and enhance intelligence gathering or provenance in criminal cases. Pollen and dust are two types of eDNA recently explored for their future forensic potential (Alotaibi et al., 2020; Young and Linacre, 2021). However, if used in criminal investigations where the eDNA

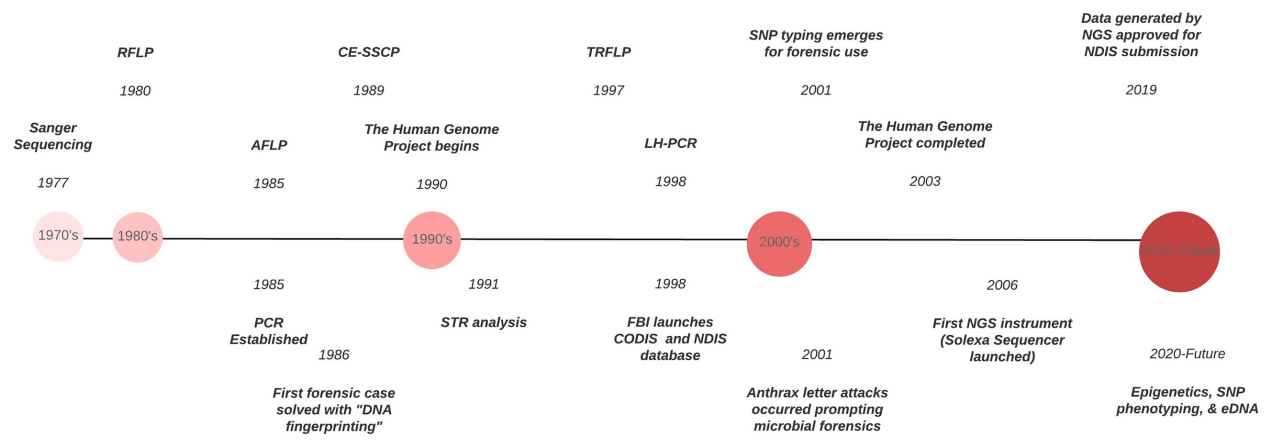

FIGURE 1 | Timeline of the evolution of DNA typing technologies from the 1970's to the present.

collected has had interaction with other environments, there must be some protocol or quality control established to account for variability that is likely to occur. This makes the prudent validation of this type of DNA analysis, essential. Limitations also arise due to lack of a database for comparison of samples and statistical analyses to evaluate the strength of a match like in the analysis of human STR profiles.

DNA has long been the gold standard in human forensic analysis because of the standardization of DNA markers, databases and statistical analyses. It has laid the foundation for these promising new technologies that will significantly enhance intelligence gathering and species identification – human and non-human – in forensic cases. In order for these methodologies to be useful in criminal investigations, they must adhere to the legal standards such as the Frye or Daubert Standards which determines if an expert testimony or evidence is admissible in court. A method can be deemed acceptable if it follows forensic guidelines set by organizations such as NIST's Organization Scientific Area Committees (OSAC), Society for Wildlife Forensic Sciences (SWFS), Scientific Working Group on DNA Analysis Methods (SWGDAM), and the International Society for Forensic Genetics (ISFG) (Linacre et al., 2011) just to name a few. These committees provide the guidelines for validation, interpretation, and quality assurance, all necessary components for DNA analysis. The US Fish and Wildlife forensic laboratory has standardized protocols for crimes against federally endangered or threatened species[1]. However, the more common limiting factors in the development of standard guidelines of non-human forensic genetic analyses across different state laboratories are the lack of consensus in methodologies, supporting allelic databases and standardized statistical analyses. Addressing those issues could lay the foundation for non-human analyses to be on par with human analyses.

AUTHOR CONTRIBUTIONS

DJ designed and wrote the manuscript. DM edited and contributed to the writing of the manuscript. Both authors contributed to the article and approved the submitted version.

ACKNOWLEDGMENTS

We would like to acknowledge the invitation by the editors to contribute to this special edition. DJ was supported by the Florida Education Fund's McKnight Doctoral Fellowship.

[1] https://www.fws.gov/lab/about.php

REFERENCES

Alotaibi, S. S., Sayed, S. M., Alosaimi, M., Alharthi, R., Banjar, A., Abdulqader, N., et al. (2020). Pollen molecular biology: Applications in the forensic palynology and future prospects: A review. *Saudi J. Biol. Sci.* 27, 1185–1190. doi: 10.1016/j.sjbs.2020.02.019

Ansorge, W. J. (2009). Next-generation DNA sequencing techniques. *N. Biotechnol.* 25, 195–203. doi: 10.1016/j.nbt.2008.12.009

Arenas, M., Pereira, F., Oliveira, M., Pinto, N., Lopes, A. M., Gomes, V., et al. (2017). Forensic genetics and genomics: Much more than just a human affair. *PLoS Genet.* 13:e1006960. doi: 10.1371/journal.pgen.1006960

Borsting, C., and Morling, N. (2015). Next generation sequencing and its applications in forensic genetics. *Forensic Sci. Int. Genet.* 18, 78–89. doi: 10.1016/j.fsigen.2015.02.002

Botstein, D., White, R. L., Skolnick, M., and Davis, R. W. (1980). Construction of a genetic linkage map in man using restriction fragment length polymorphisms. *Am. J. Hum. Genet.* 32, 314–331.

Budowle, B., and van Daal, A. (2008). Forensically relevant SNP classes. *Biotechniques* 60:610. doi: 10.2144/000112806

Butler, J. M. (2012). "Non-human DNA," in *Advanced Topics in Forensic DNA Typing*, ed. J. M. Butler (San Diego: Academic Press), 473–495.

Butler, J. M., Coble, M. D., and Vallone, P. M. (2007). STRs vs. SNPs: thoughts on the future of forensic DNA testing. *Forensic Sci. Med. Pathol.* 3, 200–205. doi: 10.1007/s12024-007-0018-1

Constantinescu, C. M., Barbarii, L. E., Iancu, C. B., Constantinescu, A., Iancu, D., and Girbea, G. (2012). Challenging DNA samples solved with MiniSTR analysis. Brief overview. *Rom. J. Leg. Med.* 20, 51–56. doi: 10.4323/rjlm.2012.51

Damaso, N., Martin, L., Kushwaha, P., and Mills, D. (2014). F-108 polymer and capillary electrophoresis easily resolves complex environmental DNA mixtures and SNPs. *Electrophoresis* 35, 3208–3211. doi: 10.1002/elps.201400069

Damaso, N., Mendel, J., Mendoza, M., von Wettberg, E. J., Narasimhan, G., and Mills, D. (2018). Bioinformatics Approach to Assess the Biogeographical Patterns of Soil Communities: The Utility for Soil Provenance. *J. Forensic. Sci.* 63, 1033–1042. doi: 10.1111/1556-4029.13741

Daniel, R., Santos, C., Phillips, C., Fondevila, M., van Oorschot, R. A., Carracedo, A., et al. (2015). A SNaPshot of next generation sequencing for forensic SNP analysis. *Forensic Sci. Int. Genet.* 14, 50–60. doi: 10.1016/j.fsigen.2014.08.013

Datwyler, S. L., and Weiblen, G. D. (2006). Genetic variation in hemp and marijuana (Cannabis sativa L.) according to amplified fragment length polymorphisms. *J. Forensic Sci.* 51, 371–375. doi: 10.1111/j.1556-4029.2006.00061.x

Editorial. (2007). Launching Forensic Science International daughter journal in 2007: Forensic Science International: Genetics. *Forensic Sci. Int. Genet.* 1, 1–2. doi: 10.1016/j.fsigen.2006.10.001

Evans, C. (2007). *The Casebook of Forensic Detection: How Science Solved 100 of the World's Most Baffling Crimes*. New York, NY: Berkley Books.

Finley, S. J., Benbow, M. E., and Javan, G. T. (2015). Potential applications of soil microbial ecology and next-generation sequencing in criminal investigations. *Appl. Soil. Ecol.* 88, 69–78. doi: 10.1016/j.apsoil.2015.01.001

Fondevila, M., Borsting, C., Phillips, C., de la Puente, M., Consortium, E. N., Carracedo, A., et al. (2017). Forensic SNP genotyping with SNaPshot: Technical considerations for the development and optimization of multiplexed SNP assays. *Forensic Sci. Rev.* 29, 57–76.

Gettings, K. B., Kiesler, K. M., Faith, S. A., Montano, E., Baker, C. H., Young, B. A., et al. (2016). Sequence variation of 22 autosomal STR loci detected by next generation sequencing. *Forensic Sci. Int. Genet.* 21, 15–21. doi: 10.1016/j.fsigen.2015.11.005

Giampaoli, S., Berti, A., Di Maggio, R. M., Pilli, E., Valentini, A., Valeriani, F., et al. (2014). The environmental biological signature: NGS profiling for forensic comparison of soils. *Forensic Sci. Int.* 240, 41–47. doi: 10.1016/j.forsciint.2014.02.028

Gill, P., Haned, H., Bleka, O., Hansson, O., Dorum, G., and Egeland, T. (2015). Genotyping and interpretation of STR-DNA: Low-template, mixtures and database matches-Twenty years of research and development. *Forensic Sci. Int. Genet.* 18, 100–117. doi: 10.1016/j.fsigen.2015.03.014

Gill, P., Jeffreys, A. J., and Werrett, D. J. (1985). Forensic application of DNA 'fingerprints'. *Nature* 318, 577–579. doi: 10.1038/318577a0

Goodwin, W., Linacre, A., and Hadi, S. (2011). *"An introduction to forensic genetics."* 2nd ed. West Sussex, UK: Wiley-Blackwell, 53–62.

Guo, F., Yu, J., Zhang, L., and Li, J. (2017). Massively parallel sequencing of forensic STRs and SNPs using the Illumina((R)) ForenSeq DNA Signature Prep Kit on the MiSeq FGx Forensic Genomics System. *Forensic Sci. Int. Genet.* 31, 135–148. doi: 10.1016/j.fsigen.2017.09.003

Habtom, H., Demaneche, S., Dawson, L., Azulay, C., Matan, O., Robe, P., et al. (2017). Soil characterisation by bacterial community analysis for forensic applications: A quantitative comparison of environmental technologies. *Forensic Sci. Int. Genet.* 26, 21–29. doi: 10.1016/j.fsigen.2016.10.005

Heather, J. M., and Chain, B. (2016). The sequence of sequencers: The history of sequencing DNA. *Genomics* 107, 1–8. doi: 10.1016/j.ygeno.2015.11.003

Javan, G. T., Finley, S. J., Abidin, Z., and Mulle, J. G. (2016). The Thanatomicrobiome: A Missing Piece of the Microbial Puzzle of Death. *Front. Microbiol.* 7:225. doi: 10.3389/fmicb.2016.00225

Javan, G. T., Finley, S. J., Smith, T., Miller, J., and Wilkinson, J. E. (2017). Cadaver Thanatomicrobiome Signatures: The Ubiquitous Nature of Clostridium Species in Human Decomposition. *Front. Microbiol.* 8:2096. doi: 10.3389/fmicb.2017.02096

Jeffreys, A. J. (2013). The man behind the DNA fingerprints: an interview with Professor Sir Alec Jeffreys. *Investig. Genet.* 4:21. doi: 10.1186/2041-2223-4-21

Jeffreys, A. J., Brookfield, J. F., and Semeonoff, R. (1985a). Positive identification of an immigration test-case using human DNA fingerprints. *Nature* 317, 818–819. doi: 10.1038/317818a0

Jeffreys, A. J., Wilson, V., and Thein, S. L. (1985b). Hypervariable 'minisatellite' regions in human DNA. *Nature* 314, 67–73. doi: 10.1038/314067a0

Jiang, H. H., Li, B., Ma, Y., Bai, S. Y., Dahmer, T. D., Linacre, A., et al. (2020). Forensic validation of a panel of 12 SNPs for identification of Mongolian wolf and dog. *Sci. Rep.* 10:13249. doi: 10.1038/s41598-020-70225-5

Kidd, K. K., Pakstis, A. J., Speed, W. C., Lagace, R., Chang, J., Wootton, S., et al. (2014). Current sequencing technology makes microhaplotypes a powerful new type of genetic marker for forensics. *Forensic Sci. Int. Genet.* 12, 215–224. doi: 10.1016/j.fsigen.2014.06.014

Kim, Y. T., Heo, H. Y., Oh, S. H., Lee, S. H., Kim, D. H., and Seo, T. S. (2015). Microchip-based forensic short tandem repeat genotyping. *Electrophoresis* 36, 1728–1737. doi: 10.1002/elps.201400477

Kitpipit, T., Thongjued, K., Penchart, K., Ouithavon, K., and Chotigeat, W. (2017). Mini-SNaPshot multiplex assays authenticate elephant ivory and simultaneously identify the species origin. *Forensic Sci. Int. Genet.* 27, 106–115. doi: 10.1016/j.fsigen.2016.12.007

Linacre, A., Gusmão, L., Hecht, W., Hellmann, A. P., Mayr, W. R., Parson, W., et al. (2011). ISFG: Recommendations regarding the use of non-human (animal) DNA in forensic genetic investigations. *Forensic Sci. Int. Genet.* 5, 501–505. doi: 10.1016/j.fsigen.2010.10.017

Liu, W. T., Marsh, T. L., Cheng, H., and Forney, L. J. (1997). Characterization of microbial diversity by determining terminal restriction fragment length polymorphisms of genes encoding 16S rRNA. *Appl. Environ. Microbiol.* 63, 4516–4522. doi: 10.1128/AEM.63.11.4516-4522.1997

Ludeman, M. J., Zhong, C., Mulero, J. J., Lagace, R. E., Hennessy, L. K., Short, M. L., et al. (2018). Developmental validation of GlobalFiler PCR amplification kit: a 6-dye multiplex assay designed for amplification of casework samples. *Int. J. Legal. Med.* 132, 1555–1573. doi: 10.1007/s00414-018-1817-5

McCord, B. R., Gauthier, Q., Cho, S., Roig, M. N., Gibson-Daw, G. C., Young, B., et al. (2019). Forensic DNA Analysis. *Anal. Chem.* 91, 673–688. doi: 10.1021/acs.analchem.8b05318

Meyers, M. S., and Foran, D. R. (2008). Spatial and temporal influences on bacterial profiling of forensic soil samples. *J. Forensic Sci.* 53, 652–660. doi: 10.1111/j.1556-4029.2008.00728.x

Miller Coyle, H., Palmbach, T., Juliano, N., Ladd, C., and Lee, H. C. (2003). An overview of DNA methods for the identification and individualization of marijuana. *Croat Med. J.* 44, 315–321.

Moreno, L. I., Galusha, M. B., and Just, R. (2018). A closer look at Verogen's Forenseq DNA Signature Prep kit autosomal and Y-STR data for streamlined analysis of routine reference samples. *Electrophoresis* 39, 2685–2693. doi: 10.1002/elps.201800087

Moreno, L. I., Mills, D. K., Entry, J., Sautter, R. T., and Mathee, K. (2006). Microbial metagenome profiling using amplicon length heterogeneity-polymerase chain reaction proves more effective than elemental analysis in discriminating soil specimens. *J. Forensic Sci.* 51, 1315–1322. doi: 10.1111/j.1556-4029.2006.00264.x

Moreno, L. I., Mills, D., Fetscher, J., John-Williams, K., Meadows-Jantz, L., and McCord, B. (2011). The application of amplicon length heterogeneity PCR (LH-PCR) for monitoring the dynamics of soil microbial communities associated with cadaver decomposition. *J. Microbiol. Methods* 84, 388–393. doi: 10.1016/j.mimet.2010.11.023

Mrkonjic Fuka, M., Gesche Braker, S. H., and Philippot, L. (2007). "Molecular Tools to Assess the Diversity and Density of Denitrifying Bacteria in Their Habitats," in *Biology of the Nitrogen Cycle*, eds H. Bothe, S. J. Ferguson, and W. E. Newton (Amsterdam: Elsevier), 313–330.

Mullis, K., Faloona, F., Scharf, S., Saiki, R., Horn, G., and Erlich, H. (1986). Specific enzymatic amplification of DNA in vitro: the polymerase chain reaction. *Cold Spring Harb. Symp. Quant. Biol.* 1, 263–273. doi: 10.1101/sqb.1986.051.01.032

Oostdik, K., Lenz, K., Nye, J., Schelling, K., Yet, D., Bruski, S., et al. (2014). Developmental validation of the PowerPlex((R)) Fusion System for analysis of casework and reference samples: A 24-locus multiplex for new database standards. *Forensic Sci. Int. Genet.* 12, 69–76. doi: 10.1016/j.fsigen.2014.04.013

Orita, M., Iwahana, H., Kanazawa, H., Hayashi, K., and Sekiya, T. (1989). Detection of polymorphisms of human DNA by gel electrophoresis as single-strand conformation polymorphisms. *Proc. Natl. Acad. Sci. U S A* 86, 2766–2770.

Osborn, A. M., Moore, E. R., and Timmis, K. N. (2000). An evaluation of terminal-restriction fragment length polymorphism (T-RFLP) analysis for the study of microbial community structure and dynamics. *Environ. Microbiol.* 2, 39–50. doi: 10.1046/j.1462-2920.2000.00081.x

Pang, J. B., Rao, M., Chen, Q. F., Ji, A. Q., Zhang, C., Kang, K. L., et al. (2020). A 124-plex Microhaplotype Panel Based on Next-generation Sequencing Developed for Forensic Applications. *Sci. Rep.* 10:1945. doi: 10.1038/s41598-020-58980-x

Sanger, F., and Coulson, A. R. (1975). A rapid method for determining sequences in DNA by primed synthesis with DNA polymerase. *J. Mol. Biol.* 94, 441–448. doi: 10.1016/0022-2836(75)90213-2

Schmedes, S. E., Sajantila, A., and Budowle, B. (2016). Expansion of Microbial Forensics. *J. Clin. Microbiol.* 54, 1964–1974. doi: 10.1128/JCM.00046-16

Schneider, P. M., Prainsack, B., and Kayser, M. (2019). The Use of Forensic DNA Phenotyping in Predicting Appearance and Biogeographic Ancestry. *Dtsch Arztebl. Int.* 52, 873–880. doi: 10.3238/arztebl.2019.0873

Suzuki, M., Rappe, M. S., and Giovannoni, S. J. (1998). Kinetic bias in estimates of coastal picoplankton community structure obtained by measurements of small-subunit rRNA gene PCR amplicon length heterogeneity. *Appl. Environ. Microbiol.* 64, 4522–4529.

SWGDAM (2019). Addendum to SWGDAM Autosomal Interpretation Guidelines for NGS.Swgdam. Available online at: https://www.swgdam.org/publications

Vidaki, A., and Kayser, M. (2018). Recent progress, methods and perspectives in forensic epigenetics. *Forensic Sci. Int. Genet.* 37, 180–195. doi: 10.1016/j.fsigen.2018.08.008

Vos, P., Hogers, R., Bleeker, M., Reijans, M., van de Lee, T., Hornes, M., et al. (1995). AFLP: a new technique for DNA fingerprinting. *Nucleic Acids Res.* 23, 4407–4414. doi: 10.1093/nar/23.21.4407

Wyman, A. R., and White, R. (1980). A highly polymorphic locus in human DNA. *Proc. Natl. Acad. Sci. U S A* 77, 6754–6758. doi: 10.1073/pnas.77.11.6754

Young, J. M., and Linacre, A. (2021). Massively parallel sequencing is unlocking the potential of environmental trace evidence. *Forensic Sci. Int. Genet.* 50:102393. doi: 10.1016/j.fsigen.2020.102393

Conflict of Interest: The authors declare that the research was conducted in the absence of any commercial or financial relationships that could be construed as a potential conflict of interest.

frontiers in Ecology and Evolution

ORIGINAL RESEARCH
published: 13 May 2021
doi: 10.3389/fevo.2021.605817

A Combined Application of Molecular Microbial Ecology and Elemental Analyses Can Advance the Understanding of Decomposition Dynamics

Chawki Bisker[1,2], *Gillian Taylor*[2,3], *Helen Carney*[2,3] *and Theresia Komang Ralebitso-Senior*[2,4]*

[1] Criminalistics Direction, National Institute of Criminalistics and Criminology, Algiers, Algeria, [2] School of Health and Life Sciences, Teesside University, Middlesbrough, United Kingdom, [3] National Horizons Centre, Darlington, United Kingdom, [4] School of Pharmacy and Biomolecular Sciences, Liverpool John Moores University, Liverpool, United Kingdom

OPEN ACCESS

Edited by:
Manuela Oliveira,
University of Porto, Portugal

Reviewed by:
Sheree J. Finley,
Alabama State University, United States
Danijela P. Miljkovic,
University of Belgrade, Serbia
Jie Liu,
Nankai University, China

***Correspondence:**
Theresia Komang Ralebitso-Senior
t.k.ralebitsosenior@ljmu.ac.uk

Specialty section:
This article was submitted to Population and Evolutionary Dynamics, a section of the journal Frontiers in Ecology and Evolution

Received: *02 December 2020*
Accepted: *06 April 2021*
Published: *13 May 2021*

Citation:
Bisker C, Taylor G, Carney H and Ralebitso-Senior TK (2021) A Combined Application of Molecular Microbial Ecology and Elemental Analyses Can Advance the Understanding of Decomposition Dynamics. Front. Ecol. Evol. 9:605817. doi: 10.3389/fevo.2021.605817

Introducing animal carbon-source to soil initiates biochemical and microbial processes that lead to its decomposition and recycling, which subsequently cause successional shifts in soil microbial community. To investigate the use of soil microbial community to inform criminal investigation, this study was designed to mimic clandestine graves. It compared the decomposition of stillborn piglets (*Sus scrofa domesticus*), as human analogues, to oak (*Quercus robur*) leaf litter and soil-only controls outdoors for 720 days. Environmental and edaphic parameters were monitored and showed soil microbial community alignment with temperature seasonality, which highlighted the importance of this abiotic factor. Denaturing gradient gel electrophoresis (DGGE) data were used to calculate Hill numbers and diversity indices of the bacterial 16S rRNA community did not distinguish mammalian- from plant-based decomposition consistently during the first or second year of the study. In contrast, the fungal 18S rRNA community allowed clear differentiation between different treatments (beta diversity) throughout the 720-day experiment and suggested the moment of the decomposing mammalian skin rupture. 16S rRNA-based NGS facilitated the identification of e.g., Pirellulaceae, Acidobacteria ii1-15_order and *Candidatus xiphinematobacter* as Year 2 bacterial markers of gravesoil at family, order and species taxonomic levels, respectively, and confirmed the similarity of the calculated Hill diversity metrics with those derived from DGGE profiling. Parallel soil elemental composition was measured by portable X-ray Fluorescence where calcium profiles for the piglet-associated soils were distinct from those without carrion. Also, soil calcium content and PMI correlated positively during the first year then negatively during the second. This study is one of the first to apply a multidisciplinary approach based on molecular and physicochemical analytical techniques to assess decomposition. It highlights the recognised potential of using soil microbial community in forensic investigations and provides a proof-of-concept for the application of a combined

molecular and elemental approach to further understand the dynamics of decomposition. In addition, it sets the scene for further research in different conditions based on Hill numbers metrics instead of the classic ecological indices for soil necrobiome richness, diversity and evenness.

Keywords: decomposition, *Sus scrofa domesticus*, microbial community succession, hill diversity indices, clandestine grave

INTRODUCTION

Death is the beginning of a series of changes in the body leading to its decomposition through two major processes, autolysis and putrefaction (Shirley et al., 2011). Decomposition involves internal changes to the body together with the action of endogenous and exogenous organisms (Pinheiro, 2006). Researchers divided this environment-dependent process (Cockle and Bell, 2017) into different stages (Megyesi et al., 2005; Goff, 2009). Although these are a convenient means for decomposition stage assessment, they are not always discernible as their supposedly distinctive characteristics usually blend with one another (Pinheiro, 2006; Knobel et al., 2018). Also, decomposition rates vary significantly depending on parameters related to: (i) the environment, such as location, atmospheric conditions and presence of clothing (Voss et al., 2011); (ii) exposure to exogenous organisms such as microbes, insects, plants (Iyengar and Hadi, 2014) and scavenging animals (Behrensmeyer, 1978); (iii) funeral care including embalming, wrapping, type of burial and coffin (Pinheiro, 2006; Tumer et al., 2013; Hau et al., 2014; Lauber et al., 2014); and (iv) cadaver physical condition which includes the circumstances of death, medical treatment, and antemortem and perimortem physical conditions of the deceased (Sutherland et al., 2013).

Various animals such as different species of birds, reptiles, fish, rodents, and mammals have been used for decomposition studies as human taphonomic proxies, with swine and murine models used the most (Ralebitso-Senior and Olakanye, 2018). Domestic pigs (*Sus scrofa domesticus*), in particular, have high anatomical, physiological, and immunological similarities with humans (Litten-Brown et al., 2010). Also, there is similarity between swine and human cadavers in terms of decomposition where putrefaction progresses at approximately the same rate to that of human bodies of comparable weight (Campobasso et al., 2001) although their body parts surface areas to volume ratios differ (Connor et al., 2018). Without access to donated human bodies and relevant ethical guidelines, animal proxies remain the best alternative to study decomposition and develop forensic investigative tools (Ralebitso-Senior and Pyle, 2018; Williams et al., 2019).

Microorganisms play significant roles in human decomposition (Bisker and Ralebitso-Senior, 2018; Bishop, 2019) and heavily affect the decomposition rate; hence Lauber et al. (2014) reported a two to three times faster decomposition in mice placed on non-sterile soil compared to those deposited on sterile soil. In addition, there is evidence that microorganisms are essential to cadaver organic residue recycling although more knowledge is required about the structure of the associated microbial communities. Furthermore, Cobaugh et al. (2015) reported the persistence of human-associated microbial species in soil, which are very distinct and scarce in nature thus making them possible biomarkers of human decomposition. Ultimately, microbial communities associated with gravesoil have the potential to be used as a tool to estimate time since death and locate clandestine burials (Metcalf et al., 2013, 2016; Finley et al., 2015a; Olakanye et al., 2015, 2017).

Denaturing gradient gel electrophoresis (DGGE) is an economical and reliable method used in many laboratories around the world, with the generated data analysed further by calculating appropriate ecological indices for richness, diversity and evenness. To date, most published research on characterisation of soil microbial communities for forensic applications have used classic diversity metrics such as Shannon-Wiener, Simpson index of concentration or those built within software/pipeline packages (Can et al., 2014; Olakanye et al., 2017; Olakanye and Ralebitso-Senior, 2018; Procopio et al., 2019). However, these metrics have known shortcomings and generate results that are not easy to interpret. In contrast, Hill numbers (^{0}D, ^{1}D, ^{2}D and Hill ratio ^{1}D/^{0}D) are equivalent to algebraic transformation of most other indices, and quantify diversity in units of modified species counts. For example, unlike Simpson's index of concentration, they preserve the doubling property and extract ecological meaning from complex data (Chao et al., 2014) allowing better interpretation of results (Chao et al., 2010). Next generation sequencing as a high throughput metagenome profiling technique has been applied widely in forensic microbial ecology studies. Its application is being improved further where processed sequencing data are analysed using the novel high-resolution approach that targets amplicon sequence variants (ASVs) instead of operational taxonomic units (OTUs) (Bolyen et al., 2018), and relevant statistical analysis.

Soil analysis in forensic investigation has evolved considerably with various inorganic and organic techniques used. While these techniques help inform investigations, their use varies from simple and practical analysis such as portable XRF (pXRF) and spectrometry that could be performed *in situ* by crime scene investigators, to more technical methods requiring highly qualified staff or necessitating laboratory work (chromatography and molecular analysis). Since it is a rapid, non-destructive, simultaneous multi-element technique (Shand and Wendler, 2014), pXRF is readily available in forensic laboratories and used widely for routine analysis of trace evidence and artefacts. This makes the expansion of its use to complement microbial community profiling of gravesoil within forensic microbial

ecology, viable and cost-effective for forensic units. pXRF is affected by factors such as soil moisture content and heterogeneity hence the importance of sample preparation prior to analysis (Ravansari and Lemke, 2018).

In order to enrich the knowledge base about carrion decomposition with the northeast of England as an example context, the following hypotheses were developed:

A. The subsurface decomposition of domestic piglet (*S. scrofa domesticus*) as a human analogue will change the surrounding soil microbial community composition distinctly from the subsurface decomposition of *Quercus robur* (oak leaves).
B. Soil microbial community signature associated with the decomposition of *S. scrofa domesticus* will persist after the decomposition of the animal proxy.
C. The composition of soil microbial community associated with decomposition is influenced by seasonal weather changes.
D. Soil elemental composition is influenced by the decomposing resource (animal vs. vegetal) and type of burial.

To test these hypotheses and explore the changes in soil microbial community biodiversity, a 2-year study was set to imitate clandestine graves. It consisted of *in situ* burials of piglets (*Sus scrofa domesticus*) as human cadaver proxies and oak (*Quercus robur*) leaf litter, with soil-only controls. Key atmospheric and edaphic variables, such as temperature, pH, humidity, and elemental composition were measured. Portable X-Ray Fluorescence was used to analyse the elemental composition during decomposition to illustrate the importance of physicochemical characterisation of gravesoil to complement microbial ecology techniques in a forensic context. The study aimed to enrich the knowledge base on subsurface decomposition using molecular microbial ecology methods supported by secondary analyses and environmental monitoring. In the long-term, this could enhance the forensic toolkit for post-mortem/post-burial interval (PMI/PBI) estimation and location of clandestine graves, and ultimately inform investigations and facilitate court proceedings.

MATERIALS AND METHODS

Experimental Design

The open air 36 m^2 study ecosystem (North Yorkshire, U.K., Lat. 53.762551°N; Long. 1.244004°W) was a woodland characterised by tree clusters of predominately oak (*Quercus robur*) and as loamy soil composed of clay (22%), silt (32%) and sand (46%) (Olakanye et al., 2017). It was used for forestry agriculture and not a human taphonomic facility. Therefore, there were no expected legacy effects as the ecosystem has, to our knowledge, never been used for decomposition research. To mitigate for lateral migration between pits while ensuring even spatial distribution, the study area was divided into three sections containing three pits each, which were dug ∼1.9 to 2.25 m apart (**Supplementary Figure 1**). Two sets of three pits each were used as triplicate piglet cadaver and oak (*Quercus robur*) leaf litter burials, respectively, with the remaining set used for soil-only controls. To minimise scavenging activity by vertebrates, each piglet was placed in a mesh wire cage prior to burial. All nine graves were monitored at monthly intervals for the first 12 months (December 2014–December 2015; Olakanye et al., 2017) then up to 24 months (January 2016–December 2016; current report) for soil temperature, pH, and microbial (bacterial and fungal) communities. Soil core samples were collected at 20–60 cm deep from all four sides of each pit using a stainless-steel soil corer (Eijkelkamp, Netherlands), which was cleaned after each sampling with water and 99.9% (v/v) ethanol (Thermo Fisher Scientific, Loughbrough, UK). The samples were then transported to the laboratory in a cold storage box containing ice packs (ca 4°C), and combined for each pit in 25 ml sterile universal tubes prior to storage at −20°C.

Environmental Monitoring

Data for rainfall, UV index, sun exposure, cloud coverage, humidity and daily atmospheric temperatures were obtained from www.worldweatheronline.co.uk. Soil temperature was recorded at each point of sampling using a Fisher Scientific portable thermometer (Fisher Scientific, Loughborough, U.K.) and further expressed in Accumulated degree-days (ADD) (Nolan et al., 2019). The ADD for each day was calculated by adding together the average positive temperatures of each day from the start of the experiment. Similarly, cumulative precipitation was calculated for each day and consisted of the rainfall (mm) accumulated between the first (01/12/2014) and last (01/12/2016) days of the study.

The average pH of each soil sample was measured electrochemically using a Hanna pH 213 microprocessor (Hanna Instruments, Bedfordshire, UK). Each soil sample (10 g) was mixed with deionised water in a 1:5 (w/v) ratio and left to settle for 30 min prior to measurement as described by Stokes et al. (2009).

Soil Mineral Composition

Mineral composition of all soil samples was assessed by portable X-Ray Fluorescence (pXRF) using a portable Niton XL3 950 GOLDD+ series Analyser (Niton UK Limited, Winchester, U.K.). To quantify the content for phosphorus, potassium, iron, calcium, magnesium and sulphur (Hopkins et al., 2000; Carter and Tibbett, 2006; Elfstrand et al., 2007; Benninger et al., 2008), soil samples were dried overnight at 105°C, ground with a mortar and pestle, sieved to 2 mm and homogenised. XRF cups (31 mm) were filled with ∼8 g of homogenised soil from each individual treatment and covered with 5 μm polypropylene film (Williams et al., 2020) before scanning at 30 s low and 60 s light beam using mining mode. Blank and standard samples were run after every 10 samples analysed. The limit of detection of pXRF used for the standard reference materials (SRM) is: P (0.03%), S (0.01%), and Mg (0.65%).

DNA Extraction

DNA was extracted from each soil sample (500 mg) from all 2 years of the study using FastDNA™ Spin Kit for Soil™ (MP Biomedicals, U.K.) according to the manufacturer's instructions and stored at −20°C until required. The concentration and purity (A_{260}/A_{280}) of each DNA extract was determined by

UV spectrophotometry (Synergy-HT microplate reader; Biotek, Bedfordshire, UK) where a ratio of 1.8–2.0 was equivalent to high quality and high purity DNA (Torsvik, 1980; Hart et al., 2015).

Polymerase Chain Reaction (PCR) and Agarose Gel Electrophoresis

DNA extracts were amplified on a Primus 96 Plus thermocycler (MWG Biotech AG, Ebersberg, Germany) using Promega 2X Master Mix containing Taq DNA polymerase (50 U ml^{-1}), dATP (400 μM), dGTP (400 μM), dCTP (400 μM), dTTP (400 μM), $MgCl_2$ (3 mM), and BSA (10 mg ml^{-1}). The V3 region of the 16S rRNA gene (location 341–534) was enzymatically amplified in the PCR using the nested primer set GC388f (5′-CGC CCG CCG CGC GCG GCG GGC GGG GCG GGG GCA CGG GGG GCC TAC GGG AGG CAG CAG-3′) and 530r (5′-ATT ACC GCG GCT GCT GG-3′) according to Muyzer et al. (1993).

Fungal 18S rRNA gene was amplified using the nested primer sets NS1f (5′- CCA GTA GTC ATA TGC TTG TC-3′) and NS8r (5′-TCC GCA GGT TCA CCT ACG GA-3′) for the first reaction, then NS1f and NS210-GCr (5′-CGC CCG CCG CGC GCG GCG GGC GGG GCG GGG GCA CGG GGG G GAA TTA CCG CGG CTG CTG GC-3′) as described by White et al. (1990). The thermal cycling conditions used were as described by Olakanye et al. (2015). Each of the 16S rRNA and 18S rRNA gene PCR amplicons were checked using a 1.5% (w/v) agarose gel electrophoresis with 1X TBE buffer and SYBR Safe (Invitrogen) staining.

Denaturing Gradient Gel Electrophoresis

Each of the bacterial 16S rRNA and fungal 18S rRNA gene amplicons (17 μl) were mixed with 5X loading buffer (3 μl) and electrophoresed on 10 and 8% (w/v) polyacrylamide gels (acrylamide/bis-acrylamide 37.5:1) using a 35–65% and 15–40% denaturing gradient, respectively. Electrophoresis was performed on a DCODE™ Universal Mutation Detection System (Bio-Rad, Hertfordshire, UK) at 60°C/110V for 16 h. The gels were observed under UV light on an Alpha Imager HP® (Alpha Innotech, Braintree, UK) after SYBR Gold (Invitrogen) staining.

Next-Generation Sequencing (NGS)

The DNA extracts from the first year of the *in situ* piglet study were processed, analysed and reported as Olakanye et al. (2017). The DNA extracts from both the first and second years of study were sequenced identically on Illumina MiSeq platform by NU-Omics (Northumbria University, Newcastle Upon Tyne, UK). The preparation and sequencing of 16S rRNA gene sequence libraries was completed according to Kozich et al. (2013). The V4 region of the bacterial 16S rRNA gene was targeted using the primers 515f (5′-GTGCCAGCMGCCGCGGTAA-3′) and 806r (5′-GGACTACHVGGGTWTCTAAT-3′) (Kozich et al., 2013; Guo et al., 2016; Pechal et al., 2018). Year 1 samples were analysed for operational taxonomic units (OTUs) with amplicon sequence variants (ASVs) assessed for year 2. Therefore, comparisons for NGS findings are made with some precaution.

Data and Statistical Analysis

pXRF readings were performed separately for each individual replicate with Microsoft Office Excel™ Professional Plus 2016 used subsequently to calculate the averages for each set of triplicate readings, and plot graphs. Phoretix 1D software (TotalLab, Newcastle, U.K.) was used to analyse DGGE images and quantify the microbial community fingerprints (Ritz et al., 2004; Chimutsa et al., 2015). Hill numbers (^{0}D, ^{1}D, ^{2}D and ratio ^{1}D/^{0}D), as measures of ecological diversity (Chao et al., 2010, 2014), were calculated using Equations 1–4 in Microsoft Office Excel™ Professional Plus 2016 based on the number and volume of the DGGE gel bands (OTU) or the NGS taxonomic classification at species level (ASV):

Hill number ^{0}D (taxa richness):

$$^0D = \sum_{i=1}^{s} pi^0 \quad (1)$$

Hill number ^{1}D (common taxa diversity):

$$^1D = e^{H'} = e^{-\sum_{i=1}^{s} pi\ lnpi} \quad (2)$$

where P_i: proportion; H': Shannon-Wiener index.

Hill number ^{2}D (dominant taxa diversity):

$$^2D = 1/\sum_{i=1}^{s} pi^2 \quad (3)$$

Hill ratio (community evenness):

$$E1:0 = {}^1D/{}^0D \quad (4)$$

All data were evaluated by a two-way ANOVA with replication followed by Tukey HSD and Bonferroni to explore the interactions using IBM® SPSS® Statistics version 25 (IBM Corporation, New York, USA).

For multivariate analysis, data were unit vector normalised, mean centred, and scaled to standard deviation. These data were then subjected to principal component analysis (PCA) to highlight correlations between weather conditions, and demonstrate the differences between fungal and bacterial ecological indices against environmental parameters. Principal co-ordinates analysis (PCoA) identified differences in bacterial community beta-diversity in response to seasonal shifts.

The raw sequencing reads resulting from next-generation sequencing of year 2 DNA extracts, which are the focus of the current manuscript, were analysed using the Quantitative Insights Into Microbial Ecology version 2 (QIIME2) software suite version 2018.8 (Bolyen et al., 2018; Hall and Beiko, 2018; Nearing et al., 2018). Denoising and filtering of the sequences were completed using the Divisive Amplicon Denoising Algorithm 2 (DADA2). QIIME2 was used to calculate diversity metrics and assign taxonomy using the classifier artefact "gg-13-8-99-515-806-nb-classifier.qza," trained on Greengenes database, trimmed to the V4 hyper-variable region of the 16S rRNA gene using the primers f515 and r806, and clustered at

99% sequence identity. Core metrics for alpha and beta-diversity were generated using QIIME2. Kruskal-Wallis test was used to determine significant differences in alpha-diversity between groups while PERMANOVA was used to assess significant differences in beta-diversity.

RESULTS

Environmental Conditions

Key environmental parameters were monitored and/or measured in the current study (**Supplementary Figure 2**) as they have a direct impact on decomposition rate, total necrobiome and microbial community functions/dynamics, in particular. Soil temperatures, which were recorded at each sampling time (**Figure 1A**) and expressed further in accumulated degree-days (**Figure 1B**), reflected the seasonal weather fluctuations. There was no statistically significant difference between the control and experimental treatments ($p = 0.87$) based on two-way ANOVA with replication. The average ($n = 3$) pH values showed that, unlike the soils associated with *S. scrofa domesticus* decomposition, control and leaf litter samples had very similar pH trends over the 24-month period (**Figure 2**), and two-way ANOVA showed significant differences between the treatments ($p = 0.04$). Cumulative precipitation was calculated at the different sampling intervals and recorded an average range of 0 to 1,400 mm over the 720 days of study (**Supplementary Figure 2A**). Overall, Principal component analysis (PCA) of the recorded weather conditions at the study site (**Figure 3**) showed that most of these parameters clustered to the right axis and correlated positively at the different sampling time points. The exceptions were snowfall and days of snow, which correlated negatively.

DGGE-Based Profiling of Soil Necrobiome

To achieve a protracted 24-month study of microbial community shifts in the subsurface necrobiome, soil samples from the first year as published by Olakanye et al. (2017) were reprocessed with new DGGE of the fungal 18S and bacterial 16S rRNA gene profiles. Denaturing gradient gel electrophoresis was used as an economical, rapid, and reliable technology that can be accessible to laboratories globally for forensic profiling of soil microbial communities. To facilitate direct temporal comparisons between treatments and gels, the fungal 18S and bacterial 16S rRNA DGGE profiles were analysed to calculate and interpret the Hill ecological indices for taxa richness (^{0}D), common taxa diversity (^{1}D), dominant taxa diversity (^{2}D) and evenness (^{1}D/^{0}D) (**Supplementary Figures 3–6**) with subsequent statistical analyses (**Table 1**).

Taxa Richness (^{0}D) Diversity (^{1}D, ^{2}D) and Evenness (^{1}D/^{0}D)

Hill number ^{0}D is the sum of the different taxa in the community and allows the assessment of community richness. The profiles of the fungal 18S rRNA gene richness (^{0}D) showed temporal differences between the control, leaf litter and piglet soil samples (**Supplementary Figure 3A**). For example, Tukey HSD and Bonferroni *post hoc* tests revealed a significant decrease in fungal community richness between day 60/ADD 258 and day 90/ADD 396. Overall, the changes in fungal richness coincided with variations in seasonal weather with a considerable decrease starting in late autumn (day 330/ ADD 3631) and lasting until the end of winter 2015 (day 360/ADD 3921). Two-way ANOVA with replication showed a significant temporal difference in fungal community richness between the control, *S. scrofa* and oak leaf litter soils ($p = 0.0002$) and between the *S. scrofa* and oak leaf litter treatments ($p = 0.01$). There were no significant differences observed between the control and experimental samples (**Table 1**). In contrast to the fungal communities, there was no significant difference in bacterial richness between the three different soils ($p = 0.179$), although significant temporal differences were recorded within each treatment ($p < 0.00$).

Hill number ^{1}D is the exponential of Shannon-Wienner index that facilitates the estimation of the community common taxa diversity, which decreased for the fungal communities in the piglet and control soils on day 30/ADD 144 and in the leaf litter treatments on day 60/ADD 258. Two-way ANOVA with replication highlighted a significant difference in fungal common taxa diversity (^{1}D) between the treatments at different sampling times ($-p<0.000$). Also, there was a significant difference in common taxa diversity between the experimental treatments ($p = 0.014$, Tukey HSD; $p = 0.015$, Bonferroni), however, no significant differences were observed between the control and experimental samples (**Table 1**). A significant difference in bacterial common taxa diversity was detected between the treatments at different time points during the second year of study ($p < 0.000$). Subsequently, *post hoc* analysis with Tukey (HSD) revealed statistical differences in the bacterial ^{1}D on days 360, 480, 660, and 720 between leaf litter and control, and leaf litter and piglet soils, but no difference between control and piglet soils. In addition, there were season-based statistically significant differences in common taxa diversity between winter 2015/day 360 and end of winter 2016/day 420, and between summer/day 600 and winter/day 720.

Hill number ^{2}D is the reciprocal of Simpson index that allows the evaluation of the dominant taxa diversity in a community. Similar to fungal ^{1}D, ^{2}D for this clade recorded a maximum increase in *Sus scrofa* soils on day 60. Two-way ANOVA with replication indicated a significant difference in fungal dominant taxa diversity between the treatments ($p = 0.018$) (**Table 1**). Unlike for ^{0}D and ^{1}D, there was a significant difference in ^{2}D between the control and piglet soil samples ($p = 0.024$, Tukey HSD; $p = 0.27$, Bonferroni), however, no significant differences were observed between the control and leaf litter, or between piglet and leaf litter soils. Similar patterns in bacterial dominant taxa diversity resulted generally between control and piglet soils, which contrasted with the leaf litter treatments. Nevertheless, significant differences were detected between the treatments at the different time points ($p = 0.0001$). Specifically, *post hoc* analysis with Tukey HSD showed statistical differences in bacterial ^{2}D on days 360, 480, 660, and 720 between leaf litter and control, and leaf litter and piglet soils, but no difference between control and piglet soils.

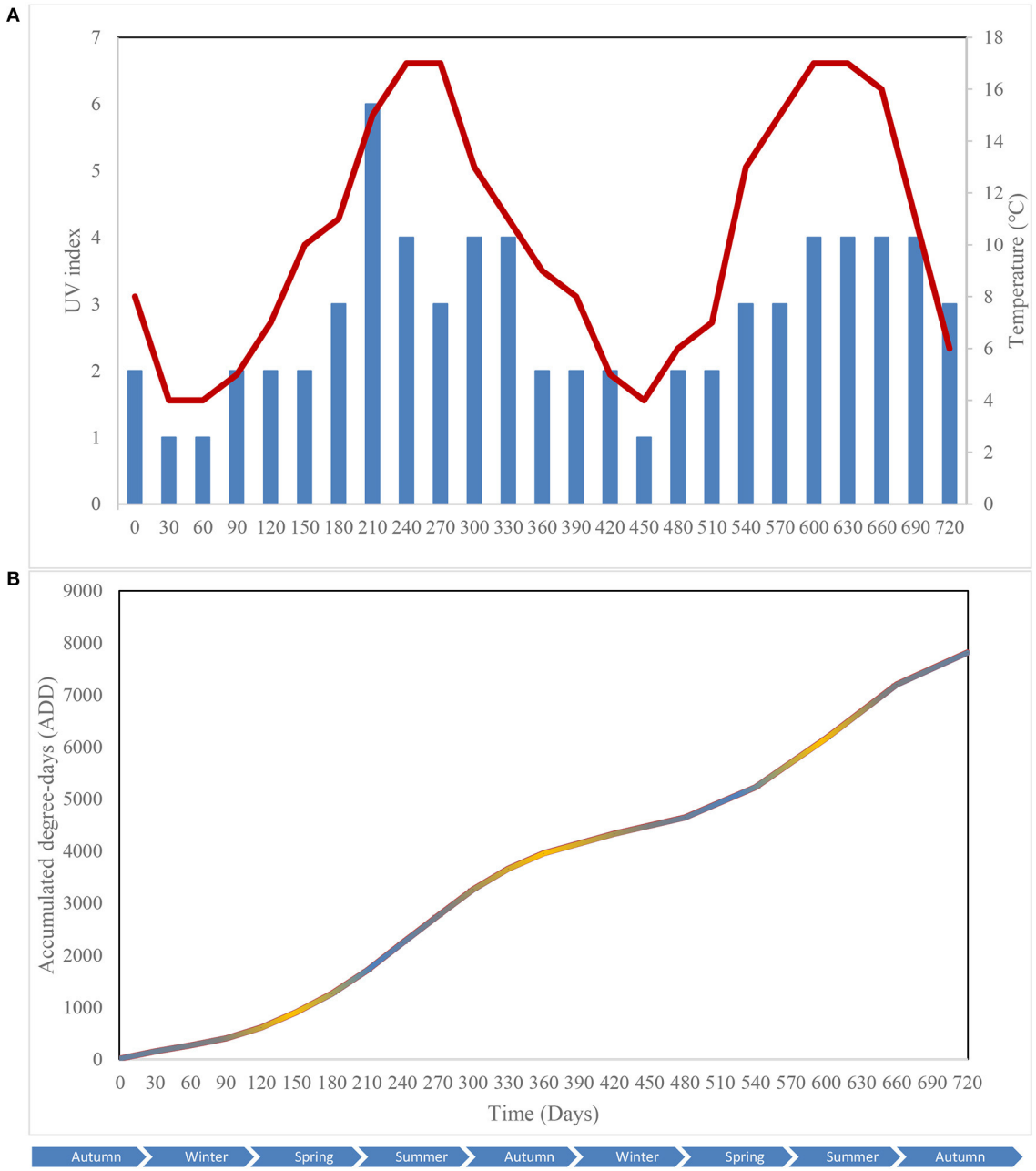

FIGURE 1 | Atmospheric temperature (•) and UV index (■) at the study site **(A)**; Accumulated degree-days (ADD) of the control (•), leaf litter (•) and *S. scrofa domesticus* (•) treatments during a 720-day *in situ* study **(B)**. Each data point is the mean of triplicate samples.

Community evenness (Hill ratio $^1D/^0D$) gives an indication of how close in number each taxon is in the community. Two-way ANOVA with replication showed no significant difference in fungal community evenness between the treatments at the different time points during the second year of the study ($p = 0.68$) (**Table 1**). However, the difference was significant for bacterial community evenness ($p < 0.00$) as reflected by *post hoc* Tukey HSD and Bonferroni tests which showed differences in the $^1D/^0D$ index between days 360, 420, and 540, and then days 600 and 660. Furthermore, significant differences were revealed between leaf litter and control, and leaf litter and piglet soils, but not between control and piglet soils.

Generally, and in contrast to those for the fungal 18S clade, all the DGGE-derived Hill numbers for bacterial 16S communities showed highly similar trends between *Sus scrofa domesticus* and control soils with pronounced increases and decreases at some specific sampling points, particularly in Year 2 of the study.

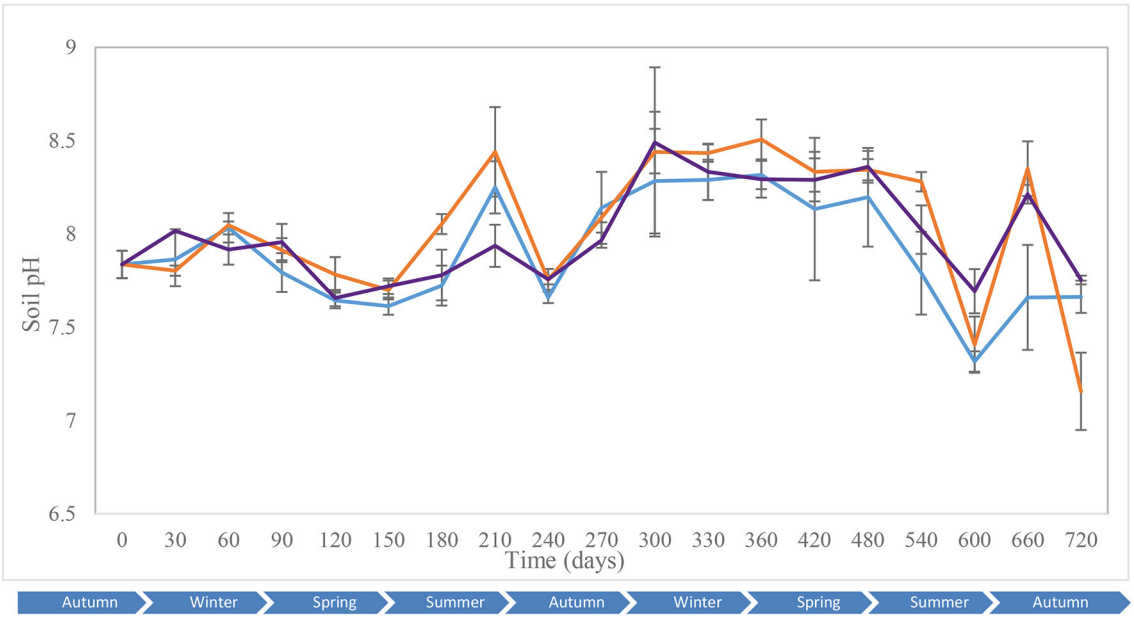

FIGURE 2 | Average ($n = 3$) soil pH of the control (•), leaf litter (•) and *S. scrofa domesticus* (•) treatments during a 720-day *in situ* study. Error bars are SEM.

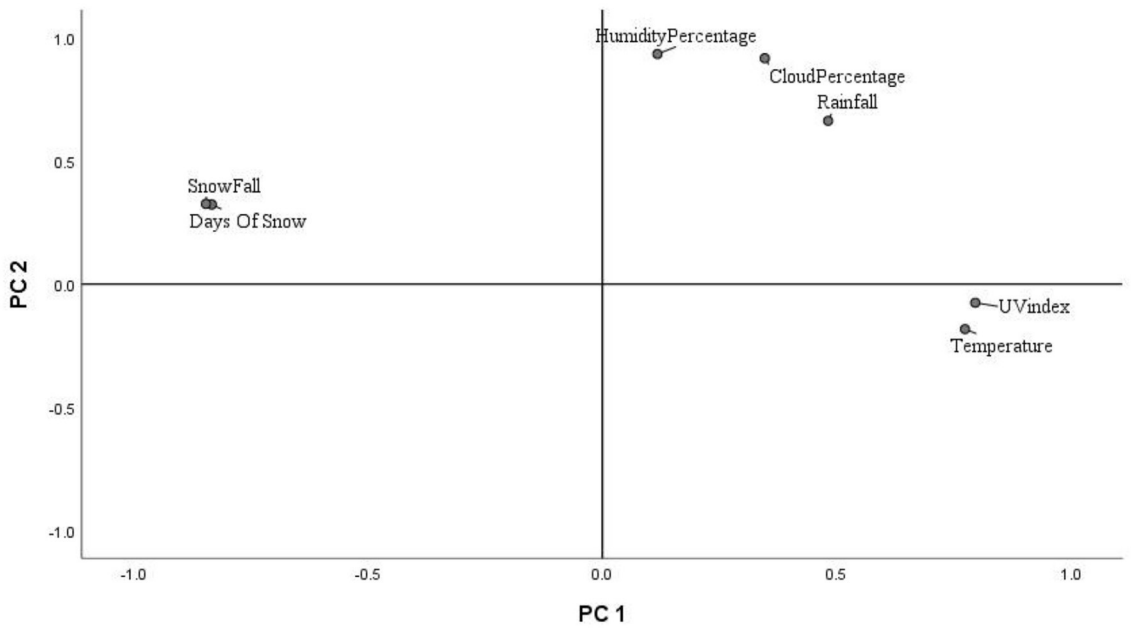

FIGURE 3 | PCA biplot of weather conditions correlation during the 720-day study.

Principal Component Analysis of Hill Ecological Indices

The principal component analysis (PCA) of the weather conditions at the site of study showed that principal component 1 (PC1) accounted for 42.98% of the variations in weather conditions while PC2 accounted for 34.14%. Temperature and UV index clustered strongly on PC1. Similarly, humidity, cloud cover and rainfall clustered and correlated strongly on PC2 at the different time points. Snowfall and days of snow correlated negatively on PC1. Principal component analysis (PCA) of the 18S rRNA fungal gene Hill ecological indices showed close clustering except for the Hill ratio $^{1}D/^{0}D$ (**Figure 4A**). Thus, ^{0}D, ^{1}D, and ^{2}D for the control and experimental treatments clustered positively on PC1. Also, PC1 accounted for 42.61%

TABLE 1 | Statistical significance for richness (^{0}D), common taxa diversity (^{1}D), dominant taxa diversity (^{2}D), and evenness (^{1}D/^{0}D) during *Sus scrofa domesticus* and oak leaf litter decomposition.

Method	Focus	Diversity metrics (Hill numbers)	ANOVA significance (*p*-value)		*Post hoc* Tukey HSD (*p* value)		
			Variation inter-treatment ANOVA	Variation in time ANOVA	Control—leaf litter	Control—piglet	Leaf litter piglet
DGGE	*Sus scrofa* 18S rRNA (Fungal community)	^{0}D	***	**	NS	NS	**
		^{1}D	*	***	NS	NS	*
		^{2}D	*	***	NS	*	NS
		^{1}D/^{0}D	NS	**	NS	NS	NS
	Sus scrofa 16S rRNA (Bacterial community)	^{0}D	NS	***	NS	NS	NS
		^{1}D	***	***	***	NS	***
		^{2}D	***	***	***	NS	***
		^{1}D/^{0}D	***	***	***	NS	***
Next-generation sequencing	*Sus scrofa* 16S rRNA (days 360,480,600 and 720)	^{0}D	NS	NS	NS	NS	NS
		^{1}D	NS	***	NS	NS	NS
		^{2}D	NS	***	NS	NS	NS
		^{1}D/^{0}D	NS	***	NS	NS	NS

*Significance ($p < 0.05$) is presented as *$P < 0.05$, **$P < 0.01$, ***$P < 0.001$, NS, not significant.*

of the variations in ecological indices while PC2 accounted for 14.21%. The different treatments' ecological indices correlated strongly and clustered together on PC1 except Hill ratio ^{1}D/^{0}D (**Figure 4A**). Cloud coverage, rainfall and humidity clustered positively on PC2.

The 16S rRNA bacterial gene PCA revealed a positive clustering of the environmental factors and all four ecological parameters for the different treatments along PC1 (**Figure 4B**). Also, control and piglet ecological indices clustered positively on PC1 and negatively on PC2, while leaf litter clustered positively on PC1 and PC2. Principal component 1 accounted for 41.56% of the variations while PC2 accounted for 19.21%. The diversity indices of piglet and control samples clustered strongly and positively on PC1, while leaf litter diversity indices clustered positively with rainfall and humidity on PC2.

Soil Bacterial Necrobiome Metabarcoding

High-throughput next generation sequencing, with the novel approach of targeting amplicon sequence variants (ASVs) instead of operational taxonomic units, has facilitated high-resolution metabarcoding of the soil necrobiome in forensic studies. The current report focuses on the second year (from day 360/month 12 to day 720/month 24) of our *in situ* piglet study, although reference is made to the results of the first year as published by Olakanye et al. (2017). Following sequencing of the bacterial 16S rRNA gene on an Illumina MiSeq^{TM} platform, sequences were denoised, reads were rarified to 4 000 and amplicon sequence variants produced by DADA2, while taxonomy was assigned based on GreenGenes database. Only the most predominant taxa were plotted while unclassified ASVs were omitted.

Phylum level resolution revealed the most predominant phyla in descending order as: Acidobacteria (19.44–35.75%), Proteobacteria (13.16–27.59%), Actinobacteria (7.00–16.54%), Planctomycetes (7.32–12.08%), Verucomicrobia (4.49–11.47%), Chloroflexi (5.61–10.00%), Bacteroidetes (3.49–11.23%), Nitrospira (0.775–2.74%), WS3_phylum (0.53–2.76%), and Firmicutes (0.34–2.22%) (**Figure 5A**). Similar patterns in Acidobacteria, Proteobacteria, Firmicutes, and Chloroflexi abundance were observed in piglet and leaf litter soils as compared to controls. However, two-way ANOVA did not detect any significant temporal differences between piglet or leaf litter soils. At order level, two-way ANOVA with replication showed a significant difference in abundance with time for the control and leaf litter treatments while there was no significant difference in piglet soils.

At family level, different members from Acidobacteria (RB40_family and mn2424_family), Chloroflexi, Chtoniobacteraceae (2.43–7.44%), Hyphomacrobiaceae (1.73–4.14%), Pirellulaceae (1.79–4.11%), Chitinophagaceae (1.12–4.61%), Gemmataceae (1.38–3.23%), Sinobacteraceae (1.23–3.09%), Gaiellaceae (1.06–3.02%), and Cytophagaceae (0.99–2.78%) were the most abundant (**Figure 5B**). Two-way ANOVA did not show any significant differences between the different treatment groups while there were significant temporal differences within the respective treatment groups, which corresponded to seasonal variation. For example, some bacterial families showed seasonal shifts for the control and leaf litter soils, although their abundances correlated negatively with temperature for piglet soils. These include Pirellulaceae, Chitinophagaceae, Gemmataceae, Hyphomicrobiaceae, Verrumicrobiaceae, Sinobacteraceae, and Commamonadaceae. Other families such as [Chthoniobacteraceae], Nitrososphaeraceae, Chitinophagaceae, Hyphomicrobiaceae, Sinobacteraceae, Commamonadaceae, Cytophagaceae, Flavobacteriaceae, Ellin6075, Myxococcales, Bacillaceae, and Saprospiraceae showed a strong positive correlation between leaf litter and piglet soil samples. In contrast, Nitrososphaeraceae, Pirellulaceae, Chitinophagaceae, Gemmataceae, Hyphomicrobiaceae, Verrumicrobiaceae, Sinobacteraceae, Commamonadaceae, Cytophagaceae,

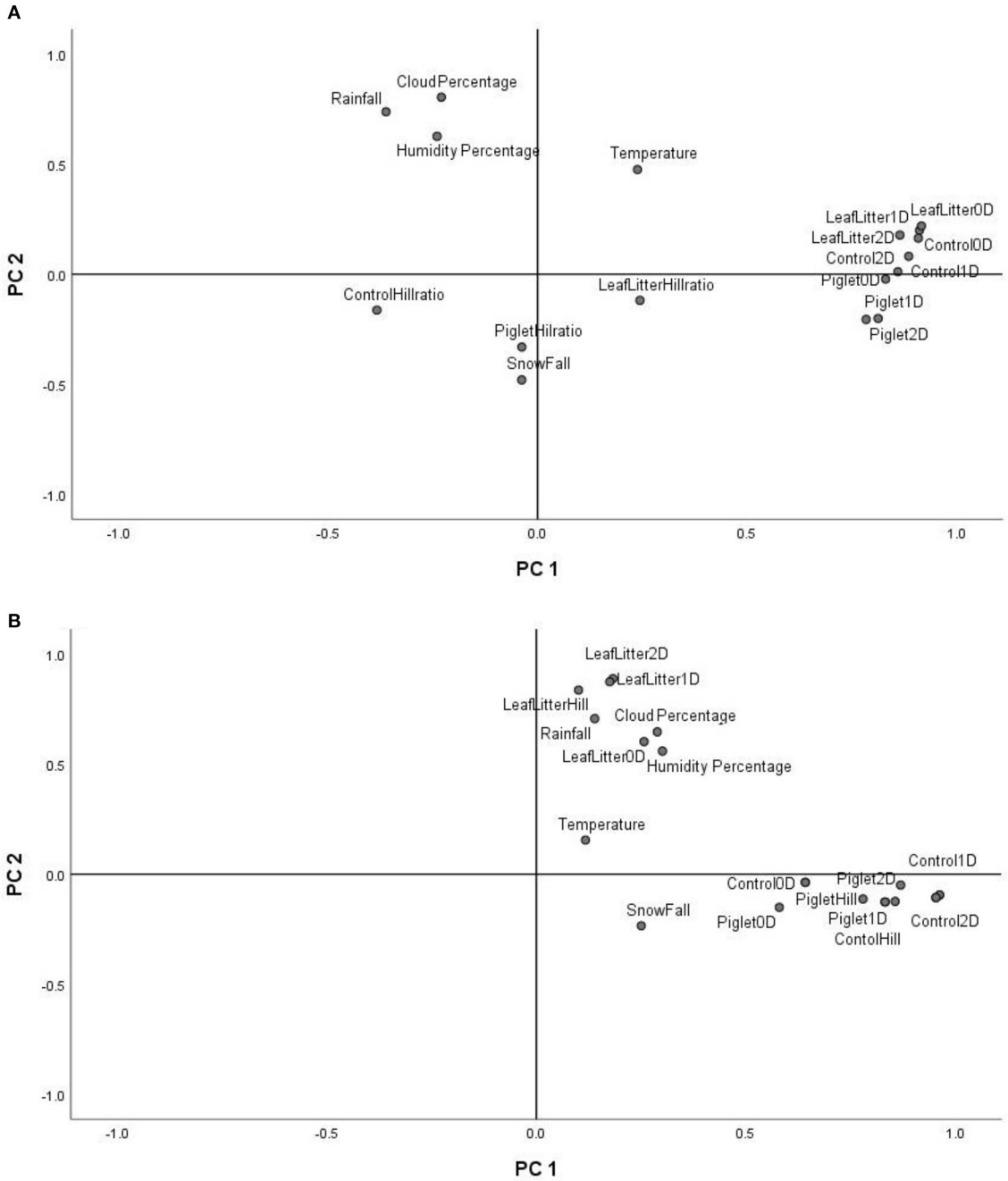

FIGURE 4 | PCA biplot of18S fungal **(A)** and 16S bacterial community **(B)** ecological indices (Hill number ^{0}D, ^{1}D, ^{2}D and Hill ratio ^{1}D/^{0}D) of the control, leaf litter and piglet soils.

Gaiellaceae, and Myxococcales correlated negatively between control and piglet soil samples.

Similar trends in genera abundance were observed between piglet and leaf litter soils from members in the iii1-15_family, mb2424_family, Chitinophagaceae_family, JG30-KF-CM45_order, CCU21_order, *Candidatus,* and *Flavobacterium*. There were significant temporal and seasonal differences in predominant genera abundances for control and oak leaf litter samples. However, no significant temporal differences were recorded in piglet soil using two-way ANOVA. As with genus level analysis, some species (**Figure 5C**) showed similar trends in abundance between piglet and leaf litter soils. These included species from iii1-15_order, RB40_family, mb2424_family, Chitinophagaceae_family,

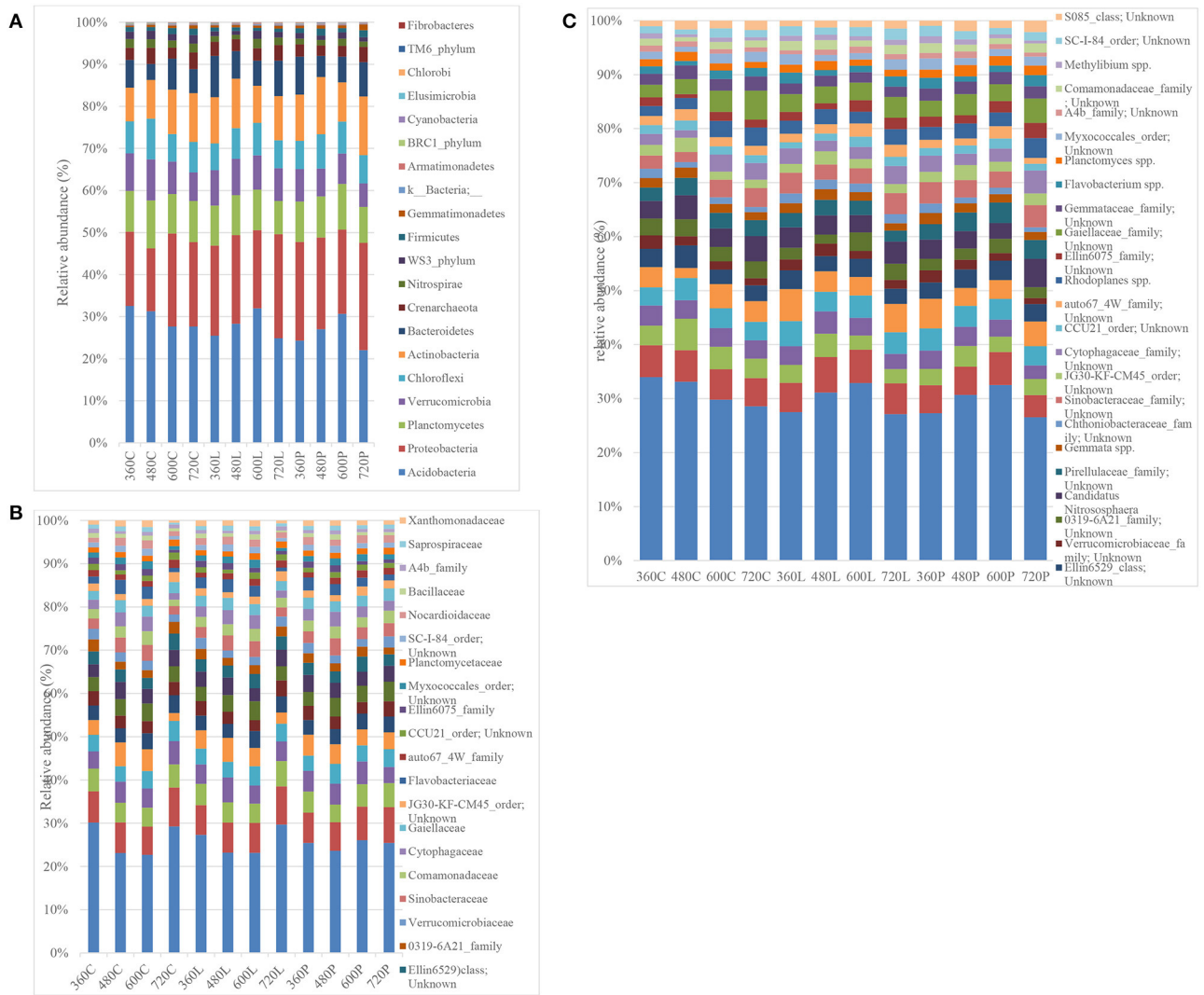

FIGURE 5 | Bacterial phylum-level **(A)**, family-level **(B)**, and species-level **(C)** resolution bar-plots of the control (C), leaf litter (L), and piglet (P) associated soils on days 360, 480, 600, and 720.

JG30-KF-CM45_order, CCU21_order, *Candidatus,* and *Flavobacterium*. Species from Ellin6529_class and *Candidatus nitrosphaera* had distinct trends in each of the piglet, leaf litter and control soils while species from Verrucomicrobiaceae and Chthoniobacteraceae family had distinct temporal trends in leaf litter soils as compared to control and piglet soils. Species from the Pirellulaceae, Gaiellaceae, Gemmataceae and Ellin6075 family reported distinct trends in piglet treatments when compared with control and leaf litter. Nonetheless, two-way ANOVA did not detect any significant temporal (seasonal) variation in the control and experimental treatments.

One-way ANOVA on ranks (Kruskal-Wallis *H* test) based on the alpha-diversity Faith phylogenetic distances (**Supplementary Figure 7**) indicated no significant differences between the control and experimental treatments during Year 2 of the study. However, principal co-ordinates analysis (PCoA) based on the beta-diversity Bray-Curtis distances (**Figure 6A**) revealed the clustering of most samples at the end of autumn (day 360; month 12) and during summer (day 600; month 20), which were more distanced by the end of winter (day 480; month 16). Also, PCoA based on weighted UNIFRAC distances (**Figure 6B**) indicated seasonal variation in the soils, with clustering toward the left for winter (day 360; month 12) and end of autumn (day 720; month 24) while most samples from spring (day 480; month 16) and summer (day 600; month 20) clustered in the centre.

Overall, dissimilarity test ANOSIM indicated significant temporal (seasonal) differences in the treatments. Likewise, PERMANOVA identified significant temporal differences while the test of homogeneity of dispersion PERMDISP did not detect any significant temporal differences in the treatments (**Table 2**), which suggests a location but no dispersion effect.

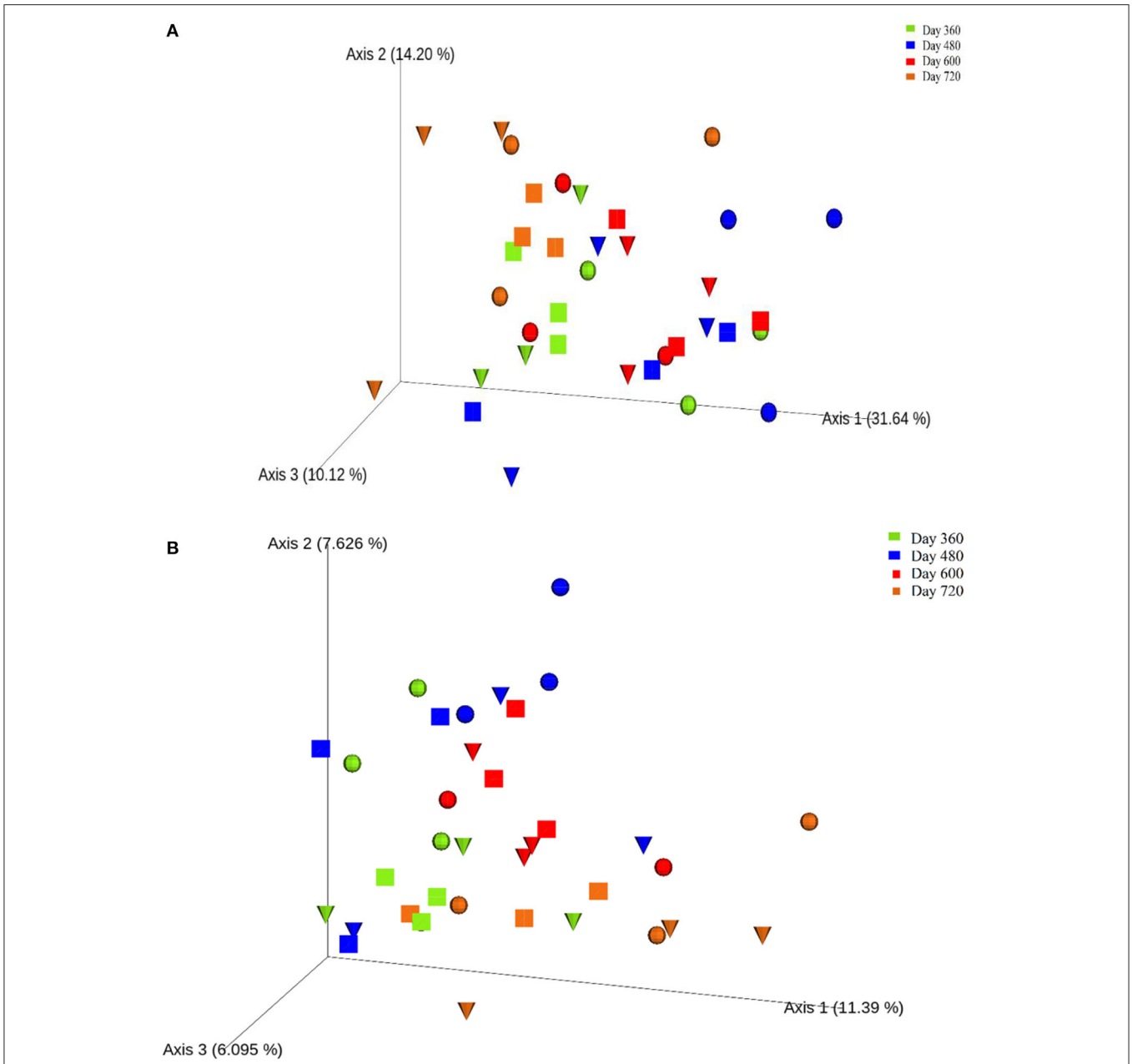

FIGURE 6 | Principal co-ordinates analysis (PCoA) ordination of the control (●), leaf litter (■) and piglet (▼) soils samples based on Bray-Curtis **(A)** and weighted UNIFRAC **(B)** distances of the observed species ASVs.

TABLE 2 | Comparison of 16S rRNA community seasonal variation using three statistical methods (*p*-value).

Groups	ANOSIM	PERMANOVA	PERMDISP
Seasonal variation treatments 16S rRNA community based on weighted UNIFRAC distances	0.02	0.003	0.207
Seasonal variation treatments 16S rRNA community based on Bray Curtis distances	0.006	0.003	0.656

NGS-Based Hill Ecological Indices

Hill numbers determined from the Year 2 NGS data were based on the numbers of species identified after assigning taxonomy. As recorded for DGGE-based bacterial profiles (**Supplementary Figure 3B**), species richness (Hill number ^{0}D) showed similar patterns for the control and piglet soils, which

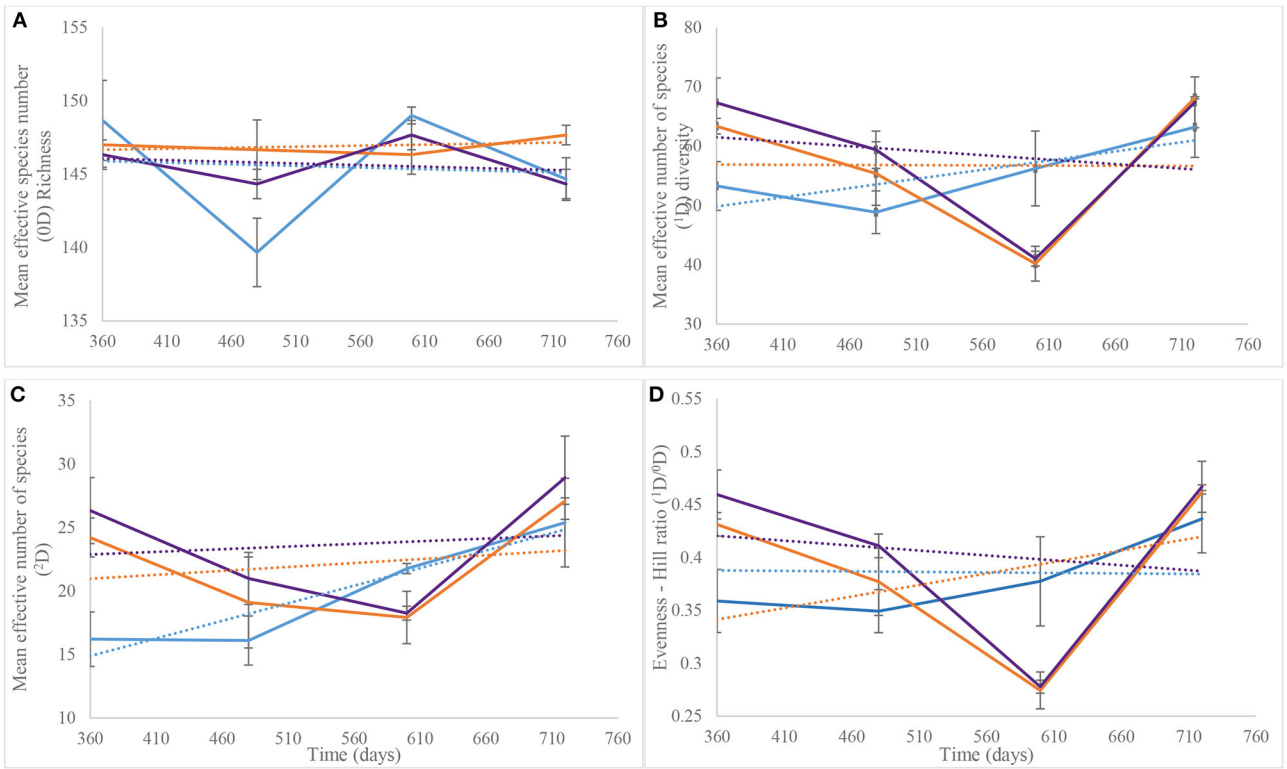

FIGURE 7 | Average ($n = 3$) taxa richness (^{0}D, **A**), common taxa diversity (^{1}D, **B**), dominant taxa diversity (^{2}D, **C**), and evenness (^{1}D/^{0}D, **D**) for bacterial communities of control (■), leaf litter (■) and piglet (■) associated soils on days 360, 480, 600, and 720. The Hill numbers were calculated using species that were identified from next generation sequencing. Each datum point is the mean of triplicate samples. Error bars are SEM.

contrasted the leaf litter soils (**Figure 7A**). Overall, two-way ANOVA with replication showed no significant difference in species richness between the control and experimental treatments during the second year of the study ($p = 0.36$) (**Table 1**). This statistical tool was applied also to the trends in **Figure 7B** and indicated a significant difference in common species diversity (^{1}D) between the control and experimental treatments at different time points ($p < 0.03$), but no significant differences between the piglet and leaf litter treatments. Comparable patterns in the diversity of dominant species (^{2}D) resulted for the *S. scrofa domesticus* and *Quercus robur* leaf litter treatments throughout the second year of the study (**Figure 7C**) and contrasted the soil-only control, but two-way ANOVA with replication indicated no significant differences between the control and experimental communities ($p = 0.14$).

Similar to the ^{2}D trends, two-way ANOVA with replication revealed a significant difference in bacterial species evenness (^{1}D/^{0}D) between the control and experimental treatments throughout Year 2 of study ($p = 0.006$) but no significant differentiation of the piglet from leaf litter soils ($p = 0.78$) (**Table 1**). Overall, the trendlines for the Hill ecological indices show: (i) increasing ^{0}D divergence from day 360 to day 720 for the control and piglet vs. the leaf litter soils; (ii) convergence in ^{1}D on day 600 with some divergence between control vs. both leaf litter and piglet treatments on day 720; (iii) divergence in ^{2}D for experimental treatments vs. control on day 360 but convergence for all three around day 700; and (iv) similar trends for ^{1}D/^{0}D (**Figure 7D**).

Soil Mineral Composition

Calcium (Ca), iron (Fe), potassium (K), phosphorus (P), sulphur (S), and magnesium (Mg) were quantified in the different soil samples collected throughout the 2-year study to assess shifts in soil mineral composition that could be exploited for forensic applications (Melis et al., 2007; Aitkenhead-Peterson et al., 2012; Stokes et al., 2013; Macdonald et al., 2014; Szelecz et al., 2018). These were used subsequently to complement subsurface microbial community profiling for a more holistic toolkit. All the blank samples tested had elemental concentrations that were below the detection limit of the equipment. Piglet soil calcium content was marked by an overall increase during the first year of the study from 2.4 5 ± 0.26% on day 0 to 7.4 2 ± 0.35% on day 360, followed by a decrease until day 720 (5.02 ± 1.75%) (**Figure 8**). Leaf litter soil calcium content increased to its highest on day 180 (7.78 ± 0.66%) and then decreased until the end of the study, while control treatments had overall minor increases in calcium with a peak on day 300 (6.04 ± 1.56%). The Fe, P and K contents for the different treatments had comparable patterns throughout the 2-year study with constant concentrations overall, except on day 240 at which Fe and

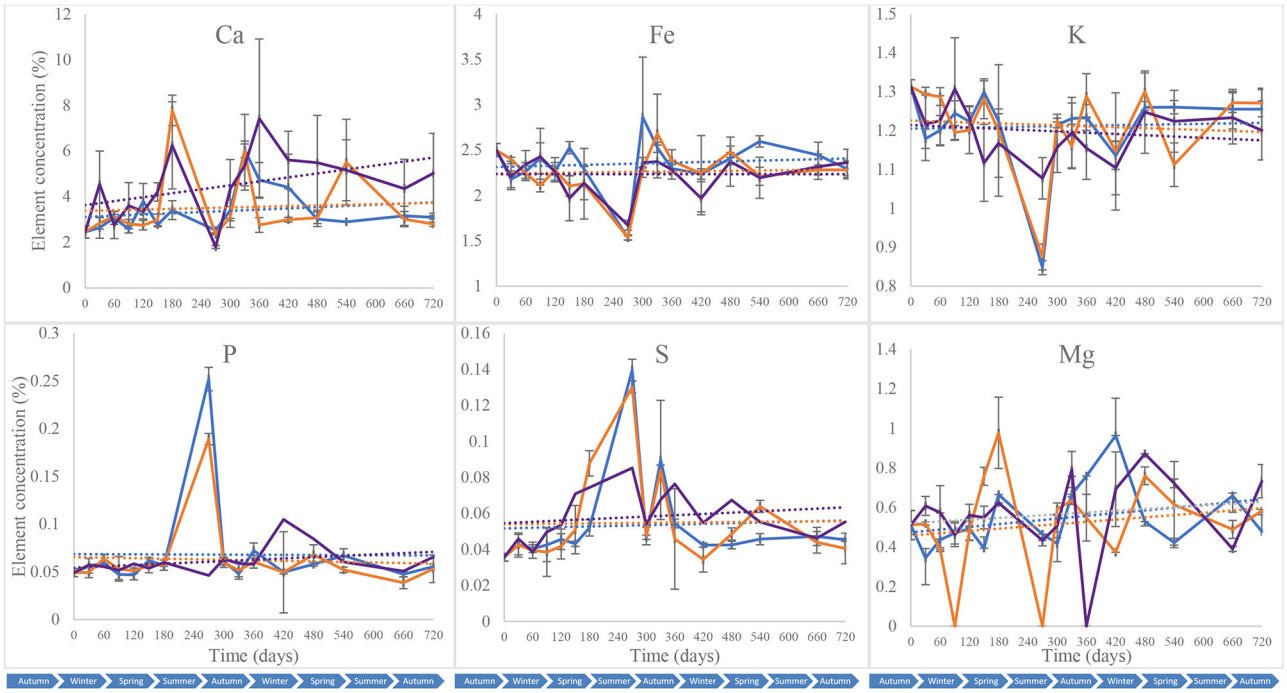

FIGURE 8 | Average ($n = 3$) soil composition in calcium (Ca), iron (Fe), potassium (K), phosphorus (P), sulphur (S), and magnesium (Mg) for control (●), leaf litter (●), and *S. Scrofa domesticus* (●) treatments. Each data point is the mean of triplicate samples. Error bars are SEM.

P decreased for the three treatments while K increased for the control and *S. scrofa* soils. Two-way ANOVA indicated a significant difference in calcium (Ca) composition between the control, piglet and leaf litter soils throughout the study ($p = 0.00$) while no significant differences were observed between the treatments for soil Fe, P, K, or S composition ($p > 0.05$). With the exception of magnesium ($p > 0.05$), significant differences were recorded for the different soil elements and between the various sampling intervals ($p < 0.00$).

DISCUSSION

Previous studies have investigated decomposition in controlled environments (Metcalf et al., 2013) and often for relatively short periods of time. Although the approach is very useful to explore the different parameters that influence decomposition separately, it does not replicate or reflect the natural conditions that would be found in forensic investigations. In contrast, the current outdoor *Sus scrofa*-based decomposition study is, to our knowledge, the longest within the forensic ecology literature. It was set outdoor in a natural, non-controlled environment, taking into consideration the inherently different atmospheric, edaphic and biotic factors at the study site in order to mimic cadaver interment in case of homicide (clandestine grave).

Atmospheric and Edaphic Conditions

Weather conditions have a significant impact on carrion decomposition and the associated soil microbial communities. For example, Carter et al. (2008) stated that temperature is one of the most important factors that affect decomposition rate as it governs biological processes. Various authors (Vass et al., 1992; Shean et al., 1993; Megyesi et al., 2005; Stokes et al., 2009) reported an inhibition of biochemical processes associated with biological activity, in general, and microbial activity, specifically, at temperatures lower than 4°C hence delayed putrefaction rates in cold and/or snowy weather. Also, UV radiation was reported to reduce litter biomass considerably (Gaxiola and Armesto, 2015) by increasing decomposition rate via photodegradation (Brandt et al., 2007). Wang et al. (2015) suggested that UV exposure time might increase litter biodegradability which would, consequently, enhance carbon supply to microorganisms and thus accelerate decomposition. The changes in fungal and bacterial richness, diversity and evenness observed during our study reflected seasonal temperature fluctuations with increases in the different ecological metrics at high temperatures, which decreased when temperatures dropped. This was reflected further by changes in the dominances of some taxa at specific intervals of the 2-year period, and highlighted the effect of temperature on microbial metabolism and biological reactions during subsurface decomposition at the current study site.

Multivariate analysis (PCA) of weather conditions revealed a positive correlation between temperature and UV index which clustered along component 1 (**Figure 3**). Similarly, rainfall, humidity and cloud coverage clustered together and correlated positively. Overall, the recorded trends aligned with the known and recognised relationships between parameters that clustered together and their related roles in decomposition. For example, rainfall which accounts for soil moisture content and partly

impacts soil temperature, affects the structure and activity of microbial communities and, hence, influences decomposition (Hyde et al., 2017). Thus, seasonal changes in rainfall and temperature coincided with the successional shifts in soil fungal and bacterial communities. PCA of the 18S fungal ecological indices (**Figure 4A**) showed high similarities in trends for richness (^{0}D) and, common (^{1}D) and dominant (^{2}D) taxa diversity of the control and experimental treatments while still permitting the distinction of leaf litter ^{0}D, ^{1}D, and ^{2}D, and piglet ^{1}D and ^{2}D from control soils. Also, the positive clustering of temperature with the ecological indices for richness and diversity highlighted the impact of this key environmental parameter on soil fungal community composition and structure, while rainfall and cloud coverage had a lesser influence on this clade. In contrast to the fungal profiles, PCA of the 16S bacterial community diversity indices (**Figure 4B**) was marked by clustering of the control and piglet soils together, but separately from leaf litter treatments, and was characterised by a distinct bacterial community. In addition, the clustering and positive correlation of the environmental factors—temperature, rainfall, cloud cover, humidity—on component 1 reflected their impact on bacterial diversity throughout the study.

The control and experimental treatments had similar pH patterns throughout the 2-year period of study. Notwithstanding this, pH did not correlate with temperature, the other abiotic factors or diversity indices, except for the fungal and bacterial Hill ratio (^{1}D/^{0}D) with which it had moderate-negative and weak correlations, respectively. Analysis of clustering amongst the ecological indices showed a strong correlation in fungal community dynamics for the control and experimental soils for the study duration. Bacterial Hill indices allowed the distinction of leaf litter soils from control and piglet soils. The similarity between controls and piglet soils was potenitally due to the small-sized piglets (1.5 kg) which created confined cadaver decomposition islands (CDIs). According to Carter et al. (2007), nutrient leaching is limited both vertically and horizontally by the cadaver size and rate of decomposition and, hence, the soil samples collected outside the cage may not have been impacted sufficiently by decomposition to then register temporal differences in the fungal and bacterial communities. In addition, the land used for the experiment was located in a woodland ecosystem with clusters of oak trees and continuous input of organic material to the surrounding soil which potentially led to the recorded microbial community similarities (Olakanye et al., 2017). Snowfall and days of snow clustered negatively on component 1 and had a moderate negative correlation with the different bacterial ecological indices which was then reflected by the decrease in bacterial diversity as exemplified during spring 2015 (day 540).

Increases in bacterial diversity for the control and experimental soils recorded during the first month of the study were probably due to the disturbance of soil during interment (Kim et al., 2013). This increase coincided with an increase in piglet soil pH which remained stable until spring (day 120). Control and leaf litter soil pH increased on day 60 (winter) and coincided with increases in bacterial richness and common taxa diversity (^{1}D) for the control, but decreases in richness, common taxa and dominant taxa diversity for the leaf litter. On day 240 (summer), bacterial community richness, diversity and evenness dropped minimally for control soils and considerably for piglet soils with similar decreases in community richness and diversity also recorded on days 360 (winter) and 660 (autumn). As also reported by Finley et al. (2015b), pH changes during decomposition lead, subsequently, to a change in the soil microbial community composition and structure. Therefore, the increase in *Sus scrofa domesticus* soil pH during the first months is attributable to the release and accumulation of ammonia-rich fluids in soil (Hopkins et al., 2000; Metcalf et al., 2016), while the subsequent decrease resulted from soil microbial communities utilisation of base cations such as K^+, Na^{2+}, or Mg^{2+}(Carter et al., 2008).

Overall, these findings highlight the importance of profiling fungal and bacterial communities in conjunction with environmental factors, and applying multivariate analyses to understand fully their interconnectedness within decomposition. The correlation of temperature with soil fungal community ecological indices, and correlation of temperature and rainfall with the bacterial community indices, demonstrate the importance of understanding the effect of the environmental factors on both universal microbial diversity and specific taxonomic glades. Hence, combining the patterns of bacterial and fungal ecological indices to climatic records could indicate the presence of a carbon source. For example, low microbial community diversity during warm seasons, or increased diversity during winter, could be indicative of a recent disturbance to soil which might be due to carrion decomposition, especially decomposition processes that usually happen during the first few months of interment.

Community Diversity Analysis Based on DGGE and Hill Numbers

To date, most forensic microbiology studies have used the Shannon-Wiener and Simpson indices to establish soil microbial community diversity during decomposition. The current study is the first to use Hill numbers as ecological indices in a forensic context for further interpretation of DGGE and NGS data to measure temporal and spatial microbial community shifts during *in situ* sub-surface decomposition.

Fungal 18S rRNA Soil Community

The overall increases in fungal taxa richness recorded for all burials on days 60/ADD 258 and 90/ADD 396 were probably due to the introduced carbon sources, which constitutes a physical disturbance to the indigenous soil microbial communities (Kim et al., 2013). Also, Tukey HSD and Bonferroni *post hoc* tests revealed a significant change during this period. This trend suggests that although it was the middle to end of winter 2015, skin rupture and nutrient release happened before day 60/ADD258 and that the piglets were potentially at the decay/active decay stage. The overall increases in fungal ^{0}D were largely sustained during the first year of the experiment and, therefore, reflected a protracted response of this clade to the presence of animal-based and plant-based sources of carbon and nitrogen in the experimental soils. Generally, a significant

difference in fungal community richness that reflected seasonal variations resulted between the two experimental treatments of piglets and oak leaf litter, and for the experimental and control soils but only at specific time points during the study.

Decreases in piglet soil fungal diversity for common (^{1}D) and dominant (^{2}D) taxa on day 30/ADD 144 were possibly caused by the introduction of the mammalian surrogates which represent a high quality nutrient resource with high water content and a narrow C:N ratio (Carter et al., 2007), selecting for specialist degraders. This contrasted the control and leaf litter soils where the pronounced decrease in ^{1}D and ^{2}D on day 60/ADD 258 (4°C) were most likely because of the lower quality carbon source (plant litter), or absence thereof (control). Generally, two-way ANOVA showed a significant difference in fungal community ^{1}D and ^{2}D between samples from different times corresponding to seasonal variations. Hence decreases in the diversity metrics from end of autumn (2014) to end of winter (2015) were followed, for example, by increases from spring until autumn particularly in the presence of leaf litter. Next generation sequencing of the 18S rRNA gene would have identified the specific indicator fungal taxa and is therefore recommended for future studies.

Although total body scores were unachievable for the subsurface burials, the generally pronounced decreases in fungal community ^{1}D and ^{2}D during the second year of study were attributed to the reduction of soil nutrients where the added substrates were largely or completely decomposed and mineralized. This highlights the need for further studies into how long the microbial community signals remain traceable within decomposition-impacted soils to still be useful for location/identification of clandestine burials, including for cases where remains have been moved. *Post hoc* Tukey HSD and Bonferroni tests facilitated the differentiation between soils with animal carbon source (piglet) and those without (control and leaf litter) but not between control and leaf litter soils based on fungal community ^{1}D and ^{2}D. Also, analysis of fungal community Hill ratio (^{1}D/^{0}D) showed temporal changes in evenness for this microbial clade. This was potentially a consequence of seasonal weather variation despite there being no significant difference between control and experimental treatments.

In summary, the 18S rRNA gene DGGE-derived richness (^{0}D) and common taxa diversity (^{1}D) allowed clear differentiation between the mammalian decomposition and that of oak leaf litter while dominant taxa diversity (^{2}D) permitted the distinction between piglet and control soils, with the resolutions more pronounced at specific intervals. Therefore, the different Hill numbers derived from fungal community profiles can be analysed for soils and conditions similar to our study specifically to establish temporal subsurface decay of mammalian or plant matter (^{0}D, ^{1}D) or no mammalian decomposition (^{2}D).

Bacterial 16S rRNA Soil Community

The initial increase in 16S rRNA bacterial community richness (^{0}D), common taxa diversity (^{1}D) and dominant taxa diversity (^{2}D) observed on day 30, concomitant with ADD 144, was due to the physical disturbance caused by digging, carbon source interment and high soil temperature (12°C) at the beginning of the study. On the other hand, the subsequent decrease in piglet soil bacterial community ^{0}D, ^{1}D, and ^{2}D at day 60/ADD 258 might be due to the influx of nutrients after the introduction of a high quality protein resource (Carter et al., 2007), which would decompose at a faster rate compared to leaf litter selecting, momentarily, for fast-growing members (r-strategists) of this clade. Lower temperatures during winter, without added nutrients, led to the decline in taxa richness and diversity for the control soils. Two-way ANOVA with replication highlighted seasonal variations in the different treatments. Furthermore, Tukey HSD and Bonferonni *post hoc* tests detected statistically significant differences between the leaf litter soils when compared to the control and *S. scrofa* based on ^{1}D, ^{2}D, and ^{1}D/^{0}D but no significant differences between control and piglet treatments. The trends were highlighted further by principal component analysis where the piglet and control ecological metrics (^{0}D, ^{1}D, ^{2}D, and ^{1}D/^{0}D) clustered along component 1, separately from the leaf litter indices. As a result, bacterial ecological analysis using Hill metrics would not afford a distinction between mammalian gravesoils from their non-burial equivalents for this and similar soils/sites.

Bacterial Community Profiling

The aim of this study was to compare soil microbial communities associated with the decomposition of stillborn piglets as human proxies and oak leaf litter in a natural setting, analyze their successional shifts in composition and structure, and determine their potential as tools for forensic investigation.

Soil Metabarcoding

Soil necrobiome metabarcoding that focused on the second year of our study identified the most predominant bacterial phyla as Acidobateria, Proteobacteria, Actinobacteria, Plancomycetes, Verrumicrobiota, Chloroflexi, Bacteroidetes, Nitrospira, and Firmicutes. This is partly in accordance with Finley et al. (2016) who reported Proteobacteria, Actinobacteria and Acidobacteria as the most abundant phyla during terrestrial decomposition and Damann et al. (2015) who reported predominances of Firmicutes, Proteobacteria, Acidobacteria, Actinobacteria, Bacteroidetes, and Chloroflexi in decomposing human bone. Also, Acidobacteria, Proteobacteria, and Bacteroidetes correlated positively with temperature. Increased abundance of Acidobacteria during the second year of study was in contrast to the findings for the first 9 months after interment where Olakanye et al. (2017) reported Proteobacteria as the most abundant phylum for these burials. Therefore, phylum-level soil metabarcoding may afford preliminary temporal resolution of a 2-year subsurface post-burial interval in sites with similar soil, environmental and climatic conditions as our study area.

Similar patterns in Acidobacteria, Proteobacteria, Firmicutes and Chloroflexi abundances were observed in piglet and leaf litter soils as compared to controls (**Figure 5A**). Thus, two-way ANOVA detected significant differences in phyla abundances between control and experimental treatments throughout the second year of study, with no significant difference between piglet and leaf litter soils. Similarly, no significant temporal changes in piglet or leaf litter soils were detected while there were significant seasonal phylum-based shifts in control soils. Singh et al. (2018)

reported a lower abundance of Chloroflexi in soil in the presence of human cadaver. This was not apparent in the current study, both in Year 1 (Olakanye et al., 2017) and Year 2, as there were no significant differences in Chloroflexi abundance between the different treatments ($p = 0.69$). In particular, two-way ANOVA with replication on the different taxa belonging to Proteobacteria and Chloroflexi showed no significant seasonal or treatment variations during the second year of study for the experimental treatments ($p > 0.05$), although control soils showed a seasonal variation in phyla abundance ($p = 0.0001$). Overall, the four phyla that presented the same patterns in piglet and leaf litter soils could help distinguish decomposition soils from soil-only controls, however, they would not detect or separate animal from plant gravesoils. Notably, the difference between controls and experimental soils during the second year of the study suggested some persistence of a microbial decomposition signature for a post-burial interval of up to 24 months. Although similarities in phylum-based succession and clock indicators between the current *Sus scrofa domesticus*-based study and those using human cadavers justify further the utility of pigs, research initiatives that directly compare these surrogates with human cadavers are essential. Only then can knowledge developed from swine decomposition studies be considered for transfer and application in criminal cases involving human remains.

Orders such as Acidobacteria iii1-15, Rhizobiales, Actinomycetales, and Saprospirales correlated positively with temperature and became more abundant in summer (day 600/ADD 6136). These were likely contributors to the recorded increases in richness as reflected by both DGGE and NGS Hill ^{0}D results at the same sampling sampling interval. In contrast, CCU21, JG30-KF-CM45, and Ellin 6529 did not correlate with temperature. Two-way ANOVA with replication showed a significant difference in taxa abundance for the control and leaf litter treatments at the different sampling times while piglet soils recorded no significant variation with time. Methylococcales, which were reported during months 0–9, were associated with piglet treatments during the second year of the experiment and had distinct successional trends from those associated with control and leaf litter soils. This order could, therefore, be used as an indicator of gravesoil in this experimental setting and conditions. In a 10-month study, Finley et al. (2016) reported a consistent abundance of Rhizobiales and Chtoniobacterales during subsurface decomposition. This was reflected in our study as these taxonomic orders correlated positively with temperature and showed seasonal variation. However, they were detected in the different treatments and, therefore, non-specific to piglet decomposition as a human analogue.

When developing their prediction model for PMI, Belk et al. (2018) found that phylum-level analysis permitted the most accurate prediction than other taxonomic levels. This contrasted the current study where phylum-level resolution, except for dominances for Proteobacteria (Year 1) and Acidobacteria (Year 2), provided no consistent differentiation between the experimental treatments. Nevertheless, most studies have focused on the use of phylum or family-level resolution (Metcalf et al., 2013; Pechal et al., 2013, 2014), which makes their findings potentially scale specific. According to Zhou and Bian (2018), microbial communities profiling at higher taxonomic resolution, of genus- or species-level, would ensure more comprehensive data analysis and probably facilitate the discovery of exploitable trends. Therefore, this approach was adopted in the current study.

At family level, the most abundant taxa recorded during the second year of the study, and hence the most likely microbial clock indicators for long PBI, were: RB40_family, mn2424_family, Chloroflexi, Chtoniobacteraceae, Hyphomacrobiaceae, Pirellulaceae, Chitinophagaceae, Gemmataceae, Sinobacteraceae, Gaiellaceae, and Cytophagaceae. The structure and dynamics of the community at family level were similar to ordinal and phyletic levels, with seasonal variations throughout the second year of the study. Pirellulaceae, Chitinophagaceae, Gemmataceae, Hyphomicrobiaceae, Sinobacteraceae, Cytophagaceae, and Gaiellaceae correlated differently according to season and/or type of treatment (**Figure 5B**). Furthermore, Sphingomonadaceae correlated negatively with temperature in the piglet and leaf litter treatments and positively in control samples. Methylophilaceae and Anaerolineaceae were reported by Olakanye et al. (2017) as potential microbial clocks for piglet and leaf litter, respectively, during the first year of the study. The results of the second year showed that Methylophilaceae correlated positively with temperature in piglet soils, however, it also correlated positively for control, which makes it non-specific to piglet soils for the late stages of temperature-related decomposition for the current scenario. On the other hand, Anaerolineaceae was not detected in any of the control or experimental treatments. Based on two-way ANOVA, there were no significant differences between the different treatment groups, however, there was a significant difference in samples collected at different times, which corresponded to seasonal variation.

Cobaugh et al. (2015) reported the persistence of microbial signatures of decomposition for more than a year after interment of a human cadaver, which would help detect clandestine graves. Similarly, Olakanye et al. (2017) used piglets instead of human cadaver and reported distinct signatures at order and family-levels during Year 1 of the current study. In contrast, the findings from Year 2 showed no detectable signatures of bacterial orders or families that could be used to establish the extent of animal decomposition in soil. This might be attributable to differences in the mass of the decomposing materials where an adult human cadaver would have a bigger and more protracted impact on the gravesoil microbial community structure and composition compared to piglets. Therefore, future experiments should compare the soil necrobiome during simultaneous subsurface decompositions of human cadavers and adult pigs where the size/weight of the interred materials are as similar as possible to establish comparison baselines and/or proof of concept.

At genus level, similar trends in abundance between piglet and leaf litter soils were observed in genera from iii1-15_family, mb2424_family, Chitinophagaceae_family, JG30-KF-CM45_order, CCU21_order, *Candidatus,* and *Flavobacterium,* which may help discriminate decomposition soils from soil-only controls. However, they did not permit the distinction between

animal-based and plant-based decomposition. Notwithstanding this, the significant temporal shifts in predominant genera abundance of control and leaf litter showed the seasonality in soil bacterial composition. No species-level markers were detected specifically for piglet decompositions during the second year of study. However, species from Sinobacteraceae and Cytophagaceae family, JG30-KF-CM45 and CCU21 order, *Rhodoplanes* spp, and *Flavobacterium* spp were present in experimental soils only, while species from Pirellulaceae, Gaiellaceae, Gemmataceae, and Ellin6075 families showed distinct shifting patterns when comparing control and leaf litter treatments. These species might, therefore, be targeted as potential markers to detect gravesoil in an outdoors crime scene with conditions similar to those of the current research setting. For method validation, the findings need to be confirmed in a controlled experimental setting to rule out the effects of the variables associated with outdoor studies where several environmental parameters are uncontrolled.

The study of alpha diversity in the different treatments was performed using Faith phylogenetic metric and complemented subsequently by Hill ecological indices analysis for a comprehensive comparison with the DGGE-based results. **Supplementary Figure 7** shows the similarity in alpha-diversity between the different treatments, especially piglet and leaf litter soils during the second year of decomposition. Also, one-way ANOVA on ranks (Kruskal-Wallis) did not show any significant differences between the control and experimental treatments for this period. This similarity might be indicative of a convergence in soil bacterial community composition due to decreased decomposition and/or amounts of mineralizable carbon sources more than a year after interment, the effect of weather conditions on soil bacterial community, and continuous input of new carbon sources in the open-air study site.

During the second year of the experiment, the Beta-diversity metric of Bray-Curtis distance showed the clustering of most of the samples at the end of autumn (day 360) and during summer (day 600), which were more distanced by the end of winter (days 480). Similarly, weighted UNIFRAC distance reflected the clustering of samples from spring (day 480) and summer (day 600) together, and separately from those of winter (day 360). These findings suggest a seasonal variation in soil bacterial community based on beta-diversity. However, there were no significant differences in beta-diversity between the control and experimental treatments.

In a study on human decomposition, Cobaugh et al. (2015) reported that cadaver-related microorganisms, that are very distinct and scarce in nature, could persist in soil and still be detected more than a year after placement, and could be used as biomarkers for human decomposition. Although the results of the current *in situ* study did not track the piglet-derived necrobiome or identify soil bacterial species associated solely with the piglet treatments, some taxa reported distinct shifts that were specific to piglet treatments and not leaf litter or control soils. Therefore, their successional shifts, and not their presence or absence, can be used as temporal indicators for post-burial interval determinations for similar study sites.

Ecological Indices of the Bacterial Community Metabarcode

Ecological indices are used typically to facilitate spatial and temporal comparisons between treatments, and across different studies. These data are often analysed parallel to those derived from next generation sequencing. In this study, we report the first time use of Hill ecological indices analysis of NGS-derived data specifically to complement, and directly compare with, the metrics calculated from DGGE community profiling. The aim was to address the limitations of each approach and test the reliability for data extrapolation between the techniques, to then inform a proposal that DGGE can be used instead of NGS by forensic microbiology laboratories with limited (financial) resources. In a similar way to Hill numbers calculated from DGGE results, Hill numbers calculated using NGS data showed seasonal shifts in diversity (^{1}D and ^{2}D) and evenness (^{1}D/^{0}D) for the different treatments. Although there was no significant difference in species richness (^{0}D) between samples collected at different seasons for Year 2 of the study, increases in the abundance of some orders on day 600 suggested an alignment between DGGE and NGS-based Hill analysis.

The current findings suggest that each taxonomic level can give additional information such as whether it is related to discriminating soil, finding decomposition markers, confirming seasonality, or checking the extent/longevity of the bacterial signature in time. NGS-based analysis of the different taxonomic levels afforded a better insight into the dynamics of the bacterial community, implying that NGS should not necessarily be replaced with DGGE. Also, analysis of bacterial community structure using the different DGGE-based Hill ecological indices calculated for all 24 months of the study did not permit a consistent distinction between control and experimental treatments. Nevertheless, the similarity in bacterial trends between piglet and leaf litter soils, and marked difference with the control community at different taxonomic levels, suggested some persistence of decomposition signature of both animal and plant-based carbon sources up to 24 months. The taxonomic resolutions from an *in situ* study, and their interpretations via Hill numbers, need to be investigated under controlled experimental settings for proof-of-concept. Furthermore, future studies should track the necrobiome of the interred mammalian surrogates parallel to that of the gravesoil to identify key markers and then determine the persistence of signature microorganisms/community after carrion decomposition.

Soil Mineral Composition

Calcium, phosphorous, potassium and magnesium are major minerals in the human body with blood concentrations dropping from 8.45 to 3.70 mg dL^{-1} for calcium, and increasing from 100.72 to 188.49 μg dL^{-1} for iron after 264 h of putrefaction (Costa et al., 2015), while sulphur and iron are trace elements necessary for biochemical functions. As a result, soil mineral composition is often included in the suite of physicochemical analyses that are used in criminal investigations, with considerable potential for preliminary location of clandestine graves. In contrast to separate

analyses, this study aimed to complement soil necrobiome metabarcoding with analysis of key elements for an enhanced toolkit for decomposition studies. Phosphorus, magnesium, calcium, potassium, iron and sulphur were selected for their importance in biological functions, nutrient recycling and microbial activity. Sulphur represents about 0.15% of pig tissue mass. It is found in protein-forming amino acids such as methionine and cysteine, which are degraded by microbial-driven decomposition to form volatile sulphur compounds that attract necrofauna insects (Statheropoulos et al., 2011; Kasper et al., 2012; Agapiou et al., 2015). Potassium is important for muscles and the nervous system functioning and has been used for the estimation of time since death based on its concentration in the vitreous humour (Ortmann et al., 2016; Cordeiro et al., 2019) and synovial fluid (Siddhamsetty et al., 2014). In addition, it is present in soil and plays an important role in plant growth and metabolism (Wang et al., 2013). Likewise, phosphorous, magnesium and calcium are important elements for biological functions and soil nutrients. Phosphorous concentration was reported to change during decomposition (Benninger et al., 2008; Stokes et al., 2009, 2013; Szelecz et al., 2018) while calcium changes underneath bison carcasses were detectable up to 7 years after interment (Melis et al., 2007).

In this study, the patterns for calcium content between piglet soils, and the control and leaf litter soils, were distinct as indicated by the trendlines (**Figure 8**). In addition, two-way ANOVA identified significant differences between the different treatments throughout the study. Calcium content increased markedly in the piglet treatments compared with control and leaf litter. This might have been due to the release of calcium from the piglets as they decomposed while the minor increase in control and leaf litter treatments calcium content was potentially due to the continuous input of oak leaves in the woodland-classified study site. Although still higher than at the beginning of the study, the decrease in calcium content during the second year might have been a result of the slower release of calcium from the piglet remains that were at the late stages of decomposition, and utilisation of the calcium already available in soil. Also, unlike potassium and phosphorous, which are mainly available in labile tissues and released during the early stages of decomposition (Szelecz et al., 2018), calcium is released continuously during the different stages of decomposition until total degradation of bones (Melis et al., 2007), probably leading to the observed statistically significant differences between the treatments throughout the study. Piglet soil calcium content had a moderate positive correlation with rainfall but did not correlate with temperature.

Further correlation analysis indicated a moderate-positive correlation in iron and potassium and a strong correlation in sulphur trends between the control and experimental treatments, which had overall similar trends throughout the study. In addition, there were significant temporal changes in soil iron content, however, there were no significant differences between the different treatments. Phosphorus content correlated very strongly between control and leaf litter soils while none of these treatments correlated with piglet soil samples. Overall, no statistically significant differences were observed when performing two-way ANOVA, which, therefore, did not allow the discernment of gravesoil from control and leaf litter soils.

The correlation of calcium and iron with decomposition observed during the study is in accordance with Costa et al. (2015) who reported a significant linear correlation of these elements with the time of blood putrefaction. Also, Marín-Roldan et al. (2013) reported a positive correlation of elements such as Mg, Na and K in swine skeletal muscles with PMI due to a variation in their concentration caused by chemical reactions in tissues. While it was not possible to determine the decomposition stages during the subsurface *S. scrofa domesticus* (piglet) study, increases in calcium content might have coincided with early and mid-stages of decomposition as these are expected to happen during the first few months of interment in the north of England (Irish et al., 2019; Procopio et al., 2019). Nevertheless, further case studies on decomposition are needed, especially on specific geo-climatic regions. On the other hand, the decrease in soil calcium content during the second year of the experiment might be attributed to the reduction in calcium released by the cadaver and, therefore, the late/advanced decomposition of the animal model. This was further confirmed when exhuming the piglets after 2 years of interment, at which point only small fragments of disarticulated bones were left while the skin, flesh, cartilage, and most of the bone tissue were completely decomposed. These findings highlight the potential of using elemental analysis, particularly for calcium, to consolidate the findings from microbial community profiling to confirm PMI/PBI and clandestine grave location.

Throughout this study, the calculated diversity metrics of ^{0}D, ^{1}D and ^{2}D correlated negatively with time while the $^{1}D/^{0}D$ evenness correlated positively with iron and potassium concentrations, and negatively with phosphorous, sulphur and magnesium (Data not shown). The patterns in piglet soil potassium, phosphorous and iron concentrations were comparable to the changes in ecological indices ^{0}D, ^{1}D, and ^{2}D during the first 5 months of the study, until day 150. Also, two-way ANOVA indicated a significant difference between soils samples collected at different times. These findings suggest that the changes in soil elemental and bacterial community composition were most probably a response to carrion decomposition.

CONCLUSIONS

The advent of culture-independent high-throughput molecular identification technologies has revolutionised the study of the microbial community allowing the characterisation of microbial species up to the strain or sub-strain level. Microorganisms are ubiquitous; they adapt to different biotopes and have predictable successions. Also, they are transferred from the cadaver to soil during decomposition and might be considered as physical evidence to be used in forensic investigation (Bishop, 2019) for gravesoil detection, PMI assessment or confirmation/exclusion of links between persons, items and locations (Oliveira and Amorim, 2018). Using the northeast of England for context, this experiment was designed to enrich the knowledge based on

carrion decomposition and test the potential of using a combined molecular microbial ecological and elemental analysis approach in decomposition studies to enhance gravesoil detection and/or PMI estimation. Overall, the study's four hypotheses were proven and accepted.

Similar to work by other researchers who investigated tissues that are typical of late decomposition stages, the second year of the current *in situ* piglet study revealed predominances of phyla such as Acidobacteria, Proteobacteria, Planctomycetes, Verrumicrobia, and Chloroflexi. Generally, phylum level analysis did not provide sufficient differentiation between treatments during the second year of the experiment but were partly indicative of shifts in temperature during subsurface decomposition. These changes in correlation could be used to distinguish soils where carrion decomposition occurred as opposed to soil only. Other key findings were of taxa at higher levels of resolution such as Methylococcales, Sinobacteraceae, *Candidatus,* and *Flavobacterium*, which, although not distinguishing mammalian from plant decomposition, differentiated experimental soils (piglet and oak leaf litter) from control-only soils. These are, therefore, potential microbial clock and clandestine grave indicators including for burials where plant material is used to cover criminal activity.

Statistical analysis of 18S rRNA gene DGGE-derived Hill ecological metrics allowed clear differentiation between mammalian decomposition and that of oak leaf litter. Also, it suggested the time at which piglet skin rupture happened (start of active decay). On the other hand, and although bacterial 16S rRNA community diversity analysis did not permit the distinction between piglet and leaf litter soils, it did delineate gravesoils from non-burial controls. For the first time in the literature, NGS-based Hill ecological metrics were calculated and compared to their DGGE equivalents while bacterial signature persistence in soil was tested over a 24-month period. Analysis of the sequencing data confirmed some similarity of the results obtained from the NGS-based and DGGE-derived diversity metrics when considering specific Hill numbers or decomposition/sampling intervals. Similarly, the elemental analysis of soil samples showed that calcium profiles of the piglet-associated soils were distinct from those without carrion.

Overall, this study achieved its aims with several key outcomes highlighted (**Supplementary Table 1**). (1) The importance of environmental and weather conditions in decomposition is evidenced by revealing the impact of seasonal temperature variation on substrate decomposition and soil microbial community composition. This includes parallel interpretation of temperature as ADD—a measure of time and heat necessary for biological functions instead of time only. (2) Likely bacterial markers that could help discriminate animal-based from plant-based decomposition are identified by NGS and provide further emphasis of the high potential of using soil microbial community characterisation in forensic investigation for the detection of gravesoil and estimation of time-since-death. (3) For the first time in forensic microbial research, we test the usefulness of Hill numbers as ecological indices to discriminate decomposition-impacted soils from controls. (4) Another novel contribution is testing the applicability and relevance for a combined approach *re* molecular and physicochemical soil analysis for enhanced precision. (5) As proposed previously (Schaldach et al., 2005; Ralebitso-Senior, 2018), we show that holistic multi-parameter approaches such as combining bacterial and fungal ecological indices, soil metabarcoding of the successional microbial community, and climatic records using multivariate analysis, have the potential to help detect gravesoil. For example, an increased microbial diversity during winter could indicate a disturbance to soil due to a recent carrion interment while a low diversity during a warm season might be the consequence of nutrient influx into soil during carrion decomposition. The application of this complementary approach in forensic cases, however, necessitates further case studies, preferably using donated human remains alone and in parallel to mammalian surrogates, and replicates/repeats for increased statistical power in order to confirm and, subsequently, validate the findings in different conditions.

DATA AVAILABILITY STATEMENT

The data generated in this article can be found in the European Nucleotide archive using the accession number PRJEB43763.

AUTHOR CONTRIBUTIONS

TR-S conceived and designed the study. CB did all the laboratory work and analysed all the study data. TR-S, GT, and HC supervised the laboratory work. CB and TR-S drafted the manuscript. All authors contributed to manuscript revision and read and approved the submitted version.

FUNDING

CB acknowledges gratefully funding from the Algerian NICC for his Ph.D. research program. TR-S acknowledges gratefully the QR-Global Challenges Research Fund (2019/2020) support from Liverpool John Moores University.

ACKNOWLEDGMENTS

Grateful acknowledgements are made to Dr. Ayodeji O. Olakanye and Professor Tim Thompson who conceived and designed the initial study with TR-S.

SUPPLEMENTARY MATERIAL

The Supplementary Material for this article can be found online at: https://www.frontiersin.org/articles/10.3389/fevo.2021.605817/full#supplementary-material

REFERENCES

Agapiou, A., Zorba, E., Mikedi, K., McGregor, L., Spiliopoulou, C., and Statheropoulos, M. (2015). Analysis of volatile organic compounds released from the decay of surrogate human models simulating victims of collapsed buildings by thermal desorption-comprehensive two-dimensional gas chromatography-time of flight mass spectrometry. *Anal. Chim. Acta* 883, 99–108. doi: 10.1016/j.aca.2015.04.024

Aitkenhead-Peterson, J. A., Owings, C. G., Alexander, M. B., Larison, N., and Bytheway, J. A. (2012). Mapping the lateral extent of human cadaver decomposition with soil chemistry. *Forensic Sci. Int.* 216, 127–134. doi: 10.1016/j.forsciint.2011.09.007

Behrensmeyer, A. K. (1978). Taphonomic and ecologic information from bone weathering. *Paleobiology* 4, 150–162. doi: 10.1017/S0094837300005820

Belk, A., Xu, Z. Z., Carter, D. O., Lynne, A., Bucheli, S., Knight, R., et al. (2018). microbiome data accurately predicts the postmortem interval using random forest regression models. *Genes* 9:104. doi: 10.3390/genes9020104

Benninger, L. A., Carter, D. O., and Forbes, S. L. (2008). The biochemical alteration of soil beneath a decomposing carcass. *Forensic Sci. Int.* 180, 70–75. doi: 10.1016/j.forsciint.2008.07.001

Bishop, A. H. (2019). The signatures of microorganisms and of human and environmental biomes can now be used to provide evidence in legal cases. *FEMS Microbiol. Lett.* 366:fnz021. doi: 10.1093/femsle/fnz021

Bisker, C., and Ralebitso-Senior, T. K. (2018). "The method debate: a state-of-the-art analysis of PMI estimation techniques," in *Forensic Ecogenomics: The Application of Microbial Ecology Analyses in Forensic Contexts*, ed T. K. Ralebitso-Senior (London: Academic Press), 61–86. doi: 10.1016/B978-0-12-809360-3.00003-5

Bolyen, E., Rideout, J. R., Dillon, M. R., Bokulich, N. A., Abnet, C. C., Gabriel, A., et al. (2018). QIIME 2 : reproducible, interactive, scalable, and extensible microbiome data science. *PeerJ*. 37, 852–857. doi: 10.1038/s41587-019-0209-9

Brandt, L. A., King, J. Y., and Milchunas, D. G. (2007). Effects of ultraviolet radiation on litter decomposition depend on precipitation and litter chemistry in a shortgrass steppe ecosystem. *Glob. Chang. Biol.* 13, 2193–2205. doi: 10.1111/j.1365-2486.2007.01428.x

Campobasso, C., Pietro, Di Vella, G., and Introna, F. (2001). Factors affecting decomposition and Diptera colonization. *Forensic Sci. Int.* 120, 18–27. doi: 10.1016/S0379-0738(01)00411-X

Can, I., Javan, G. T., Pozhitkov, A. E., and Noble, P. A. (2014). Distinctive thanatomicrobiome signatures found in the blood and internal organs of humans. *J. Microbiol. Methods* 106, 1–7. doi: 10.1016/j.mimet.2014.07.026

Carter, D. O., and Tibbett, M. (2006). Microbial decomposition of skeletal muscle tissue (*Ovis aries*) in a sandy loam soil at different temperatures. *Soil Biol. Biochem.* 38, 1139–1145. doi: 10.1016/j.soilbio.2005.09.014

Carter, D. O., Yellowlees, D., and Tibbett, M. (2007). Cadaver decomposition in terrestrial ecosystems. *Naturwissenschaften* 94, 12–24. doi: 10.1007/s00114-006-0159-1

Carter, D. O., Yellowlees, D., and Tibbett, M. (2008). Temperature affects microbial decomposition of cadavers (Rattus rattus) in contrasting soils. *Appl. Soil Ecol.* 40, 129–137. doi: 10.1016/j.apsoil.2008.03.010

Chao, A., Chiu, C. -H., and Jost, L. (2010). Phylogenetic diversity measures based on Hill numbers. *Philos. Transac. R. Soc. B Biol. Sci.* 365, 3599–3609. doi: 10.1098/rstb.2010.0272

Chao, A., Chiu, C. -H., and Jost, L. (2014). Unifying species diversity, phylogenetic diversity, functional diversity, and related similarity and differentiation measures through Hill numbers. *Ann. Rev.* 45, 297–324. doi: 10.1146/annurev-ecolsys-120213-091540

Chimutsa, M., Olakanye, A. O., Thompson, T. J. U., and Ralebitso-Senior, T. K. (2015). Soil fungal community shift evaluation as a potential cadaver decomposition indicator. *Forensic Sci. Int.* 257, 155–159. doi: 10.1016/j.forsciint.2015.08.005

Cobaugh, K. L., Schaeffer, S. M., and DeBruyn, J. M. (2015). Functional and structural succession of soil microbial communities below decomposing human cadavers. *PLoS ONE* 10:e0130201. doi: 10.1371/journal.pone.0130201

Cockle, D. L., and Bell, L. S. (2017). The environmental variables that impact human decomposition in terrestrially exposed contexts within Canada. *Sci. Just.* 57, 107–117. doi: 10.1016/j.scijus.2016.11.001

Connor, M., Baigent, C., and Hansen, E. S. (2018). Testing the use of pigs as human proxies in decomposition studies. *J. Forensic Sci.* 63, 1350–1355. doi: 10.1111/1556-4029.13727

Cordeiro, C., Ordóñez-Mayán, L., Lendoiro, E., Febrero-Bande, M., Vieira, D. N., and Muñoz-Barús, J. I. (2019). A reliable method for estimating the postmortem interval from the biochemistry of the vitreous humor, temperature and body weight. *Forensic Sci. Int.* 295, 157–168. doi: 10.1016/j.forsciint.2018.12.007

Costa, I., Carvalho, F., Magalhães, T., Guedes de Pinho, P., Silvestre, R., and Dinis-Oliveira, R. J. (2015). Promising blood-derived biomarkers for estimation of the postmortem interval. *Toxicol. Res.* 4, 1443–1452. doi: 10.1039/C5TX00209E

Damann, F. E., Williams, D. E., and Layton, A. C. (2015). Potential use of bacterial community succession in decaying human bone for estimating postmortem interval. *J. Forensic Sci.* 60, 844–850. doi: 10.1111/1556-4029.12744

Elfstrand, S., Båth, B., and Mårtensson, A. (2007). Influence of various forms of green manure amendment on soil microbial community composition, enzyme activity and nutrient levels in leek. *Appl. Soil Ecol.* 36, 70–82. doi: 10.1016/j.apsoil.2006.11.001

Finley, S. J., Benbow, M. E., and Javan, G. T. (2015a). Microbial communities associated with human decomposition and their potential use as postmortem clocks. *Int. J. Legal Med.* 129, 623–632. doi: 10.1007/s00414-014-1059-0

Finley, S. J., Benbow, M. E., and Javan, G. T. (2015b). Potential applications of soil microbial ecology and next-generation sequencing in criminal investigations. *Appl. Soil Ecol.* 88, 69–78. doi: 10.1016/j.apsoil.2015.01.001

Finley, S. J., Pechal, J. L., Benbow, M. E., Robertson, B. K., and Javan, G. T. (2016). Microbial signatures of cadaver gravesoil during decomposition. *Microb. Ecol.* 71, 524–529. doi: 10.1007/s00248-015-0725-1

Gaxiola, A., and Armesto, J. J. (2015). Understanding litter decomposition in semiarid ecosystems: linking leaf traits, UV exposure and rainfall variability. *Front. Plant Sci.* 6:140. doi: 10.3389/fpls.2015.00140

Goff, M. L. (2009). "Early Postmortem Changes and Stages of Decomposition", in *Current Concepts in Forensic Entomology*, eds J. Amendt, M. Goff, C. Campobasso, M. Grassberger (Dordrecht: Springer), 1–24. doi: 10.1007/978-1-4020-9684-6_1

Guo, J., Fu, X., Liao, H., Hu, Z., Long, L., and Yan, W. (2016). Potential use of bacterial community succession for estimating post-mortem interval as revealed by high-throughput sequencing. *Nat. Publish. Group* 2015, 1–11. doi: 10.1038/srep24197

Hall, M., and Beiko, R. G. (2018). "16S rRNA gene analysis with QIIME2," in *Microbiome Analysis*, eds R. Beiko, W. Hsiao, and J. Parkinson (New York, NY: Humana Press), 113–129. doi: 10.1007/978-1-4939-8728-3_8

Hart, M. L., Meyer, A., Johnson, P. J., and Ericsson, A. C. (2015). Comparative evaluation of DNA extraction methods from feces of multiple host species for downstream next-generation sequencing. *PLoS ONE* 10:e014333. doi: 10.1371/journal.pone.0143334

Hau, T. C., Hamzah, N. H., Lian, H. H., and Amir Hamzah, S. P. A. (2014). Decomposition process and post mortem changes: review. *Sains Malays.* 43, 1873–1882. doi: 10.17576/jsm-2014-4312-08

Hopkins, D. W., Wiltshire, P. E. J., and Turner, B. D. (2000). Microbial characteristics of soils from graves: an investigation at the interface of soil microbiology and forensic science. *Appl. Soil Ecol.* 14, 283–288. doi: 10.1016/S0929-1393(00)00063-9

Hyde, E. R., Metcalf, J. L., Bucheli, S. R., Lynne, A. M., and Knight, R. (2017). "Microbial communities associated with decomposing corpses", in *Forensic Microbiology*, eds D. O. Carter, J. K. Tomberlin, M. E. Benbow, and J. L. Metcalf (Chichester: John Wiley & Sons Ltd.), 245–273. doi: 10.1002/9781119062585.ch10

Irish, L., Rennie, S. R., Parkes, G. M. B., and Williams, A. (2019). Identification of decomposition volatile organic compounds from surface- deposited and submerged porcine remains. *Sci. Just.* 59, 503–515. doi: 10.1016/j.scijus.2019.03.007

Iyengar, A., and Hadi, S. (2014). Use of non-human DNA analysis in forensic science: a mini review.' *Med. Sci. Law* 54, 41–50. doi: 10.1177/0025802413487522

Kasper, J., Mumm, R., and Ruther, J. (2012). The composition of carcass volatile profiles in relation to storage time and climate conditions. *Forensic Sci. Int.* 223, 64–71. doi: 10.1016/j.forsciint.2012.08.001

Kim, M., Heo, E., Kang, H., and Adams, J. (2013). Changes in oil bacterial community structure with increasing disturbance frequency. *Microb. Ecol.* 66, 171–181. doi: 10.1007/s00248-013-0237-9

Knobel, Z., Ueland, M., Nizio, K. D., Patel, D., and Forbes, S. L. (2018). A comparison of human and pig decomposition rates and odour profiles in an Australian environment. *Aust. J. Forensic Sci.* 51, 557–572. doi: 10.1080/00450618.2018.1439100

Kozich, J. J., Westcott, S. L., Baxter, N. T., Highlander, S. K., and Schloss, P. D. (2013). Development of a dual-index sequencing strategy and curation pipeline for analyzing amplicon sequence data on the miseq illumina sequencing platform. *Appl. Environ. Microbiol.* 79, 5112–5120. doi: 10.1128/AEM.01043-13

Lauber, C. L., Metcalf, J. L., Keepers, K., Ackermann, G., Carter, D. O., and Knight, R. (2014). Vertebrate decomposition is accelerated by soil microbes. *Appl. Environ. Microbiol.* 80, 4920–4929. doi: 10.1128/AEM.00957-14

Litten-Brown, J. C., Corson, A. M., and Clarke, L. (2010). Porcine models for the metabolic syndrome, digestive and bone disorders: a general overview. *Animal* 4, 899–920. doi: 10.1017/S1751731110000200

Macdonald, B. C. T., Farrell, M., Tuomi, S., Barton, P. S., Cunningham, S. A., and Manning, A. D. (2014). Carrion decomposition causes large and lasting effects on soil amino acid and peptide flux. *Soil Biol. Biochem.* 69, 132–140. doi: 10.1016/j.soilbio.2013.10.042

Marín-Roldan, A., Manzoor, S., Moncayo, S., Navarro-Villoslada, F., Izquierdo-Hornillos, R. C., and Caceres, J. O. (2013). Determination of the postmortem interval by Laser Induced Breakdown Spectroscopy using swine skeletal muscles. *Spectrochim. ActaPart B Atomic Spectrosc.* 88, 186–191. doi: 10.1016/j.sab.2013.07.008

Megyesi, M. S., Nawrocki, S. P., and Haskell, N. H. (2005). Using accumulated degree-days to estimate the postmortem interval from decomposed human remains. *J. Forensic Sci.* 50, 618–626. doi: 10.1520/JFS2004017

Melis, C., Selva, N., Teurlings, I., Skarpe, C., Linnell, J. D. C., and Andersen, R. (2007). Soil and vegetation nutrient response to bison carcasses in Białowieza Primeval Forest, Poland. *Ecol. Res.* 22, 807–813. doi: 10.1007/s11284-006-0321-4

Metcalf, J. L., Wegener Parfrey, L., Gonzalez, A., Lauber, C. L., Knights, D., Ackermann, G., et al. (2013). A microbial clock provides an accurate estimate of the postmortem interval in a mouse model system. *Elife* 2:e01104. doi: 10.7554/eLife.01104

Metcalf, J. L., Xu, Z. Z., Weiss, S., Lax, S., Van Treuren, W., Hyde, E. R., et al. (2016). Microbial community assembly and metabolic function during mammalian corpse decomposition. *Science* 351, 158–162. doi: 10.1126/science.aad2646

Muyzer, G., De Waal, E. C., and Uitterlinden, A. G. (1993). Profiling of complex microbial populations by denaturing gradient gel electrophoresis analysis of polymerase chain reaction-amplified genes coding for 16S rRNA. *Appl. Environ. Microbiol.* 59, 695–700. doi: 10.1128/AEM.59.3.695-700.1993

Nearing, J. T., Douglas, G. M., Comeau, A. M., and Langille, M. G. I. (2018). Denoising the Denoisers : an independent evaluation of microbiome sequence error-correction approaches. *PeerJ.* 6:e5364. doi: 10.7717/peerj.5364

Nolan, A.-N., Mead, R. J., Maker, G., Bringans, S., Chapman, B., and Speers, S. J. (2019). Examination of the temporal variation of peptide content in decomposition fluid under controlled conditions using pigs as human substitutes. *Forensic Sci. Int.* 298, 161–168. doi: 10.1016/j.forsciint.2019.02.048

Olakanye, A. O., Nelson, A., and Ralebitso-Senior, T. K. (2017). A comparative *in situ* decomposition study using still born piglets and leaf litter from a deciduous forest. *Forensic Sci. Int.* 276, 85–92. doi: 10.1016/j.forsciint.2017.04.024

Olakanye, A. O., and Ralebitso-Senior, T. K. (2018). Soil metabarcoding identifies season indicators and differentiators of pig and *Agrostis/Festuca* spp. decomposition. *Forensic Sci. Int.* 288, 53–58. doi: 10.1016/j.forsciint.2018.04.015

Olakanye, A. O., Thompson, T., and Ralebitso-Senior, T. K. (2015). Shifts in soil biodiversity - a forensic comparison between *Sus scrofa domesticus* and vegetation decomposition. *Sci. Just.* 55, 402–407. doi: 10.1016/j.scijus.2015.07.004

Oliveira, M., and Amorim, A. (2018). Microbial forensics: new breakthroughs and future prospects. *Appl. Microbiol. Biotechnol.* 102, 10377–10391. doi: 10.1007/s00253-018-9414-6

Ortmann, J., Markwerth, P., and Madea, B. (2016). Precision of estimating the time since death by vitreous potassium - comparison of 5 different equations. *Forensic Sci. Int.* 269, 1–7. doi: 10.1016/j.forsciint.2016.10.005

Pechal, J. L., Crippen, T. L., Benbow, M. E., Tarone, A. M., Dowd, S., and Tomberlin, J. K. (2014). The potential use of bacterial community succession in forensics as described by high throughput metagenomic sequencing. *Int. J. Legal Med.* 128, 193–205. doi: 10.1007/s00414-013-0872-1

Pechal, J. L., Crippen, T. L., Tarone, A. M., Lewis, A. J., Tomberlin, J. K., and Benbow, M. E. (2013). Microbial community functional change during vertebrate carrion decomposition. *PLoS ONE* 8:e79035. doi: 10.1371/journal.pone.0079035

Pechal, J. L., Schmidt, C. J., Jordan, H. R., and Benbow, M. E. (2018). A large-scale survey of the postmortem human microbiome, and its potential to provide insight into the living health condition. *Sci. Rep.* 8, 1–15. doi: 10.1038/s41598-018-23989-w

Pinheiro, J. (2006). "Decay process of a cadaver," in A. Schmitt, E. Cunha, and J. Pinheiro, eds. *Forensic Anthropology and Medicine, Complementary Sciences From Recovery to Cause of Death* (New Jersey, NJ: Humana Press Inc.), 85–116.

Procopio, N., Ghignone, S., Williams, A., Chamberlain, A., Mello, A., and Buckley, M. (2019). Metabarcoding to investigate changes in soil microbial communities within forensic burial contexts. *Forensic Sci. Int. Genet.* 39, 73–85. doi: 10.1016/j.fsigen.2018.12.002

Ralebitso-Senior, T. K. (ed.). (2018). "Summary: an assessment of achievements, limitations, and potential of forensic ecogenomics," in *Forensic Ecogenomics: The Application of Microbial Ecology Analyses in Forensic Contexts,* (London: Academic Press), 211–234. doi: 10.1016/B978-0-12-809360-3.00009-6

Ralebitso-Senior, T. K., and Olakanye, A. O. (2018). "General Introduction: Method applications at the interface of microbial ecology and forensic investigation," in *Forensic Ecogenomics: The Application of Microbial Ecology Analyses in Forensic Contexts,* ed T. K. Ralebitso-Senior (London: Academic Press), 1–35. doi: 10.1016/B978-0-12-809360-3.00001-1

Ralebitso-Senior, T. K., and Pyle, M. K. P. (2018). "Implications of the investigative animal model," in *Forensic Ecogenomics: The Application of Microbial Ecology Analyses in Forensic Contexts,* ed T. K. Ralebitso-Senior (London: Academic Press), 87–111. doi: 10.1016/B978-0-12-809360-3.00004-7

Ravansari, R., and Lemke, L. D. (2018). Portable X-ray Fluorescence trace metal measurement in organic rich soils: pXRF response as a function of organic matter fraction. *Geoderma* 319, 175–184. doi: 10.1016/j.geoderma.2018.01.011

Ritz, K., McNicol, J. W., Nunan, N., Grayston, S., Millard, P., Atkinson, D., et al. (2004). Spatial structure in soil chemical and microbiological properties in an upland grassland. *FEMS Microbiol. Ecol.* 49, 191–205. doi: 10.1016/j.femsec.2004.03.005

Schaldach, C. M., Bench, G., DeYoreo, J. J., Esposito, T., Fergenson, D. P., Ferreira, J., et al. (2005). "Non-DNA methods for biological signatures," in *Microbial Forensics*, B. Budowle, S. E. Schutzer, and R. G. Breeze (Cambridge, MA: Elsevier), 251–294. doi: 10.1016/B978-012088483-4/50016-0

Shand, C. A., and Wendler, R. (2014). Portable X-ray Fluorescence analysis of mineral and organic soils and the influence of organic matter. *J. Geochem. Explorat.* 143, 31–42. doi: 10.1016/j.gexplo.2014.03.005

Shean, B. S., Messinger, L., and Papworth, M. (1993). Observations of differential decomposition on sun exposed v. shaded pig carrion in coastal Washington State. *J. Forensic Sci.* 38, 938–949.

Shirley, N. R., Wilson, R. J., and Jantz, L. M. (2011). Cadaver use at the University of Tennessee's Anthropological Research Facility. *Clin. Anat.* 24, 372–380. doi: 10.1002/ca.21154

Siddhamsetty, A. K., Verma, S. K., Kohli, A., Verma, A., Puri, D., and Singh, A. (2014). Exploring time of death from potassium, sodium, chloride, glucose and calcium analysis of postmortem synovial fluid in semi arid climate. *J. Forensic Leg. Med.* 28, 11–14. doi: 10.1016/j.jflm.2014.09.004

Singh, B., Minick, K. J., Strickland, M. S., Wickings, K. G., Crippen, T. L., Tarone, A. M., et al. (2018). Temporal and spatial impact of human cadaver decomposition on soil bacterial and arthropod community structure and function. *Front. Microbiol.* 8:2616. doi: 10.3389/fmicb.2017.02616

Statheropoulos, M., Agapiou, A., Zorba, E., Mikedi, K., Karma, S., Pallis, G. C., et al. (2011). Combined chemical and optical methods for monitoring the early decay stages of surrogate human models. *Forensic Sci. Int.* 210, 154–163. doi: 10.1016/j.forsciint.2011.02.023

Stokes, K. L., Forbes, S. L., and Tibbett, M. (2009). Freezing skeletal muscle tissue does not affect its decomposition in soil: evidence from temporal changes in tissue mass, microbial activity and soil chemistry based on excised samples. *Forensic Sci. Int.* 183, 6–13. doi: 10.1016/j.forsciint.2008.08.013

Stokes, K. L., Forbes, S. L., and Tibbett, M. (2013). Human versus animal: contrasting decomposition dynamics of mammalian analogues in experimental taphonomy. *J. Forensic Sci.* 58, 583–591. doi: 10.1111/1556-4029.12115

Sutherland, A., Myburgh, J., Steyn, M., and Becker, P. J. J. (2013). The effect of body size on the rate of decomposition in a temperate region of South Africa'. *Forensic Sci. Int.* 231, 257–262. doi: 10.1016/j.forsciint.2013.05.035

Szelecz, I., Koenig, I., Seppey, C. V. W., Le Bayon, R. C., and Mitchell, E. A. D. (2018). Soil chemistry changes beneath decomposing cadavers over a one-year period. *Forensic Sci. Int.* 286, 155–165. doi: 10.1016/j.forsciint.2018.02.031

Torsvik, V. L. (1980). Isolation of bacterial DNA from soil. *Soil Biol. Biochem.* 12, 15–21. doi: 10.1016/0038-0717(80)90097-8

Tumer, A. R., Karacaoglu, E., Namli, A., Keten, A., Farasat, S., Akcan, R., et al. (2013). Effects of different types of soil on decomposition: an experimental study. *Leg. Med.* 15, 149–156. doi: 10.1016/j.legalmed.2012.11.003

Vass, A. A., Bass, W. M., Wolt, J. D., Foss, J. E., and Ammons, J. T. (1992). Time since death determinations of human cadavers using soil solution. *J. Forensic Sci.* 37, 1236–1253. doi: 10.1520/JFS13311J

Voss, S. C., Cook, D. F., and Dadour, I. R. (2011). Decomposition and insect succession of clothed and unclothed carcasses in Western Australia. *Forensic Sci. Int.* 211, 67–75. doi: 10.1016/j.forsciint.2011.04.018

Wang, J., Liu, L., Wang, X., and Chen, Y. (2015). The interaction between abiotic photodegradation and microbial decomposition under ultraviolet radiation. *Glob. Chang. Biol.* 21, 2095–2104. doi: 10.1111/gcb.12812

Wang, M., Zheng, Q., Shen, Q., and Guo, S. (2013). The critical role of potassium in plant stress response. *Int. J. Mol. Sci.* 14, 7370–7390. doi: 10.3390/ijms14047370

White, T., Bruns, T., and Lee, S., (1990). "Amplification and direct sequencing of fungal ribosomal RNA genes for phylogenetics," in *PCR Protocols: A Guide to Methods and Applications*, eds M. A. Innis, D. H. Gelfand, J. J. Sninsky, and T. J. White (Cambridge, MA: Academic Press) Vol. 18, 315–322.

Williams, A., Rogers, C. J., and Cassella, J. P. (2019). Why does the UK need a Human Taphonomy Facility? *Forensic Sci. Int.* 296, 74–79. doi: 10.1016/j.forsciint.2019.01.010

Williams, R., Taylor, G., and Orr, C. (2020). pXRF method development for elemental analysis of archaeological soil. *Archaeometry* 62, 1–19. doi: 10.1111/arcm.12583

Zhou, W., and Bian, Y. (2018). Thanatomicrobiome composition profiling as a tool for forensic investigation. *Forensic Sci. Res.* 3, 105–110. doi: 10.1080/20961790.2018.1466430

Conflict of Interest: The authors declare that the research was conducted in the absence of any commercial or financial relationships that could be construed as a potential conflict of interest.

frontiers in Microbiology

ORIGINAL RESEARCH
published: 31 May 2021
doi: 10.3389/fmicb.2021.649312

Characterising Post-mortem Bacterial Translocation Under Clinical Conditions Using 16S rRNA Gene Sequencing in Two Animal Models

Lily Gates[1], Nigel J. Klein[1], Neil J. Sebire[2] and Dagmar G. Alber[1]*

[1] Department of Infection, Immunity and Inflammation, University College London Institute of Child Health, London, United Kingdom, [2] Histopathology, Great Ormond Street Hospital, London, United Kingdom

OPEN ACCESS

Edited by:
T. Komang Ralebitso-Senior, Liverpool John Moores University, United Kingdom

Reviewed by:
Marta Cohen, Sheffield Children's Hospital, United Kingdom
Gulnaz T. Javan, Alabama State University, United States

***Correspondence:**
Lily Gates
lily.gates.14@ucl.ac.uk

Specialty section:
This article was submitted to Systems Microbiology, a section of the journal Frontiers in Microbiology

Received: *04 January 2021*
Accepted: *29 April 2021*
Published: *31 May 2021*

Citation:
Gates L, Klein NJ, Sebire NJ and Alber DG (2021) Characterising Post-mortem Bacterial Translocation Under Clinical Conditions Using 16S rRNA Gene Sequencing in Two Animal Models. Front. Microbiol. 12:649312. doi: 10.3389/fmicb.2021.649312

Sudden unexpected death in infancy (SUDI) is the sudden and unexpected death of an apparently healthy infant occurring within the first year of life where the cause is not immediately obvious. It is believed that a proportion of unexplained infant deaths are due to an infection that remains undiagnosed. The interpretation of post-mortem microbiology results is difficult due to the potential false-positives, a source of which is post-mortem bacterial translocation. Post-mortem bacterial translocation is the spread of viable bacteria from highly colonised sites to extra-intestinal tissues. We hypothesise that although post-mortem bacterial translocation occurs, when carcasses are kept under controlled routine clinical conditions it is not extensive and can be defined using 16S rRNA gene sequencing. With this knowledge, implementation of the 16S rRNA gene sequencing technique into routine clinical diagnostics would allow a more reliable retrospective diagnosis of ante-mortem infection. Therefore, the aim of this study was to establish the extent of post-mortem bacterial translocation in two animal models to establish a baseline sequencing signal for the post-mortem process. To do this we used 16S rRNA gene sequencing in two animal models over a 2 week period to investigate (1) the bacterial community succession in regions of high bacterial colonisation, and (2) the bacterial presence in visceral tissues routinely sampled during autopsy for microbiological investigation. We found no evidence for significant and consistent post-mortem bacterial translocation in the mouse model. Although bacteria were detected in tissues in the piglet model, we did not find significant and consistent evidence for post-mortem bacterial translocation from the gastrointestinal tract or nasal cavity. These data do not support the concept of significant post-mortem translocation as part of the normal post-mortem process.

Keywords: post-mortem, bacterial translocation, 16S sequencing, SUDI, SIDS

INTRODUCTION

Sudden unexpected death in infancy (SUDI) is the sudden death of an apparently healthy infant occurring within the first year of life where the cause is not immediately obvious. SUDI is the leading cause of infant mortality in the developed world (Spencer and Logan, 2004; Ndu, 2016). Despite extensive post-mortem (PM) investigations into the cause of death, around 40% of SUDI cases remain unexplained and are subsequently registered as Sudden Infant Death Syndrome (SIDS) (Office for National Statistics, 2017). Infection is one of the leading causes of SUDI (Weber et al., 2008; Pryce et al., 2011b; Goldwater, 2017) and it has been hypothesised that infection is in fact responsible for a larger proportion of SUDI, but these infections remain undetected due to limited diagnostic power using current methodologies (Weber et al., 2008; Goldwater, 2009, 2017).

In diagnostic laboratories worldwide, classical bacterial culture is the gold-standard method used to identify potential causative organisms as part of routine clinical autopsy investigation (Kennedy, 2016). However, these methods are associated with many limitations, such as an increased likelihood of identifying readily culturable bacteria (Yu et al., 2019), the inability to culture all bacterial species under laboratory conditions (Hiergeist et al., 2015; Overmann et al., 2017), long incubation periods (Ombelet et al., 2019), skilled persons or high-cost equipment for bacterial identification, and the curation of only qualitative results (Rhoads et al., 2012). The interpretation of PM microbiology results generated in this way proves difficult, particularly in cases of SUDI where histological findings are often unclear (Pryce et al., 2011b; Palmiere et al., 2016).

In recent years, these caveats have encouraged the use of alternative molecular techniques, such as quantitative PCR (qPCR) targeting known pathogenic bacteria, or the sequencing of the bacterial 16S rRNA gene. The 16S rRNA gene is present in all bacterial species and each has a unique sequence. These sequences act as a bacterial fingerprint to enable bacterial identification by comparison to curated 16S reference databases, such as Greengenes, SILVA, and RDP (Wang et al., 2007; McDonald et al., 2012; Yilmaz et al., 2014). This method allows for a more detailed, unbiased determination of the bacteria present within tissues. This technique has been implemented throughout forensic literature, with particular interest placed on the use of the PM microbiome, commonly referred to as the thanatomicrobiome, as a microbial clock to determine the post-mortem interval (PMI) in advanced phases of decomposition (Javan et al., 2019; Roy et al., 2021). Still, these methods have not been widely incorporated into routine PM investigation, as their performance and interpretation remain uncertain in this setting (Fernández-Rodríguez et al., 2019).

Apparent false-positive PM microbiology results can arise due to the natural putrefaction process of the body or contamination during sample collection at autopsy (Morris et al., 2006; Riedel, 2014; Mesli et al., 2017). When positive cultures arise from visceral tissues that are believed to be sterile in life, it is often difficult to determine the relevance of such results, certainly without histological evidence of infection (Goldwater, 2009; Bryant and Sebire, 2018). PM bacterial translocation is defined as the migration of viable bacteria from highly colonised bodily sites, such as the gastrointestinal (GI) tract, to extra-intestinal tissues following death (Mesli et al., 2017).

Few studies have investigated the phenomenon of PM bacterial translocation, and those that have, typically investigate bacterial invasion under ambient conditions. Heimesaat et al. (2012) investigated PM translocation in a mouse model kept under ambient conditions using conventional bacterial culture. Results from this study showed that extra-intestinal sites including cardiac blood, kidney, liver, mesenteric lymph nodes, and spleen were invaded by intestinal bacteria as soon as 5 minutes PM (Heimesaat et al., 2012). Another study tracked fluorescently labelled *Staphylococcus aureus* following intranasal inoculation of a mouse model and found that these bacteria could be detected in all organs 1 hour PM (Burcham et al., 2016). Again, this animal model was kept under ambient conditions following sacrifice.

There is a current lack of understanding of the PM bacterial translocation process in a clinical setting where bodies are refrigerated between death and autopsy (Morris et al., 2006; Weber et al., 2010; Palmiere et al., 2016; Mesli et al., 2017). This lack of knowledge presents a greater problem when interpreting PM microbiological results during clinical autopsy and poses the question, '*is a positive result due to natural decomposition and translocation of bacterial flora or a sign of fulminant ante-mortem infection?*'. Interpretation of results requires professionals to determine whether a positive finding is a contaminant or causative of the fatal event (Balzan et al., 2007). Unlike contamination during sampling, putrefaction is a natural process that can be limited, but not completely controlled (Morris et al., 2006). Routine procedures, such as refrigeration of the body soon after death aims to limit decomposition, but the extent to which this prevents bacterial translocation has yet to be studied.

To our knowledge, PM bacterial translocation has not yet been characterised under conditions mimicking standard clinical practice using contemporary molecular approaches. Essential to the interpretation of PM microbiological results of SUDI, is a clear understanding of the natural bacterial translocation that occurs PM in this clinical setting. We hypothesise that although PM bacterial translocation occurs, it is not extensive and can be defined using 16S rRNA gene sequencing. With this knowledge, implementation of this technique into routine clinical diagnostics would then enable a more reliable retrospective diagnosis of ante-mortem infection. Therefore, the aim of this study was to establish the extent of PM bacterial translocation in two animal models to establish a baseline sequencing signal for the PM process.

We report the use of 16S rRNA gene sequencing in two separate animal models; a mouse model for ease of sampling, followed by a piglet model given its anatomical similarities to humans and ability to perform repeated sampling, to investigate bacterial presence in visceral tissues routinely sampled during autopsy for microbiological investigation. Using these animal models allowed for controlled conditions and multiple sampling time points over the study starting from time of death. We aimed to investigate (1) the bacterial community succession in regions of high bacterial colonisation, and (2) the translocation of these microbes to extra-intestinal tissue over a 2-week period PM.

MATERIALS AND METHODS

Sample Acquisition

Nine-week old C57BL/6 female mice (n = 15) that had been housed for 6 days to allow for acclimatisation and standardisation of the microbiota for another study were culled on day 0 according to Schedule 1 of the Animals (Scientific Procedures) Act 1986 and carcasses were donated to this study. Culled mice were placed into airtight freezer bags and kept on wet ice until the first sample was collected, no longer than 30 minutes PM. Tissue and blood samples were collected from one mouse per cage (C) on the following days (D) PM: D0, D3, D7, D10, and D14 (three mice sampled per day) in a sterile manner to limit contamination. Tissue samples were collected in the following order: cardiac blood, heart, lung, liver, spleen, and the lower GI tract. Mice were stored in airtight freezer bags at 4°C until sampling.

Three 1-month-old Welsh piglet carcasses were obtained from the Royal Veterinary College, London (n = 1) and a local farm (n = 2). The piglets used in this study were of a pre-weaning age. Sampling was initiated no more than 3 hours PM. Samples were obtained using sterile 16-gauge Quick-Core Biopsy Needles (Cook Medical, Ireland) on D0, D3, D7, D10, and D14 PM. On D14 PM, carcasses from the local farm were dissected using sterile scalpels. Nasal (left and right nares) and rectal swabs were obtained using polyurethane cellular foam dry swabs (MWE Medical Wire). Samples were immediately snap frozen and stored at −80°C until further analysis. Tissue type confirmation was performed using tissue-specific reverse transcriptase PCR as described in the **Supplementary Methods 1**. Piglet carcasses were stored in infant body bags at 4°C in between sampling time points.

DNA Extraction and Sequencing

DNA was extracted using the QIAamp DNA Mini Kit (Qiagen) as per the manufacturers protocol with an initial lysing step using Ribolysing Matrix B (MP Biomedicals) and bead-beating for 1 minute at 50 oscillations/second. DNA templates were amplified for sequencing using the Taq PCR Core Kit (Qiagen) and region-specific primers targeting the V3-V4 region of the 16S rRNA gene with adapters and indexes attached as previously described (Rosser et al., 2020). This method has been previously validated in-house using spike-in experiments whereby Gram-positive and Gram-negative bacteria were added to various tissue types to ensure recovery of the 16S rRNA gene (data not published). A Microbial Community Standard (Zymo Research) of known bacterial composition was used to assess bias and sequencing error rates. A post-PCR concentration of <0.5 ng/μL was considered negative. Tissue samples were amplified thrice before being considered negative. Positive samples were normalised to the desired library concentration using nuclease-free water, pooled, and sequenced on the MiSeq platform using a 500-v2 cartridge (Illumina).

Quantitative qPCR for Enterobacteriaceae and Enterococcus

See **Supplementary Methods 2, 3**.

Sequencing Data Processing and Statistical Analysis

Sequencing data was demultiplexed on the MiSeq platform. Paired-end reads were merged using FLASH (version 1.2.11) (Magoč and Salzberg, 2011) and quality filtered using VSEARCH. Taxonomic classification was carried out on the Mothur platform (version 1.44.0) (Schloss et al., 2009) using the RDP reference database with a similarity cut-off of 97%. Data was analysed using R Studio (version 1.2.5001) (RStudio Team, 2020). Samples with sequencing reads within two standard deviations from the mean number of reads within the extraction control samples were removed. The mock community was assessed for any unexpected spurious OTUs and abundances were used as a cut-off for false-positive sequence generation.

Statistical analysis was performed using R (version 3.6.3) (R Core Team, 2019) on R Studio (RStudio Team, 2020). Rarefaction curves were generated to assess species richness and appropriate random subsampling thresholds using the *vegan* package (Oksanen et al., 2019). Mouse GI tract samples were randomly subsampled at 20,000 reads. Piglet nasal and rectal swabs were randomly subsampled at 100,000 and 14,000 reads, respectively. Two samples (nasal swab P3_D10_right and rectal swab P2_D3) were excluded from downstream analysis due to low quality sequencing reads. Differences in the total number of generated sequencing reads that passed quality filtering were statistically compared between sample type and organism sampled using an independent t-test. Piglet tissues were subsampled to 500 reads prior to beta-diversity calculation. Changes in community structure in the piglet tissues (beta-diversity) was assessed with a non-metric multi-dimensional scaling (NMDS) plot based on Bray-Curtis dissimilarities between the samples. The effects of sampling day on bacterial community changes were measured by performing a permutational multivariate analysis of variance (PERMANOVA) test on Bray-Curtis dissimilarity measures using the *phyloseq* package (McMurdie and Holmes, 2013). A Kruskal-Wallis test by ranks was performed on communities at different time points to compare taxonomic differences at family level classification using the *stats* package (R Core Team, 2019). For statistical tests a $P < 0.05$ was considered significant. Figures were generated using the *ggplot2* package (Hadley, 2016) and Graphpad Prism (version 5) (Motulsky, 2007).

RESULTS

Mouse Gut Microbiota Is Relatively Stable Over the Study Period

The gut microbiome in all mice sampled at each time point were similar as expected due to their inbred nature and controlled housing environment and diet prior to this study. Based on the Bray-Curtis distances calculated for each community, there was no significant difference between communities from each mouse (P = 0.07). **Figure 1** shows the relative abundance of the top 10 bacterial families at each time point (plots for individual samples are available in **Supplementary Figure 1**).

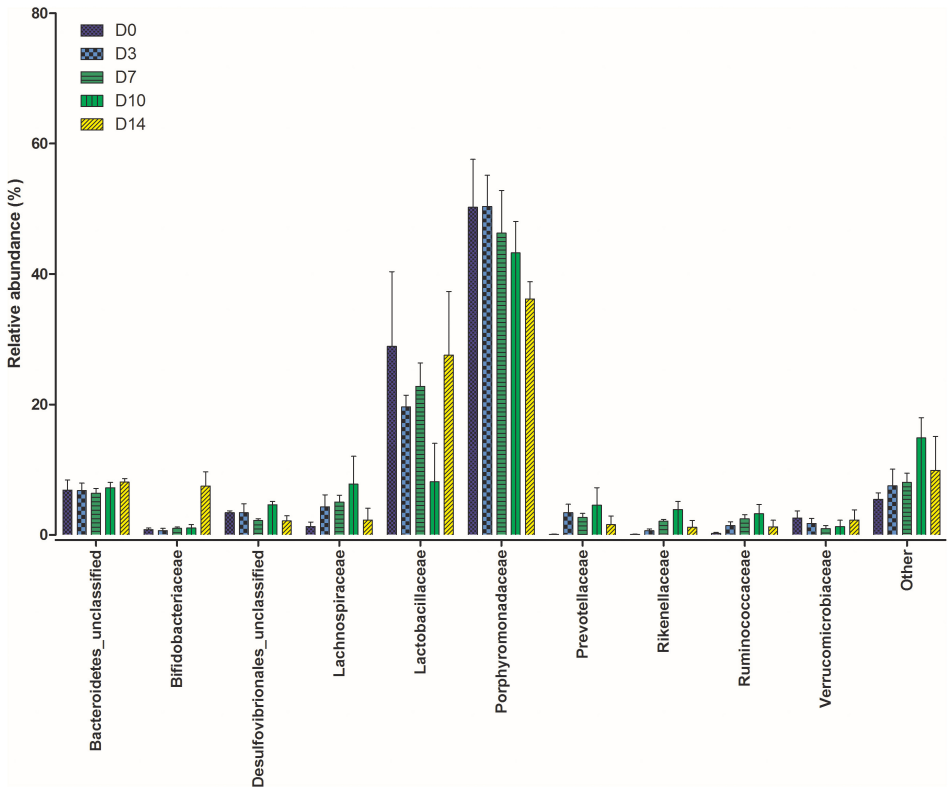

FIGURE 1 | Shifts in the relative abundance of the top 10 bacterial families present within the mouse gastrointestinal (GI) tract samples collected at five time points post mortem.

The calculated beta-diversity at each time point was compared to that of D0 to track microbiota changes over time. The first 7 days PM showed no significant changes in the gut microbiome (P = 0.096). Significant changes were, however, observed in the communities on D10 (P = 0.007) and D14 (P = 0.037) when compared to D0. To investigate bacterial families responsible for these differences a Kruskal-Wallis by rank test was performed. Dominant families did not experience any changes in rank over the study period. Significant differences were observed in Bifidobacteriaceae (P = 0.013) and Rikenellaceae (P = 0.041). At each time point from D0 to D10 Bifidobacteriaceae represented less than 1% of the total bacterial community. This was followed by a sharp increase on D14 where their relative abundance increased to 7.2%. Rikenellaceae was also present at less than 1% in the starting community. There was a steady increase to D10 where the relative abundance peaked at an average of 3.9%, which decreased again at D14 where it represented just 0.6% of the community.

Post-mortem Bacterial Translocation Could Not Be Detected in the Mouse Model

Of the 75 mouse tissue samples collected, only 4 were considered as positive for the 16S rRNA gene using the quality filtering threshold described in the methods section (positive samples are detailed in **Supplementary Table 1**). The positive tissue samples had an average of 3,267 sequencing reads (range 642–10,839). The number of sequencing reads in the tissue samples were significantly lower than those in the GI tract samples (P = 0.004). The number of successfully sequenced samples did not increase with time PM.

Operational taxonomic units (OTUs) detected in each tissue sample were cross-checked with OTUs identified in the GI tract to assess the potential translocation of bacteria from this site. Two of the four samples (C1_D3_Liver and C2_D14_Blood) did not share any OTUs with the GI tract samples collected from the same mouse at the same time point. Sample C2_D3_Liver shared all OTUs with the corresponding GI tract sample and contained bacterial families including Enterobacteriaceae, Lactobacilliaceae, and Porphyromonadaceae. These families were of high abundance in the GI tract. Sample C2_D10_Heart shared 4 of 11 OTUs identified with its corresponding GI tract sample.

Three of the four tissue samples were dominated by either Enterobacteriaceae or Enterococcus, which represented >45% of each sample. To identify whether these were truly positive reads, a specific qPCR was performed. These bacteria were identified in three gut samples from cage 2, at low relative abundances between 5 and 11%. All tissues were negative for Enterococcus. Two of the three tissues were positive for Enterobacteriaceae, but generated a very late signal with a cyclic threshold (CT) value >34 compared to the positive controls which gave an average CT value of 27.

No Trends Observed Amongst Piglets in the Rectal Swabs

The microbes within the rectal cavities were significantly different in each piglet as expected due to differences in genetics, diet and environmental conditions (P = 0.018). The relative abundance of bacterial families in each piglet are shown in **Figure 2**. The rectal swab communities progressed in a different manner over the 2-week period in each piglet. In P1, the bacterial community in the rectal cavity remained relatively stable for the first 10 days PM. On D14, an increase in Pseudomonadaceae and Moraxellaceae was observed. The dominant families in the rectal cavities in P2 and P3 included Enterobacteriaceae and Moraxellaceae. As time progressed the Bacteroidaceae and Veillonellaceae families increased in relative abundance.

Nasal Swabs Were Progressively Dominated by *Pseudomonas* spp.

Despite differences in early communities, nasal swab communities from all three piglets progressed in a similar fashion (**Figure 3**). On D0, the main bacterial families present in the nasal swabs were Enterobacteriaceae, Flavobacteriaceae, Moraxellaceae, and Pasteruellaceae. From D3 to D14, communities in different piglets began to converge and at both D10 and D14 there was no significant difference between all three piglets (P = 0.33). The convergence was largely due to the increase of Pseudomonadaceae, which began to emerge on D7 and increased in abundance until the end of the study period. On D14 PM, Pseudomonadaceae represented >90% of bacteria within the nasal cavity of each piglet.

Potential PM Bacterial Translocation Is Observed in the Piglet Model

As the piglet tissue samples were obtained using needle biopsies in a blind fashion the tissue type was confirmed using a reverse-transcriptase qPCR (successful sampling shown in **Supplementary Table 2**). The success rate of sampling the heart, the liver, and the lung in P1, P2 and P3 was 87% (13/15), 93% (14/15), and 87% (13/15), respectively (total of 40 tissue sample successfully collected). Sequencing data were obtained for 29 of these 40 tissue samples. Sequencing reads in the piglet tissues were higher than those obtained from the mouse tissues with an average of 30,960 reads from tissues across all three piglets. These read numbers were, however, significantly lower than those found in the nasal and rectal swabs (P = 0.0001). Variation amongst the reads obtained from each piglet was observed, but there were no associations with sampling day or tissue type.

Bacterial families identified in the piglet tissues were assessed using beta-diversity measures. **Figure 4** shows an NMDS plot based on calculated Bray-Curtis distances of beta-diversity. Each point on the NMDS plot represents a single tissue sample. This plot shows that the bacterial communities cluster based on the piglet they were sampled from rather than time-point or sample type. The dominant bacterial families were shared amongst tissues from the same piglet. Tissues collected from P1 were mainly dominated by Clostridiaceae_1 (7/10), P2 tissues were dominated by Moraxellaceae (4/10) and P3 tissues by Lactobacilliaceae (4/9).

As the aim of this study was to determine whether translocation occurs from sites of high colonisation to otherwise sterile tissues, OTUs present within the tissues were cross-checked with those identified in nasal and rectal swabs from

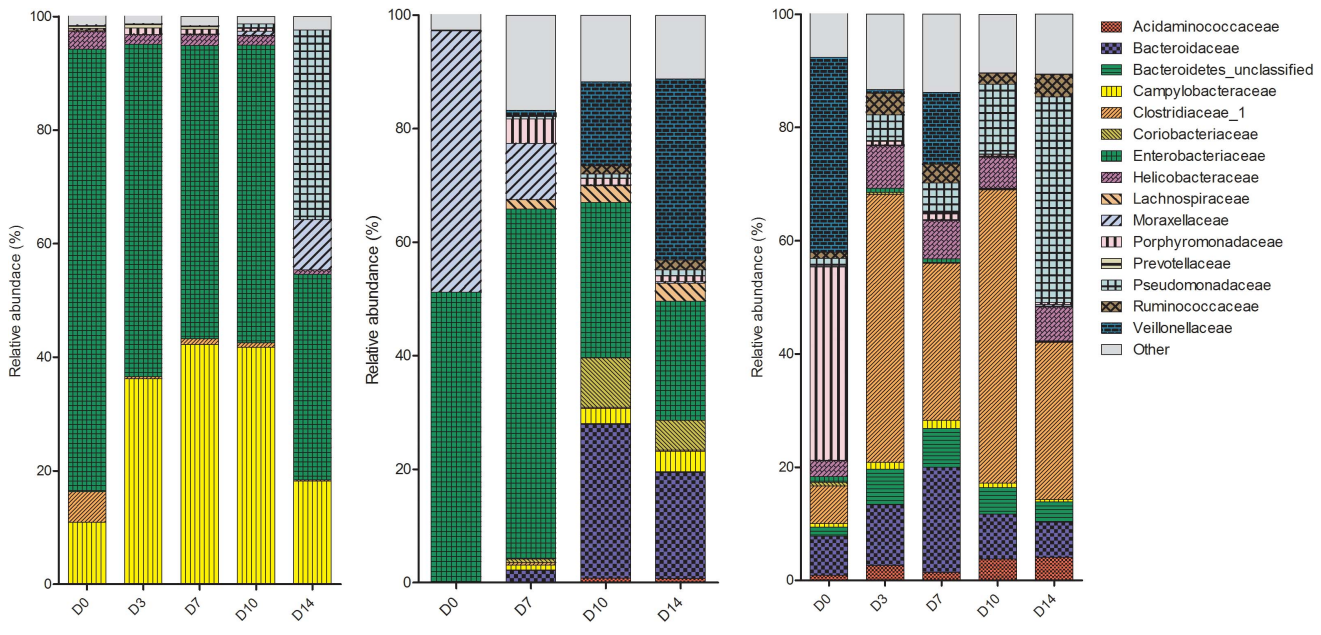

FIGURE 2 | Shifts in the relative abundance of the top 10 bacterial families in piglet rectal swabs collected from piglet 1, piglet 2, and piglet 3 (left to right). The x-axis describes the day on which the sample was collected (D0, D3, D7, D10 or D14).

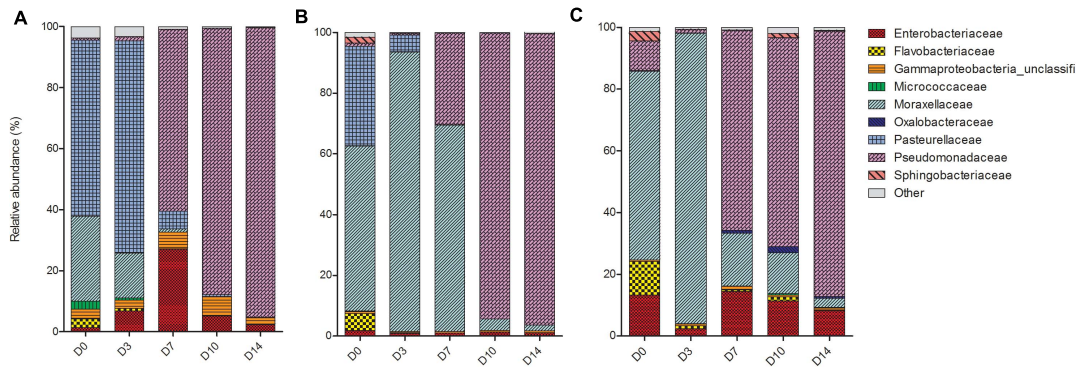

FIGURE 3 | Shifts in the relative abundance of the top 10 bacterial families in piglet nasal swabs collected from **(A)** piglet 1, **(B)** piglet 2, and **(C)** piglet 3. The x-axis describes the day on which the sample was collected (D0, D3, D7, D10, D14).

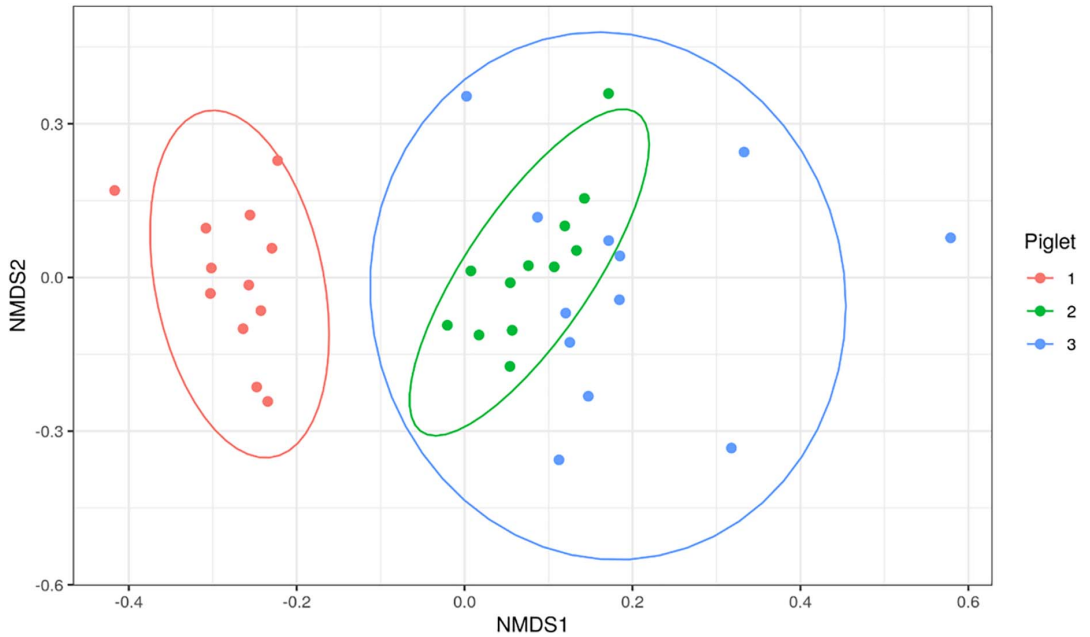

FIGURE 4 | Non-metric multi-dimensional scaling (NMDS) plot based on Bray-Curtis dissimilarity index of piglet tissue samples. Each point represents an individual piglet tissue sample. Ellipses are based on 95% confidence intervals. Colours represent the piglet from which the sample was collected.

the same piglet to identify if this was a possible source of translocation. Of the 29 sequenced samples, only 10/29 (34%) shared an OTU that was present at relative abundances >1% in the rectal swabs (**Supplementary Figure 2A**). Of the 10 samples that shared at least one OTU with the rectal swabs, the dominant OTU in 3/10 (30%) of the tissue samples was found in the rectal swabs. In comparison to the nasal swabs, 8/29 (28%) of the tissue samples shared at least one OTU present >1% in the nasal cavity, of which 1/8 (13%) shared their dominant OTU.

DISCUSSION

The aim of this study was to establish the extent of PM bacterial translocation in two animal models to establish a baseline sequencing signal for the PM process. This study provides insight into the community succession within the mouse GI tract, and the piglet nasal and rectal cavities. Our results also demonstrate that significant and consistent PM bacterial translocation was not observed in the mouse model, shown by broad-range 16S rRNA gene sequencing and confirmed with more specific, bacteria-targeted qPCR. Although bacteria were detected amongst tissues in the piglet model, we did not find evidence for true bacterial translocation from the GI tract or nasal cavity using these techniques. These data do therefore not support the concept of significant PM translocation as part of the normal PM process and demonstrate that the 16S rRNA gene sequencing technique could prove useful in diagnosis of infection PM.

Though the mouse gut microbiome was relatively stable over the first 7 days, significant changes were observed in Bifidobacteriaceae and Ruminococcaceae families at latter time points, increasing in abundance over time. These bacteria are known anaerobes, which explains their proliferation at a time when oxygen sources are low, and nutrients limited. The very slight changes in the microbiome under these conditions demonstrate the ability of the refrigeration to slow the decay process. This is in line with a study performed by Tuomisto et al. (2013) that used real-time qPCR to track six bacterial families in the stool of human autopsy cases finding no significant changes up to 5 days PM. A study that aimed to compare the thanatomicrobiome of internal organs of a rabbit model found no significant differences in the bacterial communities residing in the cecum up to 48 h PM when stored at 4°C (Lawrence et al., 2019). The bacterial communities present in the rectal cavity of the piglets showed inter-piglet variation reflecting observations in humans where the microbiome between individuals differs depending on a number of factors including genetics, age, diet, and environment (Hasan and Yang, 2019) and no trends were observed, likely due to our low sample size. The bacterial communities in P1 remained stable over the first 10 days PM reflecting results of our mouse study. In P2, although a change was observed between communities within the first 3 days there is arguably little difference observed over the remainder of the study period. The biggest shift was observed in Veillonellaceae, which are a bacterial family composed of anaerobic and microaerophilic bacteria. Their ability to thrive in such conditions explains their proliferation as time progresses. Microbial succession has been shown in various studies to be directly influenced by oxygen availability, with a longer PMI associated with a shift from aerobic to anaerobic bacteria at the completion of the bloat stage of decomposition (Hyde et al., 2013, 2015; Metcalf et al., 2013; Pechal et al., 2014; Lawrence et al., 2019).

We observed an exponential increase of Pseudomonadaceae members within the nasal cavity of the piglets as time PM increased. Studies have identified Pseudomonadaceae on porcine carcasses and are associated with food spoilage, given their ability to proliferate at low temperatures (Raposo et al., 2016). It is also interesting to note that in a recent study by Hurtado et al. (2018) who investigated the impact of PMI on microbiological results found an increase of Pseudomonas genus identification when using molecular analysis.

The mouse model used in this study failed to demonstrate ubiquitous PM translocation using 16S rRNA gene sequencing, with most samples possessing bacterial DNA loads too low to be sequenced. These results are reflected in a similar study performed on rabbit carcasses which investigated the effects of temperature on the thanatomicrobiome where they failed to amplify bacterial DNA in both lung and kidney samples due to low bacterial load (Lawrence et al., 2019). The study also obtained low sequencing reads for these visceral tissues compared to those obtained from the cecum and ileum and hypothesised that the low bacterial DNA present in these samples resulted in non-specific amplification of host DNA that then failed to align to the reference database (Lawrence et al., 2019).

The low-level detection of Enterobacteriaceae and Enterococcus in the mouse tissues and the late signal produced using a highly sensitive assay show that the bacteria are potentially present within the tissue, but at very low numbers. If this were due to translocation, it is unlikely that it would only be seen in these few tissues at seemingly random time points. This observation could therefore represent PM bacterial translocation but given the low read numbers this is unlikely. It has been found elsewhere that in human autopsies Enterobacteriaceae is found at higher numbers in autopsies performed more than 24 h after death using both molecular and conventional culture analysis (Hurtado et al., 2018). This finding is also in line with previous work that has shown poor correlation between post-mortem interval (PMI) and positive bacterial cultures in clinical autopsy investigation (Lobmaier et al., 2009; Weber et al., 2010).

We found a larger number of positive tissues and sequencing read numbers in the piglet model compared to the mouse model. The similarity of bacterial families shared between tissues collected from the same piglets suggest that these bacterial families originate from the piglet itself, rather than the external environment. Given the lack of concordance between bacterial families found in the tissues and swabs it is unlikely that these bacteria originate from such sites. Bacterial families, such as Moraxellaceae, Clostridiaceae, Flavobacteriaceae and Peptostreptococcaceae have been found in high abundance on the skin, tonsil, and nasal cavities of piglets in various studies (Lowe et al., 2012; McIntyre et al., 2016; Strube et al., 2018). It is therefore possible that these positive tissues have arisen from these sites as a result of our sampling technique.

The vast number of positive cultures that are typically detected in human SUDI PM examinations are reflected in positive piglet tissues in this study; > 80% of human PM tissues from SUDI autopsies generate positive culture results (Weber et al., 2010; Pryce et al., 2011a). In these human tissues a majority of bacteria identified are enteric bacteria (Highet, 2008), which differs from the bacterial species identified in this study. This may be due to differences in the PM translocation process or perhaps contamination occurs at a higher rate during human autopsy and tissue processing. The technique used in this study could also introduce differences in results as for a positive bacterial culture only a single viable bacteria needs to be present within the sample. Examining bacterial components using molecular targets, such as the 16S rRNA gene allow a more accurate evaluation of bacterial communities.

We acknowledge limitations of this study including the lack of skin sampling which could enhance the interpretation of bacteria within tissues. It is also important that this study was carried out on healthy animals free of known infection. If an infection were to be present in these animals the conclusions may have been different, perhaps due to increased invasive abilities of pathogenic bacteria, their disruption to commensal microbes or damage to tissue epithelium compromising barrier function. We also acknowledge that the time between death and sampling in these model organisms was also controlled as would not be the case in SUDI. Although this study could not detect PM bacterial translocation in these model organisms, it is important to note that the PM process in human subjects may differ. Given the

small sample size and the use of animal models, no clinical conclusions can be made but this study provides an insight into the investigation of PM overgrowth of bacteria and acts as a proof-of-principle study into the use of 16S rRNA gene sequencing under these circumstances.

A deeper understanding of the bacterial changes that occur PM in clinical settings will allow for improved diagnostics, particularly in cases of SUDI due to sub-clinical infection. By determining the PM process using 16S rRNA gene sequencing we have demonstrated how this technique could be incorporated into routine PM diagnosis of infection. The results of this study did not, however, provide convincing evidence to support ubiquitous PM bacterial translocation. Future works should focus on implementing this technique on PM tissues from cases of SUDI to enhance our understanding and retrospective diagnosis of fatal infection.

DATA AVAILABILITY STATEMENT

The datasets presented in this study can be found in online repositories. The names of the repository/repositories and accession number(s) can be found below: NCBI BioProject PRJNA698635.

ETHICS STATEMENT

Ethical review and approval was not required for the animal study as animals whose carcasses were used in this study were not killed for this work. No aspect of the animal's life or death was altered for the scientific purpose of the present study.

AUTHOR CONTRIBUTIONS

NS and NK came up with the conceptual idea for this study and the clinical need for such work. LG and DA devised the study plan. LG performed all the experimental work, developed bioinformatics pipelines for the data analysis and visualisation, and wrote the manuscript with consultation from NS, NK, and DA. All authors contributed to the article and approved the submitted version.

FUNDING

This work was supported by the Lullaby Trust (Grant No. 175614). DA was funded by the Reuben Foundation.

ACKNOWLEDGMENTS

We would like to thank Jan Wilhelm Bavestrello for assistance with performing the needle biopsy sampling.

SUPPLEMENTARY MATERIAL

The Supplementary Material for this article can be found online at: https://www.frontiersin.org/articles/10.3389/fmicb.2021.649312/full#supplementary-material

REFERENCES

Balzan, S., De Almeida Quadros, C., De Cleva, R., Zilberstein, B., and Cecconello, I. (2007). Bacterial translocation: overview of mechanisms and clinical impact. *J. Gastroenterol. Hepatol.* 22, 464–471. doi: 10.1111/j.1440-1746.2007.04933.x

Bryant, V., and Sebire, N. (2018). "Natural diseases causing sudden death in infancy and early childhood," in *SIDS Sudden Infant and Early Childhood Death: The Past, the Present and the Future*, eds J. R. Duncan, and R. W. Byard, (Adelaide, SA: University of Adelaide Press), doi: 10.20851/sids-25

Burcham, Z. M., Hood, J. A., Pechal, J. L., Krausz, K. L., Bose, J. L., Schmidt, C. J., et al. (2016). Fluorescently labeled bacteria provide insight on post-mortem microbial transmigration. *Forensic Sci. Int.* 264, 63–69. doi: 10.1016/j.forsciint.2016.03.019

Fernández-Rodríguez, A., Burton, J. L., Andreoletti, L., Alberola, J., Fornes, P., Merino, I., et al. (2019). Post-mortem microbiology in sudden death: sampling protocols proposed in different clinical settings. *Clin. Microbiol. Infect.* 25, 570–579. doi: 10.1016/j.cmi.2018.08.009

Goldwater, P. N. (2009). Sterile site infection at autopsy in sudden unexpected deaths in infancy. *Arch. Dis. Child.* 94, 303–307. doi: 10.1136/adc.2007.135939

Goldwater, P. N. (2017). Infection: the neglected paradigm in SIDS research. *Arch. Dis. Child.* 102, 767–772. doi: 10.1136/archdischild-2016-312327

Hadley, W. (2016). *ggplot2: Elegant Graphics for Data Analysis*. New York, NY: Springer-Verlag.

Hasan, N., and Yang, H. (2019). Factors affecting the composition of the gut microbiota, and its modulation. *PeerJ* 7:e7502. doi: 10.7717/peerj.7502

Heimesaat, M. M., Boelke, S., Fischer, A., Haag, L. M., Loddenkemper, C., Kühl, A. A., et al. (2012). Comprehensive postmortem analyses of intestinal microbiota changes and bacterial translocation in human flora associated mice. *PLoS One* 7:e40758. doi: 10.1371/journal.pone.0040758

Hiergeist, A., Gläsner, J., Reischl, U., and Gessner, A. (2015). Analyses of intestinal microbiota: culture versus sequencing. *ILAR J.* 56, 228–240. doi: 10.1093/ilar/ilv017

Highet, A. R. (2008). An infectious aetiology of sudden infant death syndrome. *J. Appl. Microbiol.* 105, 625–635. doi: 10.1111/j.1365-2672.2008.03747.x

Hurtado, J. C., Quintó, L., Castillo, P., Carrilho, C., Fernandes, F., Jordao, D., et al. (2018). Postmortem interval and diagnostic performance of the autopsy methods. *Sci. Rep.* 8:16112. doi: 10.1038/s41598-018-34436-1

Hyde, E. R., Haarmann, D. P., Lynne, A. M., Bucheli, S. R., and Petrosino, J. F. (2013). The living dead: bacterial community structure of a cadaver at the onset and end of the bloat stage of decomposition. *PLoS One* 8:e77733. doi: 10.1371/journal.pone.0077733

Hyde, E. R., Haarmann, D. P., Petrosino, J. F., Lynne, A. M., and Bucheli, S. R. (2015). Initial insights into bacterial succession during human decomposition. *Int. J. Legal. Med.* 129, 661–671. doi: 10.1007/s00414-014-1128-4

Javan, G. T., Finley, S. J., Tuomisto, S., Hall, A., Benbow, M. E., and Mills, D. E. (2019). An interdisciplinary review of the thanatomicrobiome in human decomposition. *Forensic Sci. Med. Pathol.* 15, 75–83. doi: 10.1007/s12024-018-0061-0

Kennedy, B. (2016). *Sudden Unexpected Death in Infancy and Childhood: Multi-Agency Guidelines for Care and Investigation*. London: The Royal College of Pathologists.

Lawrence, K. E., Lam, K. C., Morgun, A., Shulzhenko, N., and Löhr, C. V. (2019). Effect of temperature and time on the thanatomicrobiome of the cecum, ileum, kidney, and lung of domestic rabbits. *J. Vet. Diagn. Investig.* 31, 155–163. doi: 10.1177/1040638719828412

Lobmaier, I. V. K., Vege, Å, Gaustad, P., and Rognum, T. O. (2009). Bacteriological investigation-significance of time lapse after death. *Eur. J. Clin. Microbiol. Infect. Dis.* 28, 1191–1198. doi: 10.1007/s10096-009-0762-0

Lowe, B., Marsh, T., Isaacs-Cosgrove, N., Kirkwood, R., Kiupel, M., and Mulks, M. (2012). Defining the "core microbiome" of the microbial communities in the tonsils of healthy pigs. *BMC Microbiol.* 12:20. doi: 10.1186/1471-2180-12-20

Magoč, T., and Salzberg, S. L. (2011). FLASH: fast length adjustment of short reads to improve genome assemblies. *Bioinformatics* 27, 2957–2963. doi: 10.1093/bioinformatics/btr507

McDonald, D., Price, M. N., Goodrich, J., Nawrocki, E. P., Desantis, T. Z., Probst, A., et al. (2012). An improved Greengenes taxonomy with explicit ranks for ecological and evolutionary analyses of bacteria and archaea. *ISME J.* 6, 610–618. doi: 10.1038/ismej.2011.139

McIntyre, M. K., Peacock, T. J., Akers, K. S., and Burmeister, D. M. (2016). Initial characterization of the pig skin bacteriome and its effect on in vitro models of wound healing. *PLoS One* 11:e0166176. doi: 10.1371/journal.pone.0166176

McMurdie, P. J., and Holmes, S. (2013). phyloseq: an R package for reproducible interactive analysis and graphics of microbiome census data. *PLoS One* 8:e61217. doi: 10.1371/journal.pone.0061217

Mesli, V., Neut, C., and Hedouin, V. (2017). "Postmortem bacterial translocation," in *Forensic Microbiology*, eds D. O. Carter, J. K. Tomberlin, M. E. Benbow, and J. L. Metcalf, (Hoboken, NJ: John Wiley & Sons Ltd.)

Metcalf, J. L., Wegener Parfrey, L., Gonzalez, A., Lauber, C. L., Knights, D., Ackermann, G., et al. (2013). A microbial clock provides an accurate estimate of the postmortem interval in a mouse model system. *eLife* 2:e01104. doi: 10.7554/elife.01104

Morris, J. A., Harrison, L. M., and Partridge, S. M. (2006). Postmortem bacteriology: a re-evaluation. *J. Clin. Pathol.* 59, 1–9. doi: 10.1136/jcp.2005.028183

Motulsky, H. (2007). *GraphPad Prism5.0 Statistics Guide. Clases*. San Diego, CA: GraphPad Software, Inc.

Ndu, I. K. (2016). Sudden infant death syndrome: an unrecognized killer in developing countries. *Pediatr. Health Med. Ther.* 7, 1–4. doi: 10.2147/phmt.s99685

Office for National Statistics, (2017). *Unexpected Deaths in Infancy, England and Wales (Dataset)*. Newport: Office for National Statistics.

Oksanen, J., Blanchet, F. G., Friendly, M., Kindt, R., Legendre, P., McGlinn, D., et al. (2019). *vegan: Community Ecology Package*.

Ombelet, S., Barbé, B., Affolabi, D., Ronat, J.-B., Lompo, P., Lunguya, O., et al. (2019). Best practices of blood cultures in low- and middle-income countries. *Front. Med.* 6:131. doi: 10.3389/fmed.2019.00131

Overmann, J., Abt, B., and Sikorski, J. (2017). Present and future of culturing bacteria. *Ann. Rev. Microbiol.* 71, 711–730. doi: 10.1146/annurev-micro-090816-093449

Palmiere, C., Egger, C., Prod'Hom, G., and Greub, G. (2016). Bacterial translocation and sample contamination in postmortem microbiological analyses. *J. Forensic Sci.* 61, 367–374. doi: 10.1111/1556-4029.12991

Pechal, J. L., Crippen, T. L., Benbow, M. E., Tarone, A. M., Dowd, S., and Tomberlin, J. K. (2014). The potential use of bacterial community succession in forensics as described by high throughput metagenomic sequencing. *Int. J. Legal Med.* 128, 193–205. doi: 10.1007/s00414-013-0872-1

Pryce, J. W., Roberts, S. E. A., Weber, M. A., Klein, N. J., Ashworth, M. T., and Sebire, N. J. (2011a). Microbiological findings in sudden unexpected death in infancy: comparison of immediate postmortem sampling in casualty departments and at autopsy. *J. Clin. Pathol.* 64, 421–425. doi: 10.1136/jcp.2011.089698

Pryce, J. W., Weber, M. A., Hartley, J. C., Ashworth, M. T., Malone, M., and Sebire, N. J. (2011b). Difficulties in interpretation of post-mortem microbiology results in unexpected infant death: evidence from a multidisciplinary survey. *J. Clin. Pathol.* 64, 706–710. doi: 10.1136/jclinpath-2011-200056

R Core Team (2019). *R: A Language and Environment for Statistical Computing*. Vienna: R Foundation for Statistical Computing.

Raposo, A., Pérez, E., de Faria, C. T., Ferrús, M. A., and Carrascosa, C. (2016). "Food Spoilage by *Pseudomonas* spp.- An overview," in *Food Borne Pathogens and Antibiotic Resistance*, ed. O. V. Singh, (Hoboken, NJ: John Wiley & Sons, Inc.).

Rhoads, D. D., Cox, S. B., Rees, E. J., Sun, Y., and Wolcott, R. D. (2012). Clinical identification of bacteria in human chronic wound infections: culturing vs. 16S ribosomal DNA sequencing. *BMC Infect. Dis.* 12:321. doi: 10.1186/1471-2334-12-321

Riedel, S. (2014). The value of postmortem microbiology cultures. *J. Clin. Microbiol.* 52, 1028–1033. doi: 10.1128/JCM.03102-13

Rosser, E. C., Piper, C. J. M., Matei, D. E., Blair, P. A., Rendeiro, A. F., Orford, M., et al. (2020). Microbiota-derived metabolites suppress arthritis by amplifying aryl-hydrocarbon receptor activation in regulatory B cells. *Cell Metab.* 31, 837–851.e10. doi: 10.1016/j.cmet.2020.03.003

Roy, D., Tomo, S., Purohit, P., and Setia, P. (2021). Microbiome in death and beyond: current vistas and future trends. *Front. Ecol. Evol.* 9:630397. doi: 10.3389/fevo.2021.630397

RStudio Team, (2020). *RStudio: Integrated Development for R*. Boston, MA: Rstudio Team, PBC, doi: 10.1145/3132847.3132886

Schloss, P. D., Westcott, S. L., Ryabin, T., Hall, J. R., Hartmann, M., Hollister, E. B., et al. (2009). Introducing mothur: open-source, platform-independent, community-supported software for describing and comparing microbial communities. *Appl. Environ. Microbiol.* 75, 7537–7541. doi: 10.1128/AEM.01541-09

Spencer, N., and Logan, S. (2004). Sudden unexpected death in infancy and socioeconomic status: a systematic review. *J. Epidemiol. Commun. Health* 58, 366–373. doi: 10.1136/jech.2003.011551

Strube, M. L., Hansen, J. E., Rasmussen, S., and Pedersen, K. (2018). A detailed investigation of the porcine skin and nose microbiome using universal and Staphylococcus specific primers. *Sci. Rep.* 8:12751. doi: 10.1038/s41598-018-30689-y

Tuomisto, S., Karhunen, P. J., and Pessi, T. (2013). Time-dependent post mortem changes in the composition of intestinal bacteria using real-time quantitative PCR. *Gut Pathog.* 5:35. doi: 10.1186/1757-4749-5-35

Wang, Q., Garrity, G. M., Tiedje, J. M., and Cole, J. R. (2007). Naïve Bayesian classifier for rapid assignment of rRNA sequences into the new bacterial taxonomy. *Appl. Environ. Microbiol.* 73, 5261–5267. doi: 10.1128/AEM.00062-07

Weber, M., Klein, N., Hartley, J., Lock, P., Malone, M., and Sebire, N. (2008). Infection and sudden unexpected death in infancy: a systematic retrospective case review. *Lancet* 371, 1848–1853. doi: 10.1016/S0140-6736(08)60798-9

Weber, M. A., Hartley, J. C., Brooke, I., Lock, P. E., Klein, N. J., Malone, M., et al. (2010). Post-mortem interval and bacteriological culture yield in sudden unexpected death in infancy (SUDI). *Forensic Sci. Int.* 198, 121–125. doi: 10.1016/j.forsciint.2010.02.002

Yilmaz, P., Parfrey, L. W., Yarza, P., Gerken, J., Pruesse, E., Quast, C., et al. (2014). The SILVA and "all-species Living Tree Project (LTP)" taxonomic frameworks. *Nucleic Acids Res.* 42, D643–D648. doi: 10.1093/nar/gkt1209

Yu, X., Jiang, W., Shi, Y., Ye, H., and Lin, J. (2019). Applications of sequencing technology in clinical microbial infection. *J. Cell. Mol. Med.* 23, 7143–7150. doi: 10.1111/jcmm.14624

Conflict of Interest: The authors declare that the research was conducted in the absence of any commercial or financial relationships that could be construed as a potential conflict of interest.

frontiers in Microbiology

ORIGINAL RESEARCH
published: 02 June 2021
doi: 10.3389/fmicb.2021.647933

Estimating the Time Since Deposition of Saliva Stains With a Targeted Bacterial DNA Approach: A Proof-of-Principle Study

*Celia Díez López, Manfred Kayser and Athina Vidaki**

Department of Genetic Identification, Erasmus MC University Medical Center Rotterdam, Rotterdam, Netherlands

Information on the time when a stain was deposited at a crime scene can be valuable in forensic investigations. It can link a DNA-identified stain donor with a crime or provide a post-mortem interval estimation in cases with cadavers. The available methods for estimating stain deposition time have limitations of different types and magnitudes. In this proof-of-principle study we investigated for the first time the use of microbial DNA for this purpose in human saliva stains. First, we identified the most abundant and frequent bacterial species in saliva using publicly available 16S rRNA gene next generation sequencing (NGS) data from 1,848 samples. Next, we assessed time-dependent changes in 15 identified species using de-novo 16S rRNA gene NGS in the saliva stains of two individuals exposed to indoor conditions for up to 1 year. We selected four bacterial species, i.e., *Fusobacterium periodonticum, Haemophilus parainfluenzae, Veillonella dispar,* and *Veillonella parvula* showing significant time-dependent changes and developed a 4-plex qPCR assay for their targeted analysis. Then, we analyzed the saliva stains of 15 individuals exposed to indoor conditions for up to 1 month. Bacterial counts generally increased with time and explained 54.9% of the variation (p = <2.2E–16). Time since deposition explained ≥86.5% and ≥88.9% of the variation in each individual and species, respectively (p = <2.2E–16). Finally, based on sample duplicates we built and tested multiple linear regression models for predicting the stain deposition time at an individual level, resulting in an average mean absolute error (MAE) of 5 days (ranging 3.3–7.8 days). Overall, the deposition time of 181 (81.5%) stains was correctly predicted within 1 week. Prediction models were also assessed in stains exposed to similar conditions up to 1 month 7 months later, resulting in an average MAE of 8.8 days (ranging 3.9–16.9 days). Our proof-of-principle study suggests the potential of the DNA profiling of human commensal bacteria as a method of estimating saliva stains time since deposition in the forensic scenario, which may be expanded to other forensically relevant tissues. The study considers practical applications of this novel approach, but various forensic developmental validation and implementation criteria will need to be met in more dedicated studies in the future.

Keywords: forensic genetics, microbial forensics, stain deposition time, prediction, qPCR, bacterial DNA, saliva stains

OPEN ACCESS

Edited by:
Gulnaz T. Javan, Alabama State University, United States

Reviewed by:
Maher Noureddine, ForensiGen, United States
Aaron Michael Tarone, Texas A&M University, United States

****Correspondence:***
Athina Vidaki
a.vidaki@erasmusmc.nl

Specialty section:
This article was submitted to Systems Microbiology, a section of the journal Frontiers in Microbiology

Received: *30 December 2020*
Accepted: *14 April 2021*
Published: *02 June 2021*

Citation:
Díez López C, Kayser M and Vidaki A (2021) Estimating the Time Since Deposition of Saliva Stains With a Targeted Bacterial DNA Approach: A Proof-of-Principle Study. Front. Microbiol. 12:647933. doi: 10.3389/fmicb.2021.647933

INTRODUCTION

In routine forensic investigations, DNA profiling based on short tandem repeats (STRs) is the gold standard for identifying the individuals who left a biological sample at the crime scene (Butler, 2004). However, the presence of a person's DNA at a crime scene does not necessarily allow us to conclude that the sample donor is the perpetrator, which is typically done in court using additional (non-genetic) information. One important additional piece of information, which can be crucial to solving a case, is knowledge of the time frame when the person identified by DNA-based profiling left the biological stain at the scene. Knowing the time since deposition of a crime scene stain can help the police assess the alibis of suspects or provide investigative information to search for the right suspect. Moreover, when multiple biological traces belonging to different donors are found at a scene, information on their time since deposition may help investigators select the ones with the highest investigative value for further analysis, in cases where the time of the crime is known. Furthermore, in some missing person cases, such knowledge of the time of stain deposition on relevant items (such as clothing) might also be linked with the time a person went missing if it is unknown. In crime scenes involving (parts of) a corpse, estimation of the time since deposition of the stains found around/on the body can serve as an additional method for determining the time since death, i.e., post-mortem interval (PMI).

For estimating the time since deposition of human biological stains, the most studied molecular approach to date is the differential time-dependent degradation of human RNA, using mainly mRNA markers (Bauer et al., 2003; Anderson et al., 2011; Weinbrecht et al., 2017; Amany et al., 2018; Fu and Allen, 2019; Asaghiar and Williams, 2020), but also miRNA markers (Amany et al., 2018; Alshehhi and Haddrill, 2019). In principle, RNA decay continues *ex vivo* after a stain has been deposited, even if the biological material is dehydrated (Bauer, 2007). However, not all markers investigated for their potential time-dependent degradation are informative, as outlined in published studies, due to their reported time-stability for months (Watanabe et al., 2017; Amany et al., 2018; Alshehhi and Haddrill, 2019) or even a year (Alshehhi and Haddrill, 2019). Nevertheless, the majority of studies to date have reported the time-dependent decay of selected RNA markers, and a few have also attempted to use this for estimating the time since deposition of body fluid stains.

A qPCR-based study on degradation profiles of two human hypoxia sensitive mRNA markers up to a month obtained mean absolute error (MAE) values of 2.7, 3.5, and 6.4 days in blood, saliva, and semen stains, respectively (Asaghiar and Williams, 2020). However, the sample size was small (n = 5 for each body fluid) and stain exposure did not mimic realistic forensic scenarios. In the cases of saliva and semen, fluids were left in tubes until swabbed rather than left to dry as stains. Bauer et al. (2003) analyzed two mRNA markers in dried bloodstains using qPCR under the hypothesis that the 5′-end degrades at a faster rate than the 3′-end in mRNA, and that relative degradation could be used to estimate the time since deposition of the stains. Significant levels in mRNA degradation were only reported in stains with large deposition time differences of at least 4–5 years, resulting in very large estimation intervals of several months or even a few years. Another qPCR-based study analyzed four mRNA markers in dried bloodstains under the same previous hypothesis and reported a time estimation error of 2–4 weeks for stains exposed less than 6 months and 4–6 weeks for stains exposed between six and 12 months (Fu and Allen, 2019). Furthermore (Alshehhi and Haddrill, 2019) employed qPCR targeting two and four mRNA/miRNA markers in dried saliva and semen stains, respectively, for up to a year. On the one hand, the mRNA markers showed large fluctuation, no degradation, or were not detected at all due to the assay's sensitivity past 90 days. On the other hand, the miRNA markers remained stable across all analyzed time points, making them not suitable for investigating time-dependent changes. Lastly, another study employed RNA next-generation sequencing (NGS) to analyze the potential time-dependency of the transcripts present in dried blood, saliva, semen, and vaginal fluid stains for up to a year (Weinbrecht et al., 2017). Particularly for the saliva transcripts, abundance values decreased rapidly and erratically; hence, no comprehensive analysis could be performed. For other stains, the time-dependency of transcripts was useful for a limited time period of less than a year. Overall, a RNA-based approach for estimating the time since deposition of stains could be promising but suffers from significant drawbacks including inter-individual degradation variation.

The human microbiome has been recently proposed as a promising tool in forensic science, especially for forensically relevant topics, for which other approaches present challenges and limitations. For example, the human microbiome has proven to be a promising forensic tool for PMI estimation based on predictable succession and colonization of microorganisms over time at different body sites (Hyde et al., 2013; Adserias-Garriga et al., 2017; Pechal et al., 2018; Dash and Das, 2020). However, caution must be taken due to the environmental (Pechal et al., 2017; Dash and Das, 2020) and individual-specific (Dash and Das, 2020) factors affecting time-dependent changes. The human microbiome, particularly the skin microbiome, can also serve as a kind of "fingerprint" that is transferred to touched objects, which is promising for individual identification in cases where recovered human DNA is not sufficient for obtaining a STR profile ("touched" samples; Schmedes et al., 2017, 2018; Yang et al., 2019). Additionally, we also showed that the human microbiome is suitable for the identification of the body site of origin of human body fluid stains, which can be of great value in crime scene reconstruction. For instance, when it comes to crime scene stains that contain epithelial cells from different body sites of origin including skin, saliva, and vaginal fluids (Díez López et al., 2019), and bloodstains from different body sites of origin including venous/arterial blood, menstrual blood, nasal blood, or blood from skin injuries (Díez López et al., 2020), where previous molecular approaches such as RNA-based ones have limitations (Haas et al., 2014; Holtkotter et al., 2017; Ingold et al., 2018). On top of these previously investigated forensic microbiome applications, we envisioned it a promising tool for estimating the time since deposition of human biological stains at a crime scene, which has not been studied yet.

Particularly, the oral human microbiome has been extensively characterized (Escapa et al., 2018) and the microorganisms living in the oral cavity comprise the second largest and most diverse microbial community of the human body (Huttenhower et al., 2012) after the gut. Notably, 1 mL of saliva in healthy adults is estimated to contain approximately 100 million bacterial cells (Curtis et al., 2011). Considering the normal salivary flow rate to be around 750 mL/day, 8×10^{10} bacterial cells are shed daily from the oral surfaces (Curtis et al., 2011). As a result, human saliva samples are likely to contain a high number of bacterial cells, including dried saliva stains found at crime scenes that often are small and based on just a few microliters (μL) of liquid saliva. Additionally, it has been shown that the "core" oral microbiome, which can be defined as the taxa shared among unrelated individuals (Zaura et al., 2009), is quite large, and is larger than in other body sites such as the gut or skin (Costello et al., 2009). Finally, the oral microbiome has shown a high degree of *in vivo* time-wise stability within an individual, with no significant changes over months (Costello et al., 2009; Lazarevic et al., 2010; Zhu et al., 2012) and even a few years (Stahringer et al., 2012). The time-stable biological information of any biomarker used in forensics is crucial in investigations, especially in approaches where old crime scene samples may be used retrospectively, such as for estimating the time since stain deposition. To date, only a few studies have investigated the time-dependent changes in the microbiome in dried saliva samples exposed to indoor conditions (Dobay et al., 2019; Salzmann et al., 2019), and due to their small sample size, no meaningful conclusions could be made on how suitable the approach is for forensic purposes.

This proof-of-principle study is the first to investigate the potential of the genetic profiling of human saliva commensal bacteria for estimating the time since deposition of saliva stains, which has promising applications in future forensic scenarios. We first identified the most abundant and most frequent bacterial species in saliva from a large publicly available 16S rRNA gene NGS data set. Next, we assessed time-dependent changes in the relative abundance of the top identified bacterial target species in 16S rRNA gene NGS data produced from dried saliva stains exposed to indoor long-term conditions for up to 1 year. Based on the observed significant time-dependent changes, we further selected four bacterial species, for which we developed a multiplex qPCR assay. Finally, this assay was used to analyze dried saliva stains exposed to indoor short-term conditions with various sample storage times up to 1 month.

MATERIALS AND METHODS

Saliva Microbiome Data Sets

Publicly available human saliva 16S rRNA gene NGS data from two previously published studies were obtained from the European Bioinformatics Institute (EMBL-EBI). These studies included data from three cohorts: the American Cancer Society Cancer Prevention Study II (ACS CPS-II; N = 543; Wu et al., 2016), and the Prostate, Lung, Colorectal, and Ovarian (PLCO) Cancer Screening Trial (N = 661; Wu et al., 2016) from which the produced microbiome data was published as part of the same study; and the American Gut Project (AGP; N = 1,089; McDonald et al., 2018). The accession numbers were PRJNA434300, PRJNA434312, and PRJEB11419, respectively.

The metadata of the studies were accessed via the National Center for Biotechnology Information (NCBI) and matched to the corresponding sample identifiers using custom Python scripts to create flat metadata tables. In the first study (ACS CPS-II/PLCO), quality control sample replicates were removed to avoid data redundancy. We also discarded samples with missing metadata information for age, sex, and/or ethnicity. We also removed samples obtained from donors less than 15 years old, given that differences between adult and youth saliva microbiomes are expected (Burcham et al., 2020).

Most Abundant and Frequent Bacterial Species in Saliva

We analyzed the above-mentioned human saliva 16S rRNA gene NGS data to identify the most abundant and frequent bacterial species across individuals included in the two selected studies (**Figure 1A**). Primer sequences were obtained from the original studies and were removed from the raw sequencing reads using cutadapt (v2.6; Martin, 2011) by setting the minimum-length to 100, to discard processed reads shorter than 100 bp. The resulting FASTQ files were quality-filtered and de-noised using DADA2 (v1.12.1; Callahan et al., 2016). Parameter maxN was set to 0 in the ACS CPS-II/PLCO study to prevent unambiguous nucleotides in the sequencing reads, whereas maxN was set to 1 in the AGP study to avoid too few reads passing the filtering. Parameter maxEE for the maximum number of "expected errors" in the reads was set to 2 in the two studies. Parameter truncLen was set based on the read quality profiles, ensuring to maintain an overlap between forward and reverse reads to be merged later. Following sample inference of true sequence variants, an amplicon sequence variant (ASV) table was constructed and chimeric sequences were removed. At this point, only high-coverage samples (>1,000 reads) were chosen for downstream analysis, resulting in 525 (ACS CPS-II), 452 (PLCO), and 871 (AGP) samples.

To assign taxonomy the ASV table was processed via the *assignTaxonomy* function in DADA2 at taxonomic ranks of interest (phylum, class, order, family, genus, and species). The expanded Human Oral Microbiome Database (eHOMD; v15.2; Escapa et al., 2018) was transformed to a DADA2-compatible training format and used as the reference database. Since the eHOMD database is bacteria-exclusive, the ASV table was further compared against the SILVA SSU r132 database (Quast et al., 2013) to check for sequences assigned to Eukarya, mitochondria, or chloroplasts, which were subsequently filtered out. We additionally filtered out taxa present in less than 0.005% of relative abundance.

Finally, in each study, we ordered the bacterial species according to their relative abundance (number of bacterial species sequencing reads divided by the total number of sequencing reads) and frequency (number of samples in which the bacterial species is reported divided by the total number of

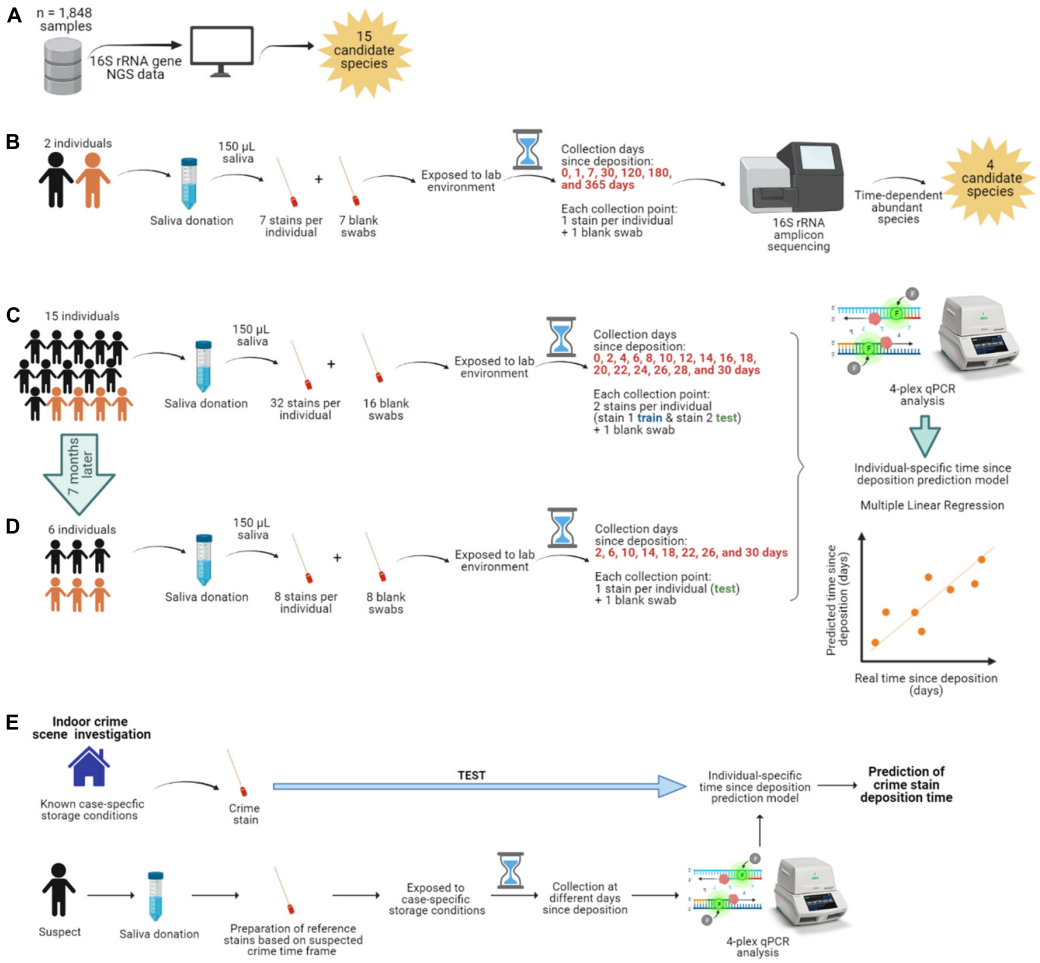

FIGURE 1 | Overview of the study. **(A)** Identification of the most abundant and frequent bacterial species in saliva from publicly available 16S rRNA gene next-generation sequencing (NGS) data. **(B)** Long-term (up to 1 year) time-dependent differentially abundance analysis in saliva stains from two individuals. The individuals are color-coded; black is female, and orange is male. **(C)** Short-term (up to 1 month) targeted analysis of species informative for time since deposition of saliva stains from 15 individuals and **(D)** from six individuals re-sampled 7 months later. **(E)** Hypothesized individualized solution to saliva trace timing as viewed in our data set.

samples). As abundant and frequent bacterial species in saliva, we selected the top 15 most common ones across the studies. The processed NGS data in the form of the relative abundance tables of the identified taxa can be found in **Supplementary Data Sheet 1**.

Saliva Collection

Sample collection, handling, and subsequent analysis adhered to the Medische Ethische Toestsings Commissie Erasmus MC (MEC-2018–1731). All individuals who donated saliva provided signed informed consent for this study. One individual included in the long-term experiment (individual No 1) was also included in the short-term one (individual No 2), with a time span of 2 years between saliva collection for each of the experiments. In summary, we included 11 females and 5 males, with an average age of 26.3 years and from various ethnic backgrounds, but mainly white Europeans (13/16). Information on our donors' sex, age, ethnicity, and sample donation can be found in **Supplementary Table 1**.

In brief, as part of donating saliva, individuals were asked to avoid all of the following for at least 1 h before saliva donation: brushing their teeth, use of mouthwash, eating food, chewing gum, and were asked to only drink non-sparkling water. Individuals were independently asked to collect saliva in their mouth for a minute and spit it into a sterile tube, repeating the process several times until reaching ∼5 mL of saliva. Subsequently, for each individual, we prepared all stains per time point, each consisting of 150 µL of saliva deposited on a sterile swab (PurFlock Ultra 6" sterile standard flock swabs, Puritan, Guilford, ME, United States). Therefore, for each individual, all saliva stains were individual samples, even though they were collected at the same time point. As a substrate, we chose sterile swabs that are routinely used in forensics, for example, to collect suspected saliva stains from objects found at the crime scene for molecular analysis. The sterile nature of the swabs also allowed us

to conclude that there was an absence of microbial contamination before the saliva was deposited.

Dried Saliva Stains

With the exception of the fresh (t0) saliva swabs that were processed straightaway, the prepared swabs were dried and directly exposed to our laboratory's environment apart from each other, for a specific time prior to bacterial DNA isolation. The swabs were stored at standard room temperature (20–25°C), with relative humidity (30-50%), and daily ambient light (8-11 h). Ambient light included both artificial and natural light sources as the swabs were placed 4 m away from a window (though not directly hit by the sun). First, for the long-term time-dependent bacterial composition analysis, saliva was collected from two individuals (**Figure 1B**). To sufficiently cover selected time points over a 1-year period, seven saliva swabs were prepared per individual (single sample replicates per time point) and processed at day 1 (t1), 7 (t2), 30 (t3), 120 (t4), 180 (t5), and 365 (t6) after deposition. Second, for the short-term time-dependent bacterial marker analysis, saliva was collected from 15 individuals (**Figure 1C**). To sufficiently cover selected time points over a 1-month period, 32 saliva swabs were prepared per individual (double replicates per time point); with the exception of one individual (No 1) for which there was insufficient volume of saliva to prepare the last time point. In this case, dried saliva swabs were processed at day 2 (t1), 4 (t2), 6 (t3), 8 (t4), 10 (t5), 12 (t6), 14 (t7), 16 (t8), 18 (t9), 20 (t10), 22 (t11), 24 (t12), 26 (t13), 28 (t14), and 30 (t15) after deposition. Additionally, six of these fifteen individuals also donated saliva 7 months after the first collection date (**Figure 1D**). For this, eight saliva swabs were prepared per individual (single replicates per time point) and processed at day 2 (t1), 6 (t2), 10 (t3), 14 (t4), 18 (t5), 22 (t6), 26 (t7), 28 (t8 for individual No 1), and 30 (t8 for the rest of individuals) after deposition, corresponding to 1-month time frame as in the first collection date. Additionally, swabs with no biological material were prepared as background blanks in both the long-term and short-term experiments and were exposed and processed in parallel at the same time points as the dried saliva stains.

Bacterial DNA Isolation and Quantification

Bacterial DNA isolation was performed with the QIAamp DNA Mini Kit (Qiagen, Germany) following the buccal swab spin protocol to simplify the isolation of DNA from human saliva samples deposited on a swab. We chose a kit that can co-isolate both the bacterial and human DNA present in the sample to simultaneously allow for STR profiling, necessary to identify the sample donor, and therefore, increasing the forensic applicability of the proposed approach. After appropriate optimization, we slightly modified the manufacturer's instructions for maximizing DNA yield. More specifically, the incubation time in step four was increased from 10 to 30 min, the elution was performed with nuclease-free water using a reduced 50 μL elution volume, spin columns were incubated for 5 min at room temperature following the addition of nuclease-free water and before centrifugation, the centrifugation time and speed were increased to 2 min and 12,000 rpm, and finally, a second elution step using the eluate was added. Isolated bacterial DNA was quantified with the Femto^{TM} Bacterial DNA Quantification kit (Zymo Research, Irvine, CA, United States) following the manufacturer's instructions on a CFX38 Touch^{TM} Real-Time PCR System (Bio-Rad, Hercules, CA, United States).

Library Preparation and Sequencing

For the long-term time-dependent bacterial composition analysis, we sequenced the obtained bacterial DNA from the dried saliva stains of the two individuals (N = 14) as well as the background controls (N = 7). To also assess the performance of the workflow we sequenced one negative control sample, one smart control (SC) sample for monitoring the library construction process and potential introduced contamination, and one positive control – a commercial microbial community DNA standard sample (ZymoBIOMICS^{TM} Microbial Community DNA Standard, ZymoResearch). Library preparation was performed using the QIAseq 16S/ITS Panel Kit (Qiagen) for sequencing the V4–V5 region of the 16S rRNA bacterial gene. Library quality control was performed with the Agilent 2100 Bioanalyzer (Agilent Technologies, Palo Alto, CA, United States) using a high sensitivity DNA chip following the manufacturer's instructions. Library quantification was performed using the KAPA Library Quantification Kit (Kapa Biosystems, Inc. Wilmington, MA, United States) following the manufacturer's instructions on a CFX384 Touch^{TM} Real-Time PCR System (Bio-Rad). Libraries were diluted down to 2 nM, or the highest possible concentration in case the library concentration was <2 nM, and pooled together for 2 × 276 bp paired-end sequencing on a MiSeq platform using the MiSeq v3 Reagent Kit (Illumina, San Diego, CA, United States).

Long-Term Time-Dependent Differential Bacterial Abundance Analysis

We performed differential abundance analysis to identify changes in the relative abundance of bacterial species over time in the 16S rRNA gene NGS data derived from the long-term dried saliva stains. Phased primer sequences were removed from the raw sequencing reads using a custom Python script. Subsequent filtering, de-noising, ASV table construction, and taxonomy annotation were carried out as previously described for the publicly available saliva microbiome data sets (section "Most abundant and frequent bacterial species in saliva"). We chose gneiss (Morton et al., 2017) for the differential abundance analysis since it acknowledges the compositional nature of microbiome data. Based on this compositional nature it is only possible to infer relative, but not absolute, abundance changes with time, since the abundance change of one species influences the abundance changes in the other species. Gneiss was run using the q2-gneiss plugin in QIIME2 (v.2019.10; Bolyen et al., 2019). Input data comprised of a microbial profile sub-selection of the 15 most abundant and most frequent bacterial species in saliva as previously identified (section "Most abundant and frequent bacterial species in saliva"). First, a bifurcating tree was built relating bacterial species to each other based on how they co-occur by using Ward's hierarchical clustering via the

correlation-clustering command. Each balance (internal nodes in the tree) is calculated by taking the log ratio of geometric means of subtrees via the *ilr-transform* command. Each balance is indicated as "*y*" followed by an ordinal number, being *y0* the first balance in the root of the constructed tree. The taxa on one side of the balance are termed as numerators and on the other side as denominators. Each log ratio's numerical value depends on the balance between the numerator's and denominator's taxa and can be either positive, negative, or null. Differences in the log ratio balances can be compared between sample groups to infer relative changes in the microbial composition. These log-transformed balances were used to construct a multivariate response linear model using the time since deposition and the individual ID as covariates using the *ols-regression* command, where 10-fold cross validation of 10 partitions showed no overfitting. The regression summary showed the contributions of the covariates to the abundances of the selected bacterial species. Balances significantly affected by the covariates were determined with a *p* value cutoff at 0.05 after Bonferroni correction. These *p* values were based on relative, rather than absolute, values resulting from inter-dependent taxa. Significant balances for time since deposition but not for individual ID were selected as the most informative for this study and used to analyze the informative bacterial species via qPCR in the short-term dried saliva stains.

4-Plex qPCR Assay Design and Optimization

Based on the differential abundance analysis results, four bacterial species were selected for qPCR analysis of the short-term dried saliva stains. The selected species were *Fusobacterium periodonticum, Haemophilus parainfluenzae, Veillonella dispar, and Veillonella parvula.* We aimed to design a suitable 4-plex qPCR assay based on TaqMan probe technology that would allow for the simultaneous analysis of all four selected bacterial species using species-specific primers that target single-copy genes. For *F. periodonticum*, *V. dispar*, and *V. parvula* we chose the beta subunit of RNA polymerase gene (rpoB) as the target gene; for *H. parainfluenzae* we chose the translation initiation factor IF-2 gene (infB).

A literature search was conducted to find previously designed suitable primers, resulting in the reverse primers for *V. dispar* and *V. parvula* (Mashima et al., 2016). The rest of the primer sequences as well as the probe sequences were manually designed using the PrimerQuest Tool (Integrated DNA Technologies, IDT, Coralville, IA, United States). The fluorescent dyes labeled to the 5′-end of the probe sequences were: 6-carboxyfluorescein (6-FAM) for *F. periodonticum*, cyanine 5 (Cy5) for *H. parainfluenzae*, Texas red-615 (TEX-615) for *V. dispar*, and hexachloro-fluorescein (HEX) for *V. parvula.* To test primer pair specificity, each pair was compared against the nucleotide collection database from the NCBI using Primer BLAST. The Autodimer software (Vallone and Butler, 2004) was also used to assess the potential formation of primer dimers and hairpins under our experimental conditions. Final primer and probe sequences are summarized in **Supplementary Table 2**.

The 4-plex qPCR assay was developed based on the CFX384 Touch^{TM} Real-Time PCR System (Bio-Rad). The assay was optimized according to various parameters including annealing temperature and primer/probe concentrations. The optimal oligo concentrations varied for each bacterial target and were determined as follows (primers/probe): *F. periodonticum* (0.7/0.5 μM), *H. parainfluenzae* (0.6/0.5 μM), *V. dispar* (0.2/0.05 μM), *and V. parvula* (0.9/0.5 μM). Synthetic double stranded DNA fragments (gBlocks, IDT) for each of the bacterial target gene fragments were used as standard samples (positive controls; **Supplementary Table 2**). Concentrations were converted to copy numbers by using the formula:

$$(C) * (M) * \left(1{*}10^{-15}\ mol/fmol\right) * \left(Avogadro's\ number\right) = copy\ number/\mu L.$$

where C is the concentration of the gBlock gene fragment in ng/μL and M is the molecular weight in fmol/ng. gBlocks were mixed in known concentrations ranging from 125,000 down to 61 copies per bacterial target gene fragment. The assay was performed in a 20 μL reaction in triplicate, including 10 μL of iQ Multiplex Powermix (Bio-Rad), 4 μL of each primer (forward and reverse), and probe mix (5X), 1 μL of 25 μM of $MgCl_2$ (Thermo Fisher Scientific, Waltham, MA, United States), 0.5 μL of 20 mg/mL of bovine serum albumin (New England Biolabs, Ipswich, MA, United States), 1 μL of bacterial DNA (corresponding to 2 ng) and 3.5 μL of nuclease-free water. The thermocycling program included an initial denaturation and polymerase activation step at 95°C for 3 min, followed by 35 PCR cycles of 95°C for 10 s and an extension step of 60°C for 45 s.

qPCR Data Analysis

Using our developed and optimized 4-plex qPCR assay we analyzed the short-term dried saliva stains of 15 individuals. The standard samples with known concentrations per bacterial target gene fragment (gBlocks) were used to create the best-fitted linearity curve. The efficiency of each qPCR assay was calculated from the slope of the serially diluted standard samples according to the equation (Kubista et al., 2006):

$$E = 10^{-(1/slope)}.$$

For each reaction, we obtained the quantification cycle (*Cq*) value, the point at which fluorescence above the threshold level is detectable. To standardize, the threshold was set to 100 relative fluorescence units (RFU) for all reactions and fragments. The copy number (cn) for each bacterial target gene fragment was calculated according to the equation:

$$cn = e^{-Cq}.$$

Since we target single-copy genes, reported copy numbers can be translated to bacterial cell counts. Between-plate variation was removed using the Factor-qPCR tool (Ruijter et al., 2015) in the stains produced at the first donation time point and 7 months later for six individuals. We set the qPCR plate ID as the variable causing the variation to be removed, while the bacterial marker and time since deposition as the variables for which preserve their effects. In some cases, the between-plate correction resulted in negative count values.

Short-Term Time-Dependent Bacterial Analysis

We aimed to investigate the statistical relationship between the time since deposition and the four selected bacteria cell counts in the short-term dried saliva stains. Since the focus was on dried saliva stains, fresh (t0) samples were excluded from this analysis. Sample duplicates collected at each time point for each donor were analyzed independently from each other to assess the magnitude of sample variation. For each analyzed stain qPCR triplicates were considered as separate samples to account for potential reaction variation. Various linear regression models were built using the *lm()* function in the lme4package (v.1.1.20; Bates et al., 2015) in R (v.3.6.1 [2019-07-05]). The linear models were based on the functions below, where C refers to the bacterial cell count, I to the individual, S to the bacterial species, and finally, *T* to the time since deposition (in days). Interactions between variables are indicated with an asterisk (*). The statistical relationship between each bacterial species cell count for each individual and the time since deposition was calculated based on the function:

$$lm\ (C \sim T).$$

The statistical relationship between the four species cell count and the time since deposition, species, and their interaction for each individual was calculated based on the function:

$$lm\ (C \sim T * S).$$

The statistical relationship between each species cell count and the time since deposition, individual, and their interaction was calculated based on the function:

$$lm\ (C \sim T * I).$$

Finally, the statistical relationship between the four species cell count and the time since deposition, species, individual, and their interaction was calculated based on the function:

$$lm\ (C \sim T * S + T * I).$$

Adjusted R^2 and p values were evaluated for all the linear models. Sample variation was assessed by testing for equality between the coefficients in the linear regression models of each of the sample duplicate sets using the Chow test implemented in the gap R-package (v.1.2.2; Zhao, 2007). Significant p values were determined with a value cutoff at 0.05 following Benjamini-Hochberg correction. All plots were generated with the ggplot2 R-package (v.3.3.2; Hadley, 2009).

Time Since Deposition Prediction Modeling

We further investigated the possibility to predict the time since deposition in the short-term dried saliva stains. We once again excluded fresh (t0) samples based on the notion that it is not feasible to collect a purely fresh saliva sample at a real crime scene. We first attempted a generalized time since deposition prediction model based on random forest (RF) regression using the randomForest R-package (v.4.6.14; Liaw and Wiener, 2002). To evaluate the generalizability of this approach and to avoid prediction biases, we built a model based on the average detected microbial DNA cell counts of the four targeted species per time point. We then used data from all time points from 14 of the analyzed individuals as the training set, while keeping all the time points of the remaining individual as the testing set. By this, the tested individual was not present in the training set to mimic real-life applications. We repeated this process 15 times given the 15 individuals in our data set. The 15 RF models were based on 5-fold cross-validation, which was repeated three times, and 500 trees with the four variables (targeted bacterial species) were sampled at each split. NA values were replaced with column medians using the *na.roughfix* command. The average performance of the generalized RF models was assessed using the mean absolute error (MAE), which measures the discrepancies between predicted and real values according to the formula below:

$$MAE = \frac{1}{n}\sum_{i=1}^{n} |yi - y|$$

where n is the total number of data points, y_i is the real value and y is the predicted value. Pearson's correlation was used to calculate the correlation (r) between real and predicted values. MAE and r were calculated with the Metrics R-package (v.0.1.4; Hamner et al., 2012).

In the individualized modeling approach, the sample duplicates collected at each time point for each donor were considered separately; namely, one duplicate was used as the training sample, while the other was used as the testing sample, mimicking a potential future forensic scenario of having both reference and crime scene samples. As predictors, we chose the bacterial cell counts of the four selected species at each time point. Multiple linear regression models were built using the *lm()* function in the lme4 R-package (Bates et al., 2015) based on the function below:

$$lm\ (T \sim C_1 + C_2 + C_3 + C_4)$$

where C refers to each bacterial species cell counts and T to the time since deposition in days. Additionally, the follow-up dried saliva stains of the selected six individuals were also analyzed as testing samples. In this case, as time since deposition predictors, we did not only consider the bacterial cell counts for the four selected species, but all the possible combinations of also one, two, and three predictor species to select the model with the lowest error for each individual. The donor-specific prediction models were evaluated based on the adjusted R^2 and p values, where significant p values were determined with a value cutoff at 0.05 following Benjamini-Hochberg correction. The average model performances were assessed using the MAE and Pearson's correlation was used to calculate the correlation (r) between real and predicted values. All plots were generated with the ggplot2 R-package (v.3.3.2; Hadley, 2009). The processed qPCR data used to build and test the prediction models can be found in **Supplementary Data Sheet 1**.

RESULTS

Selection of Most Abundant and Most Frequent Bacterial Species in Human Saliva From Large 16S rRNA Gene Sequencing Data

Publicly available 16S rRNA gene NGS data from 1,848 human saliva samples were analyzed to identify the most abundant and most frequent bacterial species across the studies they were retrieved from (Wu et al., 2016; McDonald et al., 2018). A total of 10,326,403 sequencing reads were retrieved from the ACS CPS-II/PLCO study and 31,046,365 sequencing reads from the AGP study. In the ACS CPS-II/PLCO study, 218 bacterial species from 35 families were identified, while in the AGP study 471 bacterial species from 88 families were found.

We then selected the top 15 most abundant and most frequent bacterial species from a total of 10 families that were common across these studies, namely *Actinomyces sp. HMT 180*, *Fusobacterium periodonticum*, *Granulicatella adiacens, Haemophilus parainfluenzae, Leptotrichia sp. HMT 417, Porphyromonas pasteri, Prevotella melaninogenica, Prevotella salivae, Prevotella veroralis, Rothia mucilaginosa, Streptococcus oralis subs. dentisani clade 058, Streptococcus parasanguinis clade 411, Streptococcus salivarus*, *Veillonella dispar,* and *Veillonella parvula* (**Figure 2A**). These 15 identified common species accounted for 66.0% (6,817,142) of the sequencing reads in the ACS CPS-II/PLCO study and 55.1% (17,095,402) of the sequencing reads in the AGP study. In the ACS CPS-II/PLCO study, *S. oralis subs. dentisani clade 058* was the most abundant species accounting for 24.9% (2,567,719) of the reads, whereas *L. sp. HMT 417* was the least abundant accounting for 0.59% (61,475) of the reads. In the AGP study, *R. mucilaginosa* was the most abundant species accounting for 10.7% (3,305,923) of the reads, whereas *P. salivae* was the least abundant accounting for 0.47% (146,083) of the reads. Overall, these 15 common species were similar in abundance across the analyzed studies, with the exception of *S. oralis subs. dentisani clade 058,* which was markedly more abundant in the ACS CPS-II/PLCO than in the AGP study (24.9% *vs.* 9.1% of total reads), and *R. mucilaginosa* which was more abundant in the AGP than in the ACS CPS-II/PLCO study (10.6% *vs.* 5.4% of total reads). The most frequent species was *S. oralis subs. dentisani clade 058*, which was present in 97.0% (948) of the ACS CPS-II/PLCO study's individuals, and found in 95.2% (829) of the AGP study's individuals. The less frequent species in the ACS CPS-II/PLCO study was *L. sp. HMT 417* present in 46.2% (451) of the individuals, whereas in the AGP study it was *P. veroralis* present in 33.9% (295) of the individuals.

Selection of Bacterial Species With Time-Dependent Relative Abundance in Long-Term Dried Saliva Stains Using *de-novo* 16S rRNA Gene Sequencing

We then analyzed the dried saliva stains produced from two individuals and exposed to indoor conditions for different time periods of up to 1 year. The obtained 16S rRNA microbial profiles were distinct from the background blanks (empty swabs) for each time point, indicating a low level of bacterial contamination (**Supplementary Figure 1**). We then extracted the data of the 15 most abundant and most frequent bacterial species identified in our previous *in silico* analysis (**Figure 2A**) to identify for which species their relative abundance significantly changed over time. The fit of the overall multivariate response linear model was $R^2 = 0.21$, with the time since deposition accounting for 7% and the person accounting for 15% of the bacterial variation.

A total of 13 log ratio balances (from y0 to y12) were generated as internal nodes in the built tree. Log ratio balances y4 ($p = 0.008$), y5 ($p = 0.004$), and y7 ($p = 0.022$) were significantly different for the time since deposition (**Table 1**). Balance y4 was composed of *A. sp. HMT 180, S. oralis subsp. dentisani clade 058, S. parasanguinis clade 411, P. pasteri, P. melaninogenica,* and *P. veroralis* as numerator's taxa; and *F. periodonticum, P. melaninogenica, V. dispar,* and *V. parvula* as denominator's taxa. Balance y5 was composed of *F. periodonticum, H. parainfluenzae,* and *V. dispar* as numerator's taxa; and *V. parvula* as denominator's taxa. Balance y7 was composed of *F. periodonticum,* and *H. parainfluenzae* as numerator's taxa; and *V. dispar* as denominator's taxa. It has to be noted that balance y7 is a subdivision of balance y5 numerator (**Table 1**). An overview of the generated log ratio balances, intercept, and *p* values for the time since deposition and individual person can be found in **Supplementary Table 3**.

For this study, we sub-selected the log ratio balance y5 as our reference because of its strongest significant time dependency ($p = 0.004$) in both individuals. We preferred y5 over its subdivision y7 since balances toward the root of the tree capture more information as they contain more tree tips. Furthermore, three of the four bacterial species in y5 were also present in y4, which also showed a strong significant time dependency ($p = 0.008$), albeit less strong than y5 (**Table 1**). For both individuals, there was a similar pattern in the log ratio evolution of balance y5 through time since saliva stain deposition, though the rate of change was individual-specific (**Figure 2B**). From 7 to 365 days, the general trend was the increase of the log ratios' values for both individuals. Looking at the relative abundances of the four species from balance y5 at day 7 and day 365 since deposition we observed that for *H. parainfluenzae* relative abundance increased in both individuals; for *V. dispar* and *V. parvula* relative abundances decreased in both individuals; and for *F. periodonticum* relative abundance increased in individual 1, whereas it slightly decreased in individual 2 (**Figure 2C**). Based on these results, the four species composing balance y5 were selected for developing a 4-plex qPCR assay for their targeted analysis in the short-term dried saliva stains. Parallel to the NGS analysis, the relative abundance of the four selected species in the background (blank) swabs was very low (≤1%); on average (mean ± standard deviation), as follows: *F. periodonticum* (0.008 ± 0.010), *H. parainfluenzae* (0.010 ± 0.009), *V. dispar* (0.005 ± 0.006), and *V. parvula* (0.006 ± 0.009).

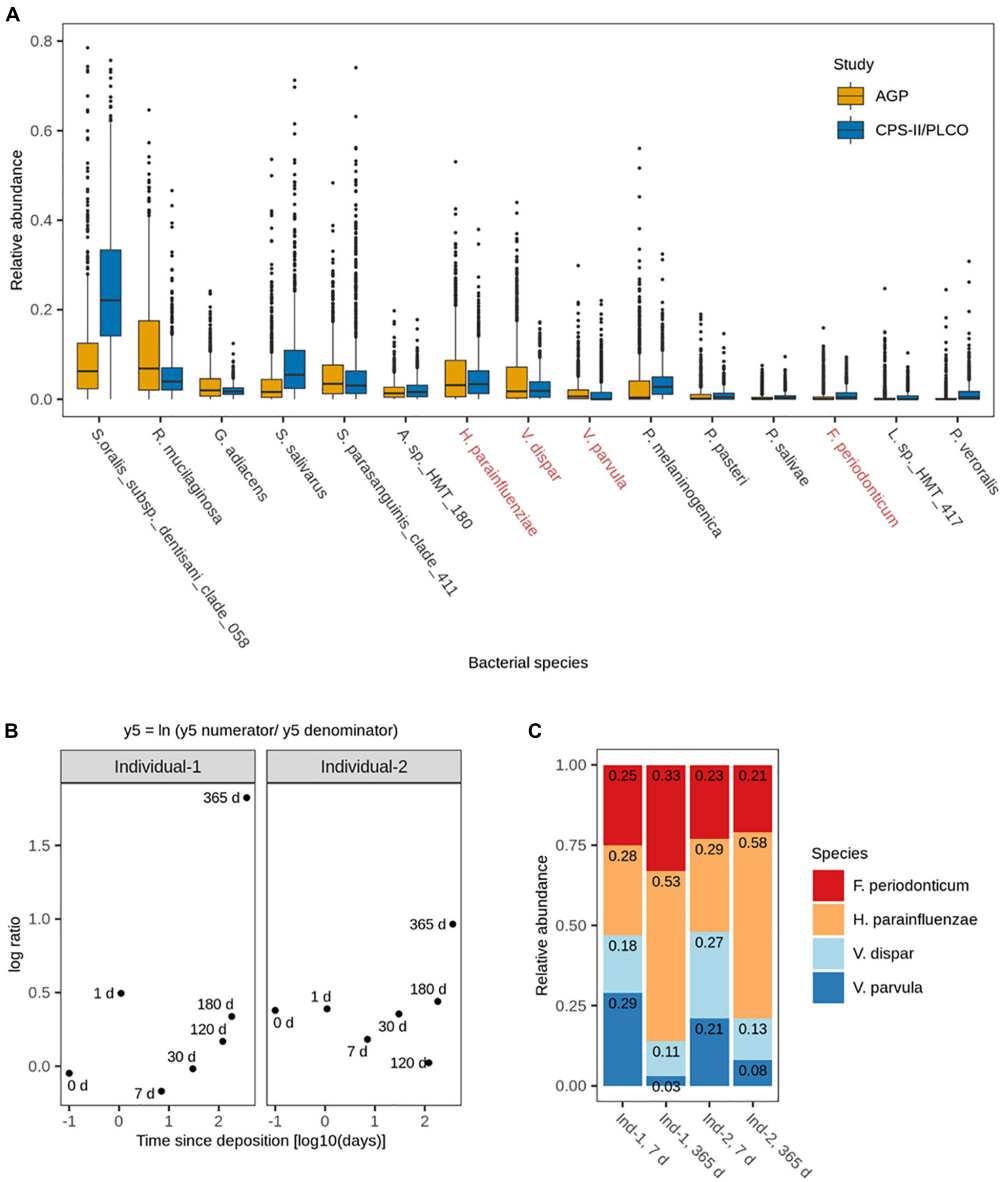

FIGURE 2 | (A) Relative abundances of the 15 most abundant and frequent bacterial species in human saliva from adults across the analyzed publicly available 16S rRNA gene NGS data sets (*N* = 1,848). Highlighted in red are the four bacterial species subsequently included in the 4-plex qPCR assay. **(B)** Log ratio balance y5, significantly different for the time since deposition in the *de-novo* generated 16S rRNA gene NGS data from the long-term (up to 1 year) dried saliva stains. Time since deposition days (*x*-axis) were log-transformed to facilitate the visualization of the earliest time points. Each dot represents a long-term dried saliva stain with its corresponding time since deposition. **(C)** Relative abundances of the four bacterial species from balance y5 (*Fusobacterium periodonticum, Haemophilus parainfluenzae, Veillonella dispar,* and *Veillonella parvula)* in the long-term (up to 1 year) dried saliva stains at day 7 and day 365 since stain deposition for both analyzed individuals.

Relationship Between Bacterial Abundance and Time Since Deposition in Short-Term Dried Saliva Stains Using Multiplex qPCR

Dried saliva stains from 15 individuals up to 1 month since deposition were analyzed using the 4-plex qPCR assay we developed. Parallel to the qPCR analysis, no signal above the set threshold was reported in the background (blank) swabs for any of the four bacterial markers and time points. The qPCR results obtained from the fresh (t0) samples confirmed that the four selected bacterial species were abundant and frequent in the saliva of all 15 individuals, although we observed high inter-individual variation within and between species. For each of the four species, the average and standard deviation (mean ± SD), as well as the minimum and maximum value (range), of qPCR-derived cell counts in 1 μL of isolated bacterial DNA solution (equivalent to 2 ng of total bacterial DNA) were as follows:

TABLE 1 | Significant log ratio balances for time since deposition in the differential abundance analysis.

Balance	Bacterial species	*p* value; time since deposition	*p* value; individual person
$y4_{numerator}$	*A. sp. HMT 180* *S. oralis subsp. dentisani clade 058* *S. parasangunis clade 411* *P. pasteri* *P. melaningenica* *P. veroralis*	0.008	0.390
$y4_{denominator}$	*F. periodonticum* *P. melaningenica* *V. dispar* *V. parvula*		
$y5_{numerator}$	*F. periodonticum* *H. parainfluenzae* *V. dispar*	0.004	0.911
$y5_{denominator}$	*V. parvula*		
$y7_{numerator}$	*F. periodonticum* *H. parainfluenzae*	0.022	0.022
$y7_{denominator}$	*V. dispar*		

The top 15 most abundant and frequent bacterial species in human saliva were sub-selected from the de-novo generated 16S rRNA gene NGS data obtained from the long-term dried saliva stains. Each balance is composed of the numerator's bacterial taxa and the denominator's bacterial taxa.

F. periodonticum (23,386 ± 24,598; range 2,698–105,567), *H. parainfluenzae* (83,854 ± 80,412; range 13,167–331,667), *V. dispar* (20,071 ± 27,406; range 399–91,937), and *V. parvula* (9,825 ± 21,354; range 309–92,347). A figure of the bacterial cell count distribution in fresh saliva samples for each of the four species can be found in **Supplementary Figure 2**.

We first investigated the time dependency of each of the four species in each individual in the dried saliva stains ranging from 2 days (t1) up to 30 days (t15) since deposition. The Chow test for equality showed no significant differences in the great majority of the compared time point swab duplicates' regressions. Exceptions were the univariate linear regressions for *F. periodonticum* in individual 2 (p = 0.010), individual 7 (p = 0.005), and individual 15 (p = 0.020) and for *H. parainfluenzae* in individual 6 (p = 0.020). We observed high inter-individual differences in terms of the amount of variation explained by time for each species' cell count (**Figures 3–6**). For example, in individual 5 the variation explained for *F. periodonticum* cell count was high in both duplicates (R^2 = 0.663, p = 1.06E–10 in duplicate 1; and R^2 = 0.522, p = 6.92E–08 in duplicate 2; **Figure 3**). However, the variation explained for *V. parvula* was much lower, even close to zero (R^2 = 0.001, p = 0.374 in duplicate 1; and R^2 = 0.062, p = 0.092 in duplicate 2; **Figure 6**). The univariate regression results including R^2 values, BH-corrected p values, and significance testing can be found in **Supplementary Table 4**.

For *F. periodonticum*, the qPCR-derived cell count increased over time for most individuals, except for individual 11, although at different rates in the different individuals. The average and standard deviation fold-change between day 2 (t1) and day 30 (t15) were 2.0 ± 0.6, range 1.1–3.3. The highest time-dependent bacterial increase was reported for individual 2 (R^2 = 0.825, p = 2.59E–14, sample duplicate 1; **Figure 3**). For *H. parainfluenzae,* the time-dependent behavior varied in an individual-specific manner meaning either increasing (individuals 1, 4, 5, 6, 7, 10, 13, and 14), decreasing (individuals 9 and 11), or barely changing (individuals 2, 3, 8, 12, and 15; **Figure 4**). For *V. dispar*, the cell count increased with time in the majority of the individuals at different rates, except individual 11. The average and standard deviation fold-change between day 2 (t1) and day 30 (t15) were 1.7 ± 1.1, range 1.1–7.0. The highest time-dependent bacterial increase was reported for individual 14 (R^2 = 0.623, p = 8.70E–10, sample duplicate 1; **Figure 5**). Lastly, for *V. parvula,* cell count increased with time for some individuals (individuals 1, 2, 4, 7, 10, 13, and 14), whereas for others it decreased (individuals 11, 12, and 15) or barely changed (individuals 3, 5, 6, and 9; **Figure 6**).

We next investigated the time dependency of the four bacterial species altogether in each individual (**Table 2**). The variation explained by time in the four species cell count varied among individuals, but it was very high in the majority of them with R^2 values ranging between 0.865 and 0.979 (p = <2.20E–16). The individual with the highest variation explained on average was individual 5 (R^2 = 0.964 in sample duplicate 1, R^2 = 0.979 in sample duplicate 2, p = <2.20E–16). The individual with the lowest variation explained on average was individual 8 (R^2 = 0.874 in duplicate 1, R^2 = 0.908 in duplicate 2, p = <2.20E–16). We also investigated the time dependency of each bacterial species considering the 15 individuals altogether (**Table 2**). The variation explained by time for each of the four bacterial species cell count in all individuals together was very high and significant. The strongest time dependency variation on average (R^2 in duplicate 1, R^2 in duplicate 2, and p value) was observed for *V. parvula* (R^2 = 0.969, R^2 = 0.948, p = <2.20E–16), followed by *H. parainfluenzae* (R^2 = 0.964, R^2 = 0.920, p = <2.20E–16), *V. dispar* (R^2 = 0.959, R^2 = 0.906, p = <2.20E–16), and finally *F. periodonticum* (R^2 = 0.941, R^2 = 0.889, p = <2.20E–16). Finally, we investigated the time dependency of the four bacterial species together in the 15 individuals altogether (**Table 2**) resulting in a significant variation, explained in the data set of R^2 = 0.544 in duplicate 1 and R^2 = 0.548 in duplicate 2, p = <2.20E–16.

Estimating the Time Since Deposition of Dried Human Saliva Stains Based on Bacterial DNA

We finally investigated the possibility of estimating the time since deposition of the dried saliva stains exposed to indoor short-term conditions of up to 1 month, using a generalized RF regression model. The correlation between real and predicted time since deposition values were very low (r = 0.11; **Supplementary Figure 3**) and the average MAE was 8 days. The real and predicted times since deposition for each individual are summarized in **Supplementary Table 5**. From these predicted values we deduced that the generalized approach was unable to discriminate between early and late times since deposition in the analyzed interval

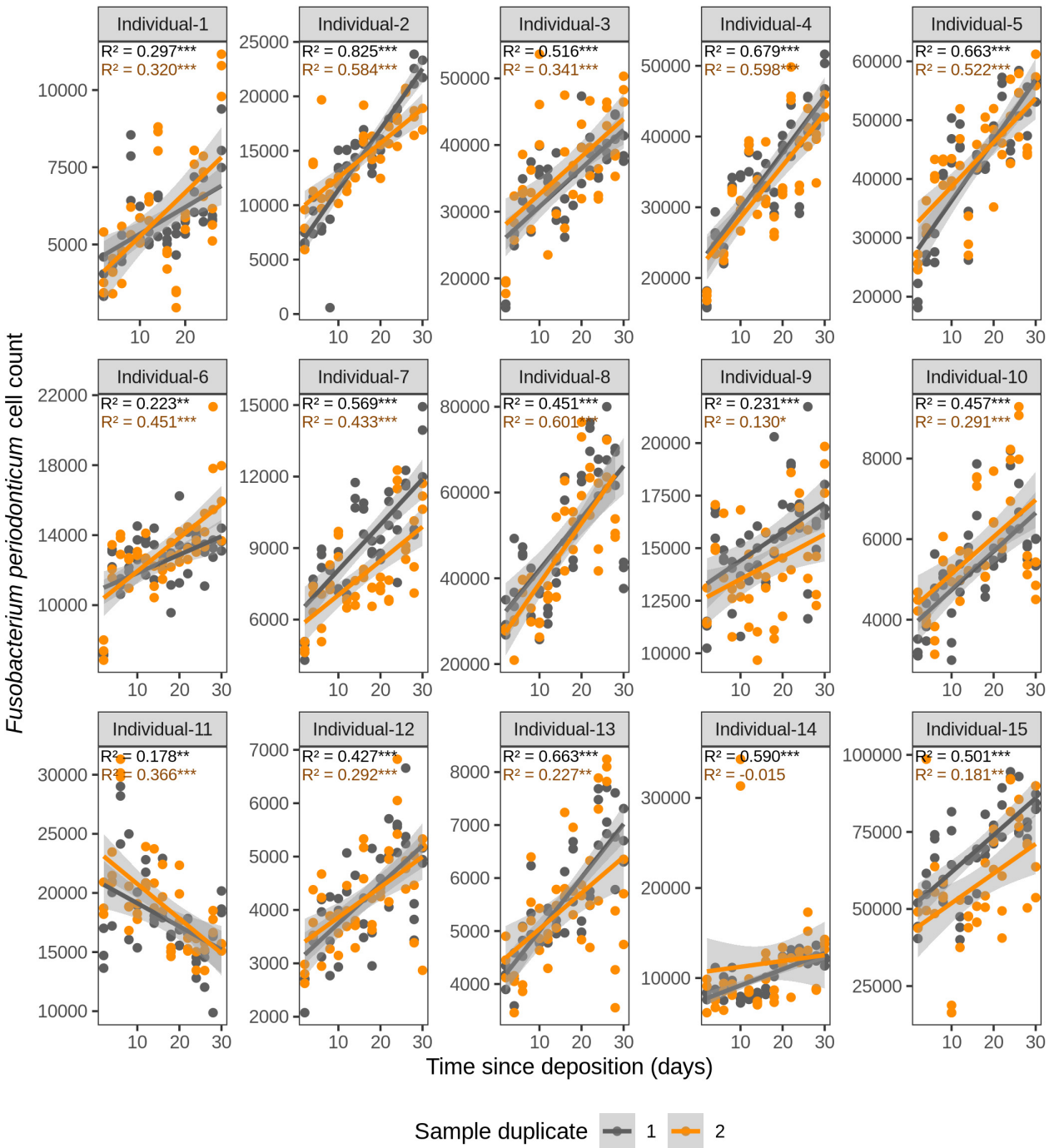

FIGURE 3 | Time-dependency of qPCR-based *Fusobacterium periodonticum* cell count for each individual in the short-term (up to 1 month) dried saliva stains from 15 individuals. Sample duplicate set 1 is indicated in gray and sample duplicate set 2 in orange. Each dot represents a qPCR-run sample triplicate. R^2 values indicate the variation explained by the time since deposition in the bacterial cell count. Asterisks indicate the significance level of the Benjamini-Hochberg corrected *p* values as follows: 0.001 "***", 0.01 "**", and 0.05 "*".

of 1 month. For instance, in individual 4 for whom all times since deposition were predicted as either 20 or 21 days and individual 7 for whom all times since deposition were predicted as 16, 17, or 18 days (**Supplementary Table 5**). Hence, the time-dependent variation in the four targeted bacterial species were surpassed by the high inter-individual variation in our data set. The high inter-individual variation can be observed using principal component analysis (PCA; **Figure 7**) where the saliva stains cluster based on the individual. Hence, because of the high inter-individual variation we observed, as

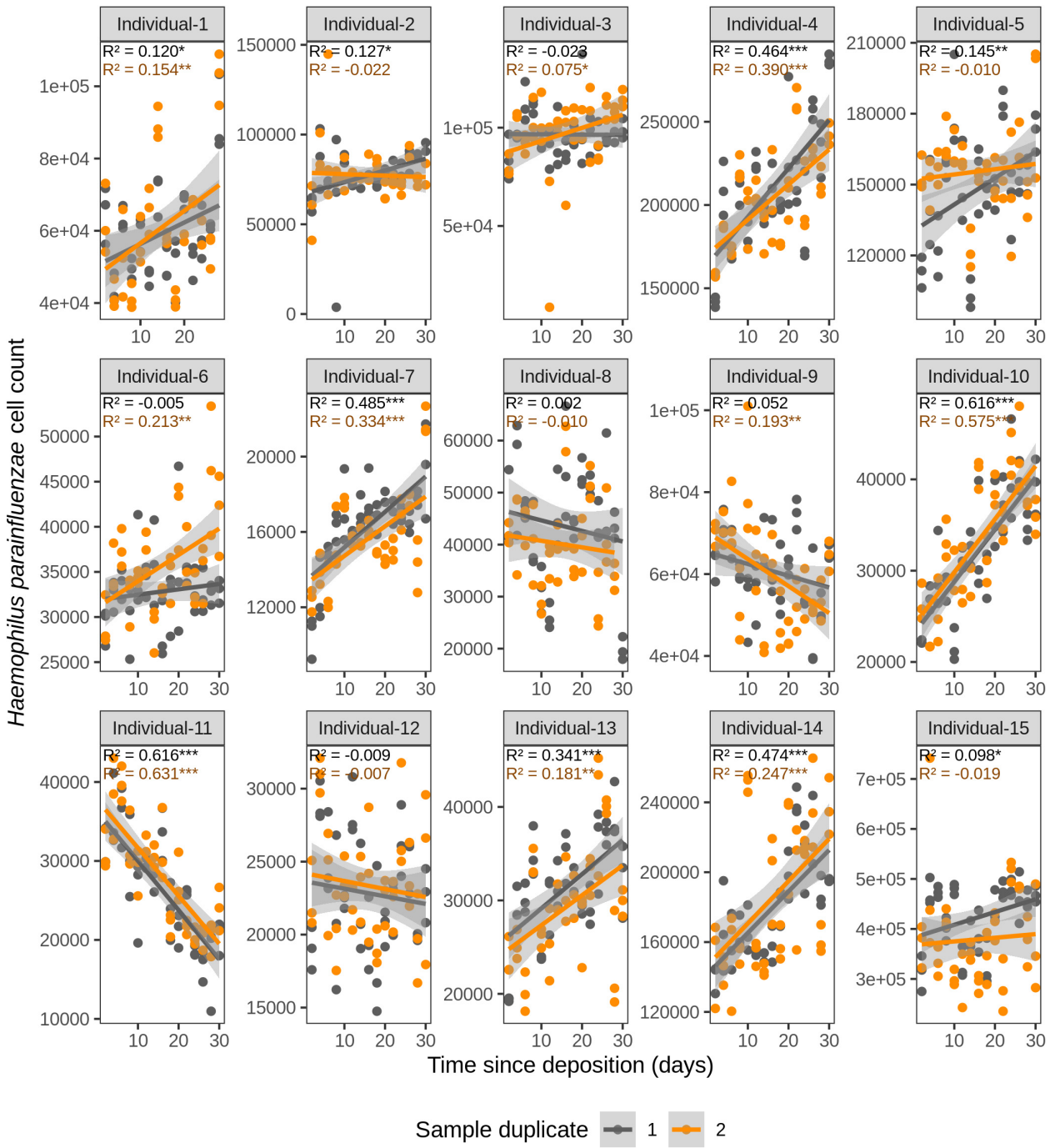

FIGURE 4 | Time-dependency of qPCR-based *Haemophilus parainfluenzae* cell count for each individual in the short-term (up to 1 month) dried saliva stains from 15 individuals. Sample duplicate set 1 is indicated in gray and sample duplicate set 2 in orange. Each dot represents a qPCR-run sample triplicate. R^2 values indicate the variation explained by the time since deposition in the bacterial cell count. Asterisks indicate the significance level of the Benjamini-Hochberg corrected *p* values as follows: 0.001 "***", 0.01 "**", and 0.05 "*".

described in section "Relationship between bacterial abundance and time since deposition in short-term dried saliva stains using multiplex qPCR," which limited the implementation of a generalized model in our data set, we built individual-specific models.

This individual-specific modeling approach enabled us to present an individualized solution to saliva trace timing in our data set, where the model training and testing data are obtained from the individual's reference saliva stored under the same environmental conditions for a specific time period

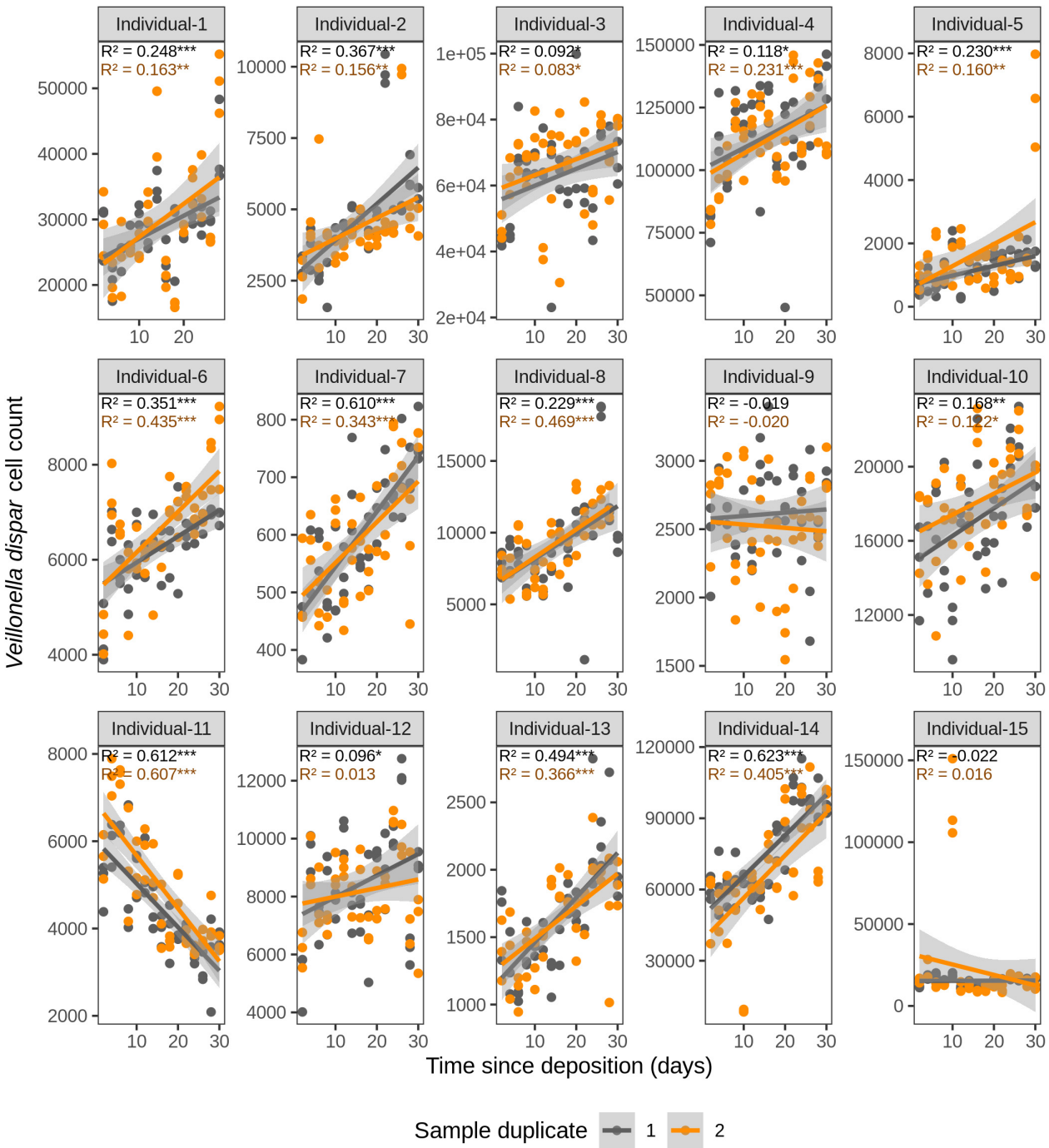

FIGURE 5 | Time-dependency of qPCR-derived *Veillonella dispar* cell count for each individual in the short-term (up to 1 month) dried saliva stains from 15 individuals. Sample duplicate set 1 is indicated in gray and sample duplicate set 2 in orange. Each dot represents a qPCR-run sample triplicate. R^2 values indicate the variation explained by the time since deposition in the bacterial cell count. Asterisks indicate the significance level of the Benjamini-Hochberg corrected *p* values as follows: 0.001 "***", 0.01 "**", and 0.05 "*".

(**Figure 1E**). We hypothesize that for certain indoor crimes where environmental conditions are rather stable, various parameters (temperature, humidity, etc.) could be measured at the crime scene when the stain is collected and applied to the reference saliva stains used to generate the model underlying data with flexibility for the time window. Consequently, in our experiments, we applied the same environmental parameters to saliva samples stored up to 1 month that we used for model training and model testing. The R^2 and BH-corrected *p* values of each individual-specific model can be found in

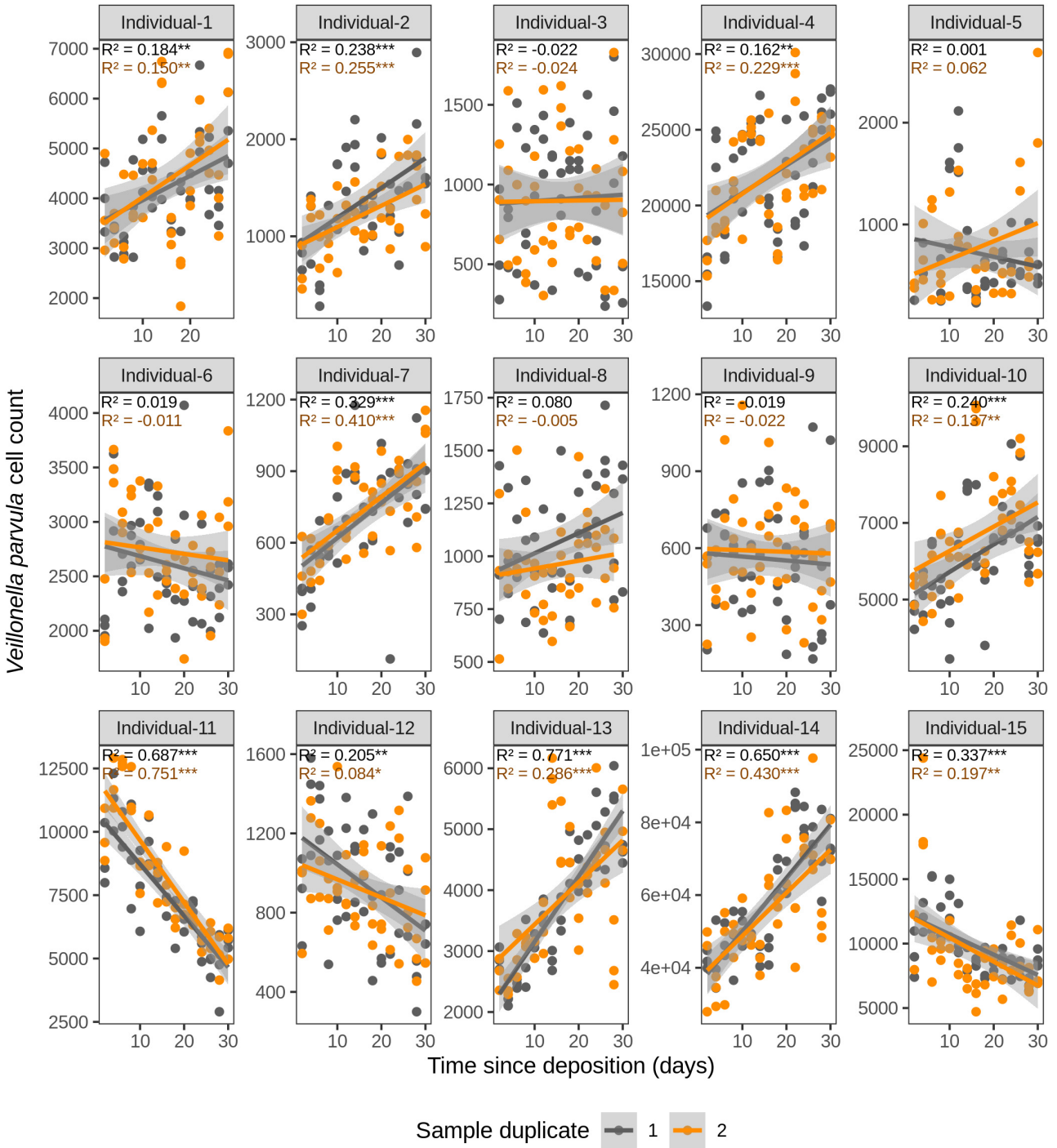

FIGURE 6 | Time-dependency of qPCR-derived *Veillonella parvula* cell count for each individual in the short-term (up to 1 month) dried saliva stains from 15 individuals. Sample duplicate set 1 is indicated in gray and sample duplicate set 2 in orange. Each dot represents a qPCR-run sample triplicate. R^2 values indicate the variation explained by the time since deposition in the bacterial cell count. Asterisks indicate the significance level of the Benjamini-Hochberg corrected *p* values as follows: 0.001 "***", 0.01 "**", and 0.05 "*".

Supplementary Table 6. Overall, the average model fit was R^2 = 0.752. The best model fit was obtained for individual 11 (R^2 = 0.921, p = 4.80E–05), whereas for individual 1 the model barely fit (R^2 = 0.178, p = 0.233).

Considering the testing stains of all 15 individuals, the average correlation between the true and predicted time since deposition was r = 0.742, while the average MAE was 5 days (16.7% of the analyzed time frame of 1 month). The model for individual 8

TABLE 2 | Time-dependency of the bacterial marker cell counts in the dried saliva stains exposed to indoor conditions up to 1 month for sample duplicate sets 1 and 2.

		Sample duplicate 1		Sample duplicate 2	
Linear regression analysis		R^2	***p* value**	R^2	***p* value**
lm(C ~ T*S)	Individual 1	0.922	<2.2E–16***	0.865	<2.2E–16***
	Individual 2	0.952		0.948	
	Individual 3	0.940		0.907	
	Individual 4	0.955		0.966	
	Individual 5	0.964		0.979	
	Individual 6	0.968		0.962	
	Individual 7	0.973		0.966	
	Individual 8	0.874		0.908	
	Individual 9	0.965		0.946	
	Individual 10	0.953		0.950	
	Individual 11	0.912		0.927	
	Individual 12	0.936		0.946	
	Individual 13	0.968		0.937	
	Individual 14	0.959		0.905	
	Individual 15	0.968		0.902	
lm(C ~ T*I)	*F. periodonticum*	0.941		0.889	
	H. parainfluenzae	0.964		0.920	
	V. dispar	0.959		0.906	
	V. parvula	0.969		0.948	
lm(C ~ T*I + T*S)	Overall	0.546		0.551	

*lm(C ~ T*S): time-dependency of the four selected bacterial species altogether in each individual, lm(C ~ T*I): time-dependency of each selected bacterial species considering the 15 individuals altogether, and lm(C ~ T*I + T*S): time-dependency of the four selected bacterial species and 15 individuals altogether. R^2 values indicate the variation explained by the time since stain deposition in the qPCR-derived bacterial cell counts. Asterisks indicate the significance level of the Benjamini-Hochberg corrected p values as follows: 0.001 "***", 0.01 "**", and 0.05 "*".*

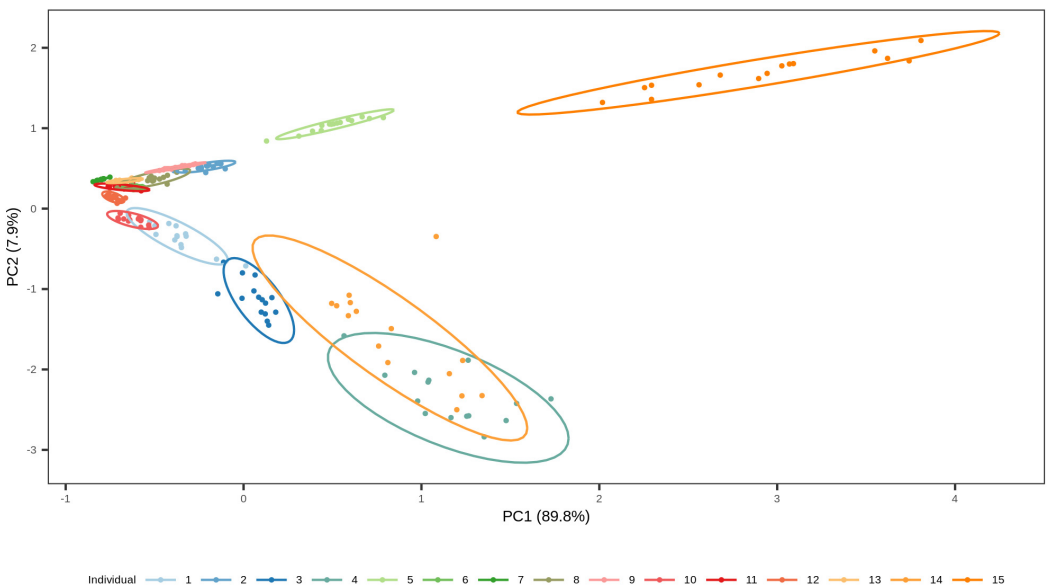

FIGURE 7 | Two-dimensional plot from principal component analysis (PCA) of the short-term dried saliva stains from 15 individuals. Projection of the counts of our four targeted species in the first two PCs together explains 97.7 % of the total variation. The stains cluster based on the individual, which highlights the high inter-individual variation in the data set.

presented the lowest MAE of 3.3 days with a correlation between real and predicted values of r = 0.905 (**Figure 8**). The model for individual 14 presented the highest MAE of 7.8 days with a correlation between real and predicted values of r = 0.235 (**Figure 8**). The real and predicted times since deposition for each individual are summarized in **Supplementary Table 5**. We

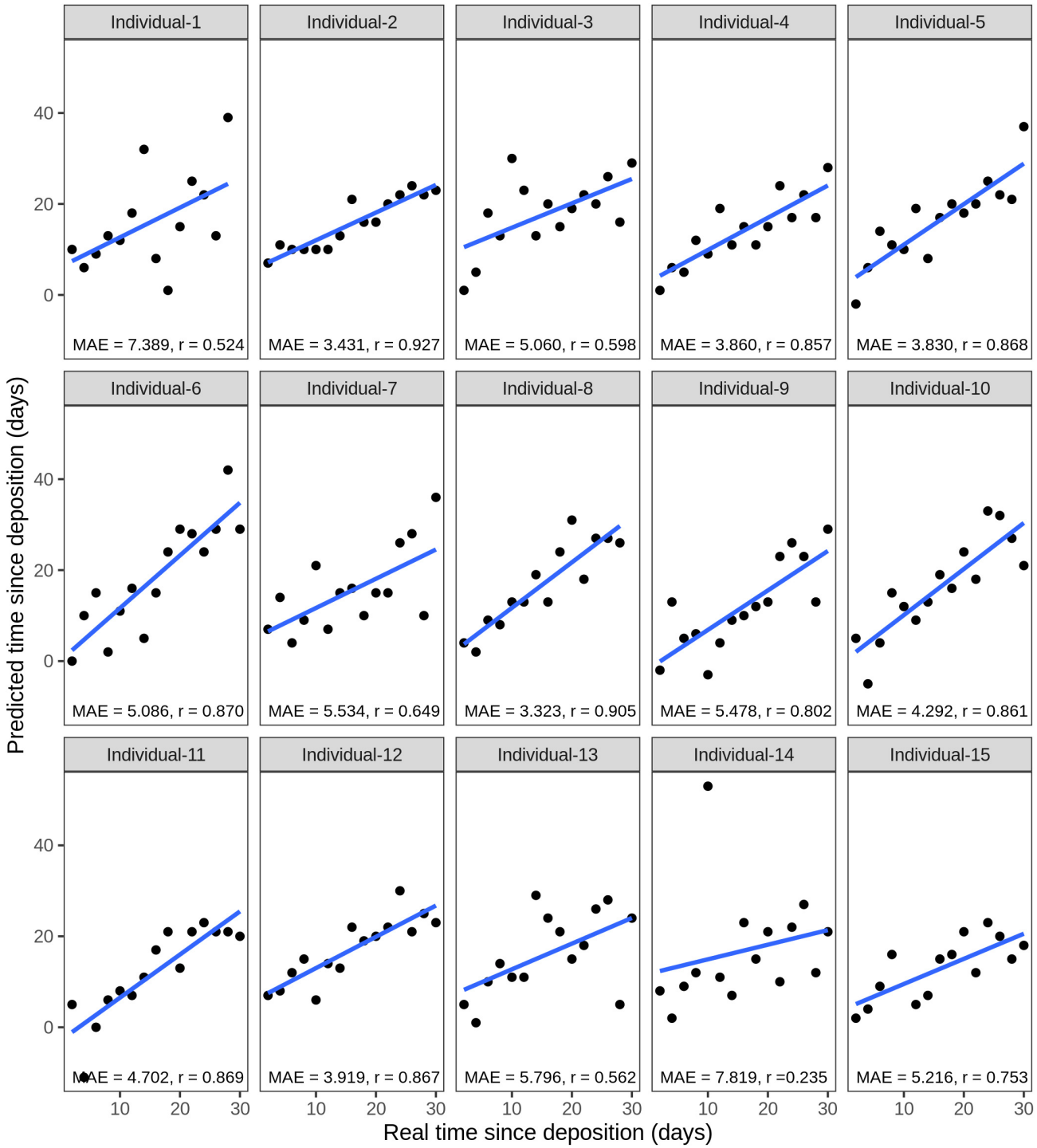

FIGURE 8 | Individual-specific model performance for the prediction of the time since deposition of saliva stains, using data of the short-term (up to 1 month) stored saliva stains based on four bacterial species from 15 individuals. Data from sample duplicates 2 were used for model testing, while data from sample duplicates 1 were used for model building. The mean absolute error (MAE) measures the discrepancies between the real and the predicted time since deposition values. The correlation between real and predicted values is indicated with *r*.

further investigated errors in the time since deposition prediction in the individual-specific approach (**Supplementary Figure 4**). There was no clear pattern relating to certain individuals or time points with lower errors. The time since deposition of eleven stains (5.0%) was correctly predicted with zero days error. In the rest of the predictions, there was a similar distribution in the

stains in which time since deposition was underestimated (113 stains, 50.9%) or overestimated (98 stains, 44.1%). In 81.5% of the cases (181 stains), the error of the predicted time since deposition fell to within 1 week (up to ±7 days error). From those, more than half of the samples fell within 3 days (±3 days error). More precisely, 16.7% (37 stains) were predicted with ±1 day; 17% (38 stains) with ±2 days; and 9% (20 stains) with ±3 days error.

Additionally, we estimated the time since deposition of short-term dried saliva stains from the six individuals that we collected and exposed to indoor conditions 7 months after the first collection time point. Considering the tested stains of all 6 individuals, the average MAE was 8.8 days (29.3% of the analyzed time frame of 1 month). The one-variable predictor model for individual 1 presented the lowest MAE of 3.9 days. The four-variable predictor model for individual 2 presented the highest MAE of 16.9 days. The MAE values of all the individual-specific models of one, two, three, and four species as predictors for time since deposition can be found in **Supplementary Table 7**.

DISCUSSION

Knowledge of the time when a human biological stain was left at a crime scene – also known as time since deposition – can be of great forensic value in assessing the alibis of known suspects, searching for suspects, selecting the stains with the highest informative value for further analysis, helping in missing person cases when the time they went missing is unknown, and in estimating PMI in scenes involving a corpse, or parts thereof. In this study, we evaluated for the first time a microbial DNA-based approach to estimating the time since deposition of dried saliva stains exposed to indoor conditions.

First, we identified the most abundant and most frequent bacterial species in human saliva samples from two publicly available 16S rRNA gene sequencing data sets (Wu et al., 2016; McDonald et al., 2018). On the one hand, we looked for abundant species to ensure their detection in forensic-type saliva samples, which are often as small as a few microliters (μL) in volume. On the other hand, we also looked for frequent species, meaning that they are more likely to be present in the general population; hence, in the great majority of saliva stains found at crime scenes. For our final choice, we focused on species that are both abundant and frequent species at the same time since taxa "exclusive" to an individual often account for a significant percentage of an individual's microbiome profile (Costello et al., 2009; Nasidze et al., 2009; Zaura et al., 2009; Lazarevic et al., 2010; Huse et al., 2012; Li et al., 2013, 2014; Hall et al., 2017). The top 15 bacterial species identified as both most abundant and most frequent in our samples belonged to genera previously reported to be predominant taxa in saliva and part of the so-called "core" oral microbiome (Costello et al., 2009; Nasidze et al., 2009; Zaura et al., 2009; Lazarevic et al., 2010; Huse et al., 2012; Li et al., 2013, 2014; Hall et al., 2017). Our observations agree with these previous studies, reporting that the saliva microbiome is dominated by just a few taxa, while most of the taxa detected per individual are rare.

Second, we analyzed the microbiome profiles of dried saliva stains exposed to our laboratory environment long-term (up to 1 year) and focused our time-dependent analysis on the previously selected 15 most abundant and frequent bacterial species. Based on differential abundance analysis, we identified four species, the abundance of which significantly changed over time since deposition: *F. periodonticum, H. parainfluenzae, V. dispar,* and *V. parvula.* It is noted that three of the species are obligate anaerobes (*F. periodonticum, V. dispar,* and *V. parvula*), while the fourth one is a facultative anaerobe (*H. parainfluenzae*). Theoretically, obligate anaerobes might be depleted upon exposure to an oxygen-rich environment such as our laboratory, as a previous study also reported this for *Veillonella* genus (Salzmann et al., 2019). We hypothesize that the selected bacterial species co-aggregate *ex vivo* with other saliva microbes forming biofilms and having access to nutrients and molecules for survival and protection. The removal of oxygen by aerobic and facultative anaerobes could create "pockets" of anoxia that support the growth of obligate anaerobes, in a process similar to what happens in human dental plaque both *in vivo* (Schaechter, 2009) and *ex vivo* (Diaz et al., 2002). Obligate anaerobic organisms can also metabolize oxygen and produce protective enzymes in response to oxidative stress (Marquis, 1995; Jabłońska and Tawfik, 2019). Additionally, the bacterial *ex vivo* co-aggregates could be advantageous for the more efficient utilization of nutrients and molecules found in saliva, as previously reported (Bradshaw et al., 1994; Kuramitsu and Ellen, 2000; Periasamy and Kolenbrander, 2009). The method we employed reported only relative abundance changes of the four species over time, though different scenarios could explain the direction of these changes. For example, the increase in the selected reference log ratio balance from 7 to 365 days since deposition could be explained by one of the following five scenarios of absolute abundance changes: (i) the numerator's taxa increased on average; (ii) the denominator's taxa decreased on average; (iii) a combination of the previous two happened; (iv) both the numerator's and denominator's taxa increased, but the numerator's taxa increased more compared to the denominator's taxa; and (v) the numerator's and denominator's taxa both decreased, but the denominator's taxa decreased more compared to the numerator's taxa.

In line with our findings, other published studies also indicated time-dependent microbiome changes in the dried saliva samples exposed to indoor conditions. Though not the main aim of their study, Salzmann et al., 2019 analyzed the microbial communities in both the fresh and dried saliva samples exposed to their laboratory environment for both 5 and 9 months. Via differential abundance analysis using DESeq2 (Love et al., 2014) they showed that four facultative and obligate anaerobic bacteria were significantly depleted upon exposure to indoor conditions: *Actinomyces, Staphylococcus, Veillonella,* and an unclassified genus from the *Leptotrichiaceae* family. However, no definitive conclusions could be drawn due to the small sample size in the study ($n = 4$, two fresh and two dried saliva stains). Moreover, the analysis employed for the differential abundance testing (DESeq2; Love et al., 2014) was originally developed for RNA-Seq data and requires further development for general use on microbiome data (Weiss et al., 2017). While the authors did not report their results at the species level, looking at the genus level two of the four

bacterial species we selected as time-dependent markers belong to the genus *Veillonella*, and one of the 15 species identified as most abundant and most frequent belong to the *Actinomyces* genus and another to the *Leptotrichiaceae* family.

We are aware of the limitation that only two individuals were studied in the differential abundance analysis of the long-term dried saliva stains. This was mainly due to the technical and financial restrictions of our NGS analysis, but we consider it sufficient for a proof of principle study. In the future, analysis of more individuals for targeted time periods will add to these results and perhaps reveal additional promising biomarkers. Our study also only analyzed the four most promising bacterial species via a targeted analysis. However, based on the promising follow-up results, future work could focus on the analysis of all the top 15 most abundant and frequent species as identified from the publically available adult human saliva 16S gene NGS data sets. The other eleven bacterial species might potentially similarly participate in an *ex vivo* microbial consortium (Kolenbrander, 2011). Hence, potential time-dependent changes in their abundance could serve as powerful additional estimators of the time since deposition of saliva stains.

Based on the four differentially abundant and frequent bacterial species, we developed a 4-plex qPCR assay to test the forensic applicability in dried saliva stains exposed to indoor short-term conditions of up to 1 month. A prerequisite for applying such a qPCR assay in a stain would be to confirm its body fluid source being saliva. For this, it is possible to apply another microbiome-based approach for the conclusive identification of saliva stains, as we recently showed in a previous study (Díez López et al., 2019). The four species targeted with the 4-plex qPCR assay were detected in the fresh saliva (t0) of all 15 analyzed individuals, confirming that they are abundant and frequent enough for forensic use. Interestingly, the qPCR-reported cell counts of our four targeted bacterial species increased with time since deposition for the majority of the analyzed individuals. However, high inter-individual differences were observed in the variation explained by time in the species abundance. Nevertheless, there was no clear relationship between a higher explained variation and initial species abundance (t0). We are not very surprised by this, as this variation between individuals could be explained by bacterial interactions. For example, other bacteria taxa present in the sample might have interacted with our targeted species in different ways (i.e., mutualism, syntrophism, commensalism, proto-cooperation, antagonism, competition, parasitism, and predation). The presence and abundance of certain nutrients and molecules in the saliva at the time since deposition could also favor or impair some of these interactions. Finally, while qPCR is a well-established and suitable method for this study, it is also possible to transfer the protocol to newer, more sensitive methods, such as digital droplet PCR, in the future.

For estimating the time since deposition of our saliva stains, we first built a generalized prediction model. By this, we attempted to estimate the time when an "unknown" test stain was deposited based on a previously established model. However, the high inter-individual variation in our data set limited the possibility of implementing such a model. Though time-dependent changes in the four targeted bacteria occurred in the short-term dried saliva stains (up to 1 month) from all the 15 analyzed individuals, the magnitude and evolution through time of those changes were very specific to each individual. As a result, the estimation of the time since deposition of an individual's stains based on a model trained with stains from other individuals was not feasible with our data set. To further explore the possibility of a generalized model, future studies might employ a much bigger sample size; not only regarding the number of individuals but also regarding the tested environmental conditions. This could enable a better understanding of whether a broad range of inter-individual and different environmental effects can be captured during model building. These effects, together with the bacterial-based time-dependent information, might result in a generalized model being applicable to unknown stains that originate from random individuals in the population, exposed to different environmental conditions.

Based on the limitation of applying a generalized model in our data set, we decided to build individual-specific models to predict the time since deposition of these short-term dried saliva stains. For each individual, we employed the first sample duplicate set for model training and the second for model testing. With this, we aimed to mimic forensic investigations with our data set, where the estimation of the time since deposition of one or various stains is possible based on a model built from a reference set of dried saliva stains from the same individual exposed to adequate storage conditions and time frames (e.g., indoor storage conditions for a particular period of time; **Figure 1E**). We acknowledge that different factors might affect the model building and accuracy; particularly, the environment the stain is exposed to; i.e., temperature, relative humidity, ambient light, availability of nutrients, and molecules, the template bacterial community present in the stain at the time of deposition (which seems to be affected by individual characteristics), and the time since deposition itself. All these factors are expected to influence the time-dependent changes in the bacterial biomarkers, which could be accounted for by an individualized solution as we do in our data set in more dedicated future studies. The reported MAE values in these individual-specific models further highlighted the observed inter-individual differences, ranging from 3.3 to 7.8 days (average of 5 days). In contrast to RNA-based studies, we did not observe increased prediction errors with increased storage times. There is only one published RNA-based study on the time since deposition estimation of dried saliva stains we can compare our results with (Asaghiar and Williams, 2020). That study reported a slightly lower MAE value (3.5 *vs.* 5 days); however, the sample size was much larger in our study (222 samples from 15 different individuals *vs.* 5 samples). A different study analyzing dried blood stains reported a time estimation error of 2–4 weeks for stains exposed less than 6 months, which we improved in our study for dried saliva stains (Fu and Allen, 2019).

This study observed an increase in the MAE values in the short-term dried saliva stains collected 7 months later, ranging from 3.9 to 16.9 days (average of 8.8 days) compared to a

range of 3.3 to 7.8 days (average of 5 days) from the first sample collection. In the same way that different environmental factors can affect the PMI of human cadavers (Belk et al., 2018; Dash and Das, 2020), the time since deposition estimation of dried body fluid stains could be affected by variations in the exposure conditions. We hypothesize that one factor affecting our predictions might be the season, since the first round of stains were collected and exposed during spring and the second round during autumn, with the consequent differences in average temperatures (slightly lower in autumn) and daylight duration (8 *vs.*11 h), even in indoor conditions (since stains were placed 4 m away from a window). It could also happen that the *in vivo* abundance of some of the four selected bacterial species varied between the two saliva collection time points, 7 months apart from each other, which could happen due to changes in an individual's health status or lifestyle habits, affecting the subsequent time-dependent bacterial abundance changes in the prepared stains. However, given the more extensive previous data sets demonstrating time-wise microbiome stability in saliva *in vivo* (Costello et al., 2009; Lazarevic et al., 2010; Stahringer et al., 2012; Zhu et al., 2012), and the absence of available information on potential changes in our volunteers' health status and lifestyle habits, our preliminary data need to be considered with care and larger data evidence needs to be established in the future.

More dedicated future research might focus on increasing the reliability of the individual-specific prediction models by, for example, increasing the model training sample size. For instance, instead of preparing and collecting dried stains every 2 days, shorter time frames could be analyzed (i.e., daily or every a few hours), which may better reflect the rapid division rates of bacterial cells when the conditions are favorable. A bigger training set would also mean the possibility of investigating more complex prediction models that can capture other time-dependent changes that are less linear. Additionally, DNA-based analysis can be reliable in time-dependent bacterial "growing" patterns but might present limitations in "decaying" patterns since living and dead cells cannot be distinguished. An alternative could be bacterial RNA-based analysis in which only the live bacterial fraction is analyzed or a combined approach of bacterial DNA/RNA analysis. Before our proposed approach is considered for future forensic applications various forensic developmental and implementation criteria will need to be met. For instance, future research should deal with the suitability of the approach under different scenarios, such as sample volume and sample substrate (e.g., cigarette butts, chewing gums, food utensils, and fabrics) as well as environmental factors (e.g., average temperature, percentage of air humidity, and ambient daylight hours).

CONCLUSION

To the best of our knowledge, this research is the first to show from a forensic standpoint, how commensal human bacteria absolute abundance changes can be used to estimate the time since deposition of dried saliva stains. We focused on the abundant and frequent commensal bacterial species of the saliva of human adults, aiming for applications in forensic-type saliva stains from the general population. We observed that, though high inter-individual variation was found, the four selected bacterial species present a high and significant correlation between their abundance in saliva stains and the time since deposition of saliva stains. The data set presents an individual-specific solution for estimating stain time since deposition. We hypothesize that this might be forensically feasible when a saliva reference sample is used to produce the prediction model underlying data based on samples stored for different time intervals under specific environmental conditions that resemble those to which the crime scene stain was exposed, such as in cases of indoor crimes, though more dedicated future research is needed to confirm our hypothesis. While we consider 1 month as a forensically realistic time frame between stain deposition at a crime scene and reference sample collection from potential suspects for the majority of forensic cases, shorter or longer time spans could be studied in more detail to analyze the extended potential forensic utility of our approach.

Our proof-of-principle study suggests that like in other forensic applications, the human microbiota has promising future forensic applications for estimating the time since deposition of a saliva stain at a crime scene. In the future, this novel approach may be expanded to other forensically relevant human stains containing microbial DNA. Before such microbiome-based stain timing can be further considered for practical forensic applications, further microbiome research is needed to better understand and model all the factors contributing to the bacterial time-dependent changes. Additionally, various forensic developmental and forensic implementation criteria will need to be met via more dedicated studies in future.

DATA AVAILABILITY STATEMENT

The processed NGS and qPCR data produced and used in this study to perform our analysis and derive our conclusions are included in **Supplementary Data Sheet 1**.

ETHICS STATEMENT

The studies involving human participants were reviewed and approved by Medische Ethische Toestsings Commissie Erasmus MC (MEC-2018–1731). The patients/participants provided their written informed consent to participate in this study.

AUTHOR CONTRIBUTIONS

AV conceptualized the work. CDL and AV designed the study with contributions by MK. CDL performed all experiments and data analyses. CDL and AV interpreted the data with contributions by MK. MK provided resources. All authors wrote the manuscript and approved its final version.

FUNDING

The work of all authors is supported by Erasmus MC University Medical Center Rotterdam. AV was additionally supported by a EUR fellowship by Erasmus University Rotterdam.

ACKNOWLEDGMENTS

We are grateful to all volunteers for their kind donation of biological samples and to the authors of ACS CPS-II, PLCO, and AGP for making their data publically available. We thank Benjamin Planterose and Diego Montiel Gonzalez (Erasmus MC) for their valuable guidance in statistical analysis, as well as Eric M.J. Bindels (Erasmus MC) for providing us with access and help in use the Illumina® MiSeq platform. Finally, we also thank Qiagen for supplying the QIAseq™ 16S/ITS Panel Kit as a prize to CDL for having been selected amongst the top 10 finalists in the 2018 Qiagen Microbiome Award (PhD student category).

SUPPLEMENTARY MATERIAL

The Supplementary Material for this article can be found online at: https://www.frontiersin.org/articles/10.3389/fmicb.2021.647933/full#supplementary-material

REFERENCES

Adserias-Garriga, J., Quijada, N. M., Hernandez, M., Rodríguez Lázaro, D., Steadman, D., and Garcia-Gil, L. J. (2017). Dynamics of the oral microbiota as a tool to estimate time since death. *Mol. Oral Microbiol.* 32, 511–516. doi: 10.1111/omi.12191

Alshehhi, S., and Haddrill, P. R. (2019). Estimating time since deposition using quantification of RNA degradation in body fluid-specific markers. *Forensic Sci. Int.* 298, 58–63. doi: 10.1016/j.forsciint.2019.02.046

Amany, T. M. K. S., Ali, A. H., and Awad, A. (2018). Validation of mRNA and microRNA profiling as tools in qPCR for estimation of the age of bloodstains. *Life Sci.* 15, 1–7. doi: 10.7537/marslsj150618.01

Anderson, S. E., Hobbs, G. R., and Bishop, C. P. (2011). Multivariate analysis for estimating the age of a bloodstain. *J. Forensic Sci.* 56, 186–193. doi: 10.1111/j.1556-4029.2010.01551.x

Asaghiar, F., and Williams, G. A. (2020). Evaluating the use of hypoxia sensitive markers for body fluid stain age prediction. *Sci. Justice* 60, 547–554. doi: 10.1016/j.scijus.2020.09.001

Bates, D., Mächler, M., Bolker, B., and Walker, S. (2015). Fitting linear mixed-effects models using lme4. *J. Stat. Softw.* 67:119129. doi: 10.18637/jss.v067.i01

Bauer, M. (2007). RNA in forensic science. *Forensic Sci. Int. Genet.* 1, 69–74. doi: 10.1016/j.fsigen.2006.11.002

Bauer, M., Polzin, S., and Patzelt, D. (2003). Quantification of RNA degradation by semi-quantitative duplex and competitive RT-PCR: a possible indicator of the age of bloodstains? *Forensic Sci. Int.* 138, 94–103. doi: 10.1016/j.forsciint.2003.09.008

Belk, A., Xu, Z. Z., Carter, D. O., Lynne, A., Bucheli, S., Knight, R., et al. (2018). Microbiome data accurately predicts the postmortem interval using random forest regression models. *Genes (Basel)* 9:104. doi: 10.3390/genes9020104

Bolyen, E., Rideout, J. R., Dillon, M. R., Bokulich, N. A., Abnet, C. C., Al-Ghalith, G. A., et al. (2019). Reproducible, interactive, scalable and extensible microbiome data science using QIIME 2. *Nat. Biotechnol.* 37, 852–857. doi: 10.1038/s41587-019-0209-9

Bradshaw, D. J., Homer, K. A., Marsh, P. D., and Beighton, D. (1994). Metabolic cooperation in oral microbial communities during growth on mucin. *Microbiology* 140, 3407–3412. doi: 10.1099/13500872-140-12-3407

Burcham, Z. M., Garneau, N. L., Comstock, S. S., Tucker, R. M., Knight, R., Metcalf, J. L., et al. (2020). Patterns of oral microbiota diversity in adults and children: a crowdsourced population study. *Sci. Rep.* 10:2133. doi: 10.1038/s41598-020-59016-0

Butler, J. M. (2004). Short tandem repeat analysis for human identity testing. *Curr. Protoc. Hum. Genet.* Chapter 14, Unit148. doi: 10.1002/0471142905.hg1408s41

Callahan, B. J., McMurdie, P. J., Rosen, M. J., Han, A. W., Johnson, A. J. A., and Holmes, S. P. (2016). DADA2: high-resolution sample inference from Illumina amplicon data. *Nat. Methods* 13:581. doi: 10.1038/nmeth.3869

Costello, E. K., Lauber, C. L., Hamady, M., Fierer, N., Gordon, J. I., and Knight, R. (2009). Bacterial community variation in human body habitats across space and time. *Science* 326, 1694–1697. doi: 10.1126/science.1177486

Curtis, M. A., Zenobia, C., and Darveau, R. P. (2011). The relationship of the oral microbiotia to periodontal health and disease. *Cell Host Microbe* 10, 302–306. doi: 10.1016/j.chom.2011.09.008

Dash, H. R., and Das, S. (2020). Thanatomicrobiome and epinecrotic community signatures for estimation of post-mortem time interval in human cadaver. *Appl. Microbiol. Biotechnol.* 104, 9497–9512. doi: 10.1007/s00253-020-10922-3

Diaz, P. I., Zilm, P. S., and Rogers, A. H. (2002). *Fusobacterium nucleatum* supports the growth of *Porphyromonas gingivalis* in oxygenated and carbon-dioxide-depleted environments. *Microbiology* 148, 467–472. doi: 10.1099/00221287-148-2-467

Díez López, C., Montiel González, D., Haas, C., Vidaki, A., and Kayser, M. (2020). Microbiome-based body site of origin classification of forensically relevant blood traces. *Forensic Sci. Int. Genet.* 47:102280. doi: 10.1016/j.fsigen.2020.102280

Díez López, C., Vidaki, A., Ralf, A., Montiel González, D., Radjabzadeh, D., Kraaij, R., et al. (2019). Novel taxonomy-independent deep learning microbiome approach allows for accurate classification of different forensically relevant human epithelial materials. *Forensic Sci. Int. Genet.* 41, 72–82. doi: 10.1016/j.fsigen.2019.03.015

Dobay, A., Haas, C., Fucile, G., Downey, N., Morrison, H. G., Kratzer, A., et al. (2019). Microbiome-based body fluid identification of samples exposed to indoor conditions. *Forensic Sci. Int. Genet.* 40, 105–113. doi: 10.1016/j.fsigen.2019.02.010

Escapa, I. F., Chen, T., Huang, Y., Gajare, P., Dewhirst, F. E., and Lemon, K. P. (2018). New insights into human nostril microbiome from the expanded human oral microbiome database (eHOMD): a resource for the microbiome of the human aerodigestive tract. *mSystems* 3:e00187-18. doi: 10.1128/mSystems.00187-18

Fu, J., and Allen, R. W. (2019). A method to estimate the age of bloodstains using quantitative PCR. *Forensic Sci. Int. Genet.* 39, 103–108. doi: 10.1016/j.fsigen.2018.12.004

Haas, C., Hanson, E., Anjos, M. J., Ballantyne, K. N., Banemann, R., Bhoelai, B., et al. (2014). RNA/DNA co-analysis from human menstrual blood and vaginal secretion stains: results of a fourth and fifth collaborative EDNAP exercise. *Forensic Sci. Int. Genet.* 8, 203–212. doi: 10.1016/j.fsigen.2013.09.009

Hadley, W. (2009). *ggplot2: Elegant Graphics for Data Analysis*. Berlin: Springer Publishing Company.

Hall, M. W., Singh, N., Ng, K. F., Lam, D. K., Goldberg, M. B., Tenenbaum, H. C., et al. (2017). Inter-personal diversity and temporal dynamics of dental, tongue, and salivary microbiota in the healthy oral cavity. *NPJ Biofilms Microbiomes* 3, 1–7. doi: 10.1038/s41522-016-0011-0

Hamner, B., Frasco, M., and LeDell, E. (2012). *Metrics: Evaluation Metrics for Machine Learning. R Package Version 01*. 1.

Holtkotter, H., Beyer, V., Schwender, K., Glaub, A., Johann, K. S., Schrenkamp, M., et al. (2017). Independent validation of body fluid-specific CpG markers and construction of a robust multiplex assay. *Forensic Sci. Int. Genet.* 29, 261–268. doi: 10.1016/j.fsigen.2017.05.002

Huse, S. M., Ye, Y. Z., Zhou, Y. J., and Fodor, A. A. (2012). A core human microbiome as viewed through 16S rRNA sequence clusters. *PLoS One* 7:e34242. doi: 10.1371/journal.pone.0034242

Huttenhower, C., Gevers, D., Knight, R., Abubucker, S., Badger, J. H., Chinwalla, A. T., et al. (2012). Structure, function and diversity of the healthy human microbiome. *Nature* 486, 207–214. doi: 10.1038/nature11234

Hyde, E. R., Haarmann, D. P., Lynne, A. M., Bucheli, S. R., and Petrosino, J. F. (2013). The living dead: bacterial community structure of a cadaver at the onset and end of the bloat stage of decomposition. *PLoS One* 8:e77733. doi: 10.1371/journal.pone.0077733

Ingold, S., Dorum, G., Hanson, E., Berti, A., Branicki, W., Brito, P., et al. (2018). Body fluid identification using a targeted mRNA massively parallel sequencing approach - results of a EUROFORGEN/EDNAP collaborative exercise. *Forensic Sci. Int. Genet.* 34, 105–115. doi: 10.1016/j.fsigen.2018.01.002

Jabłońska, J., and Tawfik, D. S. (2019). The number and type of oxygen-utilizing enzymes indicates aerobic vs. anaerobic phenotype. *Free Radic. Biol. Med.* 140, 84–92. doi: 10.1016/j.freeradbiomed.2019.03.031

Kolenbrander, P. E. (2011). Multispecies communities: interspecies interactions influence growth on saliva as sole nutritional source. *Int. J. Oral Sci.* 3, 49–54. doi: 10.4248/IJOS11025

Kubista, M., Andrade, J. M., Bengtsson, M., Forootan, A., Jonák, J., Lind, K., et al. (2006). The real-time polymerase chain reaction. *Mol. Aspects Med.* 27, 95–125. doi: 10.1016/j.mam.2005.12.007

Kuramitsu, H. K., and Ellen, R. P. (2000). *Oral Bacterial Ecology: The Molecular Basis*. Summerville, SC: Horizon Scientific.

Lazarevic, V., Whiteson, K., Hernandez, D., François, P., and Schrenzel, J. (2010). Study of inter-and intra-individual variations in the salivary microbiota. *BMC Genomics* 11:523. doi: 10.1186/1471-2164-11-523

Li, J., Quinque, D., Horz, H. P., Li, M. K., Rzhetskaya, M., Raff, J. A., et al. (2014). Comparative analysis of the human saliva microbiome from different climate zones: Alaska, Germany, and Africa. *BMC Microbiol.* 14:316. doi: 10.1186/s12866-014-0316-1

Li, K., Bihan, M., and Methé, B. A. (2013). Analyses of the stability and core taxonomic memberships of the human microbiome. *PLoS One* 8:e63139. doi: 10.1371/journal.pone.0063139

Liaw, A., and Wiener, M. (2002). Classification and regression by randomForest. *R News* 2, 18–22.

Love, M. I., Huber, W., and Anders, S. (2014). Moderated estimation of fold change and dispersion for RNA-seq data with DESeq2. *Genome Biol.* 15:550. doi: 10.1186/s13059-014-0550-8

Marquis, R. E. (1995). Oxygen metabolism, oxidative stress and acid-base physiology of dental plaque biofilms. *J. Ind. Microbiol.* 15, 198–207. doi: 10.1007/BF01569826

Martin, M. (2011). Cutadapt removes adapter sequences from high-throughput sequencing reads. *EMBnet.* 17:3. doi: 10.14806/ej.17.1.200

Mashima, I., Theodorea, C. F., Thaweboon, B., Thaweboon, S., and Nakazawa, F. (2016). Identification of *Veillonella* species in the tongue biofilm by using a novel one-step polymerase chain reaction method. *PLoS One* 11:e0157516. doi: 10.1371/journal.pone.0157516

McDonald, D., Hyde, E., Debelius, J. W., Morton, J. T., Gonzalez, A., Ackermann, G., et al. (2018). American gut: an open platform for citizen science microbiome research. *mSystems* 3:e00031-18. doi: 10.1128/mSystems.00031-18

Morton, J. T., Sanders, J., Quinn, R. A., McDonald, D., Gonzalez, A., Vázquez-Baeza, Y., et al. (2017). Balance trees reveal microbial niche differentiation. *mSystems* 2:e00162-16. doi: 10.1128/mSystems.00162-16

Nasidze, I., Li, J., Quinque, D., Tang, K., and Stoneking, M. (2009). Global diversity in the human salivary microbiome. *Genome Res.* 19, 636–643. doi: 10.1101/gr.084616.108

Pechal, J. L., Schmidt, C. J., Jordan, H. R., and Benbow, M. E. (2017). Frozen: thawing and its effect on the postmortem microbiome in two pediatric cases. *J. Forensic Sci.* 62, 1399–1405. doi: 10.1111/1556-4029.13419

Pechal, J. L., Schmidt, C. J., Jordan, H. R., and Benbow, M. E. (2018). A large-scale survey of the postmortem human microbiome, and its potential to provide insight into the living health condition. *Sci. Rep.* 8:5724. doi: 10.1038/s41598-018-23989-w

Periasamy, S., and Kolenbrander, P. E. (2009). Aggregatibacter actinomycetemcomitans builds mutualistic biofilm communities with *Fusobacterium nucleatum* and *Veillonella* species in saliva. *Infect. Immun.* 77, 3542–3551. doi: 10.1128/IAI.00345-09

Quast, C., Pruesse, E., Yilmaz, P., Gerken, J., Schweer, T., Yarza, P., et al. (2013). The SILVA ribosomal RNA gene database project: improved data processing and web-based tools. *Nucleic Acids Res.* 41, D590–D596. doi: 10.1093/nar/gks1219

Ruijter, J. M., Villalba, A. R., Hellemans, J., Untergasser, A., and van den Hoff, M. J. B. (2015). Removal of between-run variation in a multi-plate qPCR experiment. *Biomol. Detect. Quantif.* 5, 10–14. doi: 10.1016/j.bdq.2015.07.001

Salzmann, A. P., Russo, G., Aluri, S., and Haas, C. (2019). Transcription and microbial profiling of body fluids using a massively parallel sequencing approach. *Forensic Sci. Int. Genet.* 43:102149. doi: 10.1016/j.fsigen.2019.102149

Schaechter, M. (2009). *Encyclopedia of Microbiology*. Cambridge, MA: Academic Press.

Schmedes, S. E., Woerner, A. E., and Budowle, B. (2017). Forensic human identification using skin microbiomes. *Appl. Environ. Microbiol.* 83:e01672-17. doi: 10.1128/AEM.01672-17

Schmedes, S. E., Woerner, A. E., Novroski, N. M. M., Wendt, F. R., King, J. L., Stephens, K. M., et al. (2018). Targeted sequencing of clade-specific markers from skin microbiomes for forensic human identification. *Forensic Sci. Int. Genet.* 32, 50–61. doi: 10.1016/j.fsigen.2017.10.004

Stahringer, S. S., Clemente, J. C., Corley, R. P., Hewitt, J., Knights, D., Walters, W. A., et al. (2012). Nurture trumps nature in a longitudinal survey of salivary bacterial communities in twins from early adolescence to early adulthood. *Genome Res.* 22, 2146–2152. doi: 10.1101/gr.140608.112

Vallone, P. M., and Butler, J. M. (2004). AutoDimer: a screening tool for primer-dimer and hairpin structures. *Biotechniques* 37, 226–231. doi: 10.2144/04372ST03

Watanabe, K., Akutsu, T., Takamura, A., and Sakurada, K. (2017). Practical evaluation of an RNA-based saliva identification method. *Sci. Justice* 57, 404–408. doi: 10.1016/j.scijus.2017.07.001

Weinbrecht, K. D. F. J., Payton, M. E., and Allen, R. W. (2017). Time-dependent loss of mRNA transcripts from forensic stains. *Dovepress* 7, 1–12. doi: 10.2147/RRFMS.S125782

Weiss, S., Xu, Z. Z., Peddada, S., Amir, A., Bittinger, K., Gonzalez, A., et al. (2017). Normalization and microbial differential abundance strategies depend upon data characteristics. *Microbiome* 5:27. doi: 10.1186/s40168-017-0237-y

Wu, J., Peters, B. A., Dominianni, C., Zhang, Y. L., Pei, Z. H., Yang, L. Y., et al. (2016). Cigarette smoking and the oral microbiome in a large study of American adults. *ISME J.* 10, 2435–2446. doi: 10.1038/ismej.2016.37

Yang, J., Tsukimi, T., Yoshikawa, M., Suzuki, K., Takeda, T., Tomita, M., et al. (2019). Cutibacterium acnes (*Propionibacterium acnes*) 16S rRNA genotyping of microbial samples from possessions contributes to owner identification. *mSystems* 4:e00594-19. doi: 10.1128/mSystems.00594-19

Zaura, E., Keijser, B. J. F., Huse, S. M., and Crielaard, W. (2009). Defining the healthy "core microbiome" of oral microbial communities. *BMC Microbiol.* 9:259. doi: 10.1186/1471-2180-9-259

Zhao, J. H. (2007). gap: genetic analysis package. *J. Stat. Softw.* 23, 1–18. doi: 10.18637/jss.v023.i08

Zhu, X., Wang, S., Gu, Y., Li, X., Yan, H., Yan, H., et al. (2012). Possible variation of the human oral bacterial community after wearing removable partial dentures by DGGE. *World J. Microbiol. Biotechnol.* 28, 2229–2236. doi: 10.1007/s11274-012-1030-5

Conflict of Interest: The authors declare that the research was conducted in the absence of any commercial or financial relationships that could be construed as a potential conflict of interest.

frontiers in Microbiology

ORIGINAL RESEARCH
published: 07 June 2021
doi: 10.3389/fmicb.2021.689493

Characterization of Bacterial Community Dynamics of the Human Mouth Throughout Decomposition *via* Metagenomic, Metatranscriptomic, and Culturing Techniques

Emily C. Ashe[1†], André M. Comeau[2], Katie Zejdlik[3] and Seán P. O'Connell[1†]*

[1]Department of Biology, Western Carolina University, Cullowhee, NC, United States, [2]Integrated Microbiome Resource, Dalhousie University, Halifax, NS, Canada, [3]Department of Anthropology and Sociology, Forensic Osteology Research Station, Western Carolina University, Cullowhee, NC, United States

OPEN ACCESS

Edited by:
Gulnaz T. Javan,
Alabama State University,
United States

Reviewed by:
Dhrubajyoti Chattopadhyay,
Amity University, India
Jonathan J. Parrott,
Arizona State University West Campus, United States

***Correspondence:**
Seán P. O'Connell
soconnell@email.wcu.edu

†These authors have contributed equally to this work

Specialty section:
This article was submitted to Systems Microbiology, a section of the journal Frontiers in Microbiology

Received: 01 April 2021
Accepted: 06 May 2021
Published: 07 June 2021

Citation:
Ashe EC, Comeau AM, Zejdlik K and O'Connell SP (2021) Characterization of Bacterial Community Dynamics of the Human Mouth Throughout Decomposition via Metagenomic, Metatranscriptomic, and Culturing Techniques. Front. Microbiol. 12:689493. doi: 10.3389/fmicb.2021.689493

The postmortem microbiome has recently moved to the forefront of forensic research, and many studies have focused on the idea that predictable fluctuations in decomposer communities could be used as a "microbial clock" to determine time of death. Commonly, the oral microbiome has been evaluated using 16S rRNA gene sequencing to assess the changes in community composition throughout decomposition. We sampled the hard palates of three human donors over time to identify the prominent members of the microbiome. This study combined 16S rRNA sequencing with whole metagenomic (MetaG) and metatranscriptomic (MetaT) sequencing and culturing methodologies in an attempt to broaden current knowledge about how these postmortem microbiota change and might function throughout decomposition. In all four methods, Proteobacteria, Firmicutes, Actinobacteria, and Bacteroidetes were the dominant phyla, but their distributions were insufficient in separating samples based on decomposition stage or time or by donor. Better resolution was observed at the level of genus, with fresher samples from decomposition clustering away from others *via* principal components analysis (PCA) of the sequencing data. Key genera in driving these trends included *Rothia*; *Lysinibacillus*, *Lactobacillus*, *Staphylococcus*, and other Firmicutes; and yeasts including *Candida* and *Yarrowia*. The majority of cultures (89%) matched to sequences obtained from at least one of the sequencing methods, while 11 cultures were found in the same samples using all three methods. These included *Acinetobacter gerneri*, *Comamonas terrigena*, *Morganella morganii*, *Proteus vulgaris*, *Pseudomonas koreensis*, *Pseudomonas moraviensis*, *Raoutella terrigena*, *Stenotrophomonas maltophilia*, *Bacillus cereus*, *Kurthia zopfii*, and *Lactobacillus paracasei*. MetaG and MetaT data also revealed many novel insects as likely visitors to the donors in this study, opening the door to investigating them as potential vectors of microorganisms during decomposition. The presence of cultures at specific time points in decomposition, including samples for which we have MetaT

data, will yield future studies tying specific taxa to metabolic pathways involved in decomposition. Overall, we have shown that our 16S rRNA sequencing results from the human hard palate are consistent with other studies and have expanded on the range of taxa shown to be associated with human decomposition, including eukaryotes, based on additional sequencing technologies.

Keywords: postmortem interval, human decomposition, 16S rRNA community profile, metagenomics, metatranscriptomics, accumulated degree days, bacterial cultures, oral thanatomicrobiome

INTRODUCTION

The period of time between death and when a body is discovered, also called the postmortem interval (PMI), can provide crucial information when conducting a medicolegal death investigation. There are many methods investigators have used to determine a PMI, including body temperature (algor mortis), rigor mortis, livor mortis, and stage of soft tissue decomposition as well as using more circumstantial evidence – such as when a person was last seen or the last time they checked their mail (Megyesi et al., 2005; Goff, 2010). Forensic entomology, a field of study which investigates the role that various insect species and other arthropods play in decomposition, has also been used in determining PMI (Goff, 2010). These methods can provide PMI estimates that range from hours to days, weeks, months, and even years, often depending on what state of decomposition the body was found (Megyesi et al., 2005; Swift, 2006; Goff, 2010). Due to how the body decomposes, more rapid changes (e.g., algor mortis, rigor mortis, and livor mortis) occur near the beginning of decomposition and can thus provide more accurate PMI ranges (Goff, 2010). However, the interpretation of these findings is often subjective (Madea and Henssge, 2015). As these intrinsic processes subside and other information must be used, the accuracy with which PMI can be estimated begins to decrease, resulting in much wider windows for the time of death (Megyesi et al., 2005; Swift, 2006; Goff, 2010; Madea and Henssge, 2015). Often this results in skeletonized remains having PMIs that range from a day to months to sometimes years (Megyesi et al., 2005).

Recently, numerous studies have centered on analyzing the utility of the human microbiome in more accurately determining the PMI. The intrinsic nature of the human microbiome and the large role the microbial community plays in the progression of decomposition makes microbial-based PMI estimation an appealing forensic technique because it would reduce the reliance on postmortem processes that are heavily influenced by external conditions, such as forensic entomology which can often yield broad PMI estimations especially in cases with extensive decomposition or cases where physical barriers delay insect activity (Goff, 2010; Johnson et al., 2013; Javan et al., 2016). The postmortem microbiome has even shown promise in providing more accurate PMI estimates for skeletonized remains through analysis of communities present in fresh and weathered bone (Damann et al., 2015). In addition to skeletal remains, other studies have focused on the postmortem microbial communities associated with a variety of soft tissue (Javan et al., 2016). Due to its ease of access, the bacterial community of the oral cavity has been a common target for many of these studies (Hyde et al., 2013, 2015; Javan et al., 2016; Adserias-Garriga et al., 2017). The postmortem oral microbial community has been shown to exhibit distinct differences between early and late stage decomposition and to exhibit a community that is distinct from other locations in the body but not significantly different between sexes (Hyde et al., 2013; Javan et al., 2016; Adserias-Garriga et al., 2017). The microbial community of the oral cavity has also been shown to include more environment-associated taxa and become less host-associated as decomposition progresses (Adserias-Garriga et al., 2017). Distinctions between early and late stage communities appear to be driven by the bloat stage and the host-associated Actinobacteria found in the oral cavity throughout early decomposition (Hyde et al., 2013; Adserias-Garriga et al., 2017).

Carter et al. (2015) investigated how different seasons (i.e., summer vs. winter) can influence the gravesoil microbial community composition. They demonstrated that even in soils not associated with a carcass, bacterial communities were markedly different between seasons (Carter et al., 2015). Specifically, they showed how gravesoil microbial communities were more stable in winter compared to communities observed in the summer. Bashan et al. (2016) demonstrated that in healthy living individuals, the gut and oral microbiomes share universal similarities between individuals while the skin is more likely to be influenced by the environment of the host. In death, this may not hold true for the oral cavity due to its increased exposure to the environment and the lack of the immune system of the host to mitigate community changes. Compared to internal organs and bones, the oral cavity is more exposed to the external environment, making it more susceptible to environmental influences such as weather and scavenging. This likely makes the bacterial community living within the oral cavity more susceptible to seasonal variation.

This study focused on examining the postmortem succession of the bacterial communities found in the oral cavities of three human donors. The communities were assessed using 16S rRNA gene sequencing (hereafter, abbreviated 16S), total metagenomic (MetaG), and metatranscriptomic (MetaT) analyses, and culturing of bacteria on solid media. Our overarching goals were to connect patterns of microbial diversity to PMI during human decomposition and to link cultures of bacteria to distinct stages and processes throughout decomposition. While none of these methods alone provides a complete picture of the bacterial assemblages, making connections between these approaches could elucidate dynamic interactions between

populations and be used to estimate important benchmarks of the PMI.

MATERIALS AND METHODS

Donors and Sample Collection

Three donors, one male and two females, were placed in the open-air Forensic Osteology Research Station (FOREST) at Western Carolina University, located in Cullowhee, NC (coordinates 35°18'34"N 83°11'52"W). The donors were all elderly and died of natural causes (**Table 1**) and all were unembalmed. Donor 1, a male, had dentures in place when they arrived while Donor 2, a female, had a full set of teeth with some metal components and Donor 3, a female, was edentulate. Upon their arrival at the facility, each donor was immediately unclothed and placed on the ground in a supine position with no barriers to wildlife or the elements employed. Donor 2 was received in an early stage of decomposition because she had been deceased in her home for 2 days prior to discovery. All donors had been stored in the cold after death for at least 6 days before being transported to FOREST. This storage was related to legal requirements of a certified death certificate to accept donated bodies and the scheduling of transportation of bodies from across the state of North Carolina. Multiple oral swabs of the entire hard palate were taken during each sampling event; one swab was collected for DNA extraction, one for RNA extraction, and one for culturing techniques. Each donor was sampled 5–7 times throughout decomposition, including swabbed samples taken upon deposition at the facility (**Table 1**). The sampling times did not overlap between the donors, although each donor was placed in FOREST within 1–3 days after the end of the sampling period of the previous donor. Samples were collected using sterile Puritan® Hydraflock flocked swabs with a 30 mm break point and dry transport tube (Puritan Medical Products, Guilford, ME, United States). Generally, swabs were individually moistened in the field using separate aliquots of sterile molecular biology grade water prior to sample collection. The swabs intended for nucleic acid extraction were placed back in their tubes and immediately frozen on dry ice. The swabs intended for culturing were broken off on-site into a 2-ml microcentrifuge tube of sterile 15% glycerol/R2B medium (recipe is below in the Bacterial Isolates section) and placed on dry ice. The samples were immediately transported back to the lab where they were stored at −80°C.

Accumulated Degree Days

Located in the southern Appalachian Mountains, Cullowhee is a temperate climate (Cfa) that is classified as "fully humid with hot summers" (Peel et al., 2007). Because of the climate type and time of year, the donors were subjected to a wide range of environmental influences despite sampling spanning only 2 months. The facility experienced temperatures ranging from −1.7 to 32.2°C and received a total of 12.12 inches of precipitation during this time.[1] Due to this variation, accumulated degree days (ADD) were used to standardize the decomposition process between donors (**Table 1**). ADD was calculated using the temperature measurements taken from iButton Thermochron® data loggers (Maxim Integrated, San Jose, CA, United States) that were placed in holders and staked next to the head of each donor. The iButtons were set to record the temperature

[1]https://www.ncdc.noaa.gov/

TABLE 1 | Information and sampling schedule for three human donors undergoing decomposition at the Forensic Osteology Research Station (FOREST) facility in Cullowhee, NC.

Donor information	Date of death/ Cause of death	Sampling date	Sampling event	ADD	Decomposition state	Insect activity
ID: D1	4/03/2018	4/09/2018	1	0	Fresh	0
Sex, Age: M, 65	Gastric cancer	4/13/2018	2	49	Early	2
Height: 180 cm		4/16/2018	3*	89	Early	1
Weight: 54.4 kg (BMI = 16.7)		4/20/2018	4	138	Early	2
Ethnicity: White		4/23/2018	5*	168	Advanced	0
		4/27/2018	6*	222	Advanced	1
		4/30/2018	7	253	Advanced	0
ID: D2	4/23/2018	5/01/2018	1	41	Early	1
Sex, Age: F, 77	Heart disease	5/04/2018	2	106	Early	3
Height: 160 cm		5/07/2018	3	155	Early	2
Weight: 74.8 kg (BMI = 29.2)		5/11/2018	4*	223	Advanced	1
Ethnicity: White		5/14/2018	5	292	Advanced	1
ID: D3	5/11/2018	5/17/2018	1*	0	Fresh	0
Sex, Age: F, 84	Pneumonia	5/21/2018	2*	84	Early	3
Height: <140 cm		5/24/2018	3*	169	Advanced	2
Weight: <60 kg (BMI < 25)		5/28/2018	4*	291	Skeletonization	1
Ethnicity: White		6/01/2018	5*	392	Skeletonization	0

*The first sampling event coincided with when the donors were received and placed at the facility. Samples consisted of oral swabs taken from the hard palate of each donor. ADD are reported for each sampling event as is a qualitative assessment of the decomposition state (based on Megyesi et al., 2005). Insect activity is reported as: 0 = no visible insect activity, 1 = only adult flies present, 2 = adult flies and small maggots present, and 3 = large quantities of both adult flies and maggots present. (Note: For Donor 3, height and weight were not reported and upper estimates are shown.). *Samples were taken when it was raining (trace amounts of snow was present on 4/16/2018).*

every 30 min, resulting in 48 reads each day. This temperature data were then used to calculate a specific ADD for each sampling time using the following formula:

$$ADD_t = \sum_{d=0}^{d_x-1} \overline{T} + \left(\frac{\sum_{s=0}^{t} T}{t} \right) . \frac{t}{48}$$

Equation 1 Calculation of ADD. Variables are assigned as follows: t refers to the number of temperatures that were recorded prior to sampling on a given day (d), d_x is the day on which the sampling occurred, T is the temperature in Celsius, and s refers to the number of iButton temperature records (48 total per day).

Since Donor 2 was received in an early state of decomposition, their starting decomposition measurement could not be zero and was instead estimated based on the National Institute of Health's National Institute on Aging (NIA) recommendation for thermostat settings for the elderly during winter months (Calvin, 2014). According to the NIA, thermostats should be kept at an average of 69°F (20.5°C). Across 2 days, this resulted in a baseline of 41 ADD for Donor 2. Data collected from the field also included a qualitative estimate of the state of decomposition ranging from fresh, early, advanced, and skeletonization stages (Megyesi et al., 2005). Qualitative data were also recorded for insect activity for each of the donors throughout decomposition.

Nucleic Acid Extraction and Purification

Samples were thawed at 4°C prior to nucleic acid extractions for 16S rRNA gene sequencing, whole genome shotgun MetaGs, and whole genome shotgun MetaTs. DNA and RNA were both extracted and purified using QIAGEN's RNeasy® PowerMicrobiome® Kit (QIAGEN, Valencia, CA, United States) following the manufacturer's protocol. The step involving phenol/chloroform/isoamyl alcohol was not utilized and dithiothreitol (DTT) was used in lieu of β-mercaptoethanol at a ratio of 20 µl of 2 M DTT per 1 ml of lysis buffer. During the third step of both DNA and RNA extractions, samples were placed in a BioSpec Mini-BeadBeater-1 (BioSpec, Bartlesville, OK, United States) at 2,500 rpm for 1 min. During RNA extraction, 70% ethanol was used in lieu of buffer PM4 during the addition of binding salts (buffer PM3) to prevent copurification of small RNAs. DNA extracts were stored at −20°C and RNA extracts at −80°C until sequencing or complementary DNA (cDNA) synthesis could be performed. cDNA was generated using Thermo Fisher Scientific's SuperScript IV First-Strand Synthesis Kit (Thermo-Fisher Scientific, Waltham, MA, United States) following the manufacturer's protocol before sequencing.

Quantitation of Nucleic Acids

Nucleic acids were quantified using a 2100 Bioanalyzer (Agilent Technologies, Santa Clara, CA, United States). DNA was quantified using the Agilent DNA 12000 Kit and the DNA 12000 Series II Assay following the protocol detailed in the DNA 12000 Kit Quick Start Guide (Agilent Technologies) while RNA was quantified using the Agilent RNA 6000 Pico Kit and the Prokaryotic Total RNA Pico Series II Assay following the protocol detailed in the RNA 6000 Pico Kit Quick Start Guide (Agilent Technologies). One DNA sample (Donor 3, sample 3) was concentrated prior to sequencing by drying down the sample, then reconstituting it to half the original volume. cDNA was quantified using Invitrogen's Qubit® 2.0 Fluorometer with the Qubit® dsDNA HS Assay Kit (Life Technologies, Carlsbad, CA, United States) following the protocol described in the Qubit® 2.0 Fluorometer User Manual.

Library Preparation and Sequencing

Library preparation and sequencing were performed at the Integrated Microbiome Resource (IMR), located at Dalhousie University in Halifax, Nova Scotia. Libraries of the V6–V8 hypervariable region of the 16S rRNA gene were prepared using bacteria-specific primers (B969F = ACGCGHNRAA CCTTACC; BA1406R = ACGGGCRGTGWGTRCAA) as outlined in Comeau et al. (2017) and sequenced on an Illumina MiSeq using 2 × 300 bp v3 chemistry. MetaG and MetaT libraries were prepared from extracted DNA or synthesized cDNA using the Illumina Nextera Flex kit (Illumina® Inc., San Diego, CA, United States), as per the manufacturer's instructions, and sequenced on an Illumina NextSeq 550 using 2 × 150 bp HiOutput v2.5 chemistry.

16S rRNA Gene Sequence Data Analysis

Raw FASTQ files were demultiplexed on-instrument and then processed to create amplicon sequence variants (ASVs), as described in Comeau et al. (2017) and Nearing et al. (2018), using a custom SOP developed at the IMR as part of the continually evolving MicrobiomeHelper repository. The exact version of the analysis pipeline used is available at github.com/LangilleLab/microbiome_helper/wiki/Amplicon-SOP-v2-(qiime2-2019.7). In summary, custom scripts and the QIIME2 program (Bolyen et al., 2019) were used to perform read quality-control, denoising into ASVs using Deblur, and assignment of taxonomy against the SILVA reference taxonomy.

Whole Metagenomic and Metatranscriptomic Data Analysis

Similar to above, raw FASTQ files were demultiplexed on-instrument and then processed using a pipeline under development at the IMR as part of the MicrobiomeHelper repository, the current version of which is available at github.com/LangilleLab/microbiome_helper/wiki. In summary, raw reads were quality-controlled using KneadData v0.7.2[2], which employs Trimmomatic v0.36 (Bolger et al., 2014; options: SLIDINGWINDOW:4:20 MINLEN:50) and Bowtie2 v2.2.3 (Langmead and Salzberg, 2012; options: –very-sensitive –dovetail) to filter low-quality reads and screen out potential contaminant sequences against the human (GRCh38) and phiX174 genomes. "Raw" taxonomic composition was determined using Kraken2 v2.0.8 (Wood et al., 2019; option: –confidence 0.1), based upon a 150mer database built from the entire NCBI RefSeq Complete v93 database, and final taxonomic abundance profiles were

[2]http://www.github.com/biobakery/kneaddata

generated using Bracken v2.0 (Lu et al., 2017; option: -t 10). Custom PERL and Python scripts (available above) were then used to do functional mapping of reads using MMseqs2 (Steinegger and Söding, 2017) against the entire UniRef90 database[3], select the top hit for each read, map functions to Enzyme Commission (EC) numbers, and then generate either unstratified (function-only) or stratified (linking the above Kraken2 taxonomy) matrices. Two PICRUSt2 v2.2.0-b scripts (Douglas et al., 2020) were used to append functional descriptions (add_descriptions.py) to the above matrices and to generate KEGG pathway coverages (pathway_pipeline.py). Final functional coverages were normalized to reads-per-kilobase-million (RPKM). Processes were parallelized using GNU parallel (Tange, 2018).

Bacterial Isolates

All cultures were grown and isolated in fall 2018 from frozen swab materials that were vortexed in sterile Reasoner's 2A Agar (R2A formulation: 0.5 g yeast extract, 0.5 g proteose peptone, 0.5 g casamino acids, 0.5 g dextrose, 0.5 g soluble starch, 0.3 g sodium pyruvate, 0.3 g dipotassium phosphate, 0.05 g magnesium sulfate, and 15.0 g agar in 1 L distilled water) broth media without agar added (R2B), diluted, and spread plate onto either R2A plates (full strength or 1%) or 1% nutrient broth and 1% brain heart infusion agar media. These cultures were incubated at room temperature under a normal atmosphere. In total, 69 cultures were isolated, 46 of which were identified as distinct species. Fifty-three isolates were grown on R2A, while 16 isolates were cultured on the diluted media. The dilute media formulations were used in order to obtain slower growing bacteria that could have been active in decomposition or numerically abundant but difficult to detect otherwise. Once isolated, a variety of phenotypic tests were performed in order to characterize the species (Ashe, 2019).

Isolates were identified by sending cultures to GENEWIZ (GENEWIZ Inc., South Plainfield, NJ, United States) for DNA extraction and Sanger sequencing of the full 16S rRNA gene. Sequences were analyzed using BLAST in order to identify the closest sequence match for each culture (NCBI Resource Coordinators, 2016). Search parameters included blastn of 16S rRNA genes for sequences from type material and a cutoff value of 97% identity to designate an OTU. NCBI taxonomy designations were used to compare cultures to ASVs from the 16S rRNA gene sequencing and reads obtained in the MetaG and MetaT datasets.

The 16S rRNA sequences from the bacterial cultures were analyzed with the 328 ASVs (~400 bp in length) obtained from the 16S environmental sequencing. The ASVs and culture sequences were aligned using Clustal Omega followed by construction of a cladogram to group similar sequences (Madeira et al., 2019). Sequences that appeared to be closely related were compared pairwise by using BLAST and those that were ≥97% identical were considered to be the same OTU. Bracken was used to generate data to the species level for the MetaG and MetaT sequences. These data were then used to compare to OTUs from the cultured bacteria.

Statistical Analyses

Daily precipitation and temperature data between donors were analyzed using one-way ANOVA and Bonferroni *post hoc* testing using Systat 10 for Windows (SPSS, Inc., Chicago, IL). Shannon diversity (H) and evenness (E_H) of ASVs, MetaG, and MetaT reads at the species level were calculated using data that had been normalized to the sample with the lowest total number of sequences. These data were examined for statistical significance by grouping samples by donor, ADD, and decomposition stage (grouped by fresh + early vs. advanced + skeletonized) using ANOVA or *t* tests as above.

Principal components analysis was performed on data at the level of phylum and genus using BioVinci version 3.0.9 (BioVinci, Inc., San Diego, CA, United States) for each of the three sequencing methods. Proportional data were arranged by donor and sampling event for each donor across the taxonomic categories derived from the bioinformatics tool applied for each sequencing method. Vectors were also generated from the statistical output to indicate which taxa were most influential in separating the samples on the PCA plots.

RESULTS

Climate and Other Factors Affecting Decomposition

The three donors in this study were elderly and died from different natural causes (**Table 1**). Estimated body mass indices (BMI) ranged from underweight for Donor 1 to almost obese for Donor 2, with Donor 3 estimated to be on the low end of the BMI scale. No official height or weight data were available for Donor 3. The donors were placed into the decomposition facility sequentially with none of their sampling periods overlapping one another, therefore exposing them to disparate temperature regimes (**Figure 1**). Snow was observed on 16 April, which also had the coldest recorded average daily temperature. Net daily precipitation was not significantly different between any of the donors ($p = 0.08$; one-way ANOVA), with Donor 1 seeing 0–38.6 mm precipitation each day, Donor 2 receiving 0–8.4 mm rain, and Donor 3 ranging from 0 to 25.7 mm of daily rain. The mean daily temperatures were significantly different for the three donors with temperatures increasing with the placement of each donor ($p < 0.001$ for one-way ANOVA and $p < 0.01$ for pairwise comparisons using the Bonferroni *post hoc* test; **Figure 1A**). The average daily temperatures ranged from 4.9–17.7°C ($\bar{x}$ = 11.8°C), 15.5–20.8°C ($\bar{x}$ = 18.3°C), and 18.6–34.0°C ($\bar{x}$ = 24.6°C), for Donors 1, 2, and 3, respectively, resulting in higher ADD values with each subsequent donor placed in the FOREST. The slopes for ADD over time were also found to be significant ($p < 0.001$). Donor 2 was placed in the facility at an estimated ADD of 41 while the others were included in the study at

[3]www.uniprot.org/uniref

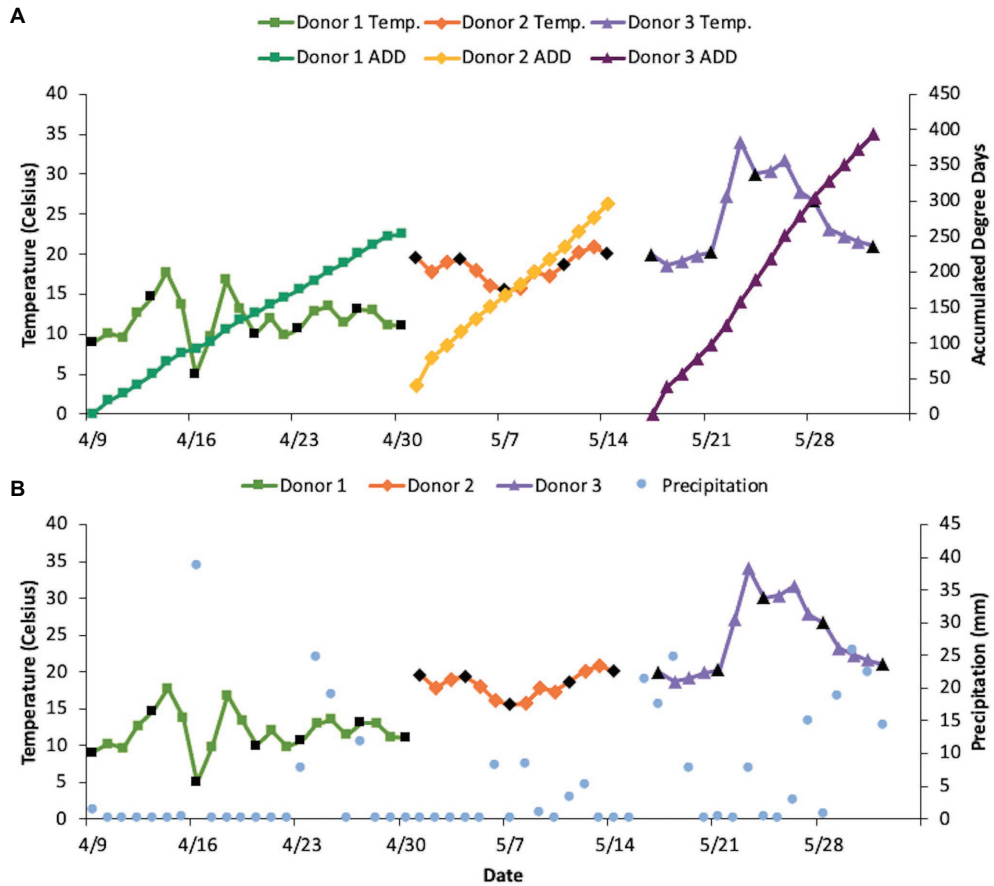

FIGURE 1 | Differences in sampling period, temperature, precipitation (mm), and accumulated degree days (ADD) between donors. Black points denote days on which samples were collected. (Note: The last collection day for each donor was not able to be included because the temperature loggers were collected during sampling, therefore an average daily temperature could not be recorded for those days). **(A)** ADD compared to the average daily temperatures for each donor. Daily temperatures were significantly different between donors based on one-way ANOVA and Bonferroni *post hoc* test ($p < 0.01$ between all pairs of donors). **(B)** Comparison of net daily precipitation and average daily temperature for each donor throughout the sampling period. Precipitation was not significantly different between donors based on one-way ANOVA ($p = 0.08$).

an ADD value of 0 after being stored cold after death for at least 6 days. The last sample for Donor 1 was taken at an ADD of 253, for Donor 2 at 292, and for Donor 3 at an ADD of 392. Donor 3 was the only of the three to reach the skeletonization stage of decomposition and, along with Donor 2, saw high amounts of insect activity throughout decomposition (**Table 1**). Additionally, camera trap footage and visible signs on the bodies revealed scavenging activity from vultures for all three donors.

Diversity Measures From the Three Sequencing Approaches

Sequencing of the samples from the three donors yielded data for all 17 samples for the three sequencing methods used. The total number of 16S sequences ranged from 1,229 to 8,594 with an average of 4,822 (**Supplementary Table 1**). These yielded a total of 328 unique ASVs, with single samples ranging from 7 to 74 ASVs each and Donor 1 having significantly fewer ASVs on average than Donors 2 and 3 (one-way ANOVA $p = 0.008$; Bonferroni test $p < 0.05$). MetaG sequencing produced 1.3×10^5–4.0×10^6 total reads at the taxonomic level of species ($\bar{x} = 2.4 \times 10^6$ reads) and 183–6,976 distinct species per sample from a total pool of 11,504 species. MetaT sequencing resulted in a range of 4.7×10^4–1.8×10^6 total reads at the level of species ($\bar{x} = 3.8 \times 10^5$ reads), a total pool of 1,797 distinct species, and 46–746 species for each sample. There were no significant differences for Shannon diversity (H) or Shannon evenness (E_H) for the 16S data based on neither ANOVA tests for data grouped by either donor or ADD range grouped into three classes (early, middle, and late) nor for *t* tests based on the fresh + early vs. the advanced + skeletonized stages of decomposition (**Supplementary Table 1**). The only significant differences seen were for MetaG data for E_H and MetaT data for H when comparing the three donors, with Donor 1 showing lower values than Donor 2, but neither showing differences from Donor 3 (one-way ANOVA $p = 0.02$; Bonferroni test $p < 0.05$, for both comparisons).

16S Taxonomic Distributions

Firmicutes dominated or co-dominated the samples collected from the donors based on the 16S sequencing, while the Proteobacteria were also found in sizable numbers in most samples and Actinobacteria were most numerous in two of the samples (**Figure 2**). PCA of these data revealed strong trends in separating samples based on Actinobacteria and Proteobacteria vs. Firmicutes with 70.7% of the variation in the dataset being explained by PC1 (**Figure 3**). Grouping of the samples was based on these phyla and no clear trends were seen based on donor or ADD, though the four earliest time points sampled were separated from almost all of the other samples based on PC2 which accounted for 27.3% of the variation. The diversity within each phylum was high for most samples and included many genera that each contributed to less than 1% of the total data (**Figure 4**). This latter case is evident for the first sample for Donor 2 and the final sample for Donor 3. *Rothia* spp. and *Lactobacillus* spp. were especially common during early decomposition and this can be seen in the PCA plot of the data in **Figure 5**, which separated early samples based on a combination of PC1 (19.4% of variance) and PC2 (18% of variance). *Lysinibacillus* spp. were only observed in large numbers (85% of the ASVs) in the third Donor 1 sample while *Streptococcus* spp., Bacillales spp., and Planococcaceae spp. were common among middle to late ADD samples. These latter two groups were influential in separating samples based on PC1 which also skewed the third sample for Donor 1, based on the high numbers of *Lysinibacillus* (**Figure 5**). *Pseudomonas* spp. was most common in the later samples.

MetaG Taxonomic Distributions

Metagenomic sequencing included reads for Chordata, Arthropoda, Ascomycota, and Streptophyta in addition to bacterial phyla (**Figure 6**). Three eukaryotic phyla were represented in most samples, with high numbers seen for Chordata for samples from Donors 1 and 2, for Arthropoda for Donor 2, and for Ascomycota in one sample each for Donor 1 and Donor 3. Streptophyta were common (>1% of the total samples) in 11 of the 17 samples. The Firmicutes and Proteobacteria were in the majority for bacteria in most samples, with higher numbers of Firmicutes being found generally in earlier samples and Proteobacteria being in higher amounts in later samples. Actinobacteria were primarily found in early and late samples, comprising up to ~25% of the community in some samples, but were generally less common. Chordates appeared to help drive the largest trend in the dataset, with Chordate-heavy samples separating in PCA from samples with high abundances of Firmicutes and Proteobacteria, based on PC1 which accounted for 43.5% of the total variation (**Figure 7**). Samples with high numbers of Firmicutes and Proteobacteria were separated based on PC2 (29.4% of total variation). Samples did not appear to cluster based on donor or ADD.

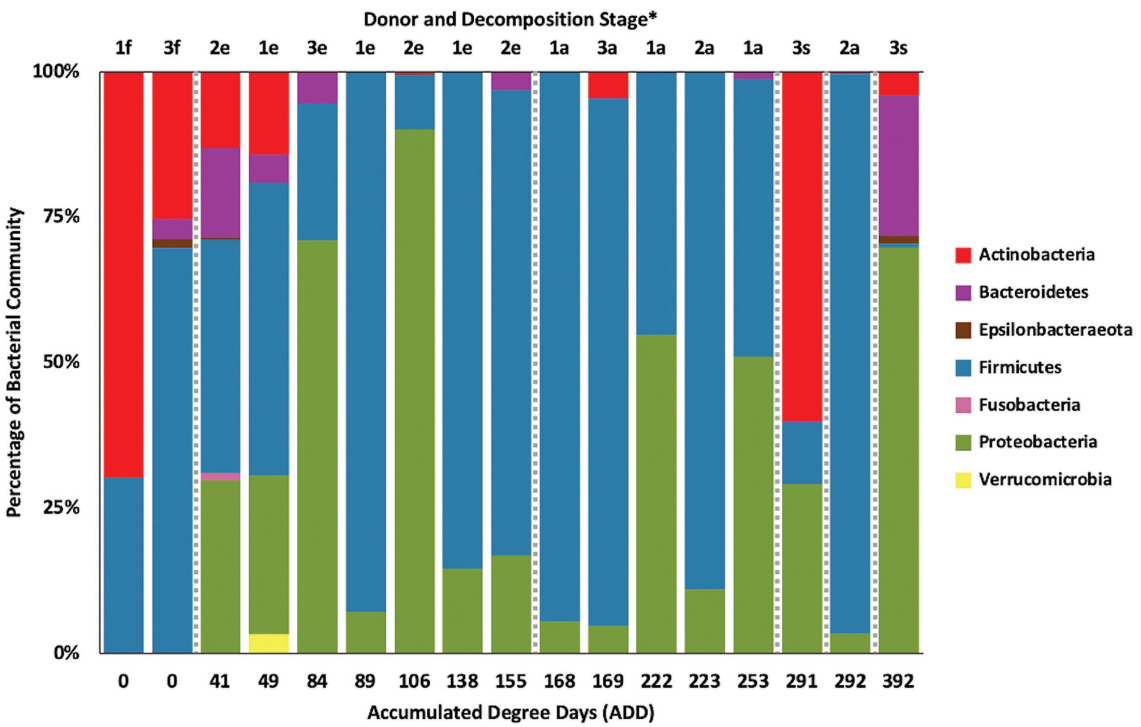

FIGURE 2 | Proportion of bacterial phyla determined from 16S rRNA gene sequencing of the V6–V8 hypervariable region from oral samples of three human donors (Donors 1, 2, and 3) during decomposition. Decomposition was assessed as ADD on the *x*-axis, and samples were also classified to an overall decomposition stage for each donor at each sampling event (*f*, fresh; *e*, early; *a*, advanced; and *s*, skeletonized).

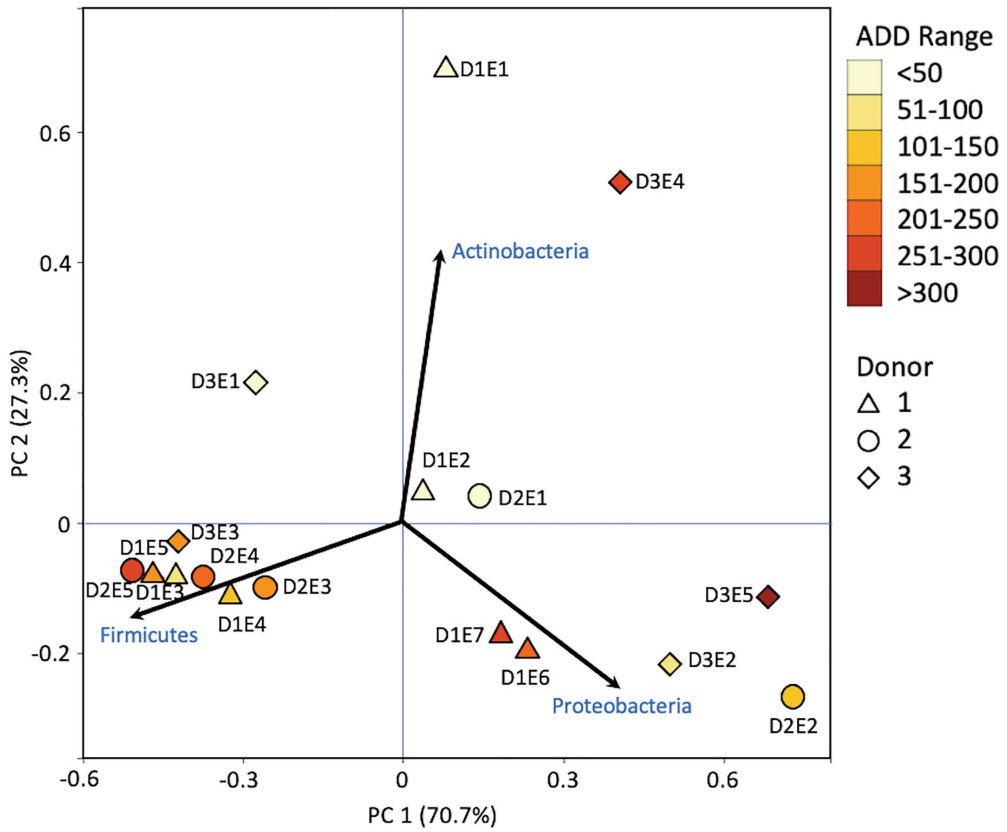

FIGURE 3 | Principal components analysis (PCA) plot for the proportional data of bacterial phyla observed from 16S rRNA gene sequencing of the V6–V8 hypervariable region from oral samples of three human donors (Donors 1, 2, and 3) during decomposition. Shading is added to the symbols [triangles for Donor 1 (D1), circles for Donor 2 (D2), and diamonds for Donor 3 (D3)] to show earlier (lighter shading) to later (darker shading) ADD and also times sampled (from E1 to E7 for D1 and E1 to E5 for D2 and D3, indicating first sample to last sample taken).

At the level of genus, MetaG samples showed high diversity, with ~15–75% of the data for each sample attributed to minor contributors, which each individually accounted for <3% of the total reads (**Figure 8**). DNA from the human donors (*Homo* and the misidentified genus *Pan*) was common in the early samples as were reads from Firmicutes, including *Lactobacillus* spp., *Lysinibacillus* spp., and *Staphylococcus* spp., while some samples included *Candida* spp. Middle samples were richer in *Ignatzschineria* spp. and later samples contained more *Oblitimonas* spp. *Yarrowia* spp. dominated one of the last samples for Donor 3 and was common only in that donor. *Penaeus* spp. (an arthropod group), *Olea* spp. (plants), and *Vagococus* spp. were found throughout the samples in generally lower amounts. *Oblitimonas* spp. and *Lysinibacillus* spp. primarily separated the five middle to late Donor 1 samples from all others in PCA, based on PC1 (23.8% of the variation) while PC2 (18.3% of the variation) separated the fourth sample from Donor 3 based on *Yarrowia* spp. (**Figure 9**). The human reads were influential in separating the earliest samples from all others based on PC1 and PC2.

MetaT Taxonomic Distributions

Metatranscriptomic sequencing analyses revealed some eukaryotic RNA throughout the sampling schedule, with Chordata most prevalent early on, Arthropoda increasing in abundance with time (due to sequences related to flies including *Drosophila* and to a lesser extent *Lucilia*, *Rhagoletis*, *Bactrocera*, and *Ceratitis*), Ascomycota fluctuating over time, and Streptophyta being in relatively low abundance most of the time (**Figure 10**). Bacterial data showed Firmicutes to be common for the early and middle sampling times and Proteobacteria generally being in secondary numbers, except for the last few samples where Proteobacteria generally outnumbered the Firmicutes. Actinobacteria were found in lower numbers in most of the samples, but were once again found primarily in early and late sampling times. The primary drivers of separating the samples using PCA were Chordata, Proteobacteria, and Firmicutes, with the latter two phyla separating samples from the other phyla based on PC1, which accounted for 51.5% of the variation in the dataset and Chordata separating samples along PC2 (**Figure 11**). The samples did not appear to follow a trend based on donor or ADD. As for the MetaG data, and to a lesser extent the 16S data, minor contributors (accounting for <3% of the data each) were found to be common in total across most of the samples (**Figure 12**). Human reads were found in the first samples taken for each donor and were more than 50% of the total for the first sample for Donor 1.

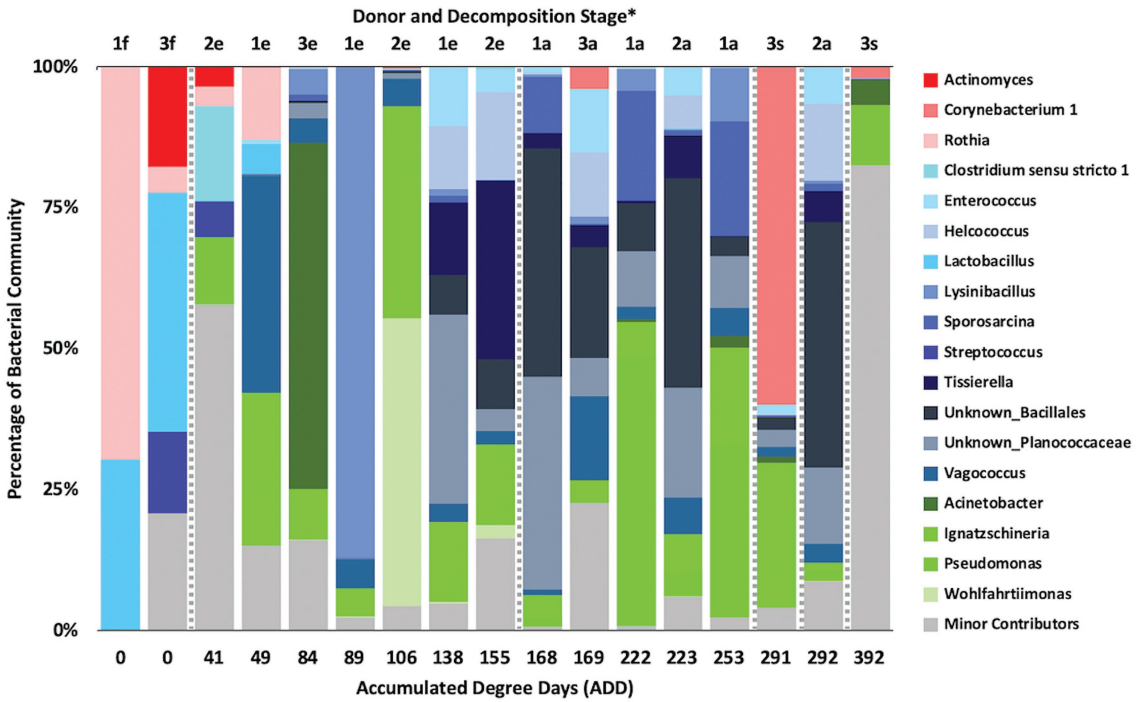

FIGURE 4 | Proportions of bacterial genera determined from 16S rRNA gene sequencing of the V6–V8 hypervariable region from oral samples of three human donors (Donors 1, 2, and 3) during decomposition. Decomposition was assessed as ADD on the *x*-axis and samples were also classified to an overall decomposition stage for each donor at each sampling event (*f*, fresh; *e*, early; *a*, advanced; and *s*, skeletonized). Minor contributors include data that accounted for <1% of the total diversity within a group.

Candida spp. was dominant in one sample (Donor 1, sample 2) while *Drosophila* spp. were observed in about two-thirds of the samples, primarily in the final two samples taken from Donor 2. *Starmera* spp. and *Yarrowia* spp. appeared in the same 10 samples, usually in abundances of <10% of the total. *Staphylococcus* spp. was common throughout the samples while other Firmicutes genera were in lower numbers much of the time. Proteobacteria such as *Escherichia* spp., *Ignatzschineria* spp., and *Oblitimonas* spp. became common and often dominant in the middle to later samples. Human reads and *Candida* spp. (positive relationships for PC1) and *Lysinibacillus* spp. (positive relationship for PC2) appeared to skew three samples in PCA analysis, with *Staphylococcus* spp. showing some influence along the negative axes for the principal components (**Figure 13**). Most samples were clustered quite close together in the negative quadrant of the plot. As in the 16S and MetaG data, *Lysinibacillus* spp. was found in notably high abundances for MetaT in the third sample for Donor 1.

Bacterial Isolates

Cultures recovered from the donors spanned the range of ADD and included 46 unique species of bacteria from a total of 69 isolates (**Table 2**). Species from the Proteobacteria accounted for the largest proportion of the isolates, with 43.5% of the cultures belonging to this phylum. Firmicutes (32.6%), Actinobacteria (19.6%), and Bacteroidetes (4.3%) accounted for the rest of the cultures. Four isolates were recovered from the same donor from multiple sampling times, including *Bacillus cereus*, *Paenarthrobacter nitroguajacolicus*, *Proteus vulgaris*, and *Pseudomonas koreensis*. Eight other cultures were obtained from more than one donor including representatives from *Dermacoccus*, *Morganella*, *Proteus*, *Providencia*, and *Staphylococcus*. Fifteen of the isolates appeared only from early samples (ADD < 100) while another 10 only appeared in late samples (ADD > 250) and 11 of the other 21 appeared in multiple ADD sampling points. Notably, cultures from *Corynebacterium* were obtained from times in which this genus was prevalent in the 16S data from the same samples (**Figure 4**), while *Pseudomonas* isolates were also recovered from corresponding sampling times that had high levels of *Pseudomonas* sequences present in the community profiles obtained from the sequencing approaches involving 16S (**Figure 4**) and MetaG (**Figure 8**). *Acinetobacter* spp. were cultured from samples that showed this genus to be common in the 16S and MetaT sequencing (**Figures 4, 12**), *Staphylococcus* spp. were common in MetaG and MetaT sampling (**Figures 8, 12**), and *Bacillus* spp. were common in MetaT sequences (**Figure 12**). Only five species, *Curtobacterium citreum*, *Dermacoccus nishinomiyaensis*, *Microbacterium saccharophilum*, and *Micrococcus aloeverae*, were not detected in the sequence data. In all, of the 46 isolates, 41 could be matched to species-level reads from at least one of the three sequencing methods, including 11 species that were seen in all three datasets (**Table 2**). These included *Acinetobacter gerneri*, *B. cereus*, *Comamonas terrigena*, *Kurthia zopfii*, *Lactobacillus paracasei*, *Morganella morganii*, *P. vulgaris*, *P. koreensis*, *Pseudomonas moraviensis*, *Raoutella terrigena*, and *Stenotrophomonas maltophilia*.

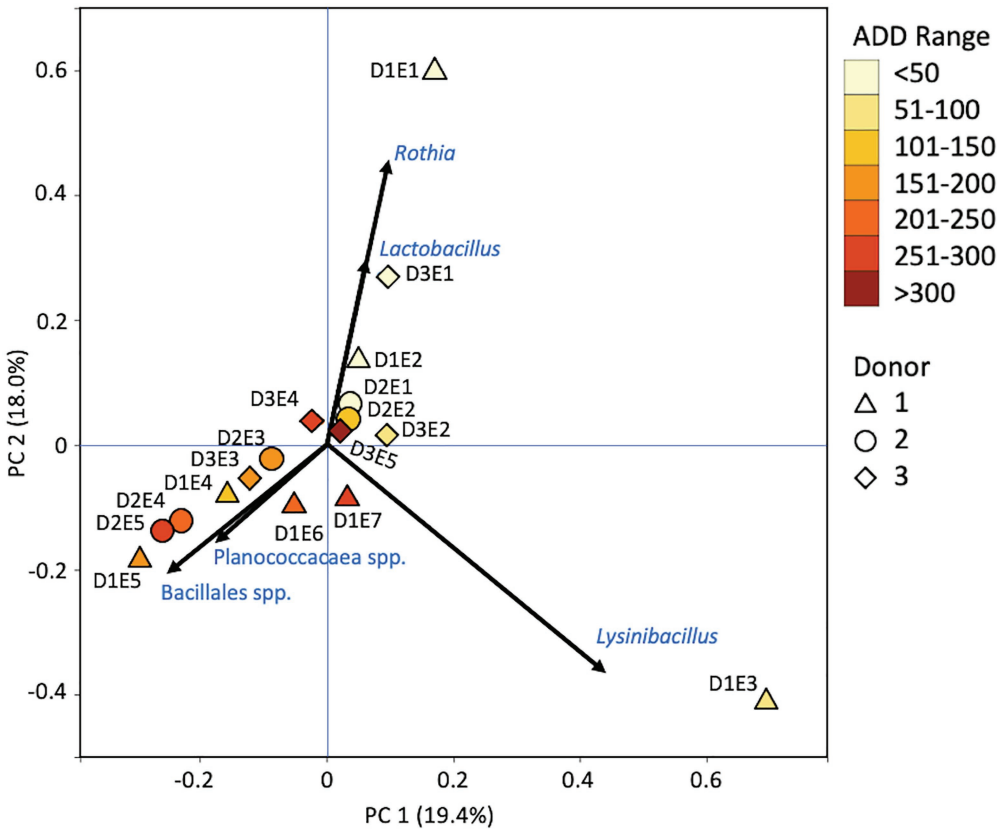

FIGURE 5 | Principal components analysis plot for the proportional data of bacterial genera observed from 16S rRNA gene sequencing of the V6–V8 hypervariable region from oral samples of three human donors (Donors 1, 2, and 3) during decomposition. Shading is added to the symbols [triangles for Donor 1 (D1), circles for Donor 2 (D2), and diamonds for Donor 3 (D3)] to show earlier (lighter shading) to later (darker shading) ADD and also times sampled (from E1 to E7 for D1 and E1 to E5 for D2 and D3, indicating first sample to last sample taken).

Nearly half of the isolates (n = 22) were assessed to match sequences that were recovered from all three donors using at least one of the sequencing techniques (**Table 2**). For example, putative sequences from *B. cereus*, *C. terrigena*, *K. zopfii*, *L. paracasei*, *M. morganii*, *P. vulgaris*, *P. koreensis*, *P. moraviensis*, *R. terrigena*, and *S. maltophilia* were recovered using 16S, MetaG, and MetaT sequencing. MetaG sequencing was most sensitive in detecting species in multiple sampling events, finding 10 or more records of the same species in the 17 samples and matching 37 of the 46 cultures obtained. MetaT sequencing found >10 matches for the same species in four cases and matched to 24 total cultures while the 16S sequencing matched 29 cultures, but only saw a maximum of 6 of the 17 sampling times reflected in the cultured species, thus suggesting lower sensitivity for detecting cultured bacteria using this method. These numbers are likely reflective of the total sequences generated by each method, with thousands (16S), millions (MetaG), and hundreds of thousands (MetaT) of sequences generated in this study (**Supplementary Table 1**). Lastly, two species, *B. cereus* and *E. faecalis*, were observed in all 17 of the samples using the MetaG method. These species were also observed in high numbers in the MetaT reads and *B. cereus* was independently cultured at least four times. A 16S ASV was related to *E. faecalis* at the 96.75% homology level (based on 400 bp), so is not reported in **Table 2** as a match.

DISCUSSION

Overview

To our knowledge, this is the first study to combine 16S sequencing with MetaG and MetaT in exploring the taxonomic diversity in human donors decomposing over time. Many studies have employed next generation sequencing of 16S amplicons from deceased human donors, e.g., Adserias-Garriga et al. (2017) from oral samples; Damann et al. (2015) from bone samples; Hyde et al. (2013) from the mouth and rectum before and after the bloat stage and GI tract after bloat; Hyde et al. (2015) from skin, mouth, and fecal material; Javan et al. (2016) from internal organs, blood, and the buccal cavity; Javan et al. (2017) from the liver and spleen; and Johnson et al. (2016) from the nose and ear cavities. Other microbiome studies based on 16S have included living humans (Costello et al., 2009; Huttenhower et al., 2012), which included samples from the mouth. Several investigations

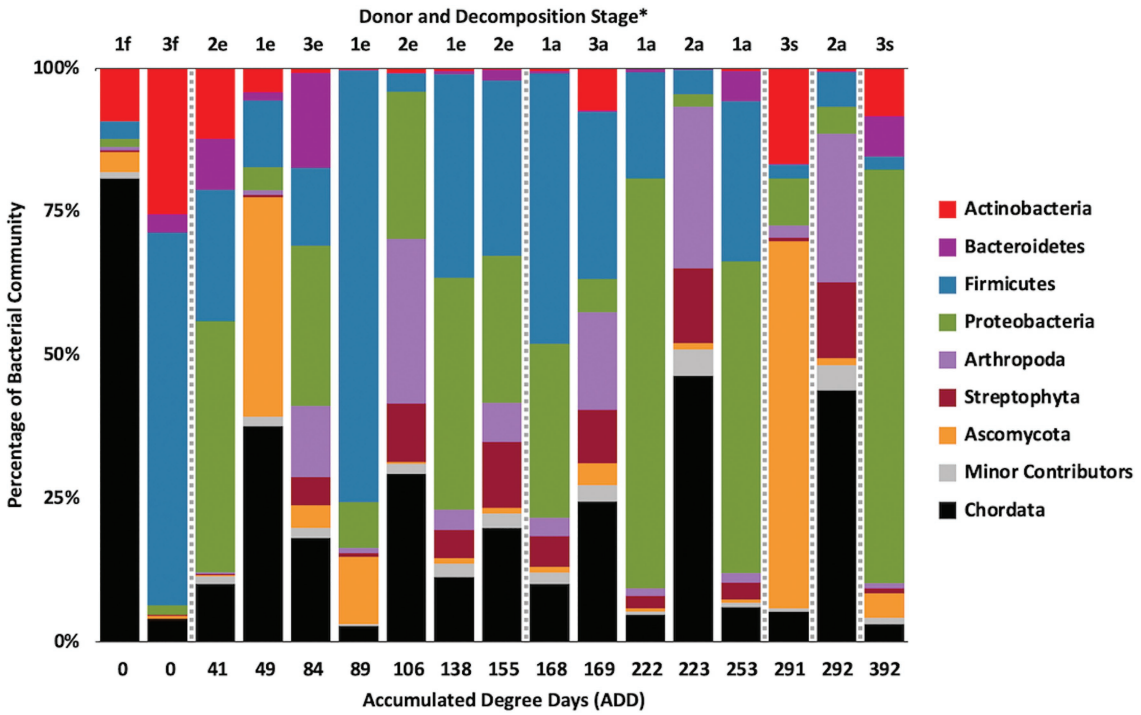

FIGURE 6 | Proportions in percentages of bacterial and eukaryotic phyla determined from shotgun metagenomic (MetaG) sequencing from oral samples of three human donors (Donors 1, 2, and 3) during decomposition. Decomposition was assessed as ADD on the *x*-axis and samples were also classified to an overall decomposition stage for each donor at each sampling event (*f*, fresh; *e*, early; *a*, advanced; and *s*, skeletonized). Minor contributors include data that accounted for <1% of the total diversity within a group.

have shown the mouth to contain unique assemblages of bacteria as compared to other locations in the body in both living (Costello et al., 2009; Huttenhower et al., 2012) and deceased humans (Hyde et al., 2013; Javan et al., 2016). Few studies have recently examined microbial cultures from decomposing human remains (Vass, 2001; Janaway et al., 2009) and none appear to have sampled the hard palate as in this study.

Climate and Other Factors Affecting Decomposition

The donors sampled in this study experienced significantly different temperature regimes during decomposition, which greatly influenced the calculated ADDs (**Figure 1**) and decomposition state (**Table 1**). While the seasonal effect as spring progressed may have had an influence on the microbial communities, there were also other compounding factors such as the presence of dentures in Donor 1, which were removed on the first day of sampling, and scavenger activity. When removing these upper dentures, a thick film of unknown origin was found along the hard palate. As for scavenger activity, vultures were spotted during sampling and their activity, which has been corroborated with higher decomposition rates, was observed by video footage, especially for Donor 3 (Bailey, 2020). Vertebrate and arthropod scavengers could have influenced the sequences we detected as they are carriers of microorganisms themselves and through their action can open up deeper tissues for microbial colonization. Due to the lack of barriers, other scavengers were likely active as well. MetaG and MetaT sequencing analyses yielded data linked to avian, rodent, carnivore, insect, and worm taxa (data not shown). Carter et al. (2015) noted faster decomposition rates in pig carcasses in summer vs. winter and also observed reduced fly activity during rainy conditions. Fewer flies and maggots were noted for Donors 1 and 3, for which it was raining at every sampling event. In all three donors, however, fly-associated bacterial taxa including *Ignatzschineria* and *Wohlfahrtiimonas* were present after the first sampling event. In addition to these variables, the time from death to placement in the decomposition facility was 6–8 days and it is unknown what changes to the microbial communities may have taken place during cold storage of the bodies (**Table 1**). For Donor 2, decomposition would have begun before storage as this individual was dead for 2 days before being discovered. In addition, this donor was obese, a factor that can aid in the acceleration of decomposition (Byard and Tsokos, 2013). Furthermore, the cause of death of the donors was different for each person and originated in organs (heart, stomach, and lungs) distant to the hard palate area that was sampled. Kaszubinski et al. (2020) demonstrated that the manner and cause of death can be linked to the beta-dispersion found in postmortem microbial communities, including those of the mouth. This may be particularly true in cases of heart disease where dysbiosis of the oral cavity has been previously linked to heart conditions (Seymour et al., 2007).

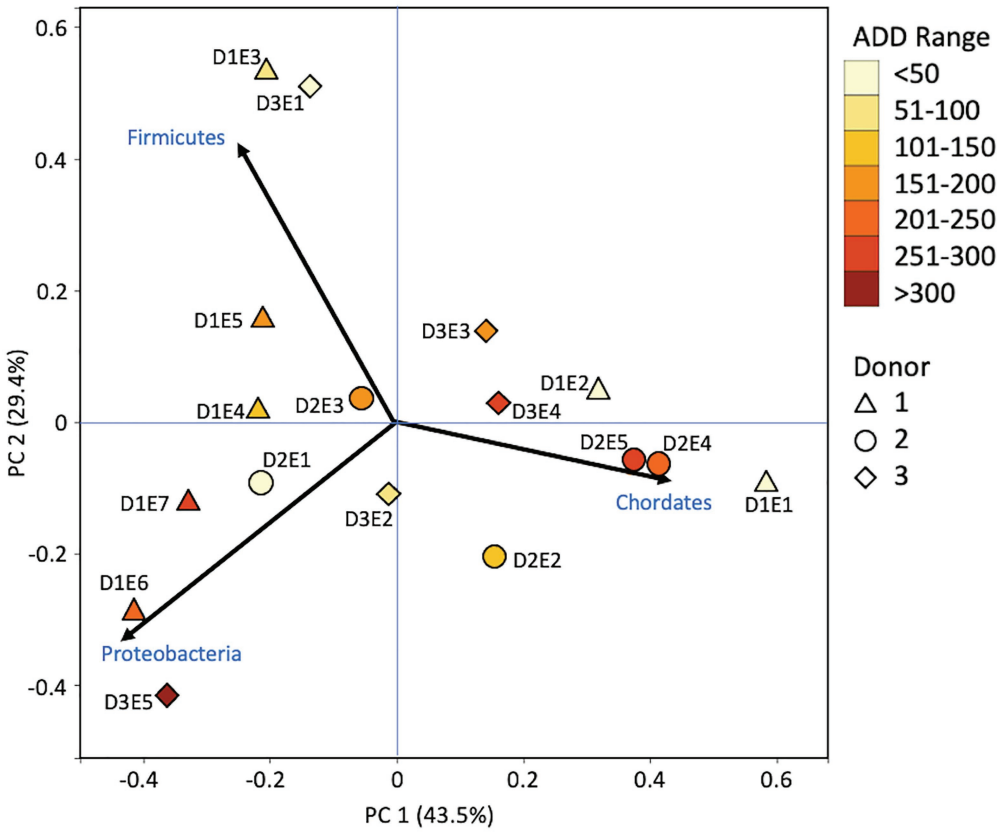

FIGURE 7 | Principal components analysis plot for the proportional data of bacterial and eukaryotic phyla observed from shotgun MetaG sequencing from oral samples of three human donors (Donors 1, 2, and 3) during decomposition. Shading is added to the symbols [triangles for Donor 1 (D1), circles for Donor 2 (D2), and diamonds for Donor 3 (D3)] to show earlier (lighter shading) to later (darker shading) ADD and also times sampled (from E1 to E7 for D1 and E1 to E5 for D2 and D3, indicating first sample to last sample taken).

16S Phylum Patterns

Based on 16S sequencing, the phyla Firmicutes and Proteobacteria are most often sampled in the human mouth before death, in recently deceased humans, and early in decomposition, while Actinobacteria and Bacteroidetes are often found in appreciable numbers (Huttenhower et al., 2012; Hyde et al., 2013, 2015; Adserias-Garriga et al., 2017). Other locations in the body show similar trends in which these four phyla are dominant in numbers in the early PMI such as for skin (Hyde et al., 2015), liver and spleen (Javan et al., 2017), and ribs (Damann et al., 2015). Our data show high numbers for Firmicutes including in the ADD values up to 50 (fresh stage of decomposition), with proportions from ~25–70% of the total; however, the first sample for Donor 1 consisted of ~75% Actinobacteria (**Figure 2**), all accounted for by the genus *Rothia* (**Figure 4**). *Rothia* has been shown to be skewed toward males (Javan et al., 2016) and especially common in early samples during decomposition (Javan et al., 2016; Adserias-Garriga et al., 2017). Donor 1 was the only male in this study and the same *Rothia* ASV found in Donor 1 was also found in the other two donors, with Donor 2 showing a second ASV for this genus. The first sample for Donor 1 showed low diversity (**Supplementary Table 1**) and otherwise only contained six distinct ASVs, all related to *Lactobacillus* spp.

Middle to later stages of decomposition have shown Firmicutes generally as the most abundant phylum with occasional dominance from Proteobacteria (Hyde et al., 2013, 2015; Adserias-Garriga et al., 2017) and, even more infrequently, Actinobacteria (Hyde et al., 2015). Our data are consistent with these findings for ADD values starting at 84 (early stage of decomposition), in which nine of 13 samples were dominated (>75% of the sequences) or co-dominated (~50% of the sequences) by Firmicutes and five of the 13 samples were dominated or co-dominated by Proteobacteria. In one sample, the second to the last for Donor 3 (291 ADD), Actinobacteria accounted for >50% of the ASVs (**Figure 2**).

The only other phyla observed for the 16S sequences included Epsilonbacteraeota (**Figure 2**), which was represented by two ASVs, one found in the first sample for both Donors 2 and 3 and was related to an uncultured *Campylobacter*, and the other found in the last sample for Donor 3 which was related to *Arcobacter*. Both of these genera contain human-associated bacteria, including well known pathogens in *Campylobacter* and bacteria from the oral and other human environments in the case of *Arcobacter* (On et al., 2017). Five unique ASVs

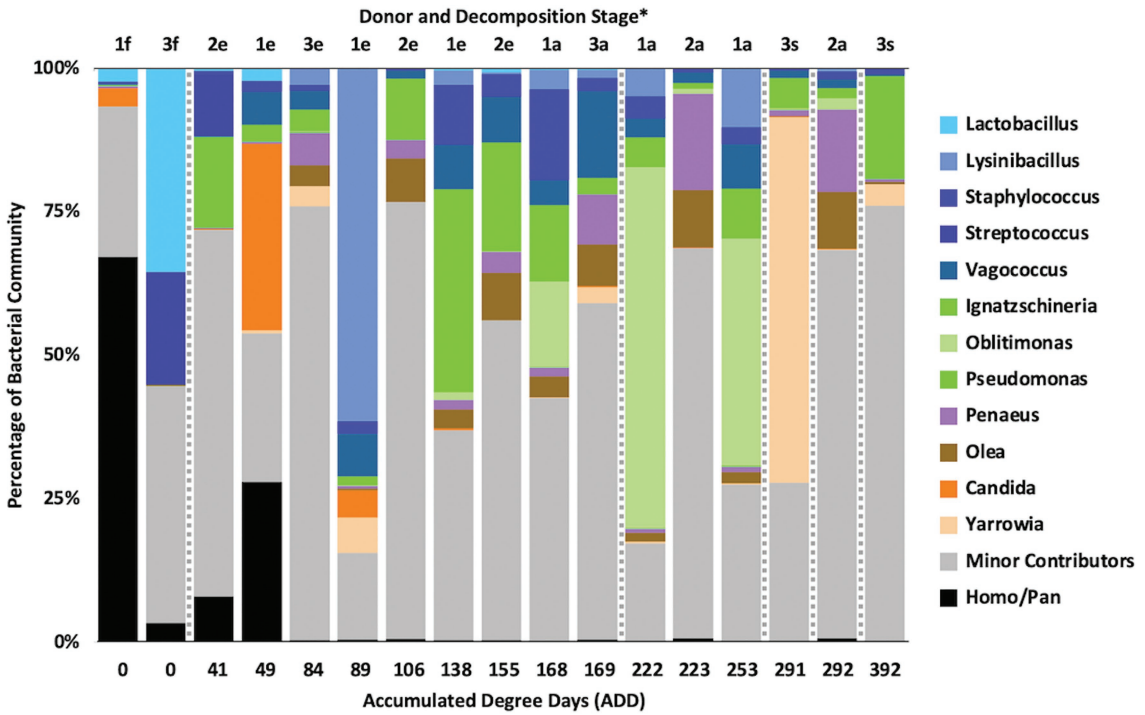

FIGURE 8 | Proportions of bacterial and eukaryotic genera determined from shotgun MetaG sequencing from oral samples of three human donors (Donors 1, 2, and 3) during decomposition. Decomposition was assessed as ADD on the *x*-axis and samples were also classified to an overall decomposition stage for each donor at each sampling event (*f*, fresh; *e*, early; *a*, advanced; and *s*, skeletonized). Minor contributors include data that accounted for <3% of the total diversity within a group.

from the phylum Fusobacteria were found, all in the first sample for Donor 2. These were related to the genera *Fusobacterium* and *Leptotrichia*, which include anaerobic fermenters and are common in oral and other locations in the body (Gupta and Sethi, 2014). Lastly, one ASV related to an uncultured species of Verrucomicrobia was found in the second sample for Donor 1. This sequence is most closely related to the genus *Akkermansia*, which includes species, found in the human gut that catabolizes mucin (Derrien et al., 2004). Some of these taxa are normally found in the GI tract, but it is not surprising to find them in the oral cavity during decomposition, especially after the bloat stage when gut contents and microbes may purge from these lower sites (Hyde et al., 2013; Adserias-Garriga et al., 2017). In our study, bloat was not observed for any of the donors due to the sampling schedule and limited access to the FOREST facility during our study.

16S Genus Patterns

Common genera observed in 16S sequenced from the mouths of human donors sampled during early stages of decomposition include *Streptococcus* (Hyde et al., 2013; Javan et al., 2016; Adserias-Garriga et al., 2017); *Prevotella* and *Veillonella* (Hyde et al., 2013; Javan et al., 2016); *Lactobacillus*, *Bacteroides*, and *Clostridium* (Hyde et al., 2013); *Corynebacterium*, *Escherichia*, and *Actinomyces* (Adserias-Garriga et al., 2017); *Rothia* (Javan et al., 2016; Adserias-Garriga et al., 2017); and *Staphylococcus* and *Haemophilus* (Javan et al., 2016). Our data include ASVs related to all of these genera with *Actinomyces*, *Rothia*, *Clostridium*, *Lactobacillus*, and *Streptococcus* showing notable numbers (~15–45% of the ASVs from at least one sample; **Figure 4**). Other genera appearing prominently in early samples in our data include *Lysinibacillus*, *Vagococcus*, *Pseudomonas*, and *Ignatzschineria*. These genera are often observed in middle to late decomposition along with *Acinetobacter*, *Enterococcus*, *Erysipelothrix*, and unresolved taxa from the families Bacillaceae and Planococcaceae (Adserias-Garriga et al., 2017). Our data showed *Enterococcus*, *Ignatzschineria*, unknown Bacillales, and unknown Planococcaceae to be common in ADD values beginning at 138 and through 292, suggesting their abundance and perhaps importance in decomposition. Other work has demonstrated that many of the above genera are abundant in the mouths of living humans, including samples specifically taken from the hard palate (Huttenhower et al., 2012), and are also generally found in decomposition of humans (Hyde et al., 2015). Johnson et al. (2016) determined that *Staphylococcus* and *Vagococcus* were good candidates for estimating PMI using a machine learning approach.

As shown above, the ASVs from our 16S sequencing yielded similar genera to those found in the mouths of living people, including some potentially associated with oral diseases (Huttenhower et al., 2012). However, at the level of species, only one of our ASVs was able to be matched to one of the sequences reported in Huttenhower et al. (2012). This was an ASV for *Lactobacillus crispatus*, which may be found in healthy

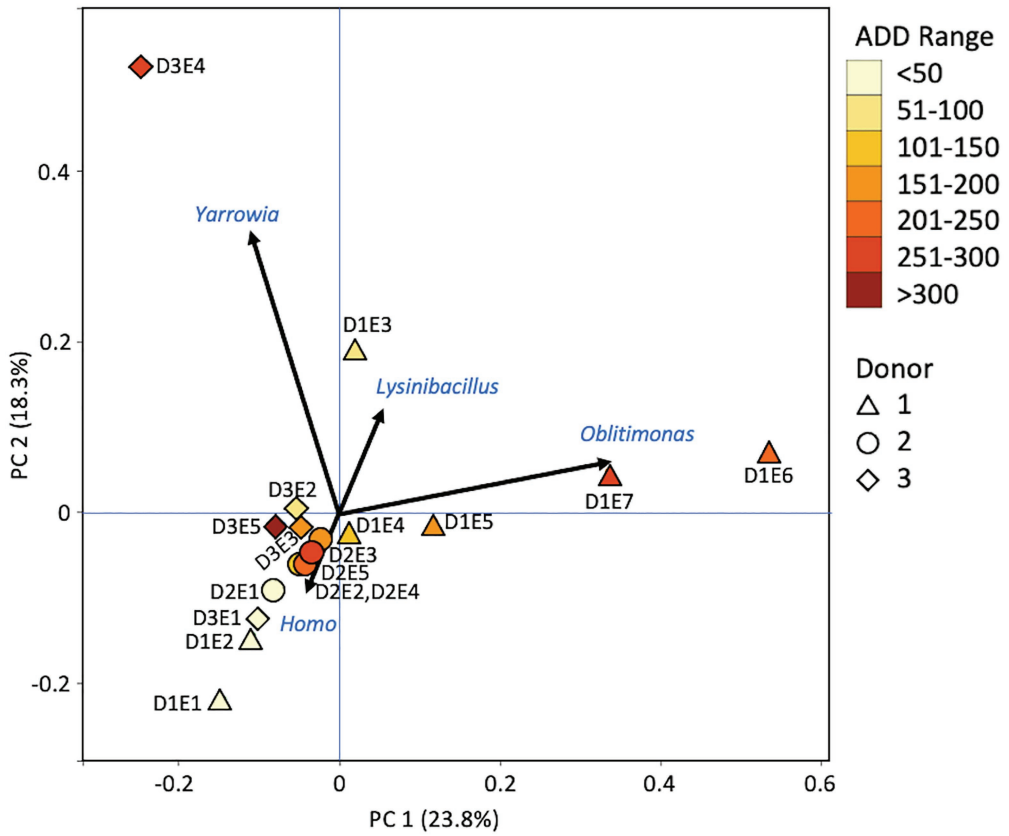

FIGURE 9 | Principal components analysis plot for the proportional data of bacterial and eukaryotic genera observed from shotgun MetaG sequencing from oral samples of three human donors (Donors 1, 2, and 3) during decomposition. Shading is added to the symbols [triangles for Donor 1 (D1), circles for Donor 2 (D2), and diamonds for Donor 3 (D3)] to show earlier (lighter shading) to later (darker shading) ADD and also times sampled (from E1 to E7 for D1 and E1 to E5 for D2 and D3, indicating first sample to last sample taken).

individuals, and was observed to be approximately a quarter of all ASVs identified in the first sample for Donor 1 and for Donor 3. It was not observed in Donor 2 and otherwise only in the second and third samples for Donor 1 as 1–2% of the total sequence records. In all other species shown to exist in the human oral cavity, our records were not able to be directly matched, largely because our output from QIIME2 produced records for uncultured bacteria or taxa with ambiguities. However, in analyzing the sequences for our ASVs against the Expanded Human Oral Microbiome Database (eHOMD; Escapa et al., 2018), another species was able to be matched to one found in the study done by Huttenhower et al. (2012) and was identified as *Rothia mucilaginosa* (100% match), which was assessed to be an opportunistic pathogen. It was only found in the three initial samples taken from all of our donors and in the second sample from Donor 1. For Donor 1, this species accounted for ~70 and ~13% of ASVs sequenced from the first and second sample, respectively. The *R. mucilaginosa* ASV comprised <5% of the total sequences for the initial samples of the other donors, lending some support to the findings of Javan et al. (2016). Commonly occurring genera in our study and the human microbiome (Huttenhower et al., 2012) were also found in the oral cavities of decomposing humans as shown in Adserias-Garriga et al. (2017) and include *Streptococcus*, *Staphylococcus*, *Rothia* (including *R. mucilaginosa*), and *Corynebacterium*. *Streptococcus parasanguinis* was a species identified in this latter study and was also determined to be among our ASVs (at a 100% match to a sequence in eHOMD), being found in a single sample, the first taken from Donor 3, which accounted for ~10% of all ASVs in the sample.

Interestingly, Adserias-Garriga et al. (2017) showed a drop in oral-associated species from as high as ~95% of all species in a donor in early decomposition to <5% of species by the end of decomposition. We examined our ASVs in a similar way and selected 51 sequences to analyze further based on their prevalence in the dataset (defined as accounting for >5% of ASVs collectively across all samples). Of these, 23 ASVs showed >97% sequence identity to eHOMD records and the others fell between 84 and 96.8% similar to 16S sequences in that database (Escapa et al., 2018). For the highly matched sequences, there were 12 species that only appeared early in decomposition from our samples, originating in ADD scores <50. These were *Schaalia* sp. HMT 180, *R. mucilaginosa*, *Prevotella* sp. HMT 313, *Granulicatella elegans*, *L. crispatus*, *L. fermentum*, *L. gasseri*, *L. paracasei*, *Streptococcus parasanguinis*, *Veillonella atypica*, *Neisseria perflava*, and

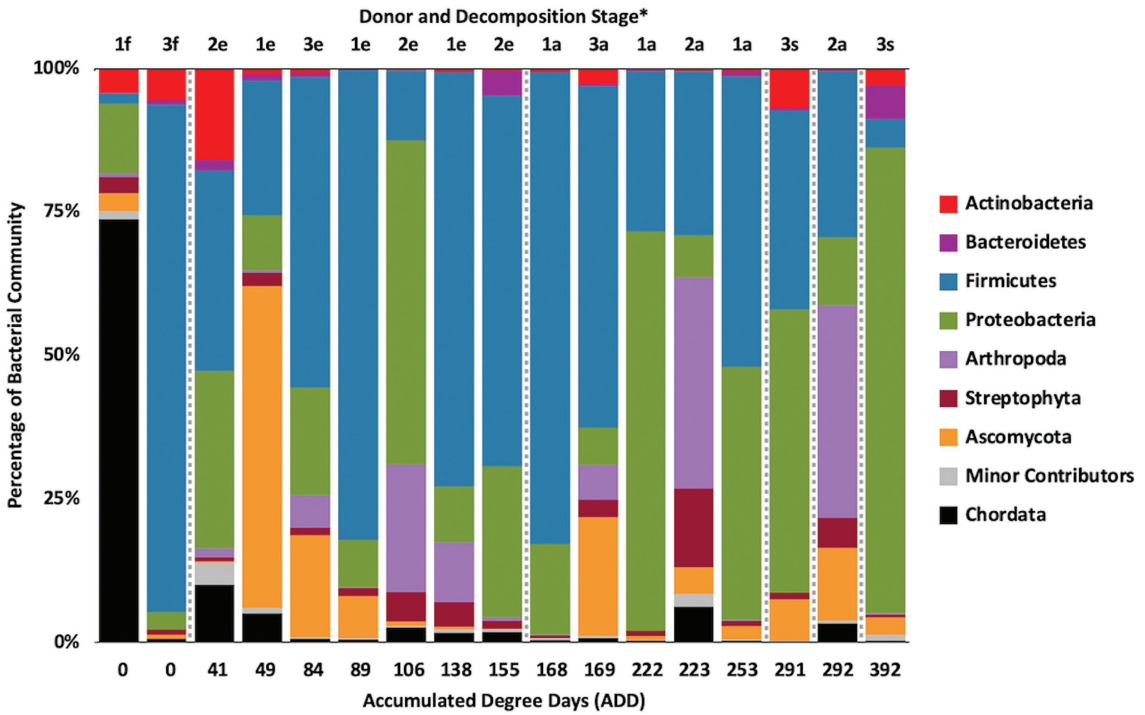

FIGURE 10 | Proportions of bacterial and eukaryotic phyla determined from shotgun metatranscriptomic (MetaT) sequencing from oral samples of three human donors (Donors 1, 2, and 3) during decomposition. Decomposition was assessed as ADD on the *x*-axis and samples were also classified to an overall decomposition stage for each donor at each sampling event (*f*, fresh; *e*, early; *a*, advanced; and *s*, skeletonized). Minor contributors include data that accounted for <1% of the total diversity within a group.

Haemophilus parainfluenzae. One poorly matched ASV to the eHOMD records was a *Vagococcus* sequence that accounted for over 38% of the sequences for the second sample for Donor 1 (ADD 49). High sequence identity matches for ASVs from late samples (>ADD 168) to oral taxa were found for *Pseudomonas stutzeri*, *Kluyvera ascorbata*, and *Corynebacterium urealyticum*. Lastly, poorer matches (all <94% sequence identity) to five ASVs were all found in the final sample from Donor 3 (392 ADD) and comprised from 6 to 13% each of the ASVs in that sample. These sequences included an unresolved taxonomic group in the Proteobacteria as well as two genera from this phylum, *Oligoflexus* and *Undibacterium*, as well as two ASVs aligned to the genus *Flavobacterium*. These results show that as decomposition progresses, fewer oral-associated bacteria are detected and an increase in taxa with low matches to the eHOMD database increased, suggesting that these taxa may come from other environments (Adserias-Garriga et al., 2017). Of the late appearing ASVs for Donor 3 with low matches to eHOMD from above, all were found to be most closely related to bacteria isolated from soil, and in one case, from a waterfall.

MetaG and MetaT Phylum Patterns

The number of numerically abundant phyla that were detected based on sequencing method was similar (7–8 phyla; **Figures 2, 6, 10**), despite the greater sequencing power of the MetaG and MetaT methods (**Supplementary Table 1**), which also picked up eukaryotic taxa. However, a total of only seven phyla were sequenced in the 16S work as compared to 66 phyla in the MetaG sequencing and 51 for MetaT. More than half of the phyla for these latter two methods were from bacteria (data not shown). For the bacteria, Actinobacteria, Firmicutes, and Proteobacteria were the most abundant phyla across the three methods, with Actinobacteria showing higher values in the 16S sequences. Unsurprisingly, these three phyla also drove the relationships seen in PCA plots, along with Chordata for the MetaG and MetaT sequence data (**Figures 3, 7, 11**). These three bacterial phyla accounted for almost all of the cultures as well (**Table 2**). Based on these results, it would appear these phyla were most numerous and important in the decomposition processes in the FOREST for the donors sampled. As shown previously, this is consistent with other studies using culture or sequencing methods when assessing bacterial diversity *via* 16S in living and decomposing humans (Vass, 2001; Janaway et al., 2009; Huttenhower et al., 2012; Hyde et al., 2013, 2015; Damann et al., 2015; Adserias-Garriga et al., 2017; Javan et al., 2017). What is not apparent, in **Figures 3, 7, 11** for the phyla in this study, is any clear trend in the plots based on decomposition time or donor. In **Figures 2, 6, 10**, one can see temporary increases or "blooms" of some taxa which help to show individual donor differences for one or two sampling events that are reflected in the PCA plots and appear to be outliers in those graphs. These include phyla in the first sample for Donor 1 and the fourth sample

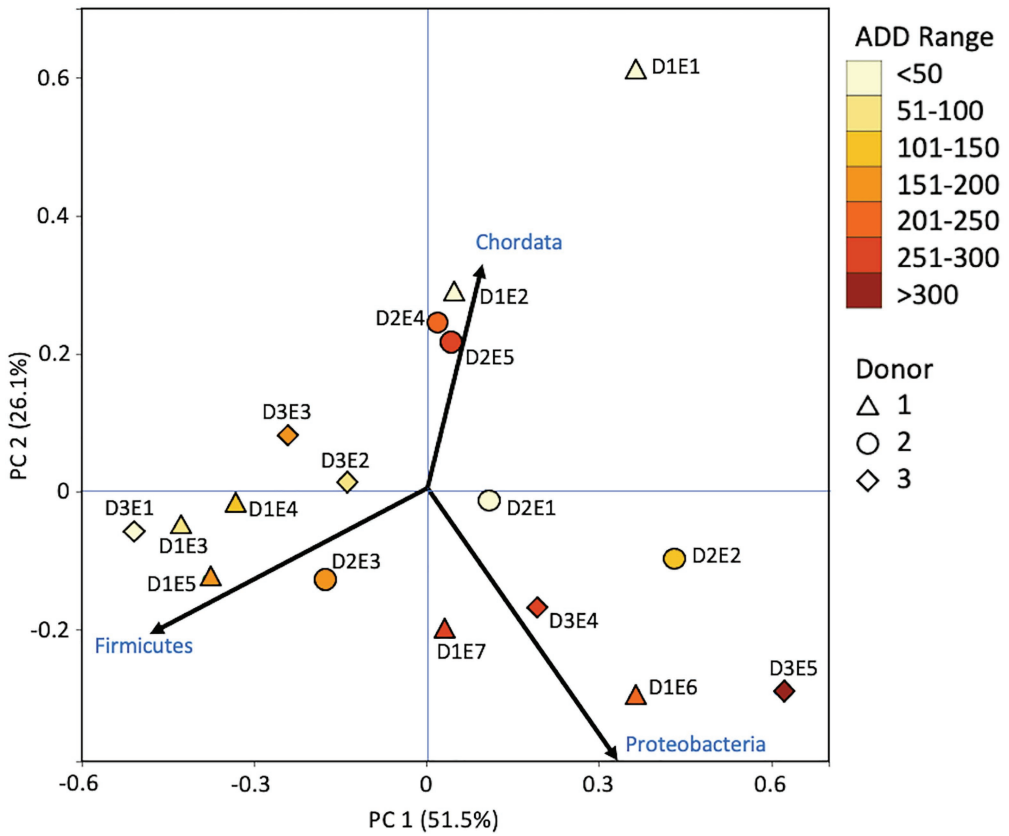

FIGURE 11 | Principal components analysis plot for the proportional data of bacterial and eukaryotic phyla observed from shotgun MetaT sequencing from oral samples of three human donors (Donors 1, 2, and 3) during decomposition. Shading is added to the symbols [triangles for Donor 1 (D1), circles for Donor 2 (D2), and diamonds for Donor 3 (D3)] to show earlier (lighter shading) to later (darker shading) ADD and also times sampled (from E1 to E7 for D1 and E1 to E5 for D2 and D3, indicating first sample to last sample taken).

for Donor 3 (Actinobacteria), the second and last sample for Donor 3 and the second sample for Donor 2 (Proteobacteria; **Figures 2, 3**); the first sample for Donor 3 and the third sample for Donor 1 (Firmicutes; **Figures 6, 7**); and the first sample for Donor 1 (**Figures 10, 11**; Chordata). These and other individual sample differences may have biological meaning, even if they are not something we can clearly define, based on lack of further data. Below we address some differences seen for the genera sequenced in this study and how some clearer patterns were observed in PCA, especially for early samples, and how some key taxa involved in the decomposition of the donors in this study may have been identified.

MetaG and MetaT Eukaryotic Genus Patterns

The MetaG and MetaT sequences included data for taxa that would be unexpected in the microflora of human mouths undergoing decomposition, including some members of the phyla Arthropoda, Chordata (non-human DNA and RNA), and Streptophyta (**Figures 6, 10**). While some of these phyla might be represented in the diet of living humans, it is unclear in many cases why they would increase in abundance through decomposition. For example, the genus *Penaeus* (all matched to *P. vannamei*, the Pacific White Shrimp) was found in all 17 of the MetaG samples and six of the MetaT samples (for Donors 1 and 2 only) and *Olea* (all sequences matched to *O. europaea*, the Common Olive tree) was found in 14 of the MetaG samples and five of the MetaT samples (Donors 1 and 2 only). This suggests a few possibilities, including that all of the donors had consumed foodstuffs with these organisms in them and that DNA or RNA from the food remained in the oral cavities and/or was released from the digestive tract into the mouth during bloat and purge. This is less easy to believe from the MetaT data as it would suggest RNA was present in inactive cellular materials. It could also mean that scavenging organisms carried plant and animal components to the mouths of the donors. It cannot be ruled out that there are as yet unsequenced nucleic acids from many understudied taxa in the sequence databases. Therefore, matches we see for our MetaG and MetaT data may be insufficient to resolve lower ranked taxa. In examining many of the minor contributors to the MetaG and MetaT sequence reads, organisms from other continents that would not be in or near the FOREST site were encountered (data not shown) and it is more plausible to presume we have detected nucleic acids from related taxa as the Kraken2

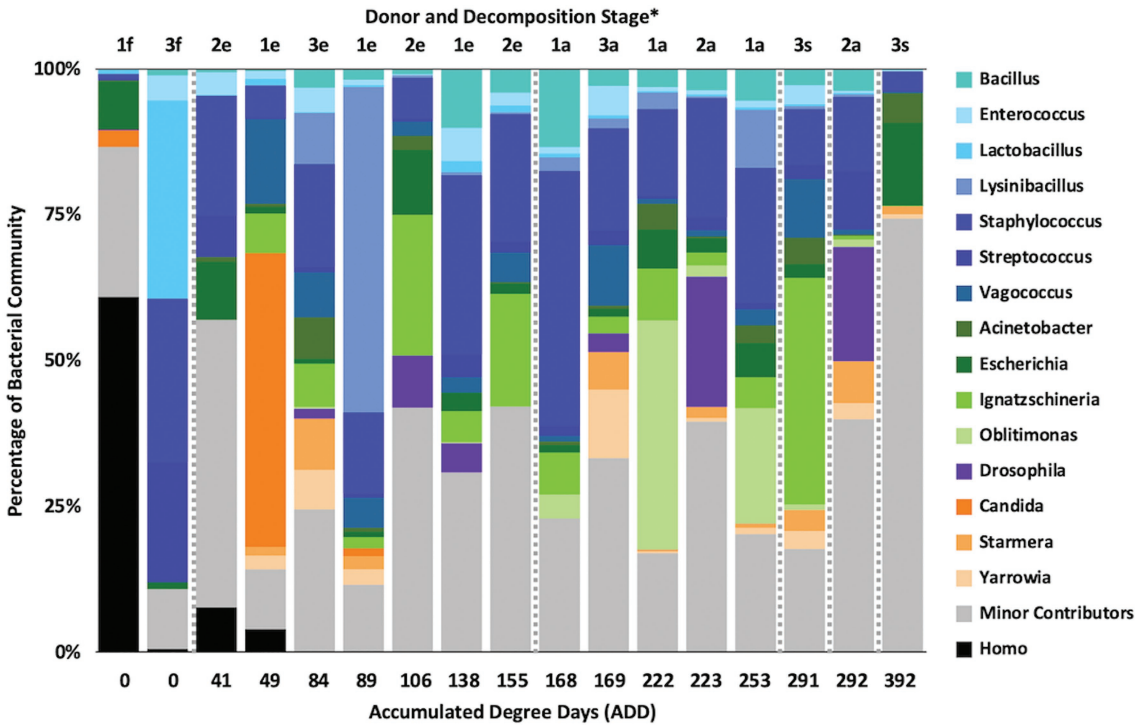

FIGURE 12 | Proportions of bacterial and eukaryotic genera determined from shotgun MetaT sequencing from oral samples of three human donors (Donors 1, 2, and 3) during decomposition. Decomposition was assessed as ADD on the *x*-axis and samples were also classified to an overall decomposition stage for each donor at each sampling event (*f*, fresh; *e*, early; *a*, advanced; and *s*, skeletonized). Minor contributors include data that accounted for <3% of the total diversity within a group.

taxonomic assignment will have a certain degree of false-positives at different confidence settings.

The presence of arthropods such as flies is not surprising as they are mobile and could be drawn to resources provided *via* decomposition (Goff, 2010). Flies and other arthropods could also serve as vectors for the nucleic acids and microbes detected in this study. Eggs and larva from insects could have also been sampled when swabbing the donors as they were observed, but not identified to any taxonomic level (**Table 1**). Perhaps surprisingly, 32 species allied to *Drosophila* were found in the MetaG reads, none of which were observed in the first sample taken, while 26 presumptive *Drosophila* species were found in MetaT reads in all but the first three samples taken for Donor 1 and the first sample taken for the other donors. To our knowledge, there is no evidence in the literature that shows fruit flies using animal remains for feeding or laying eggs and *Drosophila* spp. are consistently observed in decomposing vegetal matter (Markow and O'Grady, 2008). One laboratory investigation did report feeding fruit flies with irradiated beef and ham as part of their diet in order to detect effects of food sterilization on the genetics of the consumer (Mittler, 1979); so the use of decomposing animal tissue by *Drosophila* cannot be ruled out. In the MetaT dataset, *Drosophila* was often a major contributor to the sequences (**Figure 12**), but was always a minor contributor in the MetaG data (**Figure 8**). Donor 2 showed the most insect activity throughout sampling (**Table 1**) and had the highest values for *Drosophila* RNA sequences. More work will need to be done, including with other MetaT data yet analyzed from this study, to more precisely determine the role of these insects and whether these reads were simply misidentified or truly belong this genus. Two other insect taxa that have been identified as being important in the decomposition of humans, *Lucilia* spp. and *Phormia regina* Meigen, 1826 (Diptera: Calliphoridae; Anderson, 2000) were observed in our donors. *Lucilia cuprina* Wiedemann, 1830 (Diptera: Calliphoridae) nucleic acids were detected using MetaG and MetaT in all three donors, with the majority of the data coming from Donor 2, for which the only records from *P. regina* were also found.

Yeasts such as *Candida* and *Yarrowia* being found in nucleic acid sequences from our samples makes intuitive sense as they are often sampled from living humans (Huseyin et al., 2017) or they could be brought to decomposing bodies *via* flies or by wind dispersal. *Candida* is a well-studied genus of human-associated yeasts and is implicated in many diseases (Huffnagle and Noverr, 2013). We detected *Candida albicans* and *Candida dublinensis* in MetaG sequences in all donors across decomposition, most prominently in Donor 1 (**Figure 8**). Donor 1 and the last sample for Donor 2 also showed a match for *C. glabrata*. Only Donor 1 had any records for *Candida* in the MetaT sequences (**Figure 12**) and all three above species were represented, but only in the first three samples. It seems likely that *Candida* was present largely as a commensal of their hosts and, after death, dropped in numbers as decomposition

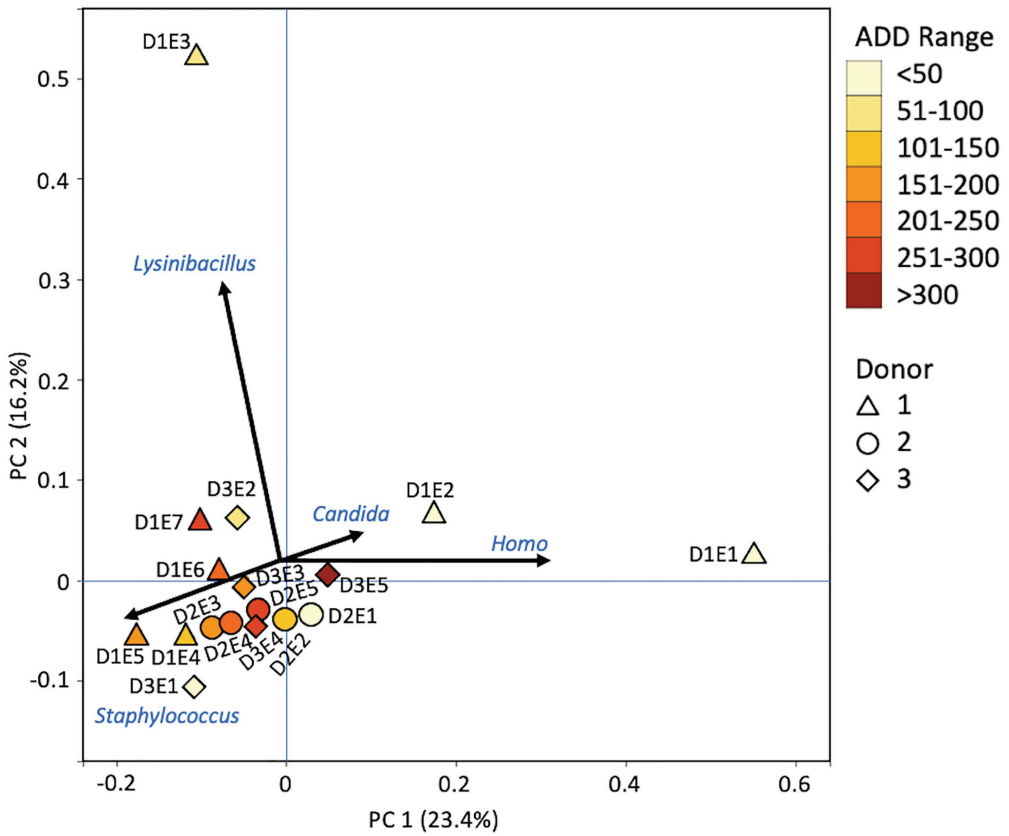

FIGURE 13 | Principal components analysis plot for the proportional data of bacterial and eukaryotic genera observed from shotgun MetaT sequencing from oral samples of three human donors (Donors 1, 2, and 3) during decomposition. Shading is added to the symbols [triangles for Donor 1 (D1), circles for Donor 2 (D2), and diamonds for Donor 3 (D3)] to show earlier (lighter shading) to later (darker shading) ADD and also times sampled (from E1 to E7 for D1 and E1 to E5 for D2 and D3, indicating first sample to last sample taken).

progressed. *Yarrowia* is a widespread yeast and almost all of our sequences in MetaG and MetaT matched to *Yarrowia lipolytica*, which has been cultured from foodstuffs, soil, hydrocarbons including fuels, wastewater, and human clinical samples (Knutsen et al., 2007). The species epitaph refers to the lipase enzymes produced by this yeast, which allows it to subsist on lipids and other complex hydrocarbons, and might explain its appearance throughout decomposition (**Figures 8, 12**). Lastly, the genus *Starmera*, seen in our MetaG as a minor contributor and more noticeably in our MetaT data (**Figure 12**), was represented by *Starmera dryadoides*, a yeast of unknown ecology, but has been associated with fig plants infested with insects (Kurtzman et al., 2011), and may have found their way to the donors through an insect or other vector.

MetaG and MetaT Bacterial Genus Patterns

At the level of genus, many more taxa were seen in the MetaG and MetaT datasets, but most were considered minor contributors in numbers to the overall microbial communities (**Figures 4, 8, 12**). *Rothia* was influential in separating some of the early samples based on PCA of the 16S data, where it was only found in in the first sample taken for all donors and in the second sample taken for Donor 1 (**Figures 4, 5**). This genus was also shown to be highly significant in MetaG data where it was only found in in the first (fresh) samples taken from each donor ($p < 0.001$). *Lysinibacillus* was important throughout all three sequencing datasets and influenced the PCA plots in all cases based on its dominance in the third sample for Donor 1. However, this genus was also common in all three methods, appearing in 12, 14, and 13 of the samples taken for the 16S, MetaG, and MetaT sequencing, respectively. *Lactobacillus* spp. played a role in separating the early samples as shown in **Figures 4, 5** for the 16S sequencing, but this genus was also present in 16 of the 17 samples taken for both the MetaG and MetaT methods, albeit in decreasing numbers past the first few sampling times. *Oblitimonas* was observed to be influential in later samples, including the MetaG data, in which it helped to separate out the last two samples from Donor 1 from the other samples (**Figure 9**). It was also found in the MetaT data where it too was common in the final Donor 1 samples. This genus was not seen in any of the 16S sequence data, but was found in 12 and 11 of the MetaG and MetaT samples taken, respectively, but never in the first sample taken from a donor. Two fungal taxa, *Yarrowia* from the MetaG data (**Figure 9**) and *Candida* from the MetaT data (**Figure 13**),

TABLE 2 | Species of bacteria recovered from three human donors undergoing decomposition at the FOREST facility in Cullowhee, NC including a name for each based on NCBI taxonomy resulting from BLAST analyses, the donor(s) and sampling event(s) that yielded each species, asnd the accumulated degree day(s; ADD) at the time(s) of sampling.

Best NCBI match	Donor	Sampling event(s)	ADD	ADD range	16S rRNA ASVs	MetaG reads	MetaT reads
Acinetobacter albensis	1	7	253	251–300	3:6*	2:3*	--
Acinetobacter gerneri	3	4	291	251–300	1:3*	2:6*	1:2*
Bacillus cereus	1	2, 4, 6, 7	49–253	0–300	2:2*	3:17*	3:14*
Bacillus mycoides	2	4	223	201–250	2:2	3:11*	1:1
Bacillus paranthracis	2	5	292	251–300	--	3:10	3:11
Bacillus simplex	2	5	292	251–300	--	3:10	--
Comamonas terrigena	3	5	392	301–400	1:3*	2:5*	1:2*
Corynebacterium striatum	3	1	0	0–50	--	1:4*	--
Corynebacterium xerosis[1]	3	3	169	151–200	1:3*	3:7*	1:1
Curtobacterium citreum[1]	3	1	0	0–50	--	--	--
Dermacoccus nishinomiyaensis	1, 3	1, 5	0.3, 168	0–200	--	--	--
Enterococcus faecalis	3	1	0	0–50	--	3:17*	3:11*
Flavobacterium saccharophilum[1]	3	5	392	301–400	--	2:2*	--
Hafnia paralvei	2	2	106	101–150	--	2:6*	1:1
Janthinobacterium lividum[1]	3	5	392	301–400	--	1:1*	1:1*
Kocuria rhizophila[1]	3	3	169	151–200	--	1:3*	--
Kurthia zopfii	3	2	84	51–100	2:3*	3:12*	2:6*
Lactobacillus paracasei	3	1	0	0–50	2:3*	2:7*	2:2*
Lactobacillus plantarum	3	1	0	0–50	1:2	3:15*	3:6*
Lysinibacillus fusiformis	3	4	291	251–300	2:2	3:10	1:1
Macrococcus canis	1	5	168	151–200	--	3:9*	1:1
Massilia putida	3	1	0	0–50	--	1:1	1:1
Microbacterium lemovicicum	1	1	0	0–50	1:1	1:2	--
Microbacterium saccharophilum[1]	1	1	0	0–50	--	--	--
Micrococcus aloeverae	1	2	49	0–50	--	--	--
Moraxella osloensis	3	1	0	0–50	--	3:10	2:2
Morganella morganii	1, 3	2, 3, 4	84–138	51–150	2:3*	3:15*	3:10*
Myroides profundi	1	6	222	201–250	2:3*	3:5*	--
Nocardia coeliaca	2	1	41	0–50	3:4	--	--
Paenarthrobacter ilicis	1	2	49	0–50	1:2*	--	--
Paenarthrobacter nicotinovorans	1, 2	1	0, 41	0–50	1:2	2:2	--
Paenarthrobacter nitroguajacolicus[1,2]	1	2, 3	49, 89	0–100	1:2*	--	--
Proteus terrae[1,2]	1, 2	3, 3, 6	89–222	51–250	2:3*	3:5*	--
Proteus vulgaris	1	3, 4	89, 138	51–150	3:6*	3:14*	2:3*
Providencia alcalifaciens[1,2]	2, 3	3	155, 169	151–200	1:1	3:12*	3:3
Providencia vermicola[1,2]	2, 3	3	155, 169	151–200	3:6*	--	--
Pseudomonas koreensis[1,2]	2	1, 2	41, 106	0–150	1:1*	2:2*	2:2*
Pseudomonas moraviensis	2	1	41	0–50	1:1*	2:2*	1:1*
Pseudomonas weihenstephanensis[1]	1	6	222	201–250	1:1	1:1	--
Raoultella terrigena	3	5	392	301–400	1:2*	2:6*	1:2*
Serratia liquefaciens	2	2	106	101–150	--	2:6*	--
Sphingomonas xinjiangensis[1]	3	3	169	151–200	--	--	--
Staphylococcus saprophyticus	1, 2	1, 5	0, 292	0–300	2:4*	3:11*	--
Staphylococcus sciuri	2, 3	2, 3	85, 155	51–200	1:1	3:12*	1:1
Staphylococcus xylosus	2	4	223	201–250	2:2*	3:12*	--
Stenotrophomonas maltophilia[1]	3	5	392	301–400	1:2*	3:11*	2:2*

*The last three columns reflect data for which similarly named taxonomic designations could be found in 16S rRNA gene sequencing, shotgun MetaG sequencing, and shotgun MetaT sequencing. The first value in each of the pairs of numbers separated by a colon in the last three columns includes how many of the three donors yielded a sequence matching the culture shown in the first column while the second number includes how many of the individual samples had a sequence match to that culture. *indicates that the culture was obtained from a sample taken from the same donor at the same sampling time as one or more of the culture-independent sequencing approaches. (For example, for Acinetobacter albensis in the first row, the 16S rRNA ASVs reports 3:6* which means that all three donors had a match to this species from this method and that six of the 17 samples recovered did. The asterisk indicates that the A. albensis culture recovered was found on the same day as one of the 16S rRNA ASVs. Where "--" is displayed indicates that a species found in culture was not detected from one of the sequencing methods).*

[1]culture grown on low nutrient media only.

[2]culture grown on low nutrient media and normal strength R2A.

helped discriminate two samples based on their high abundance. *Yarrowia* accounted for 64% of the community sequences and *Candida* for ~50%, respectively (**Figures 8, 12**). Overall, there is a pattern for the genera from the earliest sample times (first sample for each donor plus the second sample for Donor 1) to cluster in PCA plots for the 16S and MetaG data, with a weaker pattern seen for the MetaT data. A similar trend was seen at the level of phylum in another study examining oral

microbiota during human decomposition (Adserias-Garriga et al., 2017). One bacterial genus, *Comamonas*, which was not observed in high abundance in any of our data, was shown to have a highly significant result based on being most abundant in MetaT sequences from samples taken for Donor 3 that had reached skeletonization ($p < 0.001$).

Five genera were found to be in high numbers (at least 15% of the sequences obtained in a given sample) for all three sequencing methods (**Figures 4, 8, 12**). These included four from the phylum Firmicutes: *Lactobacillus*, *Lysinibacillus*, *Streptococcus*, and *Vagococcus*, and *Ignatzschineria* from Proteobacteria. The number of samples in which *Lactobacillus* appeared was 5, 16, and 16 for the 16S, MetaG, and MetaT samples, respectively, and these were most numerous in early ADD values, primarily during the fresh decomposition stage. *Streptococcus* was also most prevalent in early decomposition and was found in three of the 16S samples and all of the MetaG and MetaT samples. *Lysinibacillus*, *Vagococcus*, and *Ignatzschineria* were found in 12–16 of the samples from each sequencing method and were most commonly sampled during the early through advanced stages of decomposition. The proteobacterium *Pseudomonas* was common in 16S (12 samples) and MetaG data (16 samples), being present after the fresh stage of decomposition, except in the case of Donor 2, in which decomposition commenced before the body arrived at the FOREST site and *Pseudomonas* was found at the beginning of sampling. This genus was not observed in high numbers for any of the MetaT samples. *Staphylococcus* (Firmicutes) and *Oblitimonas* (Proteobacteria) were common in MetaG (17 and 12 samples, respectively) and MetaT data (17 and 11 samples, respectively), but not in 16S sequences. *Staphylococcus* was most commonly seen in early to advanced stages of decomposition and *Oblitimonas* was observed in advanced stages of decomposition. Cultures were also obtained for species within *Lactobacillus* (two cultures from the fresh stage of decomposition), *Lysinibacillus* (one culture from an early skeleton), *Pseudomonas* (four cultures from fresh to advanced stages of decomposition), and *Staphylococcus* (five cultures from fresh to advanced decomposition; **Table 2**).

The detection of *Lactobacillus*, *Streptococcus*, and *Staphylococcus* in fresh samples is consistent with these genera being present in the mouths of living people (Huttenhower et al., 2012), the oral environments of decomposing humans (Hyde et al., 2013; Javan et al., 2016; Johnson et al., 2016; Adserias-Garriga et al., 2017), and three *Streptococcus* species have been shown *via* MetaT of the oral microbiome in living humans to be involved in pyruvate fermentation (Jorth et al., 2014). From 10 to 185 distinct taxa at the level of species were found for *Lactobacillus* in the sequences recovered from all three methods in this study, with 16S sequencing giving the lowest number of ASVs (10) as compared to 185 sequence reads for MetaG and 35 for MetaT. Similar patterns existed for species within *Lysinibacillus* (2–37 "species"), *Pseudomonas* (9–495), *Staphylococcus* (8–52), and *Streptococcus* (11–149) with the low end of species-level sequences recovered from 16S ASVs and the high end from MetaG data. *Oblitimonas* was represented by only one sequence type, related most closely to *Oblitimonas alkaliphila*, while *Vagococcus* records were similar in returning 13–15 unique sequences each and *Ignatzschineria* ranged from 5 to 7 sequence types each. Little to no work has been done to tie specific microorganisms to metabolic functioning *in situ* during decomposition. However, all of the above genera and many species in each have been recovered in cultures (Vass, 2001; Janaway et al., 2009) from various sites on the human body during decomposition. No studies have used cultures from the hard palate to describe microbial diversity during decomposition, although many studies have examined the oral microbiota *via* 16S sequencing as referenced above.

Bacterial Isolates: Insights From Sequencing

The inability to simultaneously determine "who is there" from an environmental sample (e.g., as determined *via* culturing and/or sequencing) and "what are they doing" (e.g., putrefaction involving turnover of organic substrates or nitrogen cycling), often leaves researchers to infer how microorganisms grown in the lab may participate in their native ecosystem. MetaT could provide a vehicle to overcome this so-called "Heisenberg Uncertainty Principle" as it relates to microbial ecology (Madsen, 1998). The inclusion of cultures in this study attempted to directly link living bacteria to MetaT data from functional genes. This work continues and is beyond the scope of this paper; however, to date we have established that many of the cultures we obtained are also represented in 16S sequences, MetaG, and/or MetaT data (**Table 2**). This suggests that these cultures will be of interest in future work as we further analyze the MetaG and MetaT data for functional genes involved in specific metabolic processes.

At the present time, we can conjecture that the species observed in culture and those most commonly found across the three sequencing methods are likely active in heterotrophic pathways associated with the rich substrates provided by the tissue of the donors. Further metabolic materials come from the microbes themselves as they die and are replaced by others and *via* vectors such as flies and other arthropods that carry materials to the donors, deposit wastes, and leave young to develop in place. Species we found in culture and in MetaT sequencing include *Enterococcus faecalis*, *L. paracasei* and *L. plantarum*, *Staphylococcus sciuri*, and *Lysinibacillus fusiformis*. These species come from well-characterized and metabolically versatile genera, suggesting they probably play an active role in the postmortem microbial community (Trujillo et al., 2015). While the depth of diversity by a few dozen cultures is not as robust as the sequencing methods, these organisms can give us clues as to the metabolic and biochemical processes that happen during decomposition. Comparing their phenotypic traits with MetaT gene transcripts could indicate functions performed by these species during decomposition. Because these species were also generally encountered across sequencing methods, MetaG data might link genome information to 16S sequences, allowing us to find other genes of importance for some of these species.

In general, *Pseudomonas* spp., *Enterococcus* spp., *Staphyloccocus* spp., and *Lactobacillus* spp., e.g., have been extensively studied and are commonly associated with humans (Trujillo et al., 2015). Other species in this study may be less well-known, but have been shown to tolerate wide pH and temperature ranges and can utilize multiple forms of respiration and/or fermentation for metabolism. Some key taxa found across the methodologies in this study are heterotrophs most commonly defined by aerobic metabolic lifestyles. These include *Vagococcus* spp. (Ge et al., 2020), *Lysinibacillus* spp. (Jung et al., 2012), *Oblitimonas alkaphila* (Drobish et al., 2016), and *Ignatzschineria* spp. (Tóth et al., 2007). All four have been shown to grow at a minimum of 10°C and from slightly acidic to alkaline pH and have been recovered from a variety of sample types, including clinical specimens. Their ability to inhabit the seasonally cooler temperatures encountered by our donors concomitant with the higher pH values that accompany decomposition following putrefaction (Vass, 2001) lends credence to their presence in our study. Furthermore, *Ignatzschineria* spp. has been tied closely to human decomposition (Hyde et al., 2015; Adserias-Garriga et al., 2017). We detected 5–7 *Ignatzschineria* species in each sequencing technique, but did not recover any in pure culture.

A common estimate of how many species can be cultured from a given environment is often <1% (Amann et al., 1995) due to a variety of factors including growth media lacking required nutrients (e.g., specific organics, metals, and growth factors), separation of species from commensal or synergistic organisms, and any activation factors for rousing dormant cells or spores. We used low concentrations of organics in the media to discourage some fast-growing bacteria. We also incubated samples aerobically at room temperature. Many bacteria and yeasts that were abundant in the samples based on sequencing methods were not obtained in culture. In some cases, this was likely because the organisms were anaerobes (e.g., *Clostridium* spp.), which have been shown to be prevalent in other work (Hyde et al., 2013, 2015; Javan et al., 2017). Perhaps *Clostridium* is not as ecologically important in the mouths of donors exposed to air; indeed, it is not commonly reported in the mouths of living humans (Huttenhower et al., 2012; Escapa et al., 2018). Other taxa that escaped cultivation included species from *Ignatzschineria*, *Oblitimonas*, *Vagococcus*, *Candida*, and *Yarrowia*. Each of these genera should be cultured readily using selective media, perhaps informed by MetaG and MetaT data that will be analyzed in future work. Swabs were preserved for each donor at each sampling time, so this work could be done and would go a long way toward understanding the microbial assemblages associated with decomposition.

CONCLUSION

While the overall fluctuations of taxa observed in this study were not unlike what has been observed in similar studies, there was no apparent relationship between the length of the PMI and the bacterial community present at a given time. However, taxa from the normal human oral microbiome before death (e.g., *Lactobacillus*, *Streptococcus*, *Rothia*, and *Candida*) did give way to other genera as time progressed, e.g., *Lysinibacillus*, *Vagococcus*, *Ignatzschineria*, and *Yarrowia*. A distinction could often be made between the community from fresh vs. later sampling times, but the finer resolution required for PMI estimation was not elucidated. There were many factors that may have influenced the data in this study, including temperature, humidity, sample size, scavenger activity, and donor sex, weight, and cause of death. However, because the taxa in this study were similar to those of other studies, it is possible that, if incorporated into a comprehensive dataset, a better predictability between PMI and the thanatomicrobiome could be discerned. The approach of integrating culturing techniques alongside whole MetaG and MetaT sequencing to further examine the bacterial communities in question yielded promising data for discerning the specific roles of each taxa in human decomposition. Notably, most of the cultures were found to match data from at least one sequencing technique while 11 cultures were found to match donor and sample times from all three sequencing techniques. We will continue this work to examine prevalent functional genes from many of these species in the MetaG dataset and attempt to link the species we have cultured to expressed genes from the MetaT data. While it is beyond the scope of this paper to include such data, it offers exciting avenues of study to help the field of the postmortem microbiome to advance.

DATA AVAILABILITY STATEMENT

All high throughput reads have been assigned accession numbers ERS6384843 and ERS6384845-ERS6384860 in the European Nucleotide Archive. The culture 16S sequences are in GenBank and have been given accession numbers MZ067725-MZ067793.

AUTHOR CONTRIBUTIONS

EA and SO'C designed the experiment and oversaw the culturing and characterization of the bacterial isolates generated in this work, and EA, KZ, and SO'C received funding for the study. KZ provided access to the human donors, shared field notes throughout decomposition, and gave expert advice about decomposition processes. EA collected all samples and extracted the nucleic acids used in the study. AC conducted all of the 16S, MetaG, and MetaT sequencing and ran the bioinformatics analyses. AC, EA, and SO'C analyzed the data following bioinformatics analysis and SO'C wrote the majority of the manuscript. All authors contributed to the article and approved the submitted version.

FUNDING

Funding for this project was provided by a Western Carolina University Provost Internal Funding Support Grant (#222946) and from the Department of Biology. These provided support for the Master's work of EA who conducted the sampling and

nucleic acid extractions from this project. The funding also supported the cost of sequencing for 16S rRNA, metagenomics, and metatranscriptomics at Dalhousie University. Additional funding was provided by WCU for classroom research projects to grow and characterize bacterial isolates in this study, including sequencing costs associated with obtaining full 16S rRNA sequences from the cultures.

ACKNOWLEDGMENTS

We would like to thank the donors and their families, without whom this research would not have been possible. We would also like to thank the Forensic Osteology Research Station which is one of the few facilities in the world that provides access to exclusive research topics such as this. There were also many faculty from Western Carolina University who were instrumental in accomplishing this study, including Brittania Bintz and Tom Martin. We are indebted to the 51 students who helped us to culture bacteria from our samples and did work to characterize these isolates.

SUPPLEMENTARY MATERIAL

The Supplementary Material for this article can be found online at: https://www.frontiersin.org/articles/10.3389/fmicb.2021.689493/full#supplementary-material

REFERENCES

Adserias-Garriga, J., Quijada, N. M., Hernandez, M., Rodríguez Lázaro, D., Steadman, D., and Garcia-Gil, L. J. (2017). Dynamics of the oral microbiota as a tool to estimate time since death. *Mol Oral Microbiol* 32, 511–516. doi: 10.1111/omi.12191

Amann, R. I., Ludwig, W., and Schleifer, K. H. (1995). Phylogenetic identification and in situ detection of individual microbial cells without cultivation. *Microbiol. Rev.* 59, 143–169. doi: 10.1128/MR.59.1.143-169.1995

Anderson, G. S. (2000). Minimum and maximum development rates of some forensically important Calliphoridae (Diptera). *J. Forensic Sci.* 45, 824–832. doi: 10.1520/JFS14778J

Ashe, E. C. (2019). Thanatomicrombiome dynamics: Bacterial community succession in the human mouth throughout decomposition. master's thesis. Cullowhee (NC): Western Carolina University. Available at https://libres.uncg.edu/ir/wcu/listing.aspx?styp=ti&id=26834 (Accessed March 30, 2021).

Bailey, C. A. (2020). "The effects of scavenging on a donor from the Western Carolina University Forensic Osteology Research Station (FOREST)," in *Proceedings of the 72nd Annual Scientific Meeting of the American Academy of Forensic Sciences*; February 17–22, 2020; Anaheim, CA, 186.

Bashan, A., Gibson, T. E., Friedman, J., Carey, V. J., Weiss, S. T., Hohmann, E. L., et al. (2016). Universality of human microbial dynamics. *Nature* 534, 259–262. doi: 10.1038/nature18301

Bolger, A. M., Lohse, M., and Usadel, B. (2014). Trimmomatic: a flexible trimmer for Illumina sequence data. *Bioinformatics* 30, 2114–2120. doi: 10.1093/bioinformatics/btu170

Bolyen, E., Rideout, J. R., Dillon, M. R., Bokulich, N. A., Abnet, C. C., Al-Ghalith, G. A., et al. (2019). Reproducible, interactive, scalable and extensible microbiome data science using QIIME 2. *Nat. Biotechnol.* 37, 852–857. doi: 10.1038/s41587-019-0209-9

Byard, R. W., and Tsokos, M. (2013). The challenges presented by decomposition. *Forensic Sci. Med. Pathol.* 9, 135–137. doi: 10.1007/s12024-012-9386-2

Calvin, K. (2014). Hypothermia and older adults. National Institutes of Health (NIH). Available at: https://www.nih.gov/news-events/news-releases/hypothermia-older-adults (Accessed May 21, 2021).

Carter, D. O., Metcalf, J. L., Bibat, A., and Knight, R. (2015). Seasonal variation of postmortem microbial communities. *Forensic Sci. Med. Pathol.* 11, 202–207. doi: 10.1007/s12024-015-9667-7

Comeau, A. M., Douglas, G. M., and Langille, M. G. I. (2017). Microbiome helper: a custom and streamlined workflow for microbiome research. *MSystems* 2:e00127–116. doi: 10.1128/mSystems.00127-16

Costello, E. K., Lauber, C. L., Hamady, M., Fierer, N., Gordon, J. I., and Knight, R. (2009). Bacterial community variation in human body habitats across space and time. *Science* 326, 1694–1697. doi: 10.1126/science.1177486

Damann, F. E., Williams, D. E., and Layton, A. C. (2015). Potential use of bacterial community succession in decaying human bone for estimating postmortem interval. *J. Forensic Sci.* 60, 844–850. doi: 10.1111/1556-4029.12744

Derrien, M., Vaughan, E. E., Plugge, C. M., and de Vos, W. M. (2004). *Akkermansia muciniphila* gen. nov., sp. nov., a human intestinal mucin-degrading bacterium. *Int. J. Syst. Evol. Microbiol.* 54, 1469–1476. doi: 10.1099/ijs.0.02873-0

Douglas, G. M., Maffei, V. J., Zaneveld, J. R., Yurgel, S. N., Brown, J. R., Taylor, C. M., et al. (2020). PICRUSt2 for prediction of metagenome functions. *Nat. Biotechnol.* 38, 685–688. doi: 10.1038/s41587-020-0548-6

Drobish, A. M., Emery, B. D., Whitney, A. M., Lauer, A. C., Metcalfe, M. G., and McQuiston, J. R. (2016). *Oblitimonas alkaliphila* gen. nov., sp. nov., in the family Pseudomonadaceae, recovered from a historical collection of previously unidentified clinical strains. *Int. J. Syst. Evol. Microbiol.* 66, 3063–3070. doi: 10.1099/ijsem.0.001147

Escapa, I. F., Chen, T., Huang, Y., Gajare, P., Dewhirst, F. E., and Lemon, K. P. (2018). New insights into human nostril microbiome from the expanded human oral microbiome database (eHOMD): a resource for the microbiome of the human aerodigestive tract. *MSystems* 3:e00187–18. doi: 10.1128/mSystems.00187-18

Ge, Y., Yang, J., Lai, X.-H., Zhang, G., Jin, D., Lu, S., et al. (2020). *Vagococcus xieshaowenii* sp. nov., isolated from snow finch (*Montifringilla taczanowskii*) cloacal content. *Int. J. Syst. Evol. Microbiol.* 70, 2493–2498. doi: 10.1099/ijsem.0.004061

Goff, M. L. (2010). "Early postmortem changes and stages of decomposition," in *Current Concepts in Forensic Entomology*. eds. J. Amendt, M. L. Goff, C. P. Campobasso and M. Grassberger (Dordrecht, Netherlands: Springer), 1–24.

Gupta, R. S., and Sethi, M. (2014). Phylogeny and molecular signatures for the phylum Fusobacteria and its distinct subclades. *Anaerobe* 28, 182–198. doi: 10.1016/j.anaerobe.2014.06.007

Huffnagle, G. B., and Noverr, M. C. (2013). The emerging world of the fungal microbiome. *Trends Microbiol.* 21, 334–341. doi: 10.1016/j.tim.2013.04.002

Huseyin, C. E., O'Toole, P. W., Cotter, P. D., and Scanlan, P. D. (2017). Forgotten fungi-the gut mycobiome in human health and disease. *FEMS Microbiol. Rev.* 41, 479–511. doi: 10.1093/femsre/fuw047

Huttenhower, C., Gevers, D., Knight, R., Abubucker, S., Badger, J. H., Chinwalla, A. T., et al. (2012). Structure, function and diversity of the healthy human microbiome. *Nature* 486, 207–214. doi: 10.1038/nature11234

Hyde, E. R., Haarmann, D. P., Lynne, A. M., Bucheli, S. R., and Petrosino, J. F. (2013). The living dead: bacterial community structure of a cadaver at the onset and end of the bloat stage of decomposition. *PLoS One* 8:e77733. doi: 10.1371/journal.pone.0077733

Hyde, E. R., Haarmann, D. P., Petrosino, J. F., Lynne, A. M., and Bucheli, S. R. (2015). Initial insights into bacterial succession during human decomposition. *Int. J. Legal Med.* 129, 661–671. doi: 10.1007/s00414-014-1128-4

Janaway, R. C., Percival, S. L., and Wilson, A. S. (2009). "Decomposition of human remains," in *Microbiology and Aging: Clinical Manifestations*. ed. S. L. Percival (New York: Humana Press), 313–334.

Javan, G. T., Finley, S. J., Can, I., Wilkinson, J. E., Hanson, J. D., and Tarone, A. M. (2016). Human thanatomicrobiome succession and time since death. *Sci. Rep.* 6:29598. doi: 10.1038/srep29598

Javan, G. T., Finley, S. J., Smith, T., Miller, J., and Wilkinson, J. E. (2017). Cadaver thanatomicrobiome signatures: The ubiquitous nature of *Clostridium* species in human decomposition. *Front. Microbiol.* 8:2096. doi: 10.3389/fmicb.2017.02096

Johnson, A. P., Mikac, K. M., and Wallman, J. F. (2013). Thermogenesis in decomposing carcasses. *Forensic Sci. Int.* 231, 271–277. doi: 10.1016/j.forsciint.2013.05.031

Johnson, H. R., Trinidad, D. D., Guzman, S., Khan, Z., Parziale, J. V., DeBruyn, J. M., et al. (2016). A machine learning approach for using the postmortem skin microbiome to estimate the postmortem interval. *PLoS One* 11:e0167370. doi: 10.1371/journal.pone.0167370

Jorth, P., Turner, K. H., Gumus, P., Nizam, N., Buduneli, N., and Whiteley, M. (2014). Metatranscriptomics of the human oral microbiome during health and disease. *MBio* 5:e01012–14. doi: 10.1128/mBio.01012-14

Jung, M. Y., Kim, J.-S., Paek, W. K., Styrak, I., Park, I.-S., Sin, Y., et al. (2012). Description of *Lysinibacillus sinduriensis* sp. nov., and transfer of *Bacillus massiliensis* and *Bacillus odysseyi* to the genus *Lysinibacillus* as *Lysinibacillus massiliensis* comb. nov. and *Lysinibacillus odysseyi* comb. nov. with emended description of the genus *Lysinibacillus*. *Int. J. Syst. Evol. Microbiol.* 62, 2347–2355. doi: 10.1099/ijs.0.033837-0

Kaszubinski, S. F., Pechal, J. L., Smiles, K., Schmidt, C. J., Jordan, H. R., Meek, M. H., et al. (2020). Dysbiosis in the dead: human postmortem microbiome beta-dispersion as an indicator of manner and cause of death. *Front. Microbiol.* 11:555347. doi: 10.3389/fmicb.2020.555347

Knutsen, A. K., Robert, V., Poot, G. A., Epping, W., Figge, M., Holste-Jensen, A., et al. (2007). Polyphasic re-examination of *Yarrowia lipolytica* strains and the description of three novel *Candida* species: *Candida oslonensis* sp. nov., *Candida alimentaria* sp. nov. and *Candida hollandica* sp. nov. *Int. J. Syst. Evol. Microbiol.* 57, 2426–2435. doi: 10.1099/ijs.0.65200-0

Kurtzman, C., Fell, J. W., and Boekhout, T. (2011). *The Yeasts: A Taxonomic Study*. Amsterdam: Elsevier Science & Technology.

Langmead, B., and Salzberg, S. L. (2012). Fast gapped-read alignment with bowtie 2. *Nat. Methods* 9, 357–359. doi: 10.1038/nmeth.1923

Lu, J., Breitwieser, F. P., Thielen, P., and Salzberg, S. L. (2017). Bracken: estimating species abundance in metagenomics data. *PeerJ Comput. Sci.* 3:e104. doi: 10.7717/peerj-cs.104

Madea, B., and Henssge, C. (2015). "General remarks on estimating time of death," in *Estimation of the Time Since Death. 3rd Edn.* ed. B. Madea (Boca Raton, FL: CRC Press).

Madeira, F., Park, Y. M., Lee, J., Buso, N., Gur, T., Madhusoodanan, N., et al. (2019). The EMBL-EBI search and sequence analysis tools APIs in 2019. *Nucleic Acids Res.* 47, W636–W641. doi: 10.1093/nar/gkz268

Madsen, E. L. (1998). Epistemology of environmental microbiology. *Environ. Sci. Technol.* 32, 429–439. doi: 10.1021/es970551y

Markow, T. A., and O'Grady, P. (2008). Reproductive ecology of *Drosophila*. *Funct. Ecol.* 22, 747–759. doi: 10.1111/j.1365-2435.2008.01457.x

Megyesi, M. S., Nawrocki, S. P., and Haskell, N. H. (2005). Using accumulated degree-days to estimate the postmortem interval from decomposed human remains. *J. Forensic Sci.* 50, 618–626. doi: 10.1520/JFS2004017

Mittler, S. (1979). Failure of irradiated beef and ham to induce genetic aberrations in Drosophila. *Int. J. Radiat. Biol. Relat. Stud. Phys. Chem. Med.* 35, 583–588. doi: 10.1080/09553007914550701

NCBI Resource Coordinators (2016). Database resources of the National Center for Biotechnology Information. *Nucleic Acids Res.* 44, D7–D19. doi: 10.1093/nar/gkv1290

Nearing, J. T., Douglas, G. M., Comeau, A. M., and Langille, M. G. I. (2018). Denoising the denoisers: an independent evaluation of microbiome sequence error-correction approaches. *PeerJ* 6:e5364. doi: 10.7717/peerj.5364

On, S. L. W., Miller, W. G., Houf, K., Fox, J. G., and Vandamme, P. (2017). Minimal standards for describing new species belonging to the families Campylobacteraceae and Helicobacteraceae: *Campylobacter*, *Arcobacter*, *Helicobacter* and *Wolinella* spp. *Int. J. Syst. Evol. Microbiol.* 67, 5296–5311. doi: 10.1099/ijsem.0.002255

Peel, M. C., Finlayson, B. L., and McMahon, T. A. (2007). Updated world map of the Köppen-Geiger climate classification. *Hydrol. Earth Syst. Sci.* 11, 1633–1644. doi: 10.5194/hess-11-1633-2007

Seymour, G. J., Ford, P. J., Cullinan, M. P., Leishman, S., and Yamazaki, K. (2007). Relationship between periodontal infections and systemic disease. *Clin. Microbiol. Infect.* 13, 3–10. doi: 10.1111/j.1469-0691.2007.01798.x

Steinegger, M., and Söding, J. (2017). MMseqs2 enables sensitive protein sequence searching for the analysis of massive data sets. *Nat. Biotechnol.* 35, 1026–1028. doi: 10.1038/nbt.3988

Swift, B. (2006). "The timing of death," in *Essentials of Autopsy Practice: Current Methods and Modern Trends*. ed. G. N. Rutty (London: Springer), 189–214.

Tange, O. (2018). *GNU Parallel 2018. 1st Edn*. 112.

Tóth, E. M., Borsodi, A. K., Euzéby, J. P., Tindall, B. J., and Márialigeti, K. (2007). Proposal to replace the illegitimate genus name *Schineria* Tóth et al. 2001 with the genus name *Ignatzschineria* gen. nov. and to replace the illegitimate combination *Schineria larvae* Tóth et al. 2001 with *Ignatzschineria larvae* comb. nov. *Int. J. Syst. Evol. Microbiol.* 57, 179–180. doi: 10.1099/ijs.0.64686-0

Trujillo, M. E., Dedysh, S., DeVos, P., Hedlund, B., Kämpfer, P., Rainey, F. A., et al. (Eds.). (2015). Bergey's manual of systematics of archaea and bacteria. *1st Edn*. Wiley

Vass, A. A. (2001). Beyond the grave – understanding human decomposition. *Microbiol. Today* 28, 190–192.

Wood, D. E., Lu, J., and Langmead, B. (2019). Improved metagenomic analysis with kraken 2. *Genome Biol.* 20:257. doi: 10.1186/s13059-019-1891-0

Conflict of Interest: The authors declare that the research was conducted in the absence of any commercial or financial relationships that could be construed as a potential conflict of interest.

frontiers in Microbiology

MINI REVIEW
published: 28 July 2021
doi: 10.3389/fmicb.2021.694447

At the Interface of Life and Death: Post-mortem and Other Applications of Vaginal, Skin, and Salivary Microbiome Analysis in Forensics

*Sarah Ahannach[1], Irina Spacova[1], Ronny Decorte[2,3], Els Jehaes[4] and Sarah Lebeer[1]**

[1] Department of Bioscience Engineering, Research Group Environmental Ecology and Applied Microbiology, University of Antwerp, Antwerp, Belgium, [2] Laboratory of Forensic Genetics, Department of Forensic Medicine, University Hospitals Leuven, Leuven, Belgium, [3] Department of Imaging and Pathology, Forensic Biomedical Sciences, KU Leuven, Leuven, Belgium, [4] Forensic DNA Laboratory, Department of Forensic Medicine, Antwerp University Hospital, Edegem, Belgium

Microbial forensics represents a promising tool to strengthen traditional forensic investigative methods and fill related knowledge gaps. Large-scale microbiome studies indicate that microbial fingerprinting can assist forensics in areas such as trace evidence, source tracking, geolocation, and circumstances of death. Nevertheless, the majority of forensic microbiome studies focus on soil and internal organ samples, whereas the microbiome of skin, mouth, and especially vaginal samples that are routinely collected in sexual assault and femicide cases remain underexplored. This review discusses the current and emerging insights into vaginal, skin, and salivary microbiome-modulating factors during life (e.g., lifestyle and health status) and after death (e.g., environmental influences and post-mortem interval) based on next-generation sequencing. We specifically highlight the key aspects of female reproductive tract, skin, and mouth microbiome samples relevant in forensics. To fill the current knowledge gaps, future research should focus on the degree to which the post-mortem succession rate and profiles of vaginal, skin, and saliva microbiota are sensitive to abiotic and biotic factors, presence or absence of oxygen and other gases, and the nutrient richness of the environment. Application of this microbiome-related knowledge could provide valuable complementary data to strengthen forensic cases, for example, to shed light on the circumstances surrounding death with (post-mortem) microbial fingerprinting. Overall, this review synthesizes the present knowledge and aims to provide a framework to adequately comprehend the hurdles and potential application of vaginal, skin, and salivary post-mortem microbiomes in forensic investigations.

Keywords: post-mortem microbiome, trace evidence, microbial forensics, sexual assault, femicide, next-generation sequencing, thanatomicrobiome, epinecrotic communities

OPEN ACCESS

Edited by:
M. Eric Benbow, Michigan State University, United States

Reviewed by:
Zachary M. Burcham, Colorado State University, United States
Baneshwar Singh, Virginia Commonwealth University, United States

***Correspondence:**
Sarah Lebeer
sarah.lebeer@uantwerpen.be

Specialty section:
This article was submitted to Systems Microbiology, a section of the journal Frontiers in Microbiology

Received: *13 April 2021*
Accepted: *14 June 2021*
Published: *28 July 2021*

Citation:
Ahannach S, Spacova I, Decorte R, Jehaes E and Lebeer S (2021) At the Interface of Life and Death: Post-mortem and Other Applications of Vaginal, Skin, and Salivary Microbiome Analysis in Forensics. Front. Microbiol. 12:694447. doi: 10.3389/fmicb.2021.694447

INTRODUCTION

Violence against women is an urgent global problem, as more than one-third of women worldwide has been victim of physical and/or sexual violence in their lifetime (Devries et al., 2013; World Health Organization, 2013). Annually, 66,000 women and girls are victims of femicide, that is, intentional murder of women and girls because they are female (Geneva Declaration, 2011;

World Health Organization and Pan American Health Organization, 2012). Remarkably, only 25% of reported rape cases in Europe lead to a conviction, often due to the difficulty of providing evidence (Lovett and Kelly, 2009). Moreover, forensic experts are convinced that a large number of undetected homicides are misclassified in annual death statistics as natural deaths, suicides, or accidents (Karger et al., 2004; Ferguson and McKinley, 2019). The major obstacle is the difficulty of elucidating the circumstances surrounding death, including cause and manner (Pechal et al., 2018; Kaszubinski et al., 2020b). Traditional forensic techniques, such as human DNA profiling, can provide critical evidence by linking biological traces to crime scenes and individuals or through victim identification (Franzosa et al., 2015). However, they occasionally fall short because of human DNA degradation (Sijen, 2015; Ranjan and Surajit, 2018) and need to be complemented with alternative techniques.

Recent advances in microbial profiling have uncovered that each individual is home to complex microbial communities (Oh et al., 2016; Gilbert and Stephens, 2018). These communities inhabit all surfaces of the human body (for example, orogastrointestinal tract, respiratory tract, urogenital tract, skin) and collectively represent the human microbiota, with their microbial DNA signatures forming the microbiome (Ursell et al., 2012; Berg et al., 2020). Recent research suggests that the microbiome could greatly aid forensic casework (Clarke et al., 2017; Hampton-Marcell et al., 2017; Metcalf et al., 2017; Oliveira and Amorim, 2018; Bishop, 2019). For example, the microbiome can serve as a personal microbial fingerprint that not only can associate individuals to objects (Lax et al., 2015) and geographical locations that they came in contact with (Knight et al., 2016), but also can provide identifiable characteristics (Franzosa et al., 2015). Moreover, many microbial cells contain robust cell walls that leave them better protected against degradation compared to human cells (Sijen, 2015). Nevertheless, the focus of microbial forensics to date has been predominantly on gut and soil samples (Metcalf et al., 2013, Metcalf et al., 2016; Pechal et al., 2014; Javan et al., 2016b; Burcham et al., 2019; DeBruyn et al., 2021), whereas research on forensic implementation of the (post-mortem) microbiome of the female reproductive tract, skin, and oral cavity is lagging behind. Therefore, in this review, we provide a critical assessment of current research on the vaginal, skin, and oral/salivary microbiome in relation to their potential application in forensics, especially sexual assault and femicide cases.

RELEVANCE OF VAGINAL, SKIN, AND SALIVARY MICROBIOME DURING LIFE FOR FORENSIC CASEWORK

Vaginal, skin, and saliva samples represent some of the most commonly collected samples in forensic casework, including sexual assault cases (World Health Organization, 2003; Mont and White, 2007) and cases involving touch evidence (Burrill et al., 2019; Oorschot et al., 2019). These mucocutaneous niches are shaped by several microbiome-influencing factors (e.g., pH and oxygen) (Rojo et al., 2017; Burcham et al., 2019). However, which of these factors have the largest effect is still unknown.

Vaginal samples are routinely collected in sexual assault cases (Quaak et al., 2018; Ghemrawi et al., 2021). While their microbiome is generally neglected in forensics, the less diverse composition of vaginal microbiota, its high microbial biomass, and protected anatomical location translate into its unique potential for microbial fingerprinting (Younes et al., 2018). Depending on the women's ethnicity, the vaginal microbiome is generally dominated by Gram-positive *Lactobacillus* genera covered by a thick cell wall (i.e., *Lactobacillus crispatus*, *Lactobacillus iners*, *Lactobacillus gasseri*, and *Lactobacillus jensenii*) or a diverse microbiota dominated by non-lactobacilli such as *Bifidobacterium*, *Gardnerella*, *Atopobium*, and *Prevotella* (Ravel et al., 2010). Also fungal taxa mostly represented by *Candida* are detected, but generally in low abundances in healthy women (Chew et al., 2016). Ongoing research suggests that the vaginal microbiome composition can be correlated to individual characteristics valuable in forensics, such as health status (Ceccarani et al., 2019), ethnicity (Borgdorff et al., 2017; Gupta et al., 2017), sexual habits (Noyes et al., 2018), contraceptive use (Song et al., 2020), and pregnancy (Serrano et al., 2019), with various effect sizes that are not yet well mapped (**Figure 1**). For example, a longitudinal study found that sexual activity within 24 h of sampling has a significant negative impact on vaginal microbiome constancy as measured *via* the log Jensen–Shannon divergence rate (i.e., vaginal community deviation from constancy), independent of time in the menstrual cycle (Gajer et al., 2012). The vaginal microbiome could thus represent trace evidence in sexual assault cases indicating sexual intercourse in the last 24 h, in addition to providing links with other identifiable individual characteristics. However, whether this conclusion can be drawn from single, non-longitudinal samples after sexual intercourse needs to be investigated.

While vaginal samples are especially useful in sexual assault cases, the skin is probably the most commonly used source of forensic trace evidence, including skin under the victim's fingernails (Metcalf et al., 2017; Burrill et al., 2019). However, the unique microbial trail left behind by skin shedding (Bishop, 2019; Hampton-Marcell et al., 2020) is often overlooked. The skin microbiome is dominated by Gram-positive *Staphylococcus*, *Corynebacterium*, *Cutibacterium*, *Streptococcus*, or *Micrococcus*, although Gram-negative *Acinetobacter* are also frequently isolated (Grice and Segre, 2011). The skin microbiome composition varies depending on the body location (Costello et al., 2009; Grice and Segre, 2011), host characteristics (e.g., age, lifestyle, and cohabitation) (Ross et al., 2017), and skin care (Bouslimani et al., 2019). Importantly, the skin microbiome is at an interface between the outside world and the body that undergoes most interactions with the environment. In fact, detectable amounts of skin microbiota can be transferred to objects such as a computer keyboard and mouse (Fierer et al., 2010), shoes and phones (Lax et al., 2015), door handle, toilet seat, etc. (Flores et al., 2011). Remarkably, this is not only limited to touched surfaces, but also extends to inhabited spaces through microbial clouds which are detectable within just a few hours (Lax et al., 2014; Meadow et al., 2015). However, whether built environment microbiota can be used as trace evidence remains to be substantiated (Hampton-Marcell et al., 2020). An

important knowledge gap is to what extent the skin microbiome can be detected on touched objects after a certain amount of time, potentially even after death. Establishing this link is complicated, as it depends on environmental parameters (e.g., temperature, moisture, and UV radiation) (Fierer et al., 2010), individual shedder status (i.e., amount of epithelium deposited on a substrate) (Lowe et al., 2002; Kanokwongnuwut et al., 2018), and surface characteristics of the object (Meadow et al., 2014).

Saliva, as the primary oral cavity sample, is another widely used trace in forensic casework, especially for skin bite marks in sexual assault and child abuse cases (Chávez-Briones et al., 2015; Leake et al., 2016). The salivary microbiome is mostly dominated by the Gram-negative *Neisseria, Prevotella*, or *Veillonella* but also contains large proportions of Gram-positive *Streptococcus* taxa (e.g., *Streptococcus salivarius* and *Streptococcus oralis*) (Willis et al., 2018). Oral Gram-positive bacteria have recently been described as robust markers for highly degraded saliva samples, because of their higher resistance to degradation treatment (e.g., heat denaturation, microbial decomposition, and ultraviolet irradiation) compared to Gram-negative salivary bacteria, salivary α-amylase, and human DNA (Ohta and Sakurada, 2019). Individual characteristics that can influence the salivary microbiome composition include smoking (Belstrøm et al., 2014; Wu et al., 2016), dental hygiene (Mashima et al., 2017; Burcham et al., 2020), general and oral health (Zhou et al., 2016; Goodson et al., 2017), and socioeconomic status (Belstrøm et al., 2014; **Figure 1**). Importantly, shared environment at household level appears to more significantly determine the salivary microbiome than individual genetics (Shaw et al., 2017). Also intimate contact relevant in forensics, such as kissing (i.e., mixing of saliva), has been proposed to impact salivary microbial composition. Specifically, a transfer of approximately 80 million marker bacteria per intimate kiss of 10 s is observed, and partners have a more similar microbial community compared to unrelated

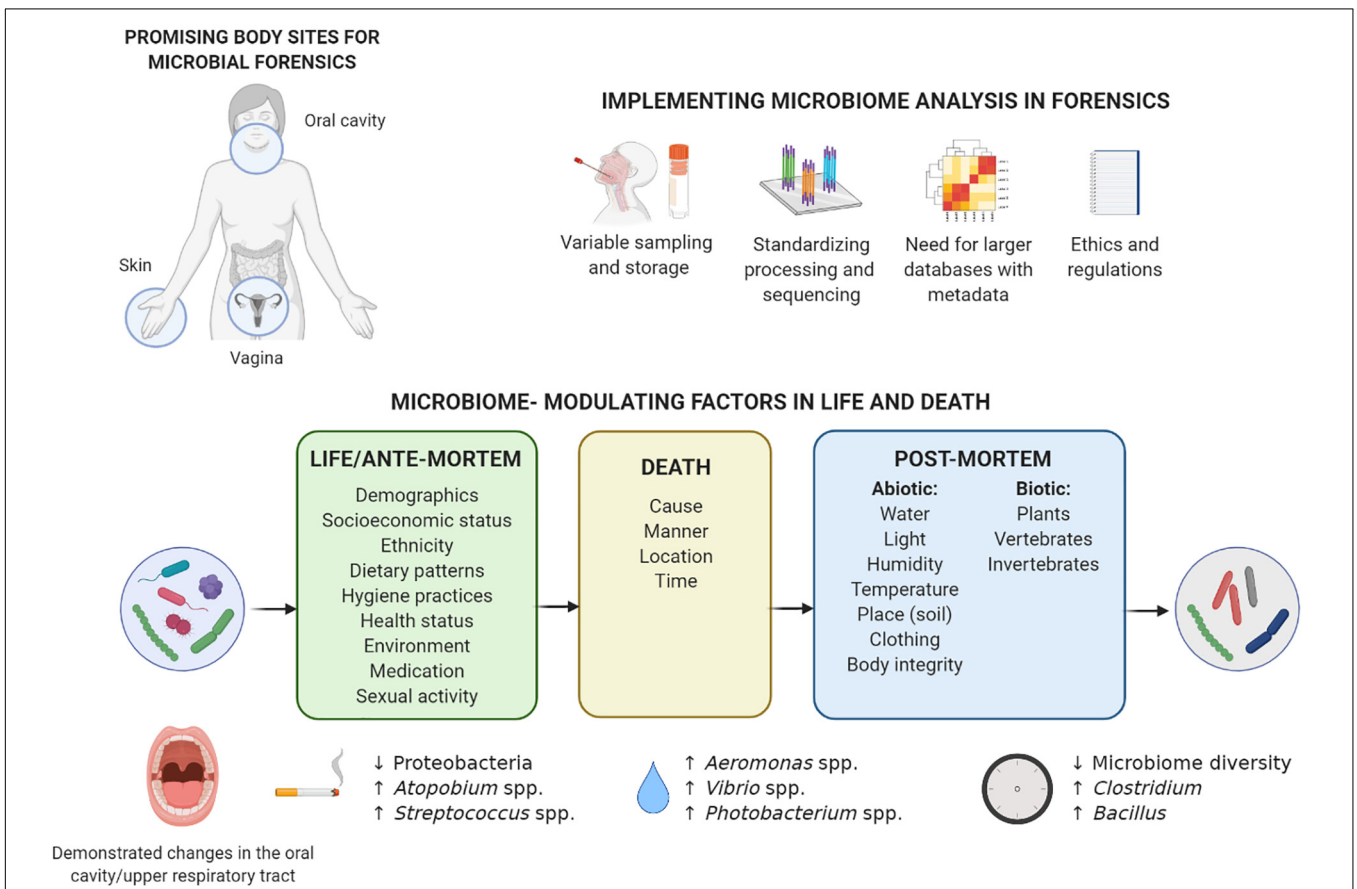

FIGURE 1 | Considerations for implementation of microbiome analysis in forensics and overview of factors in life and death that can influence the microbiome composition. The microbiome of the three body sites understudied in forensics (vagina, skin, and oral cavity) can be influenced by various individual factors during life, and these influences can sometimes also be detected after death. Death forms a turning point for the microbiome: the post-mortem microbiome is much more influenced by a range of environmental factors. Previously described microbiome-modulating factors in life and death are summarized, with some of the most prominent examples given of specific taxa in the oral cavity/upper respiratory tract associated with smoking during life (Wu et al., 2016), drowning as cause of death (Uchiyama et al., 2012; Benbow et al., 2015), and time that has passed since death (Adserias-Garriga et al., 2017b; Javan et al., 2017; García et al., 2020). More examples for the other body sites can be found in the text, although, to the best of our knowledge, no data are available on the post-mortem microbiome of the vagina. Implementation of microbiome analysis in forensics still requires extensive standardization of sampling and processing, as well as larger reference databases with metadata and an adjusted regulatory and ethical framework. Created with BioRender.com.

individuals (Kort et al., 2014). Further research into factors influencing the vaginal, skin, and oral/salivary microbiomes during life will allow their more targeted implementation in forensic casework.

THE DETRIMENTAL EFFECTS OF DEATH ON THE HUMAN MICROBIOME

While the human microbiome during life is widely studied, we are just beginning to understand the post-mortem microbial community dynamics and how it can be influenced by ante-mortem microbial communities and modulating factors. During different stages after death, many anatomical and immunological barriers break, causing fluids, chemicals, and microorganisms that normally would not interact, to come into contact with each other (Gunn and Pitt, 2012). The post-mortem process facilitates the proliferation and relocation of microorganisms throughout the body and opens a gateway of cross-kingdom ecological interactions (Goff, 2009; García et al., 2020).

The decomposition of a human body is a continuous process caused by enzymatic reactions, (bio)chemical metabolic pathways and the activity of vertebrates and invertebrates (Pechal et al., 2018). This process is divided into a series of observable stages: fresh, active decay (including bloating and leakage of effusion), advanced decay, and dry remains/skeletonized (Goff, 2009; García et al., 2020). The course of these stages is partially determined by the diverse microbial communities occupying various internal and external body sites (Hauther et al., 2015; Javan et al., 2016a). Most studies on the post-mortem microbiome focus on estimating the minimum period of time since death [i.e., post-mortem interval (PMI)] (Goff, 2009). These studies aim to predict changes in the microbial composition of internal organs (e.g., gut, brain, liver, spleen, heart, etc.), also referred to as the post-mortem microbial clock (Metcalf et al., 2013; Finley et al., 2015).

Interestingly, studies on internal organs of mice (Metcalf et al., 2013; Burcham et al., 2019), swine (Carter et al., 2015), and human bodies (Hyde et al., 2013; Can et al., 2014; Hauther et al., 2015) have observed a shift in microbial communities from predominant aerobic microorganisms such as *Staphylococcus* and Enterobacteriaceae to more facultative anaerobic bacteria such as Proteobacteria, Firmicutes, and Bacteroidetes to obligate anaerobic organisms such as *Clostridium*, and finally spore-forming microorganisms such as *Clostridium* and *Bacillus* (**Figure 1**; Hyde et al., 2015; Javan et al., 2016b, 2019; García et al., 2020). According to the "post-mortem *Clostridium* effect," *Clostridium* species can be considered important drivers of this microbial shift due to their lipolytic enzymes (Janaway et al., 2009), proteolytic functions, and rapid generation time (Javan et al., 2017). However, whether the findings from studies focusing on internal organs can be extended to mucocutaneous niches entails a different narrative.

Surprisingly, to date, no post-mortem microbiome studies have examined the vaginal microbiome succession after death (**Table 1**). This can be explained by the limited population of decomposing human bodies (mostly white males; >65 years old) studied at anthropological research facilities (Pechal et al., 2018). Nevertheless, Lutz et al. (2020) found that reproductive organs (i.e., uterus and prostate) were the last internal organs to decay. Particularly, for the nulligravid uterus (i.e., never been pregnant), the post-mortem *Clostridium* effect was not observed in contrast to the prostate and other internal organs. Of note, during life, the uterine microbiome is distinct from the vagina with a significantly lower microbial biomass and colonization by Firmicutes, Bacteroidetes, Proteobacteria, and Actinobacteria (Garcia-grau et al., 2019), and it is not clear to what degree bacterial transfer from the vagina to the uterus occurs after death. This highlights the underexplored potential of the female reproductive tract in post-mortem research.

While current research has focused on the potential of the skin microbiome as trace evidence (Tozzo et al., 2020), to the best of our knowledge, only Kodama et al. (2019) have investigated whether actual objects from real death scenes (e.g., smoking pipes, medical devices, and phones) could be linked to the hand palm of the deceased through microbiome identification. The skin microbiome on the palm of the deceased remained stable up to 60 h after death, opening a window for individual microbiome identification even after death. It is noteworthy that this persistence of the skin microbiome into the early post-mortem period opens the possibility of also applying the post-mortem skin microbiome in PMI estimation. This is especially advantageous in cases where an autopsy is not requested, and a non-invasive microbiome sampling approach is best, because the most useful body sites for PMI estimation are external sites (e.g., skin).

Another body site easily accessible for microbiome and other sampling is the oral cavity. While its application for PMI estimation is yet to be studied in large populations, an increase of Firmicutes and Actinobacteria as the PMI increased was demonstrated (Hyde et al., 2013; Adserias-Garriga et al., 2017b). Interestingly, mouth samples pre-bloating resembled the oral microbiome during life, whereas the mouth samples post-bloating contained gut bacteria such as Tenericutes that possibly migrated from the large intestine (Adserias-Garriga et al., 2017b). Overall, studies that include more body sites, like Pechal et al. (2018) and others discussed in **Table 1**, could improve estimations.

The rate and pattern of decomposition are a mosaic system associated with biotic factors (e.g., individuality of the body, intrinsic and extrinsic bacteria, other microbes, and arthropods) and abiotic factors (e.g., weather, climate, humidity, and edaphic conditions) (Hyde et al., 2013; Carter et al., 2015; Newsome et al., 2021; **Figure 1**). It is yet to be elucidated how the contact of skin and natural body openings (mouth and vagina) with the outside environment (clothing, soil, aquatic ecosystems, etc.) can differentially influence the post-mortem body site-specific microbiome. For the latter, the application of epinecrotic communities such as aquatic microbes on the post-mortem submersion interval estimation could be highly relevant in aquatic death investigations (Benbow et al., 2015; Cartozzo et al., 2021; Randall et al., 2021). While the exact effect sizes are rarely reported (Meurs, 2016), abiotic factors, such as insects and soils beneath a decomposing body (Cobaugh et al., 2015;

TABLE 1 | List of human post-mortem microbiome studies which include female reproductive tract, skin and/or oral cavity samples in the last 5 years.

Niches	Study aim	Sequencing	Population and sample size	Main outcome	Main pitfall	References
Brain, heart, liver, spleen, prostate, and **uterus**	Estimating minimum PMI and cause of death	16S rRNA gene amplicon sequencing	158 samples 40 human bodies (14 female, 26 male) 6 body sites	Reproductive organs (uterus and prostate) were the last internal organs to decay during human decomposition	Larger population size is needed to further account for variation due to (a)biotic factors	Lutz et al., 2020
Skin: nose and ear	Estimating minimum PMI	16S rRNA gene amplicon sequencing	144 samples 21 human bodies 2 body sites	Machine learning model predicted the PMI with an average error of 2 days	Model was based on only four human bodies that were sampled longitudinally	Johnson et al., 2016
Skin: left hip, right hip, left bicep, right bicep, left upper hip, right upper hip, left knee, groin, head	Understanding microbially mediated processes during decomposition on different soil substrates	16S rRNA gene amplicon sequencing 18S rRNA gene amplicon sequencing ITS amplicon sequencing	2 human bodies during winter 3 skin sites 143 days 2 human bodies during spring 8 skin sites 82 days	Soil type was not a dominant factor driving community development in the process of decomposition	Limited population size with no information on sex	Metcalf et al., 2016
Eyes, **ears**, **mouth,** nose, rectum, **thigh skin**	Estimating minimum PMI for buried bodies	16S rRNA gene amplicon sequencing	2 male bodies 10 timepoints	Multidisciplinary methodology identified temporal changes in morphology, skeletal muscle protein decomposition, entomology, and microbiome for buried bodies	Model was based on only two human bodies of which multiple samples were taken	Pittner et al., 2020
Skin: right hand palm	Linking objects at the death scene to deceased individuals	16S rRNA gene amplicon sequencing	11 male bodies 5 female bodies 30 living individuals 79 skin samples 98 object samples	Objects could be traced to deceased individual 75% of the time	Ante-mortem population was not always a demographic representation of the deceased study population	Kodama et al., 2019
Eyes, nose,**ears, mouth, umbilicus** rectum	1. Predicting the ante-mortem health condition of the deceased 2. Comparing three machine learning methods to predict PMI, location of death, and manner of death 3. Predicting cause and manner of death	16S rRNA gene amplicon sequencing	47 male bodies 141 female bodies 6 body sites 1 timepoint	1. Microbial biodiversity from the mouth could predict ante-mortem host health condition (e.g., heart disease) 2. Analysis of post-mortem microbiota from more than thee anatomic areas had limited additional value 3. Beta-dispersion, and case demographic data reflected forensic death determination	Only one timepoint (majority of cases with estimated PMI of <72 h) which does not account for variability within a body	1. Pechal et al., 2018 2. Zhang et al., 2019 3. Kaszubinski et al., 2020a

(Continued)

TABLE 1 | Continued

Niches	Study aim	Sequencing	Population and sample size	Main outcome	Main pitfall	References
Mouth: palate, tongue, inner cheek mucosa and tooth surfaces	Estimating minimum PMI	16S rRNA gene amplicon sequencing	1 male body 2 female bodies 8 timepoints 5 body sites	Post-mortem microbial succession in the oral cavity changed in a temporal way according to oxygen availability	Limited population size with large variability	Adserias-Garriga et al., 2017b
External auditory canal, eyes, nares, **mouth**, **umbilicus**, and rectum	Studying the impact of coexisting conditions such as frozen affect the human microbiome at the time of discovery	16S rRNA gene amplicon sequencing	1 male body 1 female body 3 timepoints	The microbial diversity increased throughout the thawing process	Association with time since death or cause of death	Pechal et al., 2017
Blood, brain, **buccal cavity**, heart, liver, and spleen	Estimating minimum PMI	16S rRNA gene amplicon sequencing	66 samples 27 human bodies (12 female, 15 male) 6 body sites	Microbial communities demonstrated time-, organ-, and sex-dependent changes	Niche sampling was not equal for all deceased individuals	Javan et al., 2016b
Mouth, external left/right **cheeks** external left/right **bicep** region, **torso**, and rectum	Studying outdoor decomposition under natural conditions	16S rRNA gene amplicon sequencing and 454 pyro-sequencing	1 male body 1 female body 10 timepoints	Shifts in community structure were recorded and associated with major decomposition and related events	Limited population size with large variability	Hyde et al., 2015

The bold terms refer to the most relevant niches.

Metcalf et al., 2016; Adserias-Garriga et al., 2017a; Keenan et al., 2019), seasonal variation, and distinct climates (Carter et al., 2015), but also exposure and clothing (Goff, 2009), are some of the driving determinants of the microbial succession after death. Specifically, because of lack of thermoregulation, ambient temperatures (Goff, 2009) greatly affect the shift in nutrient availability and can thereby affect microbial community dynamics. Thus, while most studies have been performed in the United States (Metcalf et al., 2013; Pechal et al., 2018; DeBruyn et al., 2021) with a few in Australia, Japan, and the United Kingdom (García et al., 2020), post-mortem microbiome research in a wider range of climates should be encouraged.

POTENTIAL HURDLES AND CONSIDERATIONS

Juries in the court of law have come to rely on physical evidence to corroborate a testimony (Shelton et al., 2007). However, before microbiome research can be reliably introduced into investigative and legislative casework, it has to be peer-reviewed, standardized, and accepted by the scientific community (Kiely, 2005).

Microbiome sequencing methods can be divided into those targeting specific parts of microbial DNA, such as the widely used 16S rRNA gene amplicon sequencing, or untargeted approaches, such as metagenomic shotgun sequencing. In-depth shotgun metagenomics is relatively new and currently more expensive than 16s rRNA gene amplicon sequencing, but it offers the advantage of sequencing the whole genetic content (microbial and human) of a sample with a higher taxonomic and functional resolution (Quince et al., 2017; Schmedes et al., 2017; Hillmann et al., 2018; Walker and Datta, 2019). However, currently, amplicon sequencing is most widely implemented and thus relies on larger available datasets with metadata on microbiome-modulating factors necessary for increasing method accuracy of machine learning–based tools (Clarke et al., 2017; Belk et al., 2018; Zhang et al., 2019), allowing for larger meta-analyses (Adams et al., 2015; Wang et al., 2018). Although both methods have specific limitations regarding taxonomic resolution, limit of specificity, and artificial bias are important when analyzing different types of samples. An integrative approach using both techniques could be implemented to rapidly advance the field, although this requires higher experimental costs (Metcalf et al., 2017; Hillmann et al., 2018).

Importantly, results of microbiome studies vary due to differences in sampling, storage, processing, and data analysis (e.g., machine learning classification models) (Clarke et al., 2017; Kaszubinski et al., 2020a). Thus, while the field expands,

forensically oriented studies should contain standardized protocols with validated techniques. These methods should ensure reproducibility, sensitivity, and quantitative accuracy while defining and delineating the limitations (e.g., expected error rates, limit of detection, and limit of specificity) (Clarke et al., 2017; Metcalf et al., 2017). Minimizing the distinct impact of these variables on microbial profiling to reduce bias and skewing of the detected microbial composition is crucial in forensic evidence.

FUTURE PERSPECTIVES AND CONCLUDING REMARKS

Microbial forensics holds much potential; however, to integrate highly dimensional microbial data into routine investigative casework, several aspects need to be clarified. A key question is to what extent and for how long various individual factors shaping the vaginal, skin, and oral/salivary microbiome during life also play a role after death. These body sites are often inhabited by Gram-positive bacteria that are potentially more resistant to environmental and temporal degradation compared to Gram-negative bacteria and human DNA. In addition, vaginal, skin, and oral/saliva samples are routinely collected as critical components of sexual assault and femicide cases. Importantly, many sensitive individual characteristics can be associated with microbiome composition; however, the magnitude of these effects requires comprehensive investigation. A better understanding of the complex human body ecosystem during life and after death is necessary with the establishment of anthropological research facilities over different continents studying diverse populations and body sites. Hereby, we can facilitate discoveries especially related to female health and safety by comprehending how the post-mortem disturbance in the body homeostasis and its microbial communities make it more susceptible to the influences of the surrounding environment. While studies and regulations are complex specifically for the forensic field, the current and potential future possibilities of microbial forensics in phenotyping, identifying individuals, minimum PMI estimation, and the source of origin of a sample are highly important to consider and develop.

AUTHOR CONTRIBUTIONS

SA, IS, and SL conceived and designed the manuscript. SA wrote the manuscript. IS made the figure. SA, IS, RD, EJ, and SL critically reviewed the manuscript and contributed with special attention towards their specific expertise. All authors contributed to the article and approved the submitted version.

ACKNOWLEDGMENTS

We want to thank the entire research group ENdEMIC of the University of Antwerp, and the Forensic DNA Laboratories of the Antwerp University Hospital and University Hospitals of Leuven. We also want to thank the following funding agencies. SA was supported by the University Research Fund (BOF-DOCPRO 37054) of the University of Antwerp. IS was supported by the IOF-POC University of Antwerp funding ReLACT (FFI190115). SL was supported by the European Research Council (ERC) grant (Lacto-be 852600).

REFERENCES

Adams, R. I., Bateman, A. C., Bik, H. M., and Meadow, J. F. (2015). Microbiota of the indoor environment: a meta-analysis. *Microbiome* 3:49. doi: 10.1186/s40168-015-0108-103

Adserias-Garriga, J., Hernández, M., Quijada, N. M., Rodríguez Lázaro, D., Steadman, D., and Garcia-Gil, J. (2017a). Daily thanatomicrobiome changes in soil as an approach of postmortem interval estimation: an ecological perspective. *Forensic Sci. Int.* 278, 388–395. doi: 10.1016/j.forsciint.2017.07.017

Adserias-Garriga, J., Quijada, M., Hernandez, N. M., Rodríguez Lázaro, D., Steadman, D., and Garcia-Gil, L. J. (2017b). Dynamics of the oral microbiota as a tool to estimate time since death. *Mol. Oral Microbiol.* 32, 511–516. doi: 10.1111/omi.12191

Belk, A., Xu, Z. Z., Carter, D. O., Lynne, A., Bucheli, S., Knight, R., et al. (2018). Microbiome data accurately predicts the postmortem interval using random forest regression models. *Genes (Basel)* 9:104. doi: 10.3390/genes9020104

Belstrøm, D., Holmstrup, P., Nielsen, C. H., Kirkby, N., Heitmann, B. L., Klepac-ceraj, V., et al. (2014). Bacterial profiles of saliva in relation to diet, lifestyle factors, and socioeconomic status. *J. Oral Microbiol.* 6:10.3402/jom.v6.23609.

Benbow, M. E., Pechal, J. L., Lang, J. M., Erb, R., and Wallace, J. R. (2015). The potential of high-throughput metagenomic sequencing of aquatic bacterial communities to estimate the postmortem submersion interval. *J. Forensic Sci.* 60, 1500–1510. doi: 10.1111/1556-4029.12859

Berg, G., Rybakova, D., Fischer, D., Cernava, T., Vergès, M. C., Charles, T., et al. (2020). Microbiome definition re-visited: old concepts and new challenges. *Microbiome* 8:103.

Bishop, A. H. (2019). The signatures of microorganisms and of human and environmental biomes can now be used to provide evidence in legal cases. *FEMS Microbiol. Lett.* 366:fnz021. doi: 10.1093/femsle/fnz021

Borgdorff, H., van der Veer, C., van Houdt, R., Alberts, C. J., de Vries, H. J., Bruisten, S. M., et al. (2017). The association between ethnicity and vaginal microbiota composition in Amsterdam, the Netherlands. *PLoS One* 12:e0181135. doi: 10.1371/journal.pone.0181135

Bouslimani, A., Silva, R., Kosciolek, T., Janssen, S., Callewaert, C., Amir, A., et al. (2019). The impact of skin care products on skin chemistry and microbiome dynamics. *BMC Biol.* 17:47. doi: 10.1186/s12915-019-0660-6

Burcham, Z. M., Garneau, N. L., Comstock, S. S., Tucker, R. M., Knight, R., Metcalf, J. L., et al. (2020). Patterns of oral microbiota diversity in adults and children: a crowdsourced population study. *Sci. Rep.* 10:2133. doi: 10.1038/s41598-020-59016-59010

Burcham, Z. M., Pechal, J. L., Schmidt, C. J., Bose, J. L., Rosch, J. W., Benbow, M. E., et al. (2019). Bacterial community succession, transmigration, and differential gene transcription in a controlled vertebrate decomposition model. *Front. Microbiol.* 10:745. doi: 10.3389/fmicb.2019.00745

Burrill, J., Daniel, B., and Frascione, N. (2019). A review of trace "Touch DNA" deposits: variability factors and an exploration of cellular composition. *Forensic Sci. Int. Genet.* 39, 8–18. doi: 10.1016/j.fsigen.2018.11.019

Can, I., Javan, G. T., Pozhitkov, A. E., and Noble, P. A. (2014). Distinctive thanatomicrobiome signatures found in the blood and internal organs of humans. *J. Microbiol. Methods* 106, 1–7. doi: 10.1016/j.mimet.2014.07.026

Carter, D. O., Metcalf, J. L., Bibat, A., and Knight, R. (2015). Seasonal variation of postmortem microbial communities. *Forensic Sci. Med. Pathol.* 11, 202–207. doi: 10.1007/s12024-015-9667-7

Cartozzo, C., Simmons, T., Swall, J., and Singh, B. (2021). Postmortem submersion interval (PMSI) estimation from the microbiome of Sus scrofa bone in a freshwater river. *Forensic Sci. Int.* 318:110480. doi: 10.1016/j.forsciint.2020.110480

Ceccarani, C., Foschi, C., Parolin, C., Antonietta, D. A., Gaspari, V., Consolandi, C., et al. (2019). Diversity of vaginal microbiome and metabolome during genital infections. *Sci. Rep.* 9:14095. doi: 10.1038/s41598-019-50410-x

Chávez-Briones, M. L., Hernández-Cortés, R., Jaramillo-Rangel, G., and Ortega-Martínez, M. (2015). Relevance of sampling and DNA extraction techniques for the analysis of salivary evidence from bite marks: a case report. *Genet. Mol. Res.* 14, 10165–10171.

Chew, S. Y., Thian, L., and Than, L. (2016). Vulvovaginal candidosis: contemporary challenges and the future of prophylactic and therapeutic approaches. *Mycoses* 56, 262–273. doi: 10.1111/myc.12455

Clarke, T. H., Gomez, A., Singh, H., Nelson, K. E., and Brinkac, L. M. (2017). Integrating the microbiome as a resource in the forensics toolkit. *Forensic Sci. Int. Genet.* 30, 141–147. doi: 10.1016/j.fsigen.2017.06.008

Cobaugh, K. L., Schaeffer, S. M., and Debruyn, J. M. (2015). Functional and structural succession of soil microbial communities below decomposing human cadavers. *PLoS One* 10:e0130201. doi: 10.1371/journal.pone.0130201

Costello, E., Lauber, C., Hamady, M., Fierer, N., Gordon, J., and Knight, R. (2009). Bacterial community variation in human body habitats across space and time. *Science* 326, 1694–1697. doi: 10.1126/science.1177486

DeBruyn, J. M., Hoeland, K. M., Taylor, L. S., Stevens, J. D., Moats, M. A., Bandopadhyay, S., et al. (2021). Comparative decomposition of humans and pigs: soil biogeochemistry, microbial activity and metabolomic profiles. *Front. Microbiol.* 11:608856. doi: 10.3389/fmicb.2020.608856

Devries, K. M., Mak, J. Y. T., García-Moreno, C., Petzold, M., Child, J. C., Falder, G., et al. (2013). The global prevalence of intimate partner violence against women. *Science* 340, 1527–1528. doi: 10.1126/science.1240937

Ferguson, C., and McKinley, A. (2019). Detection avoidance and mis/unclassified, unsolved homicides in Australia. *J. Crim. Psychol.* 10, 113–122. doi: 10.1108/JCP-09-2019-2030

Fierer, N., Lauber, C. L., Zhou, N., Mcdonald, D., Costello, E. K., and Knight, R. (2010). Forensic identi fi cation using skin bacterial communities. *Proc. Natl. Acad. Sci. U S A.* 107, 6477–6481. doi: 10.1073/pnas.1000162107

Finley, S. J., Benbow, M. E., and Javan, G. T. (2015). Microbial communities associated with human decomposition and their potential use as postmortem clocks. *Int. J. Legal Med.* 129, 623–632. doi: 10.1007/s00414-014-1059-0

Flores, G. E., Bates, S. T., Knights, D., Lauber, C. L., Stombaugh, J., Knight, R., et al. (2011). Microbial biogeography of public restroom surfaces. *PLoS One* 6:e28132. doi: 10.1371/journal.pone.0028132

Franzosa, E. A., Huang, K., Meadow, J. F., Gevers, D., and Lemon, K. P. (2015). Identifying personal microbiomes using metagenomic codes. *Proc. Natl. Acad. Sci. U S A.* 112, E2930–E2938. doi: 10.1073/pnas.1423854112

Gajer, P., Brotman, R. M., Bai, G., Sakamoto, J., Schütte, U. M. E., Zhong, X., et al. (2012). Temporal dynamics of the human vaginal microbiota. *Sci. Transl. Med.* 4:132ra52. doi: 10.1126/scitranslmed.3003605

García, M. G., Pérez-Cárceles, M. D., Osuna, E., and Legaz, I. (2020). Impact of the human microbiome in forensic sciences: a systematic review. *Appl. Environ. Microbiol.* 86:e01451-20. doi: 10.1128/AEM.01451-1420

Garcia-grau, I., Simon, C., and Moreno, I. (2019). Uterine microbiome — low biomass and high expectations. *Biol. Reprod.* 101, 1102–1114. doi: 10.1093/biolre/ioy257

Geneva Declaration (2011). *When the Victim Is a Woman in Global Burden of Armed Violence 2011: Lethal Encounters*. Cambridge: Cambridge University Press.

Ghemrawi, M., Ramírez, A., Duncan, G., Colwell, R., Dadlani, M., and Mccord, B. (2021). The genital microbiome and its potential for detecting sexual assault. *Forensic Sci. Int. Genet.* 51:102432. doi: 10.1016/j.fsigen.2020.102432

Gilbert, J. A., and Stephens, B. (2018). Microbiology of the built environment. *Nat. Rev. Microbiol.* 16, 661–670. doi: 10.1038/s41579-018-0065-65

Goff, M. L. (2009). Early post-mortem changes and stages of decomposition in exposed cadavers. *Exp. Appl. Acarol.* 49, 21–36. doi: 10.1007/s10493-009-9284-9289

Goodson, J. M., Hartman, M., Shi, P., Hasturk, H., Yaskell, T., Vargas, J., et al. (2017). The salivary microbiome is altered in the presence of a high salivary glucose concentration. *PLoS One* 12:e0170437. doi: 10.1371/journal.pone.0170437

Grice, E. A., and Segre, J. A. (2011). The skin microbiome. *Nat. Rev. Microbiol.* 9, 244–253. doi: 10.1038/nrmicro2537

Gunn, A., and Pitt, S. J. (2012). Microbes as forensic indicators. *Trop. Biomed.* 29, 311–330.

Gupta, V. K., Paul, S., and Dutta, C. (2017). Geography, ethnicity or subsistence-specific variations in human microbiome composition and diversity. *Front. Microbiol.* 8:1162. doi: 10.3389/fmicb.2017.01162

Hampton-Marcell, J. T., Larsen, P., Anton, T., Cralle, L., Sangwan, N., Lax, S., et al. (2020). Detecting personal microbiota signatures at artificial crime scenes. *Forensic Sci. Int.* 313:110351. doi: 10.1016/j.forsciint.2020.110351

Hampton-Marcell, J. T., Lopez, J. V., and Gilbert, J. A. (2017). The human microbiome: an emerging tool in forensics. *Microb. Biotechnol.* 10, 228–230. doi: 10.1111/1751-7915.12699

Hauther, K. A., Cobaugh, K. L., Jantz, L. M., Ph, D., Sparer, T. E., Ph, D., et al. (2015). Estimating time since death from postmortem human gut microbial communities. *J. Forensic Sci.* 60, 1234–1240. doi: 10.1111/1556-4029.12828

Hillmann, B., Al-ghalith, G. A., Shields-cutler, R. R., Zhu, Q., Gohl, D. M., Beckman, K. B., et al. (2018). Evaluating the information content of shallow shotgun metagenomics. *mSystems* 3:e00069-18.

Hyde, E. R., Haarmann, D. P., and Bucheli, S. R. (2015). Initial insights into bacterial succession during human decomposition. *Int. J. Leg. Med.* 129, 661–671. doi: 10.1007/s00414-014-1128-1124

Hyde, E. R., Haarmann, D. P., Lynne, A. M., Bucheli, S. R., and Petrosino, J. F. (2013). The living dead: bacterial community structure of a cadaver at the onset and end of the bloat stage of decomposition. *PLoS One* 8:e77733. doi: 10.1371/journal.pone.0077733

Janaway, R. C., Percival, S. L., and Wilson, A. S. (2009). "Decomposition of human remains," in *Microbiology and Aging: Clinical Manifestations*, ed. S. L. Percival (New York, NY: Springer), 313–334. doi: 10.1007/978-1-59745-327-1_14

Javan, G. T., Finley, S. J., Abidin, Z., and Mulle, J. G. (2016a). The thanatomicrobiome: a missing piece of the microbial puzzle of death. *Front. Microbiol.* 7:225. doi: 10.3389/fmicb.2016.00225

Javan, G. T., Finley, S. J., Can, I., Wilkinson, J. E., Hanson, J. D., and Tarone, A. M. (2016b). Human thanatomicrobiome succession and time since death. *Sci. Rep.* 6:29598. doi: 10.1038/srep29598

Javan, G. T., Finley, S. J., Smith, T., Miller, J., Wilkinson, J. E., and Cevallos, M. A. (2017). Cadaver thanatomicrobiome signatures: the ubiquitous nature of clostridium species in human decomposition. *Front. Microbiol.* 8:2096. doi: 10.3389/fmicb.2017.02096

Javan, G. T., Finley, S. J., Tuomisto, S., Hall, A., Bendow, M. E., and Mills, D. (2019). An interdisciplinary review of the thanatomicrobiome in human decomposition. *Forensic Sci. Med. Pathol.* 15, 75–83. doi: 10.1007/s12024-018-0061-0

Johnson, H. R., Trinidad, D. D., Guzman, S., Khan, Z., Parziale, V., Debruyn, J. M., et al. (2016). A machine learning approach for using the postmortem skin microbiome to estimate the postmortem interval. *PLoS One* 11:e0167370. doi: 10.1371/journal.pone.0167370

Kanokwongnuwut, P., Martin, B., Kirkbride, K. P., and Linacre, A. (2018). Shedding light on shedders. *Forensic Sci. Int. Genet.* 36, 20–25. doi: 10.1016/j.fsigen.2018.06.004

Karger, B., Lorin de la Grandmaison, G., Bajanowski, T., and Brinkmann, B. (2004). Analysis of 155 consecutive forensic exhumations with emphasis on undetected homicides. *Int. J. Legal Med.* 118, 90–94. doi: 10.1007/s00414-003-0426-z

Kaszubinski, S. F., Pechal, J. L., Schmidt, C. J., Jordan, H. R., Benbow, M. E., and Meek, M. H. (2020a). Evaluating bioinformatic pipeline performance for forensic microbiome analysis*,†,‡. *J. Forensic Sci.* 65, 513–525. doi: 10.1111/1556-4029.14213

Kaszubinski, S. F., Pechal, J. L., Smiles, K., Schmidt, C. J., and Allen, M. S. (2020b). Dysbiosis in the dead: human postmortem microbiome beta-dispersion as an indicator of manner and cause of death. *Front. Microbiol.* 11:555347. doi: 10.3389/fmicb.2020.555347

Keenan, S. W., Schaeffer, S. M., and Debruyn, J. M. (2019). Spatial changes in soil stable isotopic composition in response to carrion decomposition. *Biogeosciences* 16, 3929–3939. doi: 10.5194/bg-16-3929-2019

Kiely, T. F. (2005). *Forensic Evidence: Science and the Criminal Law*, 2nd Edition. Boca Raton, FL: CRC Press.

Knight, R., Kelley, S. T., Siegel, J., and Gregory, J. (2016). Geography and location are the primary drivers of office microbiome composition. *mSystems* 1:e00022-16. doi: 10.1128/mSystems.00022-16

Kodama, W. A., Xu, Z., Metcalf, J. L., Song, S. J., Harrison, N., Knight, R., et al. (2019). Trace evidence potential in postmortem skin microbiomes: from death scene to morgue. *J. Forensic Sci.* 64, 791–798. doi: 10.1111/1556-4029.13949

Kort, R., Caspers, M., Graaf, A., Van De, Egmond, W., Van, et al. (2014). Shaping the oral microbiota through intimate kissing. *Microbiome.* 2:41.

Lax, S., Hampton-Marcell, J. T., Gibbons, S. M., Colares, G. B., Smith, D., Eisen, J. A., et al. (2015). Forensic analysis of the microbiome of phones and shoes. *Microbiome* 3:21. doi: 10.1186/s40168-015-0082-89

Lax, S., Smith, D. P., Hampton-Marcell, J., Owens, S. M., Handley, K. M., Scott, N. M., et al. (2014). Longitudinal analysis of microbial interaction between humans and the indoor environment. *Science* 345, 1048–1052. doi: 10.1126/science.1254529

Leake, S. L., Pagni, M., Falquet, L., Taroni, F., and Greub, G. (2016). The salivary microbiome for differentiating individuals: proof of principle. *Microbes Infect.* 18, 399–405. doi: 10.1016/j.micinf.2016.03.011

Lovett, J., and Kelly, L. (2009). *Different Systems, Similar Outcomes? Tracking Attrition in Reported Rape Cases Across Europe*. London: Child and Women Abuse Studies Unit.

Lowe, A., Murray, C., Whitaker, J., Tully, G., and Gill, P. (2002). The propensity of individuals to deposit DNA and secondary transfer of low level DNA from individuals to inert surfaces. *Forensic Sci Int.* 129, 25–34. doi: 10.1016/s0379-0738(02)00207-4

Lutz, H., Vangelatos, A., Gottel, N., Osculati, A., Visona, S., Finley, S. J., et al. (2020). Effects of extended postmortem interval on microbial communities in organs of the human cadaver. *Front. Microbiol.* 11:569630. doi: 10.3389/fmicb.2020.569630

Mashima, I., Theodorea, C. F., Thaweboon, B., Thaweboon, S., Scannapieco, F. A., and Nakazawa, F. (2017). Exploring the salivary microbiome of children stratified by the oral hygiene index. *PLoS One* 12:e0185274. doi: 10.1371/journal.pone.0185274

Meadow, J. F., Altrichter, A. E., Bateman, A. C., Stenson, J., Brown, G. Z., and Green, J. L. (2015). Humans differ in their personal microbial cloud. *Peer J* 3:e1258. doi: 10.7717/peerj.1258

Meadow, J. F., Altrichter, A. E., Kembel, S. W., Moriyama, M., Connor, T. K. O., Womack, A. M., et al. (2014). Bacterial communities on classroom surfaces vary with human contact. *Microbiome* 2:7.

Metcalf, J. L., Parfrey, L. W., Gonzalez, A., Lauber, C. L., Knights, D., Ackermann, G., et al. (2013). A microbial clock provides an accurate estimate of the postmortem interval in a mouse model system. *eLife* 2:e01104. doi: 10.7554/eLife.01104

Metcalf, J. L., Xu, Z. Z., Bouslimani, A., Dorrestein, P., Carter, D. O., and Knight, R. (2017). Microbiome tools for forensic science. *Trends Biotechnol.* 35, 814–823. doi: 10.1016/j.tibtech.2017.03.006

Metcalf, J. L., Xu, Z. Z., Weiss, S., Lax, S., Treuren, W., Van, et al. (2016). Microbial community assembly and metabolic function during mammalian corpse decomposition. *Science* 351, 158–162. doi: 10.1126/science.aad2646

Meurs, J. (2016). The experimental design of postmortem studies: the effect size and statistical power. *Forensic Sci. Med. Pathol.* 12, 343–349. doi: 10.1007/s12024-016-9793-x

Mont, J. D., and White, D. (2007). *The Uses and Impacts of Medico-legal Evidence in Sexual Assault Cases: A Global Review*. Geneva: World Health Organization.

Newsome, T. M., Barton, B., Buck, J. C., DeBruyn, J., Spencer, E., Ripple, W. J., et al. (2021). Monitoring the dead as an ecosystem indicator. *Ecol. Evol.* 11, 5844–5856. doi: 10.1002/ece3.7542

Noyes, N., Cho, K.-C., Ravel, J., Forney, L. J., and Abdo, Z. (2018). Associations between sexual habits, menstrual hygiene practices, demographics and the vaginal microbiome as revealed by Bayesian network analysis. *PLoS One* 13:e0191625. doi: 10.1371/journal.pone.0191625

Oh, J., Byrd, A. L., Park, M., Kong, H. H., Segre, J. A., Oh, J., et al. (2016). Temporal stability of the human skin microbiome article temporal stability of the human skin microbiome. *Cell* 165, 854–866. doi: 10.1016/j.cell.2016.04.008

Ohta, J., and Sakurada, K. (2019). Oral gram-positive bacterial DNA-based identification of saliva from highly degraded samples. *Forensic Sci. Int. Genet.* 42, 103–112. doi: 10.1016/j.fsigen.2019.06.016

Oliveira, M., and Amorim, A. (2018). Microbial forensics: new breakthroughs and future prospects. *Appl. Microbiol. Biotechnol.* 102, 10377–10391. doi: 10.1007/s00253-018-9414-9416

Oorschot, R. A. H., Van, Goray, M., Szkuta, B., Meakin, G. E., and Kokshoorn, B. (2019). DNA transfer in forensic science: a review. *Forensic Sci. Int. Genet.* 38, 140–166. doi: 10.1016/j.fsigen.2018.10.014

Pechal, J. L., Crippen, T. L., Benbow, M. E., Tarone, A. M., Dowd, S., and Tomberlin, J. K. (2014). The potential use of bacterial community succession in forensics as described by high throughput metagenomic sequencing. *Int. J. Legal Med.* 128, 193–205. doi: 10.1007/s00414-013-0872-1

Pechal, J. L., Schmidt, C. J., Jordan, H. R., and Benbow, M. E. (2017). Frozen: thawing and its effect on the postmortem microbiome in two pediatric. *J. Forensic Sci.* 62, 1399–1405. doi: 10.1111/1556-4029.13419

Pechal, J. L., Schmidt, C. J., Jordan, H. R., and Benbow, M. E. (2018). A large-scale survey of the postmortem human microbiome, and its potential to provide insight into the living health condition. *Sci. Rep.* 8:5724. doi: 10.1038/s41598-018-23989-w

Pittner, S., Bugelli, V., Benbow, M. E., Ehrenfellner, B., Zissler, A., Campobasso, C. P., et al. (2020). The applicability of forensic time since death estimation methods for buried bodies in advanced decomposition stages. *PLoS One* 15:e0243395. doi: 10.1371/journal.pone.0243395

Quaak, F. C. A., van Duijn, T., Hoogenboom, J., Kloosterman, A. D., and Kuiper, I. (2018). Human-associated microbial populations as evidence in forensic casework. *Forensic Sci. Int. Genet.* 36, 176–185. doi: 10.1016/j.fsigen.2018.06.020

Quince, C., Walker, A. W., Simpson, J. T., Loman, N. J., and Segata, N. (2017). Shotgun metagenomics, from sampling to analysis. *Nat. Biotechnol.* 35, 833–844. doi: 10.1038/nbt.3935

Randall, S., Cartozzo, C., Simmons, T., Swall, J. L., and Singh, B. (2021). Prediction of minimum postmortem submersion interval (PMSImin) based on eukaryotic community succession on skeletal remains recovered from a lentic environment. *Forensic Sci. Int.* 323:110784. doi: 10.1016/j.forsciint.2021.110784

Ranjan, H., and Surajit, D. (2018). Microbial degradation of forensic samples of biological origin: potential threat to human DNA typing. *Mol. Biotechnol.* 60, 141–153. doi: 10.1007/s12033-017-0052-55

Ravel, J., Gajer, P., Abdo, Z., Schneider, G. M., Koenig, S. S. K., Mcculle, S. L., et al. (2010). Vaginal microbiome of reproductive-age women. *PNAS* 108, 4680–4687.

Rojo, D., Celia, M., Raczkowska, B. A., Ferrer, M., Barbas, C., Bargiela, R., et al. (2017). Exploring the human microbiome from multiple perspectives: factors altering its composition. *FEMS Microbiol. Rev.* 41, 453–478. doi: 10.1093/femsre/fuw046

Ross, A. A., Doxey, A. C., and Neufeld, J. D. (2017). The skin microbiome of cohabiting couples. *mSystems* 2:e00043-17. doi: 10.1128/mSystems.00043-17

Schmedes, S. E., Woerner, A. E., and Budowle, B. (2017). Forensic human identification using skin microbiomes. *Appl. Environ. Microbiol.* 83:e01672-17. doi: 10.1128/AEM.01672-1617

Serrano, M. G., Parikh, H. I., Brooks, J. P., Edwards, D. J., Arodz, T. J., Edupuganti, L., et al. (2019). Racioethnic diversity in the dynamics of the vaginal microbiome during pregnancy. *Nat. Med.* 25, 1001–1011. doi: 10.1038/s41591-019-0465-8

Shaw, L., Ribeiro, A. L. R., Levine, A. P., and Pontikos, N. (2017). The human salivary microbiome is shaped by shared environment rather than genetics: evidence from a large family of closely related individuals. *mBio* 8:e01237-17. doi: 10.1128/mBio.01237-17

Shelton, H. D. E., Kim, Y. S., and Barak, G. (2007). A study of juror expectations and demands concerning scientific evidence: does the "csi effect" exist? vanderbilt. *J. Entertain. Technol. Law* 9, 331–368.

Sijen, T. (2015). Molecular approaches for forensic cell type identification: on mRNA, miRNA, DNA methylation and microbial markers. *Forensic Sci. Int. Genet.* 18, 21–32. doi: 10.1016/j.fsigen.2014.11.015

Song, S. D., Acharya, K. D., Zhu, J. E., Deveney, Christen, M., Walther-Antonio, M. R. S., et al. (2020). Daily vaginal microbiota fluctuations associated with natural hormonal cycle, contraceptives, diet, and exercise. *mSphere* 5:e00593-20. doi: 10.1128/mSphere.00593-20

Tozzo, P., Angiolella, G. D., Brun, P., Castagliuolo, I., Gino, S., and Caenazzo, L. (2020). Skin microbiome analysis for forensic human identification: what do we know so far? *Microorganisms* 8:873.

Uchiyama, T., Kakizaki, E., Kozawa, S., Nishida, S., Imamura, N., and Yukawa, N. (2012). A new molecular approach to help conclude drowning as a cause of death: simultaneous detection of eight bacterioplankton species using real-time PCR assays with TaqMan probes. *Forensic Sci. Int.* 222, 11–26. doi: 10.1016/j.forsciint.2012.04.029

Ursell, L. K., Metcalf, J. L., Parfrey, L. W., and Knight, R. (2012). Defining the human microbiome. *Nutr. Rev.* 70, 38–44. doi: 10.1111/j.1753-4887.2012.00493.x

Walker, A. R., and Datta, S. (2019). Identification of city specific important bacterial signature for the MetaSUB CAMDA challenge microbiome data. *Biol. Direct.* 14:11. doi: 10.1186/s13062-019-0243-z

Wang, J., Kurilshikov, A., Radjabzadeh, D., Turpin, W., Croitoru, K., Bonder, M. J., et al. (2018). Meta-analysis of human genome-microbiome association studies: the MiBioGen consortium initiative. *Microbiome* 6:101.

Willis, J. R., González-Torres, P., Pittis, A. A., Bejarano, L. A., Cozzuto, L., Andreu-Somavilla, N., et al. (2018). Citizen science charts two major "stomatotypes" in the oral microbiome of adolescents and reveals links with habits and drinking water composition. *Microbiome* 6:218. doi: 10.1186/s40168-018-0592-593

World Health Organization (2003). *Guidelines for Medico-legal Care for Victims of Sexual Violence*. Geneva: World Health Organization.

World Health Organization (2013). *Global and Regional Estimates of Violence Against Women: Prevalence and Health Effects of Intimate Partner Violence and Non-partner Sexual Violence*. Geneva: World Health Organization.

World Health Organization, and Pan American Health Organization (2012). *Understanding and Addressing Violence Against Women: Femicide*. Geneva: World Health Organization.

Wu, J., Peters, B. A., Dominianni, C., Zhang, Y., Pei, Z., Yang, L., et al. (2016). Cigarette smoking and the oral microbiome in a large study of American adults. *ISME J.* 10, 2435–2446. doi: 10.1038/ismej.2016.37

Younes, J. A., Lievens, E., Hummelen, R., van der Westen, R., Reid, G., and Petrova, M. I. (2018). Women and their microbes: the unexpected friendship. *Trends Microbiol.* 26, 16–32. doi: 10.1016/j.tim.2017.07.008

Zhang, Y., Id, J. L. P., Schmidt, C. J., Jordan, H. R., Wang, W., Id, M. E. B., et al. (2019). Machine learning performance in a microbial molecular autopsy context: a cross-sectional postmortem human population study. *PLoS One* 14:e0213829. doi: 10.1371/journal.pone.0213829

Zhou, J., Jiang, N., Wang, S., Hu, X., Jiao, K., and He, X. (2016). Exploration of human salivary microbiomes — insights into the novel characteristics of microbial community structure in caries and caries-free subjects. *PLoS One* 11:e0147039. doi: 10.1371/journal.pone.0147039

Conflict of Interest: The authors declare that the research was conducted in the absence of any commercial or financial relationships that could be construed as a potential conflict of interest.

Publisher's Note: All claims expressed in this article are solely those of the authors and do not necessarily represent those of their affiliated organizations, or those of the publisher, the editors and the reviewers. Any product that may be evaluated in this article, or claim that may be made by its manufacturer, is not guaranteed or endorsed by the publisher.

frontiers in Ecology and Evolution

ORIGINAL RESEARCH
published: 29 July 2021
doi: 10.3389/fevo.2021.696638

Sexual Dimorphism in Growth Rate and Gene Expression Throughout Immature Development in Wild Type *Chrysomya rufifacies* (Diptera: Calliphoridae) Macquart

Meaghan L. Pimsler[1,2,3], Carl E. Hjelmen[1,4], Michelle M. Jonika[1,4], Anika Sharma[1,5], Shuhua Fu[1,6], Madhu Bala[5], Sing-Hoi Sze[6,7], Jeffery K. Tomberlin[2] and Aaron M. Tarone[1]*

[1] Tarone Lab, Department of Entomology, Texas A&M University, College Station, TX, United States, [2] FLIES Facility, Department of Entomology, Texas A&M University, College Station, TX, United States, [3] Lozier Lab, Department of Biological Science, University of Alabama, Tuscaloosa, AL, United States, [4] Blackmon Lab, Department of Biology, Texas A&M University, College Station, TX, United States, [5] MB Lab, Department of Zoology and Environmental Sciences, Punjabi University, Patiala, India, [6] Sze Lab, Department of Biochemistry and Biophysics, Texas A&M University, College Station, TX, United States, [7] Sze Lab, Department of Computer Science and Engineering, Texas A&M University, College Station, TX, United States

OPEN ACCESS

Edited by:
Gulnaz T. Javan, Alabama State University, United States

Reviewed by:
Jonathan J. Parrott, Arizona State University West Campus, United States
Sheree J. Finley, Alabama State University, United States

***Correspondence:**
Meaghan L. Pimsler
mlpimsler@gmail.com

Specialty section:
This article was submitted to Evolutionary and Population Genetics, a section of the journal Frontiers in Ecology and Evolution

Received: *17 April 2021*
Accepted: *14 May 2021*
Published: *29 July 2021*

Citation:
Pimsler ML, Hjelmen CE, Jonika MM, Sharma A, Fu S, Bala M, Sze S-H, Tomberlin JK and Tarone AM (2021) Sexual Dimorphism in Growth Rate and Gene Expression Throughout Immature Development in Wild Type Chrysomya rufifacies (Diptera: Calliphoridae) Macquart. Front. Ecol. Evol. 9:696638. doi: 10.3389/fevo.2021.696638

Reliability of forensic entomology analyses to produce relevant information to a given case requires an understanding of the underlying arthropod population(s) of interest and the factors contributing to variability. Common traits for analyses are affected by a variety of genetic and environmental factors. One trait of interest in forensic investigations has been species-specific temperature-dependent growth rates. Recent work indicates sexual dimorphism may be important in the analysis of such traits and related genetic markers of age. However, studying sexual dimorphic patterns of gene expression throughout immature development in wild-type insects can be difficult due to a lack of genetic tools, and the limits of most sex-determination mechanisms. *Chrysomya rufifacies*, however, is a particularly tractable system to address these issues as it has a monogenic sex determination system, meaning females have only a single-sex of offspring throughout their life. Using modified breeding procedures (to ensure single-female egg clutches) and transcriptomics, we investigated sexual dimorphism in development rate and gene expression. Females develop slower than males (9 h difference from egg to eclosion respectively) even at 30°C, with an average egg-to-eclosion time of 225 h for males and 234 h for females. Given that many key genes rely on sex-specific splicing for the development and maintenance of sexually dimorphic traits, we used a transcriptomic approach to identify different expression of gene splice variants. We find that 98.4% of assembled nodes exhibited sex-specific, stage-specific, to sex-by-stage specific patterns of expression. However, the greatest signal in the expression data is differentiation by developmental stage, indicating that sexual dimorphism in gene expression during development may not be investigatively important

and that markers of age may be relatively independent of sex. Subtle differences in these gene expression patterns can be detected as early as 4 h post-oviposition, and 12 of these nodes demonstrate homology with key *Drosophila* sex determination genes, providing clues regarding the distinct sex determination mechanism of *C. rufifacies*. Finally, we validated the transcriptome analyses through qPCR and have identified five genes that are developmentally informative within and between sexes.

Keywords: forensic entomology, development, transcriptome, sexual dimorphism, Calliphoridae

INTRODUCTION

Accuracy and precision in forensic science often rely upon advanced statistical analyses requiring a solid understanding of both underlying statistical distributions, as well as the factors that affect variation of measures of interest (National Research Council, 2009). These concerns apply to insect growth rates in forensic entomology, the application of the scientific study of arthropods to legal investigations. While some biologists may be focused on characterizing what is different between species, or populations of a given species, a biologist working in forensic science is generally focused on developing a model that balances broad applicability, ease of use, and accuracy and precision of predictions. Initial efforts in forensic entomology focused on the predictability of insect arrival and stability of temperature-dependent growth rates to estimate insect ages. These approaches are particularly relevant in the context of medico-legal forensic entomology, where immature insects are collected from humans or other vertebrates during death and neglect investigations. Therefore, initial efforts targeted the development of species-specific growth datasets at different stable temperatures (Byrd and Butler, 1996, 1997; Grassberger and Reiter, 2001, 2002). With technological advancements and more researchers with a broad array of backgrounds, other factors affecting temperature-dependent growth rates were identified, including stable versus fluctuating temperatures, diet, sex, presence of other species, and evidence for local adaptation (Tomberlin et al., 2009; Tarone et al., 2011; Yu et al., 2011; Picard et al., 2013; Flores et al., 2014; Yanmanee et al., 2016). However, sexual dimorphism has not historically received much attention in forensic entomology, though it is known to result in significant phenotype differences in many organisms (Hedrick and Temeles, 1989; Shine, 1989). Furthermore, many fly species (the most important group of insects in forensic entomology) demonstrate dimorphism in both final adult size and/or development rate (Stillwell et al., 2010). Both of these factors may be important in the refinement and precision of insect age estimates (Blanckenhorn et al., 2007; Zuha and Omar, 2014; Blanckenhorn et al., 2015; Frątczak-Łagiewska and Matuszewski, 2018; Matuszewski and Fratczak-Łagiewska, 2018; Patrício Macedo et al., 2018). Concerns about sexual dimorphism in forensically important species have generally focused on organismal phenotypes; however, the same consideration must be made for molecular markers of fly age (e.g., gene expression), which are gaining traction as additional information that can (but may not always, see Smith and Cook, 2020) improve precision in insect age estimates for forensic purposes (Picard et al., 2013; Jonika et al., 2020). For any sexually dimorphic trait in forensic entomology, determining if the effect of sex is functionally important for predictions is important (see Smith and Cook, 2020). Thus, some unknown proportion of genes used to predict fly age may be affected by sex, but they may be affected in ways that are relevant to fly age predictions or not.

Sexual dimorphism is a charismatic and ubiquitous example of phenotypic divergence and has been a fruitful avenue of research in evolutionary biology in understanding phenotype evolution. Focus on developmental patterns of sexually dimorphic characteristics has also yielded important insights on some of the causes of these traits (Shine, 1989; Blanckenhorn et al., 2007; Colgan et al., 2011). It is generally hypothesized that sex-specific selection pressures have led to differentiation in morphology, physiology, and behavior through sex-linked gene expression (Shearman, 2002; Mank et al., 2011; Scott et al., 2014). However, most research has focused on identifying the specific genetic or ontogenetic processes giving rise to particular characteristics, rather than transcriptome-wide patterns (Chang et al., 2011; Li et al., 2013) or relevance to predictions of insect age.

The development and maintenance of sexually dimorphic traits is ultimately controlled by the final products of the sex-determination gene cascade (Baker and Belote, 1983; Cline, 1993). Decades of research in flies, especially *Drosophila melanogaster* Meigen (Diptera: Drosophilidae), have revealed a complex hierarchy of sex-determination genes, an understanding of their modes of action and interaction, and some of the consequences of mutations at these loci (Baker et al., 1989). The most common sex determination system flies (e.g., Calliphoridae, Tephritidae, and Muscidae) is one of heteromorphic sex chromosomes and a presumed dominant *male determiner* (*M*) on the Y chromosome. The product of this *M* gene directs a positive feedback loop of sex-specific splicing of *transformer* (*tra*) and therefore *doublesex* (*dsx*), leading to a cascade of differential gene expression resulting in distinct adult sexes (Dubendorfer et al., 2002; Lagos et al., 2007; Scott et al., 2014; Sawanth et al., 2016). However, the downstream pathways leading to sexual dimorphism remain unclear in non-model organisms, limiting our ability to identify which mechanisms are conserved and which are species unique.

Genome-wide sexual dimorphism in gene expression has been extensively studied in only a few organisms, with most of the work in Diptera having been done in *D. melanogaster* (Parisi et al., 2004; Ellegren and Parsch, 2007; Morrow et al., 2008; Ghiselli et al., 2011; Grath and Parsch, 2016). Microarray and

next generation sequencing approaches have identified thousands of genes differentially expressed between the sexes in adults, not only between reproductive tissue types (Small et al., 2009), but also in somatic tissues such as the brain (Chang et al., 2011). Generally, approximately 50% of genes are sexually dimorphic in expression in adult *Drosophila*, though almost all of these differences originate in the reproductive tissues (Ranz, 2003; Parisi et al., 2004; Connallon and Knowles, 2005; Zhang et al., 2007). In comparison, there are relatively few studies of sexual dimorphism in gene expression in immature insects.

Identifying the sex of immature insects morphologically is difficult (Van Emden, 1957) and therefore challenging to study sexual dimorphism in gene expression across all developmental stages. The limited work in *D. melanogaster* has therefore relied primarily on either late-stage immature development (third instar larvae and pupae) using developing adult features such as sex-combs (Arbeitman, 2002), or the use of inbred lines, sex-lethal mutations, and transgenics (Lebo et al., 2009). However, it is not possible to use developing adult characters in earlier developmental stages, and it is unclear how sexual dimorphism in gene expression operates against a true wild-type genetic background at these stages of development as well. It is possible to differentiate between male and female-fated immatures in most species of fly though karyotyping, detection of y-linked markers, or genome size measurement (Morrow et al., 2008, 2014a,b; Salvemini et al., 2014a). However, this is an expensive and labor-intensive process that requires prior identification of useful markers, an approach impossible in study systems lacking genetic tools or dimorphic sex chromosomes (Picard et al., 2013). Therefore, a tractable system with reliable sex-specific sorting of wild-type immatures across all stages of development would be a valuable tool for understanding the ontological and evolutionary processes governing sexual dimorphism, as well as potentially increasing precision in age estimates in forensic entomology analyses.

The hairy maggot blow fly, *Chrysomya rufifacies* Macquart (Diptera: Calliphoridae), has an unusual sex-determination system (monogeny) that makes it uniquely well suited to the study of sexual dimorphism throughout development (Wilton, 1954; Ullerich, 1977). In this species, females produce genetically pre-determined single-sex offspring clutches, independent of the zygotic genome of the offspring (Ullerich, 1963, 1973, 1975, 1977, 1980, 1984). Female-producing (thelygenic) females are hypothesized to be heterozygote dominant for a factor that they incorporate into their eggs that causes their offspring to develop into fertile females (Ullerich, 1963, 1973, 1975, 1977, 1980, 1984), while male-producing (arrhenogenic) females and males are hypothesized to be homozygous recessive for this same factor. Furthermore, as *C. rufifacies* has homomorphic sex chromosomes, maternally determined sex, and limited genetic data available, it is not currently possible to use karyotyping or genome-size for immature sex-identification (Ullerich, 1973, 1975; Picard et al., 2012; Andere et al., 2020). Given the atypical nature of the sex determination system, it is also unclear if expression of known sex determination factors will be useful (Scott et al., 2014; Andere et al., 2020), though preliminary work with *doublesex* has been promising (Sze et al., 2017; Jonika et al., 2020).

The purpose of this work was to leverage the monogenic sex determination of *C. rufifacies* to study sexual dimorphism in development and gene expression in wild-type, forensically important, flies throughout their life-history. The first aim of this work was to determine whether development rate of immatures is sexually dimorphic despite the lack of variation in genome size and karyotype. We demonstrated males and females exhibit differences in development rate in both larval and puparial stages. Next, we explored patterns of gene expression throughout immature development to identify whether patterns of gene expression change throughout immature development in concert with gross morphological changes. Our results show patterns consistent with other holometabolous species, with large shifts in gene expression throughout developmental stages and within puparial development. Then, sexual dimorphism in gene expression is assessed through the application of next generation sequencing and *de novo* transcriptomics, to determine when sexual dimorphism in gene expression begins and what the patterns of differential expression are within and between stages and sexes. Our results indicate subtle differences in gene expression can be detected as early as 4 h post-oviposition and increase over developmental time. Finally, we validated the transcriptome analyses through qPCR and identify several genes that are developmentally informative within and between sexes.

MATERIALS AND METHODS

Colony Foundation and Maintenance

Larvae of *C. rufifacies* were collected from numerous carcasses in College Station, TX, United States between May and September of 2011 and eclosed adults were identified morphologically (Whitworth, 2010). Adult flies were released into a BugDorm-1 plastic cage (MegaView Science, Taiwan) and allowed to interbreed to found the laboratory colony. The colony was provided with fresh deionized water and refined sugar *ad libitum*, as well as fresh bovine blood daily as a protein source for oogenesis. Fly colonies were maintained at 28°C for a 16:8 light:dark (L:D) photoperiod for more than 10 generations before sample collection began. Sex-specific voucher specimens of this colony throughout immature development and the adult stage are at the Texas A&M University Insect Collection #716 and #717.

Sexually Dimorphic Development

To collect *C. rufifacies* larvae of a known age, flies in the colony were allowed access to an oviposition substrate of fresh beef liver in a 32.5 mL opaque plastic cup covered with a KimWipe® (Kimberly-Clark, Irving, TX, United States) moistened with deionized water for a 3-h window. After oviposition, the eggs were placed in a Percival model I-36LLVL Incubator (Percival Scientific, Perry, IA, United States) at 30°C, 75% relative humidity (RH), and a 12:12 L:D. After hatching, aliquots of 100 first instars were then transferred by paintbrush to 50 g of fresh beef liver in a 32.5 mL opaque plastic cup covered with a moistened KimWipe®in a 1.1 L canning jar with approximately

100 g of playground sand and a Wype-All on the top to prevent escape but allow airflow. This method was replicated three times per egg collection, with a total of three biological replicates. These rearing jars were then placed in a Percival model I-36LLVL Incubator (Percival Scientific, Perry, IA, United States) at 30°C, 75% RH, and a 12:12 LD. This was repeated four times for a total of 1,200 larvae in 12 jars.

Observations were made every 3 h beginning 138 h after oviposition. All individuals from each jar observed to pupate at the time of observation was placed in a labeled, capped 30 mL plastic cup. Observations continued after pupariation, and the sex of each eclosed individual was recorded. This process continued until no eclosion had been observed for 4 days, after which daily observations were made for 2 weeks in which no flies eclosed. Data were analyzed in R 3.1.3 (R Core Team, 2010) to assess survival and sex ratios. Best fit models for development rates for egg to pupariation, egg to eclosion, and pupariation to eclosion was assessed in R using AIC (base R) and AICc (MuMIn v. 1.43.15; Bartoń, 2018) with nested random effects least squared regression models, where replicate (egg collection time) and trial (aliquots of 100 larvae) were treated as random effects (**Table 1**).

One often used method to estimate insect age in forensic entomology are thermal summation models based on the accumulation of degree hours (ADH) or degree days (ADD) (Amendt et al., 2004). These models rely on the assumption that for any given species or population, the relationship between temperature and development rate is linear within optimal temperature ranges. However, these models also require knowledge of the lower developmental temperature (LDT), below which the organism cannot develop. In the case of *C. rufifacies*, the LDT has not been experimentally determined, and it is therefore necessary to estimate the LDT. One common method is to regress the development rate ($1/TDev_{Temp}$) on the *Y*-axis against the temperatures studied (Temp) on the *X*-axis (Gennard, 2007; Tarone and Benoit, 2019). Development data was extracted from two published studies using North American collected *C. rufifacies*, Byrd and Butler (1997) which used only one diet and five temperatures, and Flores et al. (2014) which used three diets and three temperatures. Linear regression models were calculated separately for each paper and diet, and the x-intercept (estimated LDT) calculated from the estimated coefficients (**Figure 1**). Sexual dimorphism in development time coefficients from the best fit models above were used in conjunction with estimated LDT to calculate the range of ADH differences between males and female for different developmental time periods.

Gene Expression Sample Collection

For each sample, a single male and female *C. rufifacies* were isolated together in a 1.1 L canning jar with approximately 100 g of playground sand, a Wype-All on the top to prevent escape but allow airflow, and refined sugar and water *ad libitum* and a 10 mL glass beaker filled with one Kim-wipe®and approximately 1 mL of fresh beef liver blood. These were kept in the incubator conditions previously mentioned (30°C, 75% RH, and a 12:12 LD). An additional 1 mL of blood was added each following day up until the 6th day post eclosion as a source of protein for oogenesis. The protein source was then excluded for 24 h. Beginning on the 7th day post-eclosion, twice each day, a 35 mL plastic cup with approximately 25 g of fresh beef liver covered with a moistened Kim-wipe®was introduced to the jar as an oviposition medium for 4 h. If a female oviposited during this time, the females were removed and flash frozen for later RNA extraction, and the progeny were allowed to develop under the same conditions listed above in a separate incubator. From a total of six different females per sex of offspring for each stage, the following samples were collected: ∼100 eggs (max of 4 h old), ∼100 first instars (12 h post oviposition), ∼10 s instars (24 h post oviposition), 2 third instars (36 h post oviposition), early pupal development (0–1 into pupariation), mid-pupal development (2–3 days into pupariation), or late pupal development (4–5 days into pupariation) (Martín-Vega et al., 2016; **Table 2**). All samples were flash frozen and stored at −80°C until RNA extraction.

RNA Preparation

RNA was extracted via TriReagent preparation according to manufacturer's protocols. Briefly, one sample (i.e., ∼100 eggs, single pupa) was macerated in 1 mL of cold TriReagent (Sigma-Aldrich Corp., St. Louis, MO, United States) in a 1.5 mL RNAse-free microfuge tube. Following this, 50 mL of ice-cold 4-bromoanisole (BAN) reagent (Molecular Research Center, Inc., Cincinnati, OH, United States) was added and the solution was vigorously mixed. Next, the tubes centrifuged at 14,000 G at 4°C for 15 min to isolate the RNA from the DNA and proteins. Approximately 500 μL of the top, clear layer was carefully removed via pipet and added to 500 μL of ice-cold 100% isopropanol. The tubes were mixed via inversion three times and allowed to rest on ice for 10 min to precipitate the RNA. The precipitate was then centrifuged at 14,000 G at 4°C for 15 min. The supernatant was completely removed, 1 mL of cold 70% ethanol was used to wash the RNA pellet, and then the pellet centrifuged at 4°C for 5 min at 14,000 G. The ethanol was eluted, and any remaining ethanol was allowed to evaporate completely. The RNA was then dissolved in a 100 μL mixture of 99 μL of DNase/RNase/Nucleotide-free water and 1 μL of SUPERase•In™ (Invitrogen, Life Technologies Incorporated, Grand Island, NY, United States).

The extracted RNA was further purified using a Qiagen RNeasy Micro Kit and on-column DNase treatment following manufacturer protocols (Qiagen Inc., Valencia, CA, United States). Sample concentration and quality and control were assessed with NanoDrop (Thermo Fisher Scientific Inc., Wilmington, DE, United States) and an Agilent 2100 BioAnalyzer (Agilent Technologies Inc., Santa Clara, CA, United States). Two samples per sex and stage were pooled based on total RNA concentration into a single library, for three libraries per sex and stage. The exception was the third instar samples, which were collected to study both immature gene expression (this work) and the molecular ecology of predation (a separate analysis). Illumina libraries were prepared under standard protocols. In total, 66 libraries were sequenced on three separate RNA Illumina HiSeq flow cells. The libraries for the following stages were prepared as 100 bp paired end reads: adult, third instar, and mid pupariation. The rest of the

TABLE 1 | Best fit model selection AIC and AICc results testing for sexual dimorphism in development rate at 30°C for *Chrysomya rufifacies.*

Developmental period	Model name	Model	df	AIC	AICc
Egg to pupariation	**Full**	**∼1 + Sex + (1| Trial:Replicate)**	**4**	***3019.862***	***3019.938***
	Trial	∼1 + Sex + (1| Trial)	4	3360.471	3360.546
	Random	∼1 + (1| Trial:Replicate)	3	3136.565	3136.61
	SexOnly	∼1 + Sex	3	3442.76	3442.805
	Null	∼1	2	3490.391	3490.413
Pupariation to eclosion	Full	∼1 + Sex + (1| Trial:Replicate)	4	2499.167	2499.242
	Trial	∼1 + Sex + (1| Trial)	4	2500.566	2500.642
	Random	∼1 + (1| Trial:Replicate)	3	2531.554	2531.6
	SexOnly	**∼1 + Sex**	**3**	***2494.722***	***2494.767***
	Null	∼1	2	2528.619	2528.642
Egg to eclosion	**Full**	**∼1 + Sex + (1| Trial:Replicate)**	**4**	***6078.737***	***6078.78***
	Trial	∼1 + Sex + (1| Trial)	4	6627.828	6627.87
	Random	∼1 + (1| Trial:Replicate)	3	6483.311	6483.337
	SexOnly	∼1 + Sex	3	6748.551	6748.576
	Null	∼1	2	6947.618	6947.631

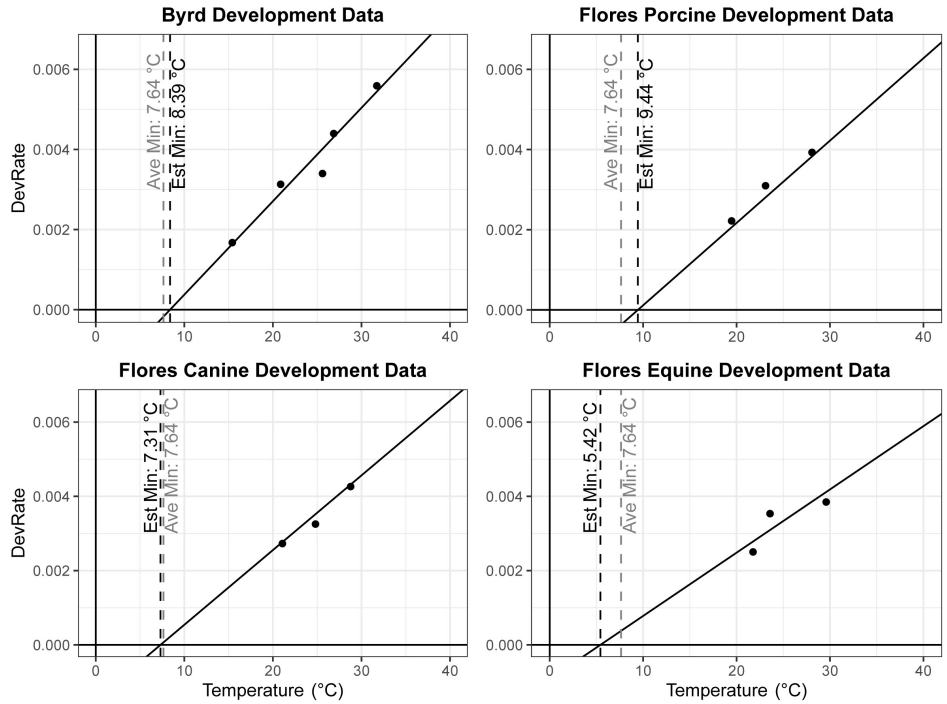

FIGURE 1 | Linear regression models to estimate lower developmental threshold of North American collected *Chrysomya rufifacies.* The estimated LDT for each data set was identified individually by calculating the x-intercept (vertical black dashed line). These estimates were averaged together and also plotted (vertical gray dashed line at 7.64°C in all panels).

libraries were prepared as 100 bp single-end reads. However, while the transcriptomes were assembled with all 66 of these libraries (PRJNA385184, PRJNA287123, PRJNA287124), the analysis presented here will focus on the 48 immature libraries (PRJNA287123, PRJNA287124).

Transcriptome Assembly

Prior to assembly, reads underwent trimming and quality control: reads were filtered to remove all sequences that contained adaptor sequences and known contaminants as defined by Illumina. The transcriptome was assembled with all 66 RNASeq libraries with ASplice (Sze et al., 2017) under a variety of k-mer (k) and k-mer coverage (c) parameters. Briefly, assemblies were generated with the ASplice algorithm on the Whole Systems Genome Initiative (WSGI) computing cluster[1]. These assemblies were then analyzed to identify potential alternative splicing patterns. This program

[1]https://genomics.tamu.edu/core-labs/tigss-hpc-cluster/

assembles reads into splicing graphs, rather than predicted transcripts, similar to SOAPdenovo2 (Luo et al., 2012). Briefly, the program produces an output of nodes connected together by edges. Nodes are sections of unambiguously aligned k-mers, and edges are the connections between nodes in alternatively spliced transcripts. While the nodes are named with numbers only, the edges are indicated in the transcriptome fasta names after a colon; i.e., NODE_1234:2345,2346 means that NODE_1234 connects with NODE_2345 and 2346. To facilitate identification of nodes of interest in the reported transcriptomes, in this manuscript we will discuss node numbers with included edges.

Once the assembly was completed for a given parameter pair, the absolute count of reads which mapped to each nodes was calculated for each library. Transcriptome nodes were compared against known *D. melanogaster* proteins using a translated Basic Local Alignment Search Tool (BLAST) search (Altschul et al., 1990). For each node, only the top BLAST hit with an *E*-value below 10^{-7} was considered, and each of these nodes were assigned the GO term(s) associated with its fly ortholog in Ensembl 2018 (Zerbino et al., 2018) using biomartr v0.9.0 (Drost and Paszkowski, 2017).

Selection of Assembly for Analyses

A total of 66 RNAseq libraries were sequenced, 33 male and 33 female. Average read length after trimming and quality control was 86.3 bp, and there was an average of 6.3×10^7 reads per library. These were assembled into 24 *de novo* transcriptome assemblies based on a range of k-mer sizes (21, 25, 31, 35, 41, and 45) and coverage cut-offs (50, 100, 200, and 500) (**Supplementary Table 1**). For the purpose of this study, the assembly with a k-mer of 31 and a coverage cutoff of 100 (31_100) was selected as the best candidate for analysis as it optimized completeness (high number of nodes, low number of single node splicing graphs) and quality (high N50, high number of *D. melanogaster* genes and transcripts detected, small "tangles") (raw data in **Supplementary Materials 1–4**). Additional details about assembly can be found in Sze et al. (2017) and Pimsler et al. (2019).

Transcriptome Analysis

RNAseq analyses used edgeR v3.22.3 (R Core Team, 2010; Robinson et al., 2010) and edgeR v3.12.1/limma v3.36.2 (Robinson et al., 2010; Ritchie et al., 2015). Raw counts were transformed to counts per million (CPM), retaining nodes $\geq$ 100 bp in length with $\geq$1 CPM in $\geq$2 samples (filtered logCPM values in **Supplementary 5**). Analysis was then conducted in two stages: (1) model-based sub-setting and multidimensional scaling (MDS) to explore broad patterns; (2) individual node-by-node differential expression analyses; (3) cluster analysis.

First, using limma *selectModel*, a best fit general linear model for each modes was selected from alternative nested models (Region, Treatment, Region + Treatment, or Full model with an interaction) using the absolute lowest Akaike's Information Criterion (AIC) score (Vuong, 1989) (results in **Supplementary Material 6**). MDS was also performed in limma, using all 81,205 nodes to investigate broad patterns of clustering of samples.

Second, we performed individual node-by-node analyses with a contrasts approach in edgeR to test for sex, stage, and sex-by-stage effects on node expression. Significance was assessed at a False Discovery Rate (FDR) $\leq$ 0.05, using Benjamini–Hochberg adjusted *P*-values of all nodes and contrasts on a per-factor basis (Benjamini and Hochberg, 1995). Of all nodes, 93,530/493,544 and 14,946/493,544 had a length of 100 bp or more or shared sequence homology with *D. melanogaster*, respectively. Of these (∼87%; 81,205/93,530), were expressed in two or more samples, and 4.5%; 3,631/81,205 of those nodes passing the cutoff were GO-annotated. GO enrichment analyses were performed with topGO v2.30.0 (Alexa and Rahnenführer, 2015) using classic method and Fisher's Exact Test with default settings (Lewin and Grieve, 2006) for biological process (BP), molecular function (MF), and cellular component (CC). We consider enrichment significant at $P \leq 0.05$, as we were primarily interested in examining functional information for nodes that were already stringently selected, and GO enrichment *P*-values do not conform to distributions typically required for FDR correction (Flight and Wentzell, 2009). For ease of visualizing GO terms in presented results, GO lists were simplified using ReViGO (Supek et al., 2011) (allowed similarity = small) (results in **Supplementary Materials 7–9**).

Finally, log counts per million (lcpm) values for all significantly differentially expressed nodes were clustered using average pairwise Pearson correlation coefficients with Cluster3.0 (de Hoon et al., 2004). Using TreeView v1.1.6r4 (Page, 1996), clusters with an average correlation of 0.85 and at least 100 nodes were included for further analysis (results in **Supplementary Material 5**). These clusters were analyzed for GO (see above), and inclusion of previously identified genes in *D. melanogaster* involved in sex determination, germline development (Lebo et al., 2009; dos Santos et al., 2015), and somatic sexual dimorphism (Lebo et al., 2009) (results in **Supplementary Material 10**).

TABLE 2 | Hours of development and proportion of development completed for each sampling group for transcriptomic analysis throughout immature development in *Chrysomya rufifacies* reared at 30°C.

Stage	Approximate hours	Proportion of development
Egg	4	1%
First instar	12	5%
Second instar	24	10%
Third instar	36	15%
Early puparial	132	52%
Mid puparial	180	71%
Late puparial	228	90%

Validation Fly Rearing

To initiate and maintain a laboratory colony, adult *C. rufifacies* (>500) were collected from decomposing animal remains in College Station, TX, United States from May to July 2017. Flies were identified using morphological features as above (TAMUIC #730) and held in a semi climate-controlled room (∼25°C, 50% RH, and a 14L:10D photoperiod) in 30 × 30 × 30 cm cages (BioQuip, Rancho Dominguez, CA, United States) at Texas A&M University, United States. To collect samples for the

validation qPCR, between November 2017 and January 2018, four separate lumite screen collapsible cages (30 × 30 × 30 cm BioQuip®Rancho Dominguez, CA, United States) of adult *C. rufifacies* flies were established in walk-in incubators (Rheem Environmental Chamber, Asheville, NC, United States) at 29 ± 1°C temperature and 60% RH. Adults were provided sugar (as carbohydrate source), fresh deionized water, and bovine blood to ensure proper egg development. After 7 days as adults, a 35 mL plastic container containing 20 g of raw fresh beef liver covered with a folded Kimwipe was provided as an oviposition medium. Eggs were collected after 4 h of exposure to the oviposition substrate. Eggs were mixed gently with a brush and approximately 200-250 eggs (0.05 g) were transferred onto a Kimwipe.

Eggs were placed in a 1 L wide mouth mason jar containing 200 g of playground sand and 100 g of fresh beef liver and were covered with Wype-all. A total of 88 jars were prepared, labeled and randomized for developmental time point collection and placement in a Percival growth chamber set at 25.0°C, 75% RH and 14:10 LD (Percival model I-36LLVL incubator). An Onset®HOBO U12-006 data logger along with Onset®TMC6-HD air, water, and soil temperature sensors (Onset Co., Pocasset, MA, United States) were placed on each shelf of the growth chambers to determine consistency in abiotic factors. Jars were inspected to ensure hatching and progression to subsequent instar and intra-puparial (sensu Martín-Vega et al., 2016) stages. Samples (12 individuals each) were collected from third instar larvae to late puparial stage (i.e., third instar, post-feeding, early puparial, mid puparial and late puparial) (Martín-Vega et al., 2016). Larval and puparial samples were collected by placing them into 15 mL Falcon tubes and flash freezing in 200 proof ethanol and dry ice. Samples were stored at −80°C until RNA extraction. Hours of development and proportion of development completed for each age group can be found in **Table 3**.

Gene Selection and Primer Design

Five target genes were selected from the 31_100 *C. rufifacies de novo* transcriptome assembly for their unique and high expression levels: *Larval serum protein-1α* (*Lsp-1α*), *Transport and Golgi organization 5* (*Tango5*), a cytochrome p450 (*Cyp28d2*), *Succinate dehydrogenase cytochrome B* (*SDCB*), *Juvenile hormone esterase binding protein* (*JHEBP*). Three reference genes, *Alpha Tubulin 84B* (*Alpha Tub84B*), *ribosomal protein 49* (*rp49*) and *Glycerol 3 phosphate dehydrogenase* (*GPDH*) were selected for expression normalization. Primers for these genes were designed and confirmed by BLAST primer design on NCBI, and node numbers (assembly 31_100) and candidate gene annotations for each of the five genes of interest can be found in **Table 4**.

TABLE 3 | Hours of development and proportion of development completed for each sampling group throughout immature development for gene expression validation in *Chrysomya rufifacies* reared at 25°C.

Stage	Approximate hours	Proportion of development
Feeding 3rd instar	120	35%
Early postfeeding	150	44%
Late postfeeding	165	49%
Early puparial	215	64%
Mid puparial	263	78%
Late puparial	335	99%

RNA Extraction, cDNA Synthesis, and Quantitative PCR

Whole larval and puparial samples were homogenized in 1000 μl of TRI-Reagent (Molecular Research Center, Inc., Cincinnati, OH, United States) and total RNA was isolated per manufacturer's instructions. BAN reagent (MRC) was used for phase separation and the RNA was precipitated in ice-cold isopropanol and washed with cold 70% ethanol. RNA was resuspended in 99 μl of DNase/RNase/Nucleotide-free water and 1 μl of SUPERase (Invitrogen). Quantification of RNA was performed using a NanoDrop 1000 Spectrophotometer (Thermo Fisher Scientific Inc, Wilmington, DE, United States). Prior to cDNA conversion, RNA extractions were treated with amplification grade DNase I (Invitrogen). RNA extractions were converted to cDNA using the High Capacity cDNA Reverse Transcriptase Kit (Applied Biosystems, Foster City, CA, United States) per manufacturer's protocol. After cDNA conversion, samples were stored at −20°C. To corroborate the absence of genomic DNA, reverse transcriptase (RT) checks were performed on all samples. RT negative controls were assayed with *rp49* primers. For Positive controls, *rp49* primers along with cDNA samples derived from the RNA of each developmental stage were used. rp49 was selected for RT check because of consistent and stable expression level throughout the development in all the samples.

Quantitative PCR (Bio-Rad Laboratories, Inc., 248 Hercules, CA, United States) was performed and in order to measure CT values and relative gene expression for each sample. 20 μL reactions containing 10 μL SSoFast^{TM} EvaGreen®Supermix (Bio-Rad Laboratories, Inc.), 2 μL cDNA, 2 μL primers, and 4 μL DNase/RNase/Nucleotide-free water were loaded onto 96-well plates and subjected to qPCR under following conditions: 40 cycles of denaturation at 94°C for 45 s, annealing and extension process at 72°C for 60 s followed by a 65°C – 95°C melt curve at increments of 0.5°C. Positive, negative, and no template controls were run on the same plate. Each sample reaction was carried out in duplicate, after which cycle threshold (CT) values were averaged per sample. Only PCR products with dissociated melt curves with single peaks were considered valid for final results. Three samples failed to pass qPCR expression cutoffs; one third instar library did not have an expression profile for any gene, and two samples (one early postfeeding third instar and one late pupariation sample) did not result in an expression profile for *Tango5*. Three libraries were excluded from analysis to balance the sampling design, randomly selected from each one in each of the other remaining developmental time points, resulting in 11 samples per sampling group.

In order to estimate relative gene expression for each gene of interest, $2^{-\Delta\ \Delta\ CT}$ was calculated for each gene by using average CT values across the replicates. The CT value for each

target gene was standardized against three reference genes (*rp49, Gpdh,* and *AlphaTub84B*) by subtracting the geometric mean of the reference genes CT from average CT of each target gene. Stability of reference genes was verified by measuring M values using the program geNorm. All reference genes had *M*-values ranging from 0.215 to 0.232, well within the recommended < 1.0 value.

Sex identification for each sample was performed as in Jonika et al. (2020). Briefly, cDNA conversion was performed on original RNA extractions, as above, for PCR amplification of the sex specific DSX gene product. Samples identified as female and male were used for sex specific analyses, whereas any samples without a confident sex identification were not included for sex specific analyses.

Statistical Analyses

Values of normalized relative gene expression were compared between developmental stages for each gene using ANOVA, where relative gene expression was the dependent variable and developmental stage was the independent variable. For sex specific comparison, gene expression was the dependent variable and sex and developmental stage were independent variables with an interaction effect included. Tukey HSD was performed as a *post hoc* test for both types of analyses with significance set at the $p < 0.05$ level.

RESULTS

Males Develop Faster Than Females

A total of 937 flies survived to eclosion, with only one of four replicates of having significantly higher than average survival (replicate B), and survival rates for the four replicates were: $^{222}/_{300}$, $^{261}/_{300}$, $^{219}/_{300}$, $^{235}/_{300}$. All replicates had sex ratios that were significantly male skewed (*t*-test, $p < 0.0001$), which has been observed before (Pimsler et al., 2019), with replicates A and B, and C and D not being significantly different from each other (*t*-test, $p > 0.05$), exhibiting a M:F ratio of $\sim$ 2:1 overall. Female overall immature development from oviposition to eclosion was 9.74 h slower than males (REML, $p < 0.0001$), with a 4.41 h difference in oviposition to pupariation time (REML, $p < 0.0001$) and a 1.41 h difference in pupariation to eclosion times (LM, $p < 0.0001$) (**Table 5** and **Figure 2**). Based on estimated lower developmental thresholds (**Figure 1**) and the model-estimated sexually dimorphic development times (**Table 5**), this represents ADH differences between males and females of 90–108 for egg hatch to pupariation, 27–32 for pupariation to eclosion, and 200–240 across all of immature development.

Most Nodes Are Differentially Expressed

We used RNAseq and a novel bioinformatic transcriptome approach that preserves splicing information to investigate ontological and sexually dimorphic patterns of gene expression throughout immature development (which depends on splicing). All analyses were conducted on a per-node basis, with a node representing an unambiguously assembled contig, where nodes are connected to each other through edges within a splicing graph. To simplify analyses and interpretation, we confined our analyses to nodes which assembled in to $\geq$100 bp in length and which were expressed in at least 2 samples, resulting in 81,205 nodes (with homology to 4,965 *D. melanogaster* genes at our conservative *a priori* BLAST cutoff).

In our preliminary approach, we explored the data by identifying best fit linear models for each node using Akaike Information Criterion (AIC) (McCarthy et al., 2012). Nearly all nodes (97.6%; 79,324/81,205 nodes; **Table 6**) were best fit by a model that included sex, developmental stage, or some combination of the two, suggesting broad genome-wide differences in gene expression throughout development. Most nodes and genes were best fit by models that included only stage. The MDS results further supported the results of the best-fit modeling, as developmental stage, rather than sex, was the primary factor affecting MDS axes 1 through 4 (see **Figure 3**).

TABLE 4 | Validation primer sequences and expected PCR product lengths.

Primers	Sequence	Product length	Node	Annotation
rp49 F	5′-ACA ATG TTA AGG AAC TCG AAG TTT TG-3′	75	–	Tarone et al., 2011
rp49 R	5′-GGA GAC ACC GTG AGC GAT TT-3′			
Gpdh F	5′-TAA GTC TGG CAA GAC CAT CCA A-3′	72	–	Wang et al., 2015
Gpdh R	5′-GTA AGG GGG CCC TGT AAC TTT-3′			
AlphaTub84B F	5′-ACG AAC AAT TGA CAG TAG CCG-3′	85	–	Wang et al., 2015
AlphaTub84B R	5′-TTT CCA TGA CGA GGA TCG CA-3′			
LSP F	5′-AGC CCG GAG ACA GAT CAT CA-3′	446	2711945	CG2559; *Lsp1α*
LSP R	5′-AAG TGA CAA ACC ACA AGC GG-3′			
SDCB F	5′-AAC ACC CTT AAC AGC CCA CA-3′	123	4022649	CG10219, *SdhD*
SDCB R	5′-AAG GTT GCC CAT GCC TCT TT-3′			
Tango5 F	5′- AGC TGG CAT TAC TTG CGG TC-3′	173	2940844	CG32675, *Tango5*
Tango5 R	5′-CAA CTA CTG GAA TGG CGG CT-3′			
JHEBP F	5′-ATC TCT TCG CCC GAT TCA CG-3′	256	586024	CG3776, *Jhebp29*
JHEBP R	5′-GCG ACT TTA ACG CTC TCA GC-3′			
p450 F	5′-CCA CAA GTG ACC GCA CAT ACT-3′	110	1153482	CG6081; *Cyp28d2*
p450 R	5′-TCT TGT TTG TCG TGA TGGCG-3′			

Next, we evaluated node-specific statistically significant patterns of gene expression (Benjamini and Hochberg, 1995) FDR $\leq$ 0.05) using *edgeR* (Robinson et al., 2010) and *limma* (Ritchie et al., 2015). First, we were interested in whether ontological gene expression patterns in *C. rufifacies* were similar to those observed in other holometabolous insects (21 pairwise comparisons, known as *contrasts*, between developmental time points). Second, we also looked for whether and when sexual dimorphism in gene expression was initiated through two approaches. We evaluated differences between the sexes within a stage (14 pairwise comparisons; e.g., male eggs versus female eggs, male mid-puparial development versus female mid-puparial development), as well as differences within development between the sexes (21 pairwise female-specific and 21 pairwise male-specific ontological gene expression patterns). Most nodes demonstrated significant differential expression in at least one pairwise contrast (98.4%; 79,922/81,205 nodes; **Supplementary Material 6**). Most of these nodes demonstrated both developmental and a sex:stage pattern of differential expression (97.6%, 78,067/79,922 nodes; **Figure 4**). All differences in node expression globally between males and females (all male samples versus all female samples) also demonstrated differential expression in other contrasts.

Immature Gene Expression

In total, 64,246 nodes were differentially expressed across all pairwise stage contrasts, representing 79.1% of all nodes passing quality and coverage cutoffs. Generally, most genes and gene ontology analyses exhibited patterns of expression consistent with those observed in *D. melanogaster* (Arbeitman, 2002). The egg stage demonstrated the most unique expression pattern, with 50,912 (6,408 annotated) nodes differentially expressed between eggs and all stages pooled together, although eggs had the second highest total number of differentially expressed nodes (62,358 nodes with 7,475 annotated compared to third instar larvae at 62,691 nodes with 7,490 annotated).

As there are simple, reliable morphological methods to identify eggs, first, second, and third instar larvae, we will limit our discussion of contrasts involving these four developmental stages. Overall, patterns of GO enrichment and dis-enrichment are in line with patterns that have been observed in other flies (Lebo et al., 2009; **Supplementary Materials 7, 8**). Eggs demonstrated increased expression of genes related to growth, cell division, and DNA replication relative to all other stages, including nodes with homology to *Drosophila* genes such as *slam* (Lecuit et al., 2002). Within and between larval stadia

TABLE 5 | *Chrysomya rufifacies* demonstrates significant sexual dimorphism in development rate in throughout immature development when reared at 30°C.

Predictors	*Estimates*	*CI*	*Statistic*	*p*	*df*
		Egg to pupariation			
(Intercept)	146.39	143.15–149.64	99.98	**<0.001**	10.36
Sex [Male]	−4.41	−5.16 to−3.66	−11.52	**<0.001**	526.93
		Random effects			
σ^2	15.09				
τ_{00}	$22.76_{Trial:Replicate}$				
ICC	0.6				
N	3_{Trial}				
	$4_{Replicate}$				
Obs.	535				
Marg. R^2/Cond. R^2	0.111/0.646				
		Pupariation to eclosion			
(Intercept)	90.11	89.78– 90.43	543.47	**<0.001**	533
Sex [Male]	−1.32	−1.75 to−0.90	−6.08	**<0.001**	533
Obs.					535
Marg. R^2/Cond. R^2	0.065/0.063				
		Egg to eclosion			
(Intercept)	234.68	230.29– 239.07	117.1	**<0.001**	11.46
Sex [Male]	−9.74	−10.59 to−8.89	−22.58	**<0.001**	925.46
		Random effects			
σ^2	36.15				
τ_{00}	$46.74_{Trial:Replicate}$				
ICC	0.56				
N	3_{Trial}				
	$4_{Replicate}$				
Obs.	937				
Marg. R^2/Cond. R^2	0.204/0.653				

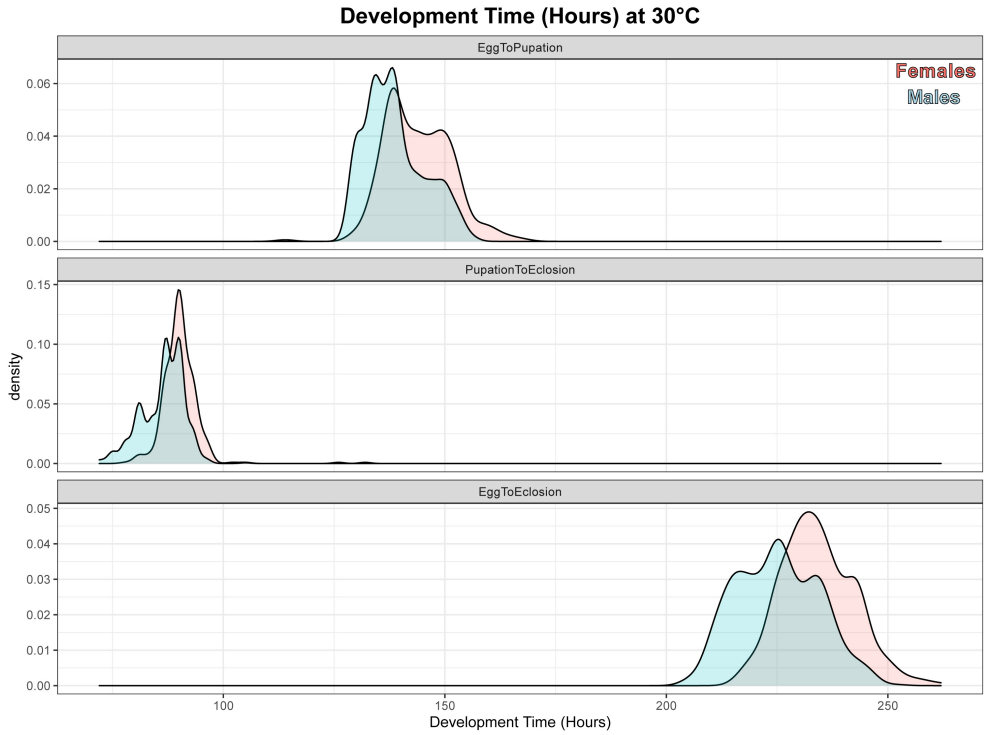

FIGURE 2 | Density plot of sexual dimorphism in development rate for *C. rufifacies* at 30°C. These are density plots of hours elapsed (*x*-axis) for male (blue) and female (red) *C. rufifacies* reared at 30°C, 12:12 LD for time elapsed from egg to pupariation **(top panel)**, pupariation to eclosion **(middle panel)**, and egg to eclosion **(bottom panel)**.

TABLE 6 | Numbers of differentially expressed nodes (DEN) as a function of stage of development and/or sex from linear models in limma.

Model name	Model formula	Total nodes (DEN)	Annotated nodes (Annotated DEN)
	Total Nodes = 81205		
None	~ 1	1881 (1182, 62.84%)	81 (50, 61.73%)
Sex	~0 + Sex	364 (293, 80.49%)	9 (8, 88.89%)
Stage	~0 + Stage	52866 (52849, 99.97%)	6413 (6412, 99.98%)
Sex + Stage	~0 + Sex + Stage	14200 (14200, 100%)	1453 (1453, 100%)
Sex: Stage	~0 + Sex + Stage + Sex*Stage	11894 (11894, 100%)	939 (939, 100%)

Nodes are assigned to a model based on only the lowest AIC and necessitates exclusion from other possible models. Therefore, any single node may be significant in additional contrasts outside of its linear model assignment. The numbers/percentages of differentially expressed nodes (in at least one sex, stage, or sex:stage contrast) assigned to each model in the individual gene analyses (FDR cutoff of ≤ 0.05) are provided in parentheses.

comparisons demonstrated enrichment of GO terms associated with vesicle transport, exocytosis, macromolecule metabolism, digestive tract, imaginal disk development, and locomotion.

A large number of nodes were differentially expressed over the course of pupariation. Early in the process, there was an enrichment of nodes related to endocytosis and the positive regulation of the Notch signaling pathway relative to mid and late pupariation. This is also the point in pupariation where male germline associated nodes became enriched, as well as regulation of gene silencing and small GTP mediated signal transduction, all of which continue until decreasing in expression late pupariation. Midway through pupariation saw the beginning of enrichment of eye morphogenesis and development, developmental programmed cell death, and the negative regulation of RAS protein signal transduction which continues through late pupariation. Mid pupariation also demonstrated an enrichment of cellular homeostasis and metabolic processes associated nodes relative to early and late pupariation. Furthermore, at the middle of pupariation, we see dis-enrichment of positive regulation of the WNT and smoothened (*hedgehog*) signaling pathways, as well as hormone biosynthetic processes, though nodes associated with these GO terms become enriched again in late pupariation. Late pupariation also demonstrated enrichment of nodes associated with antiporter activity, biological regulation, and anion transmembrane transporter activity.

Of particular interest is the identification of genes which can be used to estimate the age of an insect. We selected differentially expressed nodes based on whether they had *D. melanogaster* homology, were differentially expressed between

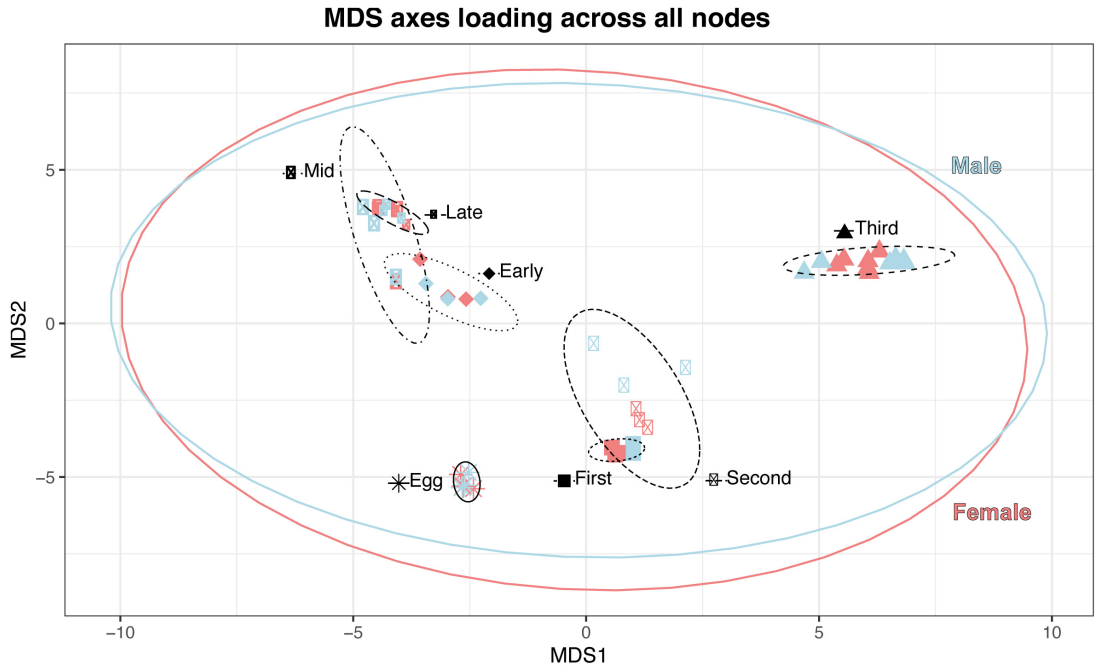

FIGURE 3 | Stage (as indicated by shape and ellipse linetype) is the most significant factor in clustering on MDS axes 1 and 2; sex (color) exhibits a smaller effect on clustering of immature samples, and the summary ellipses overlap.

puparial stages, and exhibited patterns observed in previous studies on developmental patterns of gene expression in flies. We also selected some nodes that were differentially expressed between third instar larvae and early puparial development, as these may be useful in quantifying another difficult to measure age-based phenotype, the transition from feeding to post-feeding third instar larvae. This putative list was further pruned after investigating sexual dimorphism in gene expression (below).

Differential Expression of Sex Related Genes

Eggs demonstrate differential expression of 21 sex-determination and dimorphism related genes relative to the other stages of development: three downregulated (*dsx*, *fruitless* [*fru*], and *takeout* [*to*]), one with mixed patterns (*Trithorax-like* [*Trl*]), and 11 upregulated (**Supplementary Material 6**). Of particular interest is the upregulation in eggs of *daughterless* (*da*), *Sxl*, *groucho* (*go*), and *sisterless A* (*sisA*), given past research in *C. rufifacies* (Clausen and Ullerich, 1990; Muller-Holtkamp, 1995; Andere et al., 2020) or their patterns of expression in eggs of other species (Morrow et al., 2014b; Salvemini et al., 2014b; Sawanth et al., 2016). Nodes from the gene *dsx* are not expressed until the third instar (**Figure 5**), and expression levels do not differ significantly throughout the rest of development. The expression of *fru* begins in the second instar, and remains high throughout the rest of development (**Figure 6**). The gene *to* shows two peaks, one in third instar larvae and then again late in pupariation (**Figure 6**). The gene *tra* is differentially expressed throughout development beginning in eggs and is discussed in more detail below (**Figure 7**).

Sexual Dimorphism in Gene Expression

Sexual dimorphism in expression within a stage (i.e., Female eggs versus male eggs, female late pupariation versus male pupariation) was observed in 15,268 nodes (18.8% of all nodes passing quality and coverage cutoffs). Sexual dimorphism was observed in all stages measured, including eggs (**Supplementary Material 6**). Most of these nodes did not share any homology with *D. melanogaster* at our cutoff (14,025/15,268 nodes without homology; 91.8%). The 1,243 nodes represented 876 *D. melanogaster* genes, suggesting that some of these nodes are exons or different transcripts of the same gene. A total of 2,173 nodes were differentially expressed in two or more stages.

Differences Between Male-Specific and Female-Specific Changes in Gene Expression Throughout Development

In total, 76,5757 and 74,443 nodes were differentially expressed through female-specific and male-specific development respectively (4821 and 4838 unique *D. mel* homologies), with most of these nodes overlapping (73,900; **Figure 8**). These overlapping nodes demonstrated enrichment patterns common with other fly species, including terms such as regulation of developmental processes, regulation of nervous system development, muscle structure development, and photoreceptor cell differentiation (**Supplementary Materials 7–9**).

Of greater interest, there were some specific nodes differentially expressed throughout female development only (2,682 nodes), as well as throughout male development only (2,544 nodes). However, as most nodes are not

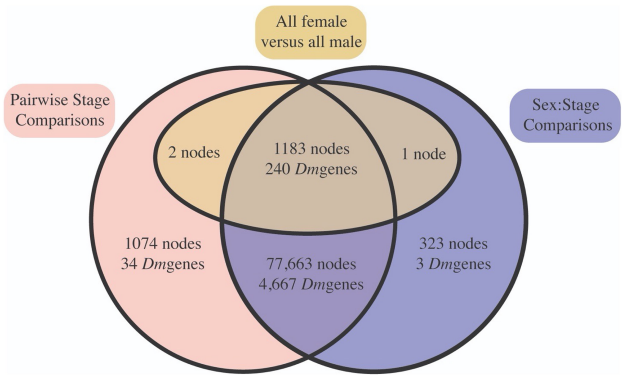

FIGURE 4 | Most differentially expressed nodes were significant in both stage (red) and sex:stage interaction (blue) contrasts, suggesting that there is broad differential expression across both development and in a sex-significant manner. This is supported by the fact that most of the nodes significant between all male and all female samples pooled across immature development (yellow) were also significant in at least one stage specific contrast. Node identities can be found in **Supplementary Material 6**.

annotated, and multiple nodes can have homology with the same *D. melanogaster* gene, the number of "genes" differentially expressed between male-specific and female-specific development is significantly smaller (88 genes and 71 genes respectively). Throughout development, male-specific unique expression demonstrates GO enrichment of appendage morphogenesis including wing development, imaginal disk development, protein modification via conjugation and/or ubiquination, and positive regulations of cell adhesion. Female-specific unique expression, on the other hand, demonstrates GO term enrichment of chorion-containing eggshell formation, pole cell migration, and a multitude of terms related to growth and cellular division, including metaphase/anaphase transition, sister chromatid separation, and nuclear division (**Supplementary Material 9**).

Most Stages Demonstrated a Male Bias in Expression of Differentially Expressed Genes

The number of differentially expressed genes, the strength (log fold change and FDR corrected *p*-values), and direction of bias generally increased throughout development (**Figure 9**). In all stages but the egg and third instar stages, more nodes demonstrated a male bias of expression and these nodes were more extremely (smaller FDR corrected *p*-values) and strongly (larger log fold change) differentially expressed (**Figure 9**). Given these stage-distinct features, embryonic, larval, and puparial dimorphism are addressed separately and in more detail below.

Differential expression is female biased in the egg stage

In the egg stage, more nodes are female biased in expression, and the outlier nodes do not exhibit homology to *Drosophila melanogaster* genes at the imposed similarity cutoff. Of the annotated genes, female eggs show an upregulation of genes related to DNA replication and endoreduplication, DNA repair, and microtubule formation related to chromosome segregation. In comparison, males demonstrate an upregulation of genes related to positive regulation of gene expression, chromatin silencing, organ development, cell localization, dorsal-ventral pattern formation, and cell division.

There were six nodes that were highly upregulated (large effect sizes and low *p*-values) in embryos destined to develop into females (**Figures 7**, **9**). Comparison to Diptera nucleotide sequences with a blastn search identified NODE_26355 as having sequence similarity to the end of (starting at exon three) *Cochliomyia macellaria transformer* (JX315619.1, 5e-30). The rest of the nodes were AT-rich sequences and demonstrated sequence similarity to each other. In addition, they demonstrate 38–43% sequence similarity to another node in a different splicing graph (NODE_13077:3370588) that joins upstream of a sequence that splices to a sequence that corresponds to exon two of *tra* in *Co. macellaria*. There is dimorphism of expression of this putative *tra* sequence (NODE_13077:3370588) with increased expression in female fated eggs relative to male fated eggs, though this homology is based on similarity of other nodes in the splicing graph to *tra* sequences isolated from other species of Calliphoridae. Thus, it appears that a female-biased AT-rich sequence upstream of exons 2 and 3 of *tra* may be connected to upregulation of that end of the gene in female *C. rufifacies* embryos.

Most larval stages exhibit male biased sexual dimorphism, and the number of genes increases throughout larval development

The larval stages did demonstrate sexual dimorphism in gene expression, and though it was more nodes than eggs, the FDR corrected *p*-values and fold changes in expression were not as extreme on average. Despite these differences, there was no significant differential expression of any of the core sex-determination genes which are important in other species of fly in either the first or second instar. Sexual dimorphism, defined as total number of nodes differentially expressed, is lowest in the first instar larvae (**Figure 9**), then increases throughout development. In the first instar, females are upregulating genes related to pH regulation, metabolic processes, and head development, while males are upregulating genes related to transmembrane transport, catabolism, response to food, and mitochondria (**Supplementary Materials 7**, **9**). In the second instar, females continue to demonstrate enrichment in head development, as well as neuron differentiation and growth and neuromuscular junction development. In comparison, male enrichment switches to GO groups related to transcription regulation, DNA synthesis, protein secretion, regulation of the JAK-STAT cascade, and dorso-ventral patterning.

Sexual dimorphism in the larval stages is most pronounced in third instar larvae. Females continue to show increased expression of genes related to a neuron maturation and differentiation, as well as broad array of GO terms, including thermosensory behavior, gene expression, splicing, and silencing, chromatin remodeling, short-term memory,

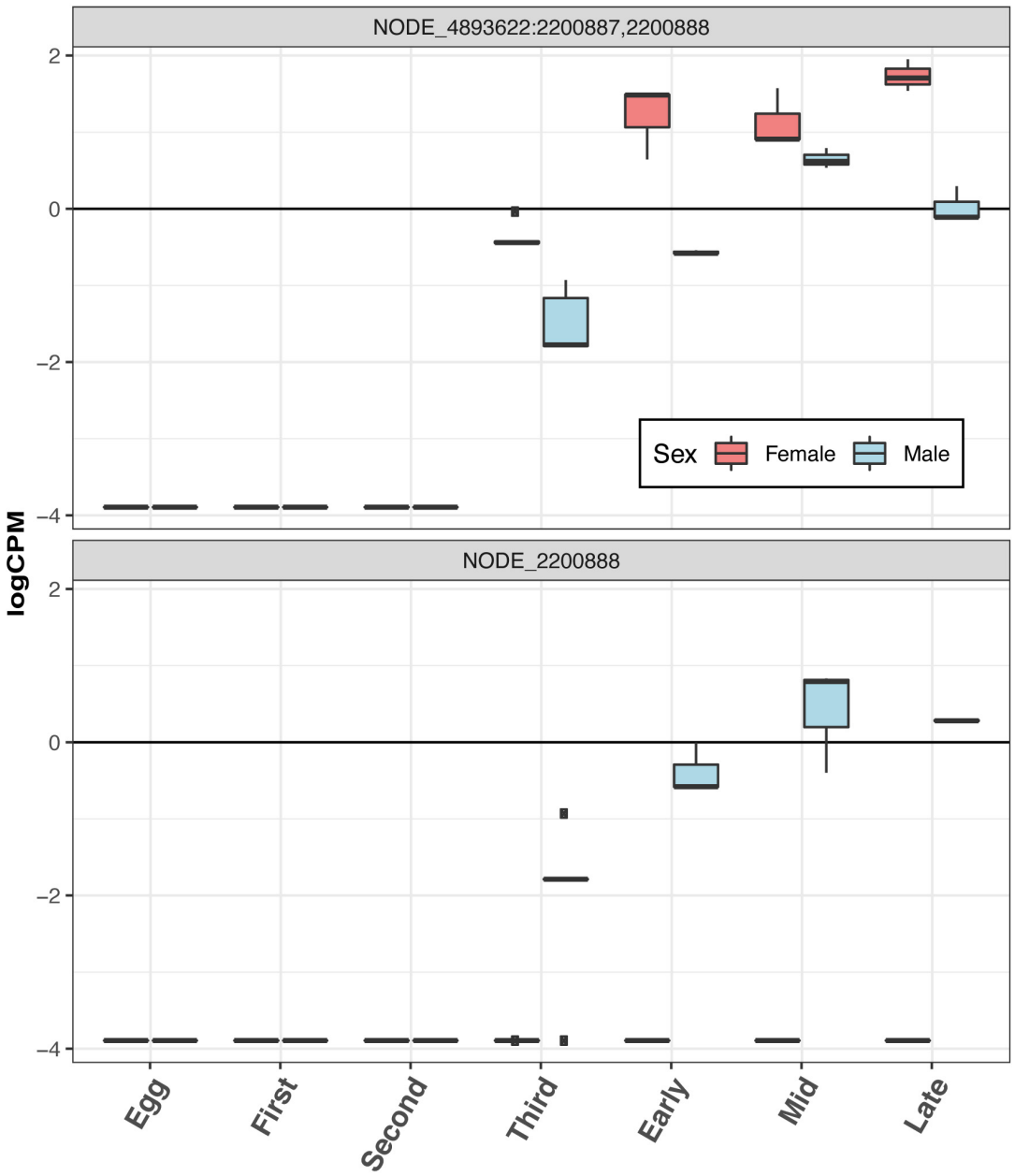

FIGURE 5 | Both nodes with homology to *D. melanogaster dsx* that passed the filtering cutoffs demonstrate sexual dimorphism in expression. In both sexes, expression is initiated in the third instar, though one node is only expressed only in males.

transmembrane transport, locomotion, and imaginal disk growth. Male third instar larvae also demonstrate a range of GO term enrichment, including shifts to metabolic processes, determination of right/left symmetry and asymmetry, imaginal disk fusion, apoptic cell clearance, cognition and memory, genital disk morphogenesis, sex differentiation, regulation of hormone metabolic processes, and the JNK cascade. Third instar is also where differential expression of the putative *tra* node NODE_13077:3370588 is most differentially expressed. Furthermore, nodes with homology to *dsx* begin to be differentially expressed in third instar, and female samples demonstrate significantly higher expression of the common *dsx* exon (NODE_4893622:2200887,2200888). Furthermore, the node with homology to the male exon of *dsx* (NODE_2200888) is also expressed only in males.

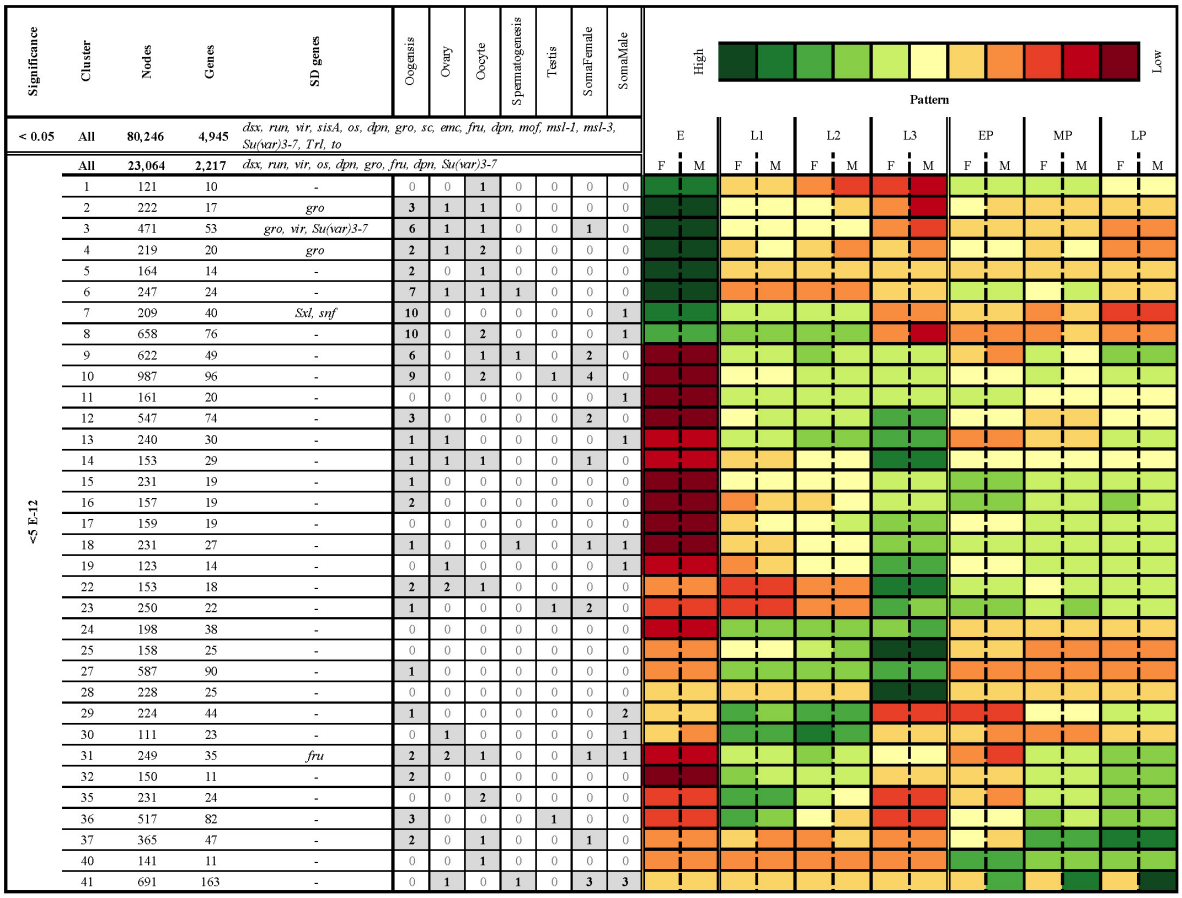

Significance	Cluster	Nodes	Genes	SD genes	Oogenesis	Ovary	Oocyte	Spermatogenesis	Testis	SomaFemale	SomaMale
< 0.05	All	80,246	4,945	*dsx, run, vir, sisA, os, dpn, gro, sc, emc, fru, dpn, mof, msl-1, msl-3, Su(var)3-7, Trl, to*							
	All	23,064	2,217	*dsx, run, vir, os, dpn, gro, fru, dpn, Su(var)3-7*							
<5 E-12	1	121	10	-	0	0	1	0	0	0	0
	2	222	17	*gro*	3	1	1	0	0	0	0
	3	471	53	*gro, vir, Su(var)3-7*	6	1	1	0	0	1	0
	4	219	20	*gro*	2	1	2	0	0	0	0
	5	164	14	-	2	0	1	0	0	0	0
	6	247	24	-	7	1	1	1	0	0	0
	7	209	40	*Ssl, snf*	10	0	0	0	0	0	1
	8	658	76	-	10	0	2	0	0	0	1
	9	622	49	-	6	0	1	1	0	2	0
	10	987	96	-	9	0	2	0	1	4	0
	11	161	20	-	0	0	0	0	0	0	1
	12	547	74	-	3	0	0	0	0	2	0
	13	240	30	-	1	1	0	0	0	0	1
	14	153	29	-	1	1	1	0	0	1	0
	15	231	19	-	1	0	0	0	0	0	0
	16	157	19	-	2	0	0	0	0	0	0
	17	159	19	-	0	0	0	0	0	0	0
	18	231	27	-	1	0	0	1	0	1	1
	19	123	14	-	0	1	0	0	0	0	1
	22	153	18	-	2	2	1	0	0	0	0
	23	250	22	-	1	0	0	0	1	2	0
	24	198	38	-	0	0	0	0	0	0	0
	25	158	25	-	0	0	0	0	0	0	0
	27	587	90	-	1	0	0	0	0	0	0
	28	228	25	-	0	0	0	0	0	0	0
	29	224	44	-	1	0	0	0	0	0	2
	30	111	23	-	0	1	0	0	0	0	1
	31	249	35	*fru*	2	2	1	0	0	1	1
	32	150	11	-	2	0	0	0	0	0	0
	35	231	24	-	0	0	2	0	0	0	0
	36	517	82	-	3	0	0	0	1	0	0
	37	365	47	-	2	0	1	0	0	1	0
	40	141	11	-	0	0	1	0	0	0	0
	41	691	163	-	0	1	0	1	0	3	3

FIGURE 6 | Clustering of all significantly differentially expressed genes (FDR < 5e-12) resulted in 41 clusters with an average Pearson correlation of 0.85 and 100 nodes or more. Columns from left to right: Level of significance (*p*-adjusted cut-off), cluster, number of nodes, number of *D. melanogaster* gene hits, *D. melanogaster* sex-related genes hits, number of hits to genes with tissue and/or sex specific patterns of expression from other species, and a heatmap of average logCPM expression in females (F) and males (M) in eggs (E), first instar (L1), second instar (L2), third instar (L3), early in pupariation (EP), mid pupariation (MP), and late in pupariation (LP). The sex-related gene hits are those genes which have been identified to play a crucial role in sex-determination and sexual-dimorphism in *D. melanogaster* (Baker et al., 1989; Erickson and Cline, 1998; Grath and Parsch, 2016). The tissue and sex-specific gene hit lists were identified *a priori* based on results from previous work in *D. melanogaster* studying somatic and gametic patterns of gene expression, including within tissues (ovaries, oocytes, and testis) and related to gametogenesis (spermatogenesis and oogenesis) (Lebo et al., 2009; Chang et al., 2011). There are three different nested sets of genes in this table. The top row (<0.05; All) represents all nodes identified as differentially expressed in the analyses. The second row represents all nodes differentially expressed in the analysis at a FDR cutoff of 5e-12. The remaining rows are all of the nodes in that set which are also in a cluster with an average Pearson correlation > 0.85 and 100 nodes or more (where to find data that produced this table).

Sexual dimorphism throughout pupariation involves many genes, and changes throughout the process

As would be expected, sexual differentiation is highest across immature development during pupariation, and increases the closer an individual is to eclosion (**Figure 9**). All stages demonstrate differential expression of the putative *tra* node and both *dsx* nodes between the sexes. Furthermore, males demonstrate enrichment of male reproduction terms, such as spermatogenesis, as well as ATP production, throughout all of pupariation.

Early in pupariation, females demonstrate enrichment in a broad array of GO terms, chemosensation, signal transduction, ion transport, ovary development, and pupariation. In contrast, while also demonstrating enrichment in a broad array of term, males mostly demonstrate parent-child enrichment of terms such as pupal development, transmembrane proton transport, ATP generation, spermatogenesis, neurogenesis, proprioception, sensory perception, JH esterase activity, and, interestingly, Y-chromosomes. However, the "Y chromosome" GO term (GO:0000806) is linked to only a single node (NODE_3701213) with homology to *Thioredoxin T* (*TrxT*, CG3315); in *D. melanogaster* the product of this gene regulates expression of genes on the Y-chromosome (Bonaccorsi et al., 1988). Several genes initially identified as demonstrating differential expression between the stages were also identified as having sexually dimorphic patterns of expression in early pupariation, including *CrLsp1α*, *CrSdhD*, and *CrJhebp29*.

Mid pupariation, females show increased expression of genes related to sensory perception, BMP signaling, cellular differentiation, establishment of chromatin silencing, R7 cell

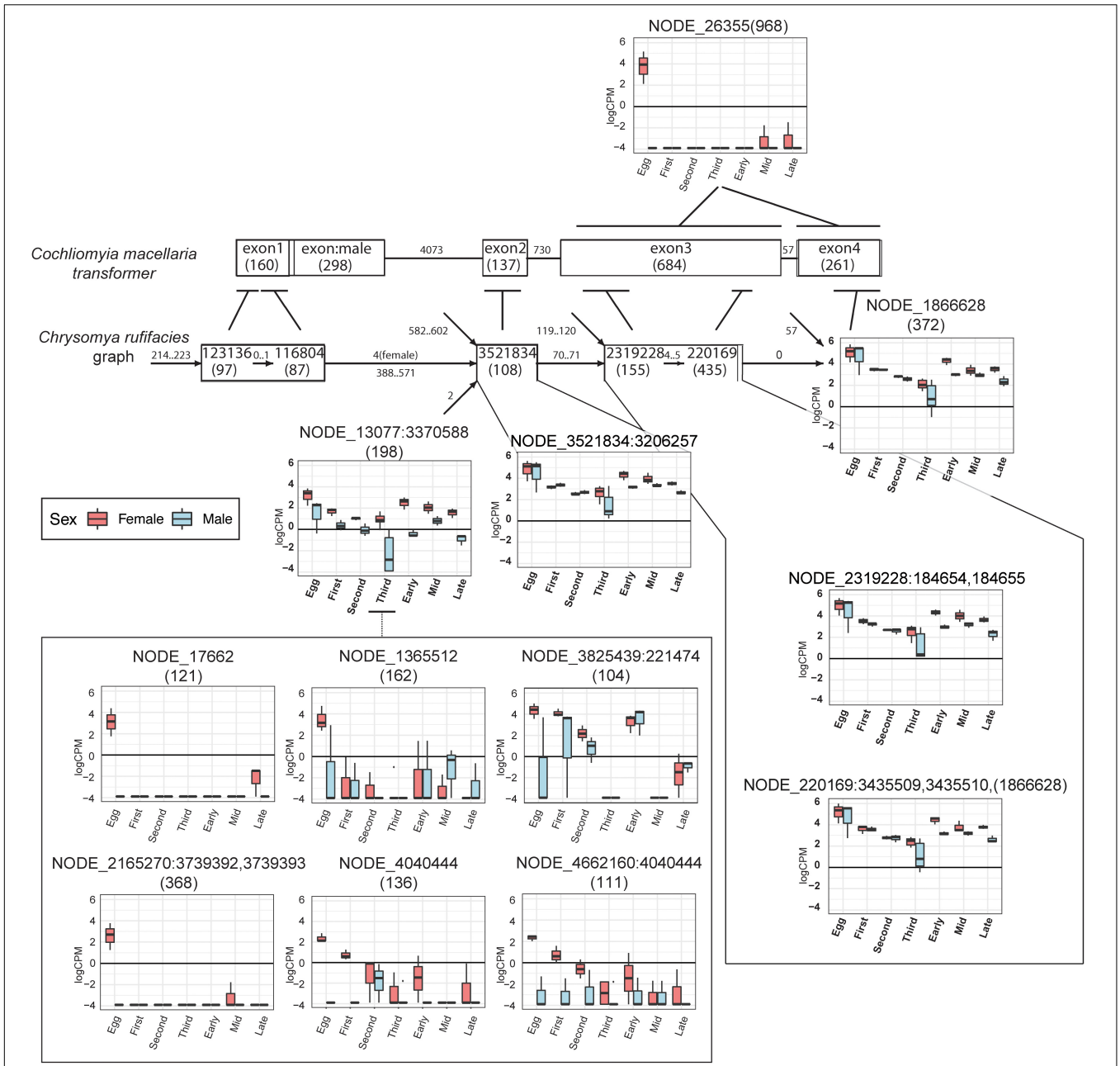

FIGURE 7 | Putative *transformer* nodes have sex- and stage- specific patterns of expression. Condensed splicing graph in 31_100 assembly of *C. rufifacies* containing nodes that have hits to the *Co. macellaria* transformer protein from translated BLAST. Also shown are upregulated nodes in *C. rufifacies* that have similarity and the *Co. macellaria* transformer gene model from accession JX315619. Within the *Co. macellaria transformer* gene model, each exon is labeled by the exon number with its length in nucleotides in parentheses. Each edge is labeled by the length of the intron between the exons. Within the *C. rufifacies* splicing graph, each node is labeled by the node number with its length in nucleotides in parentheses, and expression (*y*-axis:log counts-per-million) is plotted on a sex:stage basis (*x*-axis) for those nodes with statistically significant patterns of expression. The line leading out from each node indicates the exonic region from the BLAST hit, with the range of the local hit represented by a horizontal line near the exon. Each edge is labeled by the range of path lengths between the nodes.

development, and transmembrane transport systems, particularly those related to synaptic development. Males, on the other hand, continue to demonstrate enrichment of spermatogenesis and ATP generation, and also begin to enrich endosome organization, programmed larval cell death, salivary gland histolysis. This is also the only point in pupariation where differential expression of *sc*, a sex determination candidate with prior support (Andere et al., 2020) for driving the system, is statistically significant.

Late in pupariation, more than 2/3 of the differentially expressed genes are male biased in expression. Female upregulated genes are involved in regulation of synaptic activity,

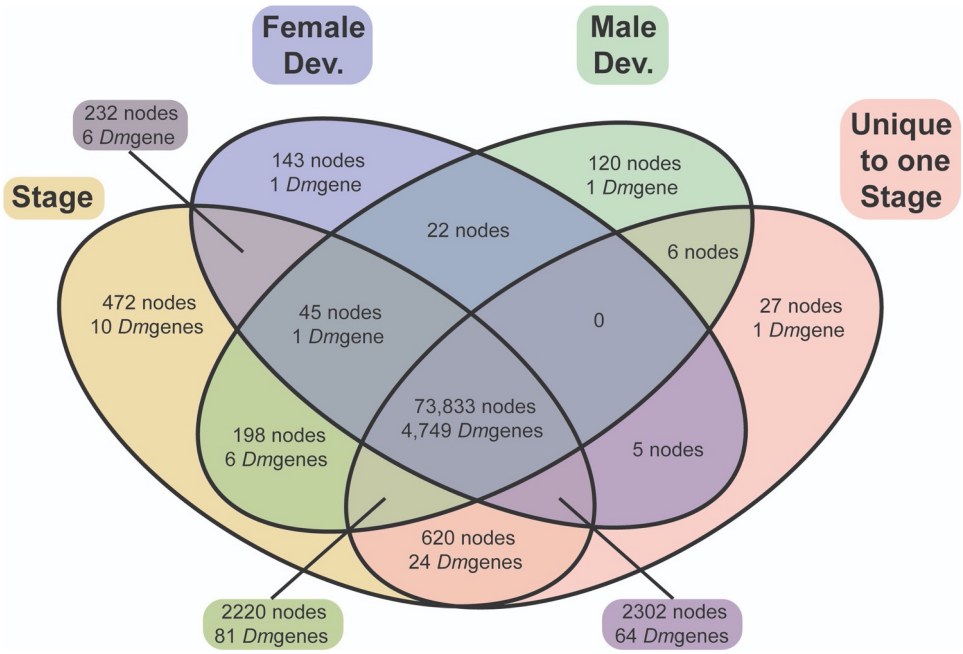

FIGURE 8 | A Venn diagram of differential expression of nodes and genes annotated with similarity to Drosophila genes. Most DEN (73,900) exhibit differential expression throughout development within both males (green) and females (blue). A similar number of nodes are expressed in a sex-specific manner throughout development in both males and females.

response to the BMP pathway, eye and wing development, renal filtration, RNA transport, pigment metabolic processes, and epidermis development. Males demonstrate enrichment of genes related to sensory perception, ATP generation, proton transport, male gamete generation, regulation of cellular pH, histolysis and cell death, axon generation and regeneration, spermatid differences and gas transport.

Clustering Identified Groups of Nodes With Similar Patterns of Expression

Using all differentially expressed nodes, we identified 38 clusters with an average Pearson Correlation Coefficient $\geq$ 0.85 and at least 100 nodes (**Figure 6**). In the interest of brevity, we will discuss only a few clusters, though each cluster may contain genes of interest to researchers investigating other questions (**Supplementary Materials 5**, **10**). For example, the nodes in cluster 4 have high expression in eggs, and sexually dimorphic patterns of gene expression in most juvenile stages (**Figure 6**). This cluster demonstrates significant enrichment of genes with GO terms related to neurogenesis, cell differentiation, sex determination, regulation of the Wnt signaling pathway, and DNA damage repair. Another cluster of interest is 22, which has high node expression in larval stages that drops off at the onset of pupariation, making genes in this cluster potentially useful for identifying postfeeding larvae. This cluster demonstrates significant enrichment of genes with GO terms related to proteolysis, transmembrane transport, and response to external stimulus and stress (including NODE_1153482 which demonstrates highest homology with a *D. melanogaster* Cytochrome p450; *Cyp28d2*). Finally, expression in cluster 36 could be useful for sex-specific age differentiation over pupariation, and demonstrates enrichment for neurological processes such as synaptic vesicle localization, long-term memory, mating, courtship behavior, and sensory perception.

qPCR Validation

All genes analyzed by qPCR in this study were significantly differentially expressed by developmental stage according to ANOVA ($p < 0.0001$). It is important to note that these potential markers were assessed in a different population, collected less than 10 generations from the wild, and under different environmental conditions than those used to identify them. The point in development where developmental stages were sampled also differed subtly. These differences are important, because they most closely reflect a realistic forensic condition, where a reference will not exactly match the rearing conditions and source population of evidentiary specimens. When comparing the directional patterns of change for each of these genes between the RNAseq expression information and the expression from the qPCR validation, the general patterns held with some variation in timing or fold change across experiments and generally occur as observed in *D. melanogaster* (Graveley et al., 2011). Gene expression was highest in third instars and early puparial samples, then decreases throughout time in puparial stages for *Larval serum protein 1α* (*Lsp1α*) and across all stages in *Cyp28d2* (**Figures 10A,B**). In *Lsp1α*, there are no significant differences in expression between larval stages and the early puparial stage; however, there is a significant decrease in expression in

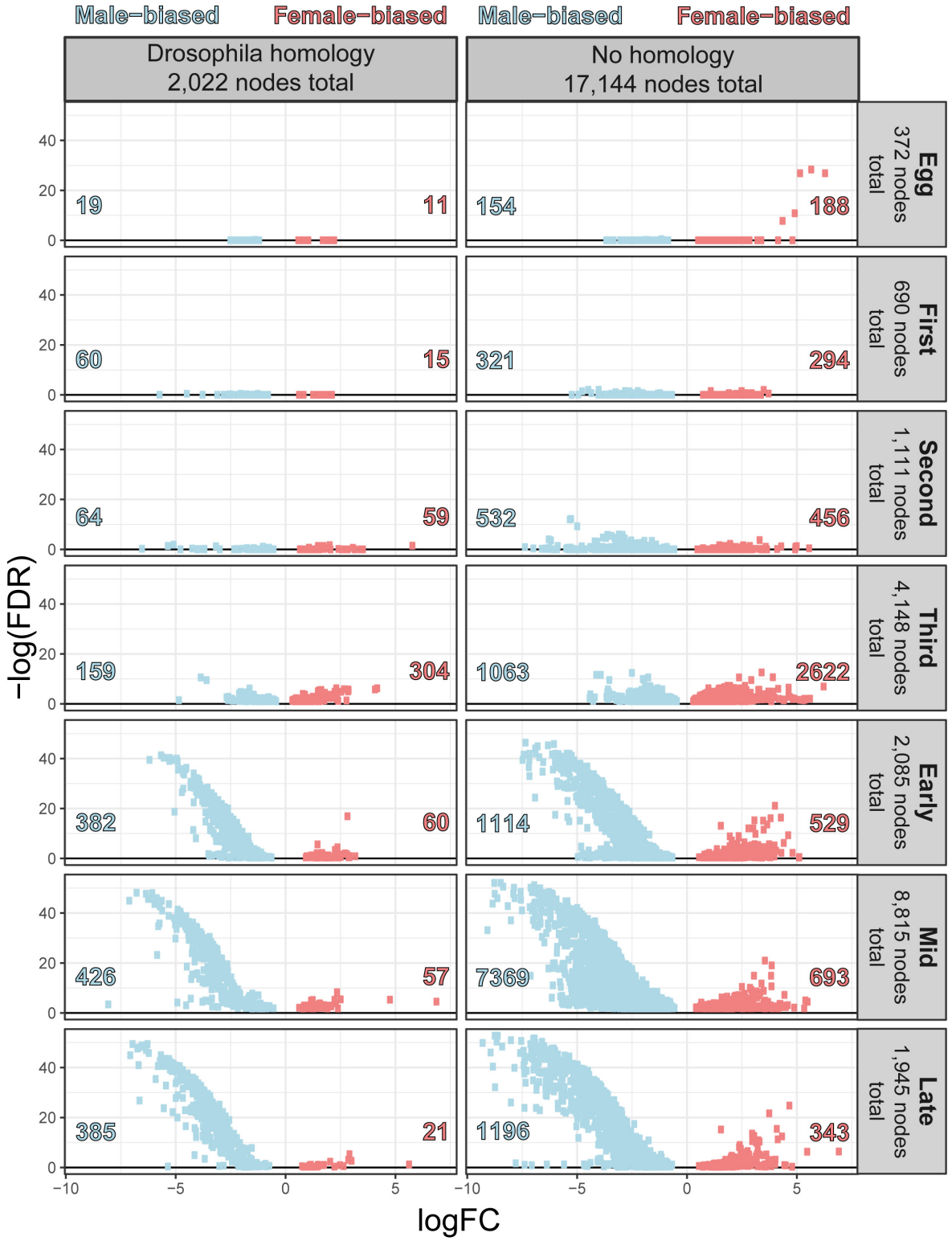

FIGURE 9 | Volcano plot of sexual dimorphism throughout immature development highlights the increasing number of nodes and strength of masculinization of *Chrysomya rufifacies'* transcriptome as development progresses.

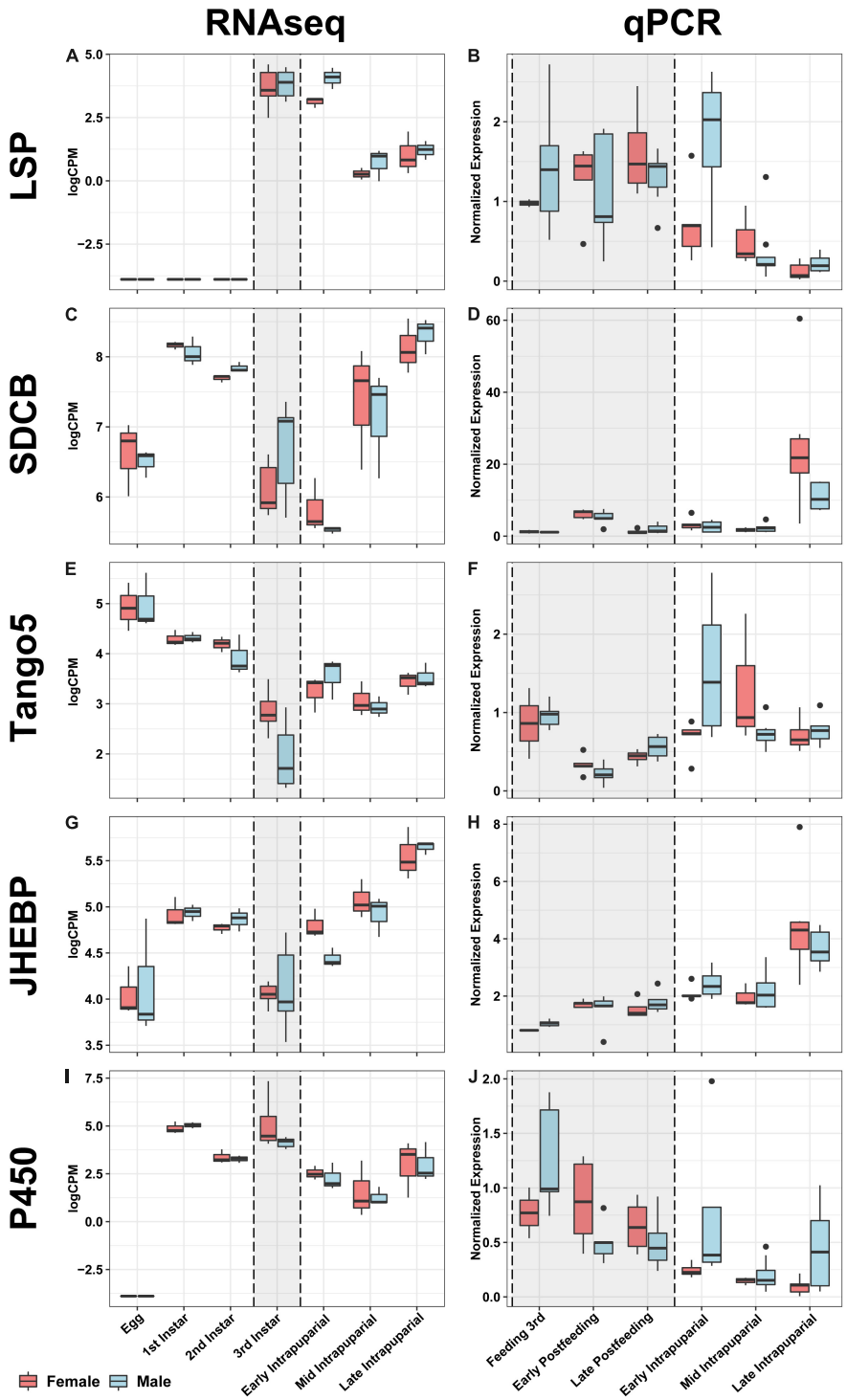

FIGURE 10 | Comparative boxplots of genes selected for validation. RNAseq expression in the left column and qPCR normalized expression in the right column for each node for which primers were designed in the rows (see **Table 4**). Each boxplot for the RNAseq column represents three separate individuals, with the exception of the third instar samples (gray background shaded box), which represents six individuals collected to evaluate gene expression correlated with facultative predatory behavior, and therefore are likely to be feeding third instars. Eleven samples were evaluated for each time point with qPCR validation, and sampling also broke up the third instar into three separate time points, all indicated in the gray shaded box; see **Table 3** and materials and methods section "Validation Fly Rearing" for more details. From left to right, top to bottom: **(A)** RNAseq expression of *Larval serum protein 1a (Lsp1a)*, **(B)** qPCR expression of *Lsp1a*, **(C)** RNAseq expression of *Succinate dehydrogenase cytochrome B (SDCB)*, **(D)** qPCR expression of *SDCB*, **(E)** RNAseq expression of *Transport and Golgi organization 5 (Tango5)*, **(F)** qPCR expression of *Tango5*, **(G)** RNAseq expression of *Juvenile hormone esterase binding protein (JHEBP)*, **(H)** qPCR expression of *JHEBP*, **(I)** RNAseq expression of a cytochrome p450 (P450), **(J)** qPCR expression of P450.

mid and late puparial stages (**Figure 10A**). In *Cyp28d2*, gene expression decreases throughout time, with lower expression in each subsequent developmental stage (**Figure 10I**). There were significant increases in expression throughout time in both *SDCB* and *Jhebp29* (**Figures 10C,D,G,H**), with highest levels at the end of pupariation. In *SDCB*, there were no significant differences in expression between larval stages and early-mid puparial stages; however, there was a significant increase in expression of this gene in the late puparial stage (**Figure 10C**). In *Jhebp29*, there was an increase in gene expression between feeding 3rd instar and postfeeding stages, however, not significantly so. In puparial development, *Jhebp29* expression significantly increased in the late puparial stage compared to early-mid puparial development (**Figure 10G,H**). *Tango5* expression was found to be significantly lower in postfeeding larval stages compared to the feeding 3rd instar larval stage (**Figure 10F**). Puparial expression did not significantly differ across time, and is not significantly different from the feeding 3rd instar expression (**Figures 10E,F**). When separated by sex, only *Tango5* in the early puparial stage and *SDCB* expression in the late puparial stage were significantly different between the sexes (**Figure 10**). In the early puparial stage, *Tango5* expression was significantly higher in males than in females, something that was seen expression data from RNAseq (**Figures 10E,F**). In the late puparial stage, *SDCB* expression was significantly higher in females than in males, yet this difference was not seen in the RNAseq data (**Figures 10C,D**).

DISCUSSION

The major goal of this project was to identify candidate genes useful for making improved predictions of *C. rufifacies* age through the use of gene expression markers. Logically, effective markers for this purpose will exhibit several features. They should be differentially expressed over development, especially among stadia whose ages are difficult to precisely predict with morphology (Anderson, 2000; Tarone and Foran, 2008; Tarone et al., 2011). Ideally, target markers will exhibit large effect sizes (e.g., off in early intra-puparial development and on at a high level at the end). However, since development time is a quantitative trait, it is expected that a variety of environmental and genetic factors, as well as their interactions, may impact either developmental progress or genes used to predict it (Tarone et al., 2015). Therefore, expression signals from target genes would ideally be robust to changes in environmental conditions (Kaneshrajah and Turner, 2004; Tarone and Foran, 2006; Fremdt et al., 2014) or genotypes (Tarone et al., 2011). One simple genetic difference found in many sexually reproducing organisms is the genetic effect of sex determination, which can impact a variety of sexually dimorphic traits. Therefore, we considered sex as a potentially major source of variation. It is also unlikely that the expression of any developmentally regulated gene is stable across all environments and genotypes (even housekeeping genes are expected to vary), so such an age prediction system will also likely be comprised of multiple genes that are less variable than other markers of age (within a point in development), respond to different environmental/genetic factors, and exhibit strong signals of change (i.e., high effect sizes) over development. The composition of such a collection of genes is likely to depend on the number of genes affected by environments, genotypes, and their interactions that exhibit characteristics desirable for predicting age. In some scenarios, it may be necessary to identify genes predictive of environments or genotypes, which can be used to correct for signals from other markers of age that exhibit large effect sizes. As an example (Frątczak-Łagiewska and Matuszewski, 2018), determined that sex alone is not useful information for improving predictions of age in a forensically informative beetle. However, improvement did occur when knowledge of sex was combined with size at maturity (Matuszewski and Fratczak-Łagiewska, 2018). Similarly, one may imagine a gene is useful in predicting age, but only when the sex of the immature fly is known, due to differences in the way the sexes developmentally regulate a gene. The inclusion of such a gene in a prediction set may be more or less desirable depending on how many genes are responsive to various inputs. Since little is known about the *C. rufifacies* transcriptomic response, we provide important baseline data that can be used to inform future decision regarding sets of age-predicting genes. Here, we evaluated gene expression across *C. rufifacies* development at 30°C and in both sexes. We identified genes that were differentially expressed over development, between sexes, and those differentially expressed across development by the sexes; identifying the relative proportions of the transcriptome that are differentially expressed by development, sex, or both. We then tested a subset of potential markers of age in a new population of flies raised at a 25°C, demonstrating that most genes (sexually dimorphic or not) performed as expected.

We present here evidence of sexual dimorphism throughout immature development against a wild-type genetic background through an assessment of two phenotypes, development rate and gene expression, in an under-studied and forensically relevant fly, *Chrysomya rufifacies*. Despite the relative lack of genetic tools in this species, broad patterns of GO enrichment were identified by leveraging sequence similarity to *D. melanogaster*. Furthermore, five genes were selected for qPCR validation based on the RNAseq results and concordance with patterns of expression in other species of fly. All genes analyzed by qPCR in this study were significantly differentially expressed by developmental stage, and two also demonstrated significant sexual dimorphism in expression. Ideal markers of age were strongly differentially expressed during development during longer developmental stages, robust to changes in the ambient temperature during rearing, and not sexually dimorphic. However, with knowledge of sex, dimorphism could be used to optimize estimate accuracy (as in Matuszewski and Fratczak-Łagiewska, 2018).

There are a few potential biases associated with the approach taken. The transcriptome was assembled with a program designed to preserve splicing information (Sze et al., 2017), as differential splicing of key sex-determination genes is responsible for many aspects of downstream sexual dimorphism. The error structure of sequences associated with this method have already been investigated, and this algorithm has been shown to be conservative and reliable (Sze et al., 2012, 2017; Pimsler et al., 2019); identifying *dsx* in *C. rufifacies*, which was

confirmed by Sanger sequencing (Jonika et al., 2020), and recovering known sequences in several other model and non-model organisms. The assembly is fragmented, which may affect its usefulness for some purposes, but for the purpose of this project it was clearly sufficient for our needs. Some of the analysis relies on similarity of transcriptome sequences to the well-known and studied organism *Drosophila melanogaster*, another higher fly, and gene ontology analyses were based on these annotations. A conservative cutoff was considered for declaring similarity to *Drosophila*, thus only 8,903 retained nodes were associated with *Drosophila* sequences, representing 4,965 genes. Unique genes or unique uses of gene products will be overlooked with such an approach, which can particularly be an issue in rapidly evolving genes, such as sex-related genes (Ellegren and Parsch, 2007; Haerty et al., 2007). However, *dsx* appears to demonstrate an expected pattern of dimorphism, as do a variety of other sequences predicted to be associated with sex determination and development. International collaborative investment in gene ontology resources (Ashburner et al., 2001) and the use of BUSCO scoring to estimate genome completeness (Waterhouse et al., 2019) suggest, however, that leveraging information from non-study species can at least serve as a useful starting point. However, care should be taken to remember potential biases and divergence from *Drosophila*, if one is interested in gene functions from the transcriptome and not the more applied interest of age prediction.

Despite these challenges, the anonymous nature of the analyses (i.e., independent of knowledge of putative node product) was expected to produce reasonable results (Sze et al., 2017). Indeed, examination of specific genes, as well as overall GO enrichment across development, demonstrated concordance with patterns observed in other species, particularly in well-studied *D. melanogaster*, across a range of transcriptomic approaches (Arbeitman, 2002; Lebo et al., 2009; Chang et al., 2011). As an example, egg gene expression is particularly enriched for genes related to patterning, growth, and cell differentiation, while larval gene expression is enriched for genes related to digestion and locomotion. Thus, in many ways *C. rufifacies* development appears to follow a similar general trajectory to *D. melanogaster* in many ways, despite their evolutionary and ecological distance from one another.

Individual genes also demonstrated conservation in pattern. For example, the gene *slam*, which is important for cleavage and polarized membrane growth and demonstrates highest expression in *D. melanogaster* eggs (Lecuit et al., 2002), was found to be uniquely expressed in the egg stage in *C. rufifacies*. Another gene that demonstrated conservation in pattern in *D. melanogaster, Bombyx mori,* and *Manduca sexta* was a juvenile hormone esterase binding product (*Jhebp29*) (Campbell et al., 1992; Liu et al., 2007; Hao et al., 2013). In *Drosophila*, the expression pattern of this gene largely matches the pattern seen in *C. rufifacies*, where lowest expression occurs in third instars and increases afterward throughout pupariation (Graveley et al., 2011).

The utility of sexual dimorphism in development rates in forensic entomology is not yet clear. In this work, we have shown that male *C. rufifacies* eclose as adults 9 h earlier at 30°C, on average, than females whose eggs were laid at the same time, and pupariate 4 h earlier. Previous work in forensically relevant species has demonstrated statistically significant sexually dimorphic development rates, though in some cases this dimorphism can too small to have a practical use in case work (Picard et al., 2013; Frątczak-Łagiewska and Matuszewski, 2018; Smith and Cook, 2020). However, given the LDT's calculated in this work, we observed that males pupariate 90-108 ADH and eclose 200–240 ADH earlier than females of the same temporal age. *Chrysomya rufifacies* can develop at relatively low temperatures (15.6°C; Byrd and Butler, 1997) and have been collected routinely as a part of indoor casework in Texas (average ambient ± std. dev.: 27.7°C ± 7.8 from Sanford, 2017). As ∼16% of cases involving *C. rufifacies* would have involved ambient temperatures of ∼20°C, this would represent a different of 16 h between male and female eclosion. Given that blow flies rarely lay eggs at night (Greenberg, 1990; Singh and Bharti, 2001; Amendt et al., 2008; Zurawski et al., 2009; Berg and Benbow, 2013), and it is common practice to use what are considered the oldest samples to estimate a minimum postmortem interval (in this case "fastest to eclose"), a 16 h difference could result in estimates that are off by a day or more (if the complete developmental timeline is relevant to a case). Clearly, more research is needed to validate the results presented here, and to identify what factors, if any, affect nocturnal oviposition in *C. rufifacies*. Results presented here indicate that there is moderate sexual dimorphism in immature development rate that is unlikely to be important in some temperatures but may have investigative importance in others – depending on what specimens/stages/sexes were sampled.

Generally, our results demonstrated that 98.4% of all nodes passing our filtering threshold were differentially expressed. Of these, most differentiated our samples by developmental time-point (99.8%), fewer nodes were sex-differentially expressed throughout development (19.1%), and very few nodes which demonstrated differential expression by sex alone (1.5%). The relatively large effect of development in differential expression is clearly demonstrated in the MDS plot (**Figure 3**), which shows the general pattern of clustering for sample types (sex:stage) across all nodes. For the purposes of estimating insect age, nodes which demonstrated significant stage-specific gene expression but which are not affected by other factors, such as sex, are the most useful (i.e., *Jhebp29*). Our results also point to sex-determination cascade genes with male and female shared exons (such as *tra* and *dsx*) which have stage-gated expression patterns as being potentially useful for age-related estimates. Additional research is required to determine how robust these patterns are with respect to other factors, such as temperature or geographic population of origin.

In concert with development-rate sexual dimorphism, sexual dimorphism in gene expression is also observed in every stage throughout immature development. Interestingly, the magnitude (p-value and $\log_2$FC) of sexual dimorphism is higher in eggs than first and second instar larvae, and is female skewed in eggs. This is likely a lingering effect of maternal contributions to their offspring (Avilés-Pagán and Orr-Weaver, 2018), although it is anticipated that embryonic samples were collected after the transition to zygotic gene expression (Kronja et al., 2014;

Navarro-Costa and Martinho, 2020). However, there is a definite masculinization of the sexually dimorphic component of the transcriptome during the rest of development, characterized by a greater number of nodes demonstrating male-biased expression with more extreme p-values and logFC's. This is directly in line with patterns observed in zebrafish (Small et al., 2009), but is also supported by findings that sex-linked gene expression dimorphism evolves and diverges more rapidly in male-linked genes (Ranz et al., 2003; Assis et al., 2012; Perry et al., 2014; Grath and Parsch, 2016). Furthermore, patterns of increasing dimorphism in gene expression over developmental time is supported by results in *D. melanogaster* (Perry et al., 2014). Additional work is needed, however, to disentangle sex-specific differences in gene expression from the effect of different development rates of males and females.

While the primary focus of this work was forensic entomology applications, these results also shed some light on the unusual sex determination mechanism of *C. rufifacies*. For example, there in an interesting connection of GO enrichment of cell cycle, underreplication, and endoreduplication in female-fated immatures relative to male-fated immatures which imply hypotheses that could explain coverage differences observed between arrhenogenic and thelygenic female genomes (Andere et al., 2020). Furthermore, the greatest increase of sexual dimorphism in gene expression coincides with the initial expression of *dsx*. Similarly, *tra* related sequences warrant further investigation, but indicate a potential role for exons 2 and 3 in embryonic cell fates. As the exact genes involved in the monogenic sex determination cascade of *C. rufifacies* have not been identified, much less their hierarchy, this serves as a promising starting point to begin to investigate critical genetic and ontological control points.

One of the main purposes of the RNA-seq work was to generate putative sequences for estimating ages of immature samples, especially puparial development, as this stage occupies a major proportion of immature development and, without dissection/imaging and detailed knowledge of development, is difficult to break into smaller portions of developmental time. Results which were upheld across RNA-seq and qPCR, especially when similar to patterns in *D. melanogaster*, support the possibility of stability of markers across genotypes and environments - more so than if they had been tested in the same conditions and population of flies (i.e., the comparison mirrors casework interests where the reference is not necessarily an exact representative of the casework sample population). Some potential markers of age were assessed further with qPCR in a different population of *C. rufifacies*, less than 10 generations out of the wild reared in different conditions. The validation qPCR tested genes demonstrated similar patterns across developmental time-points and/or sexes as seen in the RNA-seq experiment. It was anticipated that *Lsp1α* and *SdhD* would be useful for differentiating feeding 3rd instar from postfeeding 3rd instar stages, as *Lsp1α* is expressed in all instars and new white prepupae at moderate to high levels in *D. melanogaster*. However, our qPCR results indicate that *Jhebp29*, *Cyp28d2*, and *Tango5* would be a more useful panel in these larval development stages. Of the validation qPCR tested genes, *Lsp1α*, *SdhD*, and *Jhebp29* seem like ideal candidates for further work to develop a gene expression model to quantify puparial development progress. The qPCR found higher *Lsp1α* expression in the early puparial stage than later stages, with highly sexually dimorphic expression early in pupariation. While *Lsp1α* expression drops throughout puparial development, *SdhD* and *Jhebp29* have significantly higher expression in the late puparial stage than earlier stages. Aside from the sexual dimorphism in *Lsp1α* expression in early puparial development, comparison of the validation qPCR results between sexes did produce any other remarkable differences that could be found in both RNA-seq and qPCR analyses.

We have demonstrated that *C. rufifacies* is a useful organism for the study of developmental sex-specific gene expression impacts in insects against a wild-type genetic background, and provided some genetic tools with which to do so. These results set the stage for a number of downstream applications. Building upon this work will deepen our understanding of the evolution of sex determination and sexual dimorphism, especially in the case of comparison of model systems and across clades. This work has specific applications in medical entomology as well, especially for the development of new tools for the control on myiasis causing Calliphoridae. The Sterile Insect Technique (SIT), originally developed in the 1950's to control the calliphorid species *Cochliomyia hominivorax* a.k.a "the new world screwworm" (Sapti et al., 2005), has proven to be a robust tool in the control of pest insects. However, while newer applications of SIT have integrated genetic tools, the control of *Co. hominivorax* still relies upon uneconomical bisexual rearing and sorting. We have generated a list of target pathways and the genetic tools to exploit them for both SIT and the release of dominant lethal genes.

One core challenge of forensic entomology has been that individual species have their own temperature-dependent development rates (Amendt et al., 2011). As more work is done in more parts of the world, publishing pressures and theoretical developments have led to a shift in research focus away from laboratory development studies. Work in the last 10 years in this field has also highlighted the effect of carrion species and potential local adaptation on development rates (Tarone et al., 2011; Flores et al., 2014; Owings et al., 2014), though current application in forensic entomology does not always take these factors into account. The results of this work add to a growing body of data on developmental patterns of gene expression in Calliphoridae (Zehner et al., 2009; Tarone et al., 2011; Boehme et al., 2013; Fremdt et al., 2014; Zajac et al., 2015), which could be used to identify a core set of conserved genes with which to make quantitative age estimates across the Family. It is also unclear how much of an effect sex-specific development rates may have in case-work applications, as there have only been few studies so far (including this one) with flies (Smith and Cook, 2020) and beetles (Frątczak-Łagiewska and Matuszewski, 2018) of forensic importance. As noted previously (Tarone et al., 2015), any genes used to predict fly age for forensic purposes would ideally be tested across a range of genetic and environmental conditions to whittle the long list of candidates available from this and other genomic projects

down to those that are the most informative across the widest range of conditions.

CONCLUSION

This study evaluated gene expression over immature *C. rufifacies* development, leveraging the distinct sex determination system to simultaneously evaluate sexual dimorphism in development and developmental gene expression. It allowed an evaluation of the proportion of the transcriptome impacted by sex and/or development (developmental progress impacts expression the most and sex the least), in a system with no obvious morphological differences between immatures of either sex and with wild-type individuals (not mutants). The results largely align with what is known in *Drosophila*. However, it has been established that in this species, dimorphism in expression in embryos is female biased, with a major signal from *tra*, then switches to male biased expression in larvae (except third instars) and puparia that increases as development progresses and with the greatest shift in dimorphism occurring concurrent with when *dsx* expression initiates. The study sets a baseline for a set of genes that are potential markers of age, independent of and dependent on sex. Several genes were confirmed as markers of developmental progress in a way that can help separate feeding from postfeeding third instars or can break intra-puparial development into smaller portions of developmental time without detailed morphological knowledge of metamorphosis. In addition, several features of the unique sex determination system were identified that can be pursued in more detail in the future, enhancing support for, and ruling out, previous hypotheses about the sex determination system (Andere et al., 2020). Thus, this study of a forensically important insect enhances forensic application while synergistically contributing to basic evolutionary ecology (Tomberlin et al., 2011) and potentially other applications with blow flies (Yan et al., 2020).

DATA AVAILABILITY STATEMENT

Raw data files and additional results files can be accessed on Dryad (https://doi.org/10.5061/dryad.2z34tmpmx).

AUTHOR CONTRIBUTIONS

MP, JT, and AT conceived of the experimental design for the RNAseq. MP collected RNAseq samples, extracted RNA, collected sexual dimorphism in development rate data, did differential gene expression and GO analyses, and identified nodes for validation. S-HS and SF did the transcriptome assembly and *Drosophila melanogaster* annotation. AT, CH, AS, and MJ contributed to validation qPCR (samples collection, RNA extraction, qPCR, and data analysis). All authors contributed to writing and editing the manuscript.

FUNDING

Sequencing was performed by the Genomics and Bioinformatics Services at Texas A&M University and the High−Throughput Sequencing Facility of the University of North Carolina at Chapel Hill, funded through Whole Systems Genomics Initiative Catalyst, Texas AgriLife Genomics Seed grants and Texas A&M AgriLife Research funding. Bioinformatic analyses were performed on the Whole Systems Genomics Initiative Cluster and the Brazos Cluster at Texas A&M University, with A&M grants for sequencing and funding from NIJ: 2012-DN-BX-K024 to AT and S-HS partially contributing to analysis. Collection of qPCR data was supported by a Fulbright Fellowship through the Institute of International Education, New York, United States (Grant Number: 2221/DR/2017-2018) to AS. MP was supported by the TAMU Regents and Diversity Fellowships, as well as the TAMU Whole Systems Genomics Initiative Student Fellowship program and the TAMU Dissertation Fellowship.

ACKNOWLEDGMENTS

We would like to thank C. D. Jones, S. P. Srivastav, C. J. Picard, C. G. Owings, and J. A. W. Blanks for their assistance and support, as well as the TAMU Department of Entomology, the TAMU FLIES Facility, and the University of Alabama Lozier Lab.

SUPPLEMENTARY MATERIAL

The Supplementary Material for this article can be found online at: https://drive.google.com/drive/folders/1gOEI9fU0t1IY5Q_0os5_ighl9MlCqkX8

REFERENCES

Alexa, A., and Rahnenführer, J. (2015). *Gene set enrichment analysis with topGO*. Available online at: https://bioconductor.org/packages/release/bioc/vignettes/topGO/inst/doc/topGO.pdf (accessed October 30, 2020).

Altschul, S. F., Gish, W., Miller, W., Myers, E. W., and Lipman, D. J. (1990). Basic local alignment search tool. *J. Mol. Biol.* 215, 403–410. doi: 10.1016/S0022-2836(05)80360-2

Amendt, J., Krettek, R., and Zehner, R. (2004). Forensic entomology. *Naturwissenschaften* 91, 51–65. doi: 10.1007/s00114-003-0493-5

Amendt, J., Richards, C. S., Campobasso, C. P., Zehner, R., and Hall, M. J. R. (2011). Forensic entomology: applications and limitations. *Forensic Sci. Med. Pathol.* 7, 379–392. doi: 10.1007/s12024-010-9209-2

Amendt, J., Zehner, R., and Reckel, F. (2008). The nocturnal oviposition behaviour of blowflies (Diptera: Calliphoridae) in Central Europe and its forensic implications. *Forensic Sci. Int.* 175, 61–64. doi: 10.1016/j.forsciint.2007.05.010

Andere, A. A., Pimsler, M. L., Tarone, A. M., and Picard, C. J. (2020). The genomes of a monogenic fly: views of primitive sex chromosomes. *Sci. Rep.* 10, 1–12. doi: 10.1038/s41598-020-72880-0

Anderson, G. S. (2000). Minimum and maximum development rates of some forensically important Calliphoridae (Diptera). *J. Forensic Sci.* 45:14778J. doi: 10.1520/JFS14778J

Arbeitman, M. N. (2002). Gene expression during the life cycle of *Drosophila melanogaster*. *Science* 297, 2270–2275. doi: 10.1126/science.1072152

Ashburner, M., Ball, C. A., Blake, J. A., Butler, H., Cherry, J. M., Eppig, J. T., et al. (2001). Creating the Gene Ontology resource: Design and implementation. *Genome Res.* 11, 1425–1433. doi: 10.1101/gr.180801

Assis, R., Zhou, Q., and Bachtrog, D. (2012). Sex-biased transcriptome evolution in *Drosophila*. *Genome Biol. Evol.* 4, 1189–1200. doi: 10.1093/gbe/evs093

Avilés-Pagán, E. E., and Orr-Weaver, T. L. (2018). Activating embryonic development in *Drosophila*. *Semin. Cell Dev. Biol.* 84, 100–110. doi: 10.1016/j.semcdb.2018.02.019

Baker, B. S., and Belote, J. M. (1983). Sex determination and dosage compenstion in *Drosophila melanogaster*. *Annu. Rev. Genet.* 17, 345–393. doi: 10.1146/annurev.ge.17.120183.002021

Baker, B. S., Burtis, K., Goralski, T., Mattox, W., and Nagoshi, R. (1989). Molecular genetic aspects of sex determination in *Drosophila melanogaster*. *Genome* 31, 638–645. doi: 10.1139/g89-117

Bartoń, K. (2018). *MuMIn: Multi-model inference*. Vienna: R Core Team.

Benjamini, Y., and Hochberg, Y. (1995). Controlling the false discovery rate: a practical and powerful approach to multiple testing. *J. R. Stat. Soc. Ser. B* 57, 289–300. doi: 10.2307/2346101

Berg, M. C., and Benbow, M. E. (2013). Environmental factors associated with *Phormia regina* (Diptera: Calliphoridae) oviposition. *J. Med. Entomol.* 50, 451–457. doi: 10.1603/ME12188

Blanckenhorn, W. U., Dixon, A. F. G., Fairbairn, D. J., Foellmer, M. W., Gibert, P., Van Der Linde, K., et al. (2007). Proximate causes of Rensch's rule: Does sexual size dimorphism in arthropods result from sex differences in development time? *Am. Nat.* 169, 245–257. doi: 10.1086/510597

Blanckenhorn, W., Benbow, M. E., Tomberlin, J., and Tarone, A. (2015). "Quantitative genetics of life history traits in coprophagous and necrophagous insects," in *Carrion ecology, evolution, and their applications*, eds M. E. Benbow, J. K. Tomberlin, and A. M. Tarone (Boca Raton,FL: CRC Press), 333–360.

Boehme, P., Spahn, P., Amendt, J., and Zehner, R. (2013). Differential gene expression during metamorphosis: a promising approach for age estimation of forensically important *Calliphora vicina* pupae (Diptera: Calliphoridae). *Int. J. Legal Med.* 127, 243–249. doi: 10.1007/s00414-012-0699-1

Bonaccorsi, S., Pisano, C., Puoti, F., and Gatti, M. (1988). Y chromosome loops in *Drosophila melanogaster*. *Genetics* 120, 1015–1034. doi: 10.1093/genetics/120.4.1015

Byrd, J. H., and Butler, J. F. (1996). Effects of temperature on *Cochliomyia macellaria* (Diptera: Calliphoridae) development. *J. Med. Entomol.* 33, 901–905. doi: 10.1093/jmedent/33.6.901

Byrd, J. H., and Butler, J. F. (1997). Effects of temperature on *Chrysomya rufifacies* (Diptera:Calliphoridae) development. *J. Med. Entomol.* 34, 353–358. doi: 10.1093/jmedent/34.3.353

Campbell, P. M., Healy, M. J., and Oakeshott, J. G. (1992). Characterisation of juvenile hormone esterase in *Drosophila melanogaster*. *Insect Biochem. Mol. Biol.* 22, 665–677. doi: 10.1016/0965-1748(92)90045-G

Chang, P. L., Dunham, J. P., Nuzhdin, S. V., and Arbeitman, M. N. (2011). Somatic sex-specific transcriptome differences in Drosophila revealed by whole transcriptome sequencing. *BMC Genomics* 12:364. doi: 10.1186/1471-2164-12-364

Clausen, S., and Ullerich, F. H. (1990). Sequence homology between a polytene band in the genetic sex chromosomes of *Chrysomya rufifacies* and the *daughterless* gene of *Drosophila melanogaster*. *Naturwissenschaften* 77, 137–138. doi: 10.1007/bf01134479

Cline, T. W. (1993). The *Drosophila* sex determination signal: how do flies count to two? *Trends Genet.* 9, 385–390. doi: 10.1016/0168-9525(93)90138-8

Colgan, T. J., Carolan, J. C., Bridgett, S. J., Sumner, S., Blaxter, M. L., and Brown, M. J. (2011). Polyphenism in social insects: insights from a transcriptome-wide analysis of gene expression in the life stages of the key pollinator, *Bombus terrestris*. *BMC Genomics* 12:623. doi: 10.1186/1471-2164-12-623

Connallon, T., and Knowles, L. L. (2005). Intergenomic conflict revealed by patterns of sex-biased gene expression. *Trends Genet.* 21, 495–499. doi: 10.1016/j.tig.2005.07.006

de Hoon, M. J. L., Imoto, S., Nolan, J., and Miyano, S. (2004). Open source clustering software. *Bioinformatics* 20, 1453–1454. doi: 10.1093/bioinformatics/bth078

dos Santos, G., Schroeder, A. J., Goodman, J. L., Strelets, V. B., Crosby, M. A., Thurmond, J., et al. (2015). FlyBase: introduction of the *Drosophila melanogaster* Release 6 reference genome assembly and large-scale migration of genome annotations. *Nucleic Acids Res.* 43, D690–D697.

Drost, H.-G., and Paszkowski, J. (2017). Biomartr: genomic data retrieval with R. *Bioinformatics* 33:btw821. doi: 10.1093/bioinformatics/btw821

Dubendorfer, A., Hediger, M., Burghardt, G., and Bopp, D. (2002). *Musca domestica*, a window on the evolution of sex-determining mechanisms in insects. *Int. J. Dev. Biol.* 46, 75–79.

Ellegren, H., and Parsch, J. (2007). The evolution of sex-biased genes and sex-biased gene expression. *Nat. Rev. Genet.* 8, 689–698. doi: 10.1038/nrg2167

Erickson, J. W., and Cline, T. W. (1998). Key aspects of the primary sex determination mechanism are conserved across the genus *Drosophila*. *Development* 125, 3259–3268. doi: 10.1242/dev.125.16.3259

Flight, R. M., and Wentzell, P. D. (2009). Potential bias in GO::TermFinder. *Brief. Bioinform.* 10, 289–294. doi: 10.1093/bib/bbn054

Flores, M., Longnecker, M., and Tomberlin, J. K. (2014). Effects of temperature and tissue type on *Chrysomya rufifacies* (Diptera: Calliphoridae) (Macquart) development. *Forensic Sci. Int.* 245, 24–29. doi: 10.1016/j.forsciint.2014.09.023

Frątczak-Łagiewska and Matuszewski, K., and Matuszewski, S. (2018). Sex-specific developmental models for *Creophilus maxillosus* (L.) (Coleoptera: Staphylinidae): searching for larger accuracy of insect age estimates. *Int. J. Legal Med.* 132, 887–895. doi: 10.1007/s00414-017-1713-4

Fremdt, H., Amendt, J., and Zehner, R. (2014). Diapause-specific gene expression in *Calliphora vicina* (Diptera: Calliphoridae)-a useful diagnostic tool for forensic entomology. *Int. J. Legal Med.* 128:1001. doi: 10.1007/s00414-013-0920-x

Gennard, D. E. (2007). *Forensic Entomology An Introduction*. West Sussex: John Wiley & Sons Inc.

Ghiselli, F., Milani, L., Chang, P. L., Hedgecock, D., Davis, J. P., Nuzhdin, S. V., et al. (2011). De novo assembly of the Manila clam *Ruditapes philippinarum* transcriptome provides new insights into expression bias, mitochondrial doubly uniparental inheritance and sex determination. *Mol. Biol. Evol.* 29, 771–786. doi: 10.1093/molbev/msr248

Grassberger, M., and Reiter, C. (2001). Effect of temperature on *Lucilia sericata* (Diptera: Calliphoridae) development with special reference to the isomegalen- and isomorphen-diagram. *Forensic Sci. Int.* 120, 32–36. doi: 10.1016/S0379-0738(01)00413-3

Grassberger, M., and Reiter, C. (2002). Effect of temperature on development of the forensically important holarctic blow fly *Protophormia terraenovae* (Robineau-Desvoidy) (Diptera: Calliphoridae). *Forensic Sci. Int.* 128, 177–182. doi: 10.1016/S0379-0738(02)00199-8

Grath, S., and Parsch, J. (2016). Sex-biased gene expression. *Annu. Rev. Genet.* 50, 29–44. doi: 10.1146/annurev-genet-120215-035429

Graveley, B. R., Brooks, A. N., Carlson, J. W., Duff, M. O., Landolin, J. M., Yang, L., et al. (2011). The developmental transcriptome of *Drosophila melanogaster*. *Nature* 471, 473–479. doi: 10.1038/nature09715

Greenberg, B. (1990). Nocturnal oviposition behavior of blow flies (Diptera: Calliphoridae). *J. Med. Entomol.* 27, 807–810. doi: 10.1093/jmedent/27.5.807

Haerty, W., Jagadeeshan, S., Kulathinal, R. J., Wong, A., Ram, K. R., Sirot, L. K., et al. (2007). Evolution in the fast lane: Rapidly evolving sex-related genes in *Drosophila*. *Genetics* 177, 1321–1335. doi: 10.1534/genetics.107.078865

Hao, W., Zhang, Y., and Xu, Y. (2013). Identification of a juvenile hormone esterase binding protein gene and its developmental and hormone regulation in the silkworm, *Bombyx mori*. *J. Insect Physiol.* 59, 906–912. doi: 10.1016/j.jinsphys.2013.06.009

Hedrick, A. V., and Temeles, E. J. (1989). The evolution of sexual dimorphism in animals: hypotheses and tests. *Trends Ecol. Evol.* 4, 4–6. doi: 10.1016/0169-5347(89)90212-7

Jonika, M. M., Hjelmen, C. E., Faris, A. M., McGuane, A. S., and Tarone, A. M. (2020). An evaluation of differentially spliced genes as markers of sex for forensic entomology. *J. Forensic Sci.* 65, 1579–1587. doi: 10.1111/1556-4029.14461

Kaneshrajah, G., and Turner, B. (2004). *Calliphora vicina* larvae grow at different rates on different body tissues. *Int. J. Legal Med.* 118, 242–244. doi: 10.1007/s00414-004-0444-5

Kronja, I., Yuan, B., Eichhorn, S. W., Dzeyk, K., Krijgsveld, J., Bartel, D. P., et al. (2014). Widespread changes in the posttranscriptional landscape at the *Drosophila* oocyte-to-embryo transition. *Cell Rep.* 7, 1495–1508. doi: 10.1016/j.celrep.2014.05.002

Lagos, D., Koukidou, M., Savakis, C., and Komitopoulou, K. (2007). The transformer gene in *Bactrocera oleae*: the genetic switch that determines its sex fate. *Insect Mol. Biol.* 16, 221–230. doi: 10.1111/j.1365-2583.2006.00717.x

Lebo, M. S., Sanders, L. E., Sun, F., and Arbeitman, M. N. (2009). Somatic, germline and sex hierarchy regulated gene expression during *Drosophila* metamorphosis. *BMC Genomics* 10:80. doi: 10.1186/1471-2164-10-80

Lecuit, T., Samanta, R., and Wieschaus, E. (2002). *slam* encodes a developmental regulator of polarized membrane growth during cleavage of the *Drosophila* embryo. *Dev. Cell* 2, 425–436. doi: 10.1016/S1534-5807(02)00141-7

Lewin, A., and Grieve, I. C. (2006). Grouping Gene Ontology terms to improve the assessment of gene set enrichment in microarray data. *BMC Bioinformatics* 7:426. doi: 10.1186/1471-2105-7-426

Li, F., Vensko, S. P. II, Belikoff, E. J., and Scott, M. J. (2013). Conservation and sex-specific splicing of the transformer gene in the calliphorids *Cochliomyia hominivorax*, *Cochliomyia macellaria* and *Lucilia sericata*. *PLoS One* 8:e56303. doi: 10.1371/journal.pone.0056303

Liu, Z., Ho, L., and Bonning, B. (2007). Localization of a *Drosophila melanogaster* homolog of the putative juvenile hormone esterase binding protein of *Manduca sexta*. *Insect Biochem. Mol. Biol.* 37, 155–163. doi: 10.1016/j.ibmb.2006.11.003

Luo, R., Liu, B., Xie, Y., Li, Z., Huang, W., Yuan, J., et al. (2012). SOAPdenovo2: an empirically improved memory-efficient short-read de novo assembler. *Gigascience* 1:18. doi: 10.1186/2047-217X-1-18

Mank, J. E., Hosken, D. J., and Wedell, N. (2011). Some inconvenient truths about sex chromosome dosage compensation and the potential role of sexual conflict. *Evolution* 65, 2133–2144. doi: 10.1111/j.1558-5646.2011.01316.x

Martín-Vega, D., Hall, M. J. R., and Simonsen, T. J. (2016). Resolving confusion in the use of concepts and terminology in intrapuparial development studies of cyclorrhaphous Diptera. *J. Med. Entomol.* 53, 1249–1251. doi: 10.1093/jme/tjw081

Matuszewski, S., and Fratczak-Łagiewska, K. (2018). Size at emergence improves accuracy of age estimates in forensically-useful beetle *Creophilus maxillosus* L. (Staphylinidae). *Sci. Rep.* 8:2390. doi: 10.1038/s41598-018-20796-1

McCarthy, D. J., Chen, Y., and Smyth, G. K. (2012). Differential expression analysis of multifactor RNA-Seq experiments with respect to biological variation. *Nucleic Acids Res.* 40, 4288–4297. doi: 10.1093/nar/gks042

Morrow, E. H., Stewart, A. D., and Rice, W. R. (2008). Assessing the extent of genome-wide intralocus sexual conflict via experimentally enforced gender-limited selection. *J. Evol. Biol.* 21, 1046–1054. doi: 10.1111/j.1420-9101.2008.01542.x

Morrow, J. L., Riegler, M., Frommer, M., and Shearman, D. C. A. (2014a). Expression patterns of sex-determination genes in single male and female embryos of two *Bactrocera* fruit fly species during early development. *Insect Mol. Biol.* 23, 754–767. doi: 10.1111/imb.12123

Morrow, J. L., Riegler, M., Gilchrist, A. S., Shearman, D. C. A. A., and Frommer, M. (2014b). Comprehensive transcriptome analysis of early male and female *Bactrocera jarvisi* embryos. *BMC Genet.* 15:S7. doi: 10.1186/1471-2156-15-S2-S7

Muller-Holtkamp, F. (1995). The Sex-lethal gene homologue in *Chrysomya rufifacies* is highly conserved in sequence and exon-intron organization. *J. Mol. Evol.* 41, 467–477. doi: 10.1007/bf00160318

National Research Council (2009). *Strengthening Forensic Science in the United States: A Path Forward*. Washington, DC: The National Academies Press. doi: 10.17226/12589

Navarro-Costa, P., and Martinho, R. G. (2020). The emerging role of transcriptional regulation in the oocyte-to-zygote transition. *PLoS Genet.* 16:e1008602. doi: 10.1371/journal.pgen.1008602

Owings, C. G., Spiegelman, C., Tarone, A. M., and Tomberlin, J. K. (2014). Developmental variation among *Cochliomyia macellaria* Fabricius (Diptera: Calliphoridae) populations from three ecoregions of Texas, USA. *Int. J. Legal Med.* 128, 709–717. doi: 10.1007/s00414-014-1014-0

Page, R. D. M. (1996). Tree View: An application to display phylogenetic trees on personal computers. *Bioinformatics* 12, 357–358. doi: 10.1093/bioinformatics/12.4.357

Parisi, M., Nuttall, R., Edwards, P., Minor, J., Naiman, D., Lü, J., et al. (2004). A survey of ovary-, testis-, and soma-biased gene expression in *Drosophila melanogaster* adults. *Genome Biol.* 5, 1–18. doi: 10.1186/gb-2004-5-6-r40

Patrício Macedo, M., Arantes, L. C., and Tidon, R. (2018). Sexual size dimorphism in three species of forensically important blowflies (Diptera: Calliphoridae) and its implications for postmortem interval estimation. *Forensic Sci. Int.* 293, 86–90. doi: 10.1016/j.forsciint.2018.10.009

Perry, J. C., Harrison, P. W., and Mank, J. E. (2014). The ontogeny and evolution of sex-biased gene expression in *Drosophila melanogaster*. *Mol. Biol. Evol.* 31, 1206–1219. doi: 10.1093/molbev/msu072

Picard, C. J., Deblois, K., Tovar, F., Bradley, J. L., Johnston, J. S., and Tarone, A. M. (2013). Increasing precision in development-based postmortem interval estimates: what's sex got to do with it? *J. Med. Entomol.* 50, 425–431. doi: 10.1603/ME12051

Picard, C. J., Johnston, J. S., and Tarone, A. M. (2012). Genome sizes of forensically relevant Diptera. *J. Med. Entomol.* 49, 192–197. doi: 10.1603/me11075

Pimsler, M. L., Sze, S.-H., Saenz, S., Fu, S., Tomberlin, J. K., and Tarone, A. M. (2019). Gene expression correlates of facultative predation in the blow fly *Chrysomya rufifacies* (Diptera: Calliphoridae). *Ecol. Evol.* 9:5413. doi: 10.1002/ece3.5413

R Core Team (2010). *R: A language and environment for statistical computing. R Foundation for Statistical Computing*. Vienna: R Foundation for Statistical Computing, doi: ISBN 3-900051-07-0

Ranz, J. M. (2003). Sex-dependent gene expression and evolution of the *Drosophila* transcriptome. *Science* 300, 1742–1745. doi: 10.1126/science.1085881

Ranz, J. M., Castillo-Davis, C. I., Meiklejohn, C. D., and Hartl, D. L. (2003). Sex-dependent gene expression and evolution of the *Drosophila* transcriptome. *Science* 300, 1742–1745.

Ritchie, M. E., Phipson, B., Wu, D., Hu, Y., Law, C. W., Shi, W., et al. (2015). limma powers differential expression analyses for RNA-sequencing and microarray studies. *Nucleic Acids Res.* 43, e47–e47. doi: 10.1093/nar/gkv007

Robinson, M. D., McCarthy, D. J., and Smyth, G. K. (2010). edgeR: a Bioconductor package for differential expression analysis of digital gene expression data. *Bioinformatics* 26, 139–140. doi: 10.1093/bioinformatics/btp616

Salvemini, M., Amato, R. D., Petrella, V., Ippolito, D., Ventre, G., Zhang, Y., et al. (2014a). Subtractive and differential hybridization molecular analyses of *Ceratitis capitata* XX/XY versus XX embryos to search for male-specific early transcribed genes. *BMC Genet.* 15:S5. doi: 10.1186/1471-2156-15-S2-S5

Salvemini, M., Arunkumar, K. P., Nagaraju, J., Sanges, R., Petrella, V., Tomar, A., et al. (2014b). De novo assembly and transcriptome analysis of the Mediterranean fruit fly *Ceratitis capitata* early embryos. *PLoS One* 9:e114191. doi: 10.1371/journal.pone.0114191

Sanford, M. R. (2017). Insects and associated arthropods analyzed during medicolegal death investigations in Harris County, Texas, USA: January 2013-April 2016. *PLoS One* 12:1–23. doi: 10.1371/journal.pone.0179404

Sapti, M., Klassen, W., and Curtis, C. F. (2005). "History of the Sterile Insect Technique," in *Sterile Insect Technique: Principles and Practice in Area-Wide Integrated Pest Management*, eds V. A. Dyck, J. Hendrichs, and A. S. Robinson (Dordrecht: Springer), 3–36. doi: 10.1007/1-4020-4051-2_1

Sawanth, S. K., Gopinath, G., Sambrani, N., and Arunkumar, K. P. (2016). The autoregulatory loop: A common mechanism of regulation of key sex determining genes in insects. *J. Biosci.* 41, 283–294. doi: 10.1007/s12038-016-9609-x

Scott, M. J. M. J., Pimsler, M. L. M. L. M. L., and Tarone, A. M. A. M. (2014). Sex determination mechanisms in the Calliphoridae (Blow Flies). *Sex. Dev.* 8, 29–37. doi: 10.1159/000357132

Shearman, D. C. (2002). The evolution of sex determination systems in dipteran insects other than Drosophila. *Genetica* 116, 25–43.

Shine, R. (1989). Ecological causes for the evolution of sexual simorphism: a review of the evidence. *Q. Rev. Biol.* 64, 419–461. doi: 10.1086/416458

Singh, D., and Bharti, M. (2001). Further observations on the nocturnal oviposition behaviour of blow flies (Diptera: Calliphoridae). *Forensic Sci. Int.* 120, 124–126. doi: 10.1016/S0379-0738(01)00419-4

Small, C. M., Carney, G. E., Mo, Q., Vannucci, M., and Jones, A. G. (2009). A microarray analysis of sex- and gonad-biased gene expression in the zebrafish: evidence for masculinization of the transcriptome. *BMC Genomics* 10:579. doi: 10.1186/1471-2164-10-579

Smith, J. L., and Cook, A. K. (2020). First use of an entire age cohort to evaluate the role of sex in the development of the forensically important *Chrysomya megacephala* (Diptera: Calliphoridae). *J. Med. Entomol.* 57, 641–644. doi: 10.1093/jme/tjz205

Stillwell, R. C., Blanckenhorn, W. U., Teder, T., Davidowitz, G., and Fox, C. W. (2010). Sex differences in phenotypic plasticity affect variation in sexual size dimorphism in insects: from physiology to evolution. *Annu. Rev. Entomol.* 55, 227–245. doi: 10.1146/annurev-ento-112408-085500

Supek, F., Bošnjak, M., Škunca, N., and Šmuc, T. (2011). REVIGO summarizes and visualizes long lists of gene ontology terms. *PLoS One* 6:e21800. doi: 10.1371/journal.pone.0021800

Sze, S.-H. H., Dunham, J. P., Carey, B., Chang, P. L., Li, F., Edman, R. M., et al. (2012). A de novo transcriptome assembly of *Lucilia sericata* (Diptera: Calliphoridae) with predicted alternative splices, single nucleotide polymorphisms and transcript expression estimates. *Insect Mol. Biol.* 21, 205–221. doi: 10.1111/j.1365-2583.2011.01127.x

Sze, S.-H., Pimsler, M. L., Tomberlin, J. K., Jones, C. D., and Tarone, A. M. (2017). A scalable and memory-efficient algorithm for de novo transcriptome assembly of non-model organisms. *BMC Genomics* 18:387. doi: 10.1186/s12864-017-3735-1

Tarone, A. M., and Benoit, J. B. (2019). "Insect development as it relates to forensic entomology," in *Forensic Entomology: The Utility of Arthropods in Legal Investigations*, eds J. H. Byrd and K. Tomberlin (London: CRC Press), 225–252. doi: 10.4324/9781351163767-10

Tarone, A. M., and Foran, D. R. (2006). Components of developmental plasticity in a Michigan population of *Lucilia sericata* (Diptera: Calliphoridae). *J. Med. Entomol.* 43, 1023–1033. doi: 10.1093/jmedent/43.5.1023

Tarone, A. M., and Foran, D. R. (2008). Generalized additive models and *Lucilia sericata* growth: Assessing confidence intervals and error rates in forensic entomology. *J. Forensic Sci.* 53, 942–948. doi: 10.1111/j.1556-4029.2008.00744.x

Tarone, A. M., Foran, D. R., Ph, D., Foran, D. R., and Ph, D. (2011). Gene expression during blow fly development: improving the precision of age estimates in forensic entomology. *J. Forensic Sci.* 56, 112–122. doi: 10.1111/j.1556-4029.2010.01632.x

Tarone, A. M., Singh, B., and Picard, C. J. (2015). "Molecular biology in forensic entomology," in *Forensic Entomology: International Dimensions and Frontiers*, eds J. K. Tomberlin and M. E. Benbow (London: CRC Press), 297–316.

Tomberlin, J. K., Adler, P. H., Myers, H. M., and Entomol, E. (2009). Development of the black soldier fly (Diptera: Stratiomyidae) in relation to Ttemperature. *Physiol. Ecol.* 38, 930–934. doi: 10.1603/022.038.0347

Tomberlin, J. K., Benbow, M. E., Tarone, A. M. and Mohr, R. M. (2011). Basic research in evolution and ecology enhances forensics. *Trends Ecol. Evol.* 26, 53–55. doi: 10.1016/j.tree.2010.12.001

Ullerich, F. H. (1963). Geschlechtschromosomen und Geschlechtsbestimmung bei einigen Calliphorinen (Calliphoridae, Diptera). *Chromosoma* 14, 45–110. doi: 10.1007/bf00332610

Ullerich, F. H. (1973). Die genetische grundlage der monogenie beider schmeilfliege *Chrysomya rufifacies* (Calliphoridae, Diptera). *Mol. Gen. Genet.* 125, 157–172. doi: 10.1007/bf00268869

Ullerich, F. H. (1975). [Identification of the genetic sex chromosomes in the monogenic blowfly *Chrysomya rufifacies* (Calliphoridae, Diptera)]. *Chromosoma* 50, 393–419. doi: 10.1007/bf00327076

Ullerich, F. H. (1977). Production of male and female offspring in the strictly monogenic fly *Chrysomya rufifacies* after ovary transplantation. *Naturwissenschaften* 64, 277–278. doi: 10.1007/bf00438313

Ullerich, F. H. (1980). Analysis of the predetermining effect of a sex realizer by ovary transplantations in the monogenic fly *Chrysomya rufifacies*. *Wilhelm Roux's Arch. Dev. Biol.* 188, 37–43. doi: 10.1007/bf00848608

Ullerich, F. H. (1984). Analysis of sex determination in the monogenic blowfly *Chrysomya rufifacies* by pole cell transplantation. *Mol. Gen. Genet.* 193, 479–487. doi: 10.1007/bf00382087

Van Emden, F. I. (1957). The taxonomic significance of the characters of immature insects. *Annu. Rev. Entomol.* 2, 91–106. doi: 10.1146/annurev.en.02.010157.000515

Vuong, Q. H. (1989). Likelihood ratio tests for model selection and non-nested hypotheses. *Econometrica* 57:307. doi: 10.2307/1912557

Wang, X., Xiong, M., Wang, J., Lei, C., and Zhu, F. (2015). Reference gene stability of a synanthropic fly, *Chrysomya megacephala*. *Parasites Vectors* 8, 1–10. doi: 10.1186/s13071-015-1175-9

Waterhouse, R. M., Seppey, M., Simão, F. A., and Zdobnov, E. M. (2019). "Using BUSCO to assess insect genomic resources," in *Methods in Molecular Biology*, ed. J. M. Walker (New Jersey, NJ: Humana Press Inc.), 59–74. doi: 10.1007/978-1-4939-8775-7_6

Whitworth, T. (2010). Keys to the genera of species of blow flies (Diptera: Calliphoridae) of the West Indies and description of a new species of *Lucilia* Robineau-Desvoidy. *Zootaxa* 2663, 1–35. doi: 10.11646/zootaxa.2663.1.1

Wilton, D. P. (1954). *A study of a blowfly, Chrysomya rufifacies* (Macquart), with special reference to its reproductive behavior (Diptera: Calliphoridae). Ph. D. thesis. Hawaii: University of Hawaii.

Yan, Y., Williamson, M. E., Davis, R. J., Andere, A. A., Picard, C. J., and Scott, M. J., (2020). Improved transgenic sexing strains for genetic control of the Australian sheep blow fly *Lucilia cuprina* using embryo-specific gene promoters. *Molecular Genetics and Genomics* 295, 287–298. doi: 10.1007/s00438-019-01622-3

Yanmanee, S., Husemann, M., Benbow, M. E., and Suwannapong, G. (2016). Larval development rates of *Chrysomya rufifacies* Macquart, 1842 (Diptera: Calliphoridae) within its native range in South-East Asia. *Forensic Sci. Int.* 266, 63–67. doi: 10.1016/j.forsciint.2016.04.033

Yu, G., Cheng, P., Chen, Y., Li, Y., Yang, Z., Chen, Y., et al. (2011). Inoculating poultry manure with companion bacteria influences growth and development of black soldier fly (Diptera: Stratiomyidae) larvae. *Environ. Entomol.* 40, 30–35. doi: 10.1603/EN10126

Zajac, B. K., Amendt, J., Horres, R., Verhoff, M. A., and Zehner, R. (2015). De novo transcriptome analysis and highly sensitive digital gene expression profiling of *Calliphora vicina* (Diptera: Calliphoridae) pupae using MACE (Massive Analysis of cDNA Ends). *Forensic Sci. Int. Genet.* 15, 137–146. doi: 10.1016/j.fsigen.2014.11.013

Zehner, R., Amendt, J., and Boehme, P. (2009). Gene expression analysis as a tool for age estimation of blowfly pupae. *Forensic Sci. Int. Genet. Suppl. Ser.* 2, 292–293. doi: 10.1016/j.fsigss.2009.08.008

Zerbino, D. R., Achuthan, P., Akanni, W., Amode, M. R., Barrell, D., Bhai, J., et al. (2018). Ensembl 2018. *Nucleic Acids Res.* 46, D754–D761. doi: 10.1093/nar/gkx1098

Zhang, Y., Sturgill, D., Parisi, M., Kumar, S., and Oliver, B. (2007). Constraint and turnover in sex-biased gene expression in the genus *Drosophila*. *Nature* 450, 233–237. doi: 10.1038/nature06323

Zuha, R. M., and Omar, B. (2014). Developmental rate, size, and sexual dimorphism of *Megaselia scalaris* (Loew) (Diptera: Phoridae): Its possible implications in forensic entomology. *Parasitol. Res.* 113, 2285–2294. doi: 10.1007/s00436-014-3883-z

Zurawski, K. N., Benbow, M. E., Miller, J. R., and Merritt, R. W. (2009). Examination of nocturnal blow fly (Diptera: Calliphoridae) oviposition on pig carcasses in Mid-Michigan. *J. Med. Entomol.* 46, 671–679. doi: 10.1603/033.046.0335

Conflict of Interest: JT and AT are part of an NSF funded IUCRC, which includes Government and Corporate members. Most of the work done here preceded the formation of the center and no work after formation of the center was guided by any interactions with the center. No funding from the center contributed to this work.

The remaining authors declare that the research was conducted in the absence of any commercial or financial relationships that could be construed as a potential conflict of interest.

Publisher's Note: All claims expressed in this article are solely those of the authors and do not necessarily represent those of their affiliated organizations, or those of the publisher, the editors and the reviewers. Any product that may be evaluated in this article, or claim that may be made by its manufacturer, is not guaranteed or endorsed by the publisher.

Advantages of publishing in Frontiers

OPEN ACCESS
Articles are free to read for greatest visibility and readership

FAST PUBLICATION
Around 90 days from submission to decision

HIGH QUALITY PEER-REVIEW
Rigorous, collaborative, and constructive peer-review

TRANSPARENT PEER-REVIEW
Editors and reviewers acknowledged by name on published articles

Frontiers
Avenue du Tribunal-Fédéral 34
1005 Lausanne | Switzerland

Visit us: www.frontiersin.org
Contact us: frontiersin.org/about/contact

REPRODUCIBILITY OF RESEARCH
Support open data and methods to enhance research reproducibility

DIGITAL PUBLISHING
Articles designed for optimal readership across devices

FOLLOW US
@frontiersin

IMPACT METRICS
Advanced article metrics track visibility across digital media

EXTENSIVE PROMOTION
Marketing and promotion of impactful research

LOOP RESEARCH NETWORK
Our network increases your article's readership